ABSTRACT

Title of Dissertation: GENOMIC AND MICROBIOME ANALYSIS TO IMPROVE FILLET YIELD AND QUALITY TRAITS IN RAINBOW TROUT

Ridwan Olawale Ahmed
Doctor of Philosophy, 2025

Dissertation directed by: Associate Professor Mohamed Salem, Ph.D.
Department of Animal and Avian Sciences

Rainbow trout is the most widely farmed cool- and cold-water freshwater fish species in the United States. It is primarily cultivated for its fillets, rich in protein and essential fatty acids. As interest grows in enhancing the productive efficiency of rainbow trout, most breeding programs still rely heavily on traditional, pedigree-based selection. Incorporating genomic information holds promise for accelerating genetic gains, particularly for complex or lethally measured traits such as fillet yield and quality. However, even with the availability of genomic data, a substantial portion of phenotypic variation remains unexplained—an issue commonly referred to as "missing heritability."

Recently, the gut microbiome has emerged as a potential contributor to phenotypic variation through host–microbiome interactions. Some microbiome features may be heritable, which could help account for portions of the missing heritability.

In this study, we investigated the genomic and microbiome architecture of rainbow trout families from USDA breeding programs, aiming to improve fillet yield and quality traits. Fillet color, a key quality attribute influencing consumer preferences, was a major focus. Using genome-wide association studies (GWAS) and RNA-Seq, we characterized the genetic basis of variation in fillet yield and quality traits. GWAS identified SNPs within genes involved in carotenoid metabolism (e.g., β,β-carotene 15,15-dioxygenase, retinol dehydrogenase), myoglobin regulation (*ATP5F1B*), and structural maintenance of muscle tissue (*klh41b, COL28A1, CTSK*). RNA-Seq further highlighted genes involved in lipid/carotenoid metabolism, ribosomal function, mitochondrial activity, and stress response as contributors to fillet color variation.

We also integrated expression quantitative trait loci (eQTL) mapping to connect genetic variants with gene expression and phenotypic outcomes. A total of 6,275 cis-eQTLs were identified near promoter regions influencing gene expression. Notable candidate genes included *GABRR1-like*, *AZIN1*, and *ATP6V1* for body weight; *TNNI2*, *PDLIM3*, *CDK5*, and *CYP3A27* for tissue robustness; and GATD3A, PPP2R1BB, and USP6NL for muscle development. A specific A-A-C eQTL haplotype was strongly associated with elevated expression of ATP6V1. These eQTLs overlapped with regions enriched for active enhancers, making them strong candidates for inclusion in genomic selection strategies.

To assess the role of the gut microbiome, we employed both 16S rRNA gene sequencing and shotgun metagenomics to identify taxa and pathways predictive of fillet color. Fish with red fillets were enriched (LDA score > 1.5) for *Leuconostoc lactis*, *Corynebacterium variabile*, *Jeotgalicoccus halotolerans*, and *Leucobacter chromiireducens*—bacterial species with known probiotic functions and carotenoid biosynthesis capabilities. These fish also exhibited enrichment of the Methylerythritol Phosphate (MEP) pathway, which is involved in carotenoid production.

Microbiome-wide association studies (MWAS) revealed microbial taxa and metabolic pathways associated with growth traits. These included pathways such as fatty acid elongation, fatty acid oxidation II, pyruvate fermentation to isobutanol, glyoxylate cycle, mixed acid fermentation, superpathway of branched chain amino acid biosynthesis, and peptidoglycan biosynthesis II —all of which may influence growth performance in rainbow trout.

Lastly, we demonstrated the feasibility of combining low-coverage whole-genome sequencing (1x WGS) with genotype imputation and microbiome data for genomic prediction. Our findings show that combining 1x WGS with pedigree data provides predictive power that outperforms the pedigree-only-based models. Moreover, incorporating microbiome data improved prediction accuracy for body weight and muscle yield by 7.2%, and 8.6%, respectively, offering potential for substantial cumulative gains across generations.

In conclusion, this study identifies key genetic and microbiome contributors to variation in fish growth, fillet yield and quality traits in rainbow trout. Our results highlight the potential of integrating genomic and microbiome information to enhance selective breeding strategies, promote sustainable aquaculture, improve protein security, and deliver economic benefits to the U.S. aquaculture industry.

GENOMIC AND MICROBIOME ANALYSIS TO IMPROVE FILLET YIELD AND QUALITY TRAITS IN RAINBOW TROUT

by

Ridwan Olawale Ahmed

Dissertation submitted to the Faculty of the Graduate School of the

University of Maryland, College Park, in partial fulfillment

of the requirement for the degree of

Doctor of Philosophy

2025

Advisory Committee:

Mohamed Salem, Ph.D., Chair, Associate Professor

Jiuzhou Song, Ph.D. Professor

Li Ma, Ph.D., Professor

Louis Plough, Ph.D. Associate Professor

Rafet Al-Tobasei, Ph.D. Assistant Professor

Najib M. El-Sayed, Ph.D., Professor and Dean's Representative

© Copyright by

Ridwan Olawale Ahmed

2025

ACKNOWLEDGEMENTS

First, I would like to express my sincere gratitude to my advisor, Professor Mohamed Salem, for your invaluable guidance, support, and patience throughout my doctoral journey. From the time you decided to accept me into your lab, even without a scientific publication at the time, your insightful guidance, feedback, encouragement, and high standards have been instrumental in shaping this dissertation and my development as a researcher. I am most sincerely grateful.

I also appreciate all the members of my advisory committee (Professors Mohamed Salem, Jiuzhou Song, Li Ma, Louis Plough, Rafet Al-Tobasei, and Najib M. El-Sayed). Thank you all for your guidance and invaluable feedback, which shaped my dissertation.

Additionally, I would like to thank Professor Richard Kohn, Dr. Sarah Balcom, and Dr. Kris Mayo, for letting me assist in teaching and shaping the minds of future animal scientists.

I want to thank the members of Salem lab and colleagues, past and present, for their advice, assistance, and friendship: Orso (Guglielmo Raymo), Fabi (Fabiane Januario), Nour El-Husseini, and Dr. Ali Ali, our wonderful post-doc. Thank you for creating a collaborative, inspiring, and sometimes entertaining research environment.

To my parents (Mr. and Mrs. Hammed), in-laws (Alhaji and Alhaji Oladoja), and family, thank you for your unconditional love, patience, and support. Mom, Dad, and my siblings, your belief in me has been a steady source of strength, and I dedicate this work to you.

To my dearest wife, Oladoja Suleeha Olawunmi, you have been my rock, and your unwavering emotional and general support has been a survival mechanism for all these years. I will see you soon, inshaa Allah.

Lastly, I am grateful to the Department of Animal and Avian Sciences and the Graduate School for the financial and academic support that made this research possible. The department's graduate coordinators, Dr. Carol Keefer and now Dr. Zhengguo Xiao, have been of immense help not only to me but also to all the graduate students.

This dissertation is not just the result of individual effort; it reflects the collective support I have been fortunate to receive. Thank you all.

Scholarly Articles

Findings from this dissertation have been published in the following peer-reviewed research articles:

1. Ahmed, R. O., Ali, A., Al-Tobasei, R., Leeds, T., Kenney, B., & Salem, M. (2022). Weighted single-step GWAS identifies genes influencing fillet color in rainbow trout. *Genes*, *13*(8), 1331.
2. Ahmed, R. O., Ali, A., Leeds, T., & Salem, M. (2023). RNA-Seq analysis of the pyloric caecum, liver, and muscle reveals molecular mechanisms regulating fillet color in rainbow trout. *BMC genomics*, *24*(1), 579.
3. Ahmed, R. O., Ali, A., Leeds, T., & Salem, M. (2023). Fecal Microbiome Analysis Distinguishes Bacterial Taxa Biomarkers Associated with Red Fillet Color in Rainbow Trout. *Microorganisms*, *11*(11), 2704.

Table of Contents

List of Tables

List of Figures

LIST OF ABBREVIATIONS

Abbreviations	Name
ABC	ATP-binding cassette
ADP	Adenosine-di-phosphate
ANKH	Ankyrin repeat and KH domain-containing protein
ANOVA	Analysis of Variance
AP	Activator protein
ARRIVE	Animal Research: Reporting of In Vivo Experiments
ARS	Agricultural Research Service
ASV	Amplicon sequence variants
ATP	Adenosine-tri-phosphate
ATRA	All-trans-retinoic acid
BCWD	Bacteria cold water disease
BGLR	Bayesian Generalized Linear Regression
BLUP	Best Linear Unbiased Prediction
BPHL	Biephenyl hydrolase-like
BRAP	BRCA1-associated protein
BW	Body weight
CDS	Coding sequence
CLR	centered log-ratio
COA	Co-enzyme A
CRISPR	Clustered regularly interspaced short palindromic repeats
CTSC	*Cathepsin C*
CTSK	Cathepsin K
CV	Coefficient of variation
DE	Differentia Expression
DEG	Differentially Expressed Genes
DGE	Differential Gene Expression
DMA	Differential Microbiome Abundance
DNA	Deoxyribo nucleic acid
EBV	Estimated breeding value
ELAV	Embryonic Lethal, Abnormal Vision-like protein
ELOVL	Elongation of very long chain fatty acids
EST	Expressed sequence tags
EZRA	Ezrin A
FC	Fold change
FDR	False Discovery Rate
FE	Feed Efficiency
FETUB	Fetuin B

FST	Follistatin
FXR	Farnesoid X receptor
FY	Fillet yield
GABA	Gaba amino butyric acid
GALT	Gut-associated lymphoid tissues
GBLUP	Genomic Best Linear Unbiased Prediction
GCF	Genome assembly Conversion to a RefSeq Format
GCTA	Genome-wide Complex Trait Analysis
GDS	Genomic data structure
GEBV	Genomic estimated breeding value
GH	Growth hormone
GO	Gene ontology
GRM	Genomic relationship matrix
GS	Genomic selection
GWAS	Genome wide association study
HDL	High densitity lipo protein
HMGCRA	3-Hydroxy-3-methylglutaryl-CoA reductase
HWE	Hardy weinberg equilibrum
IACUC	Institutional Animal Care and Use Committee
IDT	Integrated DNA Technologies
IFNAR	Intracellular-type I interferon receptor
IGF	Insulin Growth Factor
IMAP	Immunity-associated protein
INDEL	Insertion and deletion
IPA	Ingenuity Pathway Analysis
IPKB	Ingenuity pathway knowledge base
IPP	Isopentenyl pyrophosphate
KEGG	Kyoto Encyclopedia of Genes and Genomes
LD	Linkage disequilibrum
LDA	Linear Discriminant Analysis effect size
LDLR	Low densitity lipoprotein receptor
LIPL	Lipoprotein lipase
LXR	Liver X Receptor
MAF	Minor allele frequency
MAPK	Mitogen-Activated Protein Kinase
MEP	methylerythritol phosphate
MMSDH	Methylmalonate-semialdehyde dehydrogenase
MTP	Microsomal TAG transfer protein
MWAS	Microbiomewide association study
MYOC	Myocilin
NADH	Nicotinamide Adenine Dinucleotide

NCBI	National Center for Biotechnology Information
NCCCWA	National Center for Cool and Cold Water Aquaculture
NCL	Nucleolin
NGRN	Neugrin, neurite outgrowth associated
NGS	Next generation sequencing
OORP	Oocyte-specific Oxysterol binding protein Related-Protein
PBLUP	Pedigree Best Linear Unibiased Prediction
PCA	Principal component analysis
PCR	Polymerase chain reaction
PCs	Principal components
PDLIM3	PDZ and LIM domain protein 3
PIGP	Phosphatidylinositol glycan anchor biosynthesis class P
PITA	Probability of Interaction by Target Accessibility
POS	Position
PPAR	Peroxisome Proliferator-Activated Receptor
PSV	Paralogous Sequence Variants
PWM	Position Weight Matrix
PWY	Pathway
QIIME	Quantitative Insights Into Microbial Ecology
QQ	Quantile quantile
QTL	Quantitative traits loci
RAD	Restriction-site-associated DNA
RAR	Retinoic acid receptor
RAS	Recirculatory aquaculture system
RISC	RNA-induced silencing complex
RKHS	Reproducing kernel hilbert space
RNA	Ribonucleic acid
RNS	Reactive nitrogen species
ROS	Reactive oxygen species
RPKM	Reads Per Kilobase of transcript per Million
RXR	Retinoid X Receptor
SAM	Sterile Alpha Motif
SC	Synthetic control
SD	Standard deviation
SDR	short-chain dehydrogenase/reductase
SE	Standard error
SESN	Sestrin
SNP	Single nucleotide polymorphism
SPARC	Secreted acidic cysteine rich glycoprotein
STAT	signal transducers and activators of transcription

SYNPR	Synaptoporin
TAG	Triglyceride
TCA	Tricarboxylic Acid
TF	Transcription factor
TFBS	Transcription Factor Binding Site
TFIID	Transcription initiation factor
TGF	Transforming growth factor
TNF	Tumor Necrosis Factor
TPM	Transcript per million
TRNA	Transfer RNA
TSS	Transcription start site
UCH	Ubiquitin C-terminal hydroxylase
UDPNAGSYN	UDP-N-acetyl-D-glucosamine biosynthesis
USDA	United States Department of Agriculture
UTR	Untranslated region
VCF	Variant call format
VLDL	Very low density lipo-protein
WBW	Whole body weight
WGS	Whole geneome sequence
YC	Year Class

Chapter 1: Literature Review

Introduction

Basis of Phenotypic variability and Genetic Improvement

The foundational principle of quantitative genetics, encapsulated in the equation: phenotype = genotype + environment (P = G + E), underscores the complex interplay that shapes observable traits in livestock and aquaculture species. This relationship shows that an animal's phenotype results from its genetic makeup (genotype) and the environmental conditions it experiences, including nutrition, and management practices. For animal breeders who focus on genetic improvement, the environmental component introduces what can be described as "noise" which obscures the true genetic potential of an individual animal and complicates selection decisions (Kruuk & Hadfield, 2007). To enhance the accuracy of breeding programs and accelerate genetic gains, significant efforts are devoted to minimizing environmental influences through standardized management practices, advanced statistical models, and controlled rearing systems (Vala et al., 2023). By reducing this environmental "noise", breeders can more effectively identify and propagate superior genotypes, driving progress in economically important traits, which is critical for achieving sustainable animal production.

The Genetic component

The genetic component of the phenotype, often referred to as the genotype, represents the heritable portion of an animal's traits that can be passed to subsequent generations, making it the cornerstone of selective breeding programs in livestock and aquaculture. Unlike the environmental component, which fluctuates in response to external conditions, the genotype provides a stable foundation for improving economically important traits, such as fillet yield, body weight, fillet quality, and disease resistance. Measuring this genetic contribution accurately is crucial, as it enables breeders to predict an animal's breeding value—its potential to produce superior offspring—and to separate genetic effects from environmental noise.

Over the decades, advancements in statistical tools, molecular biology, and genomics have transformed how this genetic component is estimated, thereby increasing the genetic component of the equation and reducing the "noise". Historically, the genetic component was measured through phenotypic observation and pedigree-based methods, relying on the assumption that closely related animals share more genetic material (Weigel et al., 2017). The development of quantitative genetics introduced more rigorous approaches, notably the estimation of heritability—the proportion of phenotypic variance attributable to genetic differences. Using statistical models like analysis of variance (ANOVA), researchers could partition observed variation into genetic and environmental factors based on family records (Hofer, 1998; Kruuk & Hadfield, 2007) . However, these early methods were limited by their reliance on visible traits and incomplete pedigrees, often underestimating the genetic contribution in complex, polygenic traits typical of livestock and aquaculture species.

The advent of the Best Linear Unbiased Prediction (BLUP) method in the mid-20th century marked a significant leap forward in measuring the genetic component (Henderson, 1975). Despite its success, BLUP's dependence on extensive pedigree records and inability to capture molecular variation spurred the search for more direct genetic measurement tools as DNA technologies emerged.

The Genomic Revolution

The genomic revolution, beginning in the late 20th century and accelerating with the sequencing of the genomes, introduced marker-assisted selection (MAS) (Wakchaure et al., 2015) and, later, genomic selection (GS) (Meuwissen et al., 2016) as transformative methods for assessing the genetic component.

MAS utilized specific genetic markers—such as restriction fragment length polymorphisms (RFLPs) or microsatellites—linked to quantitative trait loci (QTL) to identify animals carrying favorable alleles (Sharma et al., 2024). While effective for traits controlled by a few major genes, MAS struggled with polygenic traits prevalent in breeding programs. The Genomic selection, pioneered by Meuwissen et al. (2001), overcame this limitation by leveraging high-density single nucleotide polymorphism (SNP) panels to estimate genomic breeding values (GEBVs) across the entire genome. By analyzing thousands of SNPs simultaneously, GS captures both large- and

small-effect genetic variants, offering unprecedented accuracy in predicting genetic merit even in young animals without phenotypic records.

Today, genomic selection dominates modern breeding programs in livestock and aquaculture, supported by advances in high-throughput sequencing, bioinformatics, and statistical modeling. As genomic technologies' costs decline and computational power grows, ongoing progress promises even finer resolution, such as the incorporation of epigenetics (Gonzalez-Recio et al., 2015) and gene editing (Ruan et al., 2017), further revolutionizing how breeders harness the genotype for sustainable animal production.

Harnessing advancing Genomics to advance Genetic Improvement

The genomic revolution in animal breeding hinges on technologies like the single nucleotide polymorphism (SNP) chip, a microarray tool that genotypes thousands to millions of SNPs across an animal's genome in a single assay. In livestock and aquaculture, SNP-chips, enable genomic selection and GWAS by providing a dense map of genetic variation, allowing breeders to estimate genomic breeding values (GEBVs) with high precision (Meuwissen et al., 2001). Their advantages include cost-effectiveness relative to whole-genome sequencing, rapid processing, and scalability for large populations (Mukhopadhyay & Kumar, 2013), making them a practical choice for complex traits like growth or disease resistance. SNP-chips are the backbone of genomic selection because they balance affordability with the ability to link genetic markers to phenotypic outcomes across generations. Unlike pedigree-based methods, they directly assess an animal's DNA, enabling selection of juveniles before phenotypic data is available, thus shortening generation intervals (Koopaee & Koshkoiyeh, 2014). Unlike pedigree-based methods that rely on family averages, SNP-chips drive genomic selection by offering a direct genomic snapshot. This allows breeders to predict genetic merit in young animals—before traits like fillet yield or disease tolerance are measurable—shortening generation intervals and accelerating improvement.

Brief History of SNP-Chip Development in Rainbow Trout

The complex nature and architecture of the rainbow trout genome complicated the SNP-Chip development. The rainbow trout genome and other salmonids underwent whole genome duplication event (Allendorf & Thorgaard, 1984). It is estimated that between 25% to 50% of their

genetic loci are still duplicated, and about 50% of the genome is composed of repeat sequences (Genet et al., 2011; Guyomard et al., 2012). This complicates the discovery of true bi-allelic SNPs, with initial studies conflicting paralogous sequence variants (PSVs) ((Boussaha et al., 2012; Sanchez et al., 2009). A PSV is a single nucleotide polymorphism in a nucleotide sequence that shows duplication in two genomic regions such that the polymorphism occurs between two loci rather than between alleles of a loci (Castaño Sánchez et al., 2011).

A possible solution is to use double-haploid rainbow trout lines, where it is expected that all loci are homogeneous. This will reduce the false identification of PSVs as putative allelic SNPs (Palti et al. (2014) used restriction-site-associated DNA (RAD) sequencing on 19 homozygous double-haploid rainbow trout lines to identify 145,168 putative single-nucleotide polymorphisms (SNPs). Using results from Palti et al.(2014), and from resequencing of breeders from an outbred Norwegian commercial population, Palti et al. (2015) developed, validated, and characterized the first high-density (57K) single nucleotide polymorphism (SNP) genotyping array for rainbow trout using Affymetrix technology**.**

Whole genome resequencing of 61 unrelated samples was used to identify ~30 million SNPs across 29 chromosomes of rainbow trout (Gao et al., 2018)To ensure adequate diversity, the fish used were from double haploid lines, aquaculture hatcheries, and wild populations.

Instead of using DNA-sequence to identify SNPs, RNA-seq data can be used to identify SNPs called coding/transcribed or functional SNPs which can affect the function of a gene and have large effect on phenotypes. Using RNA-Seq whole-transcriptome analysis at low coverage of pooled cDNA samples, Salem et al. (2012) identified 361 putative SNPs with allelic imbalance in divergent populations of slow and fast-growing rainbow trout associated with growth rate. Fifty-four SNPs were validated and used to perform association analysis on 778 fish. They identified 22 SNP markers that were significantly associated with growth traits. Salem et al. (2018) and Al-Tobasei et al. (2017) also designed an Affymetrix 50K SNP chip containing 21,000 transcribed SNPs that show allelic imbalance with important rainbow trout traits, as well as 29,000 transcribed SNPs strategically placed to cover the entire genome.

Although medium-density SNP-Chips (50K to 60K) are sufficient for use in genomic selection, they may be too small for fine QTL detention and for identifying causal variants ((Kim et al., 2018; Pérez-Enciso et al., 2015). This prompted Bernard et al. (2022) to develop a high-density SNP

array (665K) for rainbow trout using preexisting SNP datasets from USDA (Gao et al., 2018; S. Liu et al., 2021), a French commercial line from "Les Fils de Charles Murgat" (Fraslin et al., 2020), and whole-genome sequencing of INRAE isogenic lines to develop an Affymetrix 665K SNP array. A total of 32,372,492 distinct SNPs were identified from these three sources, which were later streamlined to 665K SNPs of high quality based on Affymetrix quality control, prioritizing SNPs whose flanking sequence uniquely aligned to the Swanson reference genome and those with the highest minor allele frequencies.

Genomic Selection with SNP-Chip and Key Studies in Aquaculture

Genomic selection (GS) leverages SNP-Chip data to predict breeding values to identify superior individuals/animals within the population for accelerated genetic improvement in breeding programs (Meuwissen et al., 2016). Genomic selection has been widely used in livestock and is growing in use in aquaculture.

Gonzalez-Pena et al. (2016) used SNP-chip and GWAS analysis to investigate the genetic architecture of fillet yield, body weight, and carcass weight in three successive generations of rainbow trout population (2010-, 2012- and 2014-year class) from NCCCWA bred for improvement in growth performance. A univariate model of the weighted single-step GBLUP identified genomic windows that explain a maximum of 1.7% of genetic variance for any of the traits, suggesting their polygenic nature. The genes that harbor the identified SNPs were involved in maintaining a proliferative and renewable population of myogenic precursor cells. A follow-up study, utilizing additional data, employed a multiple trait model to conduct a genome-wide association study (GWAS) and also investigated the feasibility of using genomic selection to enhance these traits. Moderate heritabilities of 0.41 and 0.33 were estimated for fillet yield and body weight, respectively, with a positive correlation of 0.24 between the two traits (Garcia et al., 2023b). In comparison with using pedigree data alone, genomic selection was found to have improved the accuracy of breeding value by up to 50% for fillet yield and 44% for body weight. Even with more data used in this study (14,165 fish in pedigree, 2742 with fillet yield record, and 12,890 fish with body weight record), no significant QTL were found to be for the traits, confirming their polygenic nature (Garcia et al., 2023a).

The correlation between estimated breeding values (EBVs) and genomic breeding values (GEBVs) was higher (0.99) for body weight that can be measured directly on breeding candidates compared to 0.72-0.79 for lethally measured traits (fillet yield, fillet weight, and carcass weight) (Dianelys Gonzalez-Pena et al., 2016). The contrary was observed for the accuracy of breeding value as the accuracy of GEBVs for lethally measured traits increased more (carcass weight ~100%, fillet weight ~100%, and fillet yield ~ 320%) compared to pedigree-based EBV, while that of body weight improved by just ~6% (Dianelys Gonzalez-Pena et al., 2016).

Compared to traditional family-based selection, genomic selection can improve the accuracy of breeding value predictions for BCWD resistance because it can account for within-family genetic variation, as there is no need to phenotype the selection candidates.

In a 2016 study conducted on an experimental rainbow trout population at NCCCWA, genomic selection provided no improvement in predicting genetic merit for BCWD resistance compared to the pedigree-based BLUP model (Vallejo et al., 2016). The authors proposed that this observation was due to the relatively small sample size for the training population (583-658) used in the study.

A follow up study that used a larger training population sample size (7898) on commercial breeding population from Trout lodge, Inc. (May spawning from the 2013 Year Class) that has been selected primarily on growth showed that genomic selection increased the accuracy of breeding value by up to 108.8%, relative to that obtained using a pedigree only model (Vallejo et al., 2017). Even with a low-density SNP panel (500 SNPs), the genomic estimated breeding value for BCWD resistance was higher than the pedigree BLUP (0.50-0.56 versus 0.36) (Roger L Vallejo et al., 2018). It is customary for genomic selection models to be re-trained in every generation to increase relatedness between training and testing animals. To reduce the cost of phenotyping at every generation, Vallejo et al. (2021) proved that even without retraining the prediction model in subsequent generations, genomic selection still achieved higher accuracy compared to pedigree-based selection. Although the genomic accuracy was reduced from 0.61-0.65 (when the model was retrained in the new generation) to 0.53-0.56 (without retraining) , the accuracy without retraining was still better than the PBLUP model accuracy with retraining (0.48) and without retraining (0.22).

Using three consecutive generations of the Trout Lodge May breeding population, Liu et al. (2018) demonstrated that marker-assisted selection (MAS), which is less expensive than genomic selection, can be used to enhance resistance to BCWD in a Trout Lodge commercial population. Two haplotype markers (Omy8GCG and Omy25CG) were found to be positively correlated with family BCWD survival rates across the three generations (2013, 2015, 2017 YC), with an accuracy (0.5) equal to or greater than the accuracy of traditional family-based selection but less than the accuracy obtainable with genomic selection.

Al-Tobasei et al. (2021) investigated the utility of genomic selection for fillet yield and the potential for reducing SNP panel density in rainbow trout, examining how this would impact prediction accuracy. The genomic breeding value (GEBV) estimated using the single-step genomic best linear unbiased prediction (ssGBLUP) model outperforms the pedigree-based best linear unbiased prediction (PBLUP) by 35% and 42% for fillet yield and fillet firmness, respectively. Their study demonstrated that reducing the SNP density from 50,000 to 500-800 SNPs is possible and still achieving a predictive ability higher than that of the pedigree-based method.

Genome-wide Association Studies (GWAS) with SNP-Chip and its Relevance for Genetic Improvement

Genome-wide Association Studies scan the entire genome of animals to find statistical associations between genetic variants (like SNPs within SNP-chip) and the traits of interest (Hayes & Goddard, 2010). It is used to identify specific genomic regions and SNPs associated with traits of interest, providing a foundation for understanding both the biology and the genetic architecture of a trait (Tan et al., 2023). GWAS helps researchers understand the genetic basis of complex traits, revealing which genes and pathways are involved in regulating an economic trait. GWAS is essential for complex polygenic traits where many small-effect loci collectively shape the outcome of a phenotype. Once the SNPs/genomic regions associated with a trait are identified with GWAS, they can be prioritized for marker-assisted selection (MAS) or genomic selection models to improve its accuracy in selection programs (Luo et al., 2021; Panigrahi et al., 2022).

GWAS Case-studies in Rainbow trout

The 50K SNP-chip designed by Salem et al. (2018) were used to perform GWAS analysis for muscle yield using the 2010- and 2012-year Class USDA/NCCCWA rainbow trout growth-selected line. They identified significant SNPs on QTL windows on chromosomes 14 and 16 that together explain up to 23.20% of the additive genetic variance for muscle yield. A previous study using genomic SNP-chip on the same fish population identified no major QTLs (Dianelys Gonzalez-Pena et al., 2016), signaling the utility and efficiency of the transcribed SNP-chip. The improvement in results obtained by Salem et al. (2018) may be attributed to the use of coding/functional SNPs in their SNP-Chip, as opposed to the conventional SNP-Chip, which uses random SNPs spread all over the genome. Coding/Functional SNPs in a SNP-Chip can be used to identify causative alleles that alter protein structure or functions (Li et al., 2018).Using the same functional SNP-chip allows the reduction of SNP panel density from fifty thousand to a mere 800 SNPs, which achieves improved performance in genomic prediction than the pedigree-based BLUP method (Al-Tobasei et al., 2021).

Gonzalez-Pena et al. (2016) used SNP-chip and GWAS analysis to investigate the genetic architecture of fillet yield, body weight, and carcass weight in three successive generations of rainbow trout population (2010-, 2012-, and 2014-year class) from NCCCWA bred for improvement in growth performance. A univariate model of the weighted single-step GBLUP identified genomic windows that explain a maximum of 1.7% of genetic variance for any of the traits, suggesting their polygenic nature. The genes that harbor the identified SNPs were involved in maintaining a proliferative and renewable population of myogenic precursor cells. A follow-up to this study with additional data used a multiple trait model to perform GWAS and investigated the feasibility of using genomic selection to improve these traits. Moderate heritabilities of 0.41 and 0.33 were estimated for fillet yield and body weight, respectively, and a positive correlation of 0.24 between both traits (Garcia et al., 2023b). In comparison with using pedigree-data alone, genomic selection was found to have improved the accuracy of breeding value by up to 50% for fillet yield and 44% for body weight. Even with more data used in this study (14,165 fish in pedigree, and 2742 with fillet yield record and 12,890 fish with body weight record), no significant QTL were found to be for the traits, confirming their polygenic nature (Garcia et al., 2023a).

The correlation between estimated breeding values (EBVs) and genomic breeding values (GEBVs) was higher (0.99) for body weight that can be measured directly on breeding candidates compared

to 0.72-0.79 for lethally-measured traits (fillet yield, fillet weight, and carcass weight) (Dianelys Gonzalez-Pena et al., 2016). The contrary was observed for the accuracy of breeding value as the accuracy of GEBVs for lethally-measured traits increased more (carcass weight ~100%, fillet weight ~100%, and fillet yield ~ 320%) compared to pedigree-based EBV, while that of body weight improved by just ~6% (Dianelys Gonzalez-Pena et al., 2016).

A GWAS with a 50K SNP-chip on 789 trout identified 247 SNPs across chromosomes 4 and 14 tied to bodyweight gain, explaining significant genetic variance. GS accuracy reached 0.65, highlighting polygenic control and developmental genes (Ali et al., 2020a). A 57K SNP-chip study on 1,343 trout found highly polygenic reproduction traits (e.g., spawn weight), with six QTL explaining modest variance. GS improved BLUP accuracy by 16–37%, favoring its use over marker-assisted selection (D'Ambrosio et al., 2020).

Weighted single-step GWAS on transcribed SNP-chip was used to identify genomic regions associated with fillet yield, fillet firmness protein content, intramuscular fat, moisture content and fillet color in rainbow trout 2010 and 2012 Year Class from the NCCCWA (Ahmed et al., 2022; Ali Ali et al., 2019; Ali et al., 2020b; Mohamed Salem et al., 2018). 163 SNPs explaining at least 2% of the genetic variance for fillet yield were identified. The identified genomic regions explained up to 28% of the additive genetic variance for fillet yield with the most significant QTLs on chromosomes 14 and 16 explaining 12.71% and 10.49%, respectively. The genes in the QTLs are involve in muscle development and cell signaling, differentiation, and regulation, mitochondria regulation. They noted that the activity of one of the identified genes, citrate synthase, is 1.43-fold higher in the higher fillet yield fish families in comparison with the lower yield families (Mohamed Salem et al., 2018).

Ali et al. (2019) identified 212 and 225 SNPs associated with shear force (fillet firmness), and protein content, respectively, in rainbow trout. The SNPs are within windows that explains a minimum of 2% of the additive genetic variance for the traits. The ryanodine receptor 3 gene (RYR3) harbors four significant SNPs for both shear force and protein content. Other identified genes for filled firmness include those involved in calcium binding/ metabolism, proteolytic activities, apoptotic process, and cellular adhesion and junction while genes for protein content are involved in apoptotic process, proteolysis, lysosomal activities, cell proliferation, transcription, and methylation.

Genes associated with fillet color includes those involved in carotenoid metabolism (beta carotene genes), myoglobin homeostasis, and maintenance of muscle structural integrity (Ahmed et al., 2022)They identified SNPs within the Ubiquitin carboxyl-terminal hydrolase-10 (USP10) and β,β-carotene 15,15′-dioxygenase genes that result in non-synonymous amino acid substitutions and may impact fillet color. The trait's complex genetic architecture was evident, as the maximum percentage of additive genetic variance explained by an SNP window is 3.5% for fillet redness.

Muscle fat and moisture content can impact the quality attributes of the fillet. Ali et al. (2020b) identified 137 and 178 SNPs associated with fat and moisture content, respectively with 61 SNPs common between both traits on chromosome 19 and 29. The SNPs are located in genes involved in lipid metabolism, cytoskeleton remodeling, and protein turnover.

These studies highlight GWAS's power to dissect trait architecture, but their reliance on large, well-phenotyped populations and high-density SNP data can limit applicability in less-studied species. Nonetheless, GWAS remains essential for building reference panels and validating markers used in genomic selection.

Limitations of SNP-Chip

As widely used as it has become, the SNP-chip still has some limitations, including missing rare variants, being population-specific, and missing other population-specific markers in its pre-designed panels (Mohamed Salem et al., 2018; Ye et al., 2018). All these can contribute to reduced prediction accuracy, especially when used outside of the population used to design the SNP-chip. Despite their limitations, SNP-chips remain the most common and practical choice for genomic selection across livestock and aquaculture species, driving genetic gains in traits critical to food security. They are relatively cheaper than whole-genome sequencing and have already established pipelines for genomic analysis.

Emergence of 1X Whole-Genome Sequencing (WGS)

The advent of low-coverage (1X) whole-genome sequencing (WGS) marks an exciting frontier for GWAS and genomic selection, offering a comprehensive alternative to SNP-chips. Unlike SNP-chips, which genotype predefined markers, 1X WGS sequences the entire genome at shallow depth, imputing genotypes with computational tools to achieve high accuracy (Li et al., 2021). Its fascination lies in capturing rare variants, structural variations, and novel SNPs missed by fixed

panels, potentially uncovering hidden genetic drivers of traits. For rainbow trout, 1X WGS could refine GWAS by detecting population-specific alleles linked to environmental adaptation, enhancing selection in diverse hatchery conditions.

Low-coverage (1X) whole-genome sequencing (WGS) emerges as a next-generation tool for GWAS and GS, sequencing the entire genome at shallow depth and imputing genotypes computationally (Li et al., 2021). Unlike SNP-chips, 1X WGS captures rare variants, structural changes, and novel SNPs, offering a fuller genomic picture. In rainbow trout, it's fascinating for refining GWAS—e.g., detecting trout-specific alleles for *Piscirickettsia salmonis* resistance (Barria et al., 2022)—and enhancing GS by improving GEBV precision. Its flexibility across species, without needing custom SNP arrays, adds allure.

Advantages include richer data for polygenic traits and potential cost declines as sequencing scales. However, 1X WGS faces higher upfront costs, imputation errors (needing a reference genome), and computational complexity, limiting its immediate adoption over SNP-chips. In trout, 1X WGS could elevate GWAS resolution for traits like BCWD resistance and boost GS accuracy, but scaling to large cohorts remains challenging.

Advantages of 1X WGS include its flexibility across species without custom SNP-chip development and its potential to integrate with existing genomic pipelines. However, drawbacks include higher initial costs than SNP-chips, reliance on imputation accuracy (which requires a reference genome), and increased computational demands. For genomic selection, 1X WGS promises more precise GEBVs by leveraging full genomic data, while for GWAS, it could identify causal mutations directly. As sequencing costs drop, 1X WGS may democratize advanced breeding, though its scalability in large populations remains a hurdle compared to SNP-chips.

Limitations and Challenges of 1X Whole-Genome Sequencing (WGS)

A critical prerequisite for effective 1x WGS is a high-quality, deep-coverage (e.g., 10x–30x) WGS reference panel to enable accurate imputation of genotypes from sparse data (Liu et al., 2024). Generating this panel requires sequencing a subset of individuals at high depth, which entails a significant initial cost. The effectiveness of 1x WGS hinges on imputation accuracy, which relies on a deep-coverage reference panel tailored to the target population (Druet et al., 2014).

The bioinformatics process for 1x WGS data is computationally intensive, requiring alignment, variant calling, and imputation pipelines(Ziyada, 2023). These demand high-performance computing and expertise, unlike SNP-chip analysis, which uses simpler workflows. Despite its potential, 1x WGS may also struggle to reliably detect rare variants (MAF < 1%) due to low coverage (Li et al., 2011; Rubinacci et al., 2023), except with a large, diverse, and deeply sequenced reference panel.

RNA-seq-based Transcriptomics Analysis and its Role in Animal Breeding

While genome-wide association studies (GWAS) have become a cornerstone in identifying genetic variants linked to traits of economic importance in animals, they often leave open questions about the underlying biological mechanisms. GWAS reveals statistical associations between genetic markers and phenotypes, but it does not indicate how these markers influence biological processes (Gallagher & Chen-Plotkin, 2018). This is where RNA-seq-based differential gene expression (DGE) analysis becomes particularly valuable.

RNA-seq allows researchers to profile gene expression activity across different tissues, conditions, or phenotypic groups. After GWAS identifies genomic regions associated with traits, DGE analysis can provide a deeper layer of functional information by revealing which genes are actively involved in those traits (McDermaid et al., 2019; Weber et al., 2016). For instance, if a genomic region identified by GWAS is located near a gene that is also found to be differentially expressed between high- and low-performing animals, this convergence strengthens the evidence that the gene is truly relevant to the trait and can be regarded as a functional candidate gene (Lam et al., 2021).

Even without direct integration with GWAS, RNA-seq serves an important purpose on its own. It helps uncover gene expression signatures associated with desirable or undesirable traits, shedding light on the biological pathways and networks at play (Weber et al., 2016). This knowledge is essential for understanding trait architecture, identifying novel candidate genes, and selecting functional markers for breeding programs.

RNA-seq is also useful for eQTL analysis- to identify SNPs with regulatory effects that directly influence gene expression. The functional SNPs identified can then be prioritized for GWAS and genomic selection.

In summary, RNA-seq differential expression analysis offers functional insight that complements GWAS, enhancing our understanding of the genetic basis of traits and supporting more precise and effective breeding decisions.

RNA-seq Transcriptomics studies in Rainbow Trout

While GWAS provides insights into the genetic architecture of traits, understanding their biological underpinnings requires complementary approaches such as RNA-seq-based transcriptomics. Whole-body transcriptomic analysis showed that several immune-related genes are more expressed in the resistant line (ARS-Fp-R) compared to the control (ARS-Fp-C) and susceptible (ARS-Fp-S) lines (Marancik et al., 2014). The differentially expressed protein-coding genes include TNF receptor superfamily member 14b-like isoform x1, interleukine-1 receptor-like 1, complement c1q-like protein 4 precursor, protein nlrc3-like and GATA-binding factor 2-like isoform x2. Subsequently, Paneru et al. (2016) Identified several white muscle differentially expressed long non-coding RNA (lncRNA) in the three genetic lines when challenged with *Flavobacterium psychrophilum.* The lncRNAs showed correlated expression with their overlapping or nearby immune-relevant protein-coding genes suggesting possibly lncRNA regulation of those genes.

Liu et al. (2014) used RNA-seq analysis to investigate differentially expressed genes in the rainbow trout liver in response to handling and confinement stress initiated at the NCCCWA facility. The differentially expressed genes identified are involved in metabolic processes such as glucose metabolism, response to stimulus, regulation of cell growth, and insulin signaling pathway (Wiseman et al., 2007).

Cleveland et al. (2020) Compared the transcriptome profile in the liver and white muscle of rainbow trout selectively bred for growth (GL) and a randomly mated synthetic control line (SC) from the NCCCWA breeding program. The body weight at harvest in the GL genetic line was 20% higher than those of the SC line. They identified 145 and 36 differentially expressed genes. The genes are enriched in pathways of growth hormone/insulin-like growth factor axis (GH/IGF) and PI3K-Akt, JAK-STAT, MAPK, and cAMP signal transduction pathways. Plasma IGF-I concentration was significantly higher in the plasma of fish on the growth line. The genetic signals and pathways identified possibly contribute to the physiological mechanisms of growth performance in rainbow trout.

Ali et al. (2018) investigated the integrated transcriptomics of muscle tissue in rainbow trout families from the 2010 NCCCWA Year Class showing variability in muscle yield and muscle quality traits (fat content, shear force, and fillet color). They identified 240 and 1280 differentially expressed (DE) genes and DE long noncoding RNAs (lncRNAs), respectively. The expression of 229 DE lncRNAs shows a positive correlation with the expression of their neighboring, overlapping, or distantly located protein-coding genes. Eleven (11) DE lncRNAs were co-expressed with protein-coding genes like *LIPL* (lipoprotein lipase) and *TGF-β* (transforming growth factor-beta) that regulate muscle quality traits. Whole body weight, muscle yield, and fat content have 41 common DE protein-coding genes and 220 DE lncRNAs depicting possible pleiotropic and epistatic mechanisms in the genetic architecture of these traits. They also showed that 44 DE lncRNA has a potential sponge relationship with microRNA in regulating muscle quality traits.

Using the same fish population, 90 microRNAs were identified to show differential expression between fish families showing variability in whole body weight (WBW), muscle yield, muscle crude-fat content, muscle shear force and whiteness. MicroRNAs are important post-transcriptional regulators of genes and their expression. The micro RNA binds to its recognition or target site at the 3'UTR region of a gene's mRNA; causing downregulation of such gene (Bagga et al., 2005; Wu et al., 2006). MicroRNA-mRNA binding is very site-specific and any change in nucleotide sequence in the recognition site may have important functional consequences for the role of microRNA and phenotypes (Clop et al., 2006; Georges et al., 2006)They identified 204 SNPs on the target sites of the microRNAs and showed that these polymorphisms destroyed the miRNA-mRNA or created an illegitimate target site, with 78 of them associated with the above-mentioned traits. Overall, their study showed that variability in miRNA expression and polymorphism in their target site combine to regulate growth and muscle quality traits in rainbow trout.

The male rainbow trout typically attain sexual maturation earlier (before 2 years) than the female with attendant adverse effects on growth and fillet quality traits (Aussanasuwannakul et al., 2011; Leeds & Weber, 2019). Mono-sex female production and triploidy induction are approaches employed to prevent the possible adverse effects (Leeds & Weber, 2019). Studies have shown different sex and ploidy bias in the transcriptomics profile of matured rainbow trout. Manor et al. (2015) Showed that the diploid fish have higher expression of beta-oxidation genes (Carnitine

Palmitoyltransferase a, Carnitine Palmitoyltransferase b, Mitochondrial carnitine palmitoyltransferase I alpha1a, Acetyl-CoA Oxidase, Acetyl-CoA acyltransferase 2, Acyl-CoA dehydrogenase, very long chain) in the white muscle and visceral adipose tissue which signifies a mobilization of fatty acids within these tissues during sexual maturation in the diploid fish to provide energy for gonadogenesis. However, the sterile triploid fish has higher expression of lipogenic genes in the liver suggesting increased capacity for fatty acid synthesis and excess energy storage because of their sterile nature. They also observed similar gene expression profiles in the diploid and triploid fishes before sexual maturity. Rainbow trout are typically harvested before the onset of sexual maturation; it is, therefore, important to examine the transcriptomic profile on the fish prior to maturity. Manor et al. (2015) found that even before sexual maturity, different gene expression profiles between the male and female immature rainbow trout exist that may lead to nutrient repartitioning during maturation. In the male liver, there is a higher expression of cofactor genes (MO25—induced by energy stress, *rictor*, and Proline-rich Akt substrate of 40 kilodaltons) within the mTOR signaling pathway and genes of β-oxidation (Carnitine palmitoyltransferase b, Enoyl-CoA, hydratase/3- hydroxyacyl CoA dehydrogenase/peroxisomal bifunctional enzyme) in the liver of the male fish suggesting increased mitochondrial β-oxidation. The mTOR signaling pathway is known to be involved in growth, development and fatty acid metabolism in the liver of male fish (Laplante & Sabatini, 2012). The females had increased expression of the mTOR cofactor raptor, genes in the fatty acid synthesis pathway, and two β-oxidation genes (Carnitine palmitoyltransferase d and Mitochondrial carnitine palmitoyltransferase I alpha1a). There was no sex effect on growth parameters, but the female fish had a higher percentage of muscle yield and firmer fillets than the males.

Expression QTL Analysis and Its Relevance

Expression quantitative trait locus (eQTL) analysis is a genomic analysis that identifies genetic variants, typically single-nucleotide polymorphisms (SNPs), associated with variation in gene expression levels. By integrating genome-wide genotyping (e.g., SNP-chip or sequencing data) with transcriptomic data (e.g., RNA-Seq), eQTL analysis maps loci that influence mRNA abundance, acting as regulatory elements for gene activity (Gilad et al., 2008). Expression QTLs are classified as *cis* (acting on nearby genes, often within 1 Mb) or *trans* (affecting distant genes, often across chromosomes), providing insights into the genetic architecture of gene regulation. In

livestock and aquaculture breeding, eQTL analysis is pivotal for dissecting complex traits where gene expression mediates the link between genotype and phenotype. It complements genome-wide association studies (GWAS) by revealing regulatory mechanisms underlying trait-associated SNPs (Zeng et al., 2019; Zhu et al., 2016). The methodology involves correlating SNP genotypes with gene expression levels across a population, using statistical models like linear regression or mixed models to detect significant associations (Michaelson et al., 2009).

In dairy cattle, research on mammary gland tissue has identified thousands of cis- and trans-eQTLs regulating key milk production genes, such as *DGAT1* and *CSN2*, offering functional insights into loci previously flagged by GWAS (Cui et al., 2014). Similarly, in beef cattle, liver eQTL mapping has linked expression regulation to feed efficiency traits, highlighting regulatory roles for genes involved in lipid metabolism and energy balance (Cai et al., 2023). A study investigated the genetic basis of feather pecking behavior in 167 laying hens by combining transcriptomic and phenotypic data. The researchers identified 11,790 significant SNPs associated with 70 differentially expressed genes, with 23 SNPs showing multiple associations (Mott et al., 2022). Notably, the transcription factor KLF14 emerged as a potential key regulator influencing this behavioral disorder.

While rainbow trout has been extensively studied for quantitative trait loci (QTL) related to traits like growth, disease resistance, and fillet quality, direct eQTL studies are less common. Limited direct eQTL Studies in rainbow trout show that there is a need for such studies to provide insights into the molecular mechanisms underlying complex traits. In Pacific White Shrimp (*Litopenaeus vannamei*, a study performed genome-wide QTL and eQTL mapping to identify genes affecting growth rate (Chen et al., 2024). Using RNA-sequencing of 268 individuals, they identified 11 phenotypic QTLs and 117,525 eQTLs significantly correlated with growth rate. The integration of QTL and eQTL data pinpointed the gene *metalloreductase STEAP4* as highly associated with the growth rate of Pacific White Shrimp. An integrative genome-wide association study (GWAS) and eQTL analysis was performed to identify genetic variants associated with resistance to Vibrio harveyi infection, a major pathogen causing economic losses in yellow drum aquaculture (Huang et al., 2024). The study used 345 individuals (197 susceptible, 148 resistant) and spleen tissue transcriptomes from 78 resistant individuals. eQTL analysis revealed 49,396 eQTLs per chromosome on average, with 22.79% of SNPs significantly associated with gene expression.

They found seven SNPs within the *Zinc Finger Protein yd23210* gene that have significant associations in both GWAS and eQTL analysis, suggesting its role in immune regulation. The study provides genetic markers for molecular breeding to enhance disease resistance.

The Microbiome component: Genetic or Environmental?

The microbiome—the community of microorganisms living in and on a host—plays an increasingly recognized role in shaping phenotypic variation (Gao et al., 2023), which raises questions about its place within the classic phenotype = genotype + environment (P = G + E) framework. Unlike the host's genome, which is strictly genetic, the microbiome is not easily placeable: its composition is partly heritable, influenced by host genetics, yet it is highly responsive to environmental factors like diet, water quality, or other housing conditions (Rothschild et al., 2018; Spor et al., 2011). Some researchers argue it aligns with the environmental component due to its external origin and dynamic nature, while others, drawing on Richard Dawkins's extended phenotype concept (Dawkins, 2016), view it as an extension of the genetic component—microbial effects mediated by host genes impacting external biotic factors (Kurilshikov et al., 2017; van Opstal & Bordenstein, 2015). A related idea, the extended genotype concept, posits that the microbial metagenome, encompassing all DNA from the host-associated microbes, significantly contributes to host traits and heritability. This idea intertwines genetic and environmental influences within a holistic "holobiont" framework, which includes both the host and its microbiome(Henry et al., 2021).

This dual nature complicates its classification but underscores its evolutionary significance. In livestock and aquaculture, the microbiome's genes can enhance host resilience to stressors—such as pathogens or temperature shifts—by modulating metabolism, immunity, or nutrient uptake (Gao et al., 2023). For example, gut bacteria in rainbow trout may influence feed efficiency (Chapagain et al., 2019). This suggests that the microbiome acts as a bridge between genotype and phenotype.

Influence of the Microbiome on Phenotypic Traits

The microbiome affects phenotypic traits by interacting with host physiology in ways that traditional genetic models often overlook. In cattle, rumen microbes degrade fibrous feed, directly impacting growth rate and methane emissions—important traits (Chung et al., 2012; Tapio et al., 2017). In aquaculture, the gill and gut microbiota of fish like rainbow trout regulate immune

responses, affecting disease resistance against pathogens like *Flavobacterium psychrophilum* (Brown et al., 2019; Karami et al., 2025). These microbial contributions introduce variance in complex, polygenic traits—growth, reproduction, or other economic traits that breeding programs aim to improve. The extended phenotype hypothesis suggests that host genes indirectly shape these traits by structuring the type of microbial communities colonizing the host (Klassen, 2018).

Evidence also points to a heritable microbial component, termed "microbiability," which is the microbiome-equivalent of the commonly known heritability. Studies using 16S rRNA sequencing to quantify bacteria abundance with the bacterial matrix approach reveal that microbial profiles explain significant phenotypic variation (Ross et al., 2013). In pigs, the inclusion of microbial taxa abundance and with genomic data enhance trait predictability enhances trait predictability (Khanal et al., 2020a). This interplay suggests the microbiome is not merely noise but a measurable factor in phenotypic outcomes, offering new avenues for selection.

Integrating Microbiome Information into Genomic Prediction Models

Incorporating the holobiont into genomic prediction models holds promise to accelerate genetic gains in farmed animals and aquaculture by capturing both host and microbial contributions to complex traits. Standard genomic selection relies on genomic data to estimate breeding values, but adding microbiome data—via relative bacterial abundances or metagenomic profiles—can boost accuracy for traits like feed efficiency or disease resistance (Chakraborty et al., 2022; Weishaar et al., 2020). Linear mixed models integrating microbial information have shown microbiability values—e.g., 0.25–0.40 in dairy cattle for methane production—comparable to heritabilities of production traits (Buitenhuis et al., 2019).

There have been contrasting results, with some studies showing improved accuracy with the inclusion of microbiome information while others show no improvement.

Contrasting Results on Genomic Prediction Accuracy with Microbiome Information

Integrating microbiome data into genomic prediction models has emerged as a promising strategy to enhance breeding outcomes in livestock and aquaculture. Yet, studies reveal a spectrum of results—some demonstrating improved accuracy, others showing little or no benefit. The

microbiome's influence on phenotypic traits like growth, disease resistance, and feed efficiency suggests it could refine predictions beyond host genomic data alone. However, the variability in findings underscores the complexity of host-microbe interactions and methodological differences across species and studies.

For dairy cattle, a study integrating 16S rRNA-derived rumen microbial abundances with genomic data increased prediction accuracy for methane emissions by 7–12% over host-genome-only models, with microbiability estimates (0.28–0.40) (Difford, 2018). Similarly, in pigs, combining microbial profiles with SNP-chip data improved accuracy for fat deposition and growth traits by up to 10% (Khanal et al., 2020b)These gains come from capturing heritable microbial effects mediated by host genetics, which aligns with the *extended genotype* concept.

Conversely, other livestock studies report negligible improvement. In beef cattle, adding rumen microbiome data to genomic predictions for feed efficiency yielded no significant accuracy boost over GBLUP models, possibly due to environmental dominance over microbial composition (Li et al., 2019). A study by Saedi et al. (2024) investigated genomic prediction of methane emission in Holstein cows using both genomic data and rumen microbiome profiles. They compared the prediction accuracies of GBLUP and GMBLUP models (which integrate microbiome data). They found similar levels of accuracy: 0.21 for GBLUP, 0.20 for GMBLUP using operational taxonomic units (OTUs), and 0.19 for GMBLUP using zero-radius OTUs (ZOTUs). This suggests that including microbiome data did not significantly improve prediction accuracy over GBLUP alone. A similar outcome for milk composition in sheep study shows that the inclusion of both genetic and microbiome effects did not improve the fit of the model compared with the model with the genetic effect only (Boggio et al., 2023). Deru et al. (2024) evaluated the effect of including microbiota information, with or without host genomic information, in models predicting digestive efficiency (DE), growth, and feed efficiency (FE) traits in pigs. They observed that incorporating microbiota information did not significantly improve prediction accuracy for FE traits compared to models using host genetics alone. However, microbiota information was a good predictor for DE traits, with moderate to high prediction accuracies.

These discrepancies may reflect trait-specific microbial influence, inconsistent sampling (e.g., fecal vs. gut mucosa), or insufficient statistical power in smaller datasets. Some other explanations

for the variability in results may exist. Species-specific host-microbe dynamics differ—cattle rumen microbes have direct metabolic roles, while fish microbiota respond to water and diet, complicating consistency. Trait complexity matters: traits with strong microbial mediation (e.g., methane emissions) show more apparent benefits than polygenic traits like growth under variable conditions. Methodological choices—sampling site, sequencing depth (16S vs. metagenomics), and model type (e.g., GBLUP vs. Bayesian)—also influence outcomes. Studies showing gains often use large, controlled datasets, while null results may reflect smaller samples or environmental noise drowning microbial signals.

Summary of 16S rRNA Sequencing vs. Metagenomic Shotgun Sequencing in Microbiome Research

Microbiome research in livestock and aquaculture relies heavily on sequencing technologies to characterize microbial communities and their impact on host traits. Two primary methods—16S rRNA gene sequencing and metagenomic shotgun sequencing—offer distinct approaches to profiling these communities.

16S rRNA Sequencing: This method targets the 16S ribosomal RNA gene, a highly conserved region in bacteria and archaea, with variable regions that enable taxonomic identification (Ramazzotti & Bacci, 2018). By amplifying and sequencing specific hypervariable regions (e.g., V3–V4), 16S sequencing provides a cost-effective snapshot of microbial diversity and composition at the genus or species level (Ramazzotti & Bacci, 2018). Its advantages include low cost, minimal computational demands, and established databases like Greengenes or SILVA for taxonomic assignment (Rizal et al., 2020). However, limitations include its focus on bacteria/archaea (missing fungi, viruses, or eukaryotes), lack of functional gene information, and resolution constraints—often failing to distinguish strains or closely related species (Almeida et al., 2018).

Metagenomic Shotgun Sequencing: Unlike 16S, metagenomic shotgun sequencing captures all DNA in a sample, providing a comprehensive view of microbial diversity, including bacteria, archaea, fungi, viruses, and even host DNA contamination (Quince et al., 2017). By randomly sequencing fragmented DNA, it reveals not only taxonomy but also functional genes, metabolic

pathways, and potential antimicrobial resistance profiles (Tyagi et al., 2019). Its strengths include high resolution (down to strain level), functional insights, and independence from PCR biases (Quince et al., 2017).

Differential Microbiome Abundance: Overview and Relevance

Differential microbiome abundance (DMA) analysis identifies microbial taxa (e.g., genera, species, or operational taxonomic units, OTUs) that differ significantly in abundance between groups, such as high- vs. low-performing individuals. By comparing microbiome profiles—typically derived from 16S rRNA or shotgun sequencing—DMA pinpoints bacteria, archaea, or other microbes associated with specific conditions or traits. In livestock and aquaculture, DMA is highly relevant for uncovering microbial drivers of economically important traits which can inform breeding strategies and management practices (Forcina et al., 2022; Lakamp; O'Hara et al., 2020).

For example, in dairy cattle, Differential microbiome abundance has revealed that certain taxa, including Prevotella, are enriched in animals with high feed efficiency, suggesting a role in rumen fermentation (Jami et al., 2014; Jewell et al., 2015; Tapio et al., 2023). In rainbow trout, bacteria genera including *Clostridium, Leptotrichia and Peptostreptococcus* are more abundant in the fast-growing rainbow trout genetic line (Chapagain et al., 2019).

The relevance of differential microbiome analysis stems from its ability to connect microbial shifts to phenotypic outcomes, offering insights into host-microbe interactions that genetic models alone may miss. It shares conceptual and methodological parallels with differential gene expression (DGE) analysis, which identifies genes with varying expression levels across conditions. Both approaches aim to detect biologically meaningful differences in high-dimensional data—taxa abundances for DMA, transcript counts for DGE—between predefined groups (Lin & Peddada, 2020).

Like Differential Gene Expression (DGE) analysis, DMA's strength is its biomarker discovery—taxa for DMA, genes for DGE. DGE may directly help with marker-assisted selection or genomic selection (GS) by pinpointing causal variants and genes, while DMA's indirect effects (via host-microbe interactions) require mGWAS or microbiability models to link to genetics.

Study Objectives

The objectives of this study are to:

1. Identify candidate genes, regulatory variants, and gene expression signatures regulating the variability in fillet yield and quality traits in the rainbow trout fish population from the USDA-NCCCWA.

2. Investigating the gut microbiome and microbiome pathways as possible biomarkers for fillet yield and quality traits and identifying microbiome taxa associated with those traits.

3. Integrating genomic and microbiome information into genomic prediction to improve fillet yield and quality traits.

References

Ahmed, R. O., Ali, A., Al-Tobasei, R., Leeds, T., Kenney, B., & Salem, M. (2022). Weighted Single-Step GWAS Identifies Genes Influencing Fillet Color in Rainbow Trout. *Genes*, *13*(8), 1331.

Al-Tobasei, R., Ali, A., Garcia, A. L., Lourenco, D., Leeds, T., & Salem, M. (2021). Genomic predictions for fillet yield and firmness in rainbow trout using reduced-density SNP panels. *BMC genomics*, *22*, 1-11.

Al-Tobasei, R., Ali, A., Leeds, T. D., Liu, S., Palti, Y., Kenney, B., & Salem, M. (2017). Identification of SNPs associated with muscle yield and quality traits using allelic-imbalance analyses of pooled RNA-Seq samples in rainbow trout. *BMC genomics*, *18*(1), 1-15.

Ali, A., Al-Tobasei, R., Kenney, B., Timothy, D., & Mohamed, S. (2018). Integrated analysis of lncRNA and mRNA expression in rainbow trout families showing variation in muscle growth and fillet quality traits. Sci Rep 8, 12111. In.

Ali, A., Al-Tobasei, R., Lourenco, D., Leeds, T., Kenney, B., & Salem, M. (2019). Genome-wide association study identifies genomic loci affecting filet firmness and protein content in rainbow trout. *Frontiers in genetics*, *10*, 386.

Ali, A., Al-Tobasei, R., Lourenco, D., Leeds, T., Kenney, B., & Salem, M. (2020a). Genome-wide identification of loci associated with growth in rainbow trout. *BMC genomics*, *21*(1), 1-16.

Ali, A., Al-Tobasei, R., Lourenco, D., Leeds, T., Kenney, B., & Salem, M. (2020b). Genome-wide scan for common variants associated with intramuscular fat and moisture content in rainbow trout. *BMC genomics*, *21*(1), 1-17.

Allendorf, F. W., & Thorgaard, G. H. (1984). Tetraploidy and the evolution of salmonid fishes. *Evolutionary genetics of fishes*, 1-53.

Almeida, A., Mitchell, A. L., Tarkowska, A., & Finn, R. D. (2018). Benchmarking taxonomic assignments based on 16S rRNA gene profiling of the microbiota from commonly sampled environments. *Gigascience*, *7*(5), giy054.

Aluru, N., & Vijayan, M. M. (2009). Stress transcriptomics in fish: a role for genomic cortisol signaling. *General and comparative endocrinology*, *164*(2-3), 142-150.

Aussanasuwannakul, A., Kenney, P. B., Weber, G. M., Yao, J., Slider, S. D., Manor, M. L., & Salem, M. (2011). Effect of sexual maturation on growth, fillet composition, and texture of female rainbow trout (Oncorhynchus mykiss) on a high nutritional plane. *Aquaculture*, *317*(1-4), 79-88.

Bagga, S., Bracht, J., Hunter, S., Massirer, K., Holtz, J., Eachus, R., & Pasquinelli, A. E. (2005). Regulation by let-7 and lin-4 miRNAs results in target mRNA degradation. *Cell*, *122*(4), 553-563.

Balding, D. J. (2006). A tutorial on statistical methods for population association studies. *Nature reviews genetics*, *7*(10), 781-791.

Bernard, M., Dehaullon, A., Prchal, M., Haffray, P., Quillet, E., Dupont-Nivet, M.,…Phocas, F. (2022). Development of a high-density 665 K SNP array for rainbow trout genome-wide genotyping. *Frontiers in Genetics*, *13*, 941340.

Blay, C., Haffray, P., D'ambrosio, J., Prado, E., Dechamp, N., Nazabal, V.,…Eklouh-Molinier, C. (2021). Genetic architecture and genomic selection of fatty acid composition predicted by Raman spectroscopy in rainbow trout. *BMC genomics*, *22*, 1-19.

Boggio, G. M., Christensen, O., Legarra, A., Meynadier, A., & Marie-Etancelin, C. (2023). Microbiability of milk composition and genetic control of microbiota effects in sheep. *Journal of Dairy Science*, *106*(9), 6288-6298.

Boussaha, M., Guyomard, R., Cabau, C., Esquerré, D., & Quillet, E. (2012). Development and characterisation of an expressed sequence tags (EST)-derived single nucleotide polymorphisms (SNPs) resource in rainbow trout. *BMC genomics*, *13*(1), 1-11.

Brown, R. M., Wiens, G. D., & Salinas, I. (2019). Analysis of the gut and gill microbiome of resistant and susceptible lines of rainbow trout (Oncorhynchus mykiss). *Fish & shellfish immunology*, *86*, 497-506.

Campbell, N., LaPatra, S., Overturf, K., Towner, R., & Narum, S. (2014). Association mapping of disease resistance traits in rainbow trout using restriction site associated DNA sequencing. G3 Genes Genomes Genet. 4: 2473–81. In.

Castaño Sánchez, C., Palti, Y., & Rexroad, C. (2011). SNP analysis with duplicated fish genomes: differentiation of SNPs, paralogous sequence variants, amd multisite variants. *Next generation sequencing and whole genome selection in aquaculture*, 133-150.

Chakraborty, D., Sharma, N., Kour, S., Sodhi, S. S., Gupta, M. K., Lee, S. J., & Son, Y. O. (2022). Applications of omics technology for livestock selection and improvement. *Frontiers in Genetics*, *13*, 774113.

Chapagain, P., Arivett, B., Cleveland, B. M., Walker, D. M., & Salem, M. (2019). Analysis of the fecal microbiota of fast-and slow-growing rainbow trout (Oncorhynchus mykiss). *BMC genomics*, *20*(1), 1-11.

Chung, Y.-H., Zhou, M., Holtshausen, L., Alexander, T., McAllister, T., Guan, L.,…Beauchemin, K. (2012). A fibrolytic enzyme additive for lactating Holstein cow diets: ruminal fermentation, rumen microbial populations, and enteric methane emissions. *Journal of dairy science*, *95*(3), 1419-1427.

Cleveland, B. M., Gao, G., & Leeds, T. D. (2020). Transcriptomic response to selective breeding for fast growth in rainbow trout (Oncorhynchus mykiss). *Marine biotechnology*, *22*(4), 539-550.

Clop, A., Marcq, F., Takeda, H., Pirottin, D., Tordoir, X., Bibé, B.,…Eychenne, F. (2006). A mutation creating a potential illegitimate microRNA target site in the myostatin gene affects muscularity in sheep. *Nature genetics, 38*(7), 813-818.

Dawkins, R. (2016). *The extended phenotype: The long reach of the gene*. Oxford University Press.

Difford, G. F. (2018). *Genetic control of methane emission, feed efficiency and metagenomics in dairy cattle* Wageningen University and Research].

Déru, V., Tiezzi, F., Carillier-Jacquin, C., Blanchet, B., Cauquil, L., Zemb, O.,…Gilbert, H. (2024). The potential of microbiota information to better predict efficiency traits in growing pigs fed a conventional and a high-fiber diet. *Genetics Selection Evolution, 56*(1), 8.

D'Ambrosio, J., Morvezen, R., Brard-Fudulea, S., Bestin, A., Acin Perez, A., Guéméné, D.,…Phocas, F. (2020). Genetic architecture and genomic selection of female reproduction traits in rainbow trout. *BMC genomics, 21*, 1-14.

Evenhuis, J., Leeds, T., Marancik, D., LaPatra, S., & Wiens, G. (2015). Rainbow trout (Oncorhynchus mykiss) resistance to columnaris disease is heritable and favorably correlated with bacterial cold water disease resistance. *Journal of animal science, 93*(4), 1546-1554.

Fernando, R. L., & Garrick, D. (2013). Bayesian methods applied to GWAS. *Genome-wide association studies and genomic prediction*, 237-274.

Forcina, G., Pérez-Pardal, L., Carvalheira, J., & Beja-Pereira, A. (2022). Gut microbiome studies in livestock: achievements, challenges, and perspectives. *Animals, 12*(23), 3375.

Fraslin, C., Phocas, F., Bestin, A., Charles, M., Bernard, M., Krieg, F.,…Petitprez, F. (2020). Genetic determinism of spontaneous masculinisation in XX female rainbow trout: new insights using medium throughput genotyping and whole-genome sequencing. *Scientific Reports, 10*(1), 17693.

Gallagher, M. D., & Chen-Plotkin, A. S. (2018). The post-GWAS era: from association to function. *The American Journal of Human Genetics, 102*(5), 717-730.

Gao, G., Nome, T., Pearse, D. E., Moen, T., Naish, K. A., Thorgaard, G. H.,…Palti, Y. (2018). A new single nucleotide polymorphism database for rainbow trout generated through whole genome resequencing. *Frontiers in genetics, 9*, 363858.

Gao, Q., Liu, P., Li, Y., Song, D., Long, W., Wang, Z.,…Jiang, L. (2023). Gut microbiota, host genetics and phenotypes in aquatic animals: A review. *Aquaculture Reports, 31*, 101648.

Garcia, A., Tsuruta, S., Gao, G., Palti, Y., Lourenco, D., & Leeds, T. (2023a). Genomic selection models substantially improve the accuracy of genetic merit predictions for fillet yield and body weight in rainbow trout using a multi-trait model and multi-generation progeny testing. *Genetics Selection Evolution, 55*(1), 1-12.

Garcia, A., Tsuruta, S., Gao, G., Palti, Y., Lourenco, D., & Leeds, T. (2023b). Genomic selection models substantially improve the accuracy of genetic merit predictions for fillet yield and body weight in rainbow trout using a multi-trait model and multi-generation progeny testing. *Genetics Selection Evolution, 55*(1), 11.

Garrick, D. J., & Fernando, R. L. (2013). Implementing a QTL detection study (GWAS) using genomic prediction methodology. *Genome-wide association studies and genomic prediction*, 275-298.

Genet, C., Dehais, P., Palti, Y., Gao, G., Gavory, F., Wincker, P.,…Boussaha, M. (2011). Analysis of BAC-end sequences in rainbow trout: content characterization and assessment of synteny between trout and other fish genomes. *BMC genomics, 12*, 1-8.

Georges, M., Clop, A., Marcq, F., Takeda, H., Pirottin, D., Hiard, S.,…Bibé, B. (2006). Polymorphic Polymorphic MicroRNA–Target Interactions: A Novel Source of Phenotypic Variation. Cold Spring Harbor symposia on quantitative biology,

Gonzalez-Pena, D., Gao, G., Baranski, M., Moen, T., Cleveland, B. M., Kenney, P. B.,…Leeds, T. D. (2016). Genome-wide association study for identifying loci that affect fillet yield, carcass, and body weight traits in rainbow trout (Oncorhynchus mykiss). *Frontiers in genetics*, *7*, 203.

Guyomard, R., Boussaha, M., Krieg, F., Hervet, C., & Quillet, E. (2012). A synthetic rainbow trout linkage map provides new insights into the salmonid whole genome duplication and the conservation of synteny among teleosts. *BMC genetics*, *13*, 1-12.

Hayes, B., & Goddard, M. (2010). Genome-wide association and genomic selection in animal breeding. *Genome*, *53*(11), 876-883.

Henderson, C. (1975). Use of all relatives in intraherd prediction of breeding values and producing abilities. *Journal of Dairy Science*, *58*(12), 1910-1916.

Henry, L. P., Bruijning, M., Forsberg, S. K., & Ayroles, J. F. (2021). The microbiome extends host evolutionary potential. *Nature communications*, *12*(1), 5141.

Hofer, A. (1998). Variance component estimation in animal breeding: a review. *Journal of Animal Breeding and Genetics*, *115*(1-6), 247-265.

Jami, E., White, B. A., & Mizrahi, I. (2014). Potential role of the bovine rumen microbiome in modulating milk composition and feed efficiency. *PloS one*, *9*(1), e85423.

Jewell, K. A., McCormick, C. A., Odt, C. L., Weimer, P. J., & Suen, G. (2015). Ruminal bacterial community composition in dairy cows is dynamic over the course of two lactations and correlates with feed efficiency. *Applied and environmental microbiology*, *81*(14), 4697-4710.

Karami, A., Kania, P., Al-Jubury, A., Stefanova, D., Krych, L., Madsen, L.,…Buchmann, K. (2025). Gut microbiota in rainbow trout Oncorhynchus mykiss with different susceptibility to Flavobacterium psychrophilum infection. *Aquaculture*, *596*, 741841.

Khanal, P., Maltecca, C., Schwab, C., Fix, J., Bergamaschi, M., & Tiezzi, F. (2020a). Modeling host-microbiome interactions for the prediction of meat quality and carcass composition traits in swine. *Genetics Selection Evolution*, *52*, 1-13.

Khanal, P., Maltecca, C., Schwab, C., Fix, J., Bergamaschi, M., & Tiezzi, F. (2020b). Modeling host-microbiome interactions for the prediction of meat quality and carcass composition traits in swine. *Genetics Selection Evolution*, *52*(1), 1-13.

Kim, J. M., Santure, A., Barton, H. J., Quinn, J., Cole, E. F., Consortium, G. T. H.,…van Oers, K. (2018). A high-density SNP chip for genotyping great tit (Parus major) populations and its application to studying the genetic architecture of exploration behaviour. *Molecular Ecology Resources*, *18*(4), 877-891.

Klassen, J. L. (2018). Defining microbiome function. *Nature microbiology*, *3*(8), 864-869.

Koopaee, H. K., & Koshkoiyeh, A. E. (2014). SNPs Genotyping technologies and their applications in farm animals breeding programs. *Brazilian Archives of Biology and Technology*, *57*, 87-95.

Kruuk, L. E., & Hadfield, J. D. (2007). How to separate genetic and environmental causes of similarity between relatives. *Journal of evolutionary biology*, *20*(5), 1890-1903.

Kurilshikov, A., Wijmenga, C., Fu, J., & Zhernakova, A. (2017). Host genetics and gut microbiome: challenges and perspectives. *Trends in immunology*, *38*(9), 633-647.

Lakamp, A. Breeding for the Little Things: A Look at Including Microbiome Information in Animal Breeding.

Lam, S., Miglior, F., Fonseca, P., Gómez-Redondo, I., Zeidan, J., Suárez-Vega, A.,…Stothard, P. (2021). Identification of functional candidate variants and genes for feed efficiency in Holstein and Jersey cattle breeds using RNA-sequencing. *Journal of dairy science*, *104*(2), 1928-1950.

Laplante, M., & Sabatini, D. (2012). mTOR signaling. Cold Spring Harb Perspect Biol 4: a011593. In.

Leeds, T. D., & Weber, G. M. (2019). Effects of triploidy on genetic gains in a rainbow trout (Oncorhynchus mykiss) population selectively bred for diploid growth performance. *Aquaculture*, *505*, 481-487.

Lin, H., & Peddada, S. D. (2020). Analysis of microbial compositions: a review of normalization and differential abundance analysis. *NPJ biofilms and microbiomes*, *6*(1), 60.

Liu, S., Gao, G., Layer, R. M., Thorgaard, G. H., Wiens, G. D., Leeds, T. D.,…Palti, Y. (2021). Identification of high-confidence structural variants in domesticated rainbow trout using whole-genome sequencing. *Frontiers in Genetics*, *12*, 639355.

Liu, S., Gao, G., Palti, Y., Cleveland, B. M., Weber, G. M., & Rexroad III, C. E. (2014). RNA-seq analysis of early hepatic response to handling and confinement stress in rainbow trout. *Plos one*, *9*(2), e88492.

Liu, S., Martin, K. E., Gao, G., Long, R., Evenhuis, J. P., Leeds, T. D.,…Palti, Y. (2022). Identification of haplotypes associated with resistance to bacterial cold water disease in rainbow trout using whole-genome resequencing. *Frontiers in Genetics*, *13*, 936806.

Liu, S., Vallejo, R. L., Evenhuis, J. P., Martin, K. E., Hamilton, A., Gao, G.,…Palti, Y. (2018). Retrospective evaluation of marker-assisted selection for resistance to bacterial cold water disease in three generations of a commercial rainbow trout breeding population. *Frontiers in genetics*, *9*, 374762.

Liu, S., Vallejo, R. L., Gao, G., Palti, Y., Weber, G. M., Hernandez, A., & Rexroad, C. E. (2015). Identification of single-nucleotide polymorphism markers associated with cortisol response to crowding in rainbow trout. *Marine Biotechnology*, *17*, 328-337.

Luo, Z., Yu, Y., Xiang, J., & Li, F. (2021). Genomic selection using a subset of SNPs identified by genome-wide association analysis for disease resistance traits in aquaculture species. *Aquaculture*, *539*, 736620.

Manor, M. L., Cleveland, B. M., Weber, G. M., & Kenney, P. B. (2015). Effects of sexual maturation and feeding level on fatty acid metabolism gene expression in muscle, liver, and visceral adipose tissue of diploid and triploid rainbow trout, Oncorhynchus mykiss. *Comparative Biochemistry and Physiology Part B: Biochemistry and Molecular Biology*, *179*, 17-26.

Marancik, D., Gao, G., Paneru, B., Ma, H., Hernandez, A. G., Salem, M.,…Wiens, G. D. (2015). Whole-body transcriptome of selectively bred, resistant-, control-, and susceptible-line rainbow trout following experimental challenge with Flavobacterium psychrophilum. *Frontiers in genetics*, *5*, 453.

McDermaid, A., Monier, B., Zhao, J., Liu, B., & Ma, Q. (2019). Interpretation of differential gene expression results of RNA-seq data: review and integration. *Briefings in bioinformatics*, *20*(6), 2044-2054.

Meuwissen, T., Hayes, B., & Goddard, M. (2016). Genomic selection: A paradigm shift in animal breeding. *Animal frontiers*, *6*(1), 6-14.

Meuwissen, T. H., Hayes, B. J., & Goddard, M. (2001). Prediction of total genetic value using genome-wide dense marker maps. *genetics*, *157*(4), 1819-1829.

Momoda, T. S., Schwindt, A., Feist, G., Gerwick, L., Bayne, C., & Schreck, C. (2007). Gene expression in the liver of rainbow trout, Oncorhynchus mykiss, during the stress response. *Comparative Biochemistry and Physiology Part D: Genomics and Proteomics*, *2*(4), 303-315.

Mukhopadhyay, C., & Kumar, D. (2013). SNP chip development and genome wide association studies in livestock. *Phenomic and genomic tools for analysis of livestock genome*, *66*.

O'Hara, E., Neves, A. L., Song, Y., & Guan, L. L. (2020). The role of the gut microbiome in cattle production and health: driver or passenger? *Annual review of animal biosciences*, *8*(1), 199-220.

Opstal, E. J. v., & Bordenstein, S. R. (2015). Rethinking heritability of the microbiome. *Science*, *349*(6253), 1172-1173.

Palti, Y., Gao, G., Liu, S., Kent, M., Lien, S., Miller, M.,…Moen, T. (2015). The development and characterization of a 57 K single nucleotide polymorphism array for rainbow trout. *Molecular ecology resources*, *15*(3), 662-672.

Palti, Y., Gao, G., Miller, M. R., Vallejo, R. L., Wheeler, P. A., Quillet, E.,…Rexroad III, C. E. (2014). A resource of single-nucleotide polymorphisms for rainbow trout generated by restriction-site associated DNA sequencing of doubled haploids. *Molecular ecology resources*, *14*(3), 588-596.

Palti, Y., Vallejo, R. L., Gao, G., Liu, S., Hernandez, A. G., Rexroad III, C. E., & Wiens, G. D. (2015). Detection and validation of QTL affecting bacterial cold water disease resistance in rainbow trout using restriction-site associated DNA sequencing. *PloS one*, *10*(9), e0138435.

Paneru, B., Al-Tobasei, R., Palti, Y., Wiens, G. D., & Salem, M. (2016). Differential expression of long non-coding RNAs in three genetic lines of rainbow trout in response to infection with Flavobacterium psychrophilum. *Scientific reports*, *6*(1), 36032.

Panigrahi, M., Kumar, H., Saravanan, K., Rajawat, D., Nayak, S. S., Ghildiyal, K.,…Dutt, T. (2022). Trajectory of livestock genomics in South Asia: a comprehensive review. *Gene*, *843*, 146808.

Pérez-Enciso, M., Rincón, J. C., & Legarra, A. (2015). Sequence-vs. chip-assisted genomic selection: accurate biological information is advised. *Genetics Selection Evolution*, *47*, 1-14.

Quince, C., Walker, A. W., Simpson, J. T., Loman, N. J., & Segata, N. (2017). Shotgun metagenomics, from sampling to analysis. *Nature biotechnology*, *35*(9), 833-844.

Ramazzotti, M., & Bacci, G. (2018). 16S rRNA-based taxonomy profiling in the metagenomics era. In *Metagenomics* (pp. 103-119). Elsevier.

Rexroad, C. E., Vallejo, R. L., Liu, S., Palti, Y., & Weber, G. M. (2013). Quantitative Trait Loci Affecting Response to Crowding Stress in an F 2 Generation of Rainbow Trout Produced Through Phenotypic Selection. *Marine Biotechnology*, *15*, 613-627.

Rizal, N. S. M., Neoh, H.-m., Ramli, R., Hanafiah, A., Samat, M. N. A., Tan, T. L.,…Saw, S. H. (2020). Advantages and limitations of 16S rRNA next-generation sequencing for pathogen identification in the diagnostic microbiology laboratory: perspectives from a middle-income country. *Diagnostics*, *10*(10), 816.

Rodríguez, F. H., Flores-Mara, R., Yoshida, G. M., Barría, A., Jedlicki, A. M., Lhorente, J. P.,…Yáñez, J. M. (2019). Genome-wide association analysis for resistance to infectious

pancreatic necrosis virus identifies candidate genes involved in viral replication and immune response in rainbow trout (Oncorhynchus mykiss). *G3: Genes, Genomes, Genetics*, *9*(9), 2897-2904.

Ross, E. M., Moate, P. J., Marett, L. C., Cocks, B. G., & Hayes, B. J. (2013). Metagenomic predictions: from microbiome to complex health and environmental phenotypes in humans and cattle. *PloS one*, *8*(9), e73056.

Rothschild, D., Weissbrod, O., Barkan, E., Kurilshikov, A., Korem, T., Zeevi, D.,…Bar, N. (2018). Environment dominates over host genetics in shaping human gut microbiota. *Nature*, *555*(7695), 210-215.

Saedi, N., Ye, X., Cai, Z., Lund, M. S., & Karaman, E. (2024). Genomic prediction of methane emission using microbiome data and genomic markers in Holstein cows. In *Genomic prediction of methane emission using microbiome data and genomic markers in Holstein cows*.

Salem, M., Al-Tobasei, R., Ali, A., Lourenco, D., Gao, G., Palti, Y.,…Leeds, T. D. (2018). Genome-wide association analysis with a 50K transcribed gene SNP-chip identifies QTL affecting muscle yield in rainbow trout. *Frontiers in genetics*, *9*, 387.

Salem, M., Vallejo, R. L., Leeds, T. D., Palti, Y., Liu, S., Sabbagh, A.,…Yao, J. (2012). RNA-Seq identifies SNP markers for growth traits in rainbow trout. *PloS one*, *7*(5), e36264.

Sharma, P., Doultani, S., Hadiya, K., George, L., & Highland, H. (2024). Overview of marker-assisted selection in animal breeding. *HISTORY*, *9*, 11.

Silva, R., Vallejo, R., Evenhuis, J., Leeds, T., Gao, G., Parsons, J.,…Palti, Y. (2017). 209 Prospecting genomic regions associated with columnaris disease in two rainbow trout breeding populations. *Journal of Animal Science*, *95*(suppl_4), 103-104.

Silva, R. M., Evenhuis, J. P., Vallejo, R. L., Gao, G., Martin, K. E., Leeds, T. D.,…Lourenco, D. A. (2019). Whole-genome mapping of quantitative trait loci and accuracy of genomic predictions for resistance to columnaris disease in two rainbow trout breeding populations. *Genetics Selection Evolution*, *51*, 1-13.

Silva, R. M., Evenhuis, J. P., Vallejo, R. L., Tsuruta, S., Wiens, G. D., Martin, K. E.,…Leeds, T. D. (2019). Variance and covariance estimates for resistance to bacterial cold water disease and columnaris disease in two rainbow trout breeding populations. *Journal of animal science*, *97*(3), 1124-1132.

Spor, A., Koren, O., & Ley, R. (2011). Unravelling the effects of the environment and host genotype on the gut microbiome. *Nature Reviews Microbiology*, *9*(4), 279-290.

Sánchez, C. C., Smith, T. P., Wiedmann, R. T., Vallejo, R. L., Salem, M., Yao, J., & Rexroad, C. E. (2009). Single nucleotide polymorphism discovery in rainbow trout by deep sequencing of a reduced representation library. *Bmc Genomics*, *10*, 1-8.

Tan, X., He, Z., Fahey, A. G., Zhao, G., Liu, R., & Wen, J. (2023). Research progress and applications of genome-wide association study in farm animals. *Animal Research and One Health*, *1*(1), 56-77.

Tapio, I., Snelling, T. J., Strozzi, F., & Wallace, R. J. (2017). The ruminal microbiome associated with methane emissions from ruminant livestock. *Journal of animal science and biotechnology*, *8*, 1-11.

Tapio, M., Fischer, D., Mäntysaari, P., & Tapio, I. (2023). Rumen microbiota predicts feed efficiency of primiparous nordic red dairy cows. *Microorganisms*, *11*(5), 1116.

Tsai, H.-Y., Hamilton, A., Tinch, A. E., Guy, D. R., Bron, J. E., Taggart, J. B.,…Pong-Wong, R. (2016). Genomic prediction of host resistance to sea lice in farmed Atlantic salmon populations. *Genetics Selection Evolution*, *48*, 1-11.

Tyagi, A., Singh, B., Billekallu Thammegowda, N. K., & Singh, N. K. (2019). Shotgun metagenomics offers novel insights into taxonomic compositions, metabolic pathways and antibiotic resistance genes in fish gut microbiome. *Archives of microbiology*, *201*, 295-303.

Vala, A. G., Tomar, R., & Rathod, P. J. (2023). Speed Breeding: Accelerating Crop Improvement through Controlled Environments, Genetics, and High-Throughput Phenotyping. *Int J Adv Res Sci Eng Technol*, *10*(5), 746-749.

Vallejo, R. L., Cheng, H., Fragomeni, B. O., Gao, G., Silva, R. M., Martin, K. E.,…Palti, Y. (2021). The accuracy of genomic predictions for bacterial cold water disease resistance remains higher than the pedigree-based model one generation after model training in a commercial rainbow trout breeding population. *Aquaculture*, *545*, 737164.

Vallejo, R. L., Cheng, H., Fragomeni, B. O., Shewbridge, K. L., Gao, G., MacMillan, J. R.,…Palti, Y. (2019). Genome-wide association analysis and accuracy of genome-enabled breeding value predictions for resistance to infectious hematopoietic necrosis virus in a commercial rainbow trout breeding population. *Genetics Selection Evolution*, *51*, 1-14.

Vallejo, R. L., Evenhuis, J. P., Cheng, H., Fragomeni, B. O., Gao, G., Liu, S.,…Wiens, G. D. (2022). Genome-wide mapping of quantitative trait loci that can be used in marker-assisted selection for resistance to bacterial cold water disease in two commercial rainbow trout breeding populations. *Aquaculture*, *560*, 738574.

Vallejo, R. L., Fragomeni, B. O., Cheng, H., Gao, G., Long, R. L., Shewbridge, K. L.,…Palti, Y. (2020). Assessing accuracy of genomic predictions for resistance to infectious hematopoietic necrosis virus with progeny testing of selection candidates in a commercial rainbow trout breeding population. *Frontiers in Veterinary Science*, *7*, 590048.

Vallejo, R. L., Leeds, T. D., Fragomeni, B. O., Gao, G., Hernandez, A. G., Misztal, I.,…Palti, Y. (2016). Evaluation of genome-enabled selection for bacterial cold water disease resistance using progeny performance data in rainbow trout: insights on genotyping methods and genomic prediction models. *Frontiers in genetics*, *7*, 187840.

Vallejo, R. L., Leeds, T. D., Gao, G., Parsons, J. E., Martin, K. E., Evenhuis, J. P.,…Palti, Y. (2017). Genomic selection models double the accuracy of predicted breeding values for bacterial cold water disease resistance compared to a traditional pedigree-based model in rainbow trout aquaculture. *Genetics Selection Evolution*, *49*, 1-13.

Vallejo, R. L., Liu, S., Gao, G., Fragomeni, B. O., Hernandez, A. G., Leeds, T. D.,…Palti, Y. (2017). Similar genetic architecture with shared and unique quantitative trait loci for bacterial cold water disease resistance in two rainbow trout breeding populations. *Frontiers in genetics*, *8*, 295373.

Vallejo, R. L., Silva, R. M., Evenhuis, J. P., Gao, G., Liu, S., Parsons, J. E.,…Leeds, T. D. (2018). Accurate genomic predictions for BCWD resistance in rainbow trout are achieved using low-density SNP panels: Evidence that long-range LD is a major contributing factor. *Journal of animal breeding and genetics*, *135*(4), 263-274.

Wakchaure, R., Ganguly, S., Praveen, P., Kumar, A., Sharma, S., & Mahajan, T. (2015). Marker assisted selection (MAS) in animal breeding: a review. *J. Drug. Metab. Toxicol*, *6*(5), e127.

Weber, K. L., Welly, B. T., Van Eenennaam, A. L., Young, A. E., Porto-Neto, L. R., Reverter, A., & Rincon, G. (2016). Identification of gene networks for residual feed intake in Angus cattle using genomic prediction and RNA-seq. *PloS one*, *11*(3), e0152274.

Weigel, K., VanRaden, P., Norman, H., & Grosu, H. (2017). A 100-Year Review: Methods and impact of genetic selection in dairy cattle—From daughter–dam comparisons to deep learning algorithms. *Journal of dairy science*, *100*(12), 10234-10250.

Weishaar, R., Wellmann, R., Camarinha-Silva, A., Rodehutscord, M., & Bennewitz, J. (2020). Selecting the hologenome to breed for an improved feed efficiency in pigs—A novel selection index. *Journal of Animal Breeding and Genetics*, *137*(1), 14-22.

Wiseman, S., Osachoff, H., Bassett, E., Malhotra, J., Bruno, J., VanAggelen, G.,…Vijayan, M. M. (2007). Gene expression pattern in the liver during recovery from an acute stressor in rainbow trout. *Comparative Biochemistry and Physiology Part D: Genomics and Proteomics*, *2*(3), 234-244.

Wu, L., Fan, J., & Belasco, J. G. (2006). MicroRNAs direct rapid deadenylation of mRNA. *Proceedings of the National Academy of Sciences*, *103*(11), 4034-4039.

Ye, S., Yuan, X., Lin, X., Gao, N., Luo, Y., Chen, Z.,…Zhang, Z. (2018). Imputation from SNP chip to sequence: a case study in a Chinese indigenous chicken population. *Journal of animal science and biotechnology*, *9*, 1-12.

Yoshida, G. M., & Yáñez, J. M. (2022). Increased accuracy of genomic predictions for growth under chronic thermal stress in rainbow trout by prioritizing variants from GWAS using imputed sequence data. *Evolutionary applications*, *15*(4), 537-552.

Zhang, F., Guo, X., & Deng, H.-W. (2011). Multilocus association testing of quantitative traits based on partial least-squares analysis. *PloS one*, *6*(2), e16739.

Ødegård, J., Meuwissen, T. H., Heringstad, B., & Madsen, P. (2010). A simple algorithm to estimate genetic variance in an animal threshold model using Bayesian inference. *Genetics Selection Evolution*, *42*, 1-7.

Ødegård, J., Olesen, I., Gjerde, B., & Klemetsdal, G. (2007). Evaluation of statistical models for genetic analysis of challenge-test data on ISA resistance in Atlantic salmon (Salmo salar): prediction of progeny survival. *Aquaculture*, *266*(1-4), 70-76.

Chapter 2: Weighted Single-step GWAS identifies genes influencing fillet color in Rainbow trout

Ahmed, Ridwan O., Ali Ali, Rafet Al-Tobasei, Tim Leeds, Brett Kenney, and Mohamed Salem. "Weighted single-step GWAS identifies genes influencing fillet color in rainbow trout." *Genes* 13, no. 8 (2022): 1331.

Ridwan O. Ahmed[1], Ali Ali[1], Rafet Al-Tobasei[2], Tim Leeds[3], Brett Kenney[4,] and Mohamed Salem[1*]

[1]Department of Animal and Avian Sciences, University of Maryland, College Park, MD 20742, USA. [2]Computational Science Program, Middle Tennessee State University, Murfreesboro, TN 37132, USA. [3]United States Department of Agriculture Kearneysville, National Center for Cool and Cold Water Aquaculture, Agricultural Research Service, Kearneysville, WV, USA. [4]Division of Animal and Nutritional Sciences, West Virginia University, Morgantown, WV 26506, USA.

* Correspondence: mosalem@umd.edu [1]Department of Animal and Avian Sciences, University of Maryland, College Park, MD 20742, USA

Abstract

The visual appearance of the fish fillet is a significant determinant of consumers' purchase decisions. Depending on rainbow trout diet, a uniform bright white or reddish/pink fillet color is desirable. Factors affecting fillet color are complex ranging from the ability of live fish to accumulate carotenoids in the muscle to preharvest environmental conditions, early postmortem muscle metabolism, and storage conditions. Identifying genetic markers of fillet color is a desirable goal but, nonetheless, a challenging task for the aquaculture industry. This study used weighted, single-step GWAS to explore the genetic basis of fillet color variation in rainbow trout. We identified several SNP windows explaining up to 3.5%, 2.5%, and 1.6% of the additive genetic variance for fillet redness, yellowness, and whiteness, respectively. SNPs are located within genes implicated in carotenoid metabolism (Beta, beta-carotene 15,15'-dioxygenase, retinol dehydrogenase) and myoglobin homeostasis (ATP synthase subunit beta, mitochondrial (*ATP5F1B*)). These genes are involved in processes that influence muscle pigmentation and post-mortem flesh coloration. Other identified genes are involved in maintenance of muscle structural integrity (kelch protein 41b (*klh41b),* collagen alpha-1(XXVIII) chain (*COL28A1*), and cathepsin K (*CTSK*)) and protection against lipid oxidation (peroxiredoxin, superoxide dismutase 2 (*SOD2*), sestrin-1, Ubiquitin carboxyl-terminal hydrolase-10 (*USP10*)). A-to-G single nucleotide polymorphism in Beta, beta-carotene 15,15'-dioxygenase, and *USP10* result in isoleucine-to-valine and proline-to-leucine non-synonymous amino acid substitutions, respectively. Our observation confirms that fillet color is a complex trait regulated by many genes involved in carotenoid metabolism, myoglobin homeostasis, protection against lipid oxidation and maintenance of muscle structural integrity. The significant SNPs identified in this study could be prioritized via genomic selection in breeding programs to improve fillet color in rainbow trout.

Keywords: Fillet color, rainbow trout, GWAS, Genetic markers, Genes

Introduction

The aquaculture industry sustainably produces food fish to satisfy a growing US and worldwide demand. Rainbow trout is the most cultivated, cool, freshwater fish in the United States (Thorgaard et al., 2002). Aquaculture supplies protein with low saturated fat and cholesterol content and high omega-3 fatty acids (Harlioglu, 2012; Turchini et al., 2011). Rainbow trout are reared to produce fillets, and high production efficiency is needed to meet the ever-increasing demand for quality products. A significant constraint is lack of genetically improved fish strains with high fillet yields and good quality fillets. The industry has worked to remedy the situation by introducing breeding programs to select the best animals as parents for the next generations. Many of these breeding programs are traditional, using phenotypic information from breeding candidates and their pedigree to make selection decisions (Zenger et al., 2017). However, traditional breeding programs can be time-consuming and inefficient, especially for lethal traits like fillet yield and color that cannot be accurately measured on live fish (Ibtisham et al., 2017).

Use of genomic information in breeding programs offers a faster and more accurate method of achieving genetic progress. Achieving this goal requires an understanding of genetic architecture underlying variability in these traits. Genome-wide association (GWA) studies can identify regions of the genome associated with desired traits. GWA studies take advantage of linkage disequilibrium between SNP markers and genetic loci controlling a trait of interest. GWA studies have been conducted in the rainbow trout breeding program at National Center for Cool and Cold-Water Aquaculture (NCCCWA) for growth (Ali et al., 2020b), muscle yield (M. Salem et al., 2018), intramuscular fat (Ali et al., 2020c), and fillet firmness (A. Ali et al., 2019) and disease resistance(R. L. Vallejo et al., 2018). Another essential trait that requires attention is the fillet color; targeted in this study.

Fillet color is an important quality trait, usually influencing consumers' satisfaction and point-of-purchase decisions. There are two markets for rainbow trout fillet - one for a bright reddish/pink fillet and one for a bright white fillet. Consumers usually reject or downgrade pale yellowish fillets. Factors affecting fillet color range from genetics to environmental factors and to harvest, handling, and storage conditions (Colihueque, 2010). Postmortem fillet color stability also depends on the rate of myoglobin oxidation, which is influenced by oxidation of intramuscular lipids and mitochondrial activity (Joseph et al., 2010). Salmonids' characteristic pink/bright reddish fillet

color results from the deposition of naturally occurring carotenoid pigments or synthetic pigments added to the diets (Buttle et al., 2001). Carotenoids supplied in the diet are transported through the intestinal wall, metabolized within the cells of the intestinal linings or in the liver. The unmetabolized portion is deposited in the muscle by binding to muscle alpha-actin (Castenmiller & West, 1998; Matthews et al., 2006). Rainbow trout flesh will typically be less reddish or more whitish when the diet is not supplemented with carotenoids, as salmonids cannot synthesize carotenoids *de novo* (Storebakken & No, 1992). Atlantic salmon and rainbow trout fish fed unpigmented diet yield fillets with higher L*(lightness) and lower a*(redness), and b*(yellowness) values in comparison to fish on astaxanthin-supplemented diets (Arredondo-Figueroa et al., 2007; Thomas, 1999). Brown et al. (2016) reported a significant difference in the color retention indices (ECI, hue, and chroma) of fillets from rainbow trout fish that never received dietary astaxanthin compared to fillets from fish that received an astaxanthin-supplemented diet. Even when fed a non-pigmented diet, Crouse et al.(2018) observed significant differences in fillet redness (a*) between different rainbow trout strains fed the same diet. Red/pink pigmented rainbow trout fillets are deemed more desirable and marketed at more premium price than the white fillets (Brown et al., 2016; Folkestad et al., 2008; Forsberg & Guttormsen, 2006), but some consumers, especially in the US, may show preference for a whiter fish.

Astaxanthin, a carotenoid, which is added to the salmonid feed to improve the reddish color of the fillet, is an expensive feed ingredient, accounting for up to 30 percent of the feed cost. Therefore, development of genetically improved rainbow trout strains that more efficiently incorporate carotenoids into the muscle will benefit the aquaculture industry by improving profitability and consumer satisfaction. When fed unpigmented diets, genetically improved strains will also use naturally occurring carotenoids in the feed ingredients.

Studies in humans (Lietz et al., 2012; Yabuta et al., 2016), chicken(Le Bihan-Duval et al., 2011), mice (Hessel et al., 2007), and Atlantic salmon (Helgeland et al., 2019) identified the Beta-carotene 15,15′-oxygenase (BCO1) enzyme as responsible for variation in the ability to metabolize carotenoids. Also, a recent study on a rainbow trout line used for commercial production in France identified Bcmo1 (Beta, beta-carotene 15,15 -dioxygenase), dkk3a (dickkopf WNT signaling pathway inhibitor 3a), and bola3 (bolA family member 3) as possible genes whose functions regulate the color of rainbow trout fillets (Blay et al., 2021). However, there is still much to learn

about the genetic architecture of fillet color before it can be incorporated into breeding programs through genomic selection.

This study aims to use GWA analysis to identify genomic regions associated with fillet color traits (redness, yellowness, lightness, and whiteness) in a population of rainbow trout developed at the NCCCWA that had undergone five generations of selection for growth rate. Fish were fed an unpigmented commercial fishmeal-based diet.

Materials and Methods

Fish population and phenotype used for GWA in this study

This rainbow trout fish population used in this study was from a growth-selected line from NCCCWA as described by Leeds et al.(2016). Fish from the third (hatch-year 2010) and fourth (the hatch-year 2012) generations belonging to 197 families were included in this study. The breeding, selection, feeding, rearing, and harvesting procedure are as described in Salem et al. (2018). The fish used in this study were fed an unpigmented commercial fishmeal-based diet (42% protein, 16% fat; Ziegler Bros Inc., Gardners, PA) using automatic feeders (Arvotec, Huutokoski, Finland). Initially, young fish were fed at a daily rate of ~ 2.5% of body weight (BW), gradually reduced to approximately 0.75% of BW.

Fillet color parameters, L*, a*, b*, which represent lightness, redness, and yellowness, respectively, were obtained from fresh fillet surface using Minolta Chroma Meter CR-200 (Minolta, Model CR-300; Minolta Camera Co., Osaka, Japan). The parameters were recorded, a day after harvest, at three locations above the lateral line of the right-side fillet as described by Al-Tobasei et al.(2017). In addition to the standard color parameters, L*, a*, b*, fillet whiteness index was calculated using the equation: Whiteness = $100 - [(100 - L)^2 + a^2 + b^2]^{1/2}$ (Park, 1994). The data was obtained from 878 fish from 2 harvest years: 406 fish from hatch-year 2010 and 472 fish from hatch-year 2012.

Genotyping and Quality Control

The 878 fish were genotyped with the 50k transcribed SNP-chip developed and described in Al-Tobasei et al. (2017). PREGSF90 (Misztal et al., 2002) was used to perform quality control using

the following criteria: call rate for SNP and samples > 0.90, MAF > 0.05, monomorphic =1, and HWE < 0.15. In total, 32,868 SNPs passed the QC and were used for subsequent analysis.

Descriptive statistics

The mean and standard deviation values of each fillet color phenotype were calculated. Heritability was estimated as the ratio of additive genetic variance to total phenotypic variance. Variance components were estimated using the restricted maximum likelihood method found in AIREML in BLUPF90 software (Misztal et al., 2002) using the following linear mixed model:

$y = Xb + Z_1a + Z_2w + e$

where y is the vector of phenotypes, b is the vector of fixed effects (age, harvest group, and hatch-year), a is the vector of additive genetic effect, w is the vector of random family effect, and e is the residual effect. X and Z_1 and Z_2 are incidence matrices for the effects contained in b, a, and w, respectively.

Genome-wide Association Analysis

Weighted single-step GBLUP (wssGBLUP) approach proposed by Wang et al. (2012) was used to perform genome-wide association analysis using the BLUPF90 family programs (Misztal et al., 2002). This method allows the use of genotyped and ungenotyped animals while integrating phenotype, genotype, and pedigree information in a mixed model for single-trait analysis.

The four fillet color parameters (l, a,b, and whiteness) were analyzed using the single trait animal model in wssGBLUP according to the model below

$y = Xb + Z_1a + Z_2w + e$

where y is the vector of phenotypes, b is the vector of fixed effects, a is the vector of additive genetic effect, w is the vector of random family effect, and e is the residual effect. X and Z_1 and Z_2 are incidence matrices for the effects contained in b and a and w, respectively. The fixed effects used in this study are fish age, harvest group, and hatch-year. The assumptions are that a ~N(0, $H\sigma^2_a$) and e~ N(0, $I\sigma^2_e$), where σ^2_a and σ^2_e are the additive genetic variance and residual variance, respectively. The H is a blend of pedigree and SNP-derived matrix (Legarra et al., 2009), while *I* denote the Identity matrix. The inverse of H is used in the wssGBLUP mixed model analysis (Aguilar et al., 2010).

$$H^{-1}=A^{-1}+\begin{bmatrix}0 & 0\\ 0 & G^{-1}-A_{22}^{-1}\end{bmatrix}$$

where A^{-1} is the inverse of the pedigree relationship matrix for all animals; A_{22}^{-1} is the inverse of the pedigree relationship matrix of genotyped animals and G^{-1} is the inverse of the genomic relationship matrix. The random family effect is uncorrelated and just accounts for the fact the animals within the same family were raised in a common environment, and the covariance structure is given by $I\sigma_w^2$, where I is an identity matrix and σ_w^2 is the family variance.

AIREMLF90 was used to estimate variance components supplied to BLUPF90 to predict genomic estimated breeding values (GEBV). The inbreeding coefficient was calculated from the pedigree data of 1420 fish by RENUMF90 using the method of Meuwissen and Luo (1992).

BLUPF90 was used to predict breeding values using a weighted genomic relationship matrix(G). The SNP marker effect and new weights were then computed with POSTGSF90 (Misztal et al., 2002) using 50 adjacent SNP sliding windows. All SNPs were initially assumed to be equally weighted (i.e., given an equal weight of 1.0). The final SNP weights and SNP effects were estimated using the option "non-linear A" which allows for stable SNP weights after some iterations. Non-linear prediction assumes prior non-normal distribution of marker effect and that markers do not contribute equally to genetic variance (VanRaden, 2008). The non-linear approach resulted in greater reliability in the genomic prediction breeding value for bulls (VanRaden, 2008).

The percentage of additive genetic variance explained by each SNP window was calculated as:

$$\frac{var(a_i)}{\sigma_a^2} \times 100\% = \frac{var\left(\Sigma_{j=i}^{50} Z_j u_j\right)}{\sigma_a^2} \times 100\%$$

where a_i is the genetic value of the i^{th} window consisting of 50 adjacent SNPs, σ^2 is the total genetic variance and z_j is a vector genotype of the jth SNP for all animals; and u_j is the SNP effect of the j^{th} SNP within the ith window.

The qqman package (Turner, 2014) was used to obtain Manhattan plots for the proportion of additive genetic variance explained by each SNP window.

Identification of Candidate Genes

Genomic windows explaining at least 1% of the genetic variance were selected as possible genetic regions associated with the fillet color traits. The 1% threshold was set based on the literature obtained (Aguilar et al., 2011; Gao et al., 2019; Dianelys Gonzalez-Pena et al., 2016). The SNPs were annotated using the NCBI rainbow trout genome assembly (GCF_013265735.2) to identify SNP-harboring genes. We used a literature search to identify relevant gene pathways and functions to understand the possible mechanisms by which the candidate genes regulate the traits. Genes previously identified in literature or that were found to be related to color traits were further discussed.

MicroRNA Target Prediction

SNPs located in the 3'UTR of genes associated with fillet color in this study were investigated if their 3'UTR serves as target sites for rainbow trout microRNAs. MicroRNA targets were predicted using three algorithms *(PITA, miRanda, and TargetSpy)* from the sRNAToolbox (http://bioinfo5.ugr.es/srnatoolbox). The rainbow trout microRNA repertoire was obtained from Juanchich et al.(2016).

Results

Descriptive statistics and heritability estimates for the color traits

Table 1. Descriptive statistics of the observed phenotypes where σ^2_a , σ^2_w, and σ^2_e are the additive genetic variance, family variance, and residual variance, respectively, and h^2 is the heritability estimate.

Trait	N	Mean	SD	Min	Max	CV(%)	σ^2_a	σ^2_w	σ^2_e	h^2 (SE)
Redness	878	1.98	1.06	-0.17	5.833	0.54	0.08	0.04	0.38	0.16±0.06
Yellowness	878	4.41	1.31	-0.79	8.123	0.3	0.52	0.16	0.67	0.39±0.07
Lightness	878	44.54	2.74	38.17	54.81	0.06	1.23	0.33	4.13	0.22±0.07
Whiteness	878	44.3	2.64	38.11	54.22	0.06	1.13	0.31	3.92	0.21±0.06

There is more variation in the redness (54%) and yellowness (30%) in comparison to lightness and whiteness (6%). The heritability estimates of the traits in this population are moderate (0.16-0.39). The phenotypic correlation between lightness (L*) and whiteness color indices is 0.99 (R^2=0.98).

Genome-wide association study and QTL identification

A weighted single-step GBLUP approach was implemented in the BLUPF90 family of programs (Misztal et al., 2002) to identify SNPs associated with fillet color traits. The GWAS result for whiteness and lightness color indices follow the same pattern, as expected, because of the high phenotypic correlation. Subsequently, only the whiteness trait will be discussed further. We identified 244, 161, and 115 SNPs in genomic windows, explaining at least 1% of genetic variation in fillet redness, yellowness, and whiteness, respectively (Tables 2, 3, and Supplementary Table 1). The SNPs were identified within a genomic sliding window of 50 SNPs.

For redness (a*), chromosome 7 harbors the majority (33%) of the SNPs (80), followed by chromosome 9 (67 SNPs) (Figure 1, Table 2). Forty-five percent of the SNPs are in untranslated regions of genes, while 42% are in the coding regions. The highest peak corresponds to a SNP window on chromosome 7 that explains ~3.5% of the genetic variance.

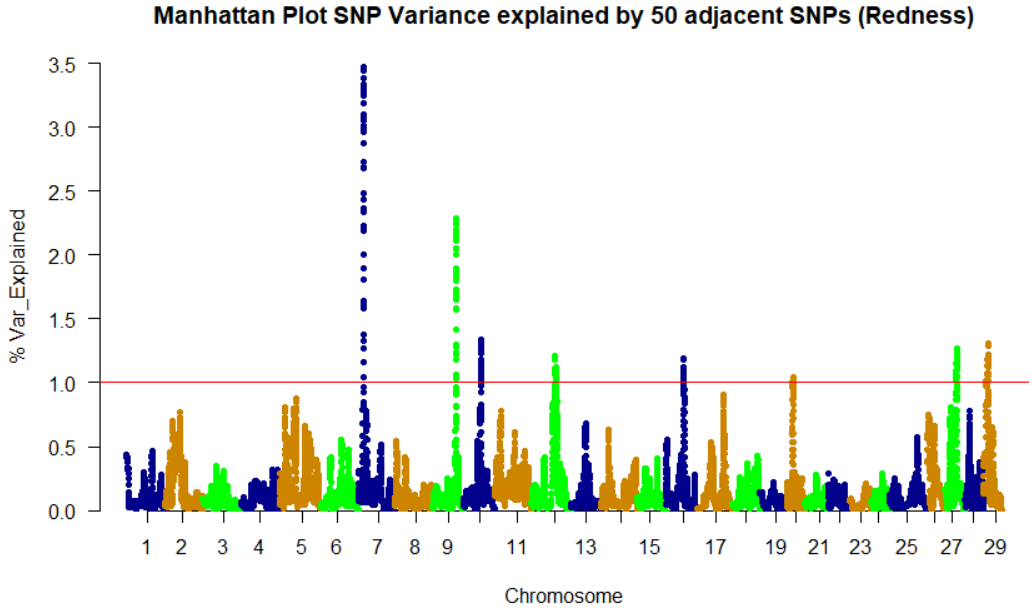

Figure 1. Manhattan plot of percent genetic variance explained by 50 adjacent SNP windows for fillet redness (a*).

For the yellowness trait (b*), most of the SNPs (66) are resident in chromosome 6 (41%), followed by 46 SNPs on chromosome 4 (29%). The peak SNP window, resident on chromosome 6 explains up to ~2.5% of genetic variance for the trait (Figure 2, Table 2). Forty percent of the SNPs are in untranslated regions (UTR), while 47% are in coding regions.

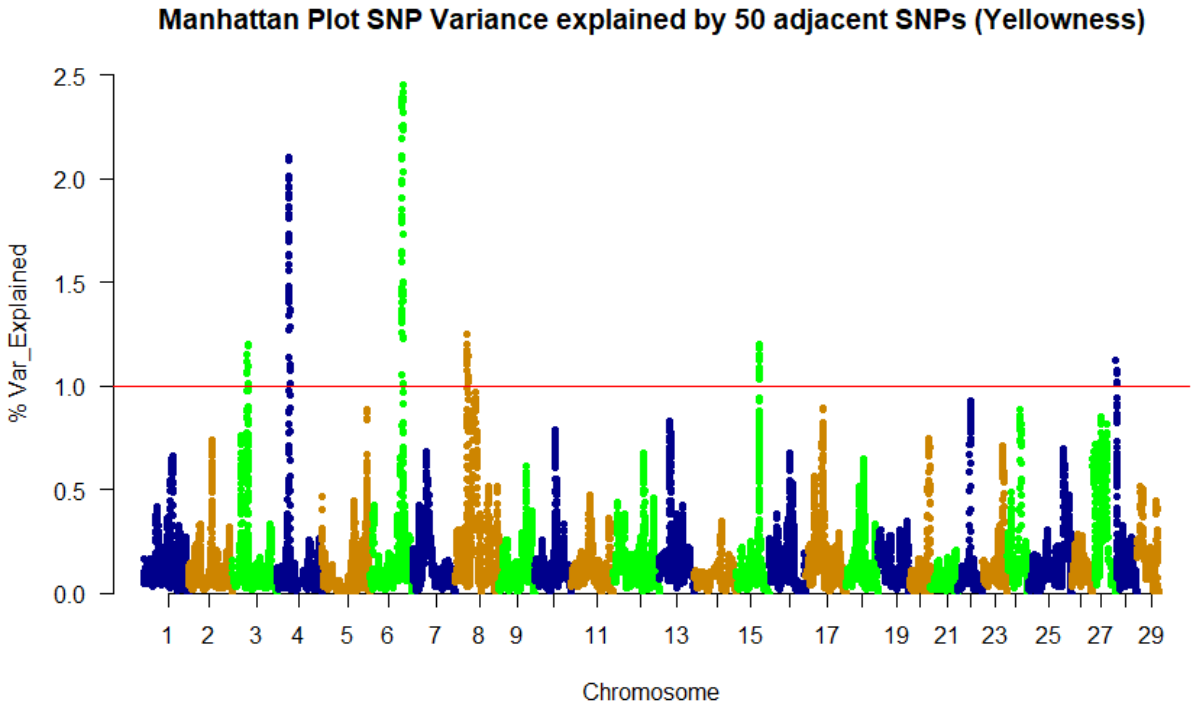

Figure 2. Manhattan plot of percent genetic variance explained by 50 adjacent SNP windows for fillet yellowness (b*).

Lightness (L*) and whiteness are similar in their genetic architecture, with peak SNP on chromosome 8 explaining only 1.6% of genetic variance for this trait (Figure 3, Table 3). 43% of the SNPs are found within gene coding regions, while 45% are located in untranslated regions.

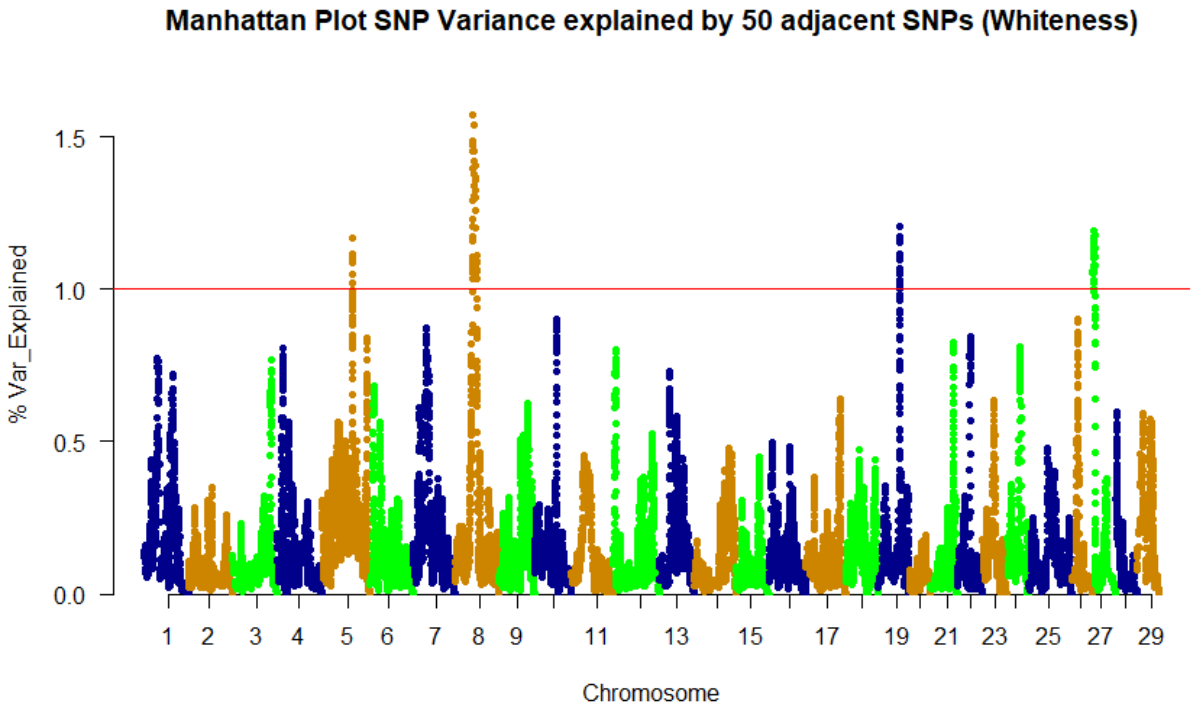

Figure 3. Manhattan plot of percent genetic variance explained by 50 adjacent SNP windows for the fillet whiteness.

Table 2: Selected SNP markers within 50 SNPs genomic sliding window explaining at least 1% of additive genetic variance for fillet redness and yellowness trait

Chr	POS	%Var	Gene ID	Gene annotation	Region/Effect
Redness					
7	10,996,914	2.43	LOC110527401	Radixin	CDS/syn
7	11,138,396	2.49	LOC110527405	Calsequestrin-2	CDS/Syn
7	11,312,252	2.73	LOC110527407	Zinc finger protein Dzip1	CDS/syn
7	11,399,310	3.45	LOC110527414	Kelch protein 41b	CDS/syn
7	11,402,881	3.47	LOC110527413	Collagen alpha-1(XXVIII) chain	3'UTR
7	11,438,574	3.29	LOC100136600	ATP synthase subunit beta, mitochondrial	CDS/syn
7	11,444,638	3.02	LOC110527417	Retinol dehydrogenase 7	CDS/syn
7	11,459,018	2.98	abcb11	Bile salt export pump	CDS/syn
7	11,477,215	2.88	LOC100136260	Cathepsin K	CDS/syn
9	52,063,734	2.27	LOC110532529	Tyrosine-protein phosphatase non-receptor type 1	3'UTR
9	52,106,708	2.26	LOC110532530	Ubiquitin-conjugating enzyme E2 variant 1	3'UTR
9	52,291,239	2.28	LOC110532539	Partner of Y14 and mago A	CDS/syn
12	53,800,425	1.1	hspb1	Heat shock protein, alpha-crystallin-related-1	3'UTR/miRNA target
Yellowness					
4	22,957,625	2.09	prdx6	Peroxiredoxin 6	CDS/syn
4	22,973,619	2.11	plpp6	Phospholipid phosphatase 6	5'UTR
4	23,074,540	2	LOC110521622	Protein PRRC2C	3'UTR
4	23,103,208	1.92	vamp4	Vesicle associated membrane protein 4	3'UTR
4	23,115,313	1.95	LOC110521624	Myocilin	CDS/Syn
6	61,578,946	1.9	LOC110526379	F-actin-methionine Sulfoxide oxidase MICAL2	5'UTR
6	61,592,297	1.99	LOC110526380	Ubiquitin carboxyl-terminal hydrolase 47	CDS/syn
6	61,666,093	2.25	LOC110526946	Beta,beta-carotene 15,15'-dioxygenase-l	CDS/Non-syn
6	61,805,211	2.11	LOC110526388	Nuclear factor of activated T-cells 5	CDS/syn

6	61,837,913	2.39	LOC110526389	Lysine--tRNA ligase	3'UTR
6	61,847,413	2.38	LOC110526390	60S ribosomal protein L13	CDS/syn
6	61,998,041	2.36	LOC110526393	Cytochrome b5	3'UTR
6	62,768,347	2.45	LOC110526402	Cysteine-rich Secretory protein LCCL domain-containing 2	3'UTR
6	62,812,905	2.32	LOC110526403	Ubiquitin carboxyl-terminal hydrolase 10	CDS/Non-syn
6	62,896,859	2.24	LOC110526405	AP-1 complex subunit gamma-1	3'UTR
6	62,961,238	2.26	LOC110526408	Myotubularin-related Protein 10	3'UTR
6	63,056,828	2.39	LOC100136691	Cyclin B2	CDS/syn

Chr= chromosome, POS =SNP Position %Var = % Variance explained, Syn=synonymous amino acid substitution, Non-Syn = non-synonymous amino acid substitution

Table 3: Selected SNP markers within 50 SNPs genomic sliding window explaining at least 1% of additive genetic variance for fillet whiteness trait

Chr	POS	Whiteness %Var	Gene ID	Gene annotation	Region/Effect
8	34,097,292	1.17	LOC110529884	Peptidyl-prolyl cis-trans isomerase FKBP1B	CDS/Syn
8	34,136,112	1.29	mut	Methylmalonyl-CoA mutase	3'UTR
8	34,495,040	1.49	sod2	Superoxide dismutase 2	3'UTR
8	34,936,875	1.57	LOC110529892	cGMP-dependent protein kinase 1	3'UTR
8	36,538,411	1.42	LOC110529899	SAM and SH3 domain-containing protein 1	3'UTR
8	37,290,793	1.54	LOC110529911	Sialomucin core protein 24	3'UTR
8	37,412,186	1.38	LOC110529910	Sestrin-1	3'UTR
8	37,829,107	1.38	ostm1	Osteopetrosis associated transmembrane protein 1	3'UTR
8	38,254,068	1.3	LOC110529920	Poly(U)-binding-splicing factor PUF60	CDS/Syn
8	39,295,098	1.37	ankh	ANKH inorganic pyrophosphate transport regulator	3UTR/miRNA target
8	40,954,559	1.3	myo10	Myosin X	3'UTR
8	40,978,990	1.36	znf622	Zinc finger protein 622	3'UTR
8	41,002,542	1.26	retreg1	Reticulophagy regulator 1	3'UTR/miRNA target
19	41,952,271	1.18	LOC110497982	Uncharacterized protein C15orf52	3'UTR
27	1,675,710	1.19	LOC110507317	Protein IWS1 homolog	3'UTR
27	3,976,684	1.18	LOC110507360	Serine/threonine-protein phosphatase 2A 65 kDa regulatory subunit A beta isoform	CDS/Syn

Chr= chromosome, POS =SNP Position %Var = % Variance explained, Syn=synonymous amino acid substitution.

MicroRNA target prediction

*Our results revealed that the 3'UTR region of ANKH (*ANKH inorganic pyrophosphate transport regulator), *RETRIG1* (reticulophagy regulator 1), and *HSPB1* (heat shock protein, alpha-crystallin-related, 1) genes are target sites for the omy-mir-1388-3p, omy-mir-219-5p, and omy-miR-724-5p micro RNAs, respectively. *An A-to-T single nucleotide substitution at the target site of* omy-mir-1388-3p *causes a loss of its miRNA target site. Likewise, a C-to-T transition at the 3'UTR of HSPB1* resulted in a loss of the target site for the omy-miR-724-5p miRNA. Single nucleotide substitution at the target site of omy-mir-219-5p does not lead to loss of the target site.

Discussion

Fillet color is an important quality trait in salmonids that influences consumers' purchasing decisions. Therefore, the industry is interested in selecting rainbow trout with superior genetic merit in their ability to produce a bright red or white fillet. Understanding the trait's genetic architecture is required to determine the best genetic improvement approach. In this study, a genome-wide association investigation identifies regions of the genome influencing variability in fillet color traits in rainbow trout.

Descriptive statistics and heritability estimates for the color traits

There is more variation in redness(a*) and yellowness(b*) in comparison to whiteness. Estimated heritability for fish in this population is low to moderate, similar to an estimate of 0.27 obtained for a rainbow trout fillet color score by Gjerde and Schaeffer (1989). A heritability estimate of 0.30 was recorded for fillet redness by Haffray et al. (2018). Blay et al. (2021) reported higher heritability estimates of 0.46, 0.45, and 0.28 for rainbow trout fillet lightness (L*), redness (a*), and yellowness (b*), respectively. Overall these studies demonstrate the possibility of achieving genetic improvement for fillet color traits through selection.

Summary of wssGWAS for fillet color traits

The SNP windows explaining the highest genetic variance are found on chromosomes 7, 6, and 8 for fillet redness, yellowness, and whiteness, respectively. The SNP-harboring genes were classified according to their function and relevance to fillet color into the following categories.

Genes involved in carotenoid metabolism

Beta, betacarotene 15,15 -dioxygenase and retinol dehydrogenase are involved in carotenoid metabolism (dela Seña et al., 2014; Lei et al., 2019; Yan et al., 2001). Fish species like Atlantic salmon and rainbow trout deposit carotenoids in their muscle that enhance the reddish coloration of the fillet (Matthews et al., 2006) and variation in carotenoid metabolism is associated with beta-carotene oxygenase 1function. Similar to the findings of this study, Beta, betacarotene 15,15 -dioxygenase was implicated in its association with rainbow trout fillet yellowness (Blay et al., 2021). Helgeland et al. (2019) identified beta-carotene oxygenase-1 (*BCO1*) and its paralogue beta-carotene oxygenase-1 (*BCO1L*) as two probable causal genes influencing flesh color in Atlantic salmon. They supported their findings with functional studies of mRNA and protein expression, which pointed to *BCO1L* as the most likely of the two genes to influence flesh color variation. Several studies have identified single nucleotide polymorphism within *BCO1* that was associated with breast meat color in chicken (Jlali et al., 2012; Jlali et al., 2014; Le Bihan-Duval et al., 2011). In the mollusk, Yesso scallop, GWAS and gene expression studies were used to confirm that PyBCO (a homolog of *BCO1* in fish) was responsible for carotenoid metabolism and subsequent muscle coloration (Li et al., 2019).

Beta, beta-carotene 15,15'-dioxygenase on chromosome 6 explains 2.2% of the phenotypic variance for yellowness, while retinol dehydrogenase-7 found on chromosome 7 explains 2.9% of the variation in the redness trait (Table 2). A-G SNP in beta,beta-carotene 15,15'-dioxygenase causes isoleucine-to-valine non-synonymous amino acid substitution. Transcriptome analysis identifies retinol dehydrogenase 12 as a candidate gene regulating body-color formation in ornamental shrimp (Huang et al., 2022). Carotenoids can serve as exogenous antioxidants to prevent oxidative damage in cells; these pigments inhibit lipid peroxidation and hemoglobin oxidation in human erythrocytes (Chiste et al., 2014).

Genes involved in myoglobin homeostasis and protection against lipid oxidation

ATP5F1B, Methylmalonyl-CoA mutase*, ABC11*, Calsequestrin, Cytochrome b5 (*CYB5*), Ubiquitin carboxyl-terminal hydrolase 10 (*USP10*), peroxiredoxin, Superoxide dismutase 2 (*SOD2*), Sestrin-1, Myosin X and Protein PRRC2C are genes that are found to affect fillet color in the study (Tables 2&3). They are known to play a role in either myoglobin homeostasis or regulation of lipid peroxidation.

ATP synthase subunit beta, mitochondrial, (*ATP5F1B*) on chromosome 7 is another identified gene explaining over 3.5% of genetic variability of fillet redness in rainbow trout (Table 2). It generates ATP from ADP through the electron transport system of the respiratory chain in the mitochondria (Grauso et al., 2019). Myoglobin is a muscle protein that binds oxygen and is responsible for muscle coloration (Ramanathan et al., 2019). Myoglobin exists in three forms: deoxymyoglobin, oxymyoglobin, and metmyoglobin. Although with low concentration of heme in the muscle, studies in salmonids have indicated that flesh color is, to some extent, dependent on the status of myoglobin (Ottestad et al., 2011; Tintchev et al., 2009).The oxymyoglobin form promotes bright-reddish coloration in beef and salmon fillet, while metmyoglobin promotes fillet lightness (L*) (Ottestad et al., 2011; Ramanathan et al., 2019).Conversion between the three myoglobin forms is influenced by the mitochondria function (Mancini & Ramanathan, 2014). Mitochondrial function can remain in postmortem muscle, influencing the conversion between the forms of myoglobin and invariably the color of the meat (Mancini & Ramanathan, 2014; Tang et al., 2005). Ramanathan et al. (2019) suggested that understanding factors that influence mitochondrial function is key to unraveling the regulation of beef color appearance. Similarly, the gene, *ATP5F1B,* may influence rainbow trout fillet color by regulating mitochondrial integrity and function. Methylmalonyl-CoA mutase regulates mitochondria function by catalyzing the isomerization of methylmalonyl-CoA to succinyl-CoA (Banerjee & Vlasie, 2002). It explains 1.29% of the genetic variability for fillet whiteness (Table 3).

Bile salt export pump *(ABCB11*) on chromosome 7 explains ~2.9% of genetic variation in fillet redness (Table 2). This gene participates in bile acid homeostasis in an ATP-dependent manner (Paulusma et al., 2009; Yabuuchi et al., 2008). It affects lipid metabolism and oxidation by regulating biliary tract lipid acid secretion through its action on bile salts excretion (Bellanti et al., 2017; Hayashi et al., 2012; Stofan & Guo, 2020). The influence of lipid oxidation on myoglobin, and thus meat color, is essential in meat color research. Post-mortem meat color stability is affected by the rate of lipid oxidation in the muscle (Joseph et al., 2010). The lipid autooxidation process generates free radicals and secondary products like aldehydes and ketones that accelerate myoglobin oxidation (Joseph et al., 2010) and, consequently, meat color deterioration (Chen et al., 2018; Faustman et al., 2010; Liu et al., 2010). Lipid peroxidation in the bile may generate pro-inflammatory agents by converting free fatty acids into lipid peroxides and aldehydes(Esterbauer et al., 1991; Grattagliano et al., 2017). Chen et al. (2018) discovered that aldehydes, a lipid

oxidation product, accelerate rate of myoglobin oxidation and promote permeability of the mitochondrial membrane. This process inhibits electron-transport chain-mediated metmyoglobin reduction and could profoundly affect fillet color stability, as discussed above with the ATP synthase subunit beta, mitochondrial (*ATP5F1B*) gene. Blay et al. (2021) identified two genes, dkk3 and bola3, known to be involved in adipogenesis, as genes harboring regulatory regions associated with fillet color. This work supports a relationship between fillet color and intramuscular fat content.

Conversion between the three myoglobin forms is influenced by mitochondrial function (Mancini & Ramanathan, 2014). Cytochrome B5, a metmyoglobin reductase, reduces ferric myoglobin (methemoglobin) to ferrous myoglobin within muscle mitochondria (Arihara et al., 1995; Seyfert et al., 2006). In this study, cytochrome b5 (*CYB5*), on chromosome 6, explained up to 2.3% of genetic variability for fillet yellowness(Table 2). This gene may play a role in the interconversion of three myoglobin forms, thereby influencing fillet coloration. Cytochrome c oxidase subunit II gene was one of the differentially expressed genes between red and chocolate ornamental shrimp (Huang et al., 2022).

Various studies have implicated ubiquitination as one of the regulatory mechanisms that determines meat quality in pork (Mora et al., 2015), lamb (Fayemi & Muchenje, 2018; Liu et al., 2016), and broiler chicken (Zheng et al., 2009). Ubiquitin carboxyl-terminal hydrolase-10 (*USP10*) is a member of the deubiquitinating enzyme family known as deubiquitinases, which include Ubiquitin C-terminal hydroxylase 1 (*UCH-L1*) (Harrigan et al., 2018). *USP10* and Ubiquitin carboxyl-terminal hydrolase 47 (both on chromosome 6), respectively, explain 2.3% and~2.0% of genetic variance associated with the yellowness phenotype in this study, (Table 2). *UCH-L1* was implicated as influencing meat quality traits in pigs (Damon et al., 2012) and sheep (Fayemi & Muchenje, 2018). *UCH-L1* reportedly regulates oxidative activity in skeletal muscle (Gao et al., 2020) and plays a role in myogenesis (Gao et al., 2017). Polymorphism (A/G) in *USP10* causes a non-synonymous change in the amino acid from Proline to leucine.

The peroxiredoxin family is a group of proteins capable of detoxifying peroxides and protecting cells against oxidation (Wu et al., 2015). Peroxiredoxin 6 (*PRDX6*), on chromosome 4, explains 2.1% of genetic variance in fillet yellowness in the present fish population (Table 2). Proteome

analysis of beef longissimus muscle revealed that peroxiredoxin-1 accounted for up to 70% of variances in color traits (L* a* b*) of muscle (ZHANG et al., 2018), and Wu et al. (2015) identified peroxiredoxin as a possible marker for beef color. Peroxiredoxin 6 enzyme protects oxymyoglobin from peroxide attack, thereby improving post-mortem color stability (Joseph et al., 2012). Activator protein (AP-1) transcription factor on chromosome 6, which explains 1.7% of genetic variance in fillet yellowness (Table 2), has been identified as a regulator of oxidative stress ((Cartwright & Scott, 2013), (Takahashi et al., 2010)). It protects the cell against reactive oxygen species. Other studies have identified a relationship between peroxiredoxin and meat quality, or color traits in beef ((Jia et al., 2009),(Subramaniyan et al., 2017),(Wu et al., 2016),(Yang et al., 2018)) and chevon ((Jia et al., 2021)). Activation of the *AP-1* transcription factor induces the expression of many antioxidants, including peroxiredoxin and glutathione reductase (Grant et al., 1996; Lee et al., 1999). It is possible that these genes (*PRDX6* and *AP-1*) function in the homeostatic regulation of myoglobin redox state, protecting oxymyoglobin against oxidation, thereby enhancing the reddish coloration of the fillet.

Superoxide dismutase 2 (*SOD2*) encodes for muscle antioxidant enzyme. This enzyme functions to reduce the damage caused by superoxide anion radicals (Chan & Decker, 1994). Nohl et al. (1978) identified superoxide dismutase as one of the agents protecting the mitochondria against lipid peroxidation and damage. Lipid oxidation and mitochondrial damage inhibit metmyoglobin reduction, and this causes muscle color deterioration (Chen et al., 2018). *SOD2* on chromosome 8 explains 1.5% of genetic variance in fillet whiteness (Table 3) in this study. A proteomics study on color stability in lamb identified *SOD2* as one of the proteins protecting the muscle against post-mortem discoloration (Gao et al., 2016). Superoxide dismutase was also a possible predictor of meat color stability in cattle (Wu et al., 2016) and chicken (Lee et al., 2013).

Sestrin-1 (*SESN-1*) on chromosome 8 explains ~1.4% of genetic variance in the fillet whiteness (Table 3). *SESN1* is known to confer resistance to oxidative stress through the regeneration of peroxiredoxins (Budanov et al., 2004; Budanov et al., 2002; Sablina et al., 2005).

Hanan & Shaklai (1995) reported a peroxidative interaction between myoglobin and myosin that regulates myoglobin homeostasis when attacked by a peroxide. *In vitro* oxidation of oxymyoglobin was significantly greater ($P<0.05$) when in the presence of myosin compared to when myosin is absent in Tuna fish and Sardine (Chaijan et al., 2007). Myosin X (*MYO10*) on chromosome 8

explains 1.3% of genetic variance for fillet whiteness (Table 3). *MYO10* encodes for a myosin protein belonging to the myosin superfamily (Sellers, 2000). Myosin X may play a role in determining fillet color through its effect on oxymyoglobin oxidation.

Protein PRRC2C is required to form stress granules [81] efficiently. It is involved in the aggregation, arrangement, and bonding of proteins and RNA molecules to form a stress granule (Nonhoff et al., 2007). Stress granules are critical for facilitating responses against oxidative and cellular stress (Byrd et al., 2016; Chen & Liu, 2017; Kobayashi et al., 2012). *Protein PRRC2C* explains 2% of the genetic variance for fillet redness in this study (Table 2).

Genes involved in maintenance of muscle structural integrity

The kelch protein 41b (*KLH41B),* Collagen alpha-1(XXVIII) chain (*COL28A1*), Myocilin *(MYOC),* F-actin-methionine sulfoxide oxidase (*MICAL2)*, and Cathepsin K (*CTSK*) are genes that are found to affect fillet color in the study. They are known to be involved in the maintenance of muscle structural integrity. *KLH4LB* on chromosome 7 explains up to 3.4% of the variance in redness trait in this study (Table 2). *KLH4LB* is involved in skeletal muscle cell differentiation, muscle fiber development, and sarcomere organization (Gupta & Beggs, 2014). Functional studies of the role of the *KLH41B* gene in zebrafish revealed that its knockout resulted in myofibrillar disorganization and muscle weakness (Gupta et al., 2013). The relationship between structure and color of fillet has been reported in literature. Kiessling et al. (2004) reported that fillets with higher L* (lightness) values were softer than those with low lightness values. Gagaoua et al. (2018) identified protein biomarkers (α-actin and connectin) for beef color traits that are also structural proteins. The structural attributes of the muscle could influence the extent of light scattering for meat (Hughes et al., 2014). In their study on mice, Ramirez-Martinez et al. (2017) showed that *KLH41B* maintains muscle function by preferentially helping stabilize nebulin, a protein needed for maintaining muscle sarcomere integrity. They revealed that proteins involved in sarcomere organization and muscle contraction regulation were downregulated in *KLH41B* knockout mice. Loss of nebulin causes nemaline myopathy in humans, a condition associated with severe muscle weakness (Ravenscroft et al., 2013).

Collagen alpha-1(XXVIII) chain (*COL28A1*) harbors SNP marker for muscle color in broiler chicken (Kong et al., 2018). The same gene explains ~3.5% variance in fillet redness in this study

(Table 2). Collagen is a connective tissue protein found in tissues. The muscle extracellular matrix is mainly composed of collagen family proteins (Bailey & Light, 1989). The relative amount and distribution of collagen fibers in the muscle can influence muscle quality (McCormick, 1999).

Cathepsin K activity was shown to influence skeletal muscle repair in mice (Ogasawara et al., 2018). Cathepsin K (*CTSK*) explains up to 2.8% of the genetic variance in fillet redness in this study (Table 2).

Myocilin *(MYOC)* encodes the protein myocilin, which is involved in regulating the actin cytoskeleton (Kwon et al., 2008). It explains 1.95% of the genetic variance in fillet yellowness in this study (Table 2).

F-actin-methionine sulfoxide oxidase (*MICAL2)* encodes methionine monooxygenase that promotes depolymerization of F-actin by mediating oxidation of residues on actin to form methionine-sulfoxide, resulting in actin filament disassembly and preventing repolymerization (Lundquist et al., 2014; Wu et al., 2018). The gene is also involved in cytoskeleton organization(Lundquist et al., 2014). It explains 1.9% of the genetic variance in fillet yellowness in this study (Table 2).

Cysteine-rich secretory protein LCCL domain-containing 2 (*CRISPLD2)* gene encodes a protein binding heparin and glycosaminoglycans and is involved in regulating the innate immune system (Lugowska et al., 2019). It was downregulated as part of the regulatory mechanisms for muscle pigmentation in broiler chickens (Tarique et al., 2014). It explains 2.45% of the genetic variance in fillet yellowness in this study (Table 2).

SNP variants alter microRNA binding sites

MicroRNAs (miRNAs) are short non-coding RNAs between 20-24 nucleotides in length and can regulate gene expression post-transcriptionally by binding to the 3'UTR of its target mRNA (Bartel, 2004; Kutter & Svoboda, 2008). This binding process can result in the formation of RNA-induced silencing complex (RISC) and subsequently repression of translation (He & Hannon, 2004). Mutation/polymorphism in miRNA and/or target 3'UTR sequence have been associated with phenotypic variation in economically important traits. A G-to-A SNP substitution in myostatin 3'UTR changes the miRNA target site and affects muscularity in sheep (Clop et al., 2006). A C/G

polymorphism in the precursor region of *microRNA affects body weight, pelvis breadth, and chest depth in chickens* (Li et al., 2015; Shi & Sun, 2017).

*The 3'UTR region of ANKH (*ANKH inorganic pyrophosphate transport regulator), *RETRIG1* (reticulophagy regulator 1), and *HSPB1* (heat shock protein, alpha-crystallin-related, 1) genes are target sites for omy-mir-1388-3p, omy-mir-219-5p, and omy-miR-724-5p microRNAs, respectively (Tables 2&3). *An A-to-T single nucleotide substitution at the target site of omy-mir-1388-3p causes a loss of its miRNA target site. Likewise, a C-to-T transition at the 3'UTR of HSPB1* resulted in a loss of the target site for the omy-miR-724-5p miRNA. Single nucleotide substitution at the target site of omy-mir-219-5p does not lead to loss of the target site.

Heat shock proteins are common effectors of the cellular stress response. Either thermal, environmental, or oxidative stress can trigger the transcription of genes encoding heat shock proteins (Arya et al., 2007; Kaźmierczuk & Kiliańska, 2009; Morimoto, 1998). Protection of oxymyoglobin against oxidative stress is required to preserve bright reddish meat coloration (Chen et al., 2018). *HSPB1* encodes for a heat shock protein that can protect against oxidative stress. Diet supplementation with antioxidant vitamins resulted in a significant drop in *HSPB1* expression in athletes after an exercise period compared with athletes fed an un-supplemented diet (Zychowska et al., 2015). Over-expression of *HSPB1* has been shown to improve stress resistance (including oxidative stress) (Alexander et al., 2022; Liu et al., 2020; X. Liu et al., 2021; Terra et al., 2019; Zychowska et al., 2015). MicroRNA can repress the translation of its target mRNA. It is possible that the loss of the *HSPB1* target site facilitates the translation of the gene and induces resistance against oxidative stress.

Another gene that exhibits loss of miRNA target site under single nucleotide polymorphism is the *ANKH (*ANKH inorganic pyrophosphate transport regulator). The gene encodes a protein that controls the extracellular level of pyrophosphate (Zhang et al., 2005). Inorganic pyrophosphate also plays an active role in oxidative stress resistance in several organisms (Gutiérrez-Luna et al., 2018; Wu et al., 2010; Yuan et al., 2019).

Conclusion

We used weighted single-step GWAS to identify genetic variants associated with variability in fillet color traits in rainbow trout. Our result confirms that fillet color is a complex trait with no

major gene but many SNP variants contributing to its regulation. We established that regulatory genes are involved in maintaining muscle structural integrity, carotenoid metabolism, or protection against myoglobin and lipid oxidation. An isoleucine-to-valine non-synonymous amino acid substitution mutation in Beta, beta-carotene 15,15'-dioxygenase explains 2.2% of the phenotypic variance for yellowness, while SNP variants in retinol dehydrogenase-7 explain 2.9% of the variance in the muscle redness.

Supplementary Information

Supplementary table 1 : SNPs and genes identified in this study explaining at least 1% of genetic variation in fillet redness, yellowness, and whiteness,

Abbreviation

GWA: Genome-wide association; HWE: Hardy–Weinberg equilibrium; LD: Linkage disequilibrium; MAF: Minor allele frequency; NCCCWA: USDA National Center of Cool and Cold Water Aquaculture; QC: Quality control; QTL: Quantitative trait loci; SNP: Single nucleotide polymorphism; UTR: Untranslated region; WssGBLUP: Weighted single-step GBLUP; YC: Year class, L,a,b,w

Funding

This study was supported by competitive grants No. 2014–67015-21602 and 2021-67015-33388 from the United States Department of Agriculture, National Institute of Food and Agriculture (MS, TL, BK), and by the USDA, Agricultural Research Service CRIS Project 1930–31000-010 "Utilizing Genetics and Physiology for Enhancing Cool and Cold Water Aquaculture Production" Agriculture (TL). The content is solely the authors' responsibility and does not necessarily represent the official views of any of the funding agents.

Availability of data and materials

All datasets generated for this study are included in the manuscript and/or the Supplementary Files. The genotypes (ped and .map files) and phenotypes are available in our previous publication (A. Ali et al., 2019).

Ethics approval and consent to participate

Institutional Animal Care and Use Committee of the United States Department of Agriculture, National Center for Cool and Cold Water Aquaculture (Leetown, WV) specifically reviewed and approved all husbandry practices used in this study (IACUC protocol #056).

References

Aguilar, I., Misztal, I., Johnson, D. L., Legarra, A., Tsuruta, S., & Lawlor, T. J. (2010). Hot topic: a unified approach to utilize phenotypic, full pedigree, and genomic information for genetic evaluation of Holstein final score. *J Dairy Sci*, *93*(2), 743-752. https://doi.org/10.3168/jds.2009-2730

Aguilar, I., Misztal, I., Legarra, A., & Tsuruta, S. (2011). Efficient computation of the genomic relationship matrix and other matrices used in single-step evaluation. *Journal of Animal Breeding and Genetics*, *128*(6), 422-428.

Al-Tobasei, R., Ali, A., Leeds, T. D., Liu, S., Palti, Y., Kenney, B., & Salem, M. (2017). Identification of SNPs associated with muscle yield and quality traits using allelic-imbalance analyses of pooled RNA-Seq samples in rainbow trout. *BMC genomics*, *18*(1), 1-15.

Alexander, C. C., Munkascy, E., Tillmon, H., Fraker, T., Scheirer, J., Holstein, D.,…Rodriguez, K. A. (2022). HspB1 Overexpression Improves Life Span and Stress Resistance in an Invertebrate Model. *J Gerontol A Biol Sci Med Sci*, *77*(2), 268-275. https://doi.org/10.1093/gerona/glab296

Ali, A., Al-Tobasei, R., Lourenco, D., Leeds, T., Kenney, B., & Salem, M. (2019). Genome-Wide Association Study Identifies Genomic Loci Affecting Filet Firmness and Protein Content in Rainbow Trout. *Front Genet*, *10*, 386. https://doi.org/10.3389/fgene.2019.00386

Ali, A., Al-Tobasei, R., Lourenco, D., Leeds, T., Kenney, B., & Salem, M. (2020a). Genome-wide identification of loci associated with growth in rainbow trout. *BMC genomics*, *21*(1), 209. https://doi.org/10.1186/s12864-020-6617-x

Ali, A., Al-Tobasei, R., Lourenco, D., Leeds, T., Kenney, B., & Salem, M. (2020b). Genome-wide scan for common variants associated with intramuscular fat and moisture content in rainbow trout. *BMC genomics*, *21*(1), 529. https://doi.org/10.1186/s12864-020-06932-0

Arihara, K., Cassens, R. G., Greaser, M. L., Luchansky, J. B., & Mozdziak, P. E. (1995). Localization of metmyoglobin-reducing enzyme (NADH-cytochrome b5 reductase) system components in bovine skeletal muscle. *Meat science*, *39*(2), 205-213.

Arredondo-Figueroa, J. L., Mora, G. I. d. l., Ponce-Palafox, J. T., Barriga-Sosa, I. d. l. A., & Vernon-Carter, E. J. (2007). Color of raw, frozen, and smoked fillets of rainbow trout (Oncorhynchus mykiss) fed diets supplemented with astaxanthin and saponified red chilli (Capsicum annuum) extracts. *Journal of Aquatic Food Product Technology*, *16*(1), 35-50.

Arya, R., Mallik, M., & Lakhotia, S. C. (2007). Heat shock genes—integrating cell survival and death. *Journal of biosciences*, *32*(3), 595-610.

Bailey, A. J., & Light, N. D. (1989). *Connective tissue in meat and meat products*. Elsevier applied science.

Banerjee, R., & Vlasie, M. (2002). Controlling the reactivity of radical intermediates by coenzyme B12-dependent methylmalonyl-CoA mutase. *Biochemical Society Transactions*, *30*(4), 621-624.

Bartel, D. P. (2004). MicroRNAs: genomics, biogenesis, mechanism, and function. *cell*, *116*(2), 281-297. https://doi.org/10.1016/s0092-8674(04)00045-5

Bellanti, F., Villani, R., Facciorusso, A., Vendemiale, G., & Serviddio, G. (2017). Lipid oxidation products in the pathogenesis of non-alcoholic steatohepatitis. *Free Radic Biol Med*, *111*, 173-185. https://doi.org/10.1016/j.freeradbiomed.2017.01.023

Blay, C., Haffray, P., Bugeon, J., D'ambrosio, J., Dechamp, N., Collewet, G.,…Corraze, G. (2021). Genetic parameters and genome-wide association studies of quality traits characterised using imaging technologies in Rainbow trout, Oncorhynchus mykiss. *Frontiers in genetics*, *12*, 219.

Brown, K. R., Barnes, M., Parker, T., & Fletcher, B. (2016). Retention of fillet coloration in rainbow trout after dietary astaxanthin cessation. *Fisheries & Aquaculture Journal*, *7*, 163.

Budanov, A. V., Sablina, A. A., Feinstein, E., Koonin, E. V., & Chumakov, P. M. (2004). Regeneration of peroxiredoxins by p53-regulated sestrins, homologs of bacterial AhpD. *Science*, *304*(5670), 596-600. https://doi.org/10.1126/science.1095569

Budanov, A. V., Shoshani, T., Faerman, A., Zelin, E., Kamer, I., Kalinski, H.,…Feinstein, E. (2002). Identification of a novel stress-responsive gene Hi95 involved in regulation of cell viability. *Oncogene*, *21*(39), 6017-6031. https://doi.org/10.1038/sj.onc.1205877

Buttle, L., Crampton, V., & Williams, P. (2001). The effect of feed pigment type on flesh pigment deposition and colour in farmed Atlantic salmon, Salmo salar L. *Aquaculture Research*, *32*(2), 103-111.

Byrd, A. K., Zybailov, B. L., Maddukuri, L., Gao, J., Marecki, J. C., Jaiswal, M.,…Chib, S. (2016). Evidence that G-quadruplex DNA accumulates in the cytoplasm and participates in stress granule assembly in response to oxidative stress. *Journal of Biological Chemistry*, *291*(34), 18041-18057.

Cartwright, G. M., & Scott, B. (2013). Redox regulation of an AP-1-like transcription factor, YapA, in the fungal symbiont Epichloe festucae. *Eukaryotic cell*, *12*(10), 1335-1348.

Castenmiller, J. J., & West, C. E. (1998). Bioavailability and bioconversion of carotenoids. *Annu Rev Nutr*, *18*(1), 19-38. https://doi.org/10.1146/annurev.nutr.18.1.19

Chaijan, M., Benjakul, S., Visessanguan, W., & Faustman, C. (2007). Interaction between fish myoglobin and myosin in vitro. *Food Chemistry*, *103*(4), 1168-1175.

Chan, K. M., & Decker, E. A. (1994). Endogenous skeletal muscle antioxidants. *Crit Rev Food Sci Nutr*, *34*(4), 403-426. https://doi.org/10.1080/10408399409527669

Chen, C., Yu, Q., Han, L., Zhang, J., & Guo, Z. (2018). Effects of aldehyde products of lipid oxidation on the color stability and metmyoglobin reducing ability of bovine Longissimus muscle. *Anim Sci J*, *89*(5), 810-816. https://doi.org/10.1111/asj.12993

Chen, L., & Liu, B. (2017). Relationships between stress granules, oxidative stress, and neurodegenerative diseases. *Oxidative medicine and cellular longevity*, *2017*.

Chisté, R. C., Freitas, M., Mercadante, A. Z., & Fernandes, E. (2014). Carotenoids inhibit lipid peroxidation and hemoglobin oxidation, but not the depletion of glutathione induced by ROS in human erythrocytes. *Life sciences*, *99*(1-2), 52-60.

Clop, A., Marcq, F., Takeda, H., Pirottin, D., Tordoir, X., Bibe, B.,…Georges, M. (2006). A mutation creating a potential illegitimate microRNA target site in the myostatin gene affects muscularity in sheep. *Nat Genet*, *38*(7), 813-818. https://doi.org/10.1038/ng1810

Colihueque, N. (2010). Genetics of salmonid skin pigmentation: clues and prospects for improving the external appearance of farmed salmonids. *Reviews in Fish Biology and Fisheries*, *20*(1), 71-86.

Crouse, C. C., Davidson, J. W., Good, C. M., May, T. C., Summerfelt, S. T., Kenney, P. B.,…Cleveland, B. M. (2018). Growth and fillet quality attributes of five genetic strains of rainbow trout (Oncorhynchus mykiss) reared in a partial water reuse system and harvested at different sizes. *Aquaculture Research*, *49*(4), 1672-1681.

Damon, M., Wyszynska-Koko, J., Vincent, A., Herault, F., & Lebret, B. (2012). Comparison of muscle transcriptome between pigs with divergent meat quality phenotypes identifies genes related to muscle metabolism and structure. *PLoS One*, *7*(3), e33763.

dela Seña, C., Riedl, K. M., Narayanasamy, S., Curley, R. W., Schwartz, S. J., & Harrison, E. H. (2014). The human enzyme that converts dietary provitamin A carotenoids to vitamin A is a dioxygenase. *Journal of biological chemistry*, *289*(19), 13661-13666.

Esterbauer, H., Schaur, R. J., & Zollner, H. (1991). Chemistry and biochemistry of 4-hydroxynonenal, malonaldehyde and related aldehydes. *Free Radic Biol Med*, *11*(1), 81-128. https://doi.org/10.1016/0891-5849(91)90192-6

Faustman, C., Sun, Q., Mancini, R., & Suman, S. P. (2010). Myoglobin and lipid oxidation interactions: mechanistic bases and control. *Meat Sci*, *86*(1), 86-94. https://doi.org/10.1016/j.meatsci.2010.04.025

Fayemi, P., & Muchenje, V. (2018). Expression of ovine ubiquitin C-terminal hydroxylase 1, pH and colour of variety meats from head-stunned Dohne Merino sheep. *South African Journal of Animal Science*, *48*(1), 88-97.

Folkestad, A., Wold, J. P., Rørvik, K.-A., Tschudi, J., Haugholt, K. H., Kolstad, K., & Mørkøre, T. (2008). Rapid and non-invasive measurements of fat and pigment concentrations in live and slaughtered Atlantic salmon (Salmo salar L.). *Aquaculture*, *280*(1-4), 129-135.

Forsberg, O. I., & Guttormsen, A. G. (2006). Modeling optimal dietary pigmentation strategies in farmed Atlantic salmon: Application of mixed-integer non-linear mathematical programming techniques. *Aquaculture*, *261*(1), 118-124.

Gagaoua, M., Bonnet, M., De Koning, L., & Picard, B. (2018). Reverse Phase Protein array for the quantification and validation of protein biomarkers of beef qualities: The case of meat color from Charolais breed. *Meat Sci*, *145*, 308-319. https://doi.org/10.1016/j.meatsci.2018.06.039

Gao, H., Antony, R., Srinivasan, R., Wu, P., Wang, X., & Li, Y. (2020). UCHL1 regulates oxidative activity in skeletal muscle. *PLoS One*, *15*(11), e0241716. https://doi.org/10.1371/journal.pone.0241716

Gao, H., Hartnett, S., & Li, Y. (2017). Ubiquitin C-Terminal Hydrolase L1 regulates myoblast proliferation and differentiation. *Biochem Biophys Res Commun*, *492*(1), 96-102. https://doi.org/10.1016/j.bbrc.2017.08.027

Gao, N., Chen, Y., Liu, X., Zhao, Y., Zhu, L., Liu, A.,…Chen, Y. (2019). Weighted single-step GWAS identified candidate genes associated with semen traits in a Duroc boar population. *BMC genomics*, *20*(1), 797. https://doi.org/10.1186/s12864-019-6164-5

Gao, X., Wu, W., Ma, C., Li, X., & Dai, R. (2016). Postmortem changes in sarcoplasmic proteins associated with color stability in lamb muscle analyzed by proteomics. *European Food Research and Technology*, *242*(4), 527-535.

Gjerde, B. a., & Schaeffer, L. (1989). Body traits in rainbow trout: II. Estimates of heritabilities and of phenotypic and genetic correlations. *Aquaculture*, *80*(1-2), 25-44.

Gonzalez-Pena, D., Gao, G., Baranski, M., Moen, T., Cleveland, B. M., Kenney, P. B.,…Leeds, T. D. (2016). Genome-wide association study for identifying loci that affect fillet yield, carcass, and body weight traits in rainbow trout (Oncorhynchus mykiss). *Frontiers in genetics*, *7*, 203.

Grant, C. M., Collinson, L. P., Roe, J. H., & Dawes, I. W. (1996). Yeast glutathione reductase is required for protection against oxidative stress and is a target gene for yAP-1 transcriptional regulation. *Molecular microbiology*, *21*(1), 171-179.

Grattagliano, I., Ciampi, S. A., & Portincasa, P. (2017). Gallbladder disease: Relevance of oxidative stress. In *Gastrointestinal Tissue* (pp. 187-194). Elsevier.

Grauso, M., Lan, A., Andriamihaja, M., Bouillaud, F., & Blachier, F. (2019). Hyperosmolar environment and intestinal epithelial cells: impact on mitochondrial oxygen consumption, proliferation, and barrier function in vitro. *Sci Rep*, *9*(1), 11360. https://doi.org/10.1038/s41598-019-47851-9

Gupta, V. A., & Beggs, A. H. (2014). Kelch proteins: emerging roles in skeletal muscle development and diseases. *Skelet Muscle*, *4*(1), 11. https://doi.org/10.1186/2044-5040-4-11

Gupta, V. A., Ravenscroft, G., Shaheen, R., Todd, E. J., Swanson, L. C., Shiina, M.,…Darras, B. T. (2013). Identification of KLHL41 mutations implicates BTB-Kelch-mediated ubiquitination as an alternate pathway to myofibrillar disruption in nemaline myopathy. *The American Journal of Human Genetics*, *93*(6), 1108-1117.

Gutiérrez-Luna, F. M., Hernández-Domínguez, E. E., Valencia-Turcotte, L. G., & Rodríguez-Sotres, R. (2018). "Pyrophosphate and pyrophosphatases in plants, their involvement in stress responses and their possible relationship to secondary metabolism". *Plant Science*, *267*, 11-19.

Haffray, P., Enez, F., Bugeon, J., Chapuis, H., Dupont-Nivet, M., Chatain, B., & Vandeputte, M. (2018). Accuracy of BLUP breeding values in a factorial mating design with mixed families and marker-based parentage assignment in rainbow trout Oncorhynchus mykiss. *Aquaculture*, *490*, 350-354.

Hanan, T., & Shaklai, N. (1995). Peroxidative interaction of myoglobin and myosin. *Eur J Biochem*, *233*(3), 930-936. https://doi.org/10.1111/j.1432-1033.1995.930_3.x

Harlioglu, A. G. (2012). Fatty acid composition, fat soluble vitamins and cholesterol content of farmed rainbow trout (Oncorhynchus mykiss). *Pakistan Journal of Zoology*, *44*(4).

Harrigan, J. A., Jacq, X., Martin, N. M., & Jackson, S. P. (2018). Deubiquitylating enzymes and drug discovery: emerging opportunities. *Nat Rev Drug Discov*, *17*(1), 57-78. https://doi.org/10.1038/nrd.2017.152

Hayashi, H., Inamura, K., Aida, K., Naoi, S., Horikawa, R., Nagasaka, H.,…Sugiyama, Y. (2012). AP2 adaptor complex mediates bile salt export pump internalization and modulates its hepatocanalicular expression and transport function. *Hepatology*, *55*(6), 1889-1900. https://doi.org/10.1002/hep.25591

He, L., & Hannon, G. J. (2004). MicroRNAs: small RNAs with a big role in gene regulation. *Nat Rev Genet*, *5*(7), 522-531. https://doi.org/10.1038/nrg1379

Helgeland, H., Sodeland, M., Zoric, N., Torgersen, J. S., Grammes, F., von Lintig, J.,…Vage, D. I. (2019). Genomic and functional gene studies suggest a key role of beta-carotene oxygenase 1 like (bco1l) gene in salmon flesh color. *Sci Rep*, *9*(1), 20061. https://doi.org/10.1038/s41598-019-56438-3

Hessel, S., Eichinger, A., Isken, A., Amengual, J., Hunzelmann, S., Hoeller, U.,…Wyss, A. (2007). CMO1 deficiency abolishes vitamin A production from beta-carotene and alters lipid metabolism in mice. *J Biol Chem*, *282*(46), 33553-33561. https://doi.org/10.1074/jbc.M706763200

Huang, Y., Zhang, L., Wang, G., & Huang, S. (2022). De novo assembly transcriptome analysis reveals the genes associated with body color formation in the freshwater ornamental shrimps Neocaridina denticulate sinensis. *Gene*, *806*, 145929. https://doi.org/10.1016/j.gene.2021.145929

Hughes, J., Oiseth, S., Purslow, P., & Warner, R. (2014). A structural approach to understanding the interactions between colour, water-holding capacity and tenderness. *Meat science*, *98*(3), 520-532.

Ibtisham, F., Zhang, L., Xiao, M., An, L., Ramzan, M. B., Nawab, A.,…Xu, Y. (2017). Genomic selection and its application in animal breeding. *The Thai Journal of Veterinary Medicine*, *47*(3), 301.

Jia, W., Zhang, R., Liu, L., Zhu, Z., Xu, M., & Shi, L. (2021). Molecular mechanism of protein dynamic change for Hengshan goat meat during freezing storage based on high-throughput proteomics. *Food Research International*, *143*, 110289.

Jia, X., Veiseth-Kent, E., Grove, H., Kuziora, P., Aass, L., Hildrum, K., & Hollung, K. (2009). Peroxiredoxin-6—a potential protein marker for meat tenderness in bovine longissimus thoracis muscle. *Journal of Animal Science*, *87*(7), 2391-2399.

Jlali, M., Graulet, B., Chauveau-Duriot, B., Chabault, M., Godet, E., Leroux, S.,…Berri, C. (2012). A mutation in the promoter of the chicken β, β-carotene 15, 15'-monooxygenase 1 gene alters xanthophyll metabolism through a selective effect on its mRNA abundance in the breast muscle. *Journal of animal science*, *90*(12), 4280-4288.

Jlali, M., Graulet, B., Chauveau-Duriot, B., Godet, E., Praud, C., Nunes, C. S.,…Duclos, M. J. (2014). Nutrigenetics of carotenoid metabolism in the chicken: a polymorphism at the β, β-carotene 15, 15'-mono-oxygenase 1 (BCMO1) locus affects the response to dietary β-carotene. *British journal of nutrition*, *111*(12), 2079-2088.

Joseph, P., Suman, S. P., Li, S., Beach, C. M., Steinke, L., & Fontaine, M. (2010). Characterization of bison (Bison bison) myoglobin. *Meat Sci*, *84*(1), 71-78. https://doi.org/10.1016/j.meatsci.2009.08.014

Joseph, P., Suman, S. P., Rentfrow, G., Li, S., & Beach, C. M. (2012). Proteomics of muscle-specific beef color stability. *J Agric Food Chem*, *60*(12), 3196-3203. https://doi.org/10.1021/jf204188v

Juanchich, A., Bardou, P., Rue, O., Gabillard, J. C., Gaspin, C., Bobe, J., & Guiguen, Y. (2016). Characterization of an extensive rainbow trout miRNA transcriptome by next generation sequencing. *BMC genomics*, *17*(1), 164. https://doi.org/10.1186/s12864-016-2505-9

Kaźmierczuk, A., & Kiliańska, Z. M. (2009). Plejotropowa aktywność białek szoku cieplnego The pleiotropic activity of heat-shock proteins. *Postepy Hig Med Dosw.(online)*, *63*, 502-521.

Kiessling, A., Espe, M., Ruohonen, K., & Mørkøre, T. (2004). Texture, gaping and colour of fresh and frozen Atlantic salmon flesh as affected by pre-slaughter iso-eugenol or CO2 anaesthesia. *Aquaculture*, *236*(1-4), 645-657.

Kobayashi, T., Winslow, S., Sunesson, L., Hellman, U., & Larsson, C. (2012). PKCα binds G3BP2 and regulates stress granule formation following cellular stress. *PloS one*, *7*(4), e35820.

Kong, H. R., Anthony, N. B., Rowland, K. C., Khatri, B., & Kong, B. C. (2018). Genome re-sequencing to identify single nucleotide polymorphism markers for muscle color traits in broiler chickens. *Asian-Australas J Anim Sci*, *31*(1), 13-18. https://doi.org/10.5713/ajas.17.0479

Kutter, C., & Svoboda, P. (2008). miRNA, siRNA, piRNA: Knowns of the unknown. In: Taylor & Francis.

Kwon, H.-S., Lee, H.-S., Rubin, J., & Tomarev, S. (2008). Myocilin May Regulate Actin Cytoskeleton Through Components of Wnt Signaling Pathway. *Investigative Ophthalmology & Visual Science*, *49*(13), 5111-5111.

Le Bihan-Duval, E., Nadaf, J., Berri, C., Pitel, F., Graulet, B., Godet, E.,…Duby, C. (2011). Detection of a Cis eQTL controlling BMCO1 gene expression leads to the identification of a QTG for chicken breast meat color. *PLoS One*, *6*(7), e14825.

Lee, J., Godon, C., Lagniel, G., Spector, D., Garin, J., Labarre, J., & Toledano, M. B. (1999). Yap1 and Skn7 control two specialized oxidative stress response regulons in yeast. *J Biol Chem*, *274*(23), 16040-16046. https://doi.org/10.1074/jbc.274.23.16040

Lee, T. T., Ciou, J. Y., Chen, C. L., & Yu, B. (2013). Effect of Echinacea purpurea L. on oxidative status and meat quality in Arbor Acres broilers. *J Sci Food Agric*, *93*(1), 166-172. https://doi.org/10.1002/jsfa.5745

Leeds, T. D., Vallejo, R. L., Weber, G. M., Gonzalez-Pena, D., & Silverstein, J. T. (2016). Response to five generations of selection for growth performance traits in rainbow trout (Oncorhynchus mykiss). *Aquaculture*, *465*, 341-351.

Legarra, A., Aguilar, I., & Misztal, I. (2009). A relationship matrix including full pedigree and genomic information. *J Dairy Sci*, *92*(9), 4656-4663. https://doi.org/10.3168/jds.2009-2061

Lei, C., Li, J., Zheng, Z., Du, X., & Deng, Y. (2019). Molecular cloning, expression pattern of beta-carotene 15,15-dioxygenase gene and association analysis with total carotenoid content in pearl oyster Pinctada fucata martensii. *Comp Biochem Physiol B Biochem Mol Biol*, *229*, 34-41. https://doi.org/10.1016/j.cbpb.2018.11.006

Li, H., Jiang, K., Wang, S., Liu, X., Kang, X., Jiang, R.,…Sun, G. (2015). Assessment of correlation between pre-miRNA-1757 polymorphism and chicken performance traits. *Genetics and Molecular Research*, *14*(4), 12184-12195.

Li, X., Wang, S., Xun, X., Zhang, M., Wang, S., Li, H.,…Li, T. (2019). A carotenoid oxygenase is responsible for muscle coloration in scallop. *Biochimica et Biophysica Acta (BBA)-Molecular and Cell Biology of Lipids*, *1864*(7), 966-975.

Lietz, G., Oxley, A., Leung, W., & Hesketh, J. (2012). Single nucleotide polymorphisms upstream from the beta-carotene 15,15'-monoxygenase gene influence provitamin A conversion efficiency in female volunteers. *J Nutr*, *142*(1), 161S-165S. https://doi.org/10.3945/jn.111.140756

Liu, F., Dai, R., Zhu, J., & Li, X. (2010). Optimizing color and lipid stability of beef patties with a mixture design incorporating with tea catechins, carnosine, and α-tocopherol. *Journal of Food Engineering*, *98*(2), 170-177.

Liu, X., Liu, Y., Jiang, Y., Zou, L., Liu, K., Liu, M.,…Chen, F. (2020). Homo-oxidized HSPB1 protects cardiomyocytes against oxidative stress via targeting Keap1/Nrf-2 signaling pathway. *Journal of Molecular and Cellular Cardiology*, *140*, 37-38.

Liu, X., Xiao, W., Jiang, Y., Zou, L., Chen, F., Xiao, W.,…Zhu, Y. (2021). Bmal1 Regulates the Redox Rhythm of HSPB1, and Homooxidized HSPB1 Attenuates the Oxidative Stress Injury of Cardiomyocytes. *Oxid Med Cell Longev*, *2021*, 5542815. https://doi.org/10.1155/2021/5542815

Liu, Y., Du, M., Li, X., Chen, L., Shen, Q., Tian, J., & Zhang, D. (2016). Role of the ubiquitin-proteasome pathway on proteolytic activity in postmortem proteolysis and tenderisation of sheep skeletal muscle. *International Journal of Food Science & Technology*, *51*(11), 2353-2359.

Lundquist, M. R., Storaska, A. J., Liu, T.-C., Larsen, S. D., Evans, T., Neubig, R. R., & Jaffrey, S. R. (2014). Redox modification of nuclear actin by MICAL-2 regulates SRF signaling. *Cell*, *156*(3), 563-576.

Luo, Z. (1992). Computing inbreeding coefficients in large populations. *Genetics Selection Evolution*, *24*(4), 305-313.

Mancini, R. A., & Ramanathan, R. (2014). Effects of postmortem storage time on color and mitochondria in beef. *Meat Sci*, *98*(1), 65-70. https://doi.org/10.1016/j.meatsci.2014.04.007

Matthews, S. J., Ross, N. W., Lall, S. P., & Gill, T. A. (2006). Astaxanthin binding protein in Atlantic salmon. *Comp Biochem Physiol B Biochem Mol Biol*, *144*(2), 206-214. https://doi.org/10.1016/j.cbpb.2006.02.007

McCormick, R. J. (1999). Extracellular modifications to muscle collagen: implications for meat quality. *Poult Sci*, *78*(5), 785-791. https://doi.org/10.1093/ps/78.5.785

Misztal, I., Tsuruta, S., Strabel, T., Auvray, B., Druet, T., & Lee, D. (2002). BLUPF90 and related programs (BGF90). Proceedings of the 7th world congress on genetics applied to livestock production,

Mora, L., Gallego, M., Aristoy, M. C., Fraser, P. D., & Toldrá, F. (2015). Peptides naturally generated from ubiquitin-60S ribosomal protein as potential biomarkers of dry-cured ham processing time. *Food Control*, *48*, 102-107.

Morimoto, R. I. (1998). Regulation of the heat shock transcriptional response: cross talk between a family of heat shock factors, molecular chaperones, and negative regulators. *Genes & development*, *12*(24), 3788-3796.

Nohl, H., Breuninger, V., & Hegner, D. (1978). Influence of mitochondrial radical formation on energy-linked respiration. *Eur J Biochem*, *90*(2), 385-390. https://doi.org/10.1111/j.1432-1033.1978.tb12615.x

Nonhoff, U., Ralser, M., Welzel, F., Piccini, I., Balzereit, D., Yaspo, M.-L.,…Krobitsch, S. (2007). Ataxin-2 interacts with the DEAD/H-box RNA helicase DDX6 and interferes with P-bodies and stress granules. *Molecular biology of the cell*, *18*(4), 1385-1396.

Ogasawara, S., Cheng, X. W., Inoue, A., Hu, L., Piao, L., Yu, C.,…Kuzuya, M. (2018). Cathepsin K activity controls cardiotoxin-induced skeletal muscle repair in mice. *J Cachexia Sarcopenia Muscle*, *9*(1), 160-175. https://doi.org/10.1002/jcsm.12248

Ottestad, S., Sørheim, O., Heia, K., Skaret, J., & Wold, J. P. (2011). Effects of storage atmosphere and heme state on the color and visible reflectance spectra of salmon (Salmo salar) fillets. *Journal of agricultural and food chemistry*, *59*(14), 7825-7831.

Park, J. W. (1994). Functional protein additives in surimi gels. *Journal of Food Science*, *59*(3), 525-527.

Paulusma, C. C., de Waart, D. R., Kunne, C., Mok, K. S., & Elferink, R. P. O. (2009). Activity of the bile salt export pump (ABCB11) is critically dependent on canalicular membrane cholesterol content. *Journal of biological chemistry*, *284*(15), 9947-9954.

Ramanathan, R., Nair, M., Hunt, M., & Suman, S. (2019). Mitochondrial functionality and beef colour: A review of recent research. *South African Journal of Animal Science*, *49*(1), 9-19.

Ramirez-Martinez, A., Cenik, B. K., Bezprozvannaya, S., Chen, B., Bassel-Duby, R., Liu, N., & Olson, E. N. (2017). KLHL41 stabilizes skeletal muscle sarcomeres by nonproteolytic ubiquitination. *Elife*, *6*, e26439. https://doi.org/10.7554/eLife.26439

Ravenscroft, G., Miyatake, S., Lehtokari, V. L., Todd, E. J., Vornanen, P., Yau, K. S.,…Laing, N. G. (2013). Mutations in KLHL40 are a frequent cause of severe autosomal-recessive nemaline myopathy. *Am J Hum Genet*, *93*(1), 6-18. https://doi.org/10.1016/j.ajhg.2013.05.004

Sablina, A. A., Budanov, A. V., Ilyinskaya, G. V., Agapova, L. S., Kravchenko, J. E., & Chumakov, P. M. (2005). The antioxidant function of the p53 tumor suppressor. *Nat Med*, *11*(12), 1306-1313. https://doi.org/10.1038/nm1320

Salem, M., Al-Tobasei, R., Ali, A., Lourenco, D., Gao, G., Palti, Y.,…Leeds, T. D. (2018). Genome-Wide Association Analysis With a 50K Transcribed Gene SNP-Chip Identifies QTL Affecting Muscle Yield in Rainbow Trout. *Front Genet*, *9*, 387. https://doi.org/10.3389/fgene.2018.00387

Sellers, J. R. (2000). Myosins: a diverse superfamily. *Biochim Biophys Acta*, *1496*(1), 3-22. https://doi.org/10.1016/s0167-4889(00)00005-7

Seyfert, M., Mancini, R. A., Hunt, M. C., Tang, J., Faustman, C., & Garcia, M. (2006). Color stability, reducing activity, and cytochrome c oxidase activity of five bovine muscles. *J Agric Food Chem*, *54*(23), 8919-8925. https://doi.org/10.1021/jf061657s

Shi, J., & Sun, G. (2017). Effect of pre-miRNA-1658 gene polymorphism on chicken growth and carcass traits. *Asian-Australas J Anim Sci*, *30*(4), 455-461. https://doi.org/10.5713/ajas.16.0305

Stofan, M., & Guo, G. L. (2020). Bile Acids and FXR: Novel Targets for Liver Diseases. *Front Med (Lausanne)*, *7*, 544. https://doi.org/10.3389/fmed.2020.00544

Storebakken, T., & No, H. K. (1992). Pigmentation of rainbow trout. *Aquaculture*, *100*(1-3), 209-229.

Subramaniyan, S. A., Kang, D. R., Jung, Y. C., Jung, J. H., Choi, Y. I., Lee, M. J.,…Shim, K. S. (2017). Comparative studies of meat quality traits and the proteome profile between low-and high-pH muscles in longissimus dorsi of Berkshire. *Canadian Journal of Animal Science*, *97*(4), 640-649.

Takahashi, M., Yamashita, K., Shiozawa, A., Ichiishi, A., Fukumori, F., & Fujimura, M. (2010). An AP-1-like transcription factor, NAP-1, regulates expression of the glutathione S-transferase and NADH: flavin oxidoreductase genes in Neurospora crassa. *Bioscience, biotechnology, and biochemistry*, *74*(4), 746-752.

Tang, J., Faustman, C., Hoagland, T. A., Mancini, R. A., Seyfert, M., & Hunt, M. C. (2005). Postmortem oxygen consumption by mitochondria and its effects on myoglobin form and stability. *J Agric Food Chem*, *53*(4), 1223-1230. https://doi.org/10.1021/jf048646o

Tarique, T., Yang, S., Mohsina, Z., Qiu, J., Yan, Z., Chen, G., & Chen, A. (2014). Identification of genes involved in regulatory mechanism of pigments in broiler chickens. *Genetics and Molecular Research*, *13*(3), 7201-7216.

Terra, L. F., Wailemann, R. A., Dos Santos, A. F., Gomes, V. M., Silva, R. P., Laporte, A.,…Lortz, S. (2019). Heat shock protein B1 is a key mediator of prolactin-induced beta-cell cytoprotection against oxidative stress. *Free Radical Biology and Medicine*, *134*, 394-405.

Thomas, A. C. (1999). *Astaxanthin in juvenile farmed Chinook salmon (Oncorhynchus tshawytscha): effective dietary levels for flesh pigmentation and influence on fatty acid profile during cold temperature storage of fillets* University of British Columbia].

Thorgaard, G. H., Bailey, G. S., Williams, D., Buhler, D. R., Kaattari, S. L., Ristow, S. S.,…Palti, Y. (2002). Status and opportunities for genomics research with rainbow trout. *Comp Biochem Physiol B Biochem Mol Biol*, *133*(4), 609-646. https://doi.org/10.1016/s1096-4959(02)00167-7

Tintchev, F., Kuhlmann, U., Wackerbarth, H., Töpfl, S., Heinz, V., Knorr, D., & Hildebrandt, P. (2009). Redox processes in pressurised smoked salmon studied by resonance Raman spectroscopy. *Food chemistry*, *112*(2), 482-486.

Turchini, G. M., Francis, D. S., Keast, R. S., & Sinclair, A. J. (2011). Transforming salmonid aquaculture from a consumer to a producer of long chain omega-3 fatty acids. *Food Chemistry*, *124*(2), 609-614.

Turner, S. D. (2014). qqman: an R package for visualizing GWAS results using QQ and manhattan plots. *Biorxiv*, 005165.

Vallejo, R. L., Silva, R. M. O., Evenhuis, J. P., Gao, G., Liu, S., Parsons, J. E.,…Palti, Y. (2018). Accurate genomic predictions for BCWD resistance in rainbow trout are achieved using low-density SNP panels: Evidence that long-range LD is a major contributing factor. *J Anim Breed Genet*. https://doi.org/10.1111/jbg.12335

VanRaden, P. M. (2008). Efficient methods to compute genomic predictions. *J Dairy Sci*, *91*(11), 4414-4423. https://doi.org/10.3168/jds.2007-0980

Wang, H., Misztal, I., Aguilar, I., Legarra, A., & Muir, W. (2012). Genome-wide association mapping including phenotypes from relatives without genotypes. *Genetics Research*, *94*(2), 73-83.

Wu, H., Yesilyurt, H. G., Yoon, J., & Terman, J. R. (2018). The MICALs are a family of F-actin dismantling oxidoreductases conserved from Drosophila to humans. *Scientific reports*, *8*(1), 1-20.

Wu, H. J., Seib, K. L., Srikhanta, Y. N., Edwards, J., Kidd, S. P., Maguire, T. L.,…Jennings, M. P. (2010). Manganese regulation of virulence factors and oxidative stress resistance in Neisseria gonorrhoeae. *J Proteomics*, *73*(5), 899-916. https://doi.org/10.1016/j.jprot.2009.12.001

Wu, W., Gao, X.-G., Dai, Y., Fu, Y., Li, X.-M., & Dai, R.-T. (2015). Post-mortem changes in sarcoplasmic proteome and its relationship to meat color traits in M. semitendinosus of Chinese Luxi yellow cattle. *Food Research International*, *72*, 98-105.

Wu, W., Yu, Q.-Q., Fu, Y., Tian, X.-J., Jia, F., Li, X.-M., & Dai, R.-T. (2016). Towards muscle-specific meat color stability of Chinese Luxi yellow cattle: A proteomic insight into post-mortem storage. *Journal of proteomics*, *147*, 108-118.

Yabuta, S., Masaki, M., & Shidoji, Y. (2016). Associations of Buccal Cell Telomere Length with Daily Intake of beta-Carotene or alpha-Tocopherol Are Dependent on Carotenoid Metabolism-related Gene Polymorphisms in Healthy Japanese Adults. *J Nutr Health Aging*, *20*(3), 267-274. https://doi.org/10.1007/s12603-015-0577-x

Yabuuchi, H., Tanaka, K., Maeda, M., Takemura, M., Oka, M., Ohashi, R., & Tamai, I. (2008). Cloning of the dog bile salt export pump (BSEP; ABCB11) and functional comparison with the human and rat proteins. *Biopharm Drug Dispos*, *29*(8), 441-448. https://doi.org/10.1002/bdd.629

Yan, W., Jang, G.-F., Haeseleer, F., Esumi, N., Chang, J., Kerrigan, M.,…Zack, D. J. (2001). Cloning and characterization of a human β, β-carotene-15, 15'-dioxygenase that is highly expressed in the retinal pigment epithelium. *Genomics*, *72*(2), 193-202.

Yang, X., Wu, S., Hopkins, D. L., Liang, R., Zhu, L., Zhang, Y., & Luo, X. (2018). Proteomic analysis to investigate color changes of chilled beef longissimus steaks held under carbon monoxide and high oxygen packaging. *Meat science*, *142*, 23-31.

Yuan, F. L., Xu, R. S., Ye, J. X., Zhao, M. D., Ren, L. J., & Li, X. (2019). Apoptotic bodies from endplate chondrocytes enhance the oxidative stress-induced mineralization by regulating PPi metabolism. *J Cell Mol Med*, *23*(5), 3665-3675. https://doi.org/10.1111/jcmm.14268

Zenger, K., Khatkar, M., Jerry, D., & Raadsma, H. (2017). The next wave in selective breeding: implementing genomic selection in aquaculture. Proc. Assoc. Advmt. Anim. Breed. Genet,

Zhang, Y., Johnson, K., Russell, R. G. G., Wordsworth, B. P., Carr, A. J., Terkeltaub, R. A., & Brown, M. A. (2005). Association of sporadic chondrocalcinosis with a− 4-basepair G-to-A transition in the 5′-untranslated region of ANKH that promotes enhanced expression of ANKH protein and excess generation of extracellular inorganic pyrophosphate. *Arthritis & Rheumatism*, *52*(4), 1110-1117.

ZHANG, Y.-m., ZHANG, X.-z., WANG, T.-t., Hopkins, D. L., MAO, Y.-w., LIANG, R.-r.,…ZHU, L.-x. (2018). Implications of step-chilling on meat color investigated using proteome analysis of the sarcoplasmic protein fraction of beef longissimus lumborum muscle. *Journal of Integrative Agriculture*, *17*(9), 2118-2125.

Zheng, Q., Zhang, Y., Chen, Y., Yang, N., Wang, X. J., & Zhu, D. (2009). Systematic identification of genes involved in divergent skeletal muscle growth rates of broiler and layer chickens. *BMC genomics*, *10*(1), 87. https://doi.org/10.1186/1471-2164-10-87

Zychowska, M., Jastrzebski, Z., Chruscinski, G., Michalowska-Sawczyn, M., & Nowak-Zaleska, A. (2015). Vitamin C, A and E supplementation decreases the expression of HSPA1A and HSPB1 genes in the leukocytes of young polish figure skaters during a 10-day training camp. *J Int Soc Sports Nutr*, *12*(1), 9. https://doi.org/10.1186/s12970-015-0069-8

Ługowska, A., Hetmańczyk-Sawicka, K., Iwanicka-Nowicka, R., Fogtman, A., Cieśla, J., Purzycka-Olewiecka, J. K.,…Lualdi, S. (2019). Gene expression profile in patients with Gaucher disease indicates activation of inflammatory processes. *Scientific reports*, *9*(1), 1-14.

Supplementary table 1 : SNPs and genes identified in this study explaining at least 1% of genetic variation in fillet redness, yellowness, and whiteness,

SNP	Chr	POS	SNP_effec	Weight	Var_explai	Var_a_hat	Trait	SNP ID	Gene ID	Gene annotation	Region
9120	7	11402881	6.80E-04	1.498768	3.474196	7.82E-08	Redness	AX-171623558	LOC110527413	collagen alpha-1(XXVIII) chain-like	3'UTR
9119	7	11399310	-1.33E-04	1.007986	3.4455	2.90E-08	Redness	AX-171597628	LOC110527414	kelch-like protein 41b	CDS
9118	7	11399286	9.47E-05	0.980311	3.380002	2.69E-08	Redness	AX-171597626	LOC110527414	kelch-like protein 41b	CDS
9114	7	11396853	-3.27E-05	0.937178	3.334715	2.45E-08	Redness	AX-171597621	LOC110527414	kelch-like protein 41b	3'UTR
9115	7	11397881	8.65E-05	0.974521	3.334395	2.86E-08	Redness	AX-171597622	LOC110527414	kelch-like protein 41b	CDS
9116	7	11399109	-3.28E-04	1.161189	3.322313	3.55E-08	Redness	AX-171597623	LOC110527414	kelch-like protein 41b	CDS
9113	7	11396815	-8.11E-05	0.970671	3.292152	2.84E-08	Redness	AX-171597620	LOC110527414	kelch-like protein 41b	3'UTR
9121	7	11438574	4.14E-06	0.917946	3.285568	2.27E-08	Redness	AX-171643678	LOC100136600	ATP synthase subunit beta, mitochondrial	CDS
9122	7	11442059	3.29E-04	1.162093	3.265931	4.05E-08	Redness	AX-171597629	LOC100136600	ATP synthase subunit beta, mitochondrial	CDS
9117	7	11399262	1.38E-04	1.011323	3.247318	3.06E-08	Redness	AX-171597624	LOC110527414	kelch-like protein 41b	CDS
9123	7	11442092	-3.13E-04	1.149001	3.184499	3.95E-08	Redness	AX-171597630	LOC100136600	ATP synthase subunit beta, mitochondrial	CDS
9124	7	11442455	2.37E-04	1.087131	3.102094	3.51E-08	Redness	AX-171597631	LOC100136600	ATP synthase subunit beta, mitochondrial	CDS
9112	7	11381734	-5.22E-05	0.950507	3.066573	1.97E-08	Redness	N/A	N/A	N/A	N/A
9125	7	11443676	2.49E-04	1.096278	3.051891	1.55E-08	Redness	AX-171597632	LOC100136600	ATP synthase subunit beta, mitochondrial	3'UTR
9127	7	11444638	-2.26E-04	1.078114	3.014607	3.45E-08	Redness	AX-171597634	LOC110527417	retinol dehydrogenase 7-like	CDS
9126	7	11444554	-1.35E-04	1.009193	3.009326	3.13E-08	Redness	AX-171597633	LOC110527417	retinol dehydrogenase 7-like	CDS
9129	7	11459018	-4.06E-04	1.228644	2.982811	4.41E-08	Redness	AX-171597636	abcb11	bile salt export pump	CDS
9128	7	11445117	-1.71E-04	1.035789	2.960005	1.18E-08	Redness	AX-171597635	LOC110527417	retinol dehydrogenase 7-like	CDS
9131	7	11477215	-6.00E-04	1.414223	2.877103	5.96E-08	Redness	AX-171597637	LOC100136260	cathepsin K	CDS
9130	7	11464878	-5.67E-05	0.953675	2.871858	2.76E-08	Redness	AX-172551847	abcb11	bile salt export pump	CDS
9111	7	11312252	1.79E-04	1.042254	2.726163	2.11E-08	Redness	AX-171641349	LOC110527407	zinc finger protein Dzip1-like	CDS
9132	7	11477251	1.28E-04	1.004033	2.686271	1.69E-08	Redness	AX-171597638	LOC100136260	cathepsin K	CDS
9133	7	11477254	-6.04E-04	1.418597	2.681329	6.00E-08	Redness	AX-171597639	LOC100136260	cathepsin K	CDS
9110	7	11138396	9.88E-05	0.983223	2.487817	1.20E-08	Redness	AX-171641342	LOC110527405	calsequestrin-2-like	CDS
9109	7	11030216	2.50E-04	1.096939	2.483659	1.55E-08	Redness	N/A	N/A	N/A	N/A
9134	7	11477335	6.00E-04	1.414339	2.48241	5.82E-08	Redness	AX-171597640	LOC100136260	cathepsin K	CDS
9108	7	10996914	-4.16E-05	0.943214	2.432493	1.41E-08	Redness	AX-171615055	LOC110527401	radixin-like	CDS
9138	7	11621269	5.03E-04	1.318741	2.364111	5.20E-08	Redness	N/A	N/A	N/A	N/A
9135	7	11477642	-3.57E-04	1.186057	2.335896	4.43E-08	Redness	AX-171597641	LOC100136260	cathepsin K	CDS
12846	9	52291239	3.88E-04	1.212535	2.283044	4.24E-08	Redness	AX-171642614	LOC110532539	partner of Y14 and mago A	CDS
12836	9	52063734	4.86E-04	1.302401	2.271036	4.89E-08	Redness	AX-171616173	LOC110532529	tyrosine-protein phosphatase non-receptor type 1-li	3'UTR
12843	9	52106708	7.00E-05	0.962865	2.259043	1.77E-08	Redness	AX-171616167	LOC110532530	ubiquitin-conjugating enzyme E2 variant 1-like	3'UTR
12844	9	52106880	-1.09E-04	0.990551	2.258232	1.86E-08	Redness	AX-171616166	LOC110532530	ubiquitin-conjugating enzyme E2 variant 1-like	3'UTR
12845	9	52106934	8.64E-05	0.974427	2.24184	1.81E-08	Redness	AX-171616165	LOC110532530	ubiquitin-conjugating enzyme E2 variant 1-like	3'UTR
9137	7	11621216	9.62E-06	0.921601	2.225852	1.77E-09	Redness	N/A	N/A	N/A	N/A
9136	7	11478430	-1.29E-04	1.005077	2.224969	2.99E-08	Redness	AX-171597642	LOC100136260	cathepsin K	3'UTR
9139	7	11621547	-5.20E-04	1.334516	2.203672	5.25E-08	Redness	N/A	N/A	N/A	N/A
12837	9	52064525	5.61E-06	0.918921	2.19514	1.82E-08	Redness	AX-171616172	LOC110532529	tyrosine-protein phosphatase non-receptor type 1-li	3'UTR
12838	9	52090273	2.33E-04	1.083974	2.19418	1.15E-08	Redness	N/A	N/A	N/A	N/A
9107	7	10991489	-3.30E-04	1.162902	2.188882	3.23E-08	Redness	AX-172563298	LOC110527401	radixin-like	3'UTR
12839	9	52104812	-9.46E-05	0.980237	2.156851	1.84E-08	Redness	AX-171616171	LOC110532530	ubiquitin-conjugating enzyme E2 variant 1-like	CDS
12847	9	52291255	1.23E-04	1.000413	2.152833	3.06E-08	Redness	AX-172560332	LOC110532539	partner of Y14 and mago A	CDS
12835	9	52062139	6.85E-05	0.961815	2.151732	2.39E-08	Redness	AX-171642620	LOC110532529	tyrosine-protein phosphatase non-receptor type 1-li	CDS
12840	9	52106061	4.13E-04	1.235037	2.148683	4.03E-08	Redness	AX-171616170	LOC110532530	ubiquitin-conjugating enzyme E2 variant 1-like	3'UTR
12834	9	51986317	-5.90E-05	0.955203	2.124331	2.05E-08	Redness	AX-171615946	LOC110532524	lysine-specific demethylase 5B-B-like	3'UTR
12848	9	52356083	-4.46E-05	0.945311	2.112818	1.02E-08	Redness	AX-171644628	LOC110532541	spermatogenesis-associated serine-rich protein 2-lik	3'UTR
12842	9	52106144	1.19E-04	0.99785	2.112331	1.81E-08	Redness	AX-171616168	LOC110532530	ubiquitin-conjugating enzyme E2 variant 1-like	3'UTR
12849	9	52418220	-3.07E-04	1.143462	2.112279	1.94E-08	Redness	AX-171616162	LOC110532542	ORM1-like protein 2	3'UTR
12850	9	52442633	-8.08E-04	1.645369	2.049723	8.07E-08	Redness	AX-171616161	LOC110532545	CD63 antigen-like	CDS
12833	9	51961346	7.73E-05	0.967985	2.038033	2.51E-08	Redness	AX-171642407	LOC110532523	ras-related protein Rap-1A-like	CDS
12841	9	52106123	-2.93E-04	1.13232	2.005924	2.00E-08	Redness	AX-171616169	LOC110532530	ubiquitin-conjugating enzyme E2 variant 1-like	3'UTR
9140	7	11621644	-5.11E-04	1.325946	2.001234	5.20E-08	Redness	N/A	N/A	N/A	N/A
12832	9	51955033	-4.68E-05	0.946846	1.90012	2.48E-08	Redness	AX-171615945	LOC110532523	ras-related protein Rap-1A-like	3'UTR
9104	7	10806779	2.53E-05	0.932133	1.899158	2.44E-08	Redness	N/A	N/A	N/A	N/A
9105	7	10807841	2.08E-05	0.92908	1.895638	2.42E-08	Redness	AX-171601275	LOC110527397	pituitary tumor-transforming gene 1 protein-interact	CDS
9106	7	10973111	1.18E-04	0.996915	1.893388	1.78E-08	Redness	AX-171615053	LOC110527400	mitogen-activated protein kinase kinase kinase kinas	3'UTR
12829	9	51756100	-2.04E-04	1.061181	1.878294	1.95E-08	Redness	AX-171615942	LOC110532512	pancreatic progenitor cell differentiation and prolife	3'UTR
12828	9	51756062	-2.01E-04	1.058627	1.867239	1.52E-08	Redness	AX-171615941	LOC110532512	pancreatic progenitor cell differentiation and prolife	3'UTR
12831	9	51885910	-4.46E-05	0.945268	1.864274	1.02E-08	Redness	AX-171642406	LOC110532517	uncharacterized LOC110532517	lnc_RNA
12830	9	51857667	-1.32E-04	1.007378	1.838727	1.87E-08	Redness	AX-171615944	LOC110532516	microtubule-associated protein RP/EB family memb	CDS
12827	9	51756019	-4.03E-05	0.942356	1.825464	1.90E-08	Redness	AX-171615940	LOC110532512	pancreatic progenitor cell differentiation and prolife	CDS
9141	7	11621880	4.98E-04	1.314087	1.810915	5.11E-08	Redness	AX-171597644	LOC110528801	xin actin-binding repeat-containing protein 2-like	3'UTR
12851	9	52449041	-3.01E-04	1.138713	1.795236	3.33E-08	Redness	AX-171622431	LOC110532545	CD63 antigen-like	CDS
12826	9	51755983	-7.97E-05	0.969676	1.733577	2.65E-08	Redness	AX-171615939	LOC110532512	pancreatic progenitor cell differentiation and prolife	CDS
12853	9	52489055	1.20E-04	0.998282	1.721084	3.11E-08	Redness	AX-171622429	LOC110532548	probable nuclear hormone receptor HR38	3'UTR
12852	9	52488934	5.80E-05	0.95452	1.718778	1.07E-08	Redness	AX-171622430	LOC110532548	probable nuclear hormone receptor HR38	3'UTR
12854	9	52493224	-1.20E-04	0.998242	1.71058	3.11E-08	Redness	AX-171619012	LOC110532548	probable nuclear hormone receptor HR38	CDS
12855	9	52493331	2.42E-04	1.091317	1.683072	1.14E-08	Redness	AX-171619011	LOC110532548	probable nuclear hormone receptor HR38	CDS
12856	9	52493665	2.59E-04	1.104222	1.682037	2.27E-08	Redness	AX-169523572	LOC110532548	probable nuclear hormone receptor HR38	CDS
12825	9	51753395	-8.98E-05	0.976864	1.658052	2.71E-08	Redness	AX-171615938	LOC110532512	pancreatic progenitor cell differentiation and prolife	5'UTR
12858	9	52544851	-2.80E-04	1.121768	1.652264	1.37E-08	Redness	N/A	N/A	N/A	N/A
12857	9	52493666	2.36E-04	1.086488	1.646531	2.22E-08	Redness	AX-171619010	LOC110532548	probable nuclear hormone receptor HR38	CDS
9142	7	11621908	-3.27E-04	1.160284	1.638109	2.00E-08	Redness	AX-171616687	LOC110528801	xin actin-binding repeat-containing protein 2-like	3'UTR
9102	7	10802585	-5.40E-05	0.951805	1.630114	1.71E-08	Redness	AX-171626660	LOC110527396	small ubiquitin-related modifier 3	3'UTR
9101	7	10779062	-3.81E-05	0.94087	1.626304	3.41E-09	Redness	AX-171626656	LOC110527395	ubiquitin carboxyl-terminal hydrolase 40-like	CDS
9103	7	10806083	2.62E-05	0.932783	1.624991	2.27E-08	Redness	N/A	N/A	N/A	N/A
9144	7	11629030	1.86E-04	1.047535	1.611114	1.35E-08	Redness	AX-171617722	LOC110528801	xin actin-binding repeat-containing protein 2-like	CDS
9143	7	11628831	9.03E-05	0.977216	1.610599	9.21E-09	Redness	AX-171617720	LOC110528801	xin actin-binding repeat-containing protein 2-like	CDS
9145	7	11629216	6.76E-05	0.961248	1.587881	8.98E-09	Redness	AX-171617723	LOC110528801	xin actin-binding repeat-containing protein 2-like	CDS

SNP	Chr	POS	SNP_effec	Weight	Var_explai	Var_a_hat	Trait	SNP ID	Gene ID	Gene annotation	Region
10884	8	34936875	0.001813	1.23193	1.592316	7.65E-07	Lightness	AX-171641	LOC11052	cGMP-dependent protein kinase 1-like	3'UTR
10887	8	37290793	0.002064	1.283892	1.563182	7.93E-07	Lightness	AX-171642	LOC11052	sialomucin core protein 24-like	3'UTR
10883	8	34495040	0.000467	0.986966	1.507177	4.13E-07	Lightness	AX-171615	sod2	superoxide dismutase 2	3'UTR
10885	8	34964577	-0.00105	1.087373	1.491242	5.56E-07	Lightness	AX-171641	LOC11052	cGMP-dependent protein kinase 1-like	CDS
10888	8	37293410	0.001865	1.242544	1.472929	7.46E-07	Lightness	N/A	N/A	N/A	N/A
10882	8	34494762	-0.00094	1.067865	1.470128	4.43E-07	Lightness	N/A	N/A	N/A	N/A
10886	8	36538411	0.000599	1.008703	1.438903	1.69E-07	Lightness	AX-172549	LOC11052	SAM and SH3 domain-containing protein 1-like	3'UTR
10895	8	40610851	-0.00205	1.281421	1.432826	7.92E-07	Lightness	N/A	N/A	N/A	N/A
10881	8	34494659	0.00046	0.98591	1.414135	4.1E-07	Lightness	N/A	N/A	N/A	N/A
10892	8	37829107	-0.00205	1.281656	1.402353	7.92E-07	Lightness	AX-171607	ostm1	osteopetrosis associated transmembrane protein 1	3'UTR
10889	8	37412186	-0.00012	0.932391	1.398128	3.86E-07	Lightness	AX-171615	LOC11052	sestrin-1-like	3'UTR
10890	8	37412232	0.001007	1.078883	1.394297	4.36E-07	Lightness	AX-171615	LOC11052	sestrin-1-like	3'UTR
10894	8	39295098	-0.00101	1.078672	1.393067	4.36E-07	Lightness	AX-172559	ankh	ANKH inorganic pyrophosphate transport regulator	3'UTR
10898	8	40978990	-0.00168	1.204807	1.381731	7.13E-07	Lightness	AX-171615	znf622	zinc finger protein 622	3'UTR
10891	8	37498606	0.001441	1.158711	1.360095	6.73E-07	Lightness	N/A	N/A	N/A	N/A
10897	8	40978642	0.000331	0.965216	1.348782	3.64E-07	Lightness	AX-172563	znf622	zinc finger protein 622	3'UTR
10893	8	38254068	-0.00033	0.965328	1.326558	4.78E-07	Lightness	AX-171642	LOC11052	poly(U)-binding-splicing factor PUF60-like	CDS
10899	8	40986889	-0.00092	1.063119	1.32395	5.9E-07	Lightness	AX-171615	znf622	zinc finger protein 622	CDS
10896	8	40954559	-0.0004	0.97649	1.322973	3.74E-07	Lightness	AX-171641	myo10	myosin X	3'UTR
10880	8	34136112	0.000851	1.05149	1.307625	4.07E-07	Lightness	AX-171615	mut	methylmalonyl-CoA mutase	3'UTR
10900	8	41002542	0.00113	1.100829	1.281443	5.78E-07	Lightness	AX-172559	retreg1	reticulophagy regulator 1	3'UTR
10877	8	34108037	0.000524	0.996426	1.242088	4.39E-07	Lightness	AX-171615	mut	methylmalonyl-CoA mutase	CDS
30686	27	1675710	0.001602	1.189789	1.238369	8.4E-07	Lightness	AX-171595	LOC11050	protein IWS1 homolog	3'UTR
30715	27	3976684	-0.00289	1.471783	1.229411	9.84E-07	Lightness	AX-171612	LOC11050	serine/threonine-protein phosphatase 2A 65 kDa reg	CDS
10879	8	34129661	4.12E-05	0.920204	1.220721	4.47E-07	Lightness	AX-171615	mut	methylmalonyl-CoA mutase	CDS
10901	8	41004613	0.001747	1.218578	1.220203	7.45E-07	Lightness	AX-899466	retreg1	reticulophagy regulator 1	3'UTR
10878	8	34114960	0.000165	0.939126	1.220038	3.43E-07	Lightness	AX-171618	mut	methylmalonyl-CoA mutase	CDS
30687	27	1676003	-0.00033	0.965299	1.215918	3.06E-07	Lightness	AX-171619	LOC11050	protein IWS1 homolog	3'UTR
30688	27	1697736	0.0022	1.313056	1.214649	7.95E-07	Lightness	AX-171637	LOC11050	protein IWS1 homolog	CDS
30691	27	1811722	0.002227	1.318837	1.202096	8.78E-07	Lightness	AX-172561	LOC11050	protein furry homolog	3'UTR
30702	27	3100140	0.002379	1.352313	1.192169	8.34E-07	Lightness	AX-172558	LOC11050	stress-associated endoplasmic reticulum protein 1-lik	3'UTR
30714	27	3947325	0.000452	0.984656	1.188657	5.67E-07	Lightness	N/A	N/A	N/A	N/A
30683	27	1501236	0.002268	1.327778	1.187138	8.1E-07	Lightness	AX-172561	atg16l1	autophagy related 16 like 1	3'UTR
10875	8	34097292	0.000976	1.073281	1.186828	5.43E-07	Lightness	AX-171622	LOC11052	peptidyl-prolyl cis-trans isomerase FKBP1B	CDS
10873	8	33468677	0.00158	1.185483	1.178851	6.98E-07	Lightness	AX-172555	LOC11053	tribbles homolog 2-like	3'UTR
30697	27	2519641	-0.00093	1.064455	1.172582	6.17E-07	Lightness	AX-171621	LOC11050	60S ribosomal protein L35a	CDS
10876	8	34104621	-0.00059	1.006811	1.171714	3.78E-07	Lightness	AX-171615	mut	methylmalonyl-CoA mutase	CDS
30699	27	2585577	0.000669	1.020407	1.171598	6.75E-07	Lightness	AX-172558	abcc5	ATP binding cassette subfamily C member 5	3'UTR
25112	19	41950961	0.00076	1.035844	1.171218	6.17E-07	Lightness	N/A	N/A	N/A	N/A
30690	27	1733783	-0.00017	0.939969	1.168386	1.25E-07	Lightness	AX-171627	kiaa1456	KIAA1456 ortholog	3'UTR
30685	27	1675054	-0.00144	1.158361	1.166494	7.52E-07	Lightness	AX-171624	LOC11050	coagulation factor IX-like	3'UTR
30684	27	1573838	0.000123	0.932639	1.165749	1.24E-07	Lightness	AX-171637	LOC11050	S-arrestin-like	CDS
30689	27	1705108	0.000651	1.017453	1.165667	6.52E-07	Lightness	AX-172554	LOC11050	arf-GAP with coiled-coil, ANK repeat and PH domain-	3'UTR
30700	27	2632164	-0.00056	1.002596	1.160491	3.88E-07	Lightness	N/A	N/A	N/A	N/A
30698	27	2582620	-0.00014	0.93504	1.159782	1.26E-07	Lightness	AX-171638	abcc5	ATP binding cassette subfamily C member 5	CDS
30713	27	3912445	-0.00013	0.933186	1.158625	8.54E-08	Lightness	AX-171612	LOC11050	myeloid leukemia factor 1-like	5'UTR
30701	27	2900304	-0.00072	1.028749	1.149915	7.29E-07	Lightness	AX-171638	LOC11050	E3 ubiquitin-protein ligase rnf168-like	5'UTR
25113	19	41952271	-0.00155	1.17934	1.142703	6.57E-07	Lightness	AX-171611	LOC11049	uncharacterized protein C15orf52-like	3'UTR
25126	19	42125868	0.002924	1.47926	1.135142	1.05E-06	Lightness	AX-171636	tmem39b	transmembrane protein 39B	CDS
25125	19	42049405	-0.00022	0.948053	1.133817	8.44E-08	Lightness	AX-172558	mthfd1	methylenetetrahydrofolate dehydrogenase, cyclohyc	CDS
10903	8	41173646	-0.00107	1.090648	1.12896	3.24E-07	Lightness	AX-171597	nol7	nucleolar protein 7	CDS
6977	5	58650420	-0.00077	1.036907	1.126468	5.2E-07	Lightness	AX-172549	LOC11052	midnolin-like	3'UTR
30716	27	3980591	0.00228	1.330526	1.126329	1.04E-06	Lightness	AX-171612	LOC11050	serine/threonine-protein phosphatase 2A 65 kDa reg	CDS
30712	27	3345790	-0.00035	0.968747	1.126166	4.57E-07	Lightness	AX-171638	LOC11050	cullin-3	CDS
25111	19	41821864	-0.00016	0.93776	1.119339	2.12E-07	Lightness	AX-171636	LOC11049	mitotic checkpoint serine/threonine-protein kinase B	CDS
30710	27	3270149	9.16E-05	0.927872	1.118839	4.42E-07	Lightness	AX-172557	LOC11050	NADPH--cytochrome P450 reductase-like	CDS
30711	27	3290825	0.001358	1.142928	1.117302	7.74E-07	Lightness	AX-171638	LOC11050	RNA-binding protein FUS-like	CDS
10874	8	34077449	0.000131	0.933903	1.117173	4.57E-07	Lightness	AX-172560	LOC11052	peptidyl-prolyl cis-trans isomerase FKBP1B	5'UTR
10864	8	33351247	0.000412	0.978134	1.116567	3.64E-07	Lightness	AX-171604	LOC11052	glycerophosphocholine phosphodiesterase GPCPD1-l	CDS

SNP	Chr	POS	SNP_effec	Weight	Var_explai	Var_a_hat	Trait	SNP ID	Gene ID	Gene annotation	Region
8673	6	62768347	0.002594	1.512593	2.453443	8.36E-07	Yellowness	AX-171641	LOC11052	cysteine-rich secretory protein LCCL domain-	3'UTR
8679	6	62987174	-0.0015	1.224655	2.417951	4.8E-07	Yellowness	AX-171614	LOC11052	uncharacterized LOC110526409	mRNA
8680	6	63056828	-0.004	1.650396	2.392732	1.01E-06	Yellowness	AX-171614	LOC10013	cyclin B2	CDS
8668	6	61837913	-0.00052	1.013279	2.390702	2.25E-07	Yellowness	AX-171641	LOC11052	lysine--tRNA ligase-like	3'UTR
8670	6	61850604	0.000701	1.04885	2.380632	2.76E-07	Yellowness	N/A	N/A	N/A	N/A
8669	6	61847413	-3.9E-05	0.922747	2.380209	3.83E-07	Yellowness	AX-171614	LOC11052	60S ribosomal protein L13-like	CDS
8678	6	62986112	0.00092	1.094327	2.375885	3.48E-07	Yellowness	AX-172561	LOC11052	uncharacterized LOC110526409	3'UTR
8671	6	61998041	-0.00121	1.157264	2.361679	2.32E-07	Yellowness	AX-171641	LOC11052	cytochrome b5-like	3'UTR
8672	6	61999079	-0.00031	0.972837	2.34677	3.85E-07	Yellowness	AX-171614	LOC11052	cytochrome b5-like	3'UTR
8674	6	62812905	-0.00255	1.498507	2.320757	8.27E-07	Yellowness	AX-171641	LOC11052	ubiquitin carboxyl-terminal hydrolase 10-like	CDS
8677	6	62961238	-0.00047	1.003892	2.257883	4.98E-08	Yellowness	AX-172548	LOC11052	myotubularin-related protein 10-like	3'UTR
8664	6	61666093	-0.00144	1.210479	2.248267	5.75E-07	Yellowness	AX-171614	LOC11052	beta,beta-carotene 15,15'-dioxygenase-like	CDS
8676	6	62896859	-0.00028	0.967022	2.23693	1.14E-07	Yellowness	AX-171614	LOC11052	AP-1 complex subunit gamma-1-like	3'UTR
8675	6	62895237	0.000666	1.041678	2.235584	1.65E-07	Yellowness	AX-172563	LOC11052	AP-1 complex subunit gamma-1-like	3'UTR
8665	6	61701306	-0.00218	1.395564	2.194166	7.25E-07	Yellowness	AX-171614	LOC11052	beta,beta-carotene 15,15'-dioxygenase-like	CDS
8666	6	61805211	0.000816	1.072355	2.109138	3.22E-07	Yellowness	AX-171641	LOC11052	nuclear factor of activated T-cells 5-like	CDS
4701	4	22973619	0.002138	1.384816	2.101947	7.66E-07	Yellowness	AX-171629	plpp6	phospholipid phosphatase 6	5'UTR
8667	6	61811098	-0.0004	0.989713	2.092843	4.61E-07	Yellowness	AX-172563	LOC11052	nuclear factor of activated T-cells 5-like	3'UTR
4700	4	22957625	0.0002	0.952044	2.087741	8.5E-08	Yellowness	AX-899681	prdx6	peroxiredoxin 6	CDS
8681	6	63056837	-0.004	1.650396	2.029983	1.01E-06	Yellowness	AX-171614	LOC10013	cyclin B2	CDS
4699	4	22956370	0.000182	0.948629	2.008355	3.99E-07	Yellowness	AX-171603	prdx6	peroxiredoxin 6	3'UTR
4703	4	23074540	-0.00136	1.192205	1.996617	5.43E-07	Yellowness	AX-171640	LOC11052	protein PRRC2C-like	3'UTR
8661	6	61592297	-0.00059	1.026254	1.989706	8.21E-08	Yellowness	AX-172556	LOC11052	ubiquitin carboxyl-terminal hydrolase 47-like	CDS
8662	6	61592695	-0.00018	0.947511	1.980228	3.25E-08	Yellowness	AX-171605	LOC11052	ubiquitin carboxyl-terminal hydrolase 47-like	CDS
8663	6	61661609	-0.00053	1.015472	1.978117	3.51E-07	Yellowness	AX-171641	LOC11052	beta,beta-carotene 15,15'-dioxygenase-like	3'UTR
4702	4	23000270	0.000614	1.031331	1.960667	2.79E-07	Yellowness	N/A	N/A	N/A	N/A
4706	4	23115313	0.001182	1.151073	1.953147	5.06E-07	Yellowness	AX-171614	LOC11052	myocilin-like	CDS
4704	4	23103208	0.000371	0.983984	1.927124	1.92E-07	Yellowness	AX-171640	vamp4	vesicle associated membrane protein 4	3'UTR
4705	4	23104063	-0.00036	0.982236	1.92524	1.87E-07	Yellowness	N/A	N/A	N/A	N/A
4707	4	23115457	-0.00099	1.108175	1.908697	4.48E-07	Yellowness	AX-171614	LOC11052	myocilin-like	CDS
8659	6	61578946	0.003213	1.650396	1.904019	9.57E-07	Yellowness	AX-171641	LOC11052	F-actin-methionine sulfoxide oxidase MICAL2	5'UTR
4710	4	23126883	-0.00105	1.122732	1.867478	3.78E-07	Yellowness	AX-171618	LOC11052	myocilin-like	CDS
4708	4	23115513	-0.00054	1.017121	1.867218	2.34E-07	Yellowness	AX-172562	LOC11052	myocilin-like	CDS
4709	4	23126838	0.000274	0.965779	1.861168	1.92E-07	Yellowness	AX-171618	LOC11052	myocilin-like	CDS
8654	6	61452701	-0.00176	1.288108	1.850532	5.07E-07	Yellowness	AX-172560	LOC11052	transcriptional enhancer factor TEF-1-like	CDS
8660	6	61586208	-0.00067	1.04272	1.848335	5.71E-07	Yellowness	AX-171615	LOC11052	ubiquitin carboxyl-terminal hydrolase 47-like	3'UTR
4698	4	22956257	-0.00014	0.941229	1.829275	1.28E-07	Yellowness	AX-171603	prdx6	peroxiredoxin 6	3'UTR
8655	6	61524139	-0.00176	1.286411	1.824078	3.11E-07	Yellowness	AX-171622	LOC11052	alpha-parvin-like	5'UTR
8656	6	61536968	0.000646	1.03768	1.810952	2.45E-07	Yellowness	AX-171622	LOC11052	F-actin-methionine sulfoxide oxidase MICAL2	CDS
4711	4	23127016	0.001362	1.191861	1.808816	3.88E-07	Yellowness	AX-171614	LOC11052	myocilin-like	3'UTR
8657	6	61537673	-0.00289	1.602525	1.787961	4.33E-07	Yellowness	AX-171622	LOC11052	F-actin-methionine sulfoxide oxidase MICAL2	CDS
4697	4	22804020	0.000273	0.965506	1.732688	2.23E-07	Yellowness	AX-172549	LOC11052	transcription factor AP-1-like	CDS
8682	6	63060976	0.004183	1.650396	1.731552	1.02E-06	Yellowness	AX-171614	LOC11052	E3 ubiquitin-protein ligase Arkadia-like	3'UTR
4712	4	23127090	0.000852	1.079935	1.720754	2.97E-07	Yellowness	AX-899477	LOC11052	myocilin-like	3'UTR
4713	4	23133434	0.001561	1.23874	1.696789	6.34E-07	Yellowness	AX-171622	itpa	inosine triphosphatase	CDS
8658	6	61560875	-0.00014	0.941122	1.646828	2.39E-07	Yellowness	AX-172561	LOC11052	F-actin-methionine sulfoxide oxidase MICAL2	CDS
8652	6	61343693	0.001312	1.180489	1.630869	3.75E-07	Yellowness	AX-171622	LOC11052	BTB/POZ domain-containing protein 10-like	5'UTR
4695	4	22697101	0.000236	0.958587	1.630603	2.14E-07	Yellowness	N/A	N/A	N/A	N/A
4696	4	22803384	0.000759	1.060701	1.629206	2.93E-07	Yellowness	AX-171625	LOC11052	transcription factor AP-1-like	CDS
8653	6	61348563	-0.00088	1.086512	1.59638	2.95E-07	Yellowness	AX-171615	LOC11052	BTB/POZ domain-containing protein 10-like	3'UTR
4714	4	23134842	-0.00214	1.38433	1.587836	8.05E-07	Yellowness	AX-172563	itpa	inosine triphosphatase	CDS
4715	4	23191213	-0.00234	1.439261	1.557448	8.83E-07	Yellowness	AX-171628	pigc	phosphatidylinositol glycan anchor biosynthes	CDS
4694	4	22622293	0.000439	0.996997	1.553898	2.04E-07	Yellowness	AX-174104	LOC11052	angiopoietin-related protein 1-like	3'UTR
8688	6	63387476	0.001684	1.268451	1.503936	6.46E-07	Yellowness	AX-171641	LOC11052	early endosome antigen 1-like	CDS
8687	6	63337422	-0.00037	0.984339	1.500878	4.59E-07	Yellowness	N/A	N/A	N/A	N/A
8683	6	63113209	0.000321	0.974482	1.497213	3.61E-07	Yellowness	AX-171614	LOC11052	SAFB-like transcription modulator	CDS
8684	6	63123436	-0.00023	0.957013	1.496547	3.82E-07	Yellowness	AX-171614	LOC11052	SAFB-like transcription modulator	CDS
8685	6	63126591	-0.00169	1.269332	1.496471	7.67E-07	Yellowness	AX-172556	LOC11052	SAFB-like transcription modulator	3'UTR
4693	4	22499940	-0.00042	0.993494	1.48027	3.11E-07	Yellowness	N/A	N/A	N/A	N/A
4720	4	23279962	-0.00119	1.153868	1.478265	5.71E-07	Yellowness	AX-171602	LOC11052	transmembrane emp24 domain-containing pr	3'UTR
8646	6	60797832	-0.00202	1.353862	1.474557	6.32E-07	Yellowness	AX-171631	LOC11052	myotubularin-related protein 13-like	3'UTR
8692	6	63690991	-0.00341	1.650396	1.4613	9.98E-07	Yellowness	AX-171614	LOC11052	E3 ubiquitin-protein ligase NEDD4-like	3'UTR
8647	6	60962928	-0.00051	1.011367	1.459396	2.79E-07	Yellowness	AX-172550	LOC11052	ADM-like	CDS
4717	4	23209006	0.00116	1.146172	1.459142	4.95E-07	Yellowness	AX-172553	LOC11052	SUN domain-containing ossification factor-lik	CDS
8691	6	63628381	-0.00027	0.964716	1.458532	1.33E-07	Yellowness	N/A	N/A	N/A	N/A
4719	4	23278852	0.000401	0.989659	1.456901	4.05E-07	Yellowness	AX-171602	LOC11052	transmembrane emp24 domain-containing pr	3'UTR
4716	4	23200735	-0.00051	1.009909	1.454131	1.38E-07	Yellowness	AX-171628	LOC11052	SUN domain-containing ossification factor-lik	CDS
8648	6	60962934	0.000265	0.964051	1.45368	4.45E-07	Yellowness	AX-171619	LOC11052	ADM-like	CDS
8690	6	63449206	0.000577	1.02405	1.451683	3.47E-07	Yellowness	AX-171605	LOC11052	transcription factor 12-like	3'UTR

SNP	Chr	POS	SNP_effec	Weight	Var_explai	Var_a_hat	Trait	SNP ID	Gene ID	Gene annotation	Region
10884	8	34936875	0.00173	1.234062	1.572888	6.95E-07	Whiteness	AX-171641	LOC11052	cGMP-dependent protein kinase 1-like	3'UTR
10887	8	37290793	0.00195	1.280835	1.540639	7.17E-07	Whiteness	AX-171642	LOC11052	sialomucin core protein 24-like	3'UTR
10883	8	34495040	0.000441	0.98641	1.488996	3.73E-07	Whiteness	AX-171615	sod2	superoxide dismutase 2	3'UTR
10885	8	34964577	-0.00101	1.089103	1.471822	5.05E-07	Whiteness	AX-171641	LOC11052	cGMP-dependent protein kinase 1-like	CDS
10882	8	34494762	-0.0009	1.068082	1.452506	4.02E-07	Whiteness	N/A	N/A	N/A	N/A
10888	8	37293410	0.00177	1.240804	1.4522	6.75E-07	Whiteness	N/A	N/A	N/A	N/A
10886	8	36538411	0.000577	1.010013	1.419253	1.53E-07	Whiteness	AX-172549	LOC11052	SAM and SH3 domain-containing protein 1-li	3'UTR
10895	8	40610851	-0.00194	1.279439	1.408324	7.16E-07	Whiteness	N/A	N/A	N/A	N/A
10881	8	34494659	0.000431	0.984688	1.397119	3.7E-07	Whiteness	N/A	N/A	N/A	N/A
10892	8	37829107	-0.00194	1.279674	1.379458	7.17E-07	Whiteness	AX-171607	ostm1	osteopetrosis associated transmembrane pr	3'UTR
10889	8	37412186	-0.00011	0.930934	1.378649	3.49E-07	Whiteness	AX-171615	LOC11052	sestrin-1-like	3'UTR
10890	8	37412232	0.000961	1.079411	1.375214	3.96E-07	Whiteness	AX-171615	LOC11052	sestrin-1-like	3'UTR
10894	8	39295098	-0.00096	1.078945	1.369999	3.95E-07	Whiteness	AX-172559	ankh	ANKH inorganic pyrophosphate transport re	3'UTR
10898	8	40978990	-0.00159	1.20456	1.358714	6.46E-07	Whiteness	AX-171615	znf622	zinc finger protein 622	3'UTR
10891	8	37498606	0.00136	1.1558	1.341195	6.07E-07	Whiteness	N/A	N/A	N/A	N/A
10897	8	40978642	0.00031	0.964349	1.326191	3.29E-07	Whiteness	AX-172563	znf622	zinc finger protein 622	3'UTR
10893	8	38254068	-0.00031	0.964114	1.304973	4.31E-07	Whiteness	AX-171642	LOC11052	poly(U)-binding-splicing factor PUF60-like	CDS
10899	8	40986889	-0.00087	1.061577	1.301531	5.33E-07	Whiteness	AX-171615	znf622	zinc finger protein 622	CDS
10896	8	40954559	-0.00038	0.975696	1.300456	3.38E-07	Whiteness	AX-171641	myo10	myosin X	3'UTR
10880	8	34136112	0.000817	1.052876	1.292619	3.7E-07	Whiteness	AX-171615	mut	methylmalonyl-CoA mutase	3'UTR
10900	8	41002542	0.00107	1.100074	1.259847	5.24E-07	Whiteness	AX-172559	retreg1	reticulophagy regulator 1	3'UTR
10877	8	34108037	0.00051	0.998256	1.228215	3.99E-07	Whiteness	AX-171615	mut	methylmalonyl-CoA mutase	CDS
25112	19	41950961	0.000786	1.047221	1.207171	5.7E-07	Whiteness	N/A	N/A	N/A	N/A
10879	8	34129661	3.73E-05	0.919839	1.206528	4.04E-07	Whiteness	AX-171615	mut	methylmalonyl-CoA mutase	CDS
10878	8	34114960	0.000145	0.93719	1.205881	3.09E-07	Whiteness	AX-171618	mut	methylmalonyl-CoA mutase	CDS
10901	8	41004613	0.00165	1.215135	1.199537	6.72E-07	Whiteness	AX-899466	retreg1	reticulophagy regulator 1	3'UTR
30686	27	1675710	0.00146	1.176359	1.193807	7.45E-07	Whiteness	AX-171595	LOC11050	protein IWS1 homolog	3'UTR
30715	27	3976684	-0.0027	1.459297	1.175444	8.79E-07	Whiteness	AX-171612	LOC11050	serine/threonine-protein phosphatase 2A 65	CDS
25113	19	41952271	-0.00142	1.168483	1.175311	5.84E-07	Whiteness	AX-171611	LOC11049	uncharacterized protein C15orf52-like	3'UTR
10875	8	34097292	0.000934	1.074368	1.173128	4.93E-07	Whiteness	AX-171622	LOC11052	peptidyl-prolyl cis-trans isomerase FKBP1B	CDS
30687	27	1676003	-0.0003	0.961859	1.172889	2.74E-07	Whiteness	AX-171619	LOC11050	protein IWS1 homolog	3'UTR
30688	27	1697736	0.00206	1.305777	1.171754	7.13E-07	Whiteness	AX-171637	LOC11050	protein IWS1 homolog	CDS
6977	5	58650420	-0.00075	1.040455	1.167423	4.74E-07	Whiteness	AX-172549	LOC11052	midnolin-like	3'UTR
10873	8	33468677	0.00148	1.18142	1.164737	6.29E-07	Whiteness	AX-172555	LOC11053	tribbles homolog 2-like	3'UTR
30691	27	1811722	0.00207	1.307151	1.159073	7.83E-07	Whiteness	AX-172561	LOC11050	protein furry homolog	3'UTR
25126	19	42125868	0.00283	1.491743	1.158158	9.58E-07	Whiteness	AX-171636	tmem39b	transmembrane protein 39B	CDS
10876	8	34104621	-0.00056	1.007125	1.158064	3.42E-07	Whiteness	AX-171615	mut	methylmalonyl-CoA mutase	CDS
25125	19	42049405	-0.00021	0.946992	1.156576	7.61E-08	Whiteness	AX-172558	mthfd1	methylenetetrahydrofolate dehydrogenase,	CDS
25111	19	41821864	-0.00016	0.93975	1.154945	1.93E-07	Whiteness	AX-171636	LOC11049	mitotic checkpoint serine/threonine-protein	CDS
30683	27	1501236	0.00212	1.319455	1.143177	7.26E-07	Whiteness	AX-172561	atg16l1	autophagy related 16 like 1	3'UTR
30702	27	3100140	0.00222	1.342656	1.140037	7.46E-07	Whiteness	AX-172558	LOC11050	stress-associated endoplasmic reticulum pro	3'UTR
30714	27	3947325	0.000443	0.986845	1.136766	5.15E-07	Whiteness	N/A	N/A	N/A	N/A
30697	27	2519641	-0.00084	1.057436	1.126376	5.52E-07	Whiteness	AX-171621	LOC11050	60S ribosomal protein L35a	CDS
30699	27	2585577	0.000671	1.02654	1.125749	6.18E-07	Whiteness	AX-172558	abcc5	ATP binding cassette subfamily C member 5	3'UTR
30690	27	1733783	-0.00017	0.941119	1.125577	1.13E-07	Whiteness	AX-171627	kiaa1456	KIAA1456 ortholog	3'UTR
30685	27	1675054	-0.0013	1.143834	1.124611	6.65E-07	Whiteness	AX-171624	LOC11050	coagulation factor IX-like	3'UTR
30684	27	1573838	0.000126	0.934026	1.124114	1.12E-07	Whiteness	AX-171637	LOC11050	S-arrestin-like	CDS
30689	27	1705108	0.000615	1.016601	1.123382	5.87E-07	Whiteness	AX-172554	LOC11050	arf-GAP with coiled-coil, ANK repeat and PH	3'UTR
6980	5	58790105	0.000711	1.033659	1.118285	4.54E-07	Whiteness	AX-171627	LOC11052	serine/threonine-protein kinase STK11-like	5'UTR
6978	5	58664012	-0.0013	1.145006	1.117352	5.21E-07	Whiteness	AX-171625	LOC11052	midnolin-like	CDS
25114	19	41952536	-0.00049	0.995157	1.116039	4.55E-07	Whiteness	AX-171611	LOC11049	uncharacterized protein C15orf52-like	mRNA
30698	27	2582620	-0.00014	0.936227	1.114689	1.14E-07	Whiteness	AX-171638	abcc5	ATP binding cassette subfamily C member 5	CDS
25124	19	42037903	-0.00021	0.947191	1.113029	1.77E-07	Whiteness	AX-171611	mthfd1	methylenetetrahydrofolate dehydrogenase,	CDS
30700	27	2632164	-0.00054	1.003676	1.112765	3.52E-07	Whiteness	N/A	N/A	N/A	N/A
10903	8	41173646	-0.00102	1.09026	1.108906	2.93E-07	Whiteness	AX-171597	nol7	nucleolar protein 7	CDS
30713	27	3912445	-0.00012	0.932384	1.108363	7.7E-08	Whiteness	AX-171612	LOC11050	myeloid leukemia factor 1-like	5'UTR
10874	8	34077449	0.000127	0.934242	1.104773	4.14E-07	Whiteness	AX-172560	LOC11052	peptidyl-prolyl cis-trans isomerase FKBP1B	5'UTR
10864	8	33351247	0.000397	0.978911	1.10269	3.31E-07	Whiteness	AX-171604	LOC11052	glycerophosphocholine phosphodiesterase (	CDS
30701	27	2900304	-0.0007	1.032455	1.102457	6.64E-07	Whiteness	AX-171638	LOC11050	E3 ubiquitin-protein ligase rnf168-like	5'UTR

CHAPTER 3: RNA-Seq analysis of the pyloric caecum, liver, and muscle reveals molecular mechanisms regulating fillet color in rainbow trout.

Ahmed, R. O., Ali, A., Leeds, T., & Salem, M. (2023). RNA-Seq analysis of the pyloric caecum, liver, and muscle reveals molecular mechanisms regulating fillet color in rainbow trout. BMC genomics, 24(1), 579.

Ridwan O. Ahmed,[1] Ali Ali,[1] Tim Leeds,[2], and Mohamed Salem[1, *]

[1]Department of Animal and Avian Sciences, University of Maryland, College Park, MD 20742, USA.

[2]United States Department of Agriculture Kearneysville, National Center for Cool and Cold Water Aquaculture, Agricultural Research Service, Kearneysville, WV 25430, USA.

Abstract

The characteristic pink-reddish color in the salmonids fillet is an important, appealing quality trait for consumers and producers. The color results from diet supplementation with carotenoids, which accounts for up to 20-30% of the feed cost. Pigment retention in the muscle is a highly variable phenotype. In this study, we aimed to understand the molecular basis for the variation in fillet color when fish families were fed an astaxanthin-supplemented diet. We used RNA-Seq to study the transcriptome profile in the pyloric caecum, liver, and muscle from fish families with pink-reddish fillet coloration (Red) versus those with lighter pale coloration (white).

More DEGs were identified in the muscle (5,148) and liver (3,180) than in the pyloric caecum (272). Genes involved in lipid/carotenoid metabolism and transport, ribosomal activities, mitochondrial functions, and stress homeostasis were uniquely enriched in the muscle and liver. For instance, the two beta carotene genes (BCO1 and BCO2) were significantly under-represented in the muscle of the red fillet group favoring more carotenoid retention. Enriched genes in the pyloric cecum were involved in intestinal absorption and transport of carotenoids and lipids. In addition, the analysis revealed the modulation of several genes with immune functions in the pyloric caecum, liver, and muscle.

The results from this study deepen our understanding of carotenoid dynamics in rainbow trout and can guide us on strategies to improve astaxanthin retention in the rainbow trout fillet.

Keywords: carotenoids, RNA-Seq, pyloric cecum, liver, muscle

Background

Carotenoids, also called tetraterpenoids, are organic molecular pigments synthesized by plants, certain bacteria, algae, and fungi (Kumari et al., 2019). Their primary function is to absorb light energy during photosynthesis and to provide photoprotection (Armstrong & Hearst, 1996). Carotenoids are structurally classified as either carotene (those without oxygen) or xanthophyll (which contains oxygen). They absorb light of wavelength between 400-550 nanometers, conferring yellow, orange, or red coloration (Kumari et al., 2019). They give characteristic color to plants like carrots, pumpkins, and tomatoes. In animals, carotenoids are used for pigmentation, as a precursor to vitamin A, as an antioxidant, and to enhance immune response (Deming & Erdman, 1999; Goodwin, 1986).

In the natural marine habitat, salmonid fish, including rainbow trout and Atlantic salmon, feed on sea algae and small crustaceans, giving the muscle pink/reddish coloration characteristics. In commercial and farmed aquaculture, synthetic carotenoids, especially astaxanthin, are added as feed additives to provide similar fillet coloration. This characteristic reddish/pink fillet coloration is an important quality criterion that can influence consumers purchasing decisions (Ahmed et al., 2022). It has been observed that only a small proportion (2-22%) of the supplied astaxanthin is deposited and retained in the muscle (Storebakken & No, 1992; Torrissen, 1989). The large disparity between the digestibility of astaxanthin in salmonids (approximately 30-50%) (No & Storebakken, 1991) and muscle retention (2-22%) (Storebakken & No, 1992) suggests that several organs between the intestine, where carotenoids are absorbed, and muscle, where it is deposited, are crucial to the understanding of carotenoid metabolism.

Understanding the mechanism of carotenoid metabolism in rainbow trout is crucial to devising strategies to improve muscle retention of the supplied astaxanthin. Most of our understanding of carotenoid metabolism comes from using beta-carotene in human studies and a few studies from fish. Due to their hydrophobic nature, carotenoids are closely associated with fatty acids and transported with them in the intestine and blood (Clevidence & Bieri, 1993; Parker, 1996). There is, therefore, a strong link between carotenoid metabolism and fat metabolism through the uptake, transport, and delivery of both compounds. Similarly, essential features of carotenoid absorption, metabolism, and transport are similar in both salmonids and mammals (Rajasingh et al., 2006). Increasing dietary lipid levels improved astaxanthin deposition and retention in rainbow trout and

Atlantic salmon fillet (Bjerkeng et al., 1997; Nickell & Bromage, 1998). Studies have shown that the gastrointestinal tract of salmon and rainbow trout consists of several regions, with the pyloric caecum, rather than the stomach or hindgut, playing the most prominent role in the digestion, absorption, and metabolism of lipid and astaxanthin (Choubert et al., 1991; Denstadli et al., 2004; Røsjø et al., 2000). Several enzymes involved in astaxanthin's absorption, metabolism, and transport are expressed in the pyloric caeca (Schmeisser et al., 2021). Several genetic factors influence carotenoid digestion in the intestine, including genes for digestive enzymes and bile acid formation that assist in carotenoid micellization, uptake of carotenoid, and transport (Desmarchelier & Borel, 2017; Harrison, 2012).

It was previously thought that the absorption of carotenoids in the intestine is passive (Reboul & Borel, 2011). Recent studies have shown that several proteins, including scavenger receptor class B (SCARB1), cluster of differentiation 36 (CD36), NPC1L1 (Niemann–Pick C1-like 1), and ABCA1 (ATP-Binding Cassette A1) (Borel et al., 2013; Reboul & Borel, 2011) facilitate carotenoid uptake in the intestine. Within the intestine, several proteins, including beta-carotene oxygenase, retinol dehydrogenases, and retinol-binding proteins, are reported to metabolize carotenoids (Helgeland et al., 2019; Lubzens et al., 2003; Madaro et al., 2020; Zoric, 2017). The unmetabolized carotenoids and retinols from the intestine are transported to the liver for further metabolism. The liver is the main metabolic organ for carotenoids in salmonids (Hardy et al., 1990; Page & Davies, 2003; Torrissen & Ingebrigtsen, 1992). The exact mechanism of carotenoid transport in the blood, liver uptake, and metabolism in rainbow trout remain a subject of continuous research. Studies have shown that astaxanthin not metabolized in the liver is repackaged into very low-density lipoproteins (VLDL) and sent into the blood again for transport and deposition in the muscle (Rajasingh et al., 2006; Tigistu-Sahle, 2012). Astaxanthin in the muscle boosts the fillet color and confers the reddish-pink fillet coloration characteristics of salmonids. During sexual maturation, carotenoids from the muscle are transferred to the skin and gonads (Bjerkeng et al., 1992).

In this study, we used RNA-Seq analysis to elucidate on the mechanisms involved in the absorption, metabolism, and deposition of astaxanthin in the muscle tissue of rainbow trout with a view to select for rainbow trout fish with a better ability to retain astaxanthin. As a result of their role in carotenoid metabolism in the literature, the pyloric caecum, liver, and muscle tissue were

selected for this study. This will shed light on the molecular basis for the development of divergent intensity of fillet coloration in rainbow trout fish fed the same diet and reared under the same experimental conditions.

2.0 Methods

2.1 Ethical statement

Husbandry practice and experimental procedures at the facility were approved by the IACUC animal study protocol of the University of Maryland, College Park, protocol number 1593175-6.

2.2 Rainbow Trout Population, Experimental Design, Treatments, and Sampling

This study was carried out using rainbow trout from a muscle yield genetic selection line developed at the National Center for Cool and Cold water aquaculture (NCCCWA). This line started as a growth-selected line in 2002 and underwent five generations of selection for improved growth performance as described by Leeds et al. (2016). Subsequent generations were selected for muscle yield as described in Cleveland et al.(2023) and Garcia et al. (2023a). Fish from the 2020-year class (YC) were included in this study and thus represent 3rd-generation families from lines selected for high (ARS-FY-H) or low (ARS-FY-L) fillet yield.

Breeding and Hatching

Briefly, the fish used for this study were from 40 families (20 full-sib families each from the ARS-FY-H and -L lines) received from the NCCCWA at 322 days post-hatch and reared at the Crane Aquaculture facility of the University of Maryland, College Park. The aquaculture facility uses a recirculating aquaculture system (RAS) with all water quality parameters closely monitored. The fish were fed an astaxanthin-supplemented diet (BioTrout 4.0mm & 6.0mm, ~ 40ppm astaxanthin) from Bio-Oregon at a feeding rate for approximately six months before harvest. At the age of between 450 to 485 days post-hatch, 442 fish were harvested (average body weight = 694.36g; SD = 173.76). The fish were taken off feed a day before harvesting. Liver, pyloric cecum, and muscle tissue were collected on the harvest day, as described below. The fish were allowed to undergo rigor mortis on ice for 48 hours and manually processed into trimmed, skinless fillets on the third day. The harvest period was done for six consecutive weeks, and sampling was done so that each week, we had a representative of one to two fish per family. Sixty fish were harvested in the first and second week, while 80 were harvested in each subsequent fish and 82 in the final week.

A section of the right fillet was collected from which color measurements were obtained in the region shown in Figure 1. The color was measured with the Minolta Chroma Meter CR-200 device (Minolta, Model CR-300; Minolta Camera Co., Osaka, Japan), which gives readings for redness (a*), yellowness (b*), and lightness (L*).

The saturation index (SI) $(a^{*2} + b^{*2})^{0.5}$ was calculated for all fish, and the average SI value for each family was used to sort the 40 families into "red fillet group" for fish families of high saturation index and "white fillet group" for fish families of low saturation index value. The saturation index describes the brightness of the color (Association, 1991). The fish from families with divergent color values (red versus white) were used for this study, five families for the pyloric caecum (3 from the red fillet group versus 2 from the white fillet group), five families for the muscle (3 from the red fillet group versus 2 from the white fillet group), and eight families for the liver (4 from the red fillet group versus 4 from the white fillet group).

2.3 RNA Extraction

The pyloric cecum, liver, and muscle tissues were collected from selected fish samples from the red and white fillet groups. The tissue samples were immediately flash-frozen in liquid nitrogen before transferring to -80ºc for storage. Total RNA was extracted from the tissues using the RNAzol reagent (Molecular Research Center Inc., USA) method following the manufacturer's instructions. The concentration of RNA was measured by NanoDrop spectrophotometer Gen 5 version 2.09.2 (BioTek Instruments, Inc., USA), and the purity was estimated by the A260:A280 ratio. Gel electrophoresis was used to confirm the integrity of the extracted RNA. RNA samples selected for library preparation had an A260:A280 ratio of 1.8-2.1. A total of ten (10), twenty-three (23), and sixteen (16) individual fish RNA samples were extracted from the pyloric caecum, liver, and muscle, respectively. The RNA were individually sequenced and used for this study.

2.4 Library Preparation and Sequencing

Library preparation was done using the Integrated DNA Technologies (IDT) xGen RNA library preparation kit with the NEB polyA selection module. The preparation is performed according to the manufacturer's instructions. Briefly, it starts with RNA fragmentation, followed by random priming and reverse transcription to generate first-strand cDNA. This follows by tailing and

adapter ligation to the 3'-end of the cDNA molecule. The final step is the PCR to increase library yield. Sequencing was performed at the Oklahoma Medical Research Foundation NGS Core, USA.

2.5 Differential Gene Expression Analyses

The rainbow trout genome annotation used was downloaded from the NCBI (**GCA_002163505.1** https://www.ncbi.nlm.nih.gov/assembly/GCF_002163495.1/**)**. Low-quality reads trimming, adapter trimming, read mapping, and differential expression analysis were performed using the CLC genomics workbench (version 22). Raw counts were used to identify differentially expressed genes (DEGs) using in-built EdgeR in the CLC genomics workbench. A gene was considered DEG when P-adj-value < 0.05 and fold change (FC) ≥ |1.5|.

2.6 KEGG Pathways and GO Analysis

Functional enrichment analysis was performed to identify KEGG (Kyoto Encyclopedia of Genes and Genomes) pathways and GO (Gene Ontology) terms based on the DEGs identified against the background (expressed) genes in the pyloric cecum, liver, and muscle. The analysis was performed using ShinyGO 0.77 (Ge et al., 2020). A cut-off of FDR-adjusted P-values of less than 0.05 was used for significant GO terms and KEGG pathways.

2.7 Canonical Pathway Analysis

To investigate the molecular mechanisms underlying carotenoid absorption and utilization, the outcome from the differential expression analysis (the DEGs, fold change, and FDR-adjusted p-values) for the muscle tissue was uploaded to the Qiagen Ingenuity Pathway Analysis (IPA) software application (Kramer et al., 2014). The DEGs were categorized into related canonical pathways based on the Ingenuity pathway knowledge base (IPKB). IPA was performed to identify canonical pathways, diseases and functions, and gene networks that are most significantly enriched from our DEGs data.

3.0 Results

3.1 Library Preparation and RNA-sequencing

A total of 1,307,592,114 raw paired-end reads (151bp long) were sequenced for the muscle (16 samples), 1,189,353,744 raw paired-end reads, 148bp for the liver (23 samples), and 699,709,530 raw paired-end reads, 151bp for the pyloric caeca (10 samples). On average, 99.9% of reads per

sample passed the quality control, producing 1,306,360,142 high-quality reads for muscle, 1,181,426,360 high-quality reads for the liver, and 699,314,138 high-quality reads for the pyloric caeca. The reads were mapped against the rainbow trout genome (https://www.ncbi.nlm.nih.gov/assembly/GCF_002163495.1/), producing an average of 90% mapping rate.

3.2 Between-Group Clusters

Principal component analysis (PCA) was conducted to observe the clustering between samples belonging to the two phenotype groups (white fillet VS red fillet) (Figure 2). There is a pattern of distinct clustering between samples from the two groups in the liver and muscle. In addition, there is a clear separation between samples from the pyloric caecum, liver, and muscle.

3.3 Differentially Expressed Genes in the Pyloric

The pyloric caecum had only 272 significant (FDR $P<0.05$) DEGs between the white and the red fillet groups. One hundred and twenty-six (126) of those genes were upregulated (Fold change ≥ 2.0), while 166 were downregulated (fold change ≤ -1.5). The complete list of DEGs and their fold change can be found in Supplementary Table 1.

The highest increase in mRNA expression in the DEGs between the white fillet versus the red fillet group was found in the gene encoding stonustoxin subunit beta-like (1256.28 FC), which confers immune-related functions. At the opposite end of the DEGs, the most downregulated genes are the protein *RD3* (retinal degeneration 3 (-439.07 FC) and *uromodulin* (-186.4 FC).

Genes encoding proteins involved in carotenoid/lipid absorption and transport are enriched in the red fillet group: CD36 antigen (-2.30 FC), phospholipid-transporting ATPase ABCA1 (-5.75 FC, FDR-adj = 0.06). Several DEGs are involved in lipid metabolism, such as apolipoprotein B-100 (-9.61 FC), ELOVL fatty acid elongase 6 (-37.51 FC), long-chain-fatty-acid--CoA ligase 3 (13.53 FC), phospholipase A and acyltransferase 4-like (4.79 FC), and phospholipid phosphatase-related protein type 4 (3.29 FC). Modulated genes involved in carotenoid metabolism are *retinoic acid receptor beta* (4.37 FC), *retinol dehydrogenase 1* (2.43 FC), and *retinoic acid receptor beta* (-3.92 FC).

Among the modulated genes in the pyloric cecum encoding proteins that have functions related to immunity include ferritin, middle subunit in the pyloric caecum (-8.89 FC), GTPase IMAP family member 8-like (34.94 FC), interferon-induced very large GTPase 1 (16.79, 6.94 FC), GTPase IMAP family member 7 (-6.4, -6.68, -43.58 FC), B-cell receptor CD22-like (-22.32 FC). Others are listed in Supplementary Table 1. There is no enriched KEGG pathway and GO terms for DEGs in the pyloric caecum.

3.4 Differentially Expressed Genes in the Liver.

There were 3,180 significant (FDR $P < 0.05$) DEGs in the liver between the white and the red fillet groups. One thousand four hundred and two (1402) of those genes are upregulated, while 1778 are down-regulated. The full list of DEGs and their fold change can be found in Supplementary Table 1. The most downregulated genes encode putative per-hexamer repeat protein 5 (-4489.25 FC), pygopus homolog 1 (-82.69 FC), and follistatin a (-75.07 FC). At the opposite end, the most upregulated genes encode pentraxin-related protein PTX3 (162.32 FC), ferritin H-3 (147.72 FC), and protein FAM163B-like (93.16 FC).

Other DEGs identified in the liver involved in chylomicron uptake include those that encode for low-density lipoprotein receptor-related protein 1 (LRP1) (-1.59 FC), LRP10 (-2.18 FC), LRP6 (-1.51, -178 FC) and basement membrane-specific heparan sulfate proteoglycan core protein (-2.06, -3.56 FC). Other significant DEGs with prominent functions in carotenoid metabolism are Apolipoprotein B-100(-6.9, -1.74, -2.38 FC), Retinol-binding protein 1 (1.44 FC), Retinol binding protein 7b, cellular (3.27 FC), retinol-binding protein 2 (2.84 FC), *BCO1* (1.46 FC), *BCO2* (-2.71 FC).

DEGs in the liver that encode for proteins with immune function include ferritin H-3 (147.7 FC), Heme oxygenase 2-like (-1.67 FC), interferon-induced very large GTPase 1 (-1.76, -2.08, 2.27 FC), GTPase IMAP family member 9 (5.66 FC). Others are listed in Supplementary Table 1. DEGs that encode proteins involved in stress homeostasis identified in the liver are listed in Supplementary Table 1.

3.41 KEGG and GO terms in the liver.

There are no significant KEGG and GO terms in the liver for the down-regulated genes. For upregulated genes between the white versus red fillet group in the liver, the KEGG pathways

enriched are ribosome (59 genes), oxidative phosphorylation (19 genes), and protein export (5 genes).

Several GO terms are significantly enriched for this group. The most significant terms involved in the biological process, as shown in Figure 3 and Supplementary Table 2, include peptide biosynthetic process, translation, amide biosynthetic process, peptide metabolic process, electron transport chain, oxidative phosphorylation, ATP metabolic process, cellular respiration.

Some of this group's most significant cellular function terms are ribosome, ribosomal subunit, ribonucleoprotein complex, large ribosomal subunit, mitochondrial inner membrane, mitochondrion, mitochondrial envelope, and others as presented in Figure 4 and Supplementary Table 2.

The most significant molecular components GO terms for this group include structural constituent of ribosome, structural molecule activity, electron transfer activity, proton transmembrane transporter activity, oxidoreduction-driven active transmembrane transporter activity, RNA binding, and cyclin-dependent protein serine/threonine kinase regulator activity as presented Figure 5 and Supplementary Table 2.

3.5 Differentially Expressed Genes in the Muscle.

There were 5148 significant (FDR $P<0.05$) DEGs between the white and the red fillet groups. Two thousand six hundred and forty-three (2643) of those genes are upregulated (Fold change > 1.5), while 2505 are downregulated (fold change > -1.5). The full list of DEGs and their fold change can be found in Supplementary Table 1. The most upregulated genes between the white versus red fillet group in the muscle encode digestive enzymes with immune functions: acidic mammalian chitinase (728.07, 575.56 FC) and gastric chitinase (565.2 FC).

The downregulated genes with the most significant fold change encode proteins with stress homeostasis function. They include heat shock protein 30 (-297.82, -151.27, -136.33, -135.52 FC), nucleotide triphosphate diphosphatase NUDT15 (-268.43 FC), and asporin (LRR class 1) (-942.47 FC).

DEGs involved in carotenoid metabolism include *albumin 1* (98.85, 86.42 FC, low-density lipoprotein receptor-related protein 2b (*LRP2B*) (-3.27 FC), low-density lipoprotein receptor-

related protein 2a (*LRP2A*) (-3.37 FC), low-density lipoprotein receptor-related protein 1Ba (*LRP1BA*) (-11.73 FC), low-density lipoprotein receptor-related protein 4 (*LRP4*) (2.61 FC), and low-density lipoprotein receptor adaptor protein 1a (*ldlrap1a*) (2.18 FC). Coronins (*coronin-2B* (-1.61 FC) and *Coronin-1C* (-18.77 FC)) are involved in the transport of astaxanthin within the muscle cells.

Several DEGs in the muscle encode proteins involved in actomyosin structure organization. They are listed in Supplementary Table 1.

DEGs that encode for proteins involved in stress homeostasis in the muscle are Tumor necrosis factor receptor superfamily member 14 (4.26 FC), glutathione peroxidase 1 (gpx1) (-1.75, -2.71 FC), probable glutathione peroxidase 8 (-2.29 FC), Superoxide dismutase (-1.9 FC), Hsp30 (-5.62, -11.59, -53.05, -55.93, -92.8, -135.53, -136.63, -151.27, -92.8, -297.82 FC) and hsp70(-3.02 FC). Others are listed in Supplementary Table 1.

DEGs involved in immune response are *ferritin, middle subunit* (-1.96, -2.01, -2.4, -2.85, -3.28,-3.5, -6.53 FC), *Cathepsin Bb* (-1.68 FC), *cathepsin K* (-1.78, -5.88, 5.75 FC), *GTPase IMAP family member 7* (3.78, 11.1, -5.06 FC), *Ladderlectin* (-8.15 FC), *tripartite motif-containing protein 35-like (5.77 FC).* Others are listed in Supplementary Table 1.

3.51 Canonical Pathways

To investigate the molecular mechanisms underlying carotenoid absorption and utilization in the muscle, the DEG list in the muscle was submitted to Ingenuity pathway analysis (IPA) core analysis from Qiagen software. The DEGs were categorized into related canonical pathways based on the Ingenuity pathway knowledge base (IPKB). IPA was performed to identify canonical pathways and 'diseases and functions' that are most significantly enriched from our DEGs data.

The top enriched canonical pathways in the muscle with a p-value less than 0.05 are presented in Figure 6. The FXR/RXR and LXR/RXR activation pathways are the most significantly enriched pathways. Others are oxidative phosphorylation and mitochondria dysfunction.

3.52 Disease and Function Analysis

The IPA also categorizes DEGs into related diseases and functions. Some diseases and functions with a p-value less than 10^{-5} and the number of representative genes involved are listed in Figure

7 and Table 1. The full list of all diseases and functions categories and the genes involved is included in Supplementary Table 3. Those functions related to lipid metabolism include disorder of lipid metabolism (P-value 1.40E-08) which is activated in the white fillet group, and uptake of lipids (P-value 1.59E-05) which is inhibited in the white fillet group. Others related to immunity with a p-value less than 0.05 include infiltration by neutrophils and cellular infiltration by phagocytes, both inhibited in the white fillet group.

Table 1. Top diseases and functions annotations identified by IPA

Categories	Diseases or Functions Annotation			p-value	# Genes
Lipid Metabolism	Metabolic Disease	Organismal Injury and Abnormalities,	Disorder of lipid metabolism	1.40E-08	17
Lipid Metabolism	Molecular Transport	Small Molecule Biochemistry	Uptake of lipid	1.59E-05	10
Molecular Transpo	Small Molecule Biochemistry		Accumulation of lipid	5.47E-07	17
Lipid Metabolism	Small Molecule Biochemistry	Vitamin and Mineral Metabolism	Metabolism of retinoid	2.97E-04	5
Lipid Metabolism	Small Molecule Biochemistry	Vitamin and Mineral Metabolism	Synthesis of cholesterol	6.31E-05	6
Lipid Metabolism	Molecular Transport	Small Molecule Biochemistry	Transport of phospholipid	2.62E-05	6
Lipid Metabolism	Molecular Transport	Small Molecule Biochemistry	Transport of steroid	2.71E-10	15
Lipid Metabolism	Molecular Transport	Small Molecule Biochemistry	Secretion of cholesterol	4.68E-10	7
Lipid Metabolism	Small Molecule Biochemistry		Homeostasis of lipid	1.29E-09	15
Lipid Metabolism	Small Molecule Biochemistry		Fatty acid metabolism	1.93E-09	27
Lipid Metabolism	Molecular Transport	Small Molecule Biochemistry	Transport of lipid	2.14E-09	17
Lipid Metabolism	Molecular Transport	Small Molecule Biochemistry	Flux of lipid	3.31E-09	13
Lipid Metabolism	Molecular Transport	Small Molecule Biochemistry	Cholesterol transport	3.49E-09	13
Lipid Metabolism	Molecular Transport	Small Molecule Biochemistry	Efflux of lipid	1.90E-08	12
Lipid Metabolism	Molecular Transport	Small Molecule Biochemistry	Concentration of lipid	2.63E-08	32
Lipid Metabolism	Small Molecule Biochemistry	Vitamin and Mineral Metabolism	Homeostasis of cholesterol	3.38E-08	10
Lipid Metabolism	Molecular Transport	Small Molecule Biochemistry	Excretion of lipid	4.04E-08	7
Lipid Metabolism	Molecular Transport	Small Molecule Biochemistry	Flux of cholesterol	7.53E-08	11
Lipid Metabolism	Small Molecule Biochemistry	Vitamin and Mineral Metabolism	Steroid metabolism	1.09E-07	15
Lipid Metabolism	Molecular Transport	Small Molecule Biochemistry	Excretion of sterol	4.28E-07	5
Lipid Metabolism	Molecular Transport	Small Molecule Biochemistry	Accumulation of lipid	5.47E-07	17
Lipid Metabolism	Molecular Transport	Small Molecule Biochemistry	Efflux of cholesterol	6.26E-07	10
Lipid Metabolism	Molecular Transport	Small Molecule Biochemistry	Uptake of cholesterol	7.27E-07	7
Lipid Metabolism	Small Molecule Biochemistry		Synthesis of lipid	9.53E-07	27
Lipid Metabolism	Molecular Transport	Small Molecule Biochemistry	Absorption of cholesterol	1.12E-06	6

3.53 KEGG Pathways and GO Terms in the Muscle

In the muscle, the KEGG pathways enriched for the upregulated genes in the white versus red fillet group, as shown in Figure 8, include metabolic pathways (122 genes), ascorbate and aldarate metabolism (6 genes), lysine degradation (11 genes), glycerophospholipid metabolism (15 genes), pentose and glucuronate interconversions (6 genes), FoxO signaling pathway (23 genes), glycerolipid metabolism (10 genes) and insulin signaling pathway (18 genes).

Several GO terms are significantly enriched for this group. The most significant terms involved in the biological process, as shown in Figure 9 and Supplementary Table 2, include complement activation, humoral immune response, immune effector process, hemostasis, activation of the immune response, regulation of body fluid levels, blood coagulation, positive regulation of immune response, coagulation, wound healing, positive regulation of immune system process, regulation of response to stimulus, response to wounding, regulation of blood coagulation, regulation of hemostasis, phosphorylation, lipid transport, lipid localization, regulation of immune response, and regulation of stress response.

The most significant GO terms for cellular components in this group, as shown in Figure 10, include extracellular space, MLL1/2 complex, MLL1 complex, histone methyltransferase complex, SWI/SNF superfamily-type complex, ATPase complex, methyltransferase complex, nucleoplasm, and transferase complex. Others are listed in Supplementary Table 2.

Some of the most significant molecular function terms for this group are Endopeptidase inhibitor activity, peptidase regulator activity, endopeptidase regulator activity, peptidase inhibitor activity, enzyme regulator activity, serine-type endopeptidase inhibitor activity, transition metal ion binding, protein serine/threonine kinase activity, protein kinase activity, oxidoreductase activity, acting on the CH-NH group of donors, NAD or NADP as acceptor, histone-lysine N-methyltransferase activity, histone methyltransferase activity, transferase activity, and transferring phosphorus-containing groups as shown in Figure 11. Others are listed in Supplementary Table 2.

For the downregulated genes between the white versus red fillet group, the KEGG pathways enriched are ribosome (85 genes), oxidative phosphorylation (61 genes), proteasome (21 genes), cardiac muscle contraction (20 genes), metabolic pathways (131 genes) and spliceosome (21 genes) as shown in Figure 12.

Several GO terms are significantly enriched for this group. The most significant terms involved in the biological process, as shown in Figure 13 and Supplementary Table 2, include peptide biosynthetic process, translation, peptide metabolic process, amide biosynthetic process, electron transport chain, ATP metabolic process, proton transmembrane transport, nucleoside triphosphate biosynthetic process, purine nucleoside triphosphate metabolic process, ATP biosynthetic process, oxidative phosphorylation, respiratory electron transport chain, mitochondrial respiratory chain complex assembly, and mitochondrial ATP synthesis coupled electron transport.

Most significant cellular components include ribosome, non-membrane-bounded organelle, mitochondrion, mitochondrial inner membrane, ribosomal subunit, ribonucleoprotein complex, mitochondrial envelope and respirasome (Figure 14, and Supplementary Table 2).

The most significant molecular function GO terms are structural constituent of ribosome, oxidoreduction-driven active transmembrane transporter activity, proton transmembrane transporter activity, electron transfer activity, cytochrome-c oxidase activity, oxidoreductase activity, acting on a heme group of donors, primary active transmembrane transporter activity, threonine-type endopeptidase activity, RNA binding, NADH dehydrogenase activity, NAD(P)H dehydrogenase (quinone) activity, NADH dehydrogenase (ubiquinone) activity, calcium ion binding, inorganic molecular entity transmembrane transporter activity, ion transmembrane transporter activity, phospholipase inhibitor activity, lipase inhibitor activity, active transmembrane transporter activity and transporter activity (Figure 15, and Supplementary Table 2).

4.0 Discussion

This study investigated molecular mechanisms influencing fillet color and the utilization of carotenoids in rainbow trout. We compared the transcriptome profile in the pyloric caecum, liver, and muscle of rainbow trout groups with 'white' versus 'red' fillets. Fish in both groups were fed astaxanthin supplemented diet. More DEGs exist in the muscle and liver than in the pyloric cecum. Metabolism of carotenoids is closely linked to lipid and fatty acid metabolism (von Lintig et al., 2020), and in agreement with this, several DEGs are involved in lipid metabolism and transport. Other DEGs have immune-related functions and are involved in stress homeostasis (Supplementary Table 1). Carotenoid absorption mainly occurs in the pyloric caecum, followed by metabolism in the liver and deposition in the muscle. The correlation between saturation index and body weight is 0.438 in our data, but the effect of body weight did not confound our result (analysis not shown here). The genetic line used for this study was selected for muscle yield, but the correlation between muscle yield and saturation index is low (0.021). How the brighter reddish fillet color selection affects muscle yield would need more investigation.

4.1 Pyloric cecum

The stonustoxin subunit beta-like (1256.28 FC) gene is the most upregulated gene in the pyloric cecum of the white fillet group in this study. LeBlanc et al. (2010) identified stonustoxin as one of the innate immune response genes upregulated in the head-kidney of Atlantic salmon injected with salmon anemia virus (ISAV) relative to the control Atlantic salmon. At the opposite end of the DEGs, the most downregulated genes are the protein *RD3* (retinal degeneration 3 (-439.07 FC) and *uromodulin* (-186.4 FC). Uromodulin protects against urinary tract infections and is an antioxidant (Schaeffer et al., 2021). It is also known that carotenoid pigments are found in the retina, acting as an antioxidant and free radical scavenger to reduce oxidative stress-induced damage (Lima et al., 2016).

4.11 Absorption of carotenoids

Carotenoids are insoluble in water and are thus absorbed and transported through their incorporation into lipids and fatty acids (von Lintig et al., 2020) by forming mixed micelle in the gut after their release from the ingesta(Bohn et al., 2019). Differences in the pigmentation between the white and red fillet groups could result from the difference in their ability to absorb, metabolize and utilize carotenoids inside the pyloric cecum. A higher content of lipase and bile fosters micellization (Bohn et al., 2017), as well as the presence of lipids in the diet (Borel, 2003). In this study, genes such as lipid droplet assembly factor, apolipoprotein B-100 (-9.6 FC), and ELOVL fatty acid elongase 6 (-37.51 FC) are downregulated in the white fillet group in the pyloric cecum probably conferring advantage to the red fillet group in their ability to form mixed micelle with astaxanthin. Although long-chain-fatty-acid--CoA ligase 3 (13.54 FC) and fatty-acid amide hydrolase 1 (4.75 FC) are also enriched in the white fillet group. Several genes involved in lipid and fatty acid metabolism were also identified to be differentially expressed in the muscle and liver. The *FXR* (farnesoid X receptor) and *HNF4-alpha* function in tandem to regulate bile acid synthesis (Chiang, 2009). Bile acids facilitate intestinal absorption and transport of lipids and other nutrients. The hepatocyte nuclear factor 1-alpha (*HNF4-alpha*) (2.29 FC) is upregulated in the pyloric cecum of the red fillet group. This upregulation might be advantageous to micellization and absorption of astaxanthin and lipid in the red fillet group. The *PPARα* (peroxisome proliferator-activated receptor α) is also reported to regulate bile acid synthesis (Chiang, 2009). The *HNF4-alpha*, *HNF4-beta*, and *PPARα* are differentially expressed in the liver and muscle.

The mixed micelles then diffuse through the mucus layer of the enterocyte, ready for absorption. Carotenoid absorption in the intestine was previously considered as a passive transport (Hollander & Ruble, 1978). However, the identification of several membrane proteins/transporters, such as CD36 and scavenger receptors, suggest otherwise (During et al., 2005; Sun, 2012). We identified that the *cd36 antigen* (-2.3 FC) is less expressed in the white fillet fish's pyloric cecum than those in the red fillet group. The *cd36 antigen* plays a role in carotenoid uptake by the intestinal cells (Reboul, 2019). They facilitate the absorption of carotenoids across the brush border membrane of the enterocyte. This suggests that the red fillet group possesses a more remarkable ability to absorb and transport astaxanthin. *CD36* was upregulated in the pyloric cecum of Atlantic salmon fed supplemented astaxanthin compared to fish fed a control diet (Schmeisser et al., 2021).

Genetic polymorphisms in the ELOVL fatty acid elongase 2 plays a significant role in carotenoid absorption in human (Borel et al., 2015a, 2015b; Borel et al., 2014). ELOVL fatty acid elongase 6 (-37.5 FC) is downregulated in the pyloric cecum of the white filet group in this study.

The white fillet group showed higher expression in *NPC1L1 Intracellular cholesterol transporter 1,* as observed in the white Chinook fish in Madaro et al. (2020). The NPC1L protein specializes in cholesterol absorption into the cell and plays a critical role in lipid metabolism (Long et al., 2021). It has been identified as one of the proteins involved in the absorption and transport of carotenoids in human and fish studies (Bohn et al., 2019; Madaro et al., 2020). It might be that absorption of carotenoids with *NPC1L* is not as efficient as with *CD36* protein that is upregulated in the red fillet group.

4.12 Metabolism of Astaxanthin inside the Enterocyte

After the uptake of the carotenoid across the apical brush border membrane and inside the enterocyte, it is reported to undergo intracellular metabolism before traveling to the basolateral side of the cell (Bohn et al., 2019). Beta-carotene 15,15'- oxygenase 1 (*BCO1*) and beta, beta-carotene 9,10'- oxygenase (*BCO2*) are enzymes that cleave beta-carotene inside the enterocyte. *BCO1* cleaves beta-carotene at its central double bond to yield retinal (a precursor of retinol and retinoic acid), while beta-carotene undergoes eccentric cleavage by *BCO2* to yield apocarotenoids (Amengual et al., 2013). Although not enriched in the pyloric cecum in this study, both enzymes are upregulated in the muscle (10.46, 3.04 FC) of the white fillet group in this study. This enrichment in the white fillet group could have implications on the retention of carotenoids in the

muscle. Enrichment in the white fillet group suggests that instead of the astaxanthin being available to boost the muscle's color, it is broken down into retinol and its derivatives. *BCO1*(1.45 FC) in the liver is upregulated in the white fillet group, while *BCO2* is downregulated (-2.70 FC). Several studies including from our lab (Ahmed et al., 2022), have identified polymorphisms in the beta carotene genes associated with fillet color traits.

Retinol dehydrogenases are a group of enzymes involved in metabolizing vitamin A and carotenoids (Clugston & Blaner, 2014; Ross & Harrison, 2007). After cleavage of carotenoids by *BCO1* and *BCO2*, they are converted into all-trans-retinoic acid and retinol. All trans-retinoic acid and retinol are further converted into retinal by retinol dehydrogenases (Ross & Harrison, 2007). The short-chain dehydrogenase gene family can also achieve this oxidation to retinal in humans (Kumar et al., 2012; Napoli, 2000; Napoli, 2012). Retinol dehydrogenase 1 (*rdh1*) (2.43 FC) and dehydrogenase/reductase (SDR family) member 12 (3.60 FC) are upregulated in the pyloric caecum of the white fillet group in this study. This might suggest the availability of more retinoic acid and its derivatives in the white fillet group due to the activities of Beta-carotene 15,15'-oxygenase 1 (*BCO1*) and beta, beta-carotene 9,10'- oxygenase (*BCO2*). Similarly, retinoic acid receptor beta (4.37FC) is upregulated in the white fillet group. Contrary to our findings, *rdh3, rdh8*, and retinal dehydrogenase 2 (*aldh1a2*) were upregulated in the pyloric caecum of the Atlantic salmon fed astaxanthin-supplemented diet compared to those on the non-astaxanthin diet (Schmeisser et al., 2021). This discrepancy might be due to differences in the design of the two experiments, i.e., absence of supplemental astaxanthin in one group of fish in Schmeisser et al. (2021) compared to our study, where both the white and red fillet group were fed supplemental astaxanthin.

Carotenoids inside the enterocyte that *BCO1* and *BCO2* do not metabolize are transported into lipoproteins and translocated to the basolateral membrane of the enterocyte (Reboul, 2019). This process is suggested to be carried out by fatty acid transport proteins and fatty acid binding proteins (Reboul, 2019). The fatty acid-binding proteins bind carotenoids and transport them within the enterocyte. Gastrotropin (Fatty acid binding protein 6) is upregulated in the pyloric cecum (8.69 FC) and muscle (2.62, 10.07 FC) of the red fillet group in this study, possibly conferring an advantage to those fish in their ability to transport astaxanthin within the pyloric caecum and

muscle cells. Fatty acid transport binding proteins were upregulated in the pylorus of red Chinook fish compared to the white Chinook Salmon (Madaro et al., 2020).

The uncleaved beta-carotene and retinyl esters are then incorporated into chylomicrons and transported into the liver (Borel et al., 1998). Beta-carotene incorporation into chylomicron has been suggested to be under the regulation of enzymes microsomal TAG transfer protein (*MTP*), apoA-IV, secretion associated Ras-related GTPase 1B (*SAR1B*) and ATP binding cassette subfamily A member 1 (*ABCA1*) (Bohn et al., 2019; Borel et al., 2015a). Indeed, *ABCA1*(-5.71 FC) was downregulated in this study's pyloric cecum and muscle of the white fillet group. *ABCA1* catalyzes the efflux of intracellular cholesterol to apolipoprotein forming high-density lipoprotein and their translocation from the cytoplasm to the extracellular membrane and into the portal blood (Brunham et al., 2006). This suggests a better ability of the red fillet group to incorporate astaxanthin into chylomicron for transport into the liver. *Apolipoprotein B-100* (9.61 FC) is also upregulated in the pyloric caecum of the red fillet group. Apolipoprotein B-100 and apolipoprotein B-48 are components of lipoproteins that transport fat and cholesterol in the form of chylomicron and very low-density lipoproteins into the blood to the liver (Olofsson & Boren, 2005). Madaro et al. (2020) also identified upregulation of ApoA-IV in the red Chinook salmon compared to white Chinook salmon suggesting more stabilization and transport of astaxanthin. Single nucleotide polymorphisms close to the *Apo* genes are also associated with flesh pigmentation in Chinook salmon (Lehnert, 2016).

4.2 Liver

On getting to the liver, chylomicrons containing carotenoids and retinyl esters are taken up by the hepatocytes through the action of cell surface several receptor proteins, including the low-density lipoprotein receptor (*LDLR*), low-density lipoprotein receptor-related protein 1 (*LRP1*), heparan sulfate proteoglycans (*HSPGs*) in human (Dallinga-Thie et al., 2010). The *LRP1* (-1.59 FC), *LRP10* (-2.18 FC), *LRP6* (-1.51, -178 FC), and *basement membrane-specific heparan sulfate proteoglycan core protein* (-2.06, -3.56 FC) were downregulated in the white fillet group in this study. *LRP1b* (3.07 FC) is upregulated in the white fillet group. This synchronized expression might suggest a comparative advantage to the red fillet group in their ability to take up chylomicrons inside the hepatocyte.

Following chylomicron uptake in the liver by cell surface receptors, carotenoids and retinyl palmitate is assumed to be released into the hepatocytes (Bohn et al., 2019). Ong (1982) suggested that retinyl palmitate is hydrolyzed by retinyl ester hydrolase to retinol and bound to retinol-binding protein, type 1 (*RBP1*). Retinol-binding protein 1 (1.44 FC), Retinol binding protein 7b, cellular (3.27 FC), and retinol-binding protein 2 (2.84 FC) are all upregulated in the white fillet group, suggesting higher availability of retinol from carotenoid cleavage. Retinol-binding proteins are involved in the intracellular transport of retinol. The beta carotene enzymes (*BCO1* and *BCO2*) in the liver can cleave carotenoids into retinal (Shmarakov et al., 2010). While *BCO1* (1.46 FC) is upregulated in the white fillet group, *BCO2* (-2.71 FC) is downregulated, unlike in the muscle, where both are differentially expressed in the same direction. Similar findings were reported by Madaro et al. (2020), where they found *BCO2* was upregulated in Chinook salmon with white phenotype, while *BCO1* was downregulated in the same phenotype group. The un-cleaved fraction of carotenoids is either stored in the hepatic stellate cells or incorporated into very low-density lipoprotein (VLDL) and secreted into the blood for transport to other tissues(Lakshman et al., 1989; Shmarakov et al., 2010).

There are no significant KEGG and GO terms in the liver for the downregulated genes. The significant KEGG pathways for the DEGs in the white versus red fillet group are ribosome and oxidative phosphorylation. It is known that oxidative phosphorylation occurs in the mitochondria, and mitochondrial activities can influence fillet color. Similarly, ribosomal activities have also been associated with fillet color in fish and skin pigmentation in mice (McGowan et al., 2008; Xiang et al., 2023; Zhang & Xie, 2019). The most significant GO terms for this group also relate to ribosome and mitochondrial activities.

4.3 Muscle

It has been suggested that astaxanthin is brought to the muscle by circulating albumin (Rajasingh et al., 2006). A radioactive study in Atlantic salmon suggested that astaxanthin is transported in the plasma via its association with serum albumin (Aas et al., 1999). Vo et al.(2021) also found upregulation of *albumin 2* in the gut of the more intense red-fleshed Atlantic salmon compared to the light-fleshed salmon. They suggested that this upregulation might confer an advantage to the red-fleshed salmon in their ability to absorb and transport astaxanthin from the gut into the blood and deposit it in the liver and muscle. In the same vein, *albumin 1* (1.89 FC) is upregulated in the

liver of the red fillet group, and this might aid in transporting carotenoids from the liver to the plasma and the muscle.

On getting to the muscle, Thomas & Harrison (2016) proposed that the extra-hepatic tissues take up the VLDL-carotenoids in an LDL-receptor-dependent manner, requiring the tissue to express LDL-receptors. In line with that proposition, low-density lipoprotein receptor-related protein 2b (*LRP2B*) (-3.27), low-density lipoprotein receptor-related protein 2a (*LRP2A*) (-3.37 FC), low-density lipoprotein receptor-related protein 1Ba (*LRP1BA*) (-11.73 FC) are downregulated in the muscle of the white fillet group in this study. Although, low-density lipoprotein receptor-related protein 4 (*LRP4*) (2.61 FC) and low-density lipoprotein receptor adaptor protein 1a (*ldlrap1a*) (2.18 FC) are upregulated in the white fillet group muscle.

Within the muscle cell, astaxanthin is deposited in the myotome and binds with actomyosin to form a complex in salmon (Rajasingh et al., 2006). Several genes involved in actomyosin structure organization (GO: 0031032) and members of their families are modulated in the muscle in this study, as stated in the results.

Schmeisser et al.(2020) suggested that astaxanthin recruits coronin for its transport inside muscle cells via actin network polymerization. They found *coronin* to be upregulated in the muscle of Atlantic salmon fed an astaxanthin-supplemented diet. Similarly, *coronin-2B* (1.61 FC) and *Coronin-1C* (18.77 FC) are both upregulated in the red fillet group muscle in this study.

Two of the most significantly enriched canonical pathways identified in the muscle are the FXR/RXR and LXR/RXR activation pathways. Studies have shown that carotenoids and their metabolites, like retinol and all-trans-retinoic acid (ATRA), can alter gene expression (Kaulmann & Bohn, 2014; Piga et al., 2014) through their interaction with nuclear receptors, including retinoic acid receptor (RAR) and retinoid X receptor (RXR) in human (Ben-Dor et al., 2001; Bohn et al., 2019; Prakash et al., 2004). The LXR/RXR activation pathway is activated in the white versus red fillet group DEGs. This might suggest more availability of retinoids in the white fillet group due to the breakdown of astaxanthin.

Other top canonical pathways are oxidative phosphorylation and mitochondria dysfunction. The result shows that oxidative phosphorylation is inhibited in the white fillet group, and mitochondrial dysfunction is activated in the same group. Disorder of mitochondrial function in the white fillet

group may be contributing to the lesser intensity of fillet color observed in the white fillet group. Mitochondrial dysfunction is a precursor to increased oxidative stress caused by the release of ROS (reactive oxygen species) and RNS (reactive nitrogen species). Reactive oxygen species and oxidative stress can deteriorate lipids, adversely affecting fillet color (Sampels, 2013; Scaife et al., 2000). The lysine degradation pathway, a KEGG pathway identified in the muscle, is confined to the mitochondria (Leandro & Houten, 2020), and mitochondria function can affect fillet color.

Regarding oxidative stress, ascorbate metabolism and FoxO signaling pathways are identified KEGG pathways enriched in the muscle. Ascorbate metabolism can be a free radical scavenger (Smirnoff, 2018). The FoxO signaling pathway also confers resistance to oxidative stress (Akasaki et al., 2014; Essers et al., 2004).

Oxidative phosphorylation is identified by both the KEGG pathway and IPA analysis. IPA analysis showed that oxidative phosphorylation is inhibited in the white fillet group. From the identified KEGG and GO terms enriched in the downregulated genes between the white and red fillet group, it is evident that activities in ribosomes and mitochondria are prevalent. Ribosomal activities have been associated with fillet color in fish and skin pigmentation in mice (McGowan et al., 2008; Xiang et al., 2023; Zhang & Xie, 2019). Ribosomal proteins in the proteome were identified as proteins whose change is associated with fillet color in grouper fish and tilapia (Xiang et al., 2023; Zhang & Xie, 2019). The role of mitochondria activity in fillet color change, especially during storage, via their actions on increasing mitochondrial respiration, function oxygen consumption, and metmyoglobin reduction has been reported in various fish species and cattle (Ramanathan et al., 2019; Singh et al., 2022; Xiang et al., 2023). Notably, ribosomal and mitochondrial activity pathways are identified in both the liver and muscle DEGs.

The IPA result also shows that there is a disorder of lipid metabolism in the white fillet group. Uptake and accumulation of lipids are inhibited in the white fillet group. As discussed above, carotenoid metabolism and utilization are closely linked with lipid metabolism; therefore, pathways and functions that inhibit the uptake and accumulation of lipids will likely inhibit the accumulation and use of carotenoids.

Concerning immunity, cellular infiltration by neutrophils, phagocytes, and leukocytes is inhibited in the white fillet group, as identified by the IPA analysis. This suggests an advantage to the red fillet group in having a better immune response. We also observed GO terms of certain biological

processes involved in the immune response in the muscle. They include complement activation, humoral immune response, immune effector process, hemostasis, activation of the immune response, blood coagulation, positive regulation of immune response, wound healing, positive regulation of immune system process, and regulation of response to stimulus.

4.6 Important Group/Class of Differentially Expressed Genes

We identified several DEGs groups that are relevant for carotenoid metabolism. One group is the Apolipoproteins, fatty acid elongases and ABC transporters. Another group is the immune and stress response genes. DEGs within each group and how they aid carotenoid metabolism and modulate stress and immune response are included in the supplementary file 4.

In summary, from our results, it appears that the ability to absorb and utilize carotenoids confer an advantage in terms of adaptation to stress. Likewise, we observed that several immune genes are modulated in this study, but more studies are needed to investigate whether it confers an advantage to the red fillet group regarding immunity.

5.0 Conclusion

We used comparative transcriptome analysis to investigate molecular mechanisms influencing the absorption and utilization of astaxanthin in the pyloric cecum, liver, and muscle of rainbow trout. We identified several genes involved in lipid/carotenoid metabolism and transport, ribosomal activities, mitochondrial functions, and stress homeostasis. The higher expression of BCO1 and BCO2 in the liver and muscle of the white fillet group suggests that these enzymes metabolize astaxanthin and reduces its availability for enriching fillet color. In addition to using carotenoid to boost fillet color, several immune-relevant and stress response genes were differentially expressed, suggesting astaxanthin's potential to provoke an immune response and be beneficial for managing stress.

List of Abbreviations

DEGs: Differentially Expressed Genes, NCCCWA: USDA National Center of Cool and Cold Water Aquaculture, FC: Fold change, GO: Gene Ontology, KEGG: Kyoto Encyclopedia of Genes and Genomes, IPA: Ingenuity Pathway Analysis, IPKB: Ingenuity pathway knowledge base, PCR: Polymerase Chain Reaction.

Ethics Declarations

Ethics approval and consent to participate

Husbandry practice and experimental procedures at the facility were approved by the IACUC animal study protocol of the University of Maryland, College Park, protocol number 1593175-6.

Availability of data and materials

All datasets generated for this study are included in the manuscript and/or the Additional Files. The raw RNA-seq data will be submitted to NCBI and released to the public upon acceptance of the manuscript.

Funding

This study was supported by competitive grants No. 2014-67015-21602, 2021-67015-33388, 2023-67015-39742 from the United States Department of Agriculture, National Institute of Food and Agriculture (M.S) and by the USDA, Agricultural Research Service CRIS Project 1930-31000-010 "Utilizing Genetics and Physiology for Enhancing Cool- and Cold-Water Aquaculture Production" (T.L.). The content is solely the authors' responsibility and does not necessarily represent the official views of any funding agents.

Authors' Information

Ridwan O. Ahmed,[1] Ali Ali,[1] Tim Leeds,[2], and Mohamed Salem[1, *]

[1]Department of Animal and Avian Sciences, University of Maryland, College Park, MD 20742, USA.

[2]United States Department of Agriculture Kearneysville, National Center for Cool and Cold Water Aquaculture, Agricultural Research Service, Kearneysville, WV 25430, USA.

Corresponding author

Correspondence to Mohamed Salem.

Figures, tables and additional files

Supplementary Information

Additional file 1: **Table S1:** Differentially expressed genes (DEGs) in the pyloric caecum, liver and muscle, and groups of DEGs. **Table S2:** KEGG and GO terms for DEGs in the liver and muscle. **Table S3**: Ingenuity Pathway Analysis (IPA) Diseases and Functions. Supplementary file 4: Important Group/Class of Differentially Expressed Genes.

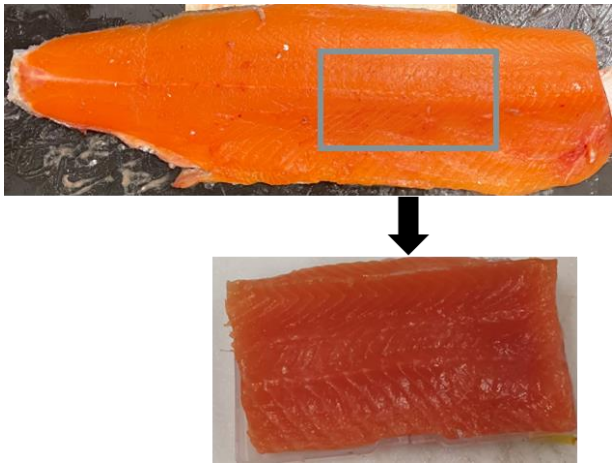

Figure 1. The region of the fillet from which the fillet color was measured.

Fig. 2

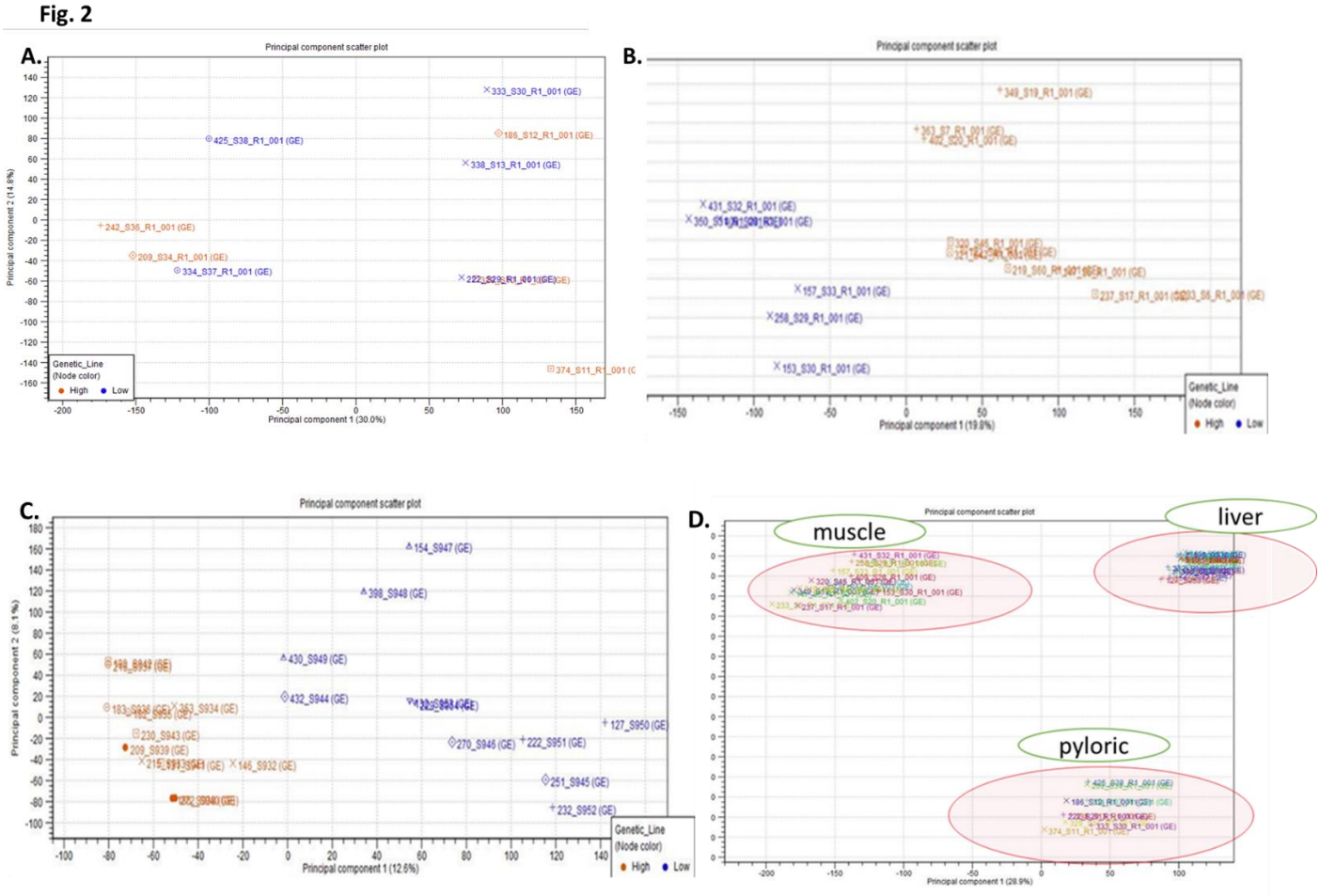

Figure 2a: Principal component analysis (PCA) performed on the gene expression data from pyloric caeca samples showing no apparent clustering. Figure 2b: PCA performed on the expression data of muscle samples showing the separation of the white (Low) and red (High) fillet groups. Figure 2c: PCA performed on the gene expression data of liver samples showing the separation of the white (Low) and red (High) fillet groups. Figure 2d: PCA performed on the expression data of pyloric cecum, liver, and muscle samples of rainbow trout. The PCA shows a clear separation of the three tissues.

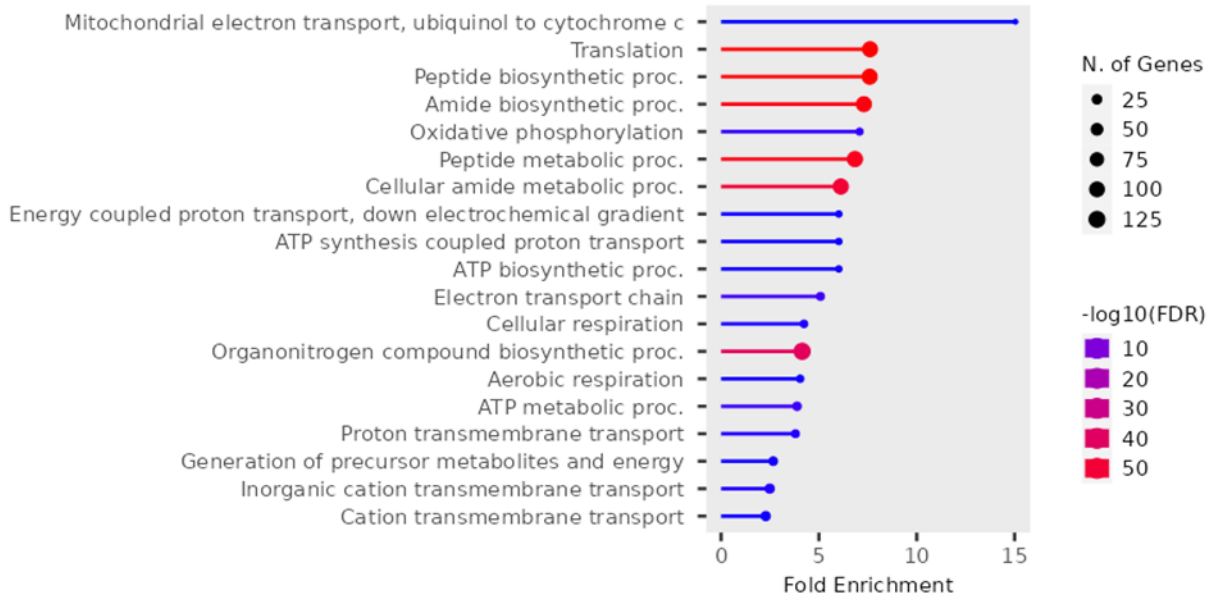

Figure 3. Enriched GO biological function terms for the upregulated genes in the liver comparing the white versus red fillet groups.

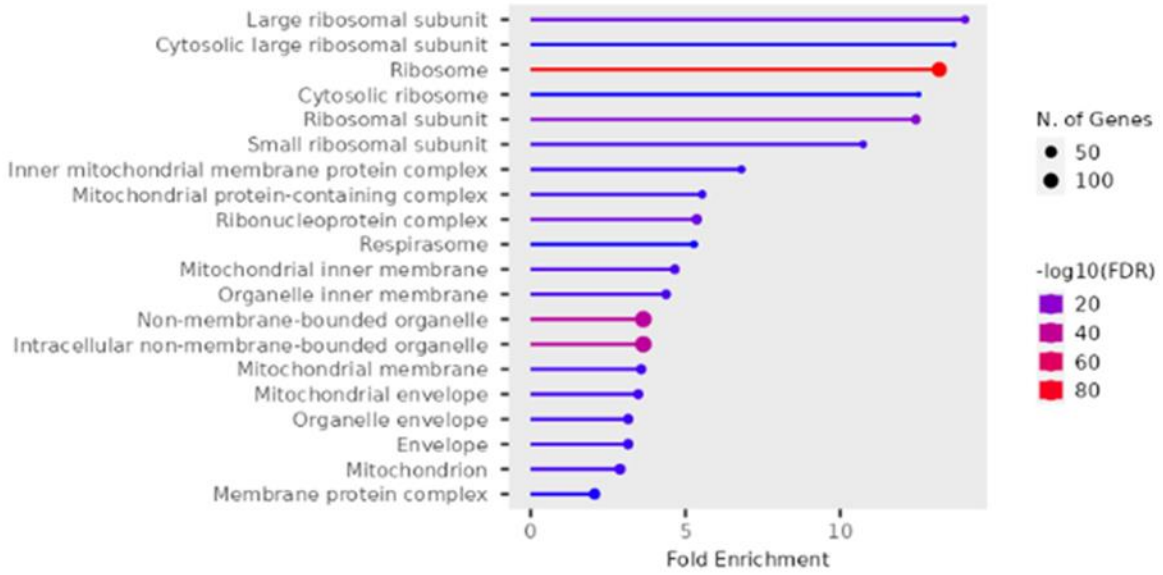

Figure 4. Enriched GO cellular function terms for the upregulated genes in the liver comparing the white versus red fillet groups.

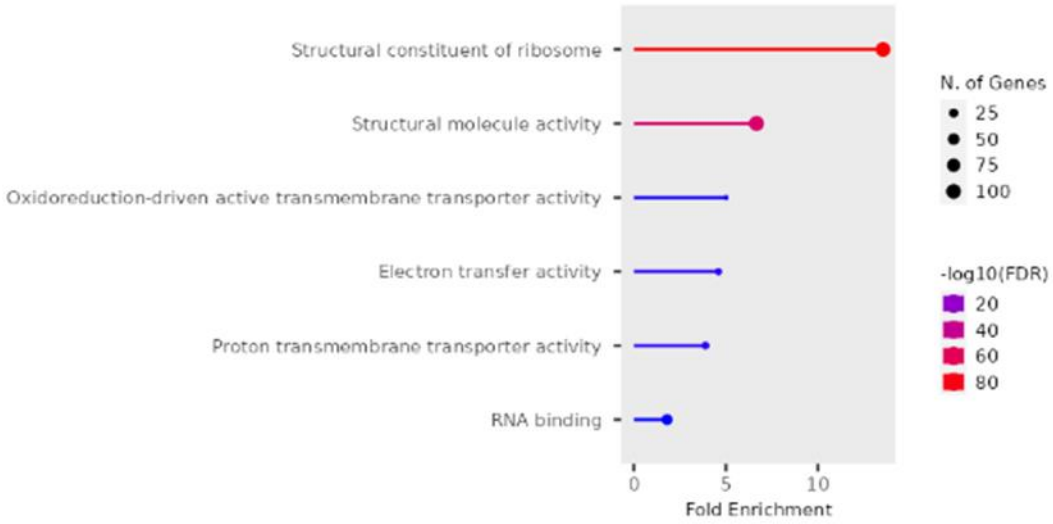

Figure 5. Enriched GO molecular function terms for the upregulated genes in the liver comparing the white versus red fillet groups.

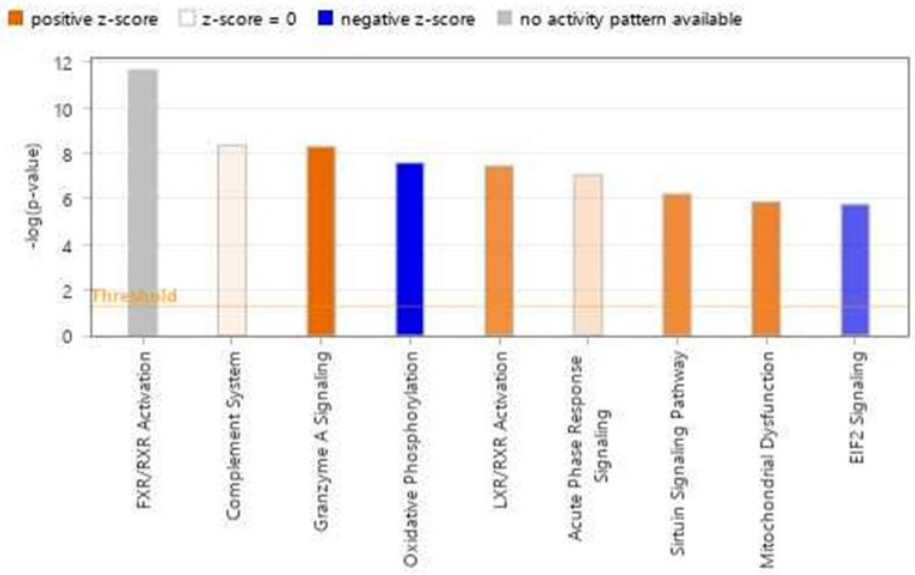

Figure 6. The topmost significant canonical pathways for the muscle DEGs

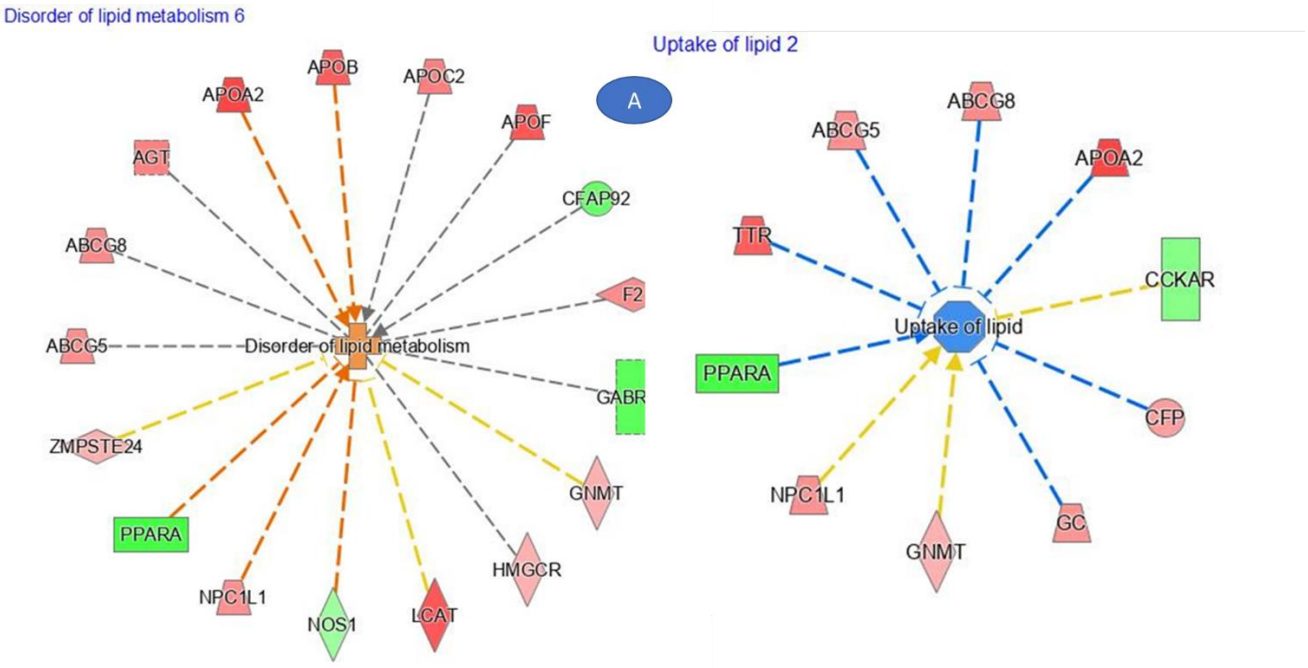

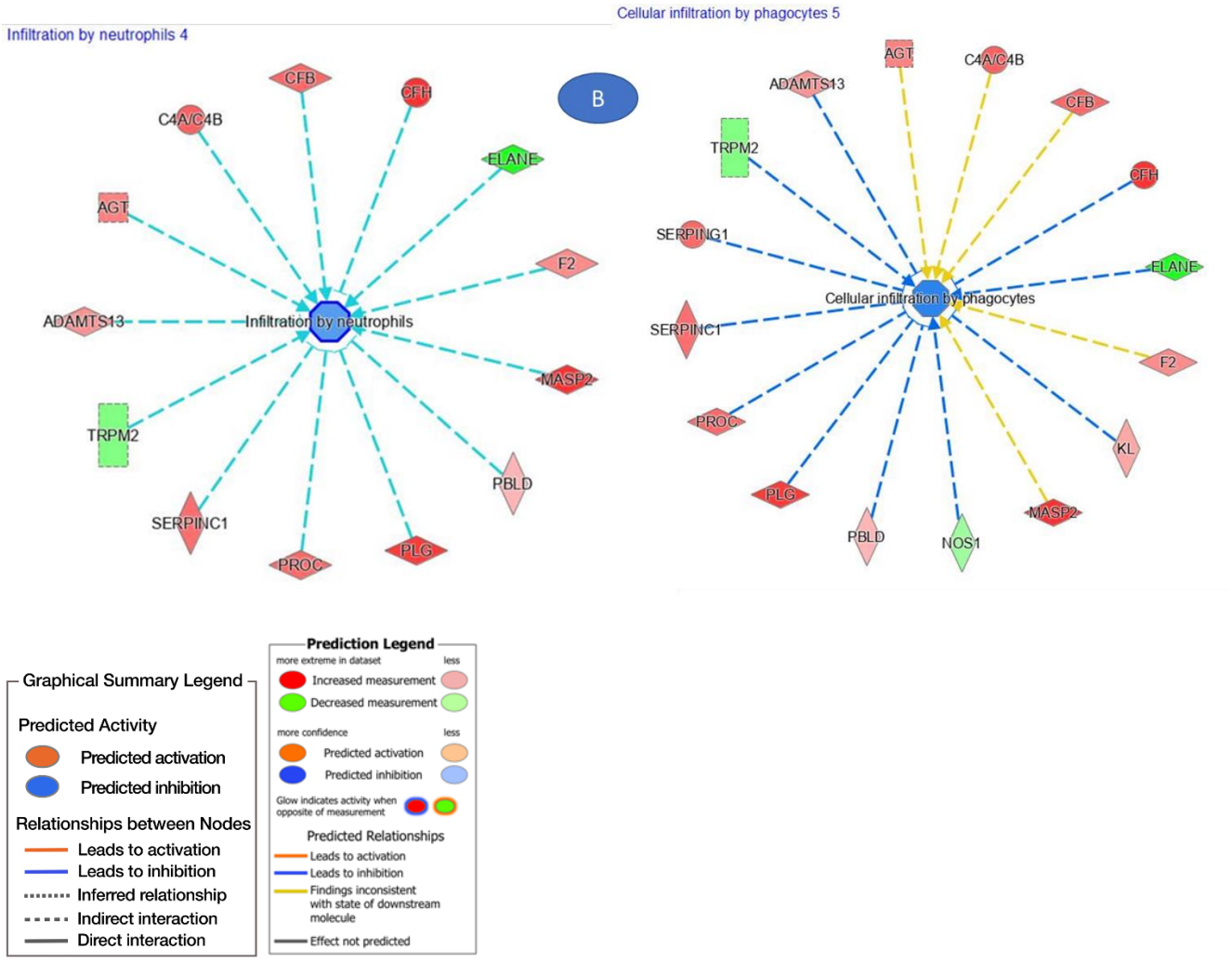

Figure 7. Modulated diseases and functions from the DEGs in the muscle a. Genes related to lipid metabolism b. Genes related to immunity.

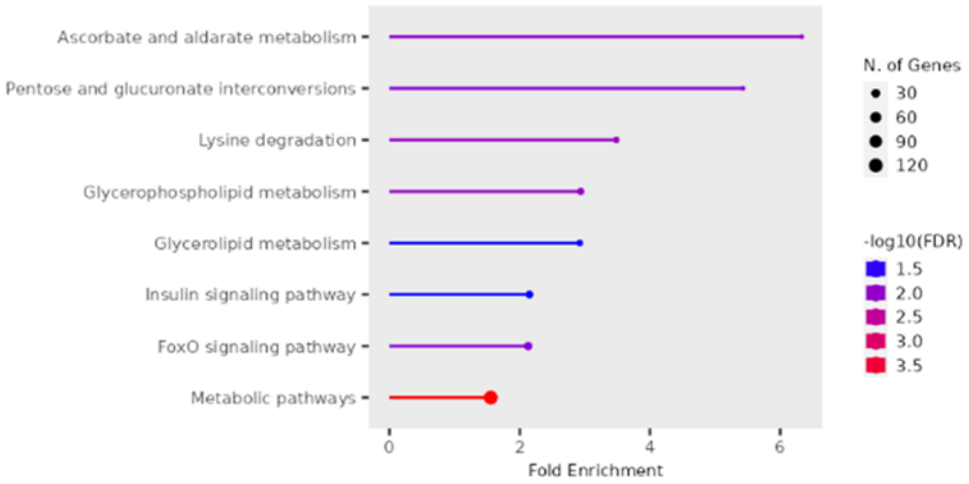

Figure 8. Enriched KEGG pathways for upregulated genes in the muscle comparing the white versus red fillet groups.

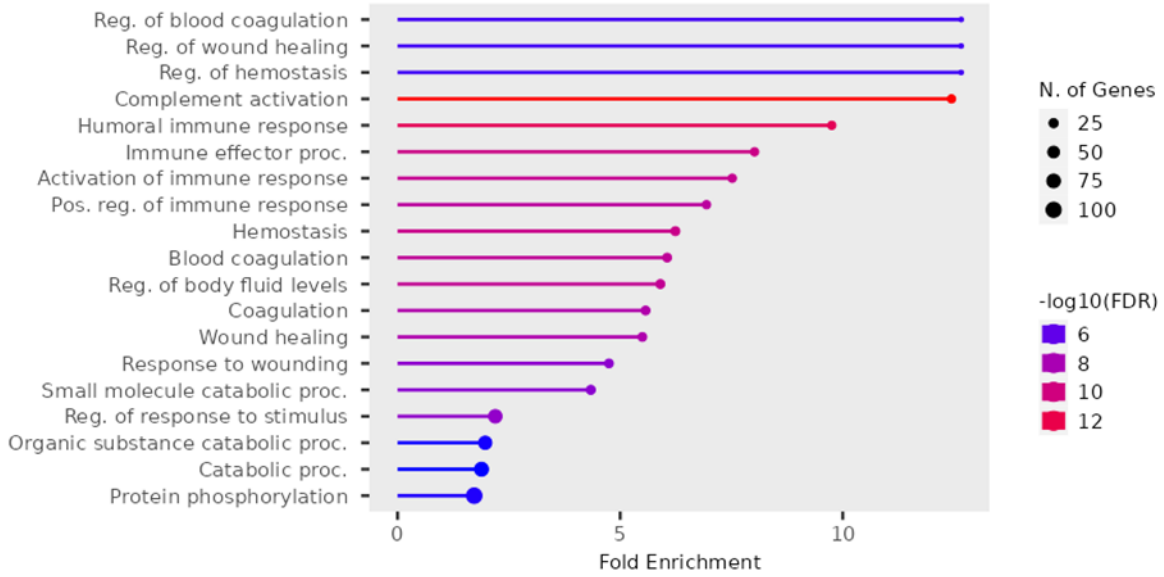

Figure 9. Enriched GO Biological process terms for the upregulated genes in the muscle comparing the white versus red fillet groups.

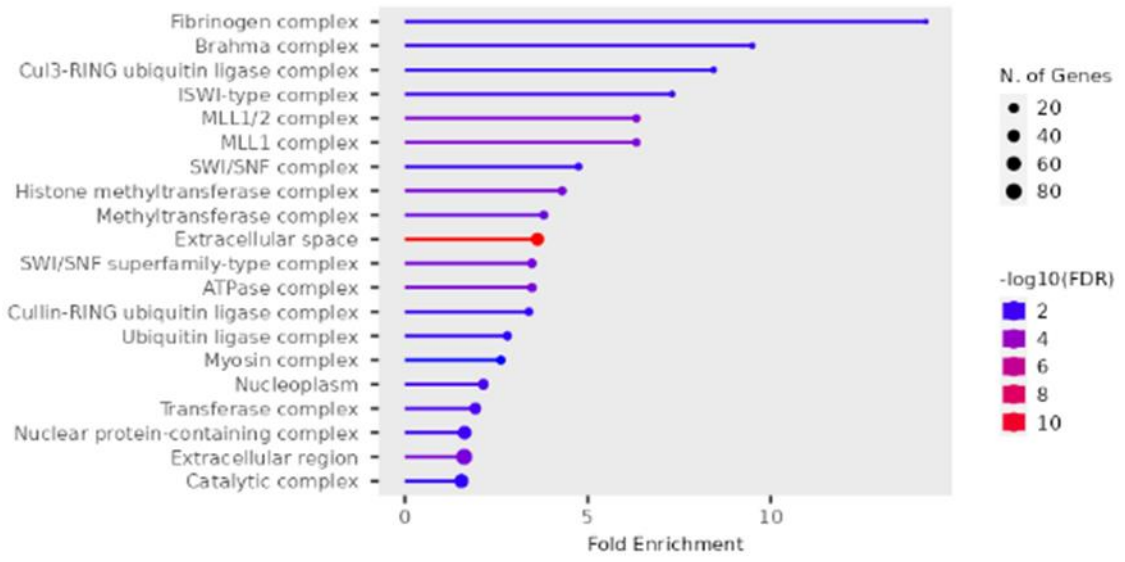

Figure 10. Enriched GO cellular component terms for the upregulated genes in the muscle comparing the white versus red fillet groups.

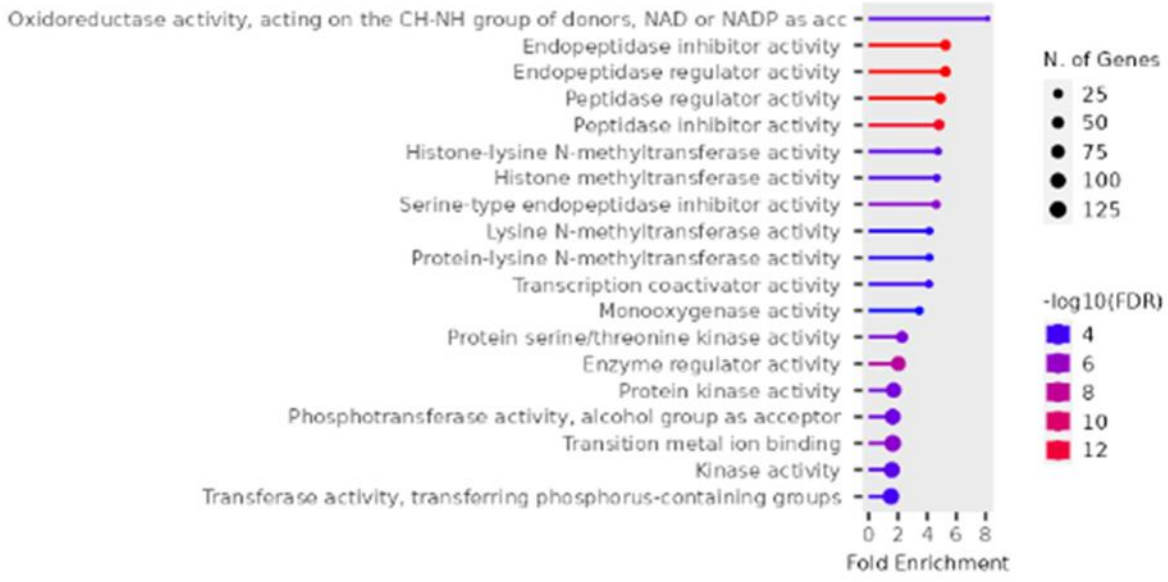

Figure 11. Enriched GO molecular function terms for the upregulated genes in the muscle comparison of the white versus red fillet groups.

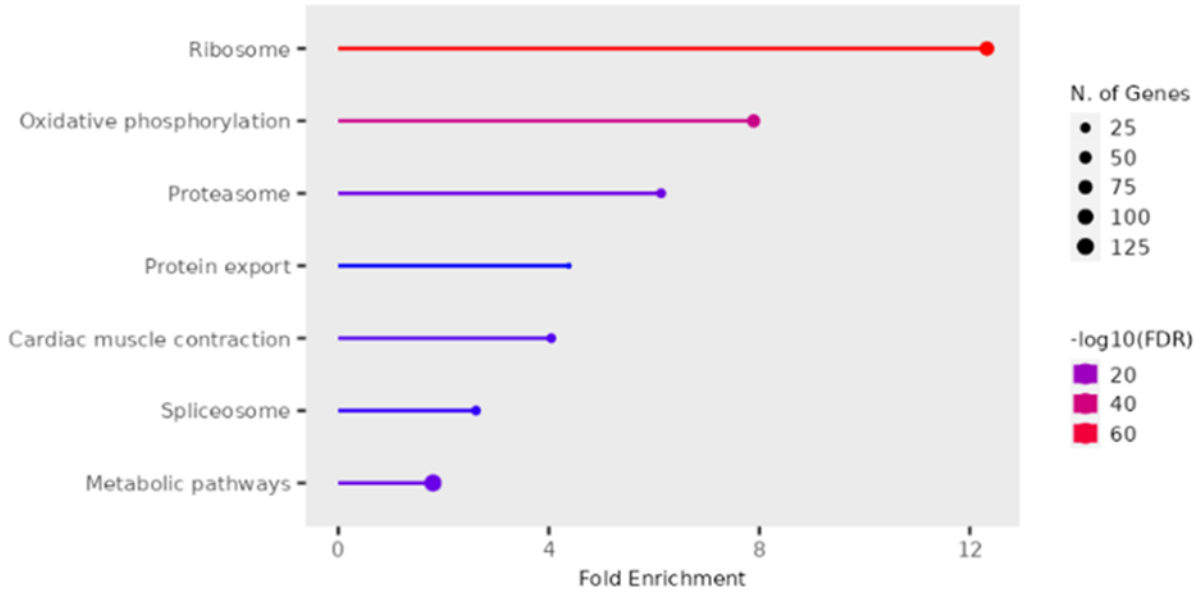

Figure 12. Enriched KEGG pathways for the downregulated genes in the muscle comparing the white versus red fillet group.

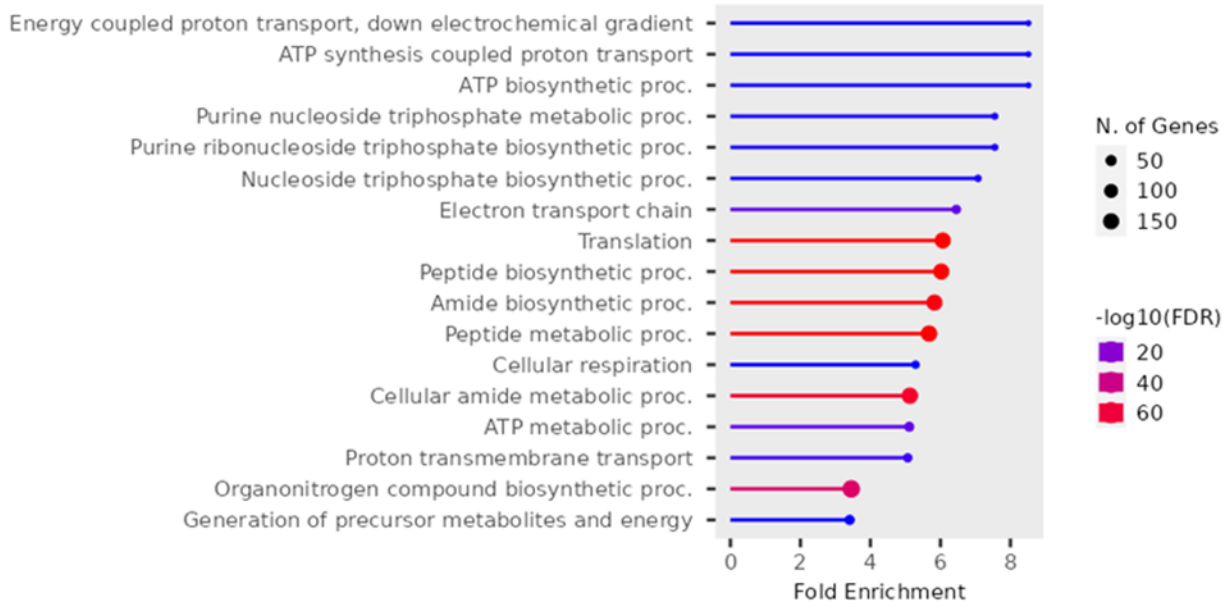

Figure 13. Enriched GO biological process for the downregulated genes in the muscle comparing white versus red fillet group.

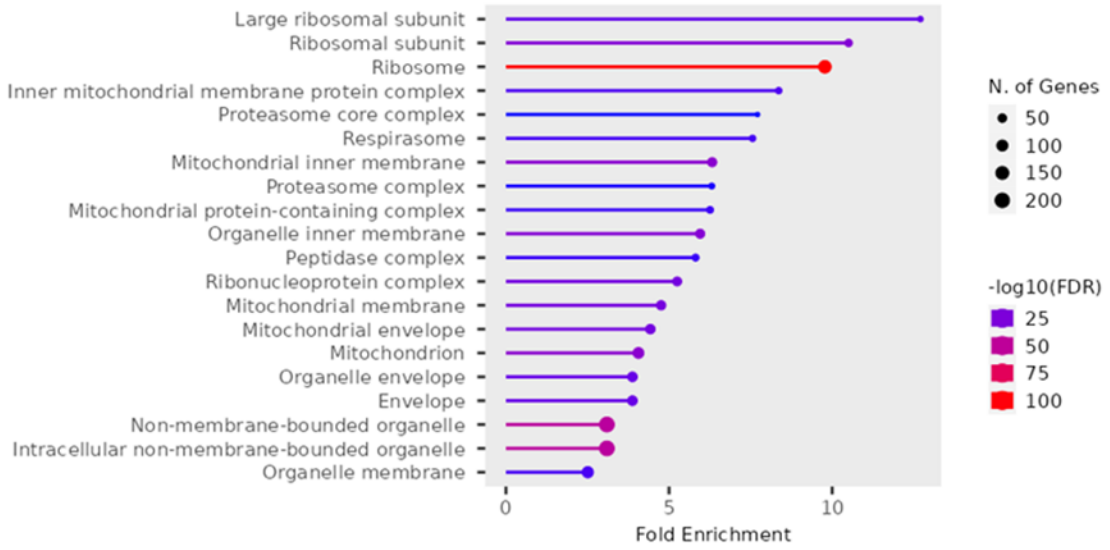

Figure 14. Enriched GO cellular component terms for the downregulated genes in the muscle comparing the white versus red fillet groups.

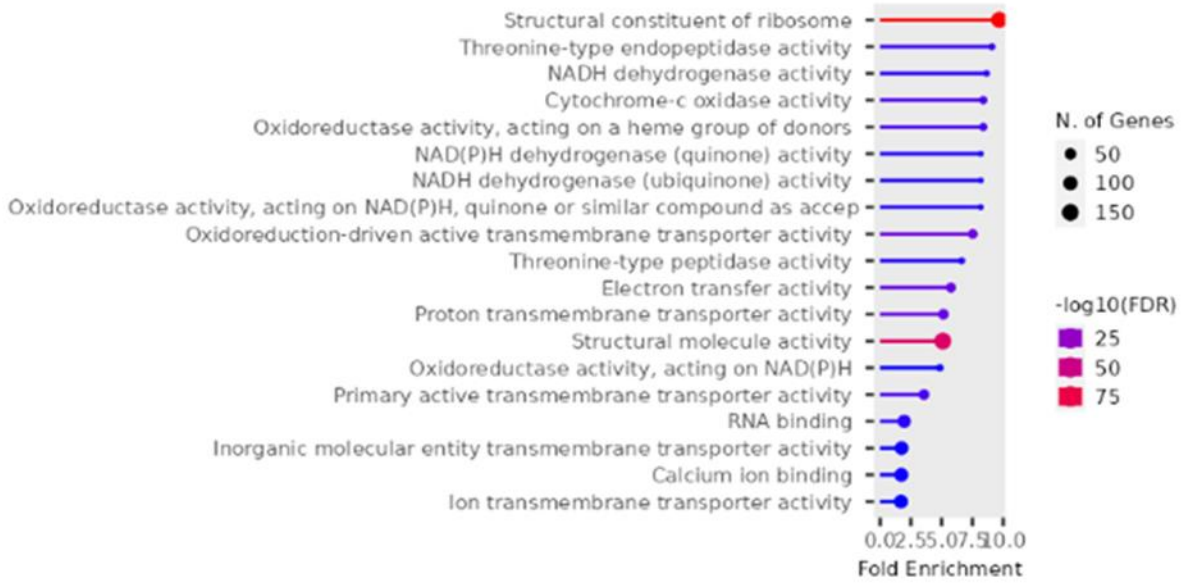

Figure 15. Enriched GO molecular function terms for the downregulated genes in the muscle comparing the white versus red fillet groups.

References

Aas, G., Bjerkeng, B., Storebakken, T., & Ruyter, B. (1999). Blood appearance, metabolic transformation and plasma transport proteins of 14C-astaxanthin in Atlantic salmon (Salmo salar L.). *Fish Physiology and Biochemistry*, *21*, 325-334.

Ahmed, R. O., Ali, A., Al-Tobasei, R., Leeds, T., Kenney, B., & Salem, M. (2022). Weighted Single-Step GWAS Identifies Genes Influencing Fillet Color in Rainbow Trout. *Genes*, *13*(8), 1331.

Akasaki, Y., Alvarez-Garcia, O., Saito, M., Caramés, B., Iwamoto, Y., & Lotz, M. K. (2014). FoxO transcription factors support oxidative stress resistance in human chondrocytes. *Arthritis & rheumatology*, *66*(12), 3349-3358.

Amengual, J., Widjaja-Adhi, M. A. K., Rodriguez-Santiago, S., Hessel, S., Golczak, M., Palczewski, K., & Von Lintig, J. (2013). Two Carotenoid Oxygenases Contribute to Mammalian Provitamin A Metabolism*♦. *Journal of Biological Chemistry*, *288*(47), 34081-34096.

Armstrong, G. A., & Hearst, J. E. (1996). Genetics and molecular biology of carotenoid pigment biosynthesis. *The FASEB Journal*, *10*(2), 228-237.

Association, A. M. S. (1991). Guidelines for meat color evaluation. proceedings: The 44th annual reciprocal meat conference. Kans, Chicago,

Ben-Dor, A., Nahum, A., Danilenko, M., Giat, Y., Stahl, W., Martin, H.-D.,…Sharoni, Y. (2001). Effects of acyclo-retinoic acid and lycopene on activation of the retinoic acid receptor and proliferation of mammary cancer cells. *Archives of Biochemistry and Biophysics*, *391*(2), 295-302.

Bjerkeng, B., Refstie, S., Fjalestad, K., Storebakken, T., Rødbotten, M., & Roem, A. (1997). Quality parameters of the flesh of Atlantic salmon (Salmo salar) as affected by dietary fat content and full-fat soybean meal as a partial substitute for fish meal in the diet. *Aquaculture*, *157*(3-4), 297-309.

Bjerkeng, B., Storebakken, T., & Liaaen-Jensen, S. (1992). Pigmentation of rainbow trout from start feeding to sexual maturation. *Aquaculture*, *108*(3-4), 333-346.

Bohn, T., Desmarchelier, C., Dragsted, L. O., Nielsen, C. S., Stahl, W., Rühl, R.,…Borel, P. (2017). Host-related factors explaining interindividual variability of carotenoid bioavailability and tissue concentrations in humans. *Molecular nutrition & food research*, *61*(6), 1600685.

Bohn, T., Desmarchelier, C., El, S. N., Keijer, J., van Schothorst, E., Rühl, R., & Borel, P. (2019). β-carotene in the human body: metabolic bioactivation pathways–from digestion to tissue distribution and excretion. *Proceedings of the Nutrition Society*, *78*(1), 68-87.

Borel, P. (2003). Factors affecting intestinal absorption of highly lipophilic food microconstituents (fat-soluble vitamins, carotenoids and phytosterols).

Borel, P., Desmarchelier, C., Nowicki, M., & Bott, R. (2015a). A combination of single-nucleotide polymorphisms is associated with interindividual variability in dietary β-carotene bioavailability in healthy men. *The Journal of Nutrition*, *145*(8), 1740-1747.

Borel, P., Desmarchelier, C., Nowicki, M., & Bott, R. (2015b). Lycopene bioavailability is associated with a combination of genetic variants. *Free Radical Biology and Medicine*, *83*, 238-244.

Borel, P., Desmarchelier, C., Nowicki, M., Bott, R., Morange, S., & Lesavre, N. (2014). Interindividual variability of lutein bioavailability in healthy men: characterization, genetic variants involved, and relation with fasting plasma lutein concentration. *The American journal of clinical nutrition*, *100*(1), 168-175.

Borel, P., Grolier, P., Mekki, N., Boirie, Y., Rochette, Y., Le Roy, B.,…Azais-Braesco, V. (1998). Low and high responders to pharmacological doses of β-carotene: proportion in the population, mechanisms involved and consequences on β-carotene metabolism. *Journal of lipid research*, *39*(11), 2250-2260.

Borel, P., Lietz, G., Goncalves, A., Szabo de Edelenyi, F., Lecompte, S., Curtis, P.,…Packard, C. (2013). CD36 and SR-BI are involved in cellular uptake of provitamin A carotenoids by Caco-2 and HEK cells, and

some of their genetic variants are associated with plasma concentrations of these micronutrients in humans. *The Journal of nutrition*, *143*(4), 448-456.

Brunham, L. R., Kruit, J. K., Iqbal, J., Fievet, C., Timmins, J. M., Pape, T. D.,…Groen, A. K. (2006). Intestinal ABCA1 directly contributes to HDL biogenesis in vivo. *The Journal of clinical investigation*, *116*(4), 1052-1062.

Chiang, J. Y. (2009). Bile acids: regulation of synthesis: thematic review series: bile acids. *Journal of lipid research*, *50*(10), 1955-1966.

Choubert, G., de la Noüe, J., & Blanc, J.-M. (1991). Apparent digestibility of canthaxanthin in rainbow trout: effect of dietary fat level, antibiotics and number of pyloric caeca. *Aquaculture*, *99*(3-4), 323-329.

Cleveland, B. M., Radler, L. M., & Leeds, T. D. Growth, fillet yield, and muscle quality traits are not affected by a genotype by diet interaction in rainbow trout consuming diets that differ in lipid content. *Journal of the World Aquaculture Society*.

Clevidence, B. A., & Bieri, J. G. (1993). [4] Association of carotenoids with human plasma lipoproteins. In *Methods in enzymology* (Vol. 214, pp. 33-46). Elsevier.

Clugston, R. D., & Blaner, W. S. (2014). Vitamin A (retinoid) metabolism and actions: What we know and what we need to know about amphibians. *Zoo biology*, *33*(6), 527-535.

Dallinga-Thie, G. M., Franssen, R., Mooij, H. L., Visser, M. E., Hassing, H. C., Peelman, F.,…Nieuwdorp, M. (2010). The metabolism of triglyceride-rich lipoproteins revisited: new players, new insight. *Atherosclerosis*, *211*(1), 1-8.

Deming, D. M., & Erdman, J. W. (1999). Mammalian carotenoid absorption and metabolism. *Pure and Applied Chemistry*, *71*(12), 2213-2223.

Denstadli, V., Vegusdal, A., Krogdahl, Å., Bakke-McKellep, A., Berge, G., Holm, H.,…Ruyter, B. (2004). Lipid absorption in different segments of the gastrointestinal tract of Atlantic salmon (Salmo salar L.). *Aquaculture*, *240*(1-4), 385-398.

Desmarchelier, C., & Borel, P. (2017). Overview of carotenoid bioavailability determinants: From dietary factors to host genetic variations. *Trends in Food Science & Technology*, *69*, 270-280.

During, A., Dawson, H. D., & Harrison, E. H. (2005). Carotenoid transport is decreased and expression of the lipid transporters SR-BI, NPC1L1, and ABCA1 is downregulated in Caco-2 cells treated with ezetimibe. *The Journal of nutrition*, *135*(10), 2305-2312.

Essers, M. A., Weijzen, S., de Vries-Smits, A. M., Saarloos, I., de Ruiter, N. D., Bos, J. L., & Burgering, B. M. (2004). FOXO transcription factor activation by oxidative stress mediated by the small GTPase Ral and JNK. *The EMBO journal*, *23*(24), 4802-4812.

Garcia, A., Tsuruta, S., Gao, G., Palti, Y., Lourenco, D., & Leeds, T. (2023). Genomic selection models substantially improve the accuracy of genetic merit predictions for fillet yield and body weight in rainbow trout using a multi-trait model and multi-generation progeny testing. *Genetics Selection Evolution*, *55*(1), 1-12.

Ge, S. X., Jung, D., & Yao, R. (2020). ShinyGO: a graphical gene-set enrichment tool for animals and plants. *Bioinformatics*, *36*(8), 2628-2629.

Goodwin, T. (1986). Metabolism, nutrition, and function of carotenoids. *Annual review of nutrition*, *6*(1), 273-297.

Hardy, R., Torrissen, O., & Scott, T. (1990). Absorption and distribution of 14C-labeled canthaxanthin in rainbow trout (Oncorhynchus mykiss). *Aquaculture*, *87*(3-4), 331-340.

Harrison, E. H. (2012). Mechanisms involved in the intestinal absorption of dietary vitamin A and provitamin A carotenoids. *Biochimica et Biophysica Acta (BBA)-Molecular and Cell Biology of Lipids*, *1821*(1), 70-77.

Helgeland, H., Sodeland, M., Zoric, N., Torgersen, J. S., Grammes, F., von Lintig, J.,…Våge, D. I. (2019). Genomic and functional gene studies suggest a key role of beta-carotene oxygenase 1 like (bco1l) gene in salmon flesh color. *Scientific reports*, *9*(1), 1-12.

Hollander, D., & Ruble Jr, P. E. (1978). beta-carotene intestinal absorption: bile, fatty acid, pH, and flow rate effects on transport. *American Journal of Physiology-Endocrinology and Metabolism*, *235*(6), E686.

Kaulmann, A., & Bohn, T. (2014). Carotenoids, inflammation, and oxidative stress—implications of cellular signaling pathways and relation to chronic disease prevention. *Nutrition research*, *34*(11), 907-929.

Krämer, A., Green, J., Pollard Jr, J., & Tugendreich, S. (2014). Causal analysis approaches in ingenuity pathway analysis. *Bioinformatics*, *30*(4), 523-530.

Kumar, S., Sandell, L. L., Trainor, P. A., Koentgen, F., & Duester, G. (2012). Alcohol and aldehyde dehydrogenases: retinoid metabolic effects in mouse knockout models. *Biochimica et Biophysica Acta (BBA)-Molecular and Cell Biology of Lipids*, *1821*(1), 198-205.

Kumari, S., Rajarani, A., Bansal, N., Dahuja, A., Praveen, S., Krishnan, V., & Kumar, S. (2019). Extraction and estimation of provitamin A carotenoids from carrot. *Omics meet Plant Biochemistry: Applications in nutritional enhancement with one health perspective*, *221*.

Lakshman, M., Asher, K., Attlesey, M., Satchithanandam, S., Mychkovsky, I., & Coutlakis, P. (1989). Absorption, storage, and distribution of beta-carotene in normal and beta-carotene-fed rats: roles of parenchymal and stellate cells. *Journal of Lipid Research*, *30*(10), 1545-1550.

Leandro, J., & Houten, S. M. (2020). The lysine degradation pathway: Subcellular compartmentalization and enzyme deficiencies. *Molecular Genetics and Metabolism*, *131*(1-2), 14-22.

LeBlanc, F., Laflamme, M., & Gagne, N. (2010). Genetic markers of the immune response of Atlantic salmon (Salmo salar) to infectious salmon anemia virus (ISAV). *Fish & Shellfish Immunology*, *29*(2), 217-232.

Leeds, T. D., Vallejo, R. L., Weber, G. M., Gonzalez-Pena, D., & Silverstein, J. T. (2016). Response to five generations of selection for growth performance traits in rainbow trout (Oncorhynchus mykiss). *Aquaculture*, *465*, 341-351.

Lehnert, S. J. (2016). *Why are salmon red? Proximate and ultimate causes of flesh pigmentation in Chinook salmon* University of Windsor (Canada)].

Lima, V. C., Rosen, R. B., & Farah, M. (2016). Macular pigment in retinal health and disease. *International journal of retina and vitreous*, *2*(1), 1-9.

Long, T., Liu, Y., Qin, Y., DeBose-Boyd, R. A., & Li, X. (2021). Structures of dimeric human NPC1L1 provide insight into mechanisms for cholesterol absorption. *Science Advances*, *7*(34), eabh3997.

Lubzens, E., Lissauer, L., Levavi-Sivan, B., Avarre, J.-C., & Sammar, M. (2003). Carotenoid and retinoid transport to fish oocytes and eggs: what is the role of retinol binding protein? *Molecular aspects of medicine*, *24*(6), 441-457.

Madaro, A., Torrissen, O., Whatmore, P., Lall, S. P., Schmeisser, J., Verlhac Trichet, V., & Olsen, R. E. (2020). Red and White Chinook Salmon (Oncorhynchus tshawytscha): differences in the transcriptome profile of muscle, liver, and pylorus. *Marine Biotechnology*, *22*(4), 581-593.

McGowan, K. A., Li, J. Z., Park, C. Y., Beaudry, V., Tabor, H. K., Sabnis, A. J.,…Myers, R. M. (2008). Ribosomal mutations cause p53-mediated dark skin and pleiotropic effects. *Nature genetics*, *40*(8), 963-970.

Napoli, J. (2000). Enzymology and biogenesis of retinoic acid. *Vitamin A and retinoids: An update of biological aspects and clinical applications*, 17-27.

Napoli, J. L. (2012). Physiological insights into all-trans-retinoic acid biosynthesis. *Biochimica et Biophysica Acta (BBA)-Molecular and Cell Biology of Lipids*, *1821*(1), 152-167.

Nickell, D., & Bromage, N. R. (1998). The effect of dietary lipid level on variation of flesh pigmentation in rainbow trout (Oncorhynchus mykiss). *Aquaculture*, *161*(1-4), 237-251.

No, H. K., & Storebakken, T. (1991). Pigmentation of rainbow trout with astaxanthin at different water temperatures. *Aquaculture*, *97*(2-3), 203-216.

Olofsson, S. O., & Boren, J. (2005). Apolipoprotein B: a clinically important apolipoprotein which assembles atherogenic lipoproteins and promotes the development of atherosclerosis. *Journal of internal medicine*, *258*(5), 395-410.

Ong, D. E. (1982). Purification and partial characterization of cellular retinol-binding protein from human liver. *Cancer Research*, *42*(3), 1033-1037.

Page, G., & Davies, S. (2003). Hepatic carotenoid uptake in rainbow trout (Oncorhynchus mykiss) using an isolated organ perfusion model. *Aquaculture*, *225*(1-4), 405-419.

Parker, R. S. (1996). Absorption, metabolism, and transport of carotenoids. *The FASEB Journal*, *10*(5), 542-551.

Piga, R., van Dartel, D., Bunschoten, A., van der Stelt, I., & Keijer, J. (2014). Role of Frizzled6 in the molecular mechanism of beta-carotene action in the lung. *Toxicology*, *320*, 67-73.

Prakash, P., Liu, C., Hu, K.-Q., Krinsky, N. I., Russell, R. M., & Wang, X.-D. (2004). β-Carotene and β-apo-14′-carotenoic acid prevent the reduction of retinoic acid receptor β in benzo [a] pyrene-treated normal human bronchial epithelial cells. *The Journal of nutrition*, *134*(3), 667-673.

Rajasingh, H., Øyehaug, L., Våge, D. I., & Omholt, S. W. (2006). Carotenoid dynamics in Atlantic salmon. *Bmc Biology*, *4*(1), 1-15.

Ramanathan, R., Nair, M., Hunt, M., & Suman, S. (2019). Mitochondrial functionality and beef colour: A review of recent research. *South African Journal of Animal Science*, *49*(1), 9-19.

Reboul, E. (2019). Mechanisms of carotenoid intestinal absorption: where do we stand? *Nutrients*, *11*(4), 838.

Reboul, E., & Borel, P. (2011). Proteins involved in uptake, intracellular transport and basolateral secretion of fat-soluble vitamins and carotenoids by mammalian enterocytes. *Progress in lipid research*, *50*(4), 388-402.

Ross, A. C., & Harrison, E. H. (2007). Vitamin A: nutritional aspects of retinoids and carotenoids. *Handbook of Vitamins, 4th Edition, USA: CRC PressTaylor & Francis Group*.

Røsjø, C., Nordrum, S., Olli, J., Krogdahl, Å., Ruyter, B., & Holm, H. (2000). Lipid digestibility and metabolism in Atlantic salmon (Salmo salar) fed medium-chain triglycerides. *Aquaculture*, *190*(1-2), 65-76.

Sampels, S. (2013). Oxidation and antioxidants in fish and meat from farm to fork. *Food industry*, 114-144.

Scaife, J., Onibi, G., Murray, I., Fletcher, T., & Houlihan, D. (2000). Influence of a-tocopherol acetate on the short-and long-term storage properties of fillets from Atlantic salmon Salmo salar fed a high lipid diet. *Aquaculture Nutrition*, *6*(1), 65.

Schaeffer, C., Devuyst, O., & Rampoldi, L. (2021). Uromodulin: roles in health and disease. *Annual Review of Physiology*, *83*, 477-501.

Schmeisser, J., Verlhac-Trichet, V., Madaro, A., Lall, S. P., Torrissen, O., & Olsen, R. E. (2021). Molecular Mechanism Involved in Carotenoid Metabolism in Post-Smolt Atlantic Salmon: Astaxanthin Metabolism During Flesh Pigmentation and Its Antioxidant Properties. *Marine Biotechnology*, *23*(4), 653-670.

Shmarakov, I., Fleshman, M. K., D'Ambrosio, D. N., Piantedosi, R., Riedl, K. M., Schwartz, S. J.,…Harrison, E. H. (2010). Hepatic stellate cells are an important cellular site for β-carotene conversion to retinoid. *Archives of biochemistry and biophysics*, *504*(1), 3-10.

Singh, A., Mittal, A., & Benjakul, S. (2022). Undesirable discoloration in edible fish muscle: Impact of indigenous pigments, chemical reactions, processing, and its prevention. *Comprehensive Reviews in Food Science and Food Safety*, *21*(1), 580-603.

Smirnoff, N. (2018). Ascorbic acid metabolism and functions: A comparison of plants and mammals. *Free Radical Biology and Medicine*, *122*, 116-129.

Storebakken, T., & No, H. K. (1992). Pigmentation of rainbow trout. *Aquaculture*, *100*(1-3), 209-229.

Sun, H. (2012). Membrane receptors and transporters involved in the function and transport of vitamin A and its derivatives. *Biochimica et Biophysica Acta (BBA)-Molecular and Cell Biology of Lipids*, *1821*(1), 99-112.

Thomas, S. E., & Harrison, E. H. (2016). Mechanisms of selective delivery of xanthophylls to retinal pigment epithelial cells by human lipoproteins. *Journal of lipid research*, *57*(10), 1865-1878.

Tigistu-Sahle, F. (2012). Lipidomics for Human Bone Marrow Mesenchymal Stem Cells.

Torrissen, O. J. (1989). Pigmentation of salmonids: interactions of astaxanthin and canthaxanthin on pigment deposition in rainbow trout. *Aquaculture*, *79*(1-4), 363-374.

Torrissen, O. J., & Ingebrigtsen, K. (1992). Tissue distribution of 14C-astaxanthin in the Atlantic salmon (Salmo salar). *Aquaculture*, *108*(3-4), 381-385.

Vo, T. T. M., Nguyen, T. V., Amoroso, G., Ventura, T., & Elizur, A. (2021). Deploying new generation sequencing for the study of flesh color depletion in Atlantic Salmon (Salmo salar). *BMC genomics*, *22*(1), 1-21.

von Lintig, J., Moon, J., Lee, J., & Ramkumar, S. (2020). Carotenoid metabolism at the intestinal barrier. *Biochimica et Biophysica Acta (BBA)-Molecular and Cell Biology of Lipids*, *1865*(11), 158580.

Xiang, H., Sun, S., Huang, H., Hao, S., Li, L., Yang, X.,…Pan, C. (2023). Proteomics study of mitochondrial proteins in tilapia red meat and their effect on color change during storage. *Food Chemistry*, *400*, 134061.

Zhang, X., & Xie, J. (2019). Analysis of proteins associated with quality deterioration of grouper fillets based on TMT quantitative proteomics during refrigerated storage. *Molecules*, *24*(14), 2641.

Zoric, N. (2017). Characterization of genes and gene products influencing carotenoid metabolism in Atlantic salmon.

Supplementary Information:

Additional file 1: **Table S1:** Differentially expressed genes (DEGs) in the pyloric caecum, liver and muscle, and groups of DEGs.

id	Chromoso	Region	Max.group	Log..fold.c	Fold.chang	P.value	FDR.p.valu	Bonferron	gene.name		Tissue
LOC11049	NC_04858	20597779.	0.93096	7.013094	129.167	5.12E-42	2.22E-37	2.22E-37	circularly permutated Ras protein 1		PYLORIC
xdh	NC_04858	60888364.	2.039765	3.709109	13.07835	3.13E-20	3.40E-16	1.36E-15	xanthine dehydrogenase		PYLORIC
LOC11893	NC_04857	101572952	5.33894	5.165782	35.89676	4.47E-15	3.88E-11	1.94E-10	NACHT, LRR and PYD domains-containing protein 12-like		PYLORIC
LOC11893	NC_04857	compleme	3.020755	3.809865	14.02438	3.85E-13	2.09E-09	1.67E-08	NACHT, LRR and PYD domains-containing protein 12-like		PYLORIC
aadacl4	NC_04857	54183222.	0.798535	4.253026	19.06726	2.26E-11	7.56E-08	9.82E-07	arylacetamide deacetylase-like 4		PYLORIC
pcolce2b	NC_04857	compleme	1.210496	4.552956	23.47341	4.56E-11	1.41E-07	1.98E-06	procollagen C-endopeptidase enhancer 2b		PYLORIC
LOC11048	NC_04857	compleme	0.355732	4.628628	24.73751	8.51E-11	2.42E-07	3.69E-06	uncharacterized LOC110489796		PYLORIC
LOC11053	NC_04856	compleme	1.624216	2.862143	7.270946	1.31E-10	3.15E-07	5.67E-06	rap guanine nucleotide exchange factor 5		PYLORIC
LOC11049	NC_04858	compleme	1.518314	6.436162	86.59198	1.75E-10	3.78E-07	7.58E-06	antimicrobial peptide NK-lysin-like		PYLORIC
LOC11053	NC_04857	73155366.	0.123917	2.735497	6.659885	1.18E-09	2.14E-06	5.14E-05	collagen alpha-1(XXVII) chain B		PYLORIC
LOC11053	NC_04856	compleme	0.147993	4.959195	31.10759	4.51E-09	6.99E-06	0.000196	monocarboxylate transporter 12-B-like		PYLORIC
aqp10a	NC_04856	compleme	20.34112	2.374555	5.185759	4.90E-09	7.34E-06	0.000213	aquaporin 10a		PYLORIC
LOC11052	NC_05057	compleme	0.047446	3.156437	8.916252	6.01E-09	8.69E-06	0.000261	zinc finger protein 644		PYLORIC
LOC11053	NC_04857	58362581.	4.55847	2.731773	6.642717	2.41E-08	3.08E-05	0.001047	butyrophilin subfamily 3 member A1		PYLORIC
LOC11052	NC_05057	42656156.	0.249876	3.155104	8.908015	3.67E-08	4.43E-05	0.001595	nuclear receptor subfamily 2 group F member 6		PYLORIC
LOC11052	NW_0234	7942..106	1.394862	4.73043	26.54613	4.62E-08	5.42E-05	0.002005	piggyBac transposable element-derived protein 4-like		PYLORIC
fbp2	NC_04857	compleme	0.039307	5.040406	32.9089	5.08E-08	5.80E-05	0.002204	fructose-1,6-bisphosphatase 2		PYLORIC
LOC11049	NC_04858	31214930.	0.092302	3.110695	8.637987	1.25E-07	0.000132	0.005416	voltage-dependent calcium channel gamma-4 subunit		PYLORIC
LOC11894	NW_0234	363207..3	0.530263	2.743208	6.695577	1.35E-07	0.00014	0.005872	gastrula zinc finger protein XlCGF17.1-like		PYLORIC
LOC11896	NC_04857	5853394..5	1.275752	4.209004	18.49424	1.39E-07	0.00014	0.006032	uncharacterized LOC118966694		PYLORIC
syt12	NC_04856	compleme	0.828593	1.5489	2.925939	1.63E-07	0.000157	0.007071	synaptotagmin XII		PYLORIC
LOC11052	NC_04857	compleme	0.036514	4.048122	16.54269	2.02E-07	0.000186	0.008752	gamma-aminobutyric acid receptor subunit rho-2-like		PYLORIC
LOC11894	NC_04859	943643..1	0.037016	4.262421	19.19184	2.86E-07	0.000253	0.012405	synaptic vesicle glycoprotein 2B-like		PYLORIC
LOC11052	NC_04857	16446388.	19.83351	2.858667	7.253448	3.56E-07	0.000297	0.015445	uncharacterized LOC110528885		PYLORIC
LOC11052	NC_04856	compleme	0.716362	3.254322	9.542199	4.31E-07	0.00035	0.018727	protein RD3		PYLORIC
LOC11049	NC_04858	compleme	0.165762	1.798172	3.477794	5.45E-07	0.000416	0.02368	semaphorin-3F		PYLORIC
LOC11053	NC_04857	48705729.	0.155274	3.5971	12.10138	5.89E-07	0.000434	0.025587	GDNF family receptor alpha-2		PYLORIC
LOC11049	NC_04858	31256900.	0.049042	5.644757	50.03121	7.87E-07	0.000551	0.034182	voltage-dependent calcium channel gamma-1 subunit		PYLORIC
LOC11053	NC_04857	compleme	0.288506	1.722411	3.299874	8.31E-07	0.000572	0.036065	phospholipid phosphatase-related protein type 4		PYLORIC
LOC11894	NC_04859	8560607..8	9.796338	2.113858	4.328473	1.08E-06	0.000713	0.047047	uncharacterized LOC118944551		PYLORIC
slc27a6	NC_04856	8250159..8	0.153598	2.350844	5.101226	1.14E-06	0.000731	0.049697	solute carrier family 27 member 6		PYLORIC
LOC11049	NC_04858	43137388.	6.058751	1.76402	3.396432	1.26E-06	0.000783	0.054802	uncharacterized LOC110499564		PYLORIC
LOC11893	NC_04857	101717789	0.146363	3.681781	12.83295	1.39E-06	0.000825	0.060211	NLR family CARD domain-containing protein 3-like		PYLORIC
LOC11049	NC_04857	compleme	334.3634	1.74417	3.350021	1.38E-06	0.000825	0.059767	galactose-specific lectin nattectin		PYLORIC
LOC11052	NC_05057	3784498..3	3.190528	1.567878	2.964684	1.66E-06	0.000951	0.072275	tripartite motif-containing protein 16		PYLORIC
LOC11894	NC_04856	compleme	0.127597	1.962686	3.897871	1.96E-06	0.001077	0.084963	rap guanine nucleotide exchange factor 5-like		PYLORIC
LOC11051	NC_04857	66393580.	0.214792	4.074914	16.85277	2.15E-06	0.001127	0.093282	uncharacterized LOC110518344		PYLORIC
LOC11053	NC_04857	compleme	0.615745	1.785637	3.447708	2.71E-06	0.001403	0.117842	alanine aminotransferase 2-like		PYLORIC
si:dkeyp-1	NC_04857	compleme	3.812366	1.622861	3.079853	2.87E-06	0.001447	0.124413	uncharacterized si:dkeyp-13a3.10		PYLORIC
LOC11053	NC_04857	34414388.	0.149617	1.391459	2.623439	2.93E-06	0.00146	0.127369	cytospin-B		PYLORIC
LOC11051	NC_04857	compleme	0.063694	10.29495	1256.283	3.05E-06	0.001473	0.132582	stonustoxin subunit beta-like		PYLORIC
LOC11050	NC_04859	29410322.	0.037627	2.035619	4.099985	3.03E-06	0.001473	0.131564	calsyntenin-2		PYLORIC
LOC11050	NC_04859	18579463.	0.069489	1.839796	3.579594	4.19E-06	0.00196	0.181779	solute carrier family 12 member 7		PYLORIC
LOC11049	NC_04857	compleme	8.100843	4.062283	16.70587	4.59E-06	0.002121	0.199401	uncharacterized LOC110497178		PYLORIC
LOC11049	NC_04856	compleme	1.316483	1.977315	3.937596	5.15E-06	0.002353	0.223489	cytoplasmic dynein 1 light intermediate chain 1		PYLORIC
LOC11049	NC_04858	compleme	0.029027	2.620559	6.149883	5.39E-06	0.002436	0.233824	gamma-2-syntrophin		PYLORIC
LOC11052	NC_04856	32734905.	1.038335	2.957639	7.768518	5.61E-06	0.002484	0.243387	vasotocin-neurophysin VT 1		PYLORIC
LOC11894	NC_04858	compleme	0.443619	3.403219	10.57964	5.75E-06	0.002523	0.249735	uncharacterized LOC118941480		PYLORIC
LOC11049	NC_04858	5196694..5	1.694705	1.619636	3.072975	5.87E-06	0.002539	0.254995	calpain-1 catalytic subunit		PYLORIC
LOC11050	NC_04858	8200364..8	1.610769	1.330895	2.515586	6.03E-06	0.002568	0.261894	gamma-aminobutyric acid receptor subunit rho-1-like		PYLORIC

id	gene name	Name	Chromoso	Region	Max group	Log_2 fold c	Fold chang	P-value	FDR p-valu	Bonferroni	
LOC11893	uncharacterized LOC118939568	LOC11893	NC_04858	compleme	7.48	10.29	1,247.89	5.36E-71	2.40E-66	2.40E-66	MUSCLE
LOC11049	acidic mammalian chitinase	LOC11049	NC_04858	52398555.	4.64	9.61	782.07	2.05E-15	1.43E-12	9.15E-11	MUSCLE
LOC11053	acidic mammalian chitinase	LOC11053	NC_04857	compleme	0.42	9.17	575.56	5.63E-09	6.33E-07	2.52E-04	MUSCLE
LOC10030	gastric chitinase	LOC10030	NC_04858	52389226.	7.95	9.14	565.2	5.77E-16	4.69E-13	2.58E-11	MUSCLE
LOC11050	pepsin A	LOC11050	NC_04858	54982792.	2.12	9.03	522.98	1.60E-13	7.02E-11	7.16E-09	MUSCLE
LOC11893	complement C3-like	LOC11893	NC_04856	compleme	2.11	8.53	368.9	1.37E-17	1.61E-14	6.13E-13	MUSCLE
ezra	ezrin a	ezra	NC_04858	44634496.	0.05	8.27	309.21	2.54E-07	1.54E-05	0.01	MUSCLE
LOC11894	uncharacterized LOC118944418	LOC11894	NC_04859	compleme	0.93	8.27	308.46	1.16E-09	1.59E-07	5.19E-05	MUSCLE
LOC11049	gastricsin	LOC11049	NC_04856	compleme	0.78	7.99	253.81	6.14E-11	1.26E-08	2.75E-06	MUSCLE
LOC11893	microfibril-associated glycoprotein 4-like	LOC11893	NC_04858	7873615..	3.16	7.87	233.19	3.38E-16	3.15E-13	1.51E-11	MUSCLE
hpxa	hemopexin a	hpxa	NC_04856	compleme	7.63	7.85	229.94	7.84E-20	1.59E-16	3.50E-15	MUSCLE
LOC11893	coagulation factor VII-like	LOC11893	NC_04858	compleme	1.1	7.49	179.86	4.32E-15	2.72E-12	1.93E-10	MUSCLE
LOC11896	uncharacterized LOC118965250	LOC11896	NC_04857	compleme	0.11	7.38	166.17	6.38E-07	3.41E-05	0.03	MUSCLE
LOC11896	uncharacterized LOC118964417	LOC11896	NC_04856	compleme	0.1	7.25	152.08	1.47E-06	6.82E-05	0.07	MUSCLE
LOC11053	hexokinase-4	LOC11053	NC_04857	compleme	0.95	7.15	141.59	1.26E-13	5.81E-11	5.65E-09	MUSCLE
cfh	complement factor H	cfh	NC_04856	90756155.	3.38	7.06	133.88	1.67E-16	1.66E-13	7.45E-12	MUSCLE
LOC11050	uncharacterized LOC110505928	LOC11050	NC_04858	compleme	0.84	7.04	131.16	7.20E-14	3.54E-11	3.22E-09	MUSCLE
LOC11049	glycerate kinase	LOC11049	NC_04858	compleme	0.07	6.99	127.5	1.85E-05	5.38E-04	0.83	MUSCLE
LOC11050	transmembrane protein 87A	LOC11050	NC_04858	compleme	0.02	6.94	122.58	9.80E-07	4.91E-05	0.04	MUSCLE
LOC11048	complement C3-like	LOC11048	NC_04856	compleme	3.19	6.86	115.99	1.18E-15	8.96E-13	5.29E-11	MUSCLE
LOC11050	vitronectin	LOC11050	NC_04859	compleme	0.68	6.82	112.9	3.30E-16	3.14E-13	1.48E-11	MUSCLE
LOC11053	intelectin	LOC11053	NC_04857	compleme	0.26	6.79	110.29	1.78E-05	5.22E-04	0.8	MUSCLE
LOC11053	platelet-derived growth factor receptor beta	LOC11053	NC_04857	49160630.	0.02	6.71	104.88	5.51E-06	2.01E-04	0.25	MUSCLE
LOC11053	albumin 1	LOC11053	NC_04858	compleme	19.41	6.63	98.85	3.68E-16	3.36E-13	1.64E-11	MUSCLE
LOC11050	alpha-2-macroglobulin	LOC11050	NC_04859	compleme	0.89	6.61	97.65	4.32E-16	3.64E-13	1.93E-11	MUSCLE
LOC11050	uncharacterized LOC110505637	LOC11050	NC_04856	5953981..	5.15	6.58	95.74	6.97E-15	4.10E-12	3.12E-10	MUSCLE
LOC11049	gastricsin	LOC11049	NC_04856	compleme	0.39	6.57	95.17	7.44E-09	8.03E-07	3.33E-04	MUSCLE
antiprot1	alpha-1-antiproteinase-like protein	antiprot1	NC_04856	32121260.	26.1	6.53	92.37	1.07E-16	1.16E-13	4.77E-12	MUSCLE
LOC11896	coagulation factor VII-like	LOC11896	NC_04857	5781376..	0.31	6.52	91.62	1.27E-08	1.23E-06	5.68E-04	MUSCLE
LOC10049	albumin 1	LOC10049	NC_04856	compleme	17.86	6.43	86.42	5.45E-17	6.25E-14	2.44E-12	MUSCLE
LOC11894	uncharacterized LOC118942975	LOC11894	NC_04858	62919976.	0.23	6.39	83.58	2.17E-05	6.14E-04	0.97	MUSCLE
LOC11894	intestinal mucin-like protein	LOC11894	NC_04859	compleme	0.15	6.38	83.48	9.49E-09	9.69E-07	4.24E-04	MUSCLE
LOC11052	apolipoprotein B-100	LOC11052	NC_04857	12071414.	1.89	6.27	77.1	3.09E-14	1.65E-11	1.38E-09	MUSCLE
LOC11049	gastricsin	LOC11049	NC_04856	compleme	0.37	6.24	75.72	2.22E-08	1.98E-06	9.93E-04	MUSCLE
shbg	sex hormone-binding globulin	shbg	NC_04857	25635682.	2.8	6.22	74.72	1.01E-17	1.25E-14	4.51E-13	MUSCLE
LOC11049	hemagglutinin/amebocyte aggregation factor	LOC11049	NC_04857	57461647.	0.45	6.22	74.64	8.61E-08	6.17E-06	3.85E-03	MUSCLE
cfbl	complement factor b, like	cfbl	NC_04859	34145403.	3.41	6.2	73.46	3.91E-16	3.43E-13	1.75E-11	MUSCLE
LOC11049	G-protein coupled receptor 183	LOC11049	NC_04858	compleme	0.04	6.18	72.39	1.31E-04	2.60E-03	1	MUSCLE
LOC11048	saxitoxin and tetrodotoxin-binding protein 2	LOC11048	NC_04857	11329907.	4.89	6.15	70.99	3.24E-14	1.70E-11	1.45E-09	MUSCLE
LOC10013	properdin	LOC10013	NC_04858	52938988.	2.09	6.14	70.65	9.97E-16	7.71E-13	4.46E-11	MUSCLE
LOC11893	haptoglobin-like	LOC11893	NC_04857	compleme	7.12	6.1	68.71	7.72E-17	8.63E-14	3.45E-12	MUSCLE
masp2	MBL associated serine protease 2	masp2	NC_04857	51173762.	0.17	6.06	66.71	1.27E-09	1.71E-07	5.66E-05	MUSCLE
LOC11048	complement C3-like	LOC11048	NC_04856	compleme	30.94	6.05	66.18	3.21E-13	1.29E-10	1.44E-08	MUSCLE
LOC11049	perforin-1	LOC11049	NC_04858	69693022.	0.07	6.04	65.67	1.11E-04	2.29E-03	1	MUSCLE
LOC11049	pepsin A	LOC11049	NC_04858	compleme	0.55	6	64.04	1.86E-08	1.69E-06	8.30E-04	MUSCLE
habp2	hyaluronan binding protein 2	habp2	NC_04856	compleme	1.97	5.94	61.43	1.88E-15	1.34E-12	8.42E-11	MUSCLE
ahsg2	alpha-2-HS-glycoprotein 2	ahsg2	NC_04859	compleme	9.54	5.93	61.09	1.10E-14	6.23E-12	4.93E-10	MUSCLE
LOC11896	lysine-specific demethylase 5C-like	LOC11896	NC_04857	compleme	0.06	5.89	59.13	1.84E-04	3.39E-03	1	MUSCLE
gk	glucokinase	gk	NC_04857	compleme	0.43	5.88	58.99	8.12E-09	8.62E-07	3.63E-04	MUSCLE

id	Chromoso	Region	Max.group	Log..fold.c	Fold.chang	P.value	FDR.p.valu	Bonferron	gene.name	
LOC11049	NC_04858	compleme	0.041348	7.342724	162.3231	4.87E-09	1.68E-06	0.00021	pentraxin-related protein PTX3	LIVER
LOC10013	NC_04857	62440267.	0.558494	7.206702	147.718	1.74E-06	0.000169	0.075049	ferritin H-3	LIVER
LOC11053	NC_04857	compleme	0.05128	6.54171	93.16462	1.84E-10	1.22E-07	7.94E-06	protein FAM163B-like	LIVER
LOC11896	NC_04856	compleme	0.337519	6.469302	88.60414	3.99E-15	1.57E-11	1.72E-10	uncharacterized LOC118964616	LIVER
LOC11048	NC_04856	28914821.	0.052972	6.400975	84.50561	4.97E-07	6.37E-05	0.021454	ectonucleoside triphosphate diphosphohydrolase 3	LIVER
dbh	NC_04857	12308661.	0.041072	6.392869	84.03214	1.59E-09	6.68E-07	6.88E-05	dopamine beta-hydroxylase (dopamine beta-monoox	LIVER
LOC11053	NC_04857	compleme	0.170535	6.1096	69.05148	9.28E-09	2.81E-06	0.000401	protein shisa-3 homolog	LIVER
LOC11053	NC_04857	compleme	0.064293	6.091861	68.20762	4.61E-08	1.01E-05	0.00199	uncharacterized LOC110531700	LIVER
LOC11894	NW_0234	compleme	1.724916	6.089839	68.11211	2.73E-12	3.69E-09	1.18E-07	toll-like receptor 13	LIVER
efcab2	NC_04858	compleme	0.12023	5.960422	62.26815	3.48E-12	4.41E-09	1.50E-07	EF-hand calcium binding domain 2	LIVER
LOC11893	NC_04858	13761395.	0.012239	5.700088	51.98734	0.000125	0.004256	1	lipopolysaccharide-induced tumor necrosis factor-alp	LIVER
LOC11050	NC_05057	compleme	0.05236	5.648749	50.16985	8.54E-06	0.000595	0.368371	histone-lysine N-methyltransferase PRDM9	LIVER
LOC11049	NC_04858	compleme	0.064319	5.644201	50.01196	1.27E-07	2.24E-05	0.005462	caspase recruitment domain-containing protein 14	LIVER
LOC11896	NC_04857	68901391.	0.330508	5.537272	46.43921	1.73E-08	4.67E-06	0.000747	uncharacterized LOC118966105	LIVER
LOC11049	NC_04858	44582635.	0.017206	5.53301	46.30224	1.61E-05	0.000941	0.692651	gonadotropin-releasing hormone II receptor-like	LIVER
dytn	NC_04858	12048979.	0.075133	5.503121	45.35283	1.14E-10	8.79E-08	4.92E-06	dystrotelin	LIVER
LOC11050	NC_04859	compleme	0.085857	5.4949	45.09515	1.31E-06	0.000134	0.056383	extracellular calcium-sensing receptor-like	LIVER
LOC11049	NW_0234	92327..97	0.096797	5.43501	43.26144	9.94E-08	1.82E-05	0.004291	toll-like receptor 13	LIVER
LOC11051	NC_04858	compleme	2.646465	5.423824	42.92732	1.43E-10	9.92E-08	6.15E-06	GTPase IMAP family member 7-like	LIVER
LOC11050	NW_0234	compleme	0.042589	5.410803	42.54163	6.28E-05	0.002537	1	tripartite motif-containing protein 16	LIVER
LOC11049	NC_04858	compleme	0.068368	5.335459	40.37693	0.000116	0.003994	1	keratin-associated protein 16-1-like	LIVER
LOC11893	NC_04856	compleme	0.053819	5.325473	40.09841	0.000251	0.007191	1	molybdopterin synthase catalytic subunit	LIVER
LOC11048	NC_05057	6651464..	0.015456	5.315315	39.81706	9.75E-06	0.000648	0.420803	visinin-like protein 1	LIVER
LOC11049	NC_04858	31595286.	0.080714	5.215606	37.15813	0.000336	0.00888	1	uncharacterized LOC110491816	LIVER
LOC11053	NC_04857	10715250.	0.018984	5.183393	36.33764	1.04E-05	0.000669	0.447831	retinal guanylyl cyclase 2-like	LIVER
LOC11894	NC_04858	compleme	0.344967	5.069497	33.57922	8.05E-10	3.86E-07	3.47E-05	uncharacterized LOC118942785	LIVER
LOC11053	NC_04857	compleme	0.100829	5.018245	32.40725	0.000373	0.009503	1	uncharacterized LOC110535241	LIVER
LOC11052	NC_04856	compleme	0.139375	4.986812	31.70882	5.15E-07	6.55E-05	0.022209	adenylate cyclase type 3	LIVER
LOC11052	NC_04858	compleme	0.279991	4.962565	31.18034	3.60E-05	0.0017	1	nucleotide triphosphate diphosphatase NUDT15	LIVER
dchs2	NC_04857	compleme	0.059803	4.962237	31.17325	8.64E-13	1.69E-09	3.73E-08	dachsous cadherin-related 2	LIVER
LOC11896	NC_04857	compleme	0.05581	4.946331	30.83145	0.000388	0.00975	1	uncharacterized LOC118965526	LIVER
LOC11893	NC_04857	67203591.	0.712254	4.853082	28.9017	1.24E-19	1.07E-15	5.33E-15	uncharacterized LOC118938472	LIVER
LOC11893	NC_04858	72706333.	1.309431	4.804334	27.94143	1.77E-07	2.94E-05	0.00765	uncharacterized LOC118939587	LIVER
LOC11049	NC_04858	27943373.	0.266328	4.618324	24.56145	6.93E-07	8.26E-05	0.029905	tubulin beta-4B chain	LIVER
LOC11048	NC_04857	63692380.	0.254549	4.535792	23.19581	1.26E-12	2.17E-09	5.43E-08	NACHT, LRR and PYD domains-containing protein 12	LIVER
pparaa	NC_04857	compleme	0.076168	4.505262	22.7101	3.90E-06	0.000318	0.168271	peroxisome proliferator-activated receptor alpha a	LIVER
LOC11894	NC_04858	61154895.	0.03319	4.489457	22.46267	0.001531	0.026195	1	uncharacterized LOC118940484	LIVER
LOC11050	NC_04856	6685900..	0.983211	4.450165	21.85914	8.71E-09	2.68E-06	0.000376	E3 ubiquitin-protein ligase NHLRC1-like	LIVER
angpt2b	NC_05057	2930144..	0.045892	4.449625	21.85097	9.11E-15	3.28E-11	3.93E-10	angiopoietin 2b	LIVER
LOC11048	NC_04857	compleme	0.006628	4.408293	21.23384	0.000377	0.009563	1	uncharacterized LOC110488755	LIVER
LOC11052	NW_0234	7942..106	9.690576	4.307394	19.79952	9.25E-11	7.83E-08	3.99E-06	piggyBac transposable element-derived protein 4-like	LIVER
LOC11896	NC_04856	49847620.	0.941379	4.307188	19.79671	9.06E-13	1.70E-09	3.91E-08	uncharacterized LOC118964840	LIVER
prr33	NC_05057	compleme	1.249934	4.269451	19.28559	4.02E-36	1.73E-31	1.73E-31	proline rich 33	LIVER
LOC11052	NC_04856	62193287.	0.097862	4.252918	19.06584	3.56E-07	4.85E-05	0.015383	uncharacterized LOC110520339	LIVER
LOC11894	NC_04858	compleme	0.24767	4.252286	19.05748	6.61E-06	0.000483	0.285186	zinc transporter zipt-7.2-like	LIVER
LOC11894	NC_05057	21906458.	0.966151	4.245023	18.96179	2.23E-13	5.34E-10	9.62E-09	uncharacterized LOC118946060	LIVER
LOC11048	NC_04857	compleme	0.015975	4.12351	17.43012	0.002433	0.035941	1	uncharacterized protein K02A2.6-like	LIVER
LOC11893	NC_04857	compleme	5.464629	4.107583	17.23875	1.37E-15	7.41E-12	5.93E-11	stonustoxin subunit beta-like	LIVER
LOC11049	NC_04858	42211247.	0.035453	4.099913	17.14734	0.003158	0.043193	1	peptidase inhibitor R3HDML	LIVER

CHAPTER 4: Fecal microbiome analysis distinguishes bacterial taxa biomarkers associated with red fillet color in rainbow trout

Ahmed, R. O., Ali, A., Leeds, T., & Salem, M. (2023). Fecal Microbiome Analysis Distinguishes Bacterial Taxa Biomarkers Associated with Red Fillet Color in Rainbow Trout. Microorganisms, 11(11), 2704.

Ridwan O. Ahmed,[1] Ali Ali,[1] Tim Leeds,[2], and Mohamed Salem[1, *]

[1]Department of Animal and Avian Sciences, University of Maryland, College Park, MD 20742, USA.

[2]United States Department of Agriculture Kearneysville, National Center for Cool and Cold Water Aquaculture, Agricultural Research Service, Kearneysville, WV 25430, USA.

Abstract

Background

The characteristic reddish-pink fillet color of rainbow trout is an important marketing trait. The gastrointestinal microbiome is vital for host health, immunity, and nutrient balance. Host genetics play a crucial role in determining the gut microbiome, and the host-microbiome interaction impacts the host's phenotypic expression. We hypothesized that fecal microbiota could be used to predict fillet color in rainbow trout. Fish were fed Astaxanthin-supplemented feed for six months, after which the 16s rDNA sequencing was used to investigate the fecal microbiome composition in rainbow trout families with reddish-pink fillet coloration (red fillet group, average saturation index = 26.50 ±2.86) compared to families with pale white fillet color (white fillet group, average saturation index = 21.21±3.53). The linear discriminant analysis effect size (LEFse) tool was used to identify bacterial biomarkers associated with fillet color. The alpha diversity measure shows no difference in the red and white fillet groups. Beta diversity PCA showed clustering of the samples along the white versus red fillet group. The red fillet group has enrichment (LDA score > 1.5) of taxa *Leuconostoc lactis, Corynebacterium variabile, Jeotgalicoccus halotolerans,* and *Leucobacter chromiireducens*. In contrast, the white fillet group has an enriched presence of *mycoplasma, Lachnoclostridium,* and *Oceanobacillus indicireducens*. The enriched bacterial taxa in the red fillet group have probiotic functions and can generate carotenoid pigments. Bacteria taxa enriched in the white fillet group are either commensal, parasitic, or capable of reducing indigo dye. The study identified specific bacterial biomarkers differentially abundant in fish families of divergent fillet color that could be used in genetic selection to improve feed carotenoid retention and reddish-pink fillet color. This work extends our understanding of carotenoid metabolism in rainbow trout through the interaction between gut microbiota and fillet color.

Keywords; Aquaculture, Microbiome, Pigmentation, carotenoids

Introduction

The characteristic reddish-pink fillet color of salmonids is an important quality criterion determining consumers' purchasing decisions. Carotenoids are organic molecular pigments synthesized by plants, certain bacteria, algae, and fungi (Kumari et al., 2019). In the natural marine habitat, salmonid fish, including rainbow trout and Atlantic salmon, feed on sea algae and small crustaceans, giving the muscle characteristic pink/reddish coloration. In commercial and farmed aquaculture, synthetic carotenoids, especially astaxanthin, are added as feed additives to provide similar fillet coloration. The astaxanthin deposition rate in the muscle of salmonids is between 1 to 22% (Torrissen, 1995; Torrissen, 1989), while up to 30-70% of astaxanthin supplied in the diet is lost in the feces (Aas et al., 1999). This poor utilization of astaxanthin is troublesome as astaxanthin is expensive and accounts for up to 25% of the feed cost (Baker et al., 2002). Therefore, it is important to investigate the mechanism of carotenoid absorption, metabolism, utilization, and deposition in salmonids, particularly the genes responsible for this metabolism and how they function. It has been suggested that there is a trade-off between the utilization of carotenoids to boost the color of the muscle and its utilization for immune defense and vitamin A production (Hill, 1999; Lozano, 1994).

The intestinal microbial community of fish has been demonstrated to be relevant in metabolism within the host (Nayak, 2010). The complex microbial community within the gastrointestinal tract is crucial in the hosts' health, immunity, and nutrient balance (Brugman & Nieuwenhuis, 2010; Cerf-Bensussan & Gaboriau-Routhiau, 2010; Viney & Riley, 2014; Wang et al., 2018). The fish host-microbial relationship is complex and has been the subject of several studies in fish species in the past (Ringø et al., 1995), including rainbow trout (Desai et al., 2012; Mansfield et al., 2010; Navarrete et al., 2012) and other fish, as reviewed by Wang et al. (2018). The fish gastrointestinal microbiome is determined by several factors, including host genetics, environmental factors, and microbial factors, like the adhesion capacity of the microbes (Wang et al., 2018). The fish gut microbiota can influence nutrient metabolism through the roles of certain enzyme-producing microbes (Camp et al., 2012; Rawls et al., 2004; Ray et al., 2012; Semova et al., 2012). The gut microbiome can also protect the fish gastrointestinal tract from infectious agents by assisting in developing and maturing the gut-associated lymphoid tissues (GALT) (Bates et al., 2007; Bates et al., 2006; Wang et al., 2018). Chapagain et al. (2019) proposed that the fecal microbiome is associated with the growth rate in rainbow trout. They reported that amylose degrading and amino

acid fermenting bacteria (Clostridium, Leptotrichia, and Peptostreptococcus) are biomarkers of fast growth, while pathogenic bacteria (Corynebacterium and Paeniclostridium) are enriched in the slow-growing fish. *Carnobacterium divergens* has been identified as having a probiotic function in Atlantic Salmon(Gildberg et al., 1995; Ringo et al., 2007). Carotenoids can alter the gut microbiota pattern in humans and mice, while certain bacteria can also produce carotenoids within the human gut (Lin & Medeiros, 2023). Bacteria referred to as carotenogenic bacteria, such as *Firmicutes, Bacteroidetes, Actinobacteria, Proteobacteria, and Verrucomicrobiota*, are capable of synthesizing carotenoids (Kanamoto et al., 2021; Misawa et al., 2022; Shindo & Misawa, 2014; Tian & Hua, 2010). Therefore, the gut microbiome has emerged as a strong candidate for factors affecting host metabolism, including possible astaxanthin metabolism.

Astaxanthin supplied in the diet must be absorbed in the intestine, transported to, and then metabolized in the liver before it is deposited in the muscle. We hypothesized that gut microbiota could function as one of the modulators of astaxanthin absorption/transport and metabolism, which affects fillet color in rainbow trout. Several microorganisms have been proposed to have carotenoid-synthesizing ability via different enzyme pathways (Ram et al., 2020). Interestingly, enzymes from different organisms can combine to generate a functional carotenoid biosynthetic pathway in the host, as reviewed by Umeno et al.(2005). The relationship between carotenoids and gut microbiome/carotenoid-producing bacteria in rainbow trout deserves further investigation. Nguyen et al. (2020) identified a significant correlation between flesh color and microbiota composition in Atlantic Salmon. Carotenoid-synthesizing bacteria families such as Bacillaceae, *Mycoplasmataceae*, *Pseudomonas*, *Phyllobacteriaceae*, and *Comamonadaceae* were enriched in the fish with more reddish flesh color, while *Pseudoalteromonadaceae*, *Enterobacteriaceae*, *Microbacteriaceae*, and *Vibrionaceae* were in high abundance in the pale individuals. Nguyen et al. (2020) identified *Carnobacterium*, a group belonging to the lactic acid bacteria, as strongly related to the flesh color and the evenness of the color between the flesh areas.

Host genetics are crucial in determining the gut microbiome (Bonder et al., 2016). Host-microbiome interaction and the ultimate impact on the host's phenotypic expression were previously reviewed in (Awany et al., 2018). Buitenhuis et al. (2019) found that the proportion of phenotypic variance of milk fatty acid composition explained by rumen microbiome could be up

to 0.26-0.42, and including microbiome information in genomic prediction can improve the predictive ability of certain milk fatty acid compositions (C15:0 and C18:3 n-3) by up to 70% (0.22 to 0.38). We hypothesized that gut microbiota is involved in the metabolism and utilization of astaxanthin supplied in the diet, thus affecting the fillet color in rainbow trout. In order to develop non-invasive microbial biomarkers that can be used to predict fillet color, we investigated the fecal microbiome composition in rainbow trout families with reddish-pink fillet color compared to families with pale white fillet color.

Materials and Methods

Ethical statement

Husbandry practices and experimental procedures at the facility were approved by the IACUC animal study protocol of the University of Maryland, College Park, protocol number 1593175-6. All methods were carried out in accordance with relevant guidelines and regulations. All methods were carried out in accordance with ARRIVE guidelines(Percie du Sert et al., 2020).

Rainbow Trout Population, Experimental Design, Treatments, and Sampling

The fish used for this study are rainbow trout from a fillet yield genetic selection line developed at the National Center for Cool and Cold Water Aquaculture (NCCCWA). This line started as a growth-selected line in 2002 and underwent five generations of selection for improved growth performance, as described by Leeds et al. (2016). Subsequent generations were selected for muscle yield, as described in Cleveland et al.(2023) and Garcia et al. (2023a). Fish from the 2020 year class were included in this study and thus represent 3rd-generation families from lines selected for high (ARS-FY-H) or low (ARS-FY-L) fillet yield. The fish (all-female and immature) were received at 322 days post-hatch and randomly allocated to 20 six-foot tanks within the Crane Aquaculture facility of the University of Maryland, College Park. The aquaculture facility uses a recirculating aquaculture system (RAS) with all water quality parameters (water temperature, dissolved oxygen, ammonia concentration) closely monitored to ensure the fish are in good condition.

The fish were fed an astaxanthin-supplemented diet(BioTrout 4.0mm & 6.0mm, up to 40ppm astaxanthin) from Bio-Oregon (Washington, USA) at 5% of their body weight from 322 days post-hatch till harvest. They were taken off feed a day before harvest. During harvest, the fish were

euthanized using physical stunning through a blow to the skull with a blunt wooden instrument, immediately followed by exsanguination. They were allowed to undergo rigor mortis on ice for 48 hours after harvest and manually processed into trimmed, skinless fillets on the third day. Fecal samples were collected from all fish at two time points per fish (March: age 380 days post-hatch, and June: age 450-485 days post-hatch) and stored in ethanol at -20°C. Mean body weights are 347.10g and 694.36g in March and June sampling time, respectively.

A 7.5cm×5cm skinless raw fillet sample was taken from the right-side fillet at a position beginning about 1.5cm before the dorsal fin and over the lateral line. All samples were prepared at a uniform thickness of 1cm to prevent the influence of fillet sample thicknesses on the color measurements. The color was measured on the collected section with the Minolta Chroma Meter CR-200 device (Minolta, Model CR-300; Minolta Camera Co., Osaka, Japan), which gives readings for redness (a*), yellowness (b*), and lightness (L*). Two measurements were taken from the same collected section, and the average value was used.

The saturation index (SI) $(a^{*2} + b^{*2})^{0.5}$ was calculated for all fish, and the average SI value for each family was used to sort the 40 families into "red fillet group" for fish families of high saturation index and "white fillet group" for fish families of low saturation index value. This study used two families from the white (five fish each) group and two from the red fillet (five fish each) group. The saturation index describes the brightness of the color (Association, 1991).

DNA extraction.

A commercial DNA extraction kit (ZymoBIOMICS®-96 MagBead DNA Kit, Zymo Research, Irvine, CA) was used to isolate bacterial DNA from the fecal samples (n = 20 samples total from 5 fish each from the red and white fillet groups), following the manufacturer's instructions.

Library preparation

The samples were processed and analyzed for microbiome analysis using the targeted sequencing service of Zymo Research, Irvine, CA. The Quick-16STM Plus NGS Library Prep Kit (Zymo Research, Irvine, CA) was used to target the bacterial 16S rRNA gene. The primer set (Quick-16STM Primer Set V3-V4) was designed to amplify the V3-V4 region of the 16S rRNA gene. These primers were custom-designed by Zymo Research to provide the best coverage of the 16S rRNA gene and maintain high sensitivity. The sequencing library was prepared such that PCR

reactions were performed in real-time to control cycles and limit the formation of PCR chimera. The final PCR product was quantified using qPCR fluorescence readings and pooled together using equal molarity. The pooled library was cleaned with the Select-a-Size DNA Clean and Concentrator (Zymo Research, Irvine, CA). Library quantification was done using TapeStation (Agilent Technologies, Santa Clara, CA) and Qubit (Thermo Fisher Scientific, Waltham, WA).

The ZymoBIOMICS® Microbial Community DNA Standard (Zymo Research, Irvine, CA) was used as a positive control with each targeted library preparation. Negative controls (i.e., blank extraction control and blank library preparation control) were used to assess the bioburden level carried by the wet-lab process. Illumina MiSeq with a v3 reagent kit (600 cycles) was used to sequence the final library. The sequencing was performed using a 10% PhiX spike-in.

Bioinformatics and statistical analyses:

Unique amplicon sequences were identified from raw reads, and chimeric sequences were removed using the Dada2 pipeline (Callahan et al., 2016). Taxonomy assignment was performed using Uclust from Qiime v.1.9.1 and a 16S rRNA database internally designed and curated as a reference by the Zymo Research Database. QIIME v.1.9.1 was used for composition visualization, alpha-diversity, and beta-diversity analyses (Caporaso et al., 2010). Taxonomic groups with significant abundance among different groups were identified by linear discriminant analysis for effect size (LEfSe), with the time of sample collection as a covariate (Segata et al., 2011) using default settings. Those default settings were α parameters with pairwise tests set to 0.05 for both class normality and subclass tests, and the threshold on the logarithmic score of linear discriminate analysis was set to 1.5. PCoA plots were performed with internal scripts. For each sample collection time (March and June), we also separately used LEfSe analysis to identify taxonomic groups showing differential abundance between the red and the white fillet group (α_value = 0.05, LDA>3).

Results

Mean saturation index (S.I) values between the red versus white fillet group.

The mean S.I value of fish in the red and white fillet group is 26.50 ± 2.86 and 21.21 ± 3.53, respectively, as shown in Figure 1. This difference is significant at $P < 0.05$.

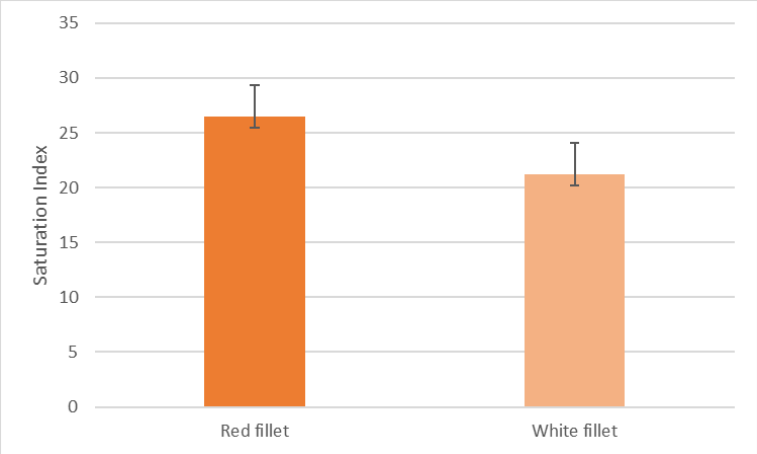

Figure 1: Mean saturation index (S.I) values between the red versus white fillet group

Fecal microbiome overall assessment:

A total of 9,898,390 16s rDNA raw sequences were obtained, with a range of 403,666 to 628,334 sequences per sample. A total of 17 bacteria phyla were identified: four (Firmicutes, Fusobacteria, Proteobacteria, Tenericutes) account for over 97% of the total sequences (Table 1). Bacteria were identified from 290 genera, with 6 genera (Enterococcus, Lactobacillus, Peptostreptococcus, Romboutsia, Cetobacterium, and Mycoplasma) representing 70% of the total sequences. A total of 51 orders, 30 classes, and 100 families were identified.

Table 1. The percentage taxa abundance of the major phyla and genera identified in the fecal samples.

Phyla	Red fillet group	White fillet group	Total
Firmicutes	22.73	23.73	46.46
Fusobacteria	16.31	6.52	22.83
Proteobacteria	2.41	2.71	5.12
Tenericutes	7.58	15.10	22.68
Others	1.10	1.81	2.91
Genera			
Enterococcus	4.81	0.35	5.17
Lactobacillus	2.71	3.61	6.32
Peptostreptococcus	1.71	6.32	8.02
Romboutsia	4.86	0.40	5.27
Cetobacterium	16.30	6.52	22.82
Mycoplasma	7.57	15.10	22.67
Others	12.19	17.55	29.74

Fecal microbiota composition in red and white fillet fish

Alpha and beta diversity

The alpha diversity assessment by Wilcoxon rank sum test shows no significant difference between the red and the white fillet group at P = 0.05, as shown in Figure 2. The effect of time of sample collection within a group is non-significant.

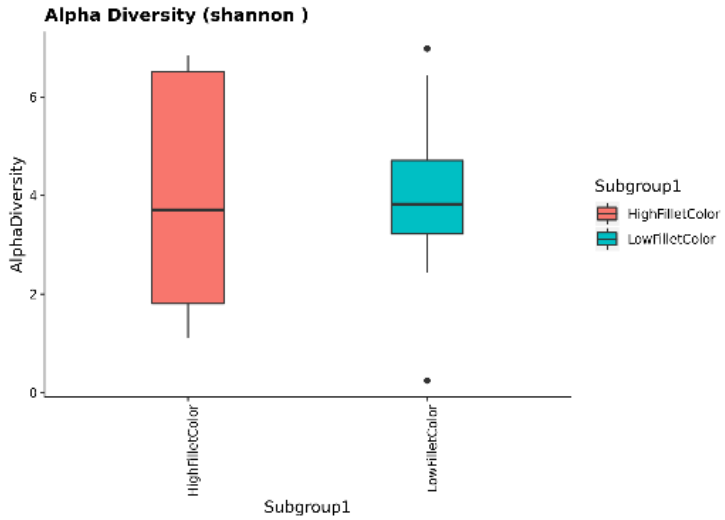

Figure 2: Alpha diversity values between the red (high fillet color) and white (low fillet color) groups.

The principal component analysis (PCA) of the beta diversity index calculated by the Bray-Curtis dissimilarity using unique amplicon sequence variants (ASV) showed clustering of the samples along the white versus red fillet group (Figure 3). Principal components 1 and 2 explain about 33.19% and 22.42% of the total variation in the data, respectively. It shows that the samples from the white fillet group have a more similar microbial community than those from the red fillet group.

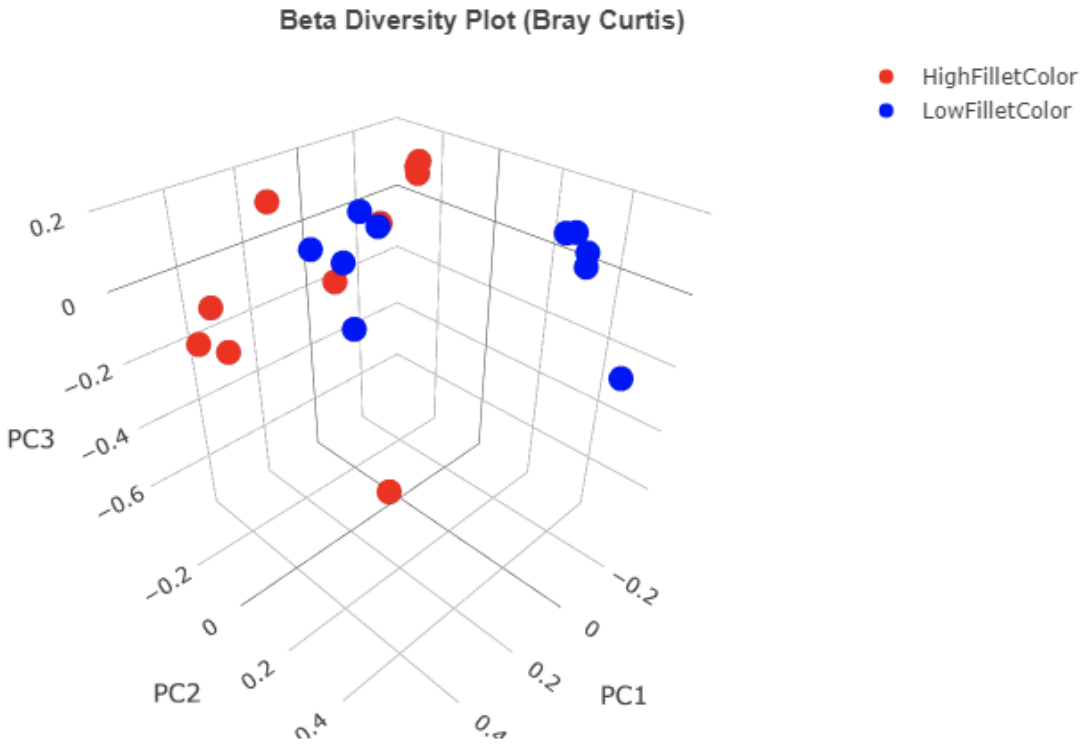

Figure 3: PCA of the beta diversity index showing the red (high fillet color) and white (low fillet color) group clustering.

Figure 4. Linear discriminate analysis score of differentially enriched taxa in fecal samples from the red (high) and white (low) fillet group.

Linear discriminant analysis for effect size.

Fecal samples were collected at two time points from the fish used in this study: after three and six months (March and June 2021). Figure 4 and Supplementary Table 1 show the phyla, classes, orders, families, and genera with a linear discriminate analysis score greater than 1.5 and a p-value less than 0.05 between the two groups when all samples are combined for microbiome composition analyses.

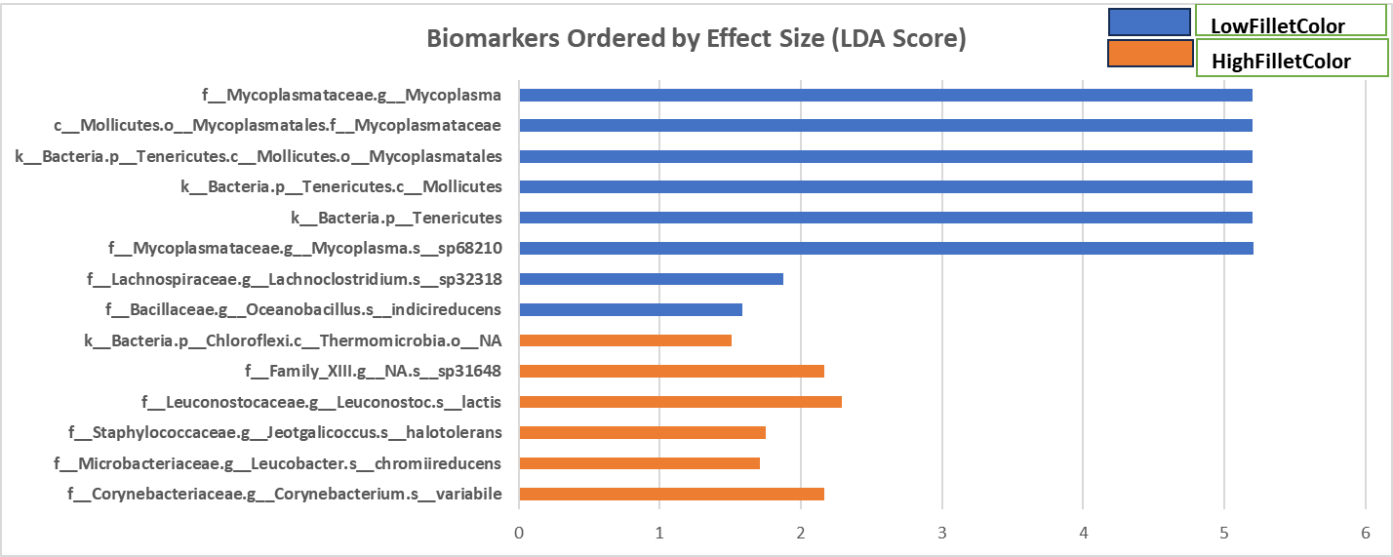

Figure 4. Linear discriminate analysis score of differentially enriched taxa in fecal samples from the red (high) and white (low) fillet group.

Fecal samples from the red fillet group had more taxa enriched of phyla Actinobacteria and Firmicutes and classes Actinobacteria, Clostridia, and Bacilli. The genera enriched in this group include *Leucobacter, Jeotgalicoccus, Corynebacterium*, and *Leuconostoc*. In contrast, fecal samples from the white fillet fish had more bacterial taxa enriched from phyla Tenericutes and Firmicutes and classes Mollicutes bacilli and clostridia. The genera enriched in this group are *Lachnoclostridium*, *Oceanobacillus*, and *Mycoplasma*.

In analyzing March and June sampling separately, the LEfSE analysis for the March samples revealed the same differentially enriched taxonomic groups as those observed in the combined analysis (supplementary table 1). However, when June fecal samples were analyzed separately, only genera *Mycoplasma* and *Terrisporobacter* were enriched in the white fillet group (supplementary table 1).

Discussion

In this study, we investigated the gut microbiome composition in rainbow trout families with reddish-pink fillet (red fillet group) coloration compared to families with pale white fillet (white fillet group) color to identify bacterial biomarkers associated with fillet color.

There is a significant difference between the color value (saturation index) between the white and the red fillet group. This difference indicates that the red fillet group had more of the desired reddish/pink fillet coloration, and the red group can retain more of the supplemented feed pigment astaxanthin into the fish's muscular tissue.

The alpha diversity measure describes the number of bacteria taxa in each sample. There is no significant difference in the alpha diversity measure between the red and the white fillet group. On the other hand, the beta diversity PCA plot showed a separation in the bacteria taxa composition between the red and the white fillet group.

The LEFSe tool was used to identify candidate biomarkers for fillet color in rainbow trout. As discussed below, we found specific taxa indicators of the fillet color groups.

Bacterial taxa enriched in the red fillet fish

The taxa *Leuconostoc lactis, Corynebacterium variabile, Jeotgalicoccus halotolerans, and Leucobacter chromiireducens* are significantly more abundant in the red fillet group.

Leuconostoc lactis is a gram positive, facultative anerobic lactic acid bacterium. It has been reported to have probiotic and prebiotic effects in the intestinal tract of fish (Lee et al., 2019; Zhang et al., 2013). It shows a better adaptive and colonization strategy in the intestine of black porgy fish due to its tolerance to a wide range of pH, bile, trypsin, and pepsin (Zhang et al., 2013). These properties might be favorable to the host's health and contribute to improving the fillet quality of the red fillet group fish.

The bacteria genus *Corynebacterium*, enriched in the red fillet group, includes a diverse group of non-pathogenic species (Brennan et al., 2002). *Corynebacterium variabile* can metabolize lactate and has been shown to contribute to the development of flavor and textural properties of cheese during the ripening process (Schröder et al., 2011). *Corynebacterium variabile,* through the production of pigments, has been suggested as one of the surface bacteria on cheese that

contributes to the color development and intensity of the Irish red-smear cheese (Mounier et al., 2006). The potential of carotenoid production from other bacteria of the genus *Corynebacterium* has been previously reported (Heider et al., 2012; Shahidi et al., 1998; Starr & Saperstein, 1953; Wariso et al., 2006). They mostly use dimethylallyl pyrophosphate as a precursor in the methylerythritol phosphate pathway to generate carotenoids (Heider et al., 2012).

Jeotgalicoccus halotolerans is a gram-positive, anaerobic bacterium first isolated from the Korean fermented seafood jeotgal (Yoon et al., 2003). It is enriched in the red fillet group. This bacterium is reported to be both halophilic and halotolerant; that is, it can survive both in the absence of salt and high salt concentrations. Halotrophic bacteria have been reported in the literature as capable of producing carotenoid pigments (Asker & Ohta, 1999; Calegari-Santos et al., 2016; de Lourdes Moreno et al., 2012; Oren, 2010). The carotenoids produced by this group of bacteria are essential for survival in environments where carotenoids can play a role in membrane stabilization and protection against reactive oxygen species (Yatsunami et al., 2014). *Jeotgalicoccus halotolerans* belongs to the order Bacillales.

Leucobacter chromiireducens is a bacterium first isolated from a chromium-contaminated environment, showing it is resistant to chromate stress (Morais et al., 2004). It is classified as a heavy-metal degrader and possesses chromium reduction ability, which can be used to reduce chromium contamination (Zhu et al., 2008). The bacteria were enriched in the gut microbiome of fish reared in a polluted river, functioning as a chromium degrader (Bharti et al., 2022). One mechanism by which *Leucobacter* bacteria respond to chromate stress is to increase the cellular production of carotenoids (Sturm et al., 2018). Carotenoid production can reduce the concentration of reactive oxygen species and increase cell membrane stability (Chen & Tian, 2021; Sturm et al., 2018). This bacterium's carotenoid production mechanism might contribute to the red fillet by increasing muscle carotenoid content.

Nguyen et al. (2020) identified *Carnobacterium* as strongly associated with reddish-pink fillet color in Atlantic salmon. *Carnobacterium* is a bacteria genus belonging to the lactic acid bacteria group, just as *Leuconostoc lactis*, identified as a marker of the red-fillet group in this study. They produce lactic acid as a metabolic end-product of carbohydrate fermentation. *Corynebacterium variabile,* also identified in the red fillet group, can ferment lactic acid. The lactic acid bacteria contribute to the host's health by acting as probiotics and protecting against diseases (He et al.,

2017). Feeding *Carnobacterium* to rainbow trout increased their survival rate during infection challenge trials (Robertson et al., 2000).

Bacterial taxa enriched in the white fillet fish

Mycoplasma (g), *lachnoclostridium* (g) and *Oceanobacillus indicireducens* are associated with the white fillet color. The bacteria of class mollicutes is the most enriched in the white fillet group. Mycoplasmas (class mollicutes) are small and widespread in humans, plants, animals, and insects. Most of them live as commensals in the host, while others are parasitic, causing chronic infection (Razin & Hayflick, 2010). Another bacterium enriched in the white fillet group is the *Oceanobacillus indicireducens*. It is a facultatively alkaliphilic strain capable of reducing indigo dye extract from *Indigofera tinctoria* plant through fermentation (Hirota et al., 2013). Indigo is used to color textiles, and its reduced state is necessary to facilitate solubility in water (Chavan, 2015). *Lachnoclostridium is a gram-positive, obligate anaerobic, spore-forming bacterial genus under the class Clostridia* (Dandachi et al., 2021). *Species under this genus has been identified as markers of several diseases and metabolic conditions in human, such as* colorectal adenoma (Liang et al., 2020), atherosclerosis (Cai et al., 2022), and serum circulating acetate levels (Nogal et al., 2021).

Similar bacterial taxa as those discussed above were differentially enriched in the March sampling group when analyzed as a stand-alone. However, *Mycoplasma* (genus) and *Terrisporobacter* (genus), found in the white fillet group, were the only enriched taxa when the June samples were analyzed alone. *Terrisporobacter* is an anaerobic acetogenic and pathogenic bacterium capable of degrading carbon sources like xylose and cellobiose (Y. Chen et al., 2021; Cheng et al., 2016; Guo et al., 2023). Differences in bacteria composition were observed in human studies due to differences in fecal sample collection time (Jones et al., 2021; Taft et al., 2014).

Conclusion

The gut microbiome can contribute to phenotypic variation in the host animal. Thus, this study aimed to understand the difference in microbiome composition between two rainbow trout groups with divergent fillet colors. We identified bacteria taxa differentially enriched in white and red-fillet rainbow trout genetic families. The bacteria taxa identified have diverse metabolic pathways that may affect host physiology and fillet color and thus may serve as biomarkers for fillet color.

The bacterial taxa community enriched in the red fillet group has probiotic functions and can generate carotenoid pigments, while Mycoplasma, a bacteria taxon that can be pathogenic, is enriched in the white fillet group. This study extends our understanding of the relationship between gut microbiome and fillet color in rainbow trout. The differential abundance of these bacteria taxa could be incorporated into genomic prediction models to accelerate genetic improvement of fillet color in rainbow trout.

Abbreviations

ASV: amplicon sequence variants, SI: Saturation Index, LEfSe: linear discriminant analysis for effect size, NCCCWA: National Center for Cool and Cold-water Aquaculture

Ethics Declarations

Ethics approval and consent to participate

Husbandry practice and experimental procedures at the facility were approved by the IACUC animal study protocol of the University of Maryland, College Park, protocol number 1593175-6. All methods were carried out in accordance with relevant guidelines and regulations. All methods were carried out in accordance with ARRIVE guidelines.

Availability of data and materials

All datasets generated for this study are included in the manuscript and/or the Additional Files. . All raw sequence data generated in this study has been deposited in NCBI under BioProject accession number PRJNA974903, https://www.ncbi.nlm.nih.gov/bioproject/PRJNA974903

Funding

This study was supported by competitive grants No. 2021-67015-33388, 2023-67015-39742 from the United States Department of Agriculture, National Institute of Food and Agriculture (M.S) and by the USDA, Agricultural Research Service CRIS Project 8082-31000-013 “Integrated Research Approaches for Improving Production Efficiency in Rainbow Trout” (T. L). The content is solely the authors’ responsibility and does not necessarily represent the official views of any funding agents.

Authors’ Information

Ridwan O. Ahmed,[1] Ali Ali,[1] Tim Leeds,[2], and Mohamed Salem[1, *]

[1]Department of Animal and Avian Sciences, University of Maryland, College Park, MD 20742, USA.

[2]United States Department of Agriculture Kearneysville, National Center for Cool and Cold Water Aquaculture, Agricultural Research Service, Kearneysville, WV 25430, USA.

Corresponding author

Correspondence to Mohamed Salem.

Figures, tables and additional files

Electronic Supplementary Materials

Additional file 1: **Table S1:** Bacteria biomarkers identified by LEfSE for the March, June and combined March and June analysis with their effect sizes

References

Aas, G., Bjerkeng, B., Storebakken, T., & Ruyter, B. (1999). Blood appearance, metabolic transformation and plasma transport proteins of 14C-astaxanthin in Atlantic salmon (Salmo salar L.). *Fish Physiology and Biochemistry*, *21*, 325-334.

Aguilar, I., Misztal, I., Johnson, D. L., Legarra, A., Tsuruta, S., & Lawlor, T. J. (2010). Hot topic: a unified approach to utilize phenotypic, full pedigree, and genomic information for genetic evaluation of Holstein final score. *J Dairy Sci*, *93*(2), 743-752. https://doi.org/10.3168/jds.2009-2730

Aguilar, I., Misztal, I., Legarra, A., & Tsuruta, S. (2011). Efficient computation of the genomic relationship matrix and other matrices used in single-step evaluation. *Journal of Animal Breeding and Genetics*, *128*(6), 422-428.

Ahmed, R. O., Ali, A., Al-Tobasei, R., Leeds, T., Kenney, B., & Salem, M. (2022). Weighted Single-Step GWAS Identifies Genes Influencing Fillet Color in Rainbow Trout. *Genes*, *13*(8), 1331.

Akasaki, Y., Alvarez-Garcia, O., Saito, M., Caramés, B., Iwamoto, Y., & Lotz, M. K. (2014). FoxO transcription factors support oxidative stress resistance in human chondrocytes. *Arthritis & rheumatology*, *66*(12), 3349-3358.

Al-Tobasei, R., Ali, A., Garcia, A. L., Lourenco, D., Leeds, T., & Salem, M. (2021). Genomic predictions for fillet yield and firmness in rainbow trout using reduced-density SNP panels. *BMC genomics*, *22*, 1-11.

Al-Tobasei, R., Ali, A., Leeds, T. D., Liu, S., Palti, Y., Kenney, B., & Salem, M. (2017). Identification of SNPs associated with muscle yield and quality traits using allelic-imbalance analyses of pooled RNA-Seq samples in rainbow trout. *BMC genomics*, *18*(1), 1-15.

Alexander, C. C., Munkascy, E., Tillmon, H., Fraker, T., Scheirer, J., Holstein, D.,…Rodriguez, K. A. (2022). HspB1 Overexpression Improves Life Span and Stress Resistance in an Invertebrate Model. *J Gerontol A Biol Sci Med Sci*, *77*(2), 268-275. https://doi.org/10.1093/gerona/glab296

Ali, A., Al-Tobasei, R., Kenney, B., Timothy, D., & Mohamed, S. (2018). Integrated analysis of lncRNA and mRNA expression in rainbow trout families showing variation in muscle growth and fillet quality traits. Sci Rep 8, 12111. In.

Ali, A., Al-Tobasei, R., Lourenco, D., Leeds, T., Kenney, B., & Salem, M. (2019). Genome-wide association study identifies genomic loci affecting filet firmness and protein content in rainbow trout. *Frontiers in genetics*, *10*, 386.

Ali, A., Al-Tobasei, R., Lourenco, D., Leeds, T., Kenney, B., & Salem, M. (2019). Genome-Wide Association Study Identifies Genomic Loci Affecting Filet Firmness and Protein Content in Rainbow Trout. *Front Genet*, *10*, 386. https://doi.org/10.3389/fgene.2019.00386

Ali, A., Al-Tobasei, R., Lourenco, D., Leeds, T., Kenney, B., & Salem, M. (2020a). Genome-wide identification of loci associated with growth in rainbow trout. *BMC genomics*, *21*(1), 1-16.

Ali, A., Al-Tobasei, R., Lourenco, D., Leeds, T., Kenney, B., & Salem, M. (2020a). Genome-wide identification of loci associated with growth in rainbow trout. *BMC genomics*, *21*(1), 209. https://doi.org/10.1186/s12864-020-6617-x

Ali, A., Al-Tobasei, R., Lourenco, D., Leeds, T., Kenney, B., & Salem, M. (2020b). Genome-wide scan for common variants associated with intramuscular fat and moisture content in rainbow trout. *BMC genomics*, *21*(1), 1-17.

Ali, A., Al-Tobasei, R., Lourenco, D., Leeds, T., Kenney, B., & Salem, M. (2020b). Genome-wide scan for common variants associated with intramuscular fat and moisture content in rainbow trout. *BMC genomics*, *21*(1), 529. https://doi.org/10.1186/s12864-020-06932-0

Allendorf, F. W., & Thorgaard, G. H. (1984). Tetraploidy and the evolution of salmonid fishes. *Evolutionary genetics of fishes*, 1-53.

Almeida, A., Mitchell, A. L., Tarkowska, A., & Finn, R. D. (2018). Benchmarking taxonomic assignments based on 16S rRNA gene profiling of the microbiota from commonly sampled environments. *Gigascience*, *7*(5), giy054.

Amengual, J., Widjaja-Adhi, M. A. K., Rodriguez-Santiago, S., Hessel, S., Golczak, M., Palczewski, K., & Von Lintig, J. (2013). Two Carotenoid Oxygenases Contribute to Mammalian Provitamin A Metabolism*♦. *Journal of Biological Chemistry*, *288*(47), 34081-34096.

Andrews, S. (2010). FastQC: a quality control tool for high throughput sequence data. In: Cambridge, United Kingdom.

Arihara, K., Cassens, R. G., Greaser, M. L., Luchansky, J. B., & Mozdziak, P. E. (1995). Localization of metmyoglobin-reducing enzyme (NADH-cytochrome b5 reductase) system components in bovine skeletal muscle. *Meat science*, *39*(2), 205-213.

Armstrong, G. A., & Hearst, J. E. (1996). Genetics and molecular biology of carotenoid pigment biosynthesis. *The FASEB Journal*, *10*(2), 228-237.

Arredondo-Figueroa, J. L., Mora, G. I. d. l., Ponce-Palafox, J. T., Barriga-Sosa, I. d. l. A., & Vernon-Carter, E. J. (2007). Color of raw, frozen, and smoked fillets of rainbow trout (Oncorhynchus mykiss) fed diets supplemented with astaxanthin and saponified red chilli (Capsicum annuum) extracts. *Journal of Aquatic Food Product Technology*, *16*(1), 35-50.

Arya, R., Mallik, M., & Lakhotia, S. C. (2007). Heat shock genes—integrating cell survival and death. *Journal of biosciences*, *32*(3), 595-610.

Asker, D., & Ohta, Y. (1999). Production of canthaxanthin by extremely halophilic bacteria. *Journal of bioscience and bioengineering*, *88*(6), 617-621.

Association, A. M. S. (1991). Guidelines for meat color evaluation. proceedings: The 44th annual reciprocal meat conference. Kans, Chicago,

Aussanasuwannakul, A., Kenney, P. B., Weber, G. M., Yao, J., Slider, S. D., Manor, M. L., & Salem, M. (2011). Effect of sexual maturation on growth, fillet composition, and texture of female rainbow trout (Oncorhynchus mykiss) on a high nutritional plane. *Aquaculture*, *317*(1-4), 79-88.

Awany, D., Allali, I., Dalvie, S., Hemmings, S., Mwaikono, K. S., Thomford, N. E.,…Chimusa, E. R. (2018). Host and Microbiome Genome-Wide Association Studies: Current State and Challenges. *Front Genet*, *9*, 637. https://doi.org/10.3389/fgene.2018.00637

Bagga, S., Bracht, J., Hunter, S., Massirer, K., Holtz, J., Eachus, R., & Pasquinelli, A. E. (2005). Regulation by let-7 and lin-4 miRNAs results in target mRNA degradation. *Cell*, *122*(4), 553-563.

Bailey, A. J., & Light, N. D. (1989). *Connective tissue in meat and meat products*. Elsevier applied science.

Baker, R., Pfeiffer, A.-M., Schöner, F.-J., & Smith-Lemmon, L. (2002). Pigmenting efficacy of astaxanthin and canthaxanthin in fresh-water reared Atlantic salmon, Salmo salar. *Animal Feed Science and Technology*, *99*(1-4), 97-106.

Banerjee, R., & Vlasie, M. (2002). Controlling the reactivity of radical intermediates by coenzyme B12-dependent methylmalonyl-CoA mutase. *Biochemical Society Transactions*, *30*(4), 621-624.

Bartel, D. P. (2004). MicroRNAs: genomics, biogenesis, mechanism, and function. *cell*, *116*(2), 281-297. https://doi.org/10.1016/s0092-8674(04)00045-5

Bates, J. M., Akerlund, J., Mittge, E., & Guillemin, K. (2007). Intestinal alkaline phosphatase detoxifies lipopolysaccharide and prevents inflammation in zebrafish in response to the gut microbiota. *Cell host & microbe*, *2*(6), 371-382.

Bates, J. M., Mittge, E., Kuhlman, J., Baden, K. N., Cheesman, S. E., & Guillemin, K. (2006). Distinct signals from the microbiota promote different aspects of zebrafish gut differentiation. *Developmental biology*, *297*(2), 374-386.

Beghini, F., McIver, L. J., Blanco-Míguez, A., Dubois, L., Asnicar, F., Maharjan, S.,…Thomas, A. M. (2021). Integrating taxonomic, functional, and strain-level profiling of diverse microbial communities with bioBakery 3. *elife*, *10*, e65088.

Bellanti, F., Villani, R., Facciorusso, A., Vendemiale, G., & Serviddio, G. (2017). Lipid oxidation products in the pathogenesis of non-alcoholic steatohepatitis. *Free Radic Biol Med*, *111*, 173-185. https://doi.org/10.1016/j.freeradbiomed.2017.01.023

Ben-Dor, A., Nahum, A., Danilenko, M., Giat, Y., Stahl, W., Martin, H.-D.,…Sharoni, Y. (2001). Effects of acyclo-retinoic acid and lycopene on activation of the retinoic acid receptor and proliferation of mammary cancer cells. *Archives of Biochemistry and Biophysics*, *391*(2), 295-302.

Bernard, M., Dehaullon, A., Prchal, M., Haffray, P., Quillet, E., Dupont-Nivet, M.,…Phocas, F. (2022). Development of a high-density 665 K SNP array for rainbow trout genome-wide genotyping. *Frontiers in Genetics*, *13*, 941340.

Bharti, M., Nagar, S., Khurana, H., & Negi, R. K. (2022). Metagenomic insights to understand the role of polluted river Yamuna in shaping the gut microbial communities of two invasive fish species. *Archives of Microbiology*, *204*(8), 509.

Bjerkeng, B., Refstie, S., Fjalestad, K., Storebakken, T., Rødbotten, M., & Roem, A. (1997). Quality parameters of the flesh of Atlantic salmon (Salmo salar) as affected by dietary fat content and full-fat soybean meal as a partial substitute for fish meal in the diet. *Aquaculture*, *157*(3-4), 297-309.

Bjerkeng, B., Storebakken, T., & Liaaen-Jensen, S. (1992). Pigmentation of rainbow trout from start feeding to sexual maturation. *Aquaculture*, *108*(3-4), 333-346.

Blay, C., Haffray, P., Bugeon, J., D'ambrosio, J., Dechamp, N., Collewet, G.,…Corraze, G. (2021). Genetic parameters and genome-wide association studies of quality traits characterised using imaging technologies in Rainbow trout, Oncorhynchus mykiss. *Frontiers in genetics*, *12*, 219.

Boggio, G. M., Christensen, O., Legarra, A., Meynadier, A., & Marie-Etancelin, C. (2023). Microbiability of milk composition and genetic control of microbiota effects in sheep. *Journal of Dairy Science*, *106*(9), 6288-6298.

Bohn, T., Desmarchelier, C., Dragsted, L. O., Nielsen, C. S., Stahl, W., Rühl, R.,…Borel, P. (2017). Host-related factors explaining interindividual variability of carotenoid bioavailability and tissue concentrations in humans. *Molecular nutrition & food research*, *61*(6), 1600685.

Bohn, T., Desmarchelier, C., El, S. N., Keijer, J., van Schothorst, E., Rühl, R., & Borel, P. (2019). β-carotene in the human body: metabolic bioactivation pathways–from digestion to tissue distribution and excretion. *Proceedings of the Nutrition Society*, *78*(1), 68-87.

Bonder, M. J., Kurilshikov, A., Tigchelaar, E. F., Mujagic, Z., Imhann, F., Vila, A. V.,…Zhernakova, A. (2016). The effect of host genetics on the gut microbiome. *Nat Genet*, *48*(11), 1407-1412. https://doi.org/10.1038/ng.3663

Borel, P. (2003). Factors affecting intestinal absorption of highly lipophilic food microconstituents (fat-soluble vitamins, carotenoids and phytosterols).

Borel, P., Desmarchelier, C., Nowicki, M., & Bott, R. (2015a). A combination of single-nucleotide polymorphisms is associated with interindividual variability in dietary β-carotene bioavailability in healthy men. *The Journal of Nutrition*, *145*(8), 1740-1747.

Borel, P., Desmarchelier, C., Nowicki, M., & Bott, R. (2015b). Lycopene bioavailability is associated with a combination of genetic variants. *Free Radical Biology and Medicine*, *83*, 238-244.

Borel, P., Desmarchelier, C., Nowicki, M., Bott, R., Morange, S., & Lesavre, N. (2014). Interindividual variability of lutein bioavailability in healthy men: characterization, genetic variants involved, and relation with fasting plasma lutein concentration. *The American journal of clinical nutrition*, *100*(1), 168-175.

Borel, P., Grolier, P., Mekki, N., Boirie, Y., Rochette, Y., Le Roy, B.,…Azais-Braesco, V. (1998). Low and high responders to pharmacological doses of β-carotene: proportion in the population, mechanisms involved and consequences on β-carotene metabolism. *Journal of lipid research*, *39*(11), 2250-2260.

Borel, P., Lietz, G., Goncalves, A., Szabo de Edelenyi, F., Lecompte, S., Curtis, P.,…Packard, C. (2013). CD36 and SR-BI are involved in cellular uptake of provitamin A carotenoids by Caco-2 and HEK cells, and some of their genetic variants are associated with plasma concentrations of these micronutrients in humans. *The Journal of nutrition*, *143*(4), 448-456.

Boussaha, M., Guyomard, R., Cabau, C., Esquerré, D., & Quillet, E. (2012). Development and characterisation of an expressed sequence tags (EST)-derived single nucleotide polymorphisms (SNPs) resource in rainbow trout. *BMC genomics*, *13*(1), 1-11.

Brennan, N. M., Ward, A. C., Beresford, T. P., Fox, P. F., Goodfellow, M., & Cogan, T. M. (2002). Biodiversity of the bacterial flora on the surface of a smear cheese. *Applied and Environmental Microbiology*, *68*(2), 820-830.

Brown, K. R., Barnes, M., Parker, T., & Fletcher, B. (2016). Retention of fillet coloration in rainbow trout after dietary astaxanthin cessation. *Fisheries & Aquaculture Journal*, *7*, 163.

Brown, R. M., Wiens, G. D., & Salinas, I. (2019). Analysis of the gut and gill microbiome of resistant and susceptible lines of rainbow trout (Oncorhynchus mykiss). *Fish & shellfish immunology*, *86*, 497-506.

Brugman, S., & Nieuwenhuis, E. E. (2010). Mucosal control of the intestinal microbial community. *Journal of Molecular Medicine*, *88*, 881-888.

Brunham, L. R., Kruit, J. K., Iqbal, J., Fievet, C., Timmins, J. M., Pape, T. D.,…Groen, A. K. (2006). Intestinal ABCA1 directly contributes to HDL biogenesis in vivo. *The Journal of clinical investigation*, *116*(4), 1052-1062.

Budanov, A. V., Sablina, A. A., Feinstein, E., Koonin, E. V., & Chumakov, P. M. (2004). Regeneration of peroxiredoxins by p53-regulated sestrins, homologs of bacterial AhpD. *Science*, *304*(5670), 596-600. https://doi.org/10.1126/science.1095569

Budanov, A. V., Shoshani, T., Faerman, A., Zelin, E., Kamer, I., Kalinski, H.,…Feinstein, E. (2002). Identification of a novel stress-responsive gene Hi95 involved in regulation of cell viability. *Oncogene*, *21*(39), 6017-6031. https://doi.org/10.1038/sj.onc.1205877

Buitenhuis, B., Lassen, J., Noel, S. J., Plichta, D. R., Sørensen, P., Difford, G. F., & Poulsen, N. A. (2019). Impact of the rumen microbiome on milk fatty acid composition of Holstein cattle. *Genetics Selection Evolution*, *51*(1), 1-8.

Busch, A. W., & Montgomery, B. L. (2015). Interdependence of tetrapyrrole metabolism, the generation of oxidative stress and the mitigative oxidative stress response. *Redox biology*, *4*, 260-271.

Buttle, L., Crampton, V., & Williams, P. (2001). The effect of feed pigment type on flesh pigment deposition and colour in farmed Atlantic salmon, Salmo salar L. *Aquaculture Research*, *32*(2), 103-111.

Byrd, A. K., Zybailov, B. L., Maddukuri, L., Gao, J., Marecki, J. C., Jaiswal, M.,…Chib, S. (2016). Evidence that G-quadruplex DNA accumulates in the cytoplasm and participates in stress granule assembly in response to oxidative stress. *Journal of Biological Chemistry*, *291*(34), 18041-18057.

Cai, W., Zhang, Y., Chang, T., Wang, Z., Zhu, B., Chen, Y.,…Gao, H. (2023). The eQTL colocalization and transcriptome-wide association study identify potentially causal genes responsible for economic traits in Simmental beef cattle. *Journal of Animal Science and Biotechnology*, *14*(1), 78.

Cai, Y.-Y., Huang, F.-Q., Lao, X., Lu, Y., Gao, X., Alolga, R. N.,…Liu, B. (2022). Integrated metagenomics identifies a crucial role for trimethylamine-producing Lachnoclostridium in promoting atherosclerosis. *NPJ biofilms and microbiomes*, *8*(1), 11.

Calegari-Santos, R., Diogo, R. A., Fontana, J. D., & Bonfim, T. M. B. (2016). Carotenoid production by halophilic archaea under different culture conditions. *Current microbiology*, *72*, 641-651.

Callahan, B. J., McMurdie, P. J., Rosen, M. J., Han, A. W., Johnson, A. J. A., & Holmes, S. P. (2016). DADA2: High-resolution sample inference from Illumina amplicon data. *Nature methods*, *13*(7), 581-583.

Camp, J. G., Jazwa, A. L., Trent, C. M., & Rawls, J. F. (2012). Intronic cis-regulatory modules mediate tissue-specific and microbial control of angptl4/fiaf transcription. *PLoS genetics*, *8*(3), e1002585.

Caporaso, J. G., Kuczynski, J., Stombaugh, J., Bittinger, K., Bushman, F. D., Costello, E. K.,…Gordon, J. I. (2010). QIIME allows analysis of high-throughput community sequencing data. *Nature methods*, *7*(5), 335-336.

Cartwright, G. M., & Scott, B. (2013). Redox regulation of an AP-1-like transcription factor, YapA, in the fungal symbiont Epichloe festucae. *Eukaryotic cell*, *12*(10), 1335-1348.

Castaño Sánchez, C., Palti, Y., & Rexroad, C. (2011). SNP analysis with duplicated fish genomes: differentiation of SNPs, paralogous sequence variants, amd multisite variants. *Next generation sequencing and whole genome selection in aquaculture*, 133-150.

Castenmiller, J. J., & West, C. E. (1998). Bioavailability and bioconversion of carotenoids. *Annu Rev Nutr*, *18*(1), 19-38. https://doi.org/10.1146/annurev.nutr.18.1.19

Cerf-Bensussan, N., & Gaboriau-Routhiau, V. (2010). The immune system and the gut microbiota: friends or foes? *Nature Reviews Immunology*, *10*(10), 735-744.

Chaijan, M., Benjakul, S., Visessanguan, W., & Faustman, C. (2007). Interaction between fish myoglobin and myosin in vitro. *Food Chemistry*, *103*(4), 1168-1175.

Chakraborty, D., Sharma, N., Kour, S., Sodhi, S. S., Gupta, M. K., Lee, S. J., & Son, Y. O. (2022). Applications of omics technology for livestock selection and improvement. *Frontiers in Genetics*, *13*, 774113.

Chan, K. M., & Decker, E. A. (1994). Endogenous skeletal muscle antioxidants. *Crit Rev Food Sci Nutr*, *34*(4), 403-426. https://doi.org/10.1080/10408399409527669

Chapagain, P., Arivett, B., Cleveland, B. M., Walker, D. M., & Salem, M. (2019). Analysis of the fecal microbiota of fast-and slow-growing rainbow trout (Oncorhynchus mykiss). *BMC genomics*, *20*(1), 1-11.

Chavan, R. (2015). Indigo dye and reduction techniques. In *Denim* (pp. 37-67). Elsevier.

Chen, C., Yu, Q., Han, L., Zhang, J., & Guo, Z. (2018). Effects of aldehyde products of lipid oxidation on the color stability and metmyoglobin reducing ability of bovine Longissimus muscle. *Anim Sci J*, *89*(5), 810-816. https://doi.org/10.1111/asj.12993

Chen, J., & Tian, Y. (2021). Hexavalent chromium reducing bacteria: mechanism of reduction and characteristics. *Environmental Science and Pollution Research*, *28*, 20981-20997.

Chen, L., & Liu, B. (2017). Relationships between stress granules, oxidative stress, and neurodegenerative diseases. *Oxidative medicine and cellular longevity*, *2017*.

Chen, X., Peng, M., Yang, C., Li, Q., Feng, P., Zhu, W.,…Zhao, Y. (2024). Genome-wide QTL and eQTL mapping reveal genes associated with growth rate trait of the Pacific white shrimp (Litopenaeus vannamei). *BMC genomics*, *25*(1), 414.

Chen, Y., Xie, Y., Zhong, R., Liu, L., Lin, C., Xiao, L.,…Everaert, N. (2021). Effects of xylo-oligosaccharides on growth and gut microbiota as potential replacements for antibiotic in weaning piglets. *Frontiers in microbiology*, *12*, 641172.

Cheng, M. P., Domingo, M.-C., Lévesque, S., & Yansouni, C. P. (2016). A case report of a deep surgical site infection with Terrisporobacter glycolicus/T. Mayombei and review of the literature. *BMC Infectious Diseases*, *16*, 1-4.

Chiang, J. Y. (2009). Bile acids: regulation of synthesis: thematic review series: bile acids. *Journal of lipid research*, *50*(10), 1955-1966.

Chisté, R. C., Freitas, M., Mercadante, A. Z., & Fernandes, E. (2014). Carotenoids inhibit lipid peroxidation and hemoglobin oxidation, but not the depletion of glutathione induced by ROS in human erythrocytes. *Life sciences*, *99*(1-2), 52-60.

Choubert, G., de la Noüe, J., & Blanc, J.-M. (1991). Apparent digestibility of canthaxanthin in rainbow trout: effect of dietary fat level, antibiotics and number of pyloric caeca. *Aquaculture*, *99*(3-4), 323-329.

Chung, Y.-H., Zhou, M., Holtshausen, L., Alexander, T., McAllister, T., Guan, L.,…Beauchemin, K. (2012). A fibrolytic enzyme additive for lactating Holstein cow diets: ruminal fermentation, rumen microbial populations, and enteric methane emissions. *Journal of dairy science*, *95*(3), 1419-1427.

Cleveland, B. M., Gao, G., & Leeds, T. D. (2020). Transcriptomic response to selective breeding for fast growth in rainbow trout (Oncorhynchus mykiss). *Marine biotechnology*, *22*(4), 539-550.

Cleveland, B. M., Radler, L. M., & Leeds, T. D. Growth, fillet yield, and muscle quality traits are not affected by a genotype by diet interaction in rainbow trout consuming diets that differ in lipid content. *Journal of the World Aquaculture Society*.

Clevidence, B. A., & Bieri, J. G. (1993). [4] Association of carotenoids with human plasma lipoproteins. In *Methods in enzymology* (Vol. 214, pp. 33-46). Elsevier.

Clop, A., Marcq, F., Takeda, H., Pirottin, D., Tordoir, X., Bibe, B.,…Georges, M. (2006). A mutation creating a potential illegitimate microRNA target site in the myostatin gene affects muscularity in sheep. *Nat Genet*, *38*(7), 813-818. https://doi.org/10.1038/ng1810

Clop, A., Marcq, F., Takeda, H., Pirottin, D., Tordoir, X., Bibé, B.,…Eychenne, F. (2006). A mutation creating a potential illegitimate microRNA target site in the myostatin gene affects muscularity in sheep. *Nature genetics*, *38*(7), 813-818.

Clugston, R. D., & Blaner, W. S. (2014). Vitamin A (retinoid) metabolism and actions: What we know and what we need to know about amphibians. *Zoo biology*, *33*(6), 527-535.

Colihueque, N. (2010). Genetics of salmonid skin pigmentation: clues and prospects for improving the external appearance of farmed salmonids. *Reviews in Fish Biology and Fisheries*, *20*(1), 71-86.

Crouse, C. C., Davidson, J. W., Good, C. M., May, T. C., Summerfelt, S. T., Kenney, P. B.,…Cleveland, B. M. (2018). Growth and fillet quality attributes of five genetic strains of rainbow trout (Oncorhynchus mykiss) reared in a partial water reuse system and harvested at different sizes. *Aquaculture Research*, *49*(4), 1672-1681.

Cui, X., Hou, Y., Yang, S., Xie, Y., Zhang, S., Zhang, Y.,…Sun, D. (2014). Transcriptional profiling of mammary gland in Holstein cows with extremely different milk protein and fat percentage using RNA sequencing. *BMC genomics*, *15*, 1-15.

Dallinga-Thie, G. M., Franssen, R., Mooij, H. L., Visser, M. E., Hassing, H. C., Peelman, F.,…Nieuwdorp, M. (2010). The metabolism of triglyceride-rich lipoproteins revisited: new players, new insight. *Atherosclerosis*, *211*(1), 1-8.

Damon, M., Wyszynska-Koko, J., Vincent, A., Herault, F., & Lebret, B. (2012). Comparison of muscle transcriptome between pigs with divergent meat quality phenotypes identifies genes related to muscle metabolism and structure. *PLoS One*, *7*(3), e33763.

Dandachi, I., Anani, H., Hadjadj, L., Brahimi, S., Lagier, J.-C., Daoud, Z., & Rolain, J.-M. (2021). Genome analysis of Lachnoclostridium phocaeense isolated from a patient after kidney transplantation in Marseille. *New Microbes and New Infections*, *41*, 100863.

Dawkins, R. (2016). *The extended phenotype: The long reach of the gene*. Oxford University Press.

de Lourdes Moreno, M., Sánchez-Porro, C., García, M. T., & Mellado, E. (2012). Carotenoids' production from halophilic bacteria. *Microbial Carotenoids from Bacteria and Microalgae: Methods and Protocols*, 207-217.

dela Seña, C., Riedl, K. M., Narayanasamy, S., Curley, R. W., Schwartz, S. J., & Harrison, E. H. (2014). The human enzyme that converts dietary provitamin A carotenoids to vitamin A is a dioxygenase. *Journal of biological chemistry*, *289*(19), 13661-13666.

Deming, D. M., & Erdman, J. W. (1999). Mammalian carotenoid absorption and metabolism. *Pure and Applied Chemistry*, *71*(12), 2213-2223.

Denstadli, V., Vegusdal, A., Krogdahl, Å., Bakke-McKellep, A., Berge, G., Holm, H.,…Ruyter, B. (2004). Lipid absorption in different segments of the gastrointestinal tract of Atlantic salmon (Salmo salar L.). *Aquaculture*, *240*(1-4), 385-398.

Desai, A. R., Links, M. G., Collins, S. A., Mansfield, G. S., Drew, M. D., Van Kessel, A. G., & Hill, J. E. (2012). Effects of plant-based diets on the distal gut microbiome of rainbow trout (Oncorhynchus mykiss). *Aquaculture*, *350*, 134-142.

Desmarchelier, C., & Borel, P. (2017). Overview of carotenoid bioavailability determinants: From dietary factors to host genetic variations. *Trends in Food Science & Technology*, *69*, 270-280.

Difford, G. F. (2018). *Genetic control of methane emission, feed efficiency and metagenomics in dairy cattle* Wageningen University and Research].

Druet, T., Macleod, I., & Hayes, B. (2014). Toward genomic prediction from whole-genome sequence data: impact of sequencing design on genotype imputation and accuracy of predictions. *Heredity*, *112*(1), 39-47.

During, A., Dawson, H. D., & Harrison, E. H. (2005). Carotenoid transport is decreased and expression of the lipid transporters SR-BI, NPC1L1, and ABCA1 is downregulated in Caco-2 cells treated with ezetimibe. *The Journal of nutrition*, *135*(10), 2305-2312.

Déru, V., Tiezzi, F., Carillier-Jacquin, C., Blanchet, B., Cauquil, L., Zemb, O.,…Gilbert, H. (2024). The potential of microbiota information to better predict efficiency traits in growing pigs fed a conventional and a high-fiber diet. *Genetics Selection Evolution*, *56*(1), 8.

D'Ambrosio, D. N., Clugston, R. D., & Blaner, W. S. (2011). Vitamin A metabolism: an update. *Nutrients*, *3*(1), 63-103.

D'Ambrosio, J., Morvezen, R., Brard-Fudulea, S., Bestin, A., Acin Perez, A., Guéméné, D.,…Phocas, F. (2020). Genetic architecture and genomic selection of female reproduction traits in rainbow trout. *BMC genomics*, *21*, 1-14.

Essers, M. A., Weijzen, S., de Vries-Smits, A. M., Saarloos, I., de Ruiter, N. D., Bos, J. L., & Burgering, B. M. (2004). FOXO transcription factor activation by oxidative stress mediated by the small GTPase Ral and JNK. *The EMBO journal*, *23*(24), 4802-4812.

Esterbauer, H., Schaur, R. J., & Zollner, H. (1991). Chemistry and biochemistry of 4-hydroxynonenal, malonaldehyde and related aldehydes. *Free Radic Biol Med*, *11*(1), 81-128. https://doi.org/10.1016/0891-5849(91)90192-6

Faustman, C., Sun, Q., Mancini, R., & Suman, S. P. (2010). Myoglobin and lipid oxidation interactions: mechanistic bases and control. *Meat Sci*, *86*(1), 86-94. https://doi.org/10.1016/j.meatsci.2010.04.025

Fayemi, P., & Muchenje, V. (2018). Expression of ovine ubiquitin C-terminal hydroxylase 1, pH and colour of variety meats from head-stunned Dohne Merino sheep. *South African Journal of Animal Science*, *48*(1), 88-97.

Folkestad, A., Wold, J. P., Rørvik, K.-A., Tschudi, J., Haugholt, K. H., Kolstad, K., & Mørkøre, T. (2008). Rapid and non-invasive measurements of fat and pigment concentrations in live and slaughtered Atlantic salmon (Salmo salar L.). *Aquaculture*, *280*(1-4), 129-135.

Forcina, G., Pérez-Pardal, L., Carvalheira, J., & Beja-Pereira, A. (2022). Gut microbiome studies in livestock: achievements, challenges, and perspectives. *Animals*, *12*(23), 3375.

Forsberg, O. I., & Guttormsen, A. G. (2006). Modeling optimal dietary pigmentation strategies in farmed Atlantic salmon: Application of mixed-integer non-linear mathematical programming techniques. *Aquaculture*, *261*(1), 118-124.

Frank, A., & Groll, M. (2017). The methylerythritol phosphate pathway to isoprenoids. *Chemical Reviews*, *117*(8), 5675-5703.

Fraslin, C., Phocas, F., Bestin, A., Charles, M., Bernard, M., Krieg, F.,…Petitprez, F. (2020). Genetic determinism of spontaneous masculinisation in XX female rainbow trout: new insights using medium throughput genotyping and whole-genome sequencing. *Scientific Reports*, *10*(1), 17693.

Gagaoua, M., Bonnet, M., De Koning, L., & Picard, B. (2018). Reverse Phase Protein array for the quantification and validation of protein biomarkers of beef qualities: The case of meat color from Charolais breed. *Meat Sci*, *145*, 308-319. https://doi.org/10.1016/j.meatsci.2018.06.039

Gallagher, M. D., & Chen-Plotkin, A. S. (2018). The post-GWAS era: from association to function. *The American Journal of Human Genetics*, *102*(5), 717-730.

Gao, G., Nome, T., Pearse, D. E., Moen, T., Naish, K. A., Thorgaard, G. H.,…Palti, Y. (2018). A new single nucleotide polymorphism database for rainbow trout generated through whole genome resequencing. *Frontiers in genetics*, *9*, 363858.

Gao, H., Antony, R., Srinivasan, R., Wu, P., Wang, X., & Li, Y. (2020). UCHL1 regulates oxidative activity in skeletal muscle. *PLoS One*, *15*(11), e0241716. https://doi.org/10.1371/journal.pone.0241716

Gao, H., Hartnett, S., & Li, Y. (2017). Ubiquitin C-Terminal Hydrolase L1 regulates myoblast proliferation and differentiation. *Biochem Biophys Res Commun*, *492*(1), 96-102. https://doi.org/10.1016/j.bbrc.2017.08.027

Gao, N., Chen, Y., Liu, X., Zhao, Y., Zhu, L., Liu, A.,…Chen, Y. (2019). Weighted single-step GWAS identified candidate genes associated with semen traits in a Duroc boar population. *BMC genomics*, *20*(1), 797. https://doi.org/10.1186/s12864-019-6164-5

Gao, Q., Liu, P., Li, Y., Song, D., Long, W., Wang, Z.,…Jiang, L. (2023). Gut microbiota, host genetics and phenotypes in aquatic animals: A review. *Aquaculture Reports*, *31*, 101648.

Gao, X., Wu, W., Ma, C., Li, X., & Dai, R. (2016). Postmortem changes in sarcoplasmic proteins associated with color stability in lamb muscle analyzed by proteomics. *European Food Research and Technology*, *242*(4), 527-535.

Garcia, A., Tsuruta, S., Gao, G., Palti, Y., Lourenco, D., & Leeds, T. (2023a). Genomic selection models substantially improve the accuracy of genetic merit predictions for fillet yield and body weight in rainbow trout using a multi-trait model and multi-generation progeny testing. *Genetics Selection Evolution*, *55*(1), 1-12.

Garcia, A., Tsuruta, S., Gao, G., Palti, Y., Lourenco, D., & Leeds, T. (2023b). Genomic selection models substantially improve the accuracy of genetic merit predictions for fillet yield and body weight in rainbow trout using a multi-trait model and multi-generation progeny testing. *Genetics Selection Evolution*, *55*(1), 11.

Ge, S. X., Jung, D., & Yao, R. (2020). ShinyGO: a graphical gene-set enrichment tool for animals and plants. *Bioinformatics*, *36*(8), 2628-2629.

Genet, C., Dehais, P., Palti, Y., Gao, G., Gavory, F., Wincker, P.,…Boussaha, M. (2011). Analysis of BAC-end sequences in rainbow trout: content characterization and assessment of synteny between trout and other fish genomes. *BMC genomics*, *12*, 1-8.

Georges, M., Clop, A., Marcq, F., Takeda, H., Pirottin, D., Hiard, S.,…Bibé, B. (2006). Polymorphic Polymorphic MicroRNA–Target Interactions: A Novel Source of Phenotypic Variation. Cold Spring Harbor symposia on quantitative biology,

Gilad, Y., Rifkin, S. A., & Pritchard, J. K. (2008). Revealing the architecture of gene regulation: the promise of eQTL studies. *Trends in genetics*, *24*(8), 408-415.

Gildberg, A., Johansen, A., & Bøgwald, J. (1995). Growth and survival of Atlantic salmon (Salmo salar) fry given diets supplemented with fish protein hydrolysate and lactic acid bacteria during a challenge trial with Aeromonas salmonicida. *Aquaculture*, *138*(1-4), 23-34.

Gjerde, B. a., & Schaeffer, L. (1989). Body traits in rainbow trout: II. Estimates of heritabilities and of phenotypic and genetic correlations. *Aquaculture*, *80*(1-2), 25-44.

Gonzalez-Pena, D., Gao, G., Baranski, M., Moen, T., Cleveland, B. M., Kenney, P. B.,…Leeds, T. D. (2016). Genome-wide association study for identifying loci that affect fillet yield, carcass, and body weight traits in rainbow trout (Oncorhynchus mykiss). *Frontiers in genetics*, *7*, 203.

González-Recio, O., Toro, M. A., & Bach, A. (2015). Past, present, and future of epigenetics applied to livestock breeding. *Frontiers in genetics*, *6*, 305.

Goodwin, T. (1986). Metabolism, nutrition, and function of carotenoids. *Annual review of nutrition*, *6*(1), 273-297.

Grant, C. M., Collinson, L. P., Roe, J. H., & Dawes, I. W. (1996). Yeast glutathione reductase is required for protection against oxidative stress and is a target gene for yAP-1 transcriptional regulation. *Molecular microbiology*, *21*(1), 171-179.

Grattagliano, I., Ciampi, S. A., & Portincasa, P. (2017). Gallbladder disease: Relevance of oxidative stress. In *Gastrointestinal Tissue* (pp. 187-194). Elsevier.

Grauso, M., Lan, A., Andriamihaja, M., Bouillaud, F., & Blachier, F. (2019). Hyperosmolar environment and intestinal epithelial cells: impact on mitochondrial oxygen consumption, proliferation, and barrier function in vitro. *Sci Rep*, *9*(1), 11360. https://doi.org/10.1038/s41598-019-47851-9

Guo, G., Wu, Y., Liu, Y., Wang, Z., Xu, G., Wang, X.,…Zhu, Q. (2023). Exploring the causal effects of the gut microbiome on serum lipid levels: A two-sample Mendelian randomization analysis. *Frontiers in microbiology*, *14*, 1113334.

Gupta, V. A., & Beggs, A. H. (2014). Kelch proteins: emerging roles in skeletal muscle development and diseases. *Skelet Muscle*, *4*(1), 11. https://doi.org/10.1186/2044-5040-4-11

Gupta, V. A., Ravenscroft, G., Shaheen, R., Todd, E. J., Swanson, L. C., Shiina, M.,…Darras, B. T. (2013). Identification of KLHL41 mutations implicates BTB-Kelch-mediated ubiquitination as an alternate pathway to myofibrillar disruption in nemaline myopathy. *The American Journal of Human Genetics*, *93*(6), 1108-1117.

Gutiérrez-Luna, F. M., Hernández-Domínguez, E. E., Valencia-Turcotte, L. G., & Rodríguez-Sotres, R. (2018). "Pyrophosphate and pyrophosphatases in plants, their involvement in stress responses and their possible relationship to secondary metabolism". *Plant Science*, *267*, 11-19.

Guyomard, R., Boussaha, M., Krieg, F., Hervet, C., & Quillet, E. (2012). A synthetic rainbow trout linkage map provides new insights into the salmonid whole genome duplication and the conservation of synteny among teleosts. *BMC genetics*, *13*, 1-12.

Haffray, P., Enez, F., Bugeon, J., Chapuis, H., Dupont-Nivet, M., Chatain, B., & Vandeputte, M. (2018). Accuracy of BLUP breeding values in a factorial mating design with mixed families and marker-based parentage assignment in rainbow trout Oncorhynchus mykiss. *Aquaculture*, *490*, 350-354.

Hanan, T., & Shaklai, N. (1995). Peroxidative interaction of myoglobin and myosin. *Eur J Biochem*, *233*(3), 930-936. https://doi.org/10.1111/j.1432-1033.1995.930_3.x

Hardy, R., Torrissen, O., & Scott, T. (1990). Absorption and distribution of 14C-labeled canthaxanthin in rainbow trout (Oncorhynchus mykiss). *Aquaculture*, *87*(3-4), 331-340.

Harlioglu, A. G. (2012). Fatty acid composition, fat soluble vitamins and cholesterol content of farmed rainbow trout (Oncorhynchus mykiss). *Pakistan Journal of Zoology*, *44*(4).

Harrigan, J. A., Jacq, X., Martin, N. M., & Jackson, S. P. (2018). Deubiquitylating enzymes and drug discovery: emerging opportunities. *Nat Rev Drug Discov*, *17*(1), 57-78. https://doi.org/10.1038/nrd.2017.152

Harrison, E. H. (2012). Mechanisms involved in the intestinal absorption of dietary vitamin A and provitamin A carotenoids. *Biochimica et Biophysica Acta (BBA)-Molecular and Cell Biology of Lipids*, *1821*(1), 70-77.

Hayashi, H., Inamura, K., Aida, K., Naoi, S., Horikawa, R., Nagasaka, H.,…Sugiyama, Y. (2012). AP2 adaptor complex mediates bile salt export pump internalization and modulates its hepatocanalicular expression and transport function. *Hepatology*, *55*(6), 1889-1900. https://doi.org/10.1002/hep.25591

Hayes, B., & Goddard, M. (2010). Genome-wide association and genomic selection in animal breeding. *Genome*, *53*(11), 876-883.

He, L., & Hannon, G. J. (2004). MicroRNAs: small RNAs with a big role in gene regulation. *Nat Rev Genet*, *5*(7), 522-531. https://doi.org/10.1038/nrg1379

He, S., Ran, C., Qin, C., Li, S., Zhang, H., De Vos, W. M.,…Zhou, Z. (2017). Anti-infective effect of adhesive probiotic Lactobacillus in fish is correlated with their spatial distribution in the intestinal tissue. *Scientific reports*, *7*(1), 1-12.

Heider, S. A., Peters-Wendisch, P., & Wendisch, V. F. (2012). Carotenoid biosynthesis and overproduction in Corynebacterium glutamicum. *BMC microbiology*, *12*, 1-11.

Helgeland, H., Sodeland, M., Zoric, N., Torgersen, J. S., Grammes, F., von Lintig, J.,…Vage, D. I. (2019). Genomic and functional gene studies suggest a key role of beta-carotene oxygenase 1 like (bco1l) gene in salmon flesh color. *Sci Rep*, *9*(1), 20061. https://doi.org/10.1038/s41598-019-56438-3

Helgeland, H., Sodeland, M., Zoric, N., Torgersen, J. S., Grammes, F., von Lintig, J.,…Våge, D. I. (2019). Genomic and functional gene studies suggest a key role of beta-carotene oxygenase 1 like (bco1l) gene in salmon flesh color. *Scientific reports*, *9*(1), 1-12.

Henderson, C. (1975). Use of all relatives in intraherd prediction of breeding values and producing abilities. *Journal of Dairy Science*, *58*(12), 1910-1916.

Henry, L. P., Bruijning, M., Forsberg, S. K., & Ayroles, J. F. (2021). The microbiome extends host evolutionary potential. *Nature communications*, *12*(1), 5141.

Hessel, S., Eichinger, A., Isken, A., Amengual, J., Hunzelmann, S., Hoeller, U.,…Wyss, A. (2007). CMO1 deficiency abolishes vitamin A production from beta-carotene and alters lipid metabolism in mice. *J Biol Chem*, *282*(46), 33553-33561. https://doi.org/10.1074/jbc.M706763200

Hill, G. E. (1999). Is there an immunological cost to carotenoid-based ornamental coloration? *The American Naturalist*, *154*(5), 589-595.

Hirota, K., Aino, K., Nodasaka, Y., & Yumoto, I. (2013). Oceanobacillus indicireducens sp. nov., a facultative alkaliphile that reduces an indigo dye. *International Journal of Systematic and Evolutionary Microbiology*, *63*(Pt_4), 1437-1442.

Hofer, A. (1998). Variance component estimation in animal breeding: a review. *Journal of Animal Breeding and Genetics*, *115*(1-6), 247-265.

Hollander, D., & Ruble Jr, P. E. (1978). beta-carotene intestinal absorption: bile, fatty acid, pH, and flow rate effects on transport. *American Journal of Physiology-Endocrinology and Metabolism*, *235*(6), E686.

Huang, Y., Li, J., Li, W., & Han, F. (2024). Integrative GWAS and eQTL analysis identifies genes associated with resistance to Vibrio harveyi infection in yellow drum (Nibea albiflora). *Frontiers in Marine Science*, *11*, 1435469.

Huang, Y., Zhang, L., Wang, G., & Huang, S. (2022). De novo assembly transcriptome analysis reveals the genes associated with body color formation in the freshwater ornamental shrimps Neocaridina denticulate sinensis. *Gene*, *806*, 145929. https://doi.org/10.1016/j.gene.2021.145929

Hughes, J., Oiseth, S., Purslow, P., & Warner, R. (2014). A structural approach to understanding the interactions between colour, water-holding capacity and tenderness. *Meat science*, *98*(3), 520-532.

Ibtisham, F., Zhang, L., Xiao, M., An, L., Ramzan, M. B., Nawab, A.,…Xu, Y. (2017). Genomic selection and its application in animal breeding. *The Thai Journal of Veterinary Medicine*, *47*(3), 301.

Ichiyama, S., Shimokata, K., & Tsukamura, M. (1988). Relationship between mycobacterial species and their carotenoid pigments. *Microbiology and immunology*, *32*(5), 473-479.

Jami, E., White, B. A., & Mizrahi, I. (2014). Potential role of the bovine rumen microbiome in modulating milk composition and feed efficiency. *PloS one*, *9*(1), e85423.

Jewell, K. A., McCormick, C. A., Odt, C. L., Weimer, P. J., & Suen, G. (2015). Ruminal bacterial community composition in dairy cows is dynamic over the course of two lactations and correlates with feed efficiency. *Applied and environmental microbiology*, *81*(14), 4697-4710.

Jia, W., Zhang, R., Liu, L., Zhu, Z., Xu, M., & Shi, L. (2021). Molecular mechanism of protein dynamic change for Hengshan goat meat during freezing storage based on high-throughput proteomics. *Food Research International*, *143*, 110289.

Jia, X., Veiseth-Kent, E., Grove, H., Kuziora, P., Aass, L., Hildrum, K., & Hollung, K. (2009). Peroxiredoxin-6—a potential protein marker for meat tenderness in bovine longissimus thoracis muscle. *Journal of Animal Science*, *87*(7), 2391-2399.

Jlali, M., Graulet, B., Chauveau-Duriot, B., Chabault, M., Godet, E., Leroux, S.,…Berri, C. (2012). A mutation in the promoter of the chicken β, β-carotene 15, 15'-monooxygenase 1 gene alters xanthophyll metabolism through a selective effect on its mRNA abundance in the breast muscle. *Journal of animal science*, *90*(12), 4280-4288.

Jlali, M., Graulet, B., Chauveau-Duriot, B., Godet, E., Praud, C., Nunes, C. S.,…Duclos, M. J. (2014). Nutrigenetics of carotenoid metabolism in the chicken: a polymorphism at the β, β-carotene 15, 15'-mono-oxygenase 1 (BCMO1) locus affects the response to dietary β-carotene. *British journal of nutrition*, *111*(12), 2079-2088.

Jones, J., Reinke, S. N., Ali, A., Palmer, D. J., & Christophersen, C. T. (2021). Fecal sample collection methods and time of day impact microbiome composition and short chain fatty acid concentrations. *Scientific reports*, *11*(1), 13964.

Joseph, P., Suman, S. P., Li, S., Beach, C. M., Steinke, L., & Fontaine, M. (2010). Characterization of bison (Bison bison) myoglobin. *Meat Sci*, *84*(1), 71-78. https://doi.org/10.1016/j.meatsci.2009.08.014

Joseph, P., Suman, S. P., Rentfrow, G., Li, S., & Beach, C. M. (2012). Proteomics of muscle-specific beef color stability. *J Agric Food Chem*, *60*(12), 3196-3203. https://doi.org/10.1021/jf204188v

Juanchich, A., Bardou, P., Rue, O., Gabillard, J. C., Gaspin, C., Bobe, J., & Guiguen, Y. (2016). Characterization of an extensive rainbow trout miRNA transcriptome by next generation sequencing. *BMC genomics*, *17*(1), 164. https://doi.org/10.1186/s12864-016-2505-9

Kanamoto, H., Nakamura, K., & Misawa, N. (2021). Carotenoid production in oleaginous yeasts. *Carotenoids: Biosynthetic and Biofunctional Approaches*, 153-163.

Karami, A., Kania, P., Al-Jubury, A., Stefanova, D., Krych, L., Madsen, L.,…Buchmann, K. (2025). Gut microbiota in rainbow trout Oncorhynchus mykiss with different susceptibility to Flavobacterium psychrophilum infection. *Aquaculture*, *596*, 741841.

Kaulmann, A., & Bohn, T. (2014). Carotenoids, inflammation, and oxidative stress—implications of cellular signaling pathways and relation to chronic disease prevention. *Nutrition research*, *34*(11), 907-929.

Kaźmierczuk, A., & Kiliańska, Z. M. (2009). Plejotropowa aktywność białek szoku cieplnego The pleiotropic activity of heat-shock proteins. *Postepy Hig Med Dosw.(online)*, *63*, 502-521.

Khanal, P., Maltecca, C., Schwab, C., Fix, J., Bergamaschi, M., & Tiezzi, F. (2020a). Modeling host-microbiome interactions for the prediction of meat quality and carcass composition traits in swine. *Genetics Selection Evolution*, *52*(1), 1-13.

Khanal, P., Maltecca, C., Schwab, C., Fix, J., Bergamaschi, M., & Tiezzi, F. (2020b). Modeling host-microbiome interactions for the prediction of meat quality and carcass composition traits in swine. *Genetics Selection Evolution*, *52*, 1-13.

Kiessling, A., Espe, M., Ruohonen, K., & Mørkøre, T. (2004). Texture, gaping and colour of fresh and frozen Atlantic salmon flesh as affected by pre-slaughter iso-eugenol or CO2 anaesthesia. *Aquaculture*, *236*(1-4), 645-657.

Kim, J. M., Santure, A., Barton, H. J., Quinn, J., Cole, E. F., Consortium, G. T. H.,…van Oers, K. (2018). A high-density SNP chip for genotyping great tit (Parus major) populations and its application to studying the genetic architecture of exploration behaviour. *Molecular Ecology Resources*, *18*(4), 877-891.

Klassen, J. L. (2018). Defining microbiome function. *Nature microbiology*, *3*(8), 864-869.

Kobayashi, T., Winslow, S., Sunesson, L., Hellman, U., & Larsson, C. (2012). PKCα binds G3BP2 and regulates stress granule formation following cellular stress. *PloS one*, *7*(4), e35820.

Kong, H. R., Anthony, N. B., Rowland, K. C., Khatri, B., & Kong, B. C. (2018). Genome re-sequencing to identify single nucleotide polymorphism markers for muscle color traits in broiler chickens. *Asian-Australas J Anim Sci*, *31*(1), 13-18. https://doi.org/10.5713/ajas.17.0479

Koopaee, H. K., & Koshkoiyeh, A. E. (2014). SNPs Genotyping technologies and their applications in farm animals breeding programs. *Brazilian Archives of Biology and Technology*, *57*, 87-95.

Kruuk, L. E., & Hadfield, J. D. (2007). How to separate genetic and environmental causes of similarity between relatives. *Journal of evolutionary biology*, *20*(5), 1890-1903.

Krämer, A., Green, J., Pollard Jr, J., & Tugendreich, S. (2014). Causal analysis approaches in ingenuity pathway analysis. *Bioinformatics*, *30*(4), 523-530.

Kumar, S., Sandell, L. L., Trainor, P. A., Koentgen, F., & Duester, G. (2012). Alcohol and aldehyde dehydrogenases: retinoid metabolic effects in mouse knockout models. *Biochimica et Biophysica Acta (BBA)-Molecular and Cell Biology of Lipids*, *1821*(1), 198-205.

Kumari, S., Rajarani, A., Bansal, N., Dahuja, A., Praveen, S., Krishnan, V., & Kumar, S. (2019). Extraction and estimation of provitamin A carotenoids from carrot. *Omics meet Plant Biochemistry: Applications in nutritional enhancement with one health perspective*, *221*.

Kurilshikov, A., Wijmenga, C., Fu, J., & Zhernakova, A. (2017). Host genetics and gut microbiome: challenges and perspectives. *Trends in immunology*, *38*(9), 633-647.

Kutter, C., & Svoboda, P. (2008). miRNA, siRNA, piRNA: Knowns of the unknown. In: Taylor & Francis.

Kwon, H.-S., Lee, H.-S., Rubin, J., & Tomarev, S. (2008). Myocilin May Regulate Actin Cytoskeleton Through Components of Wnt Signaling Pathway. *Investigative Ophthalmology & Visual Science*, *49*(13), 5111-5111.

Lakamp, A. Breeding for the Little Things: A Look at Including Microbiome Information in Animal Breeding.

Lakshman, M., Asher, K., Attlesey, M., Satchithanandam, S., Mychkovsky, I., & Coutlakis, P. (1989). Absorption, storage, and distribution of beta-carotene in normal and beta-carotene-fed rats: roles of parenchymal and stellate cells. *Journal of Lipid Research*, *30*(10), 1545-1550.

Lam, S., Miglior, F., Fonseca, P., Gómez-Redondo, I., Zeidan, J., Suárez-Vega, A.,…Stothard, P. (2021). Identification of functional candidate variants and genes for feed efficiency in Holstein and Jersey cattle breeds using RNA-sequencing. *Journal of dairy science*, *104*(2), 1928-1950.

Langmead, B., & Salzberg, S. L. (2012). Fast gapped-read alignment with Bowtie 2. *Nature methods*, *9*(4), 357-359.

Laplante, M., & Sabatini, D. (2012). mTOR signaling. Cold Spring Harb Perspect Biol 4: a011593. In.

Le Bihan-Duval, E., Nadaf, J., Berri, C., Pitel, F., Graulet, B., Godet, E.,…Duby, C. (2011). Detection of a Cis eQTL controlling BMCO1 gene expression leads to the identification of a QTG for chicken breast meat color. *PLoS One*, *6*(7), e14825.

Leandro, J., & Houten, S. M. (2020). The lysine degradation pathway: Subcellular compartmentalization and enzyme deficiencies. *Molecular Genetics and Metabolism*, *131*(1-2), 14-22.

LeBlanc, F., Laflamme, M., & Gagne, N. (2010). Genetic markers of the immune response of Atlantic salmon (Salmo salar) to infectious salmon anemia virus (ISAV). *Fish & Shellfish Immunology*, *29*(2), 217-232.

Lee, J., Godon, C., Lagniel, G., Spector, D., Garin, J., Labarre, J., & Toledano, M. B. (1999). Yap1 and Skn7 control two specialized oxidative stress response regulons in yeast. *J Biol Chem*, *274*(23), 16040-16046. https://doi.org/10.1074/jbc.274.23.16040

Lee, S., Park, J., Jang, J.-K., Lee, B.-H., & Park, Y.-S. (2019). Structural analysis of gluco-oligosaccharides produced by Leuconostoc lactis and their prebiotic effect. *Molecules*, *24*(21), 3998.

Lee, T. T., Ciou, J. Y., Chen, C. L., & Yu, B. (2013). Effect of Echinacea purpurea L. on oxidative status and meat quality in Arbor Acres broilers. *J Sci Food Agric*, *93*(1), 166-172. https://doi.org/10.1002/jsfa.5745

Leeds, T. D., Vallejo, R. L., Weber, G. M., Gonzalez-Pena, D., & Silverstein, J. T. (2016). Response to five generations of selection for growth performance traits in rainbow trout (Oncorhynchus mykiss). *Aquaculture*, *465*, 341-351.

Leeds, T. D., & Weber, G. M. (2019). Effects of triploidy on genetic gains in a rainbow trout (Oncorhynchus mykiss) population selectively bred for diploid growth performance. *Aquaculture*, *505*, 481-487.

Legarra, A., Aguilar, I., & Misztal, I. (2009). A relationship matrix including full pedigree and genomic information. *J Dairy Sci*, *92*(9), 4656-4663. https://doi.org/10.3168/jds.2009-2061

Lehnert, S. J. (2016). *Why are salmon red? Proximate and ultimate causes of flesh pigmentation in Chinook salmon* University of Windsor (Canada)].

Lei, C., Li, J., Zheng, Z., Du, X., & Deng, Y. (2019). Molecular cloning, expression pattern of beta-carotene 15,15-dioxygenase gene and association analysis with total carotenoid content in pearl oyster Pinctada fucata martensii. *Comp Biochem Physiol B Biochem Mol Biol*, *229*, 34-41. https://doi.org/10.1016/j.cbpb.2018.11.006

Leonardi, R., Zhang, Y.-M., Rock, C. O., & Jackowski, S. (2005). Coenzyme A: back in action. *Progress in lipid research*, *44*(2-3), 125-153.

Li, G., Martínez-Bonet, M., Wu, D., Yang, Y., Cui, J., Nguyen, H. N.,…Westra, H.-J. (2018). High-throughput identification of noncoding functional SNPs via type IIS enzyme restriction. *Nature genetics*, *50*(8), 1180-1188.

Li, H., Jiang, K., Wang, S., Liu, X., Kang, X., Jiang, R.,…Sun, G. (2015). Assessment of correlation between pre-miRNA-1757 polymorphism and chicken performance traits. *Genetics and Molecular Research*, *14*(4), 12184-12195.

Li, X., Wang, S., Xun, X., Zhang, M., Wang, S., Li, H.,…Li, T. (2019). A carotenoid oxygenase is responsible for muscle coloration in scallop. *Biochimica et Biophysica Acta (BBA)-Molecular and Cell Biology of Lipids*, *1864*(7), 966-975.

Li, Y., Sidore, C., Kang, H. M., Boehnke, M., & Abecasis, G. R. (2011). Low-coverage sequencing: implications for design of complex trait association studies. *Genome research*, *21*(6), 940-951.

Liang, J. Q., Li, T., Nakatsu, G., Chen, Y.-X., Yau, T. O., Chu, E.,…Chan, F. K. (2020). A novel faecal Lachnoclostridium marker for the non-invasive diagnosis of colorectal adenoma and cancer. *Gut*, *69*(7), 1248-1257.

Lietz, G., Oxley, A., Leung, W., & Hesketh, J. (2012). Single nucleotide polymorphisms upstream from the beta-carotene 15,15'-monoxygenase gene influence provitamin A conversion efficiency in female volunteers. *J Nutr*, *142*(1), 161S-165S. https://doi.org/10.3945/jn.111.140756

Lima, V. C., Rosen, R. B., & Farah, M. (2016). Macular pigment in retinal health and disease. *International journal of retina and vitreous*, *2*(1), 1-9.

Lin, D., & Medeiros, D. M. (2023). The microbiome as a major function of the gastrointestinal tract and its implication in micronutrient metabolism and chronic diseases. *Nutrition Research*.

Lin, H., & Peddada, S. D. (2020). Analysis of microbial compositions: a review of normalization and differential abundance analysis. *NPJ biofilms and microbiomes*, *6*(1), 60.

Liu, F., Dai, R., Zhu, J., & Li, X. (2010). Optimizing color and lipid stability of beef patties with a mixture design incorporating with tea catechins, carnosine, and α-tocopherol. *Journal of Food Engineering*, *98*(2), 170-177.

Liu, S., Gao, G., Layer, R. M., Thorgaard, G. H., Wiens, G. D., Leeds, T. D.,…Palti, Y. (2021). Identification of high-confidence structural variants in domesticated rainbow trout using whole-genome sequencing. *Frontiers in Genetics*, *12*, 639355.

Liu, S., Gao, G., Palti, Y., Cleveland, B. M., Weber, G. M., & Rexroad III, C. E. (2014). RNA-seq analysis of early hepatic response to handling and confinement stress in rainbow trout. *Plos one*, *9*(2), e88492.

Liu, S., Martin, K. E., Snelling, W. M., Long, R., Leeds, T. D., Vallejo, R. L.,…Palti, Y. (2024). Accurate genotype imputation from low-coverage whole-genome sequencing data of rainbow trout. *G3: Genes, Genomes, Genetics*, *14*(9), jkae168.

Liu, S., Vallejo, R. L., Evenhuis, J. P., Martin, K. E., Hamilton, A., Gao, G.,…Palti, Y. (2018). Retrospective evaluation of marker-assisted selection for resistance to bacterial cold water disease in three generations of a commercial rainbow trout breeding population. *Frontiers in genetics*, *9*, 374762.

Liu, X., Liu, Y., Jiang, Y., Zou, L., Liu, K., Liu, M.,…Chen, F. (2020). Homo-oxidized HSPB1 protects cardiomyocytes against oxidative stress via targeting Keap1/Nrf-2 signaling pathway. *Journal of Molecular and Cellular Cardiology*, *140*, 37-38.

Liu, X., Xiao, W., Jiang, Y., Zou, L., Chen, F., Xiao, W.,…Zhu, Y. (2021). Bmal1 Regulates the Redox Rhythm of HSPB1, and Homooxidized HSPB1 Attenuates the Oxidative Stress Injury of Cardiomyocytes. *Oxid Med Cell Longev*, *2021*, 5542815. https://doi.org/10.1155/2021/5542815

Liu, Y., Du, M., Li, X., Chen, L., Shen, Q., Tian, J., & Zhang, D. (2016). Role of the ubiquitin-proteasome pathway on proteolytic activity in postmortem proteolysis and tenderisation of sheep skeletal muscle. *International Journal of Food Science & Technology*, *51*(11), 2353-2359.

Long, T., Liu, Y., Qin, Y., DeBose-Boyd, R. A., & Li, X. (2021). Structures of dimeric human NPC1L1 provide insight into mechanisms for cholesterol absorption. *Science Advances*, *7*(34), eabh3997.

Lozano, G. A. (1994). Carotenoids, parasites, and sexual selection. *Oikos*, 309-311.

Lu, J., Breitwieser, F. P., Thielen, P., & Salzberg, S. L. (2017). Bracken: estimating species abundance in metagenomics data. *PeerJ Computer Science*, *3*, e104.

Lubzens, E., Lissauer, L., Levavi-Sivan, B., Avarre, J.-C., & Sammar, M. (2003). Carotenoid and retinoid transport to fish oocytes and eggs: what is the role of retinol binding protein? *Molecular aspects of medicine*, *24*(6), 441-457.

Lundquist, M. R., Storaska, A. J., Liu, T.-C., Larsen, S. D., Evans, T., Neubig, R. R., & Jaffrey, S. R. (2014). Redox modification of nuclear actin by MICAL-2 regulates SRF signaling. *Cell*, *156*(3), 563-576.

Luo, Z. (1992). Computing inbreeding coefficients in large populations. *Genetics Selection Evolution*, *24*(4), 305-313.

Luo, Z., Yu, Y., Xiang, J., & Li, F. (2021). Genomic selection using a subset of SNPs identified by genome-wide association analysis for disease resistance traits in aquaculture species. *Aquaculture*, *539*, 736620.

Madaro, A., Torrissen, O., Whatmore, P., Lall, S. P., Schmeisser, J., Verlhac Trichet, V., & Olsen, R. E. (2020). Red and White Chinook Salmon (Oncorhynchus tshawytscha): differences in the transcriptome profile of muscle, liver, and pylorus. *Marine Biotechnology*, *22*(4), 581-593.

Mancini, R. A., & Ramanathan, R. (2014). Effects of postmortem storage time on color and mitochondria in beef. *Meat Sci*, *98*(1), 65-70. https://doi.org/10.1016/j.meatsci.2014.04.007

Manor, M. L., Cleveland, B. M., Weber, G. M., & Kenney, P. B. (2015). Effects of sexual maturation and feeding level on fatty acid metabolism gene expression in muscle, liver, and visceral adipose tissue of diploid and triploid rainbow trout, Oncorhynchus mykiss. *Comparative Biochemistry and Physiology Part B: Biochemistry and Molecular Biology*, *179*, 17-26.

Mansfield, G. S., Desai, A. R., Nilson, S. A., Van Kessel, A. G., Drew, M. D., & Hill, J. E. (2010). Characterization of rainbow trout (Oncorhynchus mykiss) intestinal microbiota and inflammatory marker gene expression in a recirculating aquaculture system. *Aquaculture*, *307*(1-2), 95-104.

Marancik, D., Gao, G., Paneru, B., Ma, H., Hernandez, A. G., Salem, M.,…Wiens, G. D. (2015). Whole-body transcriptome of selectively bred, resistant-, control-, and susceptible-line rainbow trout following experimental challenge with Flavobacterium psychrophilum. *Frontiers in genetics*, *5*, 453.

Martin, M. (2011). Cutadapt removes adapter sequences from high-throughput sequencing reads. *EMBnet. journal*, *17*(1), 10-12.

Matthews, S. J., Ross, N. W., Lall, S. P., & Gill, T. A. (2006). Astaxanthin binding protein in Atlantic salmon. *Comp Biochem Physiol B Biochem Mol Biol*, *144*(2), 206-214. https://doi.org/10.1016/j.cbpb.2006.02.007

McCormick, R. J. (1999). Extracellular modifications to muscle collagen: implications for meat quality. *Poult Sci*, *78*(5), 785-791. https://doi.org/10.1093/ps/78.5.785

McDermaid, A., Monier, B., Zhao, J., Liu, B., & Ma, Q. (2019). Interpretation of differential gene expression results of RNA-seq data: review and integration. *Briefings in bioinformatics*, *20*(6), 2044-2054.

McGowan, K. A., Li, J. Z., Park, C. Y., Beaudry, V., Tabor, H. K., Sabnis, A. J.,…Myers, R. M. (2008). Ribosomal mutations cause p53-mediated dark skin and pleiotropic effects. *Nature genetics*, *40*(8), 963-970.

McMurdie, P. J., & Holmes, S. (2013). phyloseq: an R package for reproducible interactive analysis and graphics of microbiome census data. *PloS one*, *8*(4), e61217.

Meuwissen, T., Hayes, B., & Goddard, M. (2016). Genomic selection: A paradigm shift in animal breeding. *Animal frontiers*, *6*(1), 6-14.

Meuwissen, T. H., Hayes, B. J., & Goddard, M. (2001). Prediction of total genetic value using genome-wide dense marker maps. *genetics*, *157*(4), 1819-1829.

Michaelson, J. J., Loguercio, S., & Beyer, A. (2009). Detection and interpretation of expression quantitative trait loci (eQTL). *Methods*, *48*(3), 265-276.

Misawa, N., Maoka, T., & Takemura, M. (2022). Carotenoids: Carotenoid and apocarotenoid analysis—Use of E. coli to produce carotenoid standards. In *Methods in Enzymology* (Vol. 670, pp. 87-137). Elsevier.

Misztal, I., Tsuruta, S., Strabel, T., Auvray, B., Druet, T., & Lee, D. (2002). BLUPF90 and related programs (BGF90). Proceedings of the 7th world congress on genetics applied to livestock production,

Mora, L., Gallego, M., Aristoy, M. C., Fraser, P. D., & Toldrá, F. (2015). Peptides naturally generated from ubiquitin-60S ribosomal protein as potential biomarkers of dry-cured ham processing time. *Food Control*, *48*, 102-107.

Morais, P. V., Francisco, R., Branco, R., Chung, A. P., & Da Costa, M. S. (2004). Leucobacter chromiireducens sp. nov, and Leucobacter aridicollis sp. nov., two new species isolated from a chromium contaminated environment. *Systematic and applied microbiology*, *27*(6), 646-652.

Morimoto, R. I. (1998). Regulation of the heat shock transcriptional response: cross talk between a family of heat shock factors, molecular chaperones, and negative regulators. *Genes & development*, *12*(24), 3788-3796.

Mott, A. C., Mott, A., Preuß, S., Bennewitz, J., Tetens, J., & Falker-Gieske, C. (2022). eQTL analysis of laying hens divergently selected for feather pecking identifies KLF14 as a potential key regulator for this behavioral disorder. *Frontiers in genetics*, *13*, 969752.

Mounier, J., Irlinger, F., Leclercq-Perlat, M.-N., Sarthou, A.-S., Spinnler, H.-E., Fitzgerald, G. F., & Cogan, T. M. (2006). Growth and colour development of some surface ripening bacteria with Debaryomyces hansenii on aseptic cheese curd. *Journal of dairy research*, *73*(4), 441-448.

Mukhopadhyay, C., & Kumar, D. (2013). SNP chip development and genome wide association studies in livestock. *Phenomic and genomic tools for analysis of livestock genome*, *66*.

Napoli, J. (2000). Enzymology and biogenesis of retinoic acid. *Vitamin A and retinoids: An update of biological aspects and clinical applications*, 17-27.

Napoli, J. L. (2012). Physiological insights into all-trans-retinoic acid biosynthesis. *Biochimica et Biophysica Acta (BBA)-Molecular and Cell Biology of Lipids*, *1821*(1), 152-167.

Navarrete, P., Magne, F., Araneda, C., Fuentes, P., Barros, L., Opazo, R.,…Romero, J. (2012). PCR-TTGE analysis of 16S rRNA from rainbow trout (Oncorhynchus mykiss) gut microbiota reveals host-specific communities of active bacteria. *PloS one*, *7*(2), e31335.

Nayak, S. K. (2010). Role of gastrointestinal microbiota in fish. *Aquaculture research*, *41*(11), 1553-1573.

Nguyen, C. D., Amoroso, G., Ventura, T., & Elizur, A. (2020). Assessing the pyloric caeca and distal gut microbiota correlation with flesh color in Atlantic salmon (Salmo salar L., 1758). *Microorganisms*, *8*(8), 1244.

Nguyen, C. D., Amoroso, G., Ventura, T., Minich, J. J., & Elizur, A. (2020). Atlantic salmon (Salmo salar L., 1758) gut microbiota profile correlates with flesh pigmentation: cause or effect? *Marine Biotechnology*, *22*, 786-804.

Nickell, D., & Bromage, N. R. (1998). The effect of dietary lipid level on variation of flesh pigmentation in rainbow trout (Oncorhynchus mykiss). *Aquaculture*, *161*(1-4), 237-251.

No, H. K., & Storebakken, T. (1991). Pigmentation of rainbow trout with astaxanthin at different water temperatures. *Aquaculture*, *97*(2-3), 203-216.

Nogal, A., Louca, P., Zhang, X., Wells, P. M., Steves, C. J., Spector, T. D.,…Menni, C. (2021). Circulating levels of the short-chain fatty acid acetate mediate the effect of the gut microbiome on visceral fat. *Frontiers in microbiology*, *12*, 711359.

Nohl, H., Breuninger, V., & Hegner, D. (1978). Influence of mitochondrial radical formation on energy-linked respiration. *Eur J Biochem*, *90*(2), 385-390. https://doi.org/10.1111/j.1432-1033.1978.tb12615.x

Nonhoff, U., Ralser, M., Welzel, F., Piccini, I., Balzereit, D., Yaspo, M.-L.,…Krobitsch, S. (2007). Ataxin-2 interacts with the DEAD/H-box RNA helicase DDX6 and interferes with P-bodies and stress granules. *Molecular biology of the cell*, *18*(4), 1385-1396.

Numa, S., Bortz, W. M., & Lynen, F. (1965). Regulation of fatty acid synthesis at the acetyl-CoA carboxylation step. *Advances in enzyme regulation*, *3*, 407-423.

O'Hara, E., Neves, A. L., Song, Y., & Guan, L. L. (2020). The role of the gut microbiome in cattle production and health: driver or passenger? *Annual review of animal biosciences*, *8*(1), 199-220.

Ogasawara, S., Cheng, X. W., Inoue, A., Hu, L., Piao, L., Yu, C.,…Kuzuya, M. (2018). Cathepsin K activity controls cardiotoxin-induced skeletal muscle repair in mice. *J Cachexia Sarcopenia Muscle*, *9*(1), 160-175. https://doi.org/10.1002/jcsm.12248

Olofsson, S. O., & Boren, J. (2005). Apolipoprotein B: a clinically important apolipoprotein which assembles atherogenic lipoproteins and promotes the development of atherosclerosis. *Journal of internal medicine*, *258*(5), 395-410.

Ong, D. E. (1982). Purification and partial characterization of cellular retinol-binding protein from human liver. *Cancer Research*, *42*(3), 1033-1037.

Opstal, E. J. v., & Bordenstein, S. R. (2015). Rethinking heritability of the microbiome. *Science*, *349*(6253), 1172-1173.

Oren, A. (2010). Industrial and environmental applications of halophilic microorganisms. *Environmental technology*, *31*(8-9), 825-834.

Ottestad, S., Sørheim, O., Heia, K., Skaret, J., & Wold, J. P. (2011). Effects of storage atmosphere and heme state on the color and visible reflectance spectra of salmon (Salmo salar) fillets. *Journal of agricultural and food chemistry*, *59*(14), 7825-7831.

Page, G., & Davies, S. (2003). Hepatic carotenoid uptake in rainbow trout (Oncorhynchus mykiss) using an isolated organ perfusion model. *Aquaculture*, *225*(1-4), 405-419.

Palti, Y., Gao, G., Liu, S., Kent, M., Lien, S., Miller, M.,…Moen, T. (2015). The development and characterization of a 57 K single nucleotide polymorphism array for rainbow trout. *Molecular ecology resources*, *15*(3), 662-672.

Palti, Y., Gao, G., Miller, M. R., Vallejo, R. L., Wheeler, P. A., Quillet, E.,…Rexroad III, C. E. (2014). A resource of single-nucleotide polymorphisms for rainbow trout generated by restriction-site associated DNA sequencing of doubled haploids. *Molecular ecology resources*, *14*(3), 588-596.

Paneru, B., Al-Tobasei, R., Palti, Y., Wiens, G. D., & Salem, M. (2016). Differential expression of long non-coding RNAs in three genetic lines of rainbow trout in response to infection with Flavobacterium psychrophilum. *Scientific reports*, *6*(1), 36032.

Panigrahi, M., Kumar, H., Saravanan, K., Rajawat, D., Nayak, S. S., Ghildiyal, K.,…Dutt, T. (2022). Trajectory of livestock genomics in South Asia: a comprehensive review. *Gene*, *843*, 146808.

Park, J. W. (1994). Functional protein additives in surimi gels. *Journal of Food Science*, *59*(3), 525-527.

Parker, R. S. (1996). Absorption, metabolism, and transport of carotenoids. *The FASEB Journal*, *10*(5), 542-551.

Paulusma, C. C., de Waart, D. R., Kunne, C., Mok, K. S., & Elferink, R. P. O. (2009). Activity of the bile salt export pump (ABCB11) is critically dependent on canalicular membrane cholesterol content. *Journal of biological chemistry*, *284*(15), 9947-9954.

Percie du Sert, N., Hurst, V., Ahluwalia, A., Alam, S., Avey, M. T., Baker, M.,…Dirnagl, U. (2020). The ARRIVE guidelines 2.0: Updated guidelines for reporting animal research. *Journal of Cerebral Blood Flow & Metabolism*, *40*(9), 1769-1777.

Piga, R., van Dartel, D., Bunschoten, A., van der Stelt, I., & Keijer, J. (2014). Role of Frizzled6 in the molecular mechanism of beta-carotene action in the lung. *Toxicology*, *320*, 67-73.

Prakash, P., Liu, C., Hu, K.-Q., Krinsky, N. I., Russell, R. M., & Wang, X.-D. (2004). β-Carotene and β-apo-14′-carotenoic acid prevent the reduction of retinoic acid receptor β in benzo [a] pyrene-treated normal human bronchial epithelial cells. *The Journal of nutrition*, *134*(3), 667-673.

Pérez-Enciso, M., Rincón, J. C., & Legarra, A. (2015). Sequence-vs. chip-assisted genomic selection: accurate biological information is advised. *Genetics Selection Evolution*, *47*, 1-14.

Quince, C., Walker, A. W., Simpson, J. T., Loman, N. J., & Segata, N. (2017). Shotgun metagenomics, from sampling to analysis. *Nature biotechnology*, *35*(9), 833-844.

Rajasingh, H., Øyehaug, L., Våge, D. I., & Omholt, S. W. (2006). Carotenoid dynamics in Atlantic salmon. *Bmc Biology*, *4*(1), 1-15.

Ram, S., Mitra, M., Shah, F., Tirkey, S. R., & Mishra, S. (2020). Bacteria as an alternate biofactory for carotenoid production: A review of its applications, opportunities and challenges. *Journal of Functional Foods*, *67*, 103867.

Ramanathan, R., Nair, M., Hunt, M., & Suman, S. (2019). Mitochondrial functionality and beef colour: A review of recent research. *South African Journal of Animal Science*, *49*(1), 9-19.

Ramazzotti, M., & Bacci, G. (2018). 16S rRNA-based taxonomy profiling in the metagenomics era. In *Metagenomics* (pp. 103-119). Elsevier.

Ramirez-Martinez, A., Cenik, B. K., Bezprozvannaya, S., Chen, B., Bassel-Duby, R., Liu, N., & Olson, E. N. (2017). KLHL41 stabilizes skeletal muscle sarcomeres by nonproteolytic ubiquitination. *Elife*, *6*, e26439. https://doi.org/10.7554/eLife.26439

Ravenscroft, G., Miyatake, S., Lehtokari, V. L., Todd, E. J., Vornanen, P., Yau, K. S.,…Laing, N. G. (2013). Mutations in KLHL40 are a frequent cause of severe autosomal-recessive nemaline myopathy. *Am J Hum Genet*, *93*(1), 6-18. https://doi.org/10.1016/j.ajhg.2013.05.004

Rawls, J. F., Samuel, B. S., & Gordon, J. I. (2004). Gnotobiotic zebrafish reveal evolutionarily conserved responses to the gut microbiota. *Proceedings of the National Academy of Sciences*, *101*(13), 4596-4601.

Ray, A. K., Ghosh, K., & Ringø, E. (2012). Enzyme-producing bacteria isolated from fish gut: a review. *Aquaculture Nutrition*, *18*(5), 465-492.

Razin, S., & Hayflick, L. (2010). Highlights of mycoplasma research—an historical perspective. *Biologicals*, *38*(2), 183-190.

Reboul, E. (2019). Mechanisms of carotenoid intestinal absorption: where do we stand? *Nutrients*, *11*(4), 838.

Reboul, E., & Borel, P. (2011). Proteins involved in uptake, intracellular transport and basolateral secretion of fat-soluble vitamins and carotenoids by mammalian enterocytes. *Progress in lipid research*, *50*(4), 388-402.

Ringø, E., Salinas, I., Olsen, R., Nyhaug, A., Myklebust, R., & Mayhew, T. (2007). Histological changes in intestine of Atlantic salmon (Salmo salar L.) following in vitro exposure to pathogenic and probiotic bacterial strains. *Cell and tissue research*, *328*, 109-116.

Ringø, E., Strøm, E., & Tabachek, J. A. (1995). Intestinal microflora of salmonids: a review. *Aquaculture research*, *26*(10), 773-789.

Rizal, N. S. M., Neoh, H.-m., Ramli, R., Hanafiah, A., Samat, M. N. A., Tan, T. L.,…Saw, S. H. (2020). Advantages and limitations of 16S rRNA next-generation sequencing for pathogen identification in the diagnostic microbiology laboratory: perspectives from a middle-income country. *Diagnostics*, *10*(10), 816.

Robertson, P., O'Dowd, C., Burrells, C., Williams, P., & Austin, B. (2000). Use of Carnobacterium sp. as a probiotic for Atlantic salmon (Salmo salar L.) and rainbow trout (Oncorhynchus mykiss, Walbaum). *Aquaculture*, *185*(3-4), 235-243.

Rodríguez-Concepción, M. (2010). Supply of precursors for carotenoid biosynthesis in plants. *Archives of Biochemistry and Biophysics*, *504*(1), 118-122.

Rohmer, M. (1999). The discovery of a mevalonate-independent pathway for isoprenoid biosynthesis in bacteria, algae and higher plants. *Natural product reports*, *16*(5), 565-574.

Ross, A. C., & Harrison, E. H. (2007). Vitamin A: nutritional aspects of retinoids and carotenoids. *Handbook of Vitamins, 4th Edition, USA: CRC PressTaylor & Francis Group*.

Ross, E. M., Moate, P. J., Marett, L. C., Cocks, B. G., & Hayes, B. J. (2013). Metagenomic predictions: from microbiome to complex health and environmental phenotypes in humans and cattle. *PloS one*, *8*(9), e73056.

Rothschild, D., Weissbrod, O., Barkan, E., Kurilshikov, A., Korem, T., Zeevi, D.,…Bar, N. (2018). Environment dominates over host genetics in shaping human gut microbiota. *Nature*, *555*(7695), 210-215.

Ruan, J., Xu, J., Chen-Tsai, R. Y., & Li, K. (2017). Genome editing in livestock: Are we ready for a revolution in animal breeding industry? *Transgenic research*, *26*, 715-726.

Rubinacci, S., Hofmeister, R. J., Sousa da Mota, B., & Delaneau, O. (2023). Imputation of low-coverage sequencing data from 150,119 UK Biobank genomes. *Nature Genetics*, *55*(7), 1088-1090.

Ryter, S. W., & Tyrrell, R. M. (2000). The heme synthesis and degradation pathways: role in oxidant sensitivity: heme oxygenase has both pro-and antioxidant properties. *Free Radical Biology and Medicine*, *28*(2), 289-309.

Røsjø, C., Nordrum, S., Olli, J., Krogdahl, Å., Ruyter, B., & Holm, H. (2000). Lipid digestibility and metabolism in Atlantic salmon (Salmo salar) fed medium-chain triglycerides. *Aquaculture*, *190*(1-2), 65-76.

Sablina, A. A., Budanov, A. V., Ilyinskaya, G. V., Agapova, L. S., Kravchenko, J. E., & Chumakov, P. M. (2005). The antioxidant function of the p53 tumor suppressor. *Nat Med*, *11*(12), 1306-1313. https://doi.org/10.1038/nm1320

Saedi, N., Ye, X., Cai, Z., Lund, M. S., & Karaman, E. (2024). Genomic prediction of methane emission using microbiome data and genomic markers in Holstein cows. In *Genomic prediction of methane emission using microbiome data and genomic markers in Holstein cows*.

Salem, M., Al-Tobasei, R., Ali, A., Lourenco, D., Gao, G., Palti, Y.,…Leeds, T. D. (2018). Genome-Wide Association Analysis With a 50K Transcribed Gene SNP-Chip Identifies QTL Affecting Muscle Yield in Rainbow Trout. *Front Genet*, *9*, 387. https://doi.org/10.3389/fgene.2018.00387

Salem, M., Al-Tobasei, R., Ali, A., Lourenco, D., Gao, G., Palti, Y.,…Leeds, T. D. (2018). Genome-wide association analysis with a 50K transcribed gene SNP-chip identifies QTL affecting muscle yield in rainbow trout. *Frontiers in genetics*, *9*, 387.

Salem, M., Vallejo, R. L., Leeds, T. D., Palti, Y., Liu, S., Sabbagh, A.,…Yao, J. (2012). RNA-Seq identifies SNP markers for growth traits in rainbow trout. *PloS one*, *7*(5), e36264.

Sampels, S. (2013). Oxidation and antioxidants in fish and meat from farm to fork. *Food industry*, 114-144.

Scaife, J., Onibi, G., Murray, I., Fletcher, T., & Houlihan, D. (2000). Influence of a-tocopherol acetate on the short-and long-term storage properties of fillets from Atlantic salmon Salmo salar fed a high lipid diet. *Aquaculture Nutrition*, *6*(1), 65.

Schaeffer, C., Devuyst, O., & Rampoldi, L. (2021). Uromodulin: roles in health and disease. *Annual Review of Physiology*, *83*, 477-501.

Schmeisser, J., Verlhac-Trichet, V., Madaro, A., Lall, S. P., Torrissen, O., & Olsen, R. E. (2021). Molecular Mechanism Involved in Carotenoid Metabolism in Post-Smolt Atlantic Salmon: Astaxanthin Metabolism During Flesh Pigmentation and Its Antioxidant Properties. *Marine Biotechnology*, *23*(4), 653-670.

Schröder, J., Maus, I., Trost, E., & Tauch, A. (2011). Complete genome sequence of Corynebacterium variabile DSM 44702 isolated from the surface of smear-ripened cheeses and insights into cheese ripening and flavor generation. *BMC genomics*, *12*(1), 1-23.

Segata, N., Izard, J., Waldron, L., Gevers, D., Miropolsky, L., Garrett, W. S., & Huttenhower, C. (2011). Metagenomic biomarker discovery and explanation. *Genome biology*, *12*, 1-18.

Sellers, J. R. (2000). Myosins: a diverse superfamily. *Biochim Biophys Acta*, *1496*(1), 3-22. https://doi.org/10.1016/s0167-4889(00)00005-7

Semova, I., Carten, J. D., Stombaugh, J., Mackey, L. C., Knight, R., Farber, S. A., & Rawls, J. F. (2012). Microbiota regulate intestinal absorption and metabolism of fatty acids in the zebrafish. *Cell host & microbe*, *12*(3), 277-288.

Seyfert, M., Mancini, R. A., Hunt, M. C., Tang, J., Faustman, C., & Garcia, M. (2006). Color stability, reducing activity, and cytochrome c oxidase activity of five bovine muscles. *J Agric Food Chem*, *54*(23), 8919-8925. https://doi.org/10.1021/jf061657s

Shahidi, F., & Brown, J. A. (1998). Carotenoid pigments in seafoods and aquaculture. *Critical Reveiws in Food Science*, *38*(1), 1-67.

Sharma, P., Doultani, S., Hadiya, K., George, L., & Highland, H. (2024). Overview of marker-assisted selection in animal breeding. *HISTORY*, *9*, 11.

Shi, J., & Sun, G. (2017). Effect of pre-miRNA-1658 gene polymorphism on chicken growth and carcass traits. *Asian-Australas J Anim Sci*, *30*(4), 455-461. https://doi.org/10.5713/ajas.16.0305

Shindo, K., & Misawa, N. (2014). New and rare carotenoids isolated from marine bacteria and their antioxidant activities. *Marine drugs*, *12*(3), 1690-1698.

Shmarakov, I., Fleshman, M. K., D'Ambrosio, D. N., Piantedosi, R., Riedl, K. M., Schwartz, S. J.,…Harrison, E. H. (2010). Hepatic stellate cells are an important cellular site for β-carotene conversion to retinoid. *Archives of biochemistry and biophysics*, *504*(1), 3-10.

Singh, A., Mittal, A., & Benjakul, S. (2022). Undesirable discoloration in edible fish muscle: Impact of indigenous pigments, chemical reactions, processing, and its prevention. *Comprehensive Reviews in Food Science and Food Safety*, *21*(1), 580-603.

Smirnoff, N. (2018). Ascorbic acid metabolism and functions: A comparison of plants and mammals. *Free Radical Biology and Medicine*, *122*, 116-129.

Spor, A., Koren, O., & Ley, R. (2011). Unravelling the effects of the environment and host genotype on the gut microbiome. *Nature Reviews Microbiology*, *9*(4), 279-290.

Starr, M. P., & Saperstein, S. (1953). Thiamine and the carotenoid pigments of Corynebacterium poinsettiae. *Archives of Biochemistry and Biophysics*, *43*(1), 157-168.

Stofan, M., & Guo, G. L. (2020). Bile Acids and FXR: Novel Targets for Liver Diseases. *Front Med (Lausanne)*, *7*, 544. https://doi.org/10.3389/fmed.2020.00544

Storebakken, T., & No, H. K. (1992). Pigmentation of rainbow trout. *Aquaculture*, *100*(1-3), 209-229.

Sturm, G., Brunner, S., Suvorova, E., Dempwolff, F., Reiner, J., Graumann, P.,…Gescher, J. (2018). Chromate resistance mechanisms in Leucobacter chromiiresistens. *Applied and Environmental Microbiology*, *84*(23), e02208-02218.

Subramaniyan, S. A., Kang, D. R., Jung, Y. C., Jung, J. H., Choi, Y. I., Lee, M. J.,…Shim, K. S. (2017). Comparative studies of meat quality traits and the proteome profile between low-and high-pH muscles in longissimus dorsi of Berkshire. *Canadian Journal of Animal Science*, *97*(4), 640-649.

Sun, H. (2012). Membrane receptors and transporters involved in the function and transport of vitamin A and its derivatives. *Biochimica et Biophysica Acta (BBA)-Molecular and Cell Biology of Lipids*, *1821*(1), 99-112.

Sánchez, C. C., Smith, T. P., Wiedmann, R. T., Vallejo, R. L., Salem, M., Yao, J., & Rexroad, C. E. (2009). Single nucleotide polymorphism discovery in rainbow trout by deep sequencing of a reduced representation library. *Bmc Genomics*, *10*, 1-8.

Taft, D. H., Ambalavanan, N., Schibler, K. R., Yu, Z., Newburg, D. S., Ward, D. V., & Morrow, A. L. (2014). Intestinal microbiota of preterm infants differ over time and between hospitals. *Microbiome*, *2*, 1-12.

Takahashi, M., Yamashita, K., Shiozawa, A., Ichiishi, A., Fukumori, F., & Fujimura, M. (2010). An AP-1-like transcription factor, NAP-1, regulates expression of the glutathione S-transferase and NADH: flavin oxidoreductase genes in Neurospora crassa. *Bioscience, biotechnology, and biochemistry*, *74*(4), 746-752.

Tan, X., He, Z., Fahey, A. G., Zhao, G., Liu, R., & Wen, J. (2023). Research progress and applications of genome-wide association study in farm animals. *Animal Research and One Health*, *1*(1), 56-77.

Tang, J., Faustman, C., Hoagland, T. A., Mancini, R. A., Seyfert, M., & Hunt, M. C. (2005). Postmortem oxygen consumption by mitochondria and its effects on myoglobin form and stability. *J Agric Food Chem*, *53*(4), 1223-1230. https://doi.org/10.1021/jf048646o

Tapio, I., Snelling, T. J., Strozzi, F., & Wallace, R. J. (2017). The ruminal microbiome associated with methane emissions from ruminant livestock. *Journal of animal science and biotechnology*, *8*, 1-11.

Tapio, M., Fischer, D., Mäntysaari, P., & Tapio, I. (2023). Rumen microbiota predicts feed efficiency of primiparous nordic red dairy cows. *Microorganisms*, *11*(5), 1116.

Tarique, T., Yang, S., Mohsina, Z., Qiu, J., Yan, Z., Chen, G., & Chen, A. (2014). Identification of genes involved in regulatory mechanism of pigments in broiler chickens. *Genetics and Molecular Research*, *13*(3), 7201-7216.

Terra, L. F., Wailemann, R. A., Dos Santos, A. F., Gomes, V. M., Silva, R. P., Laporte, A.,…Lortz, S. (2019). Heat shock protein B1 is a key mediator of prolactin-induced beta-cell cytoprotection against oxidative stress. *Free Radical Biology and Medicine*, *134*, 394-405.

Thomas, A. C. (1999). *Astaxanthin in juvenile farmed Chinook salmon (Oncorhynchus tshawytscha): effective dietary levels for flesh pigmentation and influence on fatty acid profile during cold temperature storage of fillets* University of British Columbia].

Thomas, S. E., & Harrison, E. H. (2016). Mechanisms of selective delivery of xanthophylls to retinal pigment epithelial cells by human lipoproteins. *Journal of lipid research*, *57*(10), 1865-1878.

Thorgaard, G. H., Bailey, G. S., Williams, D., Buhler, D. R., Kaattari, S. L., Ristow, S. S.,…Palti, Y. (2002). Status and opportunities for genomics research with rainbow trout. *Comp Biochem Physiol B Biochem Mol Biol*, *133*(4), 609-646. https://doi.org/10.1016/s1096-4959(02)00167-7

Tian, B., & Hua, Y. (2010). Carotenoid biosynthesis in extremophilic Deinococcus–Thermus bacteria. *Trends in microbiology*, *18*(11), 512-520.

Tigistu-Sahle, F. (2012). Lipidomics for Human Bone Marrow Mesenchymal Stem Cells.

Tintchev, F., Kuhlmann, U., Wackerbarth, H., Töpfl, S., Heinz, V., Knorr, D., & Hildebrandt, P. (2009). Redox processes in pressurised smoked salmon studied by resonance Raman spectroscopy. *Food chemistry*, *112*(2), 482-486.

Torrissen, O. (1995). Strategies for salmonid pigmentation. *Journal of Applied ichthyology*, *11*(3-4), 276-281.

Torrissen, O. J. (1989). Pigmentation of salmonids: interactions of astaxanthin and canthaxanthin on pigment deposition in rainbow trout. *Aquaculture*, *79*(1-4), 363-374.

Torrissen, O. J., & Ingebrigtsen, K. (1992). Tissue distribution of 14C-astaxanthin in the Atlantic salmon (Salmo salar). *Aquaculture*, *108*(3-4), 381-385.

Turchini, G. M., Francis, D. S., Keast, R. S., & Sinclair, A. J. (2011). Transforming salmonid aquaculture from a consumer to a producer of long chain omega-3 fatty acids. *Food Chemistry*, *124*(2), 609-614.

Turner, S. D. (2014). qqman: an R package for visualizing GWAS results using QQ and manhattan plots. *Biorxiv*, 005165.

Tyagi, A., Singh, B., Billekallu Thammegowda, N. K., & Singh, N. K. (2019). Shotgun metagenomics offers novel insights into taxonomic compositions, metabolic pathways and antibiotic resistance genes in fish gut microbiome. *Archives of microbiology*, *201*, 295-303.

Umeno, D., Tobias, A. V., & Arnold, F. H. (2005). Diversifying carotenoid biosynthetic pathways by directed evolution. *Microbiology and molecular biology reviews*, *69*(1), 51-78.

Vala, A. G., Tomar, R., & Rathod, P. J. (2023). Speed Breeding: Accelerating Crop Improvement through Controlled Environments, Genetics, and High-Throughput Phenotyping. *Int J Adv Res Sci Eng Technol*, *10*(5), 746-749.

Vallejo, R. L., Cheng, H., Fragomeni, B. O., Gao, G., Silva, R. M., Martin, K. E.,…Palti, Y. (2021). The accuracy of genomic predictions for bacterial cold water disease resistance remains higher than the pedigree-based model one generation after model training in a commercial rainbow trout breeding population. *Aquaculture*, *545*, 737164.

Vallejo, R. L., Leeds, T. D., Fragomeni, B. O., Gao, G., Hernandez, A. G., Misztal, I.,…Palti, Y. (2016). Evaluation of genome-enabled selection for bacterial cold water disease resistance using progeny performance data in rainbow trout: insights on genotyping methods and genomic prediction models. *Frontiers in genetics*, *7*, 187840.

Vallejo, R. L., Leeds, T. D., Gao, G., Parsons, J. E., Martin, K. E., Evenhuis, J. P.,…Palti, Y. (2017). Genomic selection models double the accuracy of predicted breeding values for bacterial cold water disease resistance compared to a traditional pedigree-based model in rainbow trout aquaculture. *Genetics Selection Evolution*, *49*, 1-13.

Vallejo, R. L., Silva, R. M., Evenhuis, J. P., Gao, G., Liu, S., Parsons, J. E.,…Leeds, T. D. (2018). Accurate genomic predictions for BCWD resistance in rainbow trout are achieved using low-density SNP panels: Evidence that long-range LD is a major contributing factor. *Journal of animal breeding and genetics*, *135*(4), 263-274.

Vallejo, R. L., Silva, R. M. O., Evenhuis, J. P., Gao, G., Liu, S., Parsons, J. E.,…Palti, Y. (2018). Accurate genomic predictions for BCWD resistance in rainbow trout are achieved using low-density SNP panels: Evidence that long-range LD is a major contributing factor. *J Anim Breed Genet*. https://doi.org/10.1111/jbg.12335

VanRaden, P. M. (2008). Efficient methods to compute genomic predictions. *J Dairy Sci*, *91*(11), 4414-4423. https://doi.org/10.3168/jds.2007-0980

Viney, M. E., & Riley, E. M. (2014). From immunology to eco-immunology: more than a new name. *Eco-immunology: evolutive aspects and future perspectives*, 1-19.

Vo, T. T. M., Nguyen, T. V., Amoroso, G., Ventura, T., & Elizur, A. (2021). Deploying new generation sequencing for the study of flesh color depletion in Atlantic Salmon (Salmo salar). *BMC genomics*, *22*(1), 1-21.

von Lintig, J., Moon, J., Lee, J., & Ramkumar, S. (2020). Carotenoid metabolism at the intestinal barrier. *Biochimica et Biophysica Acta (BBA)-Molecular and Cell Biology of Lipids*, *1865*(11), 158580.

Vranová, E., Coman, D., & Gruissem, W. (2013). Network analysis of the MVA and MEP pathways for isoprenoid synthesis. *Annual review of plant biology*, *64*(1), 665-700.

Wakchaure, R., Ganguly, S., Praveen, P., Kumar, A., Sharma, S., & Mahajan, T. (2015). Marker assisted selection (MAS) in animal breeding: a review. *J. Drug. Metab. Toxicol*, *6*(5), e127.

Wang, A. R., Ran, C., Ringø, E., & Zhou, Z. G. (2018). Progress in fish gastrointestinal microbiota research. *Reviews in Aquaculture*, *10*(3), 626-640.

Wang, H., Misztal, I., Aguilar, I., Legarra, A., & Muir, W. (2012). Genome-wide association mapping including phenotypes from relatives without genotypes. *Genetics Research*, *94*(2), 73-83.

Wariso, B. A., Kester, A. S., & Thomas, R. D. (2006). Isolation and partial characterization of carotenoid mutants of Corynebacterium poinsettiae ATCC 9682. *Global Journal of Pure and Applied Sciences*, *12*(2), 203-210.

Weber, K. L., Welly, B. T., Van Eenennaam, A. L., Young, A. E., Porto-Neto, L. R., Reverter, A., & Rincon, G. (2016). Identification of gene networks for residual feed intake in Angus cattle using genomic prediction and RNA-seq. *PloS one*, *11*(3), e0152274.

Weigel, K., VanRaden, P., Norman, H., & Grosu, H. (2017). A 100-Year Review: Methods and impact of genetic selection in dairy cattle—From daughter–dam comparisons to deep learning algorithms. *Journal of dairy science*, *100*(12), 10234-10250.

Weishaar, R., Wellmann, R., Camarinha-Silva, A., Rodehutscord, M., & Bennewitz, J. (2020). Selecting the hologenome to breed for an improved feed efficiency in pigs—A novel selection index. *Journal of Animal Breeding and Genetics*, *137*(1), 14-22.

Weiss, S., Xu, Z. Z., Peddada, S., Amir, A., Bittinger, K., Gonzalez, A.,…Birmingham, A. (2017). Normalization and microbial differential abundance strategies depend upon data characteristics. *Microbiome*, *5*, 1-18.

Wiseman, S., Osachoff, H., Bassett, E., Malhotra, J., Bruno, J., VanAggelen, G.,…Vijayan, M. M. (2007). Gene expression pattern in the liver during recovery from an acute stressor in rainbow trout. *Comparative Biochemistry and Physiology Part D: Genomics and Proteomics*, *2*(3), 234-244.

Wood, D. E., Lu, J., & Langmead, B. (2019). Improved metagenomic analysis with Kraken 2. *Genome biology*, *20*, 1-13.

Wu, H., Yesilyurt, H. G., Yoon, J., & Terman, J. R. (2018). The MICALs are a family of F-actin dismantling oxidoreductases conserved from Drosophila to humans. *Scientific reports*, *8*(1), 1-20.

Wu, H. J., Seib, K. L., Srikhanta, Y. N., Edwards, J., Kidd, S. P., Maguire, T. L.,…Jennings, M. P. (2010). Manganese regulation of virulence factors and oxidative stress resistance in Neisseria gonorrhoeae. *J Proteomics*, *73*(5), 899-916. https://doi.org/10.1016/j.jprot.2009.12.001

Wu, L., Fan, J., & Belasco, J. G. (2006). MicroRNAs direct rapid deadenylation of mRNA. *Proceedings of the National Academy of Sciences*, *103*(11), 4034-4039.

Wu, W., Gao, X.-G., Dai, Y., Fu, Y., Li, X.-M., & Dai, R.-T. (2015). Post-mortem changes in sarcoplasmic proteome and its relationship to meat color traits in M. semitendinosus of Chinese Luxi yellow cattle. *Food Research International*, *72*, 98-105.

Wu, W., Yu, Q.-Q., Fu, Y., Tian, X.-J., Jia, F., Li, X.-M., & Dai, R.-T. (2016). Towards muscle-specific meat color stability of Chinese Luxi yellow cattle: A proteomic insight into post-mortem storage. *Journal of proteomics*, *147*, 108-118.

Xiang, H., Sun, S., Huang, H., Hao, S., Li, L., Yang, X.,…Pan, C. (2023). Proteomics study of mitochondrial proteins in tilapia red meat and their effect on color change during storage. *Food Chemistry*, *400*, 134061.

Yabuta, S., Masaki, M., & Shidoji, Y. (2016). Associations of Buccal Cell Telomere Length with Daily Intake of beta-Carotene or alpha-Tocopherol Are Dependent on Carotenoid Metabolism-related Gene Polymorphisms in Healthy Japanese Adults. *J Nutr Health Aging*, *20*(3), 267-274. https://doi.org/10.1007/s12603-015-0577-x

Yabuuchi, H., Tanaka, K., Maeda, M., Takemura, M., Oka, M., Ohashi, R., & Tamai, I. (2008). Cloning of the dog bile salt export pump (BSEP; ABCB11) and functional comparison with the human and rat proteins. *Biopharm Drug Dispos*, *29*(8), 441-448. https://doi.org/10.1002/bdd.629

Yan, W., Jang, G.-F., Haeseleer, F., Esumi, N., Chang, J., Kerrigan, M.,…Zack, D. J. (2001). Cloning and characterization of a human β, β-carotene-15, 15′-dioxygenase that is highly expressed in the retinal pigment epithelium. *Genomics*, *72*(2), 193-202.

Yang, X., Wu, S., Hopkins, D. L., Liang, R., Zhu, L., Zhang, Y., & Luo, X. (2018). Proteomic analysis to investigate color changes of chilled beef longissimus steaks held under carbon monoxide and high oxygen packaging. *Meat science*, *142*, 23-31.

Yatsunami, R., Ando, A., Yang, Y., Takaichi, S., Kohno, M., Matsumura, Y.,…Fujita, N. (2014). Identification of carotenoids from the extremely halophilic archaeon Haloarcula japonica. *Frontiers in microbiology*, *5*, 100.

Ye, S., Yuan, X., Lin, X., Gao, N., Luo, Y., Chen, Z.,…Zhang, Z. (2018). Imputation from SNP chip to sequence: a case study in a Chinese indigenous chicken population. *Journal of animal science and biotechnology*, *9*, 1-12.

Yoon, J.-H., Lee, K.-C., Weiss, N., Kang, K. H., & Park, Y.-H. (2003). Jeotgalicoccus halotolerans gen. nov., sp. nov. and Jeotgalicoccus psychrophilus sp. nov., isolated from the traditional Korean fermented seafood jeotgal. *International Journal of Systematic and Evolutionary Microbiology*, *53*(2), 595-602.

Yuan, F. L., Xu, R. S., Ye, J. X., Zhao, M. D., Ren, L. J., & Li, X. (2019). Apoptotic bodies from endplate chondrocytes enhance the oxidative stress-induced mineralization by regulating PPi metabolism. *J Cell Mol Med*, *23*(5), 3665-3675. https://doi.org/10.1111/jcmm.14268

Zeng, B., Lloyd-Jones, L. R., Montgomery, G. W., Metspalu, A., Esko, T., Franke, L.,…Quyyumi, A. A. (2019). Comprehensive multiple eQTL detection and its application to GWAS interpretation. *Genetics*, *212*(3), 905-918.

Zenger, K., Khatkar, M., Jerry, D., & Raadsma, H. (2017). The next wave in selective breeding: implementing genomic selection in aquaculture. Proc. Assoc. Advmt. Anim. Breed. Genet,

Zhang, W., Liu, M., & Dai, X. (2013). Biological characteristics and probiotic effect of Leuconostoc lactis strain isolated from the intestine of black porgy fish. *Brazilian journal of microbiology*, *44*, 685-691.

Zhang, X., & Xie, J. (2019). Analysis of proteins associated with quality deterioration of grouper fillets based on TMT quantitative proteomics during refrigerated storage. *Molecules*, *24*(14), 2641.

Zhang, Y., Johnson, K., Russell, R. G. G., Wordsworth, B. P., Carr, A. J., Terkeltaub, R. A., & Brown, M. A. (2005). Association of sporadic chondrocalcinosis with a− 4-basepair G-to-A transition in the 5′-untranslated region of ANKH that promotes enhanced expression of ANKH protein and excess generation of extracellular inorganic pyrophosphate. *Arthritis & Rheumatism*, *52*(4), 1110-1117.

ZHANG, Y.-m., ZHANG, X.-z., WANG, T.-t., Hopkins, D. L., MAO, Y.-w., LIANG, R.-r.,…ZHU, L.-x. (2018). Implications of step-chilling on meat color investigated using proteome analysis of the sarcoplasmic protein fraction of beef longissimus lumborum muscle. *Journal of Integrative Agriculture*, *17*(9), 2118-2125.

Zheng, Q., Zhang, Y., Chen, Y., Yang, N., Wang, X. J., & Zhu, D. (2009). Systematic identification of genes involved in divergent skeletal muscle growth rates of broiler and layer chickens. *BMC genomics*, *10*(1), 87. https://doi.org/10.1186/1471-2164-10-87

Zhu, W., Yang, Z., Ma, Z., & Chai, L. (2008). Reduction of high concentrations of chromate by Leucobacter sp. CRB1 isolated from Changsha, China. *World Journal of Microbiology and Biotechnology*, *24*, 991-996.

Zhu, Z., Zhang, F., Hu, H., Bakshi, A., Robinson, M. R., Powell, J. E.,…Visscher, P. M. (2016). Integration of summary data from GWAS and eQTL studies predicts complex trait gene targets. *Nature genetics*, *48*(5), 481-487.

Ziyada, A. M. A. (2023). *Evaluation of Low Coverage Whole Genome Sequencing Genotype Imputation Strategies* Hamad Bin Khalifa University (Qatar)].

Zoric, N. (2017). Characterization of genes and gene products influencing carotenoid metabolism in Atlantic salmon.

Zychowska, M., Jastrzebski, Z., Chruscinski, G., Michalowska-Sawczyn, M., & Nowak-Zaleska, A. (2015). Vitamin C, A and E supplementation decreases the expression of HSPA1A and HSPB1 genes in the leukocytes of young polish figure skaters during a 10-day training camp. *J Int Soc Sports Nutr*, *12*(1), 9. https://doi.org/10.1186/s12970-015-0069-8

Ługowska, A., Hetmańczyk-Sawicka, K., Iwanicka-Nowicka, R., Fogtman, A., Cieśla, J., Purzycka-Olewiecka, J. K.,…Lualdi, S. (2019). Gene expression profile in patients with Gaucher disease indicates activation of inflammatory processes. *Scientific reports*, *9*(1), 1-14.

Electronic Supplementary Materials

Additional file 1: **Table S1:** Bacteria biomarkers identified by LEfSE for the March, June and combined March and June analysis with their effect sizes

Combined March and June Analysis

Feature	Effect Size	Class	LDA Score	p-value
k__Bacteria.p__Actinobacteria.c__Actinobacteria.o__Corynebacteriales.f__Corynebacteriaceae.g__Corynebacterium.s__variabile	2.460279	HighFilletColor	2.167119	0.035999
k__Bacteria.p__Actinobacteria.c__Actinobacteria.o__Micrococcales.f__Microbacteriaceae.g__Leucobacter.s__chromiireducens	1.933653	HighFilletColor	1.713324	0.03057
k__Bacteria.p__Firmicutes.c__Bacilli.o__Bacillales.f__Staphylococcaceae.g__Jeotgalicoccus.s__halotolerans	2.048807	HighFilletColor	1.752627	0.03057
k__Bacteria.p__Firmicutes.c__Bacilli.o__Lactobacillales.f__Leuconostocaceae.g__Leuconostoc.s__lactis	2.596861	HighFilletColor	2.289649	0.045098
k__Bacteria.p__Firmicutes.c__Clostridia.o__Clostridiales.f__Family_XIII.g__NA.s__sp31648	2.449172	HighFilletColor	2.165685	0.03057
k__Bacteria.p__Chloroflexi.c__Thermomicrobia.o__NA	1.798919	HighFilletColor	1.508759	0.03057
k__Bacteria.p__Firmicutes.c__Bacilli.o__Bacillales.f__Bacillaceae.g__Oceanobacillus.s__indicireducens	1.735656	LowFilletColor	1.585663	0.03057
k__Bacteria.p__Firmicutes.c__Clostridia.o__Clostridiales.f__Lachnospiraceae.g__Lachnoclostridium.s__sp32318	2.08618	LowFilletColor	1.878955	0.013002
k__Bacteria.p__Tenericutes.c__Mollicutes.o__Mycoplasmatales.f__Mycoplasmataceae.g__Mycoplasma.s__sp68210	5.542538	LowFilletColor	5.21029	0.000425
k__Bacteria.p__Tenericutes	5.599575	LowFilletColor	5.20413	0.008151
k__Bacteria.p__Tenericutes.c__Mollicutes	5.599575	LowFilletColor	5.20413	0.008151
k__Bacteria.p__Tenericutes.c__Mollicutes.o__Mycoplasmatales	5.599535	LowFilletColor	5.204078	0.008151
k__Bacteria.p__Tenericutes.c__Mollicutes.o__Mycoplasmatales.f__Mycoplasmataceae	5.599535	LowFilletColor	5.204078	0.008151
k__Bacteria.p__Tenericutes.c__Mollicutes.o__Mycoplasmatales.f__Mycoplasmataceae.g__Mycoplasma	5.599535	LowFilletColor	5.20409	0.008151

March Only

Feature	Effect Size	Class	LDA Score	p-value
k__Bacteria.p__Firmicutes.c__Bacilli.o__Lactobacillales.f__Lactobacillaceae.g__Lactobacillus.s__NA	4.729421	HighFilletColor	4.182668	0.047202
k__Bacteria.p__Firmicutes.c__Clostridia.o__Clostridiales.f__Clostridiaceae.g__Clostridium.s__paraputrificum	3.713004	HighFilletColor	3.375249	0.026388
k__Bacteria.p__Firmicutes.c__Clostridia.o__Clostridiales.f__Lachnospiraceae.g__Blautia.s__sp31973	3.555528	HighFilletColor	3.190258	0.046533
k__Bacteria.p__Firmicutes.c__Clostridia.o__Clostridiales.f__Peptostreptococcaceae.g__Peptostreptococcus.s__sp34369	4.111319	HighFilletColor	3.707897	0.009023
k__Bacteria.p__Actinobacteria.c__Actinobacteria.o__Corynebacteriales	3.654374	HighFilletColor	3.171965	0.02828
k__Bacteria.p__Actinobacteria.c__Actinobacteria.o__Corynebacteriales.f__Corynebacteriaceae	3.590111	HighFilletColor	3.235213	0.016294
k__Bacteria.p__Actinobacteria.c__Actinobacteria.o__Corynebacteriales.f__Corynebacteriaceae.g__Corynebacterium	3.590111	HighFilletColor	3.235213	0.016294
k__Bacteria.p__Actinobacteria.c__Coriobacteriia	3.689085	HighFilletColor	3.326591	0.047202
k__Bacteria.p__Actinobacteria.c__Coriobacteriia.o__Coriobacteriales	3.689085	HighFilletColor	3.326591	0.047202
k__Bacteria.p__Actinobacteria.c__Coriobacteriia.o__Coriobacteriales.f__Coriobacteriaceae	3.689085	HighFilletColor	3.326591	0.047202
k__Bacteria.p__Firmicutes.c__Bacilli.o__Bacillales.f__Staphylococcaceae	4.061747	HighFilletColor	3.455292	0.047202
k__Bacteria.p__Firmicutes.c__Bacilli.o__Bacillales.f__Staphylococcaceae.g__Staphylococcus	3.695903	HighFilletColor	3.190773	0.047202
k__Bacteria.p__Firmicutes.c__Bacilli.o__Lactobacillales.f__Lactobacillaceae	4.996334	HighFilletColor	4.392649	0.047202
k__Bacteria.p__Firmicutes.c__Bacilli.o__Lactobacillales.f__Lactobacillaceae.g__Lactobacillus	4.98236	HighFilletColor	4.372701	0.047202
k__Bacteria.p__Firmicutes.c__Clostridia.o__Clostridiales.f__Clostridiaceae	4.576466	HighFilletColor	4.086803	0.009023
k__Bacteria.p__Firmicutes.c__Clostridia.o__Clostridiales.f__Clostridiaceae.g__Clostridium	4.573573	HighFilletColor	4.091112	0.009023
k__Bacteria.p__Firmicutes.c__Clostridia.o__Clostridiales.f__Lachnospiraceae.g__NA	3.714008	HighFilletColor	3.339591	0.026388
k__Bacteria.p__Firmicutes.c__Clostridia.o__Clostridiales.f__NA.g__NA	3.564272	HighFilletColor	3.117375	0.015971
k__Bacteria.p__Tenericutes.c__Mollicutes.o__Mycoplasmatales.f__Mycoplasmataceae.g__Mycoplasma.s__sp68210	5.624225	LowFilletColor	5.316488	0.007058
k__Bacteria.p__Tenericutes	5.701664	LowFilletColor	5.297908	0.016294
k__Bacteria.p__Tenericutes.c__Mollicutes	5.701664	LowFilletColor	5.297908	0.016294
k__Bacteria.p__Tenericutes.c__Mollicutes.o__Mycoplasmatales	5.701664	LowFilletColor	5.297908	0.016294
k__Bacteria.p__Tenericutes.c__Mollicutes.o__Mycoplasmatales.f__Mycoplasmataceae	5.701664	LowFilletColor	5.297908	0.016294
k__Bacteria.p__Tenericutes.c__Mollicutes.o__Mycoplasmatales.f__Mycoplasmataceae.g__Mycoplasma	5.701664	LowFilletColor	5.297927	0.016294

June Only

Feature	Effect Size	Class	LDA Score	p-value
k__Bacteria.p__Firmicutes.c__Clostridia.o__Clostridiales.f__Peptostreptococcaceae.g__Terrisporobacter.s__sp34390_sp34393	3.214297	LowFilletColor	3.254878	0.018603
k__Bacteria.p__Tenericutes.c__Mollicutes.o__Mycoplasmatales.f__Mycoplasmataceae.g__Mycoplasma.s__sp68210	5.441842	LowFilletColor	5.174622	0.046533

Addendum to chapter 4 after publication

Here, we used shotgun metagenomics sequencing to investigate pathways associated with fillet color (High = 29, Low = 24). The fillet color was measured with the Minolta Chroma Meter CR-200 device (Minolta, Model CR-300; Minolta Camera Co., Osaka, Japan), which gives readings for redness (a*), yellowness (b*), and lightness (L*). Two measurements were taken from the same collected section, and the average value was used. The saturation index (SI) $(a^*2 + b^*2)^{0.5}$ was calculated for all fish and used to sort the 40 families into "red fillet group" for fish families

of high saturation index and "white fillet group" for fish families of low saturation index value. The saturation index describes the brightness of the color (Association, 1991).

Metagenomics Shotgun Sequencing

Unlike 16S, metagenomic shotgun sequencing captures all DNA in a sample, providing a comprehensive view of microbial diversity, including bacteria, archaea, fungi, viruses, and even host DNA contamination (Quince et al., 2017). By randomly sequencing fragmented DNA, it reveals not only taxonomy but also functional genes, metabolic pathways, and potential antimicrobial resistance profiles (Tyagi et al., 2019). Its strengths include high resolution (down to strain level), functional insights, and independence from PCR biases (Quince et al., 2017).

Methods

Fecal DNA Extraction, Library preparation, and Metagenomic sequencing

DNA was extracted from fecal samples using the ZymoBIOMICS®-96 MagBead DNA Kit (Zymo Research, Irvine, CA) and following the manufacturer's instructions. The genomic DNA extracted was used to prepare the library following Illumina® DNA Library Prep Kit (Illumina, San Diego, CA) with up to 500 ng DNA input following the manufacturer's protocol using unique dual-index 10 bp barcodes with Nextera® adapters (Illumina, San Diego, CA). All libraries were pooled in equal abundance. The final pool was quantified using qPCRand TapeStation® (Agilent Technologies, Santa Clara, CA). The final library was profiled with shotgun metagenomic sequencing on the NovaSeq X or 6000® (Illumina, San Diego, CA) platform.

The ZymoBIOMICS® Microbial Community Standard (Zymo Research, Irvine, CA) was used as a positive control for each DNA extraction. The ZymoBIOMICS® Microbial Community DNA Standard (Zymo Research, Irvine, CA) was used as a positive control for each library preparation. Negative controls (i.e. blank extraction control, blank library preparation control) were included to assess the level of bioburden carried by the wet-lab process.

Metagenomics Sequence Data Processing and Analysis

The paired raw reads were checked for quality control using FastQC (Andrews, 2010). This was followed by trimming the Illumina Nexterra adapter sequences and low-quality reads using a minimum base quality of 20 Phred and length of 70bp with Cutadapt (v48) (Martin, 2011). Furthermore, host and human sequence contaminations in the trimmed reads were removed using bowtie2 (v2.5.4) (Langmead & Salzberg, 2012) using rainbow trout (Refseq assembly accession: GCA_013265735.3) and human (Refseq assembly accession: GCF_000001405.40) assemblies. The unmapped data were considered clean reads, free of human and host contamination. The resulting clean reads were used for subsequent analysis.

Taxonomic Classification, Abundance Estimation, and Functional Profiling

Clean paired reads from each sample were classified with the Kraken2 standard database(Wood et al., 2019). The Kraken2 database contains complete genomes in the RefSeq database for the bacterial, archaeal, and viral domains. Subsequently, the classification rate and abundance estimate of each specie-level taxon were also calculated using Bracken (Lu et al., 2017). For metagenomic taxonomic abundance data manipulation and analysis, we used the phyloseq and DESeq2 (version

1.46.0) in R version 4.4.1 (McMurdie & Holmes, 2013). The impact of divergent phenotypes on overall microbial diversity was estimated using alpha and beta diversity. As diversity analysis may be affected by sequencing depth (Weiss et al., 2017), a rarefaction of the species-level abundance was done before the analysis. The abundance was rarified to the smallest column sum per sample. The MetaPhlAn3 (Beghini et al., 2021) software which profiles functional taxonomy was also used to complement the kraken2 taxonomic profiles.

The functional profiling was done by mapping the paired metagenomic reads to the HUMAnN3 database (Beghini et al., 2021). The HUMAnN3 software (Beghini et al., 2021) profile genes, pathways, KOs, and GO terms from the metagenomic reads using the UniRef90 database and report the abundance of each gene and pathway detected.

Results and Discussion

Alpha and Beta Diversity

The alpha and Beta diversity show no significant difference when comparing the High and low Saturation Index groups.

Metaphlan

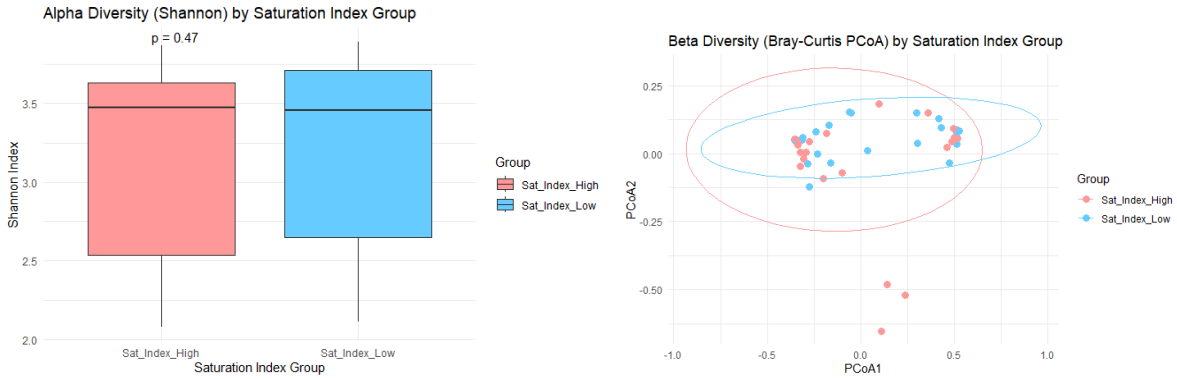

Supplementary Figure 1: Alpha and Beta diversity plots comparing High and low Saturation Index groups.

Differential Pathway Abundance

Using DESeq2, we identified 79 significant pathways (p-adj < 0.1) (Supplementary File 2) that show differential abundance between the high and low Saturation Index (Redness) groups, respectively. The pathways (top 20 for DESeq2) are shown in the Figure below.

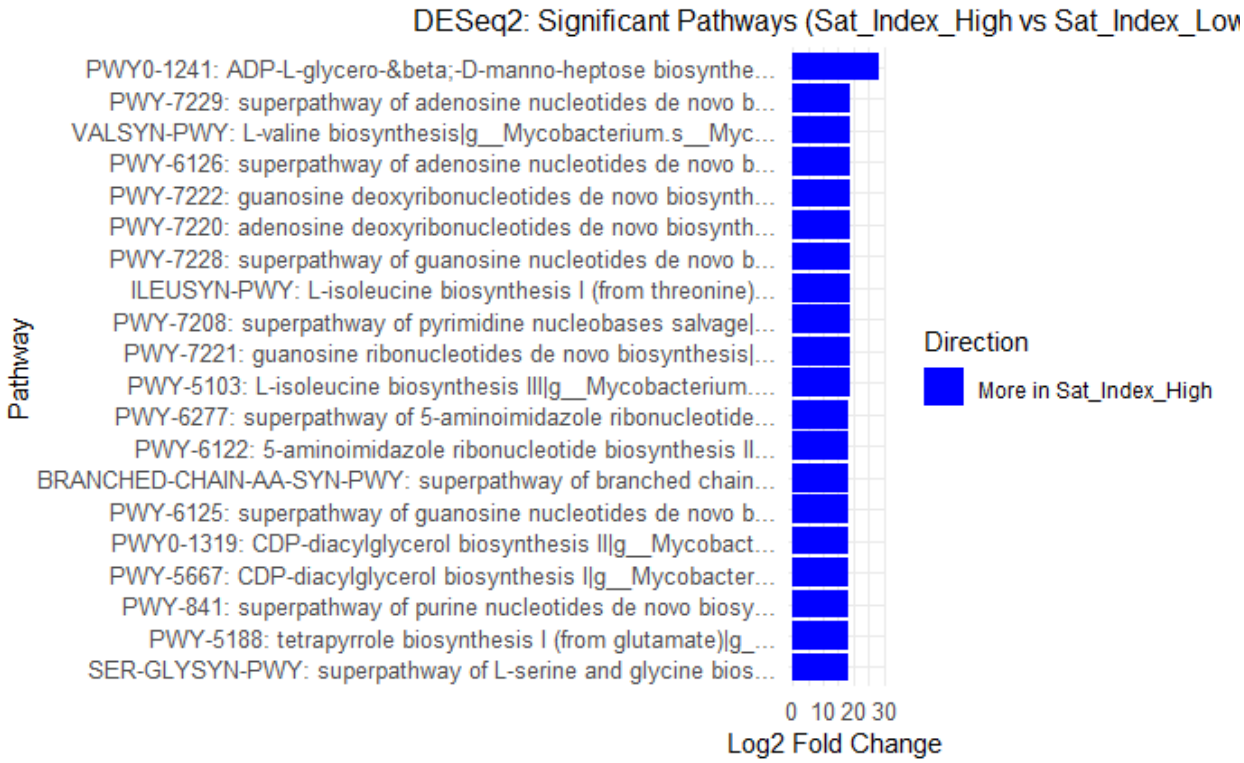

Supplementary Figure 2: Differential abundance pathways between the High (29) and low (24) Saturation Index groups.. The Saturation Index is an indication of the brightness of the reddish coloration of the fillet.

The pathways enriched in the low Saturation Index group are glycolysis IV, CMP-3-deoxy-D-manno-octulosonate biosynthesis, TRNA-CHARGING-PWY: tRNA charging, the Super pathway of N-acetylglucosamine, N-acetylmannosamine, and N-acetylneuraminate degradation, and Stachyose degradation.

Differential Abundant Pathways and their Relationship with Fillet color

Mycobacterium species are known to produce carotenoids like β-carotene and lycopene, often as a stress response (Ichiyama et al., 1988) . The MEP (methylerythritol phosphate) pathway (NONMEVIPP-PWY) in *Mycobacterium sp. YC-RL4* is likely the primary route for carotenoid synthesis, supported by lipid, amino acid, and cofactor pathways. Pathways associated with *Mycobacterium* species are more abundant in the high saturation index group.

The literature provides evidence that some of the microbiome pathways—particularly those from *Mycobacterium sp. YC_RL4*—may contribute to carotenoid production and enhancement of fillet coloration. The Methylerythritol Phosphate (MEP) Pathway produces isopentenyl pyrophosphate

(IPP), a precursor for terpenoids, including carotenoids (Rodriguez-Concepcion, 2010; Rohmer, 1999; Vranova et al., 2013). This is a central pathway for microbial carotenoid biosynthesis.

The Coenzyme A Biosynthesis Pathways (COA-PWY, COA-PWY-1, PANTOSYN-PWY, PANTO-PWY, PWY-7851) synthesize coenzyme A and its precursors (e.g., phosphopantothenate), which are critical for acetyl-CoA production (Leonardi et al., 2005). Acetyl-CoA is a substrate in the MEP pathway and fatty acid biosynthesis (Frank & Groll, 2017; Numa et al., 1965), both linked to carotenoid production. Coenzyme A supports lipid metabolism, which is crucial for carotenoid transport and storage in fish muscle as lipid-soluble pigments. Increased coenzyme A availability could enhance carotenoid incorporation into fillets.

The Fatty Acid and Phospholipid Biosynthesis pathways (FASYN-INITIAL-PWY, PHOSLIPSYN-PWY, PWY-5667) produce fatty acids and phospholipids, which form lipid carriers for carotenoids. Carotenoids are lipophilic and require lipid matrices for absorption and deposition (Parker, 1996). Enhanced lipid synthesis in *Mycobacterium* could improve carotenoid bioavailability in fish diets, promoting pigment deposition in muscle tissue for vibrant fillet color.

The Retinol Biosynthesis (PWY-6857), Supplementary file 2, pathway produces retinol (vitamin A), derived from β-carotene cleavage (D'Ambrosio et al., 2011). While not directly a carotenoid, it indicates active carotenoid metabolism.

The tetrapyrrole and heme Biosynthesis pathways (HEME-BIOSYNTHESIS-II, PWY-5188, PWY-5918 are involved in heme and porphyrin biosynthesis, which can influence oxidative stress and iron metabolism (Busch & Montgomery, 2015; Ryter & Tyrrell, 2000). Antioxidant balance is critical for carotenoid preservation in tissues.

16s rDNA microbiome sequencing versus metagenomics

Using 16s microbiome sequencing, we showed that bacterial taxa such as *Leuconostoc lactis*, *Corynebacterium variabile*, *Jeotgalicoccus halotolerans*, and *Leucobacter chromiireducens* are more abundant in the rainbow trout fish families with better reddish fillet coloration. A shortcoming of the 16S approach is that it cannot provide direct functional information and pathways, unlike shotgun metagenomics. We subsequently used shotgun metagenomics to investigate genes, pathways, and provide functional insights into how the microbiome taxa function to influence fillet coloration. We identified pathways associated with *Mycobacterium* species, capable of producing carotenoids, to be more abundant in the red fillet family. The primary pathway is the MEP (methylerythritol phosphate) pathway, supported by lipid, amino acid, and cofactor pathways.

Supplementary File 2: Pathways that show differential abundance between the High and Low Saturation Index groups.

baseMean	log2FoldChar	lfcSE	stat	pvalue	padj	Pathway
1707.667	-1.66784	0.549054	-3.03767	0.002384	0.084066	PWY-1042: glycolysis IV| unclassified
1900.435	-2.01557	0.668524	-3.01496	0.00257	0.08946	TRNA-CHARGING-PWY: tRNA charging| unclassified
839.6575	-2.44608	0.728066	-3.3597	0.00078	0.032098	GLCMANNANAUT-PWY: superpathway of N-acetylglucosamine, N-acetylmannosamine and N-acetylneuraminate degradati
930.5241	-2.30727	0.731045	-3.15613	0.001599	0.058657	PWY-6527: stachyose degradation| unclassified
757.6726	-3.54273	1.049617	-3.37526	0.000737	0.030803	PWY-1269: CMP-3-deoxy-D-manno-octulosonate biosynthesis
736.9323	-3.5779	1.198408	-2.98554	0.002831	0.097285	PWY-1269: CMP-3-deoxy-D-manno-octulosonate biosynthesis| unclassified
30.49658	9.610895	2.909434	3.303355	0.000955	0.038713	ORNDEG-PWY: superpathway of ornithine degradation| unclassified
10.07338	9.810173	3.081643	3.183423	0.001455	0.054882	PWY-6857: retinol biosynthesis
10.02994	9.774769	3.081657	3.17192	0.001514	0.056321	PWY-6857: retinol biosynthesis| unclassified
12.58951	-12.07	3.08169	-3.91669	8.98E-05	0.003869	FASYN-INITIAL-PWY: superpathway of fatty acid biosynthesis initiation (E. coli)
7.777869	-11.3857	3.082086	-3.69416	0.000221	0.009359	FASYN-INITIAL-PWY: superpathway of fatty acid biosynthesis initiation (E. coli)| unclassified
14.06387	9.953051	3.082151	3.229255	0.001241	0.048201	PWY-6928: superpathway of cholesterol degradation I (cholesterol oxidase)
14.06387	9.953051	3.082151	3.229255	0.001241	0.048201	PWY-6947: superpathway of cholesterol degradation II (cholesterol dehydrogenase)
13.96069	9.9394	3.082155	3.224822	0.001261	0.048201	PWY-6928: superpathway of cholesterol degradation I (cholesterol oxidase)| unclassified
13.96069	9.9394	3.082155	3.224822	0.001261	0.048201	PWY-6947: superpathway of cholesterol degradation II (cholesterol dehydrogenase)| unclassified
11.41958	9.62206	3.08222	3.121795	0.001798	0.064574	PWY-6944: androstenedione degradation I (aerobic)
11.39078	9.616997	3.082222	3.120151	0.001808	0.064574	PWY-6944: androstenedione degradation I (aerobic)| unclassified
20.8295	28.61029	3.090551	9.257341	2.1E-20	5.69E-17	PWY0-1241: ADP-L-glycero-β-D-manno-heptose biosynthesis| unclassified
48.70927	18.71607	3.101011	6.035472	1.58E-09	4.19E-07	PWY-7229: superpathway of adenosine nucleotides de novo biosynthesis I| g__Mycobacterium.s__Mycobacterium_sp_YC_RL
48.01104	18.69957	3.101012	6.030153	1.64E-09	4.19E-07	VALSYN-PWY: L-valine biosynthesis| g__Mycobacterium.s__Mycobacterium_sp_YC_RL4
46.59156	18.67324	3.101012	6.02166	1.73E-09	4.19E-07	PWY-6126: superpathway of adenosine nucleotides de novo biosynthesis II| g__Mycobacterium.s__Mycobacterium_sp_YC_R
46.21732	18.67192	3.101012	6.021235	1.73E-09	4.19E-07	PWY-7220: adenosine deoxyribonucleotides de novo biosynthesis II| g__Mycobacterium.s__Mycobacterium_sp_YC_RL4
46.21732	18.67192	3.101012	6.021235	1.73E-09	4.19E-07	PWY-7222: guanosine deoxyribonucleotides de novo biosynthesis II| g__Mycobacterium.s__Mycobacterium_sp_YC_RL4
44.64677	18.65672	3.101012	6.016333	1.78E-09	4.19E-07	PWY-7228: superpathway of guanosine nucleotides de novo biosynthesis I| g__Mycobacterium.s__Mycobacterium_sp_YC_RL
44.08595	18.64241	3.101012	6.011719	1.84E-09	4.19E-07	ILEUSYN-PWY: L-isoleucine biosynthesis I (from threonine)| g__Mycobacterium.s__Mycobacterium_sp_YC_RL4
42.66577	18.62717	3.101013	6.006803	1.89E-09	4.19E-07	PWY-7208: superpathway of pyrimidine nucleobases salvage| g__Mycobacterium.s__Mycobacterium_sp_YC_RL4
41.4518	18.60442	3.101013	5.999466	1.98E-09	4.19E-07	PWY-7221: guanosine ribonucleotides de novo biosynthesis| g__Mycobacterium.s__Mycobacterium_sp_YC_RL4
41.37552	18.60365	3.101013	5.999217	1.98E-09	4.19E-07	PWY-5103: L-isoleucine biosynthesis III| g__Mycobacterium.s__Mycobacterium_sp_YC_RL4
39.11424	18.5628	3.101013	5.986044	2.15E-09	4.19E-07	PWY-6122: 5-aminoimidazole ribonucleotide biosynthesis II| g__Mycobacterium.s__Mycobacterium_sp_YC_RL4
39.11424	18.5628	3.101013	5.986044	2.15E-09	4.19E-07	PWY-6277: superpathway of 5-aminoimidazole ribonucleotide biosynthesis| g__Mycobacterium.s__Mycobacterium_sp_YC_R
37.97222	18.54213	3.101014	5.979377	2.24E-09	4.19E-07	BRANCHED-CHAIN-AA-SYN-PWY: superpathway of branched chain amino acid biosynthesis| g__Mycobacterium.s__Mycoba
35.37735	18.48845	3.101015	5.962064	2.49E-09	4.19E-07	PWY-6125: superpathway of guanosine nucleotides de novo biosynthesis II| g__Mycobacterium.s__Mycobacterium_sp_YC_R
30.41957	18.38489	3.101016	5.928667	3.05E-09	4.19E-07	PWY-5667: CDP-diacylglycerol biosynthesis I| g__Mycobacterium.s__Mycobacterium_sp_YC_RL4
30.41957	18.38489	3.101016	5.928667	3.05E-09	4.19E-07	PWY0-1319: CDP-diacylglycerol biosynthesis II| g__Mycobacterium.s__Mycobacterium_sp_YC_RL4
28.62697	18.33949	3.101017	5.914025	3.34E-09	4.19E-07	PWY-841: superpathway of purine nucleotides de novo biosynthesis I| g__Mycobacterium.s__Mycobacterium_sp_YC_RL4
26.88026	18.29992	3.101018	5.901261	3.61E-09	4.19E-07	PWY-5188: tetrapyrrole biosynthesis I (from glutamate)| g__Mycobacterium.s__Mycobacterium_sp_YC_RL4
25.09175	18.24584	3.101019	5.883822	4.01E-09	4.19E-07	SER-GLYSYN-PWY: superpathway of L-serine and glycine biosynthesis I| g__Mycobacterium.s__Mycobacterium_sp_YC_RL4
24.72466	18.23921	3.101019	5.881682	4.06E-09	4.19E-07	PWY66-399: gluconeogenesis III| g__Mycobacterium.s__Mycobacterium_sp_YC_RL4
23.64216	18.20007	3.10102	5.86906	4.38E-09	4.19E-07	PWY-6121: 5-aminoimidazole ribonucleotide biosynthesis I| g__Mycobacterium.s__Mycobacterium_sp_YC_RL4
23.61045	18.20104	3.10102	5.86937	4.37E-09	4.19E-07	PWY-7977: L-methionine biosynthesis IV| g__Mycobacterium.s__Mycobacterium_sp_YC_RL4
22.57137	18.17949	3.101021	5.86242	4.56E-09	4.19E-07	GLYOXYLATE-BYPASS: glyoxylate cycle| g__Mycobacterium.s__Mycobacterium_sp_YC_RL4
22.56261	18.18033	3.101021	5.862693	4.55E-09	4.19E-07	TCA-GLYOX-BYPASS: superpathway of glyoxylate bypass and TCA| g__Mycobacterium.s__Mycobacterium_sp_YC_RL4
22.35905	18.17505	3.101021	5.86099	4.6E-09	4.19E-07	PWY-6124: inosine-5'-phosphate biosynthesis II| g__Mycobacterium.s__Mycobacterium_sp_YC_RL4
21.93281	18.16157	3.101021	5.856641	4.72E-09	4.19E-07	PWY-5686: UMP biosynthesis II| g__Mycobacterium.s__Mycobacterium_sp_YC_RL4
21.93281	18.16157	3.101021	5.856641	4.72E-09	4.19E-07	PWY-7790: UMP biosynthesis III| g__Mycobacterium.s__Mycobacterium_sp_YC_RL4
21.93281	18.16157	3.101021	5.856641	4.72E-09	4.19E-07	PWY-7791: UMP biosynthesis III| g__Mycobacterium.s__Mycobacterium_sp_YC_RL4
21.43057	18.14644	3.101022	5.851762	4.86E-09	4.19E-07	TCA: TCA cycle I (prokaryotic)| g__Mycobacterium.s__Mycobacterium_sp_YC_RL4
20.76612	18.11721	3.101023	5.842333	5.15E-09	4.19E-07	UDPNAGSYN-PWY: UDP-N-acetyl-D-glucosamine biosynthesis I| g__Mycobacterium.s__Mycobacterium_sp_YC_RL4
20.68886	18.11739	3.101023	5.842393	5.15E-09	4.19E-07	PWY-6969: TCA cycle V (2-oxoglutarate synthase)| g__Mycobacterium.s__Mycobacterium_sp_YC_RL4

CHAPTER 5: Integrative eQTL and GWAS Mapping Reveals Cis-Regulatory Variants Associated with Growth Traits in Rainbow Trout

Abstract

Unraveling the genetic architecture of growth in fish requires integrative approaches that link genomic variation to gene expression and downstream biological function. In this study, we performed expression quantitative trait loci (eQTL) analysis by integrating whole-genome SNP data with transcriptomic profiles to investigate growth traits—body weight, muscle yield, and condition factor—in *Oncorhynchus mykiss* (rainbow trout).

We identified 234,630 putative cis-eQTLs and over 5.3 million trans-eQTLs, revealing widespread regulatory variation across the genome. A filtered set of 6,275 promoter-proximal cis-eQTLs was integrated with GWAS and differential gene expression data to prioritize candidate genes associated with growth. These included **GABRR1-like**, **AZIN1**, and **ATP6V1** for body weight; **TNNI2**, **PDLIM3**, **CDK5**, and **CYP3A27** for robustness; and **GATD3A**, **PPP2R1BB**, and **USP6NL** for muscle development. Many eQTL SNPs were located within active enhancer regions.

Pathway enrichment analysis highlighted roles in MAPK signaling, oxidative phosphorylation, glycolysis/gluconeogenesis, and the tricarboxylic acid (TCA) cycle. Haplotype analysis identified a specific variant combination significantly associated with elevated **ATP6V1** expression.

These results advance our understanding of the regulatory basis of growth traits in rainbow trout and improve the resolution of genotype-to-phenotype associations in the context of fish growth.

INTRODUCTION

Growth is a complex and highly polygenic trait regulated by interactions among genetic, environmental, and physiological factors. Understanding the molecular mechanisms underlying growth variation is essential for advancing functional genomics and improving predictive models of phenotypes from genotype. In vertebrates, including fish, growth is influenced by a network of pathways related to cellular proliferation, energy metabolism, endocrine signaling, and structural development.

Rainbow trout (Oncorhynchus mykiss) is a well-established model for studying complex traits in teleosts, owing to its fully sequenced genome, availability of genomic tools, and diverse phenotypic datasets. Previous studies have shown that traits related to growth—such as body weight, muscle yield, and condition factor—are governed by numerous genetic variants, each contributing modest effect (A. Ali et al., 2020; Gonzalez-Pena et al., 2016; Hu et al., 2013; Reis Neto et al., 2019). Despite numerous genome-wide association studies (GWAS), most associated loci explain only a small proportion of phenotypic variance, limiting their utility for trait prediction and interpretation. Many of these variants lie in non-coding regions, making functional characterization challenging.

Transcriptomic analyses have provided additional insights into the molecular basis of growth. For instance, differential expression studies have implicated genes involved in the growth hormone/insulin-like growth factor (GH/IGF) axis, PI3K-Akt, JAK-STAT, and MAPK pathways in muscle and liver tissues of fast-growing versus slow-growing rainbow trout families(Cleveland et al., 2020; Codina et al., 2006; Danzmann et al., 2016; Hou et al., 2020; Reindl et al., 2011). These studies also highlighted roles for protein metabolism, myogenesis, lipid processing, redox regulation, and regulatory contributions from long non-coding RNAs.

However, connecting expression profiles to specific causal variants remains a challenge. Expression quantitative trait loci (eQTL) mapping bridges this gap by integrating gene expression and genotype data to identify variants that regulate gene expression. eQTLs can act locally (cis-eQTLs), typically within or near the gene they influence, or distantly (trans-eQTLs), affecting genes on different loci or chromosomes(Võsa et al., 2021). These regulatory variants can illuminate the mechanisms through which genetic differences influence complex traits by modulating transcriptional activity.

To date, there has been limited eQTL mapping in rainbow trout, with the only prior effort using microarray data and a small number of genetic markers to explore acclimation to seawater (Le Bras et al., 2010). With the advent of high-throughput RNA-sequencing and dense genome-wide SNP datasets, it is now feasible to conduct comprehensive eQTL analyses in this species.

In this study, we performed genome-wide eQTL analysis to identify genetic variants associated with gene expression variation in rainbow trout and to investigate their potential roles in regulating growth-related traits. By integrating eQTL mapping with GWAS and differential gene expression

data, we aim to prioritize candidate genes and regulatory variants that contribute to the genetic architecture of growth.

2.0 METHODOLOGY

2.1 Ethical statement

Husbandry practices and experimental procedures at the facility were approved by the University of Maryland, College Park, IACUC animal study protocol, protocol number 1593175-6.

2.2 Rainbow trout population, rearing, and harvest

The fish population used and their rearing were described in our previous publication (Ahmed et al., 2023). The rainbow trout population is from a muscle yield genetic selection line developed at the National Center for Cool and Cold Water Aquaculture (NCCCWA). This line started in 2002 as a growth-selected line for five consecutive generations before it was switched to a muscle yield line in 2014, as described in Cleveland et al. (2023). The fish used in this study were from the 2020-year class (YC) representing third-generation families. Phenotypic data and white muscle samples were collected from 442 females between 450- and 485-days post-hatch. The fish, representing 40 families, were received from the NCCCWA at 322 days post-hatch and reared at the University of Maryland, College Park's Crane Aquaculture facility. The fish were reared in a recirculating aquaculture system (RAS) with closely monitored water quality parameters.

At harvest, whole-body weight, fillet yield, and body length measurements were obtained from individual fish. The condition factor was calculated as (10^5*Body weight/Body length^3). A small piece of white muscle tissue was collected on the day of harvest for RNA extraction.

2.3 RNA extraction

According to their phenotypic values, the fish were classified as either “High” or “Low” family for each trait. Total RNA was extracted from the tissues using the RNAzol reagent as described in Ahmed et al. (2023). We used 24 (four families), 23 (four families), 48 (eight families), and 94 (17 families) samples for body weight, muscle yield, condition factor, and genetic line, respectively (Table 1).

Table 1. The number of fish samples and families per trait

	Body weight	Muscle yield	Condition Factor	Genetc Line
High	12 (2 families)	12 (2 families)	24 (4 families)	50 (8 families)
Low	12 (2 families)	11 (2 families)	24 (4 families)	44 (9 families)

2.4 Library preparation and sequencing

One library preparation per sample was done as described in Ahmed et al. (2023). It was prepared using the Integrated DNA Technologies (IDT) xGen kit with the NEB polyA selection module. The steps include RNA fragmentation, random priming, and reverse transcription to

generate first-strand cDNA, tailing and adapter ligation to the 3'-end of the cDNA molecule, and PCR. Sequencing was performed at the Oklahoma Medical Research Foundation NGS Core, USA, using an Illumina NovaSeq -S4 Instrument and paired-end 150-cycle sequencing.

2.5 Differential Gene Expression Analyses

The differential gene expression analysis procedure is described in Ahmed et al. (2023) and is summarized here. The process involves downloading the rainbow trout genome annotation from NCBI, trimming low-quality reads, performing adapter trimming, mapping reads, and conducting differential expression analysis using the CLC Genomics Workbench (version 23). Raw counts were used to identify differentially expressed genes (DEGs) using DESeq2 (version 1.46.0) in R. A gene was considered a DEG when the P-adjusted value was less than 0.05, logfold change ± 1. The parameters for each procedure step in the CLC genomics workbench can be accessed in Supplementary File 1.

2.6 Tissue DNA extraction, genotyping, and quality control (QC)

2.11.1 DNA Extraction

DNA extraction was carried from tissue samples using a modified salting-out protocol (Salem et al., 2012). DNA quality was assessed using gel electrophoresis, while DNA quantity was measured using Qubit fluorometry (Catalog# Q32853).

2.6.2 Library Preparation and Sequencing

Libraries were generated using a modified protocol with the Illumina Nextera DNA Flex Library Preparation kit. Sequencing libraries were paired-end with an average insert size of approximately 350 bp. Library quality was assessed using TapeStation (Agilent), and final libraries were quantified by fluorometry prior to pooling. Adapter sequences utilized for libraries were standard Illumina adapters. The sequencing was performed on an Illumina NovaSeq 6000 (Paired End Reads 2x150).

Each library, prepared from a single fish, was subjected to low-pass whole-genome sequencing for genotyping. The samples were sequenced to an average coverage of 1x, and the imputation of genotypes was performed using Loimpute v0.18 by Gencove, Inc. (New York, NY), based on the imputation model developed by Rubinacci et al. (2023). Several studies have shown that low-pass sequencing could be a cost-efficient alternative to genotyping arrays and produce comparable quality(Wasik et al., 2021).

2.6.3 Quality control

Quality control (QC) was done using VCFtools (Danecek et al., 2011), with the following parameters: a threshold for minor allele frequency of 5% (–maf 0.05), a Hardy-Weinberg equilibrium threshold of 1e-06 (- hwe 1e-06), a maximum allele count of 2 (- max-allele 2), and a

maximum missingness rate of 0.5 (- max-missing 0.5). A total of 14,115,938 SNPs were retained for the eQTL analysis.

2.7 Expression Quantitative Loci (eQTL) Mapping

We identified eQTL in rainbow trout using 120 samples from muscle (90), liver (20), and pyloric cecum (10) obtained from fish divergent for muscle yield and quality traits. A preliminary filtering procedure was carried out prior to analysis. The genes selected for eQTL have a minimum TPM (transcripts per kilobase per million mapped reads) threshold value of 0.01, and expression in at least 90% of the samples. Quantile normalization was performed on each gene.

The association between the SNPs and gene expression was performed using the MatrixeQTL package with the General Linear Model option (Shabalin, 2012), correcting for covariates including RNA sequencing batch, tissue type, fish family, and whether the fish belonged to the "high" or "low" family. Following the analysis, cis-eQTL was defined as gene expression associated with SNPs within a range of ±1 Mb from the transcription start site (TSS) of the genes. All remaining SNP-gene pairs were defined as trans-eQTL(Grieve et al., 2008; Võsa et al., 2021). Multiple testing was corrected with a false discovery rate (FDR) with a significance threshold at $q = 0.05$.

2.8 Genotype Quality Control and Genome-wide Association Analysis

Quality control of the pre-processed genotype data was performed using PLINK 2.0 (Chang et al., 2015) with the following filters applied: removing SNPs with a minor allele frequency (MAF) of less than 0.05, those with a call rate of less than 90%, and those that failed the Hardy-Weinberg equilibrium (HWE) test at a p-value of 0.001. Following quality control, 441 animals and 5,027,164 SNPs were available for the genome-wide association study (GWAS) analysis. The relatedness within the rainbow trout samples used was assessed with PCA, and the first five principal components were used as covariates in the GWAS analysis.

The genome-wide association analysis was conducted using a single-trait fixed-effect linear model implemented in PLINK. The p-values were adjusted for multiple testing, and significant GWAS variants are considered those with FDR_BH (False Discovery Rate-adjusted p-value using the Benjamini-Hochberg method) less than 0.05.

For the subsequent analysis, we focused on cis-eQTL variants located within 10 kb of a gene's transcription start site (TSS), as this region is enriched for core regulatory elements likely to affect gene expression. From this set, we identified variants that were also significant in the GWAS, as well as genes that were differentially expressed.

2.9 Haplotype-based Association Analysis

We performed haplotype-based association analysis with gene expression for the three body weight candidate eQTL variants associated with *V-type proton ATPase* (LOC110485500). To investigate

the association between haplotypes formed by single-nucleotide polymorphisms (SNPs) and *V-type proton ATPase* gene expression, we performed haplotype-based association analyses using two complementary methods: haplotype-specific score tests (`haplo.score`) and linear regression with haplotype probabilities (`haplo.design`). Both methods utilized the `haplo.stats` package (version 1.8.7) in R (version 4.2.0) (Sinnwell et al., 2007). The analyses focused on three SNPs (2_27318690_A_G, 2_27311612_A_G, and 2_27321356_C_G).

2.9.1 Haplotype Data Preparation

Genotype data for the three SNPs were extracted from a larger SNP matrix (genotype file used for eQTL analysis) and coded as 0 (homozygous reference), 1 (heterozygous), or 2 (homozygous alternate). Genotypes were recoded into allele pairs (e.g., `A/A`, `A/G`, `G/G` for `2_27318690_A_G` and `2_27311612_A_G`; `C/C`, `C/G`, `G/G` for `2_27321356_C_G`) and converted into a six-column allele matrix (two alleles per SNP) using a custom script. This matrix was processed with `haplo.stats::setupGeno` to generate a haplotype data matrix, where alleles were numerically encoded (e.g., `A` = 1, `G` = 2; `C` = 1, `G` = 2). Haplotype frequencies were estimated using the expectation-maximization algorithm implemented in `haplo.stats::haplo.em`, with locus labels specified as `2_27311612_A_G, 2_27318690_A_G` and `2_27321356_C_G`.

2.9.2 Haplotype Score Test (`haplo.score`)

The `haplo.score` method was used to test the association between estimated haplotypes and *V-type proton ATPase* expression without covariate adjustment. This approach, based on Schaid et al. (2002), employs a score test to evaluate whether haplotype frequencies differ between individuals with varying expression levels, assuming an additive haplotype effect. The method models *V-type proton ATPase* expression as a continuous trait (Gaussian distribution) and calculates haplotype-specific scores, which reflect the direction and strength of association (positive for increased expression, negative for decreased expression).

2.9.3 Linear Regression with Haplotype Probabilities

To account for potential confounders and quantify haplotype effects, we conducted linear regression using haplotype probabilities derived from `haplo.stats::haplo.design`. This method, also based on Schaid et al. (2002), constructs a design matrix of posterior probabilities for each haplotype, representing the expected number of haplotype copies (ranging from 0 to 2) per individual under an additive model. Haplotypes with frequencies ≥ 0.1 and at least 20 copies (`min.count = 20`) were included to ensure sufficient statistical power, resulting in two dominant haplotypes (`A-A-C` and `G-G-G`) for analysis. The regression model included *V-type proton ATPase* expression as the dependent variable, haplotype probabilities as primary predictors, and covariates (tissue type, DNA sequencing batch, RNA sequencing batch) to adjust for technical and biological variability. The model was fitted using the `lm` function in R, with coefficients, standard errors, t-values, and p-values reported to assess the significance and magnitude of haplotype

effects. The adjusted R-squared was calculated to evaluate the proportion of expression variance explained by the model.

2.10 KEGG pathways and GO analysis

Functional enrichment analysis was performed to identify KEGG (Kyoto Encyclopedia of Genes and Genomes) pathways and GO (Gene Ontology) terms. The analysis was performed using ShinyGO 0.77 (Ge et al., 2020) with the default setting. For significant GO terms and KEGG pathways, a cut-off of FDR-adjusted P-values of less than 0.05 was used.

2.11 Transcription Factor Binding Sites Prediction and eQTL Variants Impact Analysis

We used the "TFBSTools" version 1.44.0 (Tan & Lenhard, 2016) and "JASPAR2018" version 1.44.0 (Rauluseviciute et al., 2024) R packages for the Transcription Factor Binding Sites (TFBS) prediction. A 20-bp nucleotide sequence around the cis-eQTL SNP variant, 10 kb upstream of the TSS, was used, and the tools predicted whether the presence of the reference or alternative allele of a SNP variant resulted in the gain or loss of the transcription factor binding site. We used the human transcription factor binding motifs provided by JASPAR for the prediction since transcription factors are relatively conserved among organisms (Chen & Rajewsky, 2007; Villar et al., 2014). A minimum score threshold of 80-90% was used to select only strong binding sites.

We then compared predicted transcription factors between reference sequences (located around the cis-eQTL variant) and alternative sequences (containing the alternative SNP allele) to identify potential gains or losses of TFBS caused by the presence of the reference or alternative allele.

3.0 RESULTS

3.1 eQTL Analysis

The eQTL analysis investigated associations between SNPs and gene expression levels for 542,578,507 cis- and 608,927,160,581 trans-SNP-gene pairs. The QQplot in Fig. 1A showed that the distribution of the observed p-values of cis-eQTL displayed an earlier departure from the diagonal than that of trans-eQTL, indicating that cis-eQTL were easier to detect than trans-eQTL. In total, we identified 234,630 significant cis-SNP-gene associations (FDR < 0.05) (Supplementary file 2) and 5,300,774 trans-SNP-gene associations (FDR < 0.05) (Supplementary file 2b). There were 2,308 and 28,645 unique cis and trans eQTL genes, respectively. The cis-eQTLs were clustered around the TSS (Figure 1B).

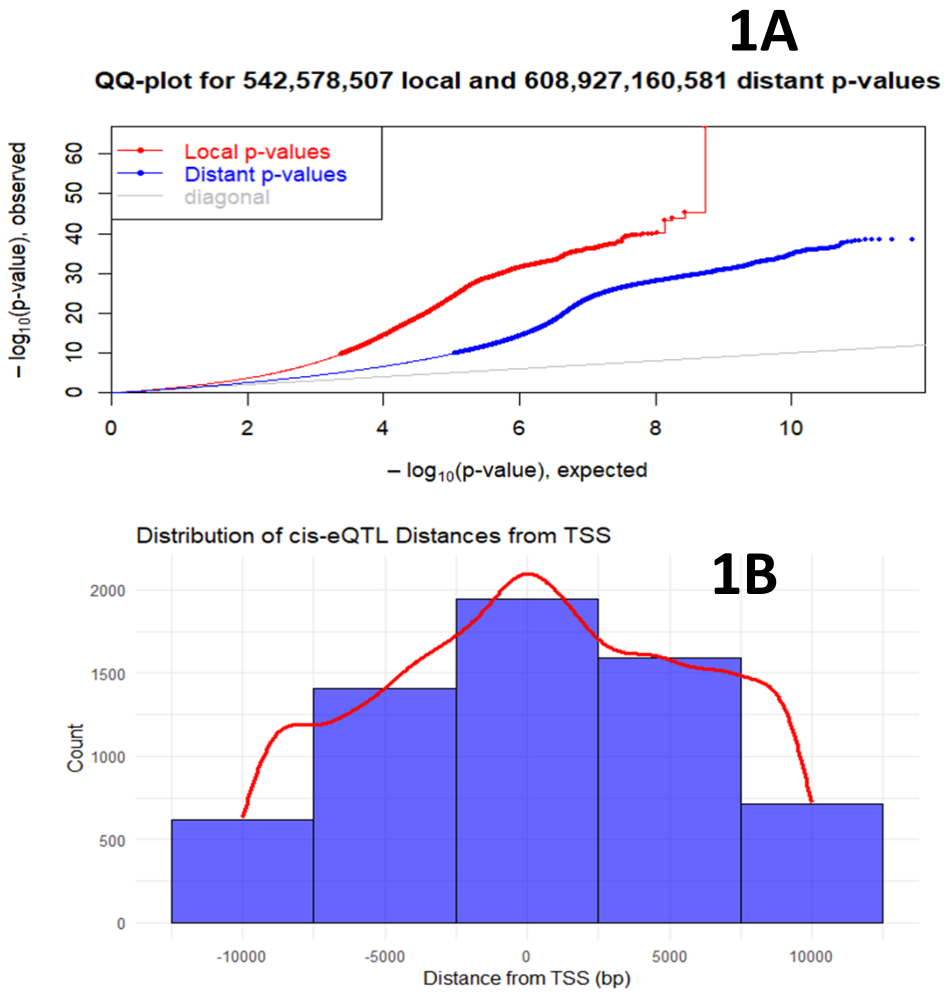

Figure 1A. QQ-plot of -Log10(*p* value) of eQTL analysis using MatrixEQTL, 1B. Distribution of cis-eQTLs 10kb around the transcription start site (TSS).

After filtering, we identified 6,275 cis-eQTL variants located within 10 kb of the TSS, encompassing the promoter regions of their associated genes. These are the variants used for downstream candidate prioritization. Candidate genes were selected from this refined eQTL set. To further prioritize regulatory variants and target genes, we integrated genome-wide association study (GWAS) results and differential gene expression analysis related to growth and muscle yield traits in rainbow trout.

3.2 Differential Gene Expression Analysis

3.2.1 Phenotypic difference between the High and Low families

The average phenotype in the high and low families for each trait is shown in Figure 2. The difference between the high and low groups is statistically significant ($p<0.01$).

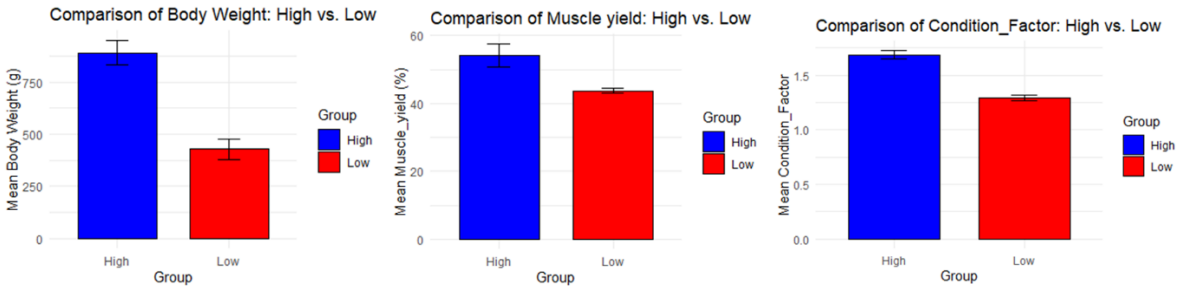

Figure 2. The average phenotype values for fish belonging to the High and Low fish for each trait. This consists of 24 VS 24, 12 VS 12, and 12 VS 11 samples for Condition Factor, Body weight, and Muscle yield, respectively. For the genetic line, we used 50 ARS-FY-H and 44 ARS-FY-L samples.

3.2.2 RNA-sequencing data

A total of 1,487,578,810 raw paired-end reads (150bp) were sequenced for muscle yield (23 samples), 1,465,724,860 for body weight (24 samples), and 2,958,449,886 for condition factor (48 samples), respectively. The reads were mapped against the rainbow trout genome (https://www.ncbi.nlm.nih.gov/assembly/GCF_002163495.1/), resulting in an average mapping

percentage of 90%, 89%, and 91% for muscle yield, body weight, and the condition factor, respectively.

3.2.3 Differentially expressed genes (DEGs)

3.2.3.1 Muscle yield

There are 513 significant (FDR < 0.05, logfold change ± 1) differentially expressed genes (DEGs) between the high and the low muscle yield families. Two hundred and twenty-five (225) genes are upregulated in the high muscle yield families, while 288 genes are downregulated. The complete list of DEGs is available in Supplementary File 1.

The most upregulated genes are involved in neuronal and cytoskeletal activities, including *CADPS2* (*calcium-dependent secretion activator*) (5.55-fold change), *neurexin-1a* (4.50-fold change), *protein bicaudal D homolog 1* (4.83-fold change), and *SAMD12* (*sterile alpha motif domain-containing 12*) (3.42-fold change). The enriched pathways for muscle yield differentially expressed genes include the pentose phosphate pathway, amino acid biosynthesis, glycolysis/gluconeogenesis, tight junction regulation, regulation of the actin cytoskeleton, and oxidative phosphorylation (Supplementary file 1, Figure 3).

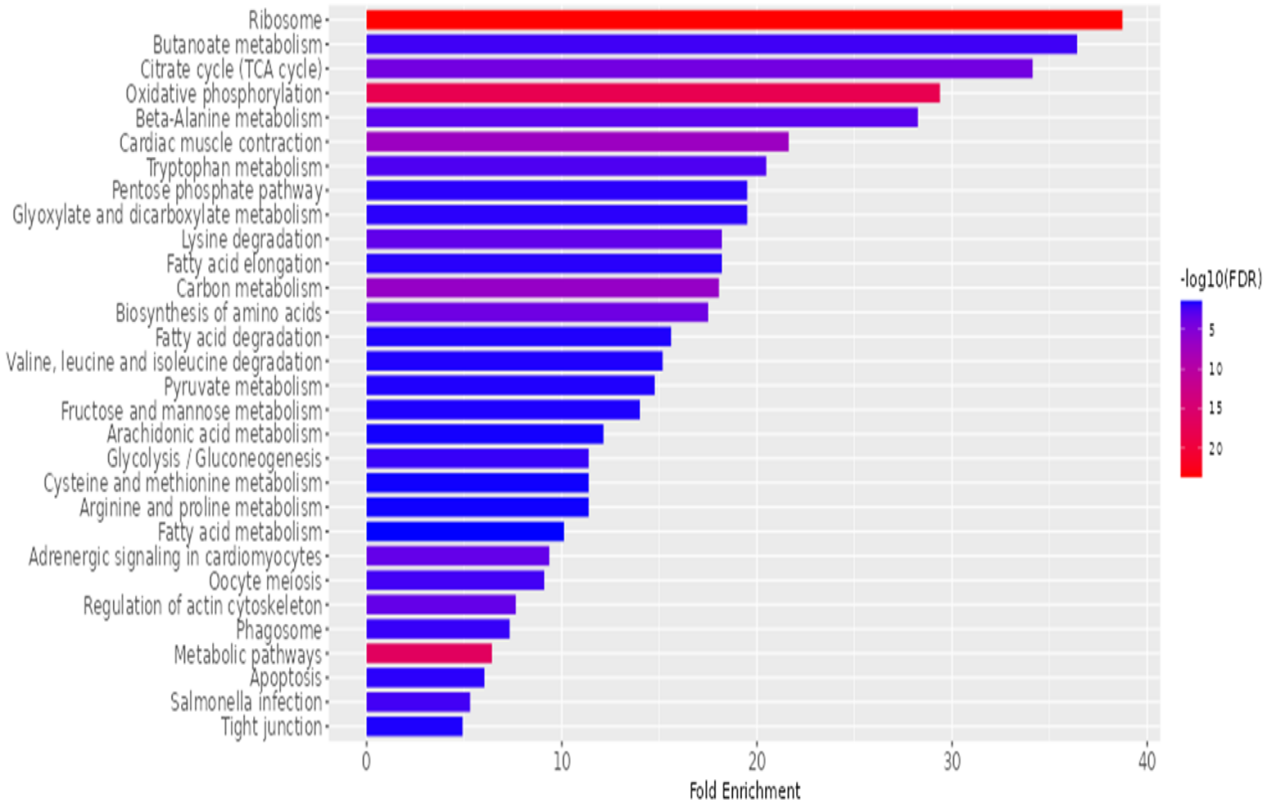

Figure 3. Enriched KEGG pathways for the muscle yield differentially expressed genes

3.2.3.2 Body weight

There are 383 significant (FDR < 0.05) differentially expressed genes (DEGs) between the high- and low-body weight families. Two hundred and fifty-one (257) genes are upregulated, while 126 are downregulated. The complete list of DEGs and their fold change can be found in Supplementary file 1.

The most upregulated genes are myosin-7 (5.05-fold change), troponin (3.17-fold change), and *ATP2A1* (*ATPase sarcoplasmic/endoplasmic reticulum Ca2+-transporting 1*, 2.87-fold change). The most downregulated genes in the high body weight family are *complement C3* (5.6-fold decrease), *apolipoprotein B-100* (4.5-fold decrease), *fibrinogen beta chain* (3.8-fold decrease), *apolipoprotein A-I* (3.3-fold reduction), and *apolipoprotein A-II* (3.2-fold reduction).. A consistent pattern of reduced expression of apolipoproteins involved in lipid transport suggests diminished systemic lipid mobilization in the high body weight group, potentially favoring local lipid utilization within muscle tissue.

The body weight DEGs are enriched in pathways related to the TCA cycle, oxidative phosphorylation, pyruvate metabolism, propanoate, tryptophan, and butanoate metabolism, the PPAR signaling pathway, and carbon metabolism (Supplementary file 1, Figure 4).

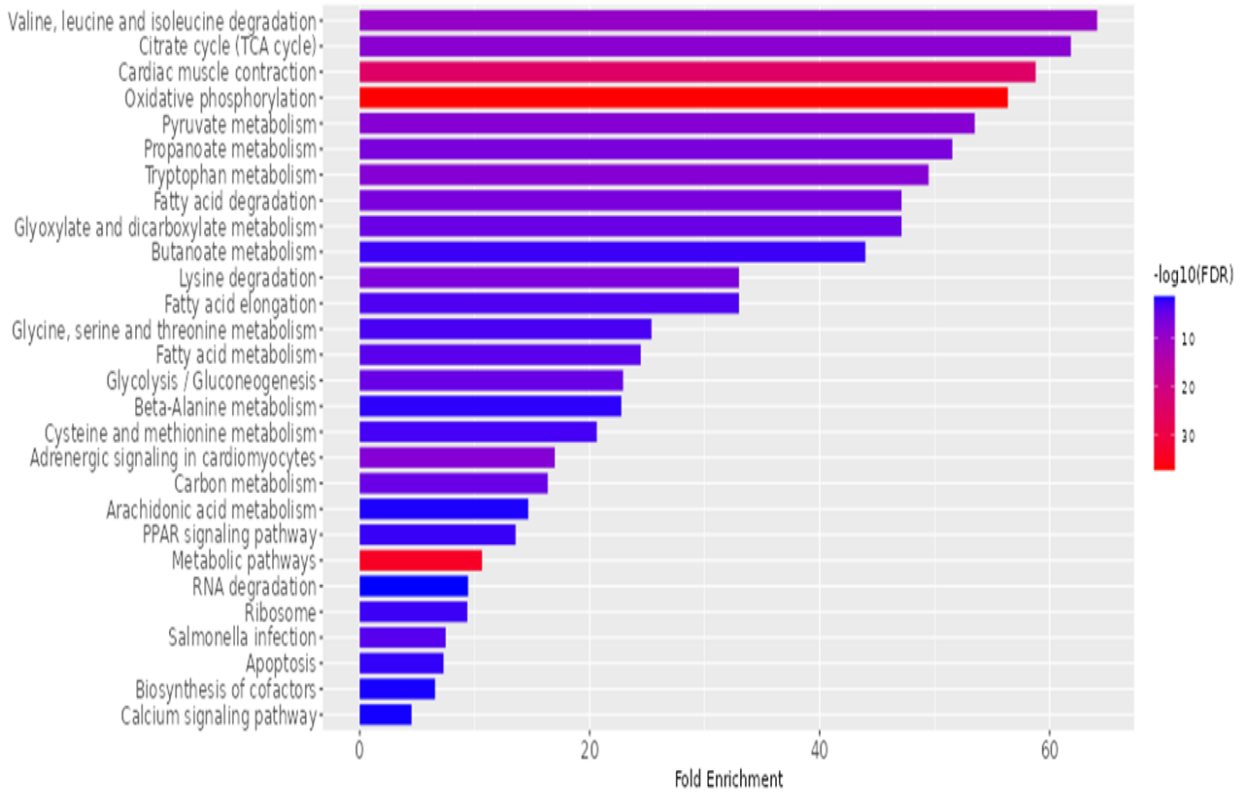

Figure 4. Enriched KEGG pathways for the body weight differentially expressed genes

3.2.3.3 Condition Factor

Four thousand fifty-one (4051) genes are differentially expressed (FDR < 0.05) between the high- and low-condition factor families. The high condition factor family has a higher expression of genes associated with growth, tissue maintenance and cellular integrity, including *Follistatin (FST)* (2.91 FC) involved in muscle development, *Secreted acidic cysteine rich glycoprotein (SPARC)* (2.54 FC) involved in extracellular matrix, and *Phosphatidylinositol glycan anchor biosynthesis class P (PIGP)* (2.94 FC) involved in membrane anchoring. Genes downregulated in the high condition factor family are linked to inflammation, stress responses, and altered metabolism. Examples of inflammatory mediator genes are the *LECT2 neutrophil chemotactic factor* (-3.42 log2 FC), lipid transport (*Apolipoprotein A-I-1* (-3.28 log2FC), *Apolipoprotein A-I-2* (-3.28 log2 FC), and ribosomal proteins (*60S ribosomal protein L29 RL29* (-2.06 log2 FC)).

The most upregulated genes in the high condition factor family include *Probable 6-protein-coupled receptor 139* (10.74-fold change), *KH domain-containing RNA binding protein* (10.74-fold change), *OORP* (7.80-fold change), and *reticulon-4 receptor-like* (7.52-fold change). The most downregulated genes are *Envoplakin* (-13.58 FC), *Complement component 8 gamma* (-11.65 FC), *LECT2 neutrophil chemotactic factor* (-10.70 FC), *Apolipoprotein A-I-2* (-9.73 FC), and *Apolipoprotein A-I-1* (-9.72 FC).

KEGG pathway analysis (Figure 5, Supplementary file 1) reveals the enrichment of ribosome, spliceosome, citric acid cycle, oxidative phosphorylation, tight junction, regulation of the actin cytoskeleton, ubiquitin-mediated proteolysis, MAPK signaling, and metabolic pathways.

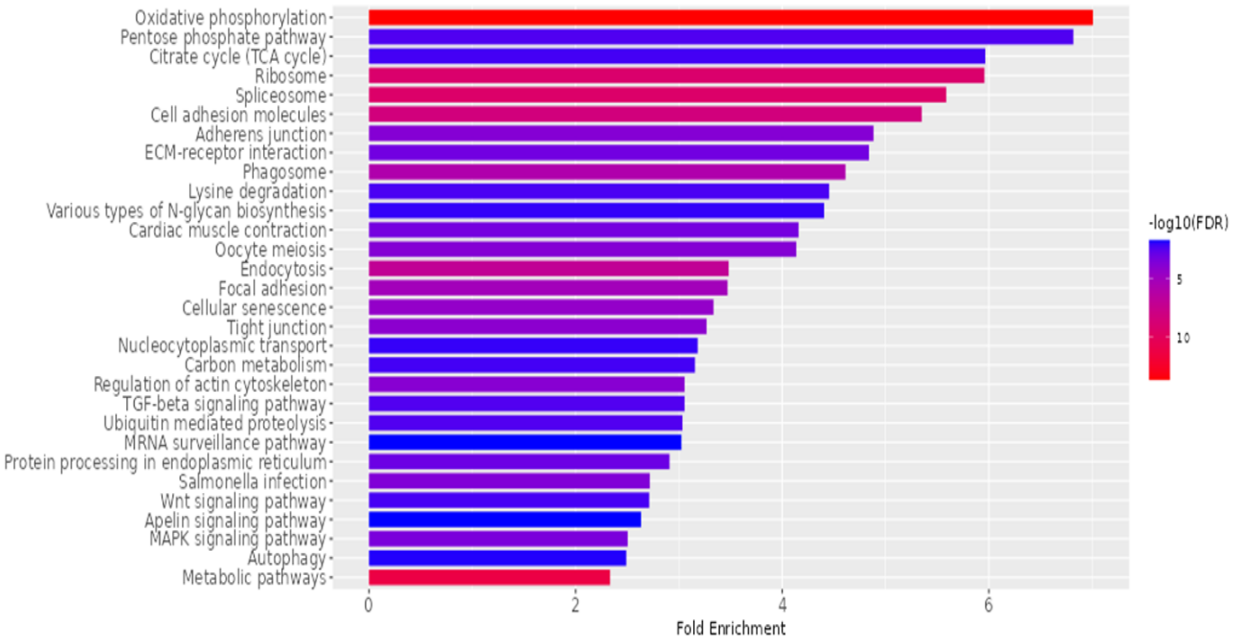

Figure 5. Enriched terms for the condition factor differentially expressed genes

3.2.3.4 Genetic Line (ARS-FY-H vs ARS-FY-L)

There are 1,163 differentially expressed genes between the genetic lines (ARS-FY-H vs ARS-FY-L). The ARS-FY-H line has higher expression of genes involved in cytoskeletal functions and lipid and protein metabolism. The most upregulated genes in the ARS-FY-H include *EZRIN A* (*EZRA* 778,184 FC), *Carboxypeptidase A1* (*CBPA1* 123,512 FC), *Phospholipase B1 membrane-associated-like* (76175 FC), *3-hydroxy-3-methylglutaryl-CoA reductase* (*HMGCRA* 15609 FC), and *Ladder lectin-like* (12972 FC). The most downregulated genes include *Thyroid hormone responsive* (-1155 FC), *Alpha-2-HS-glycoprotein 1* (-1016 FC), *Fetuin B* (*FETUB*, -302 FC), *Complement factor H* (-82 FC), and *pentraxin* (-49 FC). KEGG pathway (Figure 6, Supplementary file 1) analysis reveals that the differentially expressed genes are involved in steroid biosynthesis, the TCA cycle, carbon metabolism, the Apelin signaling pathway, oxidative phosphorylation, Gap junction, the MAPK signaling pathway, and Adrenergic signaling in cardiomyocytes.

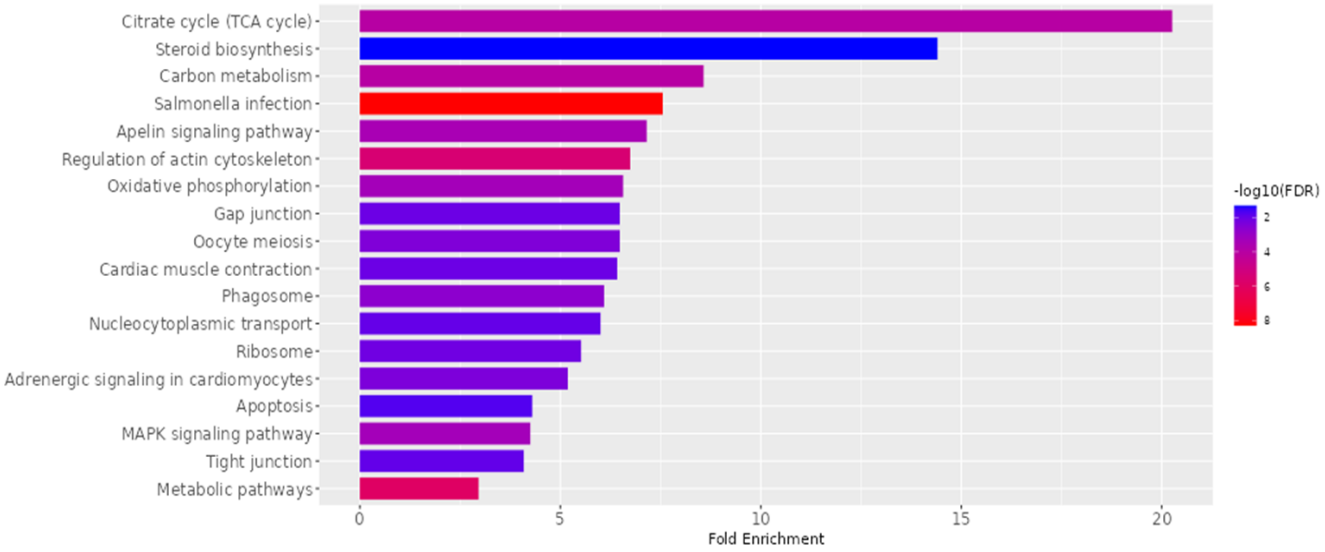

Figure 6. Enriched terms for the differentially expressed genes between genetic lines

3.3 Genome-wide association analysis

The GWAS analysis identified 17,152; 203, and 3,693 significant associations (FDR_BH <0.05) for body weight, muscle yield, and condition factor, respectively (Supplementary file 3). Manhattan plot obtained using the qqman package in R (Turner, 2014), and the qqplot is shown in Figure 7. The plots for other traits are available in Supplementary File 3.

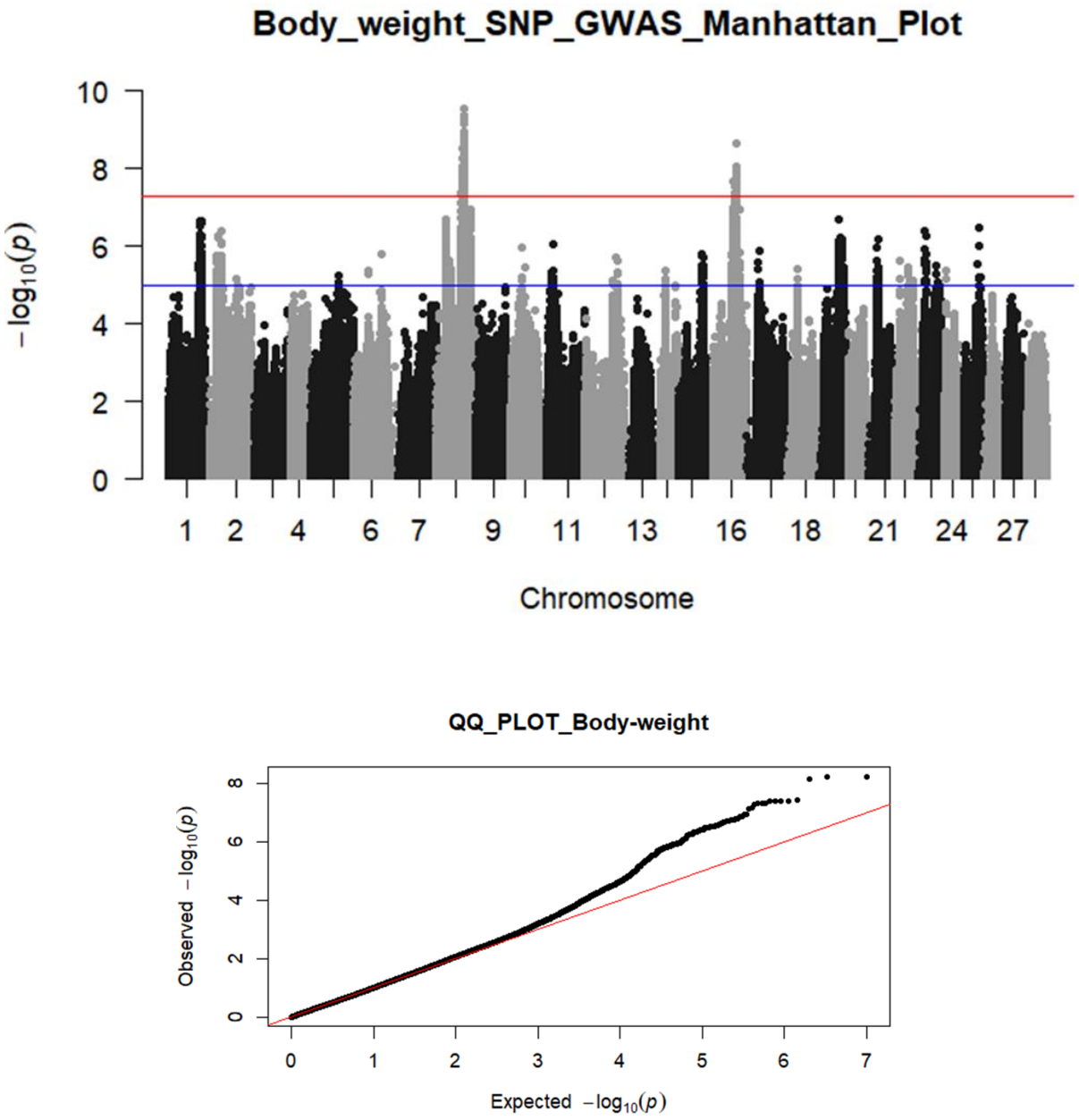

Figure 7. The Manhattan (top) and qqplot (bottom) for body weight GWAS results

Next, we integrated differentially expressed genes and GWAS-significant variants to prioritize candidate genes from the eQTL analysis. Candidate genes discussed here are those that (1) harbor GWAS-significant variants, (2) are identified as significant cis-eQTLs, and (3) have variants located within 10 kb of the TSS of the associated gene. We prioritized candidate genes using the DEGs list instead for muscle yield and condition factor, where no SNPs met all three criteria, i.e.

candidate genes selected are those DEGs that harbor eQTL-SNPs located within 10 kb of the TSS of cis-eQTL genes.

3.4 Prioritized Candidate Genes

3.4.1 Cis-eQTL prioritized for body weight

After prioritization, we identified four cis-eQTLs equivalent to two candidate genes for body weight. These body weight candidate genes are *gamma-amino butyric acid receptor subunit rho-1-like, and V-type proton ATPase.* Figure 8 illustrates how cis-eQTL variants affect the expression of candidate genes. The 2_27311612_A_G eQTL variant is within the *antizyme inhibitor 1 gene body* and the promoter of the nearby gene (*V-type proton ATPase).*

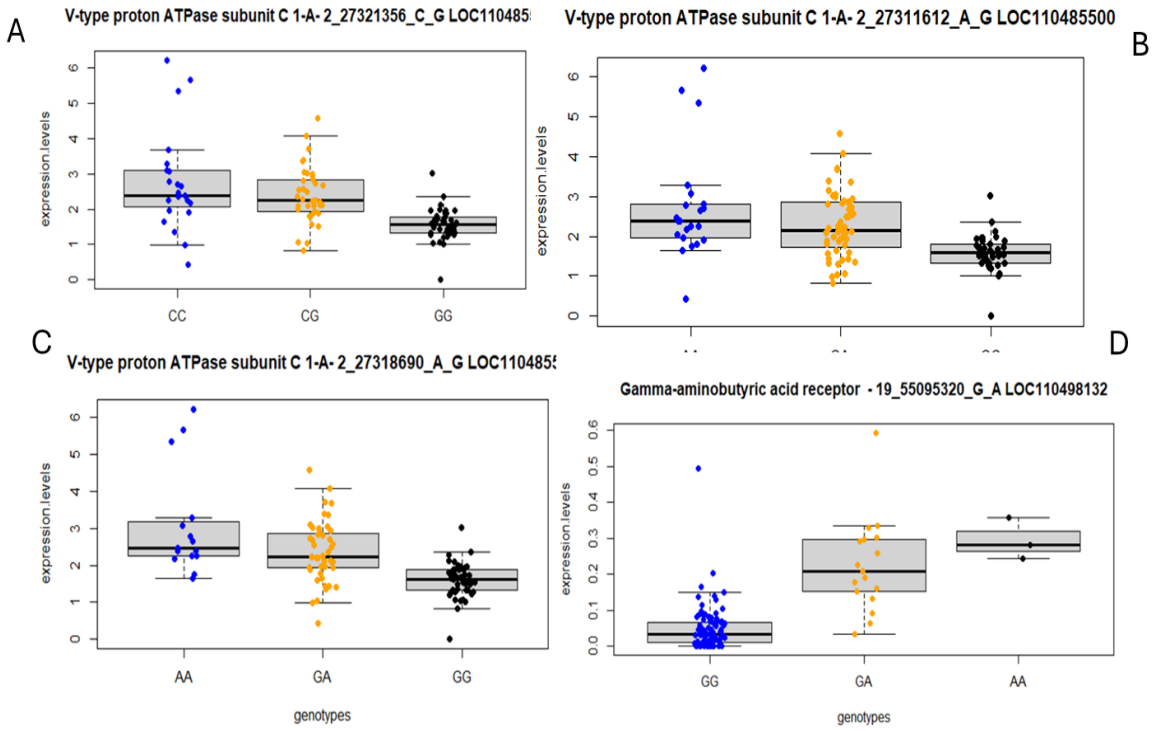

Figure 8. Body weight candidate eQTL genes. Three of the eQTL variants affect LOC11048500 (V-type proton ATPase subunit C1, A-C), while one variant affects LOC110498132 (gamma-aminobutyric acid receptor subunit rho-1-like, D). The eQTL genotypes are on the X-axis, and the expression of the eQTL genes is on the Y-axis.

3.4.2 Haplotype-based Association Analysis

The three SNPs associated with *V-type proton ATPase 2* expression were used for haplotype-based analysis using two complementary methods: haplo.score and regression analysis. The haplo.score method cannot adjust for covariates, unlike the regression analysis. This identified six possible haplotypes whose frequencies are shown in Figure 9A. The dominant haplotypes are G-G-G (56.5%) and A-A-C (31%). The likelihood ratio test with a p-value of 0 shows strong evidence of linkage disequilibrium between 2_27318690_A_G, 2_27311612_A_G, and 2_27321356_C_G, indicating that the alleles at these loci are not inherited independently.

The haplo.score method identifies two haplotypes (A-A-C, G-G-G) significantly associated with *V-type proton ATPase 2* expression. The A-A-C has a positive hap-score (5.99), indicating that fish with this haplotype tend to have a higher expression level than the baseline. The G-G-G haplotype has a negative hap-score (-4.30) and is associated with a decreased *V-type proton ATPase 2* expression. The linear regression analysis, which adjusts for covariates, identifies only the A-A-C (effect size = 0.836) haplotype as significantly and positively associated with the *V-type proton ATPase 2* expression. The adjusted R-square shows that the regression model explains ~ 36 % of *V-type proton ATPase 2* expression variance. Figure 9B is a boxplot of the *V-type proton ATPase 2* expression levels for fish samples grouped by the two dominant haplotypes, which shows that the G-G-G haplotype is associated with decreased expression.

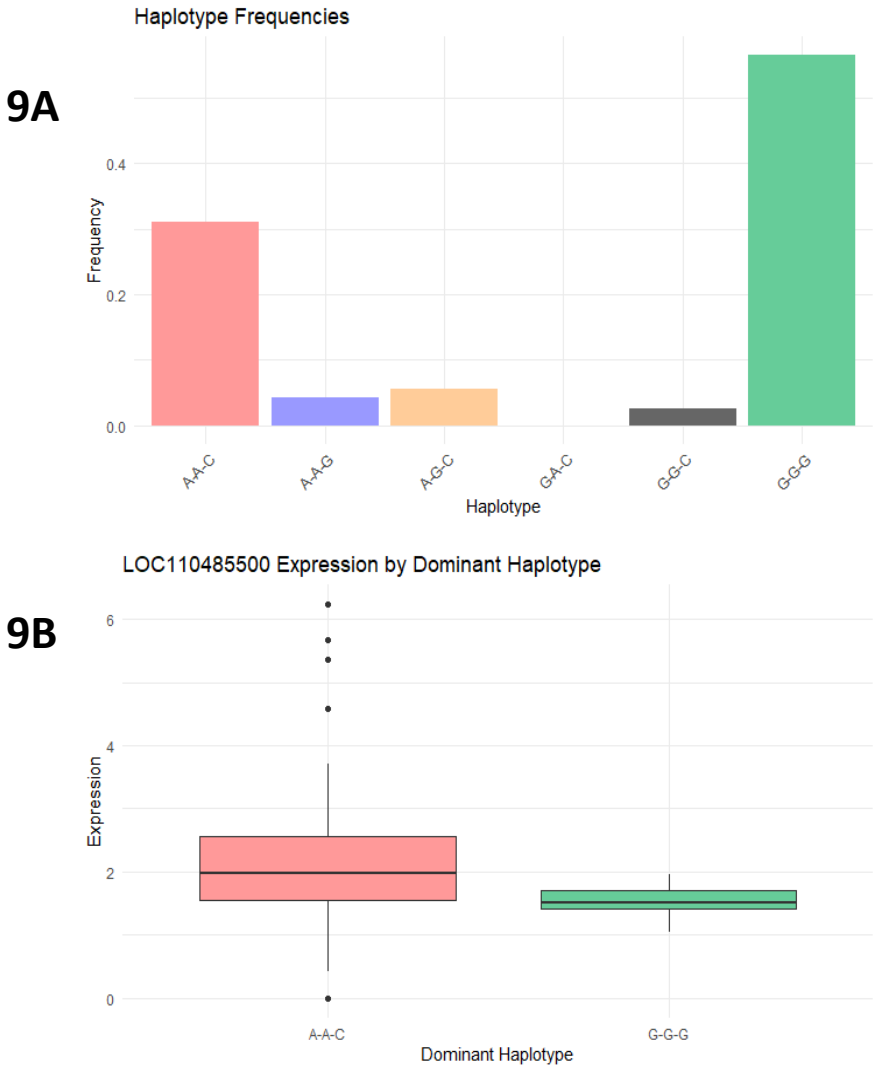

Figure 9A. Haplotype frequencies for the six possible haplotypes of the 2_27318690_A_G, 2_27311612_A_G, and 2_27321356_C_G loci. 9B. Box plot showing *V-type proton ATPase 2* expression levels by the dominant and significant haplotypes (A-A-C and G-G-G). A-A-C haplotype is associated with higher expression, while G-G-G is associated with lower expression

We used the newly developed epigenome annotation maps/ UCSC browser (Salem M, 2024; Salem et al., 2024) to investigate the chromatin state of the regions around the candidate SNPs (Figure 10) in six tissues (muscle, liver, kidney, intestine, spleen, and brain).

Figure 10 shows that the eQTL SNP (*V-type proton ATPase 2,* POS: 27321356*)* is flanked by strong enhancers (red color) in the liver. In other tissues, the SNP is flanked by weak enhancers (dark green) in the white muscle, and intestine, an active TSS state (purple) in the spleen, and quiescent enhancers (light green) in the kidney.

The eQTL SNP (POS: 27311612) is flanked by strong enhancers in the liver (Red color), weak enhancers (dark green) flanked the SNP in the white muscle. The eQTL SNP 27318690_A_G was surrounded by strong enhancers (red) in the intestine and liver (Figure 10). It was surrounded by poised enhancers (blue) in the spleen, weak enhancers (dark green) in the white muscle, brain, and kidney.

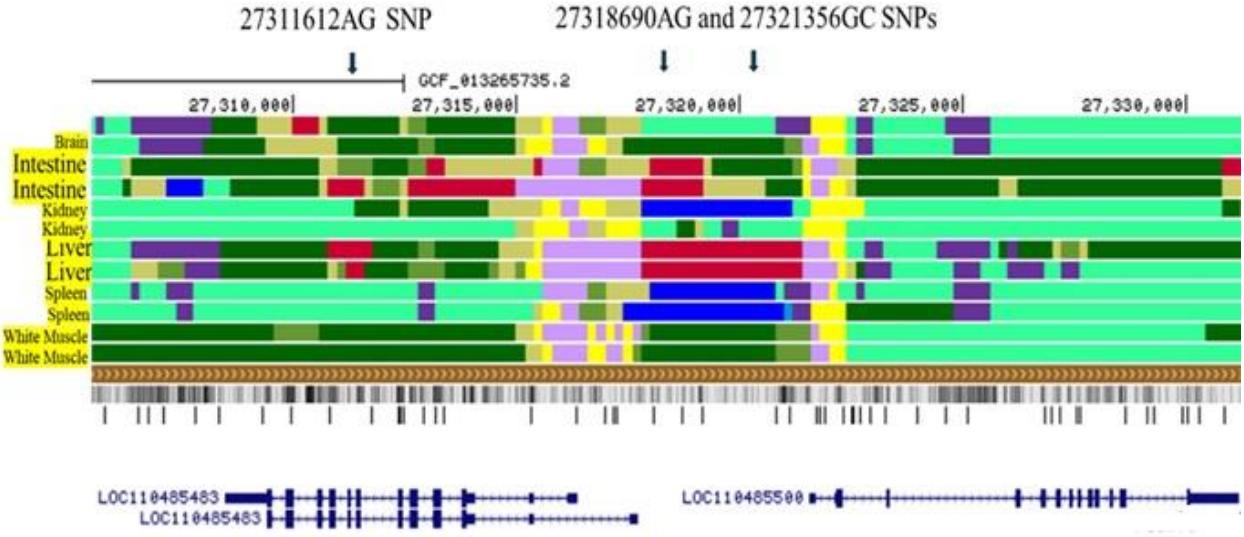

Figure 10. UCSC genome browser tracks showing the landscape of chromatin state around the eQTL SNPs (27311612_AG, 27318690_AG, and 27321356_GC, indicated by arrows) affecting LOC110485500 (*V-type proton ATPase 2*). The 27311612_AG , 27318690_AG, and 27321356_GC are 9938bp, 2860bp, and 194bp to the *V-type proton ATPase 2* TSS, respectively. Red indicates strong enhancers, dark green signifies weak enhancers, and purple indicates active TSS states. The light green signifies quiescent enhancers, while blue indicates poised enhancers.

3.4.3 Transcription Factor Binding Sites Prediction and eQTL Variants Impact Analysis

For body weight candidate genes whose variants are located 10 kb of the TSS, TFBSTools predicted that polymorphisms at the eQTL variant resulted in a loss or gain of the TF binding site for several transcription factors. As shown in Figure 11A, for the 19_55095320_G_A cis-QTL variant in the *gamma-aminobutyric acid receptor subunit rho-1-like*, the polymorphism at the eQTL variant resulted in the loss of sites for two transcription factors (NKX2-3, NKX2-8) and a gain of a BARHL2 transcription factor binding site. Similarly, the 2_27318690_A_G and 2_27321356_C_G eQTL variants in the V-*type proton ATPase subunit C 1-A* resulted in the loss

of one (NKX2-8) (Figure 11B) and thirteen (Figure 11C) transcription factor binding sites, respectively (Figure 11, Supplementary file 3).

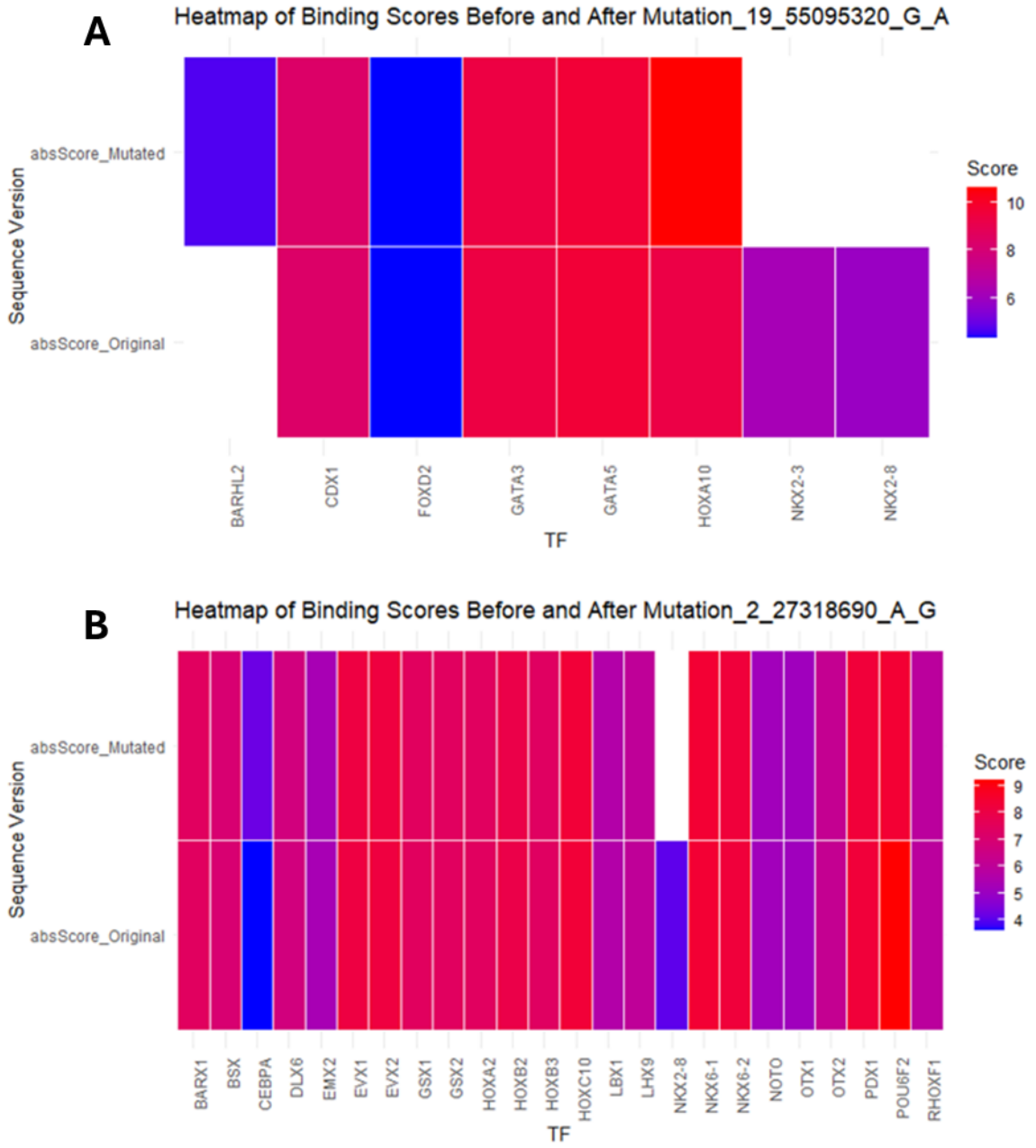

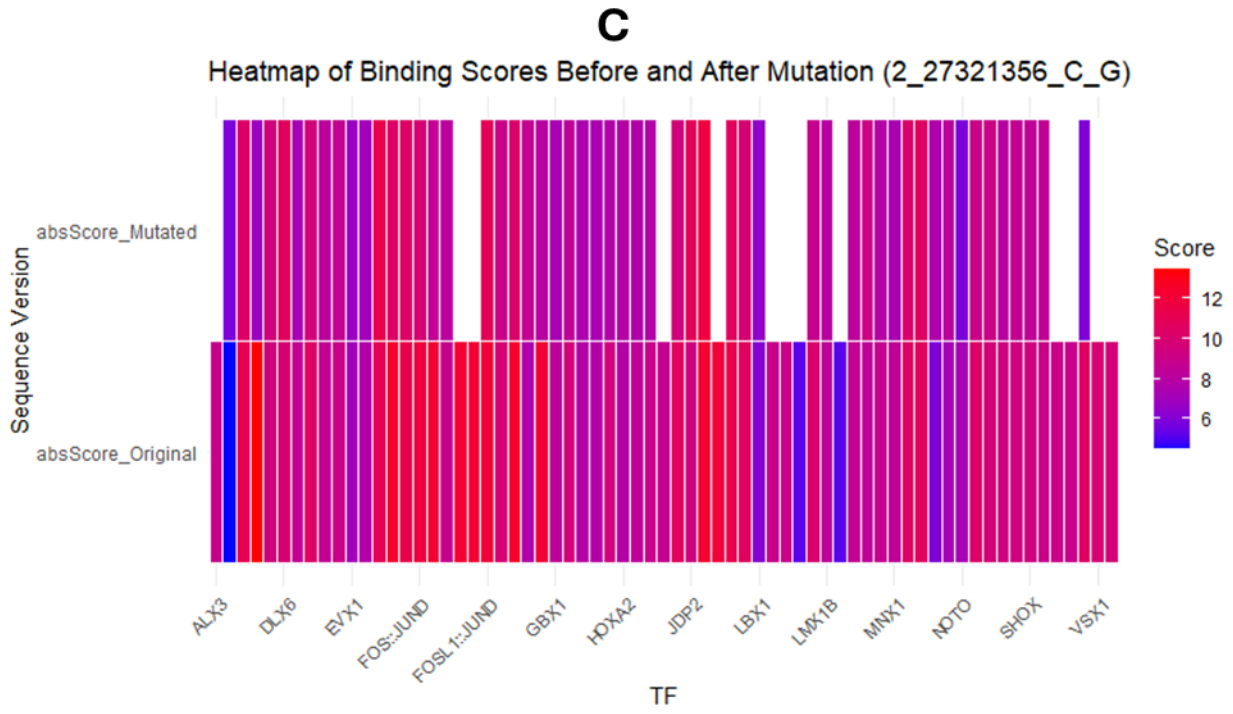

Figure 11. Predicted gain/loss of TFBS for the body weight eQTL variants. The absScore is a numerical value representing the raw score of how well a given DNA sequence matches the binding motif (PWM) of a transcription factor. A higher absScore indicates a better match to the PWM. Two Transcription Factors (TFs) were lost and one was gained as a result of the 19_55095320_G_A eQTL variant (Fig. 11A). One (Fig. 11 B) and thirteen (Fig. 11C) TFs lost and 13 TFs were lost as a result of the 2_27318690_A_G and 2_27321356_C_G eQTL variants, respectively.

3.4.4 Cis-eQTL Prioritized for muscle yield, condition factor and genetic line

The muscle yield and condition factor have no GWAS-significant SNP within the 10kb TSS; thus, their differentially expressed genes were used for prioritization. Using the differentially expressed genes for filtering, four candidate genes were identified for muscle yield (Figure 12) with 83 eQTL variants near the TSS. The genes are *GATD3A, uncharacterized LOC110486628, PPP2R1BB (protein phosphatase 2 regulatory subunit A beta, also known as protein phosphatase 2A regulatory subunit B)*, and *USP6 N-terminal-like protein*.

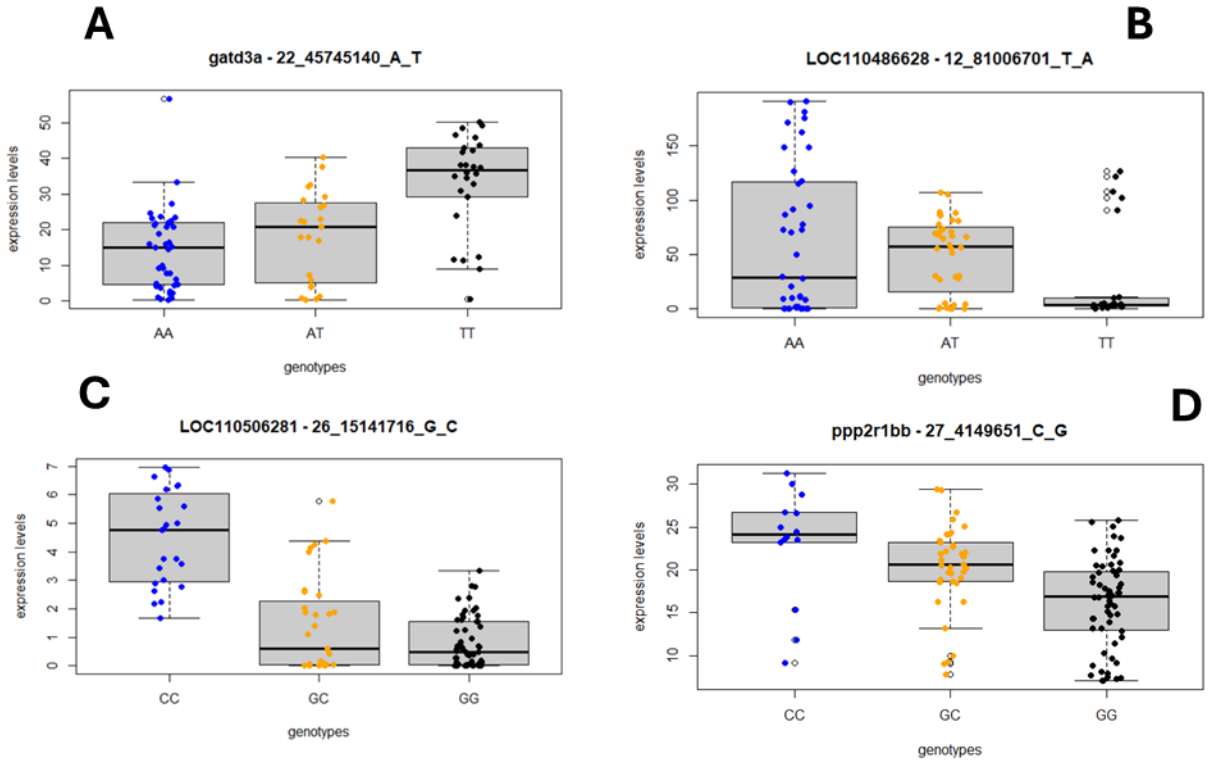

Figure 12. Muscle yield candidate genes (A; *GATD3A, B; uncharacterized LOC110486628, C; PPP2R1BB (protein phosphatase 2 regulatory subunit A beta,* and D; *USP6 N-terminal-like protein)* and their significant SNP eQTL variants. The eQTL genotypes are on the X-axis, and the expression of the eQTL genes is on the Y-axis.

The condition factor has 51 candidate genes with 549 eQTLs around the TSS. These genes can be classified into those that affects growth, muscle development and metabolism including: *Troponin 1 fast skeletal muscle (TNNI2), PDZ and LIM domain protein 3 (PDLIM3), Cyclin-dependent-like kinase 5 (CDK5), Cytochrome P450 3A27-like (CYP3A27), Biephenyl hydrolase-like (BPHL), Arylamine N-acetyl transferase (BPHL), Arylamine N-acetyltransferase (NAT-10)*; those involved in immunity and stress response: *Cathepsin C (CTSC), Intracellular-type I interferon receptor (IFNAR), Immunoglobulin superfamily member 21 (IGSF21), BRCA1-associated protein (BRAP), DnaJ (Hsp40) homolog, subfamily C, member 6 (DNAJC6)*; those involved in neurological and endocrine regulation including: *Apoptosis antagonizing transcription factor (AATF), ELAV-like RNA binding protein 1a (ELAVL1a), Neugrin, neurite outgrowth associated (NGRN), Synaptoporin (SYNPR) & Synaptic vesicle glycoprotein 2Ca (SV2Ca)*; those involved in Cellular and structural maintenance: *Centrosomal protein 290 (CEP290), Epithelial stromal interaction 1 (EPSTI1), USP6 N-terminal-like protein (USP6NL), Nucleolin (NCL)* and those involved in Transcription, RNA Processing, and Gene Regulation which *includes RNA-*

binding protein 34-like (RBM34), Transcription initiation factor TFIID subunit 1 (TAF1), Pseudouridine synthase-like 1 (PUS1).

Figure 13 shows the gene expression plots for two condition factor candidate genes, *Troponin 1 fast skeletal muscle (TNNI2*) and *PDZ and LIM domain protein 3 (PDLIM3)*.

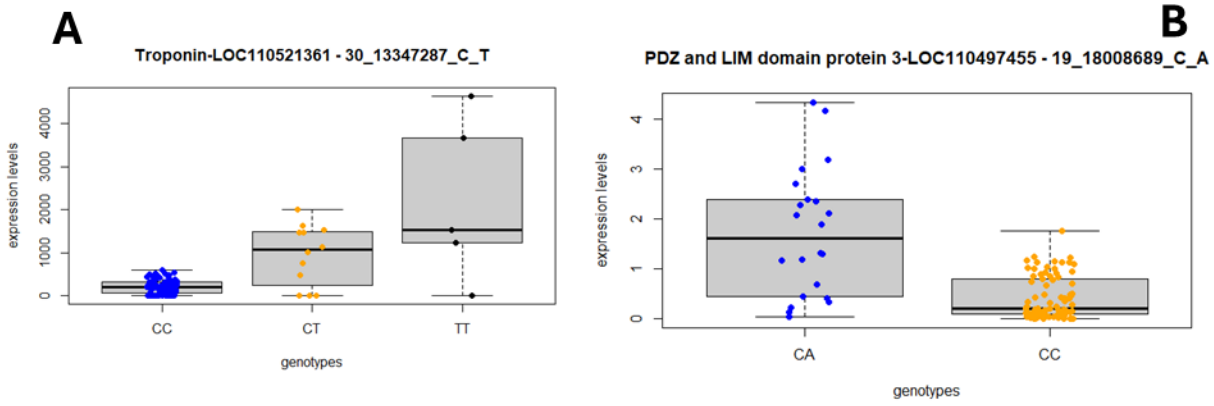

Figure 13. Gene expression plots for Troponin 1 fast skeletal muscle (TNNI2) (A) and *PDZ and LIM domain protein 3 (PDLIM3)* (B). The eQTL genotypes are on the X-axis, and the expression of the eQTL genes is on the Y-axis.

Sixteen candidate genes and 190 eQTL significant variants were identified for the Genetic line (ARS-FY-H vs ARS-FY-L). Candidate genes for the genetic line trait are involved in pathways related to muscle cell proliferation, differentiation, metabolism, protein synthesis, and stress responses. The genes are listed in Supplementary File 2. Figure 14 shows the gene expression plot for eQTL SNPs associated with candidate genes for the genetic line. The *USP6 N-terminal-like protein* and its eQTL SNP are identified as a common candidate gene for muscle yield, condition factor, and the genetic line trait.

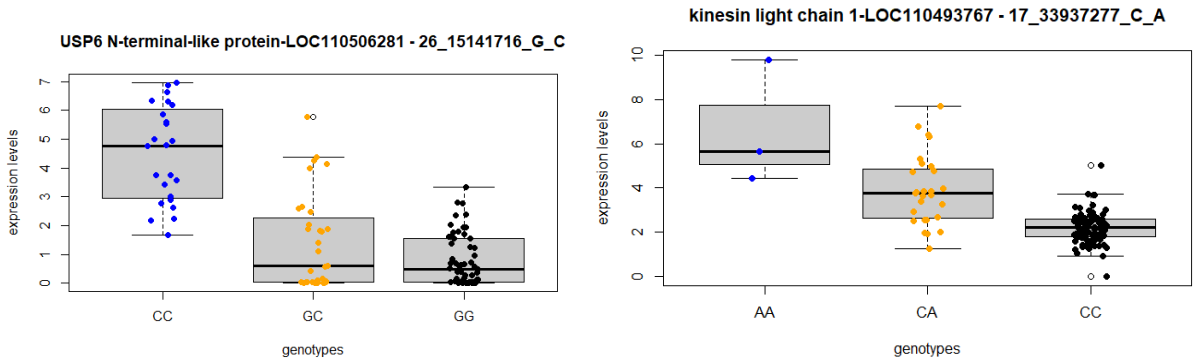

Figure 14. The eQTL plots for two genetic line candidate genes (*USP6 (5A)* and *kinesin light chain (B)*). The eQTL genotypes are on the X-axis, and the expression of the eQTL genes is on the Y-axis.

3.5 Trans-eQTL Summary

A total of 5,300,774 trans eQTLs were identified, with 28,645 unique trans-eQTL genes involved in cardiac muscle contraction, oxidative phosphorylation, cell adhesion molecules, regulation of actin cytoskeleton, glycolysis/gluconeogenesis, MAPK signaling pathway, FoxO signaling pathway, Apelin signaling pathway, and Focal adhesion (Figure 15, Supplementary file 2). The trans-eQTL list contains 1329, 171, and 1071 unique GWAS-significant SNPs for body weight, muscle yield, and condition factor, respectively (Supplementary file 2).

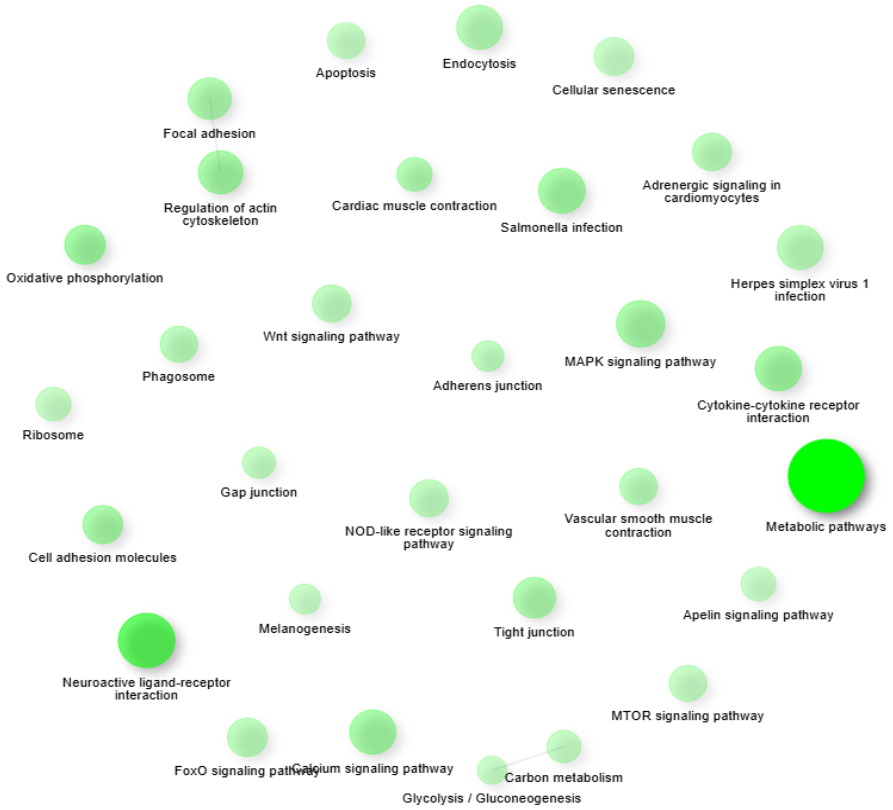

Figure 15. Enriched pathways for the trans-eQTL genes

4.0 DISCUSSION

Growth traits such as body weight, muscle yield, and tissue robustness represent complex biological phenotypes regulated by multiple genetic and transcriptional mechanisms. Understanding the gene regulatory networks that drive these phenotypes is critical for elucidating how somatic tissues grow and remodel across the lifespan.

Body weight reflects the cumulative outcome of diverse growth-regulatory processes, including energy metabolism, cellular proliferation, and hormonal signaling. Genes identified in this study, including those involved in mitochondrial energy production and calcium handling, highlight the coordinated regulation of bioenergetics and muscle contractility during growth.

Skeletal muscle is a metabolically active tissue central to locomotion, metabolism, and somatic growth. In teleosts, post-embryonic muscle growth occurs via both hyperplasia and hypertrophy (Johnston et al., 2011; Rescan, 2019; Rowlerson, 2001), making rainbow trout a valuable model for studying vertebrate muscle development. The fish used in this study have been selected for improved muscle growth and designated as high (ARS-FY-H) and low (ARS-FY-L) genetic lines.

The condition factor is an index that measures the relative robustness of fish and tells us about their overall well-being (Williams & Schneider, 2000). It is calculated as a length-weight factor (10^5*Body weight/Body length^3). It also reflects the degree of nourishment and can vary by sex, age, season, and degree of gonad development of the fish (Froese, 2006). The condition factor has been reported to be correlated with the relative muscle thickness and fat content in Plaice and California sardine Sardinops sagax fishes, respectively (Clark, 1928; Heincke, 1908).

We have previously used genome-wide association studies to identify candidate genes for growth traits in rainbow trout (Ali Ali et al., 2020; Salem et al., 2018). One method for identifying candidate genes with direct functional impact on the phenotype is through eQTL analysis. Expression quantitative trait loci (eQTL) studies associate genotypic variation with gene expression. A comprehensive eQTL study in rainbow trout is lacking. Here, we performed eQTL analysis using 120 samples and 14,115,938 SNP variants, which could serve as a mini catalogue of rainbow trout eQTLs. Thereafter, we used GWAS and differential gene expression analysis to prioritize the eQTL variants and identified candidate genes with causal variants contributing to growth traits in rainbow trout.

4.1 eQTL Genes, Gene-expression, and their relationship with growth traits

We conducted eQTL analysis to understand the global genotypic regulation of gene expression and its influence on growth traits in rainbow trout. The expression quantitative traits analysis (eQTL) revealed 234,630 cis and 5,300,774 trans-SNP-gene associations for rainbow trout. We focused more on the cis-acting QTLs since they tend to have a larger effect size and have a more localized effect on gene expression, making them easier to pinpoint and link to specific phenotypic changes (Wang et al., 2024; Westra & Franke, 2014).

As shown in Figure 2, most of the cis-eQTL clustered around their respective genes' TSS in line with observations from other eQTL studies from cattle (Cai et al., 2023) and human (Consortium et al., 2015). We further filtered the cis-eQTLs to focus on only those variants within 10kb of the TSS. These are known to be enriched for promoter and enhancer regulatory elements (Consortium, 2020) with a higher probability of affecting the expression of their eQTL genes.

Our analysis revealed 3, 4, 51, and 16 candidate genes for body weight, muscle yield, condition factor, and genetic line, respectively. These candidate genes, whose expression levels are regulated by cis-eQTL variants are potential functional genes for further investigation. The *USP6 N-terminal-like protein* is identified as a common candidate gene for muscle yield, genetic line, and condition factor.

Candidate genes for body weight are *gamma-amino butyric acid receptor subunit rho-1-like, antizyme inhibitor 1, and V-type proton ATPase.* The *gamma-amino butyric acid receptor subunit rho-1-like* gene encodes a subunit of the GABA receptor, which is pivotal in inhibitory neurotransmission within the central nervous system (Ghit et al., 2021), but the gene may also be expressed in the muscle (Ong & Kerr, 1990; Watanabe et al., 2002). In fish species, including

rainbow trout, GABA has been implicated in regulating the secretion of gonadotrophin hormones that play roles in growth and development (Kah et al., 1992; Mananos et al., 1999). In murine models, alterations in GABRR1 expression have been associated with changes in body weight, suggesting a possible role in growth regulation (Shao et al., 2021) Antizyme inhibitor 1 regulates polyamine levels by inhibiting antizymes, which are proteins that suppress polyamine synthesis and promote the degradation of polyamines. Elevated polyamine levels have been linked to increased cell growth and hypertrophy (Lee & MacLean, 2011; Tabbaa et al., 2021), which may influence growth and body weight. The *V-type proton ATPase 2* eQTL SNPs are located in active enhancers region of the genome (Figure 9), which reinforces findings from the eQTL analysis that these eQTL SNPs influence the expression of their respective genes. The V-Type Proton ATPase complex is crucial for acidifying intracellular compartments and is involved in various cellular processes, including protein degradation, nutrient absorption, and pH regulation (Collins & Forgac, 2020; Eaton et al., 2021). The proper functioning of this enzyme is crucial for maintaining cellular homeostasis and metabolic efficiency; any disruptions in its activity can affect metabolic processes integral to growth and body weight regulation. There is a strong upregulation of muscle-specific genes (myosin, troponin, and myomesin) and a calcium-handling protein (*ATP2A1*) in the high body weight family, suggesting enhanced contraction, muscle development, and repair. Genes involved in energy metabolism, including mitochondrial activities (*COX1, COX2, ND6, ND2, ATP5MC3B*), as well as fatty acid metabolism (*FABP3, CPT1A, ACADE9*), are enriched in the high-body weight family, indicating an increased energy production to support body growth.

The muscle yield candidate genes are *GATD3A, uncharacterized LOC110486628, PPP2R1BB (protein phosphatase 2 regulatory subunit A beta b*, and *USP6 N-terminal-like protein*. The Protein phosphatase 2A (PP2A) is a serine/threonine phosphatase involved in various cellular processes, including cell growth and division (Janssens & Goris, 2001). The regulatory subunit encoded by *PPP2R1BB* modulates PP2A activity. In zebrafish (*Danio rerio*), *PPP2R1BB* interacts with other PP2A subunits and regulatory proteins, suggesting a role in cell cycle regulation(Wlodarchak & Xing, 2016). The *ppp2r1bb* may, therefore, influence muscle cell proliferation and growth. The USP6 N-terminal-like protein is one of the ubiquitin-specific proteases involved in protein degradation and turnover (Hegde, 2004; Hochstrasser, 1996)—processes vital for muscle development and remodeling, as well as muscle atrophy and growth(Bilodeau et al., 2016; Wing et al., 2011). There is upregulation of genes associated with cytoskeletal dynamics, neuromuscular stability, and signaling in the high muscle yield family. The *CADPS2* and *neurexin-1a* genes are critical for neurotransmitter activities, hormonal release, and protection of neuromuscular junction integrity. These may imply enhanced signaling and neuromuscular activity to support hyperplasia in the high muscle yield family.

The fifty-one candidate genes for condition factor are involved in several biological pathways and systems. They include those that have influence on growth and muscle development (*troponin, PDZ and LIM domain protein, cyclin-dependent-like kinase 5*), influence metabolic and energy

pathways (*cytochrome P450 3A27, methylmalonate-semialdehyde dehydrogenase*), influence neurological and endocrine regulation (*Apoptosis antagonizing transcription factor, ELAV-like RNA binding protein 1a, Neugrin neurite outgrowth associated, synaptoporin and synaptic vesicle glycoprotein 2ca*), those that affects cellular regulation and structural maintenance (*centrosomal protein 290 CEP290, Epithelial stromal interaction 1 EPSTI1, USP6 N-terminal-like protein USP6NL, nucleolin NCL*), and those involved in transcription, RNA processing and gene regulation (*RNA-binding protein 34-like RBM34, Transcription initiation factor TFIID subunit 1 TAF1, Pseudouridine synthase-like 1 PUS1*). The Synaptic vesicle glycoprotein 2Ca, typically referred to as *SVC2C* (Synaptic vesicle glycoprotein 2C) is a member of the synaptic vesicle protein family, which plays a role in neurotransmitter release and synaptic function throughout the brain (Dunn et al., 2017; Rossi et al., 2022). Asch et al. (2022) associated lower synaptic density in humans, particularly in those with obesity and higher body mass index. They found a lower synaptic index in overweight individuals and a negative correlation between synaptic density and body mass index. The *SV2C* (Synaptic Vesicle Glycoprotein 2C) was identified as a promising candidate gene for growth traits in Simmental beef cattle (An et al., 2020). Genes associated with growth, tissue maintenance, and cellular integrity are more expressed in the high condition factor family. This suggests that the fish are in a state of enhanced anabolic activity and are better equipped to build and maintain tissue functions. Similarly, the genes downregulated in the high condition factor family are associated with inflammation, stress responses, and altered metabolism, suggesting that fish with the low condition factor may be experiencing physiological stress, immune activation, and metabolic shifts.

Sixteen candidate genes were identified for the Genetic lines (ARS-FY-H vs ARS-FY-L). These genes are involved in pathways related to muscle cell proliferation, differentiation, metabolism, protein synthesis, and stress responses. The ARS-FY-H genetic line was selected for its improved muscle growth compared to the ARS-FY-L line. Candidate genes identified for Genetic line influence muscle growth through pathways related to muscle cell growth proliferation, differentiation (*apoptosis antagonizing transcription factor AATF, dual specificity tyrosine phosphorylation-regulated kinase 3 DYRK3, USP6 N-terminal-like protein*), protein synthesis and muscle development (*eukaryotic translation initiation factor 4E-binding protein 2 EIF4EBP2, ribonuclease inhibitor-like RNHIL, nucleolin NCL*), energy metabolism and nutrient utilization (*cytochrome P450 3A27 CYP3A27, methylmalonate-semialdehyde dehydrogenase MMSDH, 1-acyl-sn-glyerol-3-phosphate acyltransferase gamma AGPAT3*), and muscle fiber maintenance and cytoskeletal function (*kinesin light chain 1, cystatin-B*). One of those genes, the USP6 N-terminal-like protein, which is involved in protein trafficking and cellular growth and may play a role in muscle fiber expansion (Su et al., 2022).

4.2 Transcription Factor Binding Sites Prediction, eQTL Variants Impact and Haplotype Analysis

Transcription factors are trans-acting proteins that interact with specific nucleotide sequences located around the genes' promoter region (Sassone-Corsi & Borrelli, 1986). The interaction with sequences, known as transcription factor binding sites (TFBS), is one of the mechanisms responsible for regulating gene expression (Wong et al., 2017). We utilized bioinformatic tools to predict transcription factors that bind to the nucleotide sequences surrounding the body weight cis-eQTL variants identified in the study and how the polymorphism of these variants can affect the ability of transcription factors to bind to their transcription factor binding sites (TFBS).

The cis-eQTL variants and candidate genes for body weight are presented in Figure 8. The 2_27321356_C_G eQTL variant is flanked by strong enhancers in the liver and weak enhancers in the white muscle, brain, and intestine (Figure 9). Some of the transcription factors that have lost their binding ability due to polymorphisms at the 2_27321356_C_G eQTL variants in the V-*type proton ATPase subunit C 1-A* gene have been implicated in regulating body weight. For example, the FOSL1::JUN, JUN::JUNB, and FOSL1::JUNB transcription factors, collectively known as the AP-1 Complex, have been linked to body weight regulation. They are AP-1 (Activator Protein-1) transcription factors, which are known to regulate adipogenesis, inflammation, and energy metabolism(Bose et al., 2024; Luther et al., 2014). The ALX3 (ALX Homeobox 3) is a homeobox transcription factor, and homeobox genes and transcription factors are known to play significant roles in promoting adipogenesis and energy balance(Du et al., 2013; Yang et al., 2025).

The haplotype analysis demonstrates that the A-A-C haplotype (A at 2_27318690_A_G, A at 2_27311612_A_G, and C at 2_27321356_C_G) is strongly associated with increased *V-type proton ATPase 2* expression. In contrast, the G-G-G haplotype is associated with decreased expression. This analysis provides evidence that the combination of A at 2_27318690_A_G, A at 2_27311612_A_G, and C at 2_27321356_C_G may enhance transcription of *V-type proton ATPase 2*. Given that these eQTL variants are located within 10kb of the TSS of *V-type proton ATPase 2* and the UCSC genome browser track shows that they are located in active enhancer region, this suggest that polymorphisms within this eQTL variants and haplotypes regulate gene expression by determining the ability of the enhancers to interact with promoter for *V-type proton ATPase 2* gene expression regulation. Functional studies like CRISPR can be used to validate the relationship between polymorphisms at the eQTL variants associated with *V-type proton ATPase 2* and their relationship with body weight in rainbow trout.

5.0 CONCLUSION

In conclusion, this study presents a comprehensive eQTL analysis in rainbow trout, integrating genomic, transcriptomic, and association data to identify regulatory variants and genes associated with growth traits. Our findings underscore the importance of cis-regulatory variation in shaping

gene expression profiles linked to somatic growth. By leveraging multi-omics data, we identified key candidate genes—such as *gamma-aminobutyric acid receptor subunit rho-1-like, antizyme inhibitor 1, ATP6V1, TNNI2, PDLIM3, CDK5, CYP3A27, and USP6NL*—that regulate muscle development, cellular metabolism, and tissue integrity. These genes and pathways are involved in fundamental biological processes rather than aquaculture-specific outcomes, broadening our understanding of the molecular networks that underlie post-embryonic muscle growth in vertebrates. This eQTL atlas offers a resource for future studies on the transcriptional and epigenetic regulation of vertebrate growth.

REFERENCES

Aas, G., Bjerkeng, B., Storebakken, T., & Ruyter, B. (1999). Blood appearance, metabolic transformation and plasma transport proteins of 14C-astaxanthin in Atlantic salmon (Salmo salar L.). *Fish Physiology and Biochemistry*, *21*, 325-334.

Abraham, G., Kowalczyk, A., Loi, S., Haviv, I., & Zobel, J. (2010). Prediction of breast cancer prognosis using gene set statistics provides signature stability and biological context. *BMC bioinformatics*, *11*, 1-15.

Aguilar, I., Misztal, I., Johnson, D. L., Legarra, A., Tsuruta, S., & Lawlor, T. J. (2010). Hot topic: a unified approach to utilize phenotypic, full pedigree, and genomic information for genetic evaluation of Holstein final score. *J Dairy Sci*, *93*(2), 743-752. https://doi.org/10.3168/jds.2009-2730

Aguilar, I., Misztal, I., Legarra, A., & Tsuruta, S. (2011). Efficient computation of the genomic relationship matrix and other matrices used in single-step evaluation. *Journal of Animal Breeding and Genetics*, *128*(6), 422-428.

Ahmed, R. O., Ali, A., Al-Tobasei, R., Leeds, T., Kenney, B., & Salem, M. (2022). Weighted Single-Step GWAS Identifies Genes Influencing Fillet Color in Rainbow Trout. *Genes*, *13*(8), 1331.

Ahmed, R. O., Ali, A., Leeds, T., & Salem, M. (2023). RNA-Seq analysis of the pyloric caecum, liver, and muscle reveals molecular mechanisms regulating fillet color in rainbow trout. *BMC genomics*, *24*(1), 579.

Akasaki, Y., Alvarez-Garcia, O., Saito, M., Caramés, B., Iwamoto, Y., & Lotz, M. K. (2014). FoxO transcription factors support oxidative stress resistance in human chondrocytes. *Arthritis & rheumatology*, *66*(12), 3349-3358.

Al-Tobasei, R., Ali, A., Garcia, A. L., Lourenco, D., Leeds, T., & Salem, M. (2021). Genomic predictions for fillet yield and firmness in rainbow trout using reduced-density SNP panels. *BMC genomics*, *22*, 1-11.

Al-Tobasei, R., Ali, A., Leeds, T. D., Liu, S., Palti, Y., Kenney, B., & Salem, M. (2017). Identification of SNPs associated with muscle yield and quality traits using allelic-imbalance analyses of pooled RNA-Seq samples in rainbow trout. *BMC genomics*, *18*(1), 1-15.

Alexander, C. C., Munkascy, E., Tillmon, H., Fraker, T., Scheirer, J., Holstein, D.,…Rodriguez, K. A. (2022). HspB1 Overexpression Improves Life Span and Stress Resistance in an Invertebrate Model. *J Gerontol A Biol Sci Med Sci*, *77*(2), 268-275. https://doi.org/10.1093/gerona/glab296

Ali, A., Al-Tobasei, R., Kenney, B., Timothy, D., & Mohamed, S. (2018). Integrated analysis of lncRNA and mRNA expression in rainbow trout families showing variation in muscle growth and fillet quality traits. Sci Rep 8, 12111. In.

Ali, A., Al-Tobasei, R., Lourenco, D., Leeds, T., Kenney, B., & Salem, M. (2019). Genome-Wide Association Study Identifies Genomic Loci Affecting Filet Firmness and Protein Content in Rainbow Trout. *Front Genet*, *10*, 386. https://doi.org/10.3389/fgene.2019.00386

Ali, A., Al-Tobasei, R., Lourenco, D., Leeds, T., Kenney, B., & Salem, M. (2019). Genome-wide association study identifies genomic loci affecting filet firmness and protein content in rainbow trout. *Frontiers in genetics*, *10*, 386.

Ali, A., Al-Tobasei, R., Lourenco, D., Leeds, T., Kenney, B., & Salem, M. (2020a). Genome-wide identification of loci associated with growth in rainbow trout. *BMC genomics*, *21*(1), 209. https://doi.org/10.1186/s12864-020-6617-x

Ali, A., Al-Tobasei, R., Lourenco, D., Leeds, T., Kenney, B., & Salem, M. (2020b). Genome-wide identification of loci associated with growth in rainbow trout [Article]. *BMC genomics*, *21*(1), Article 209. https://doi.org/10.1186/s12864-020-6617-x

Ali, A., Al-Tobasei, R., Lourenco, D., Leeds, T., Kenney, B., & Salem, M. (2020a). Genome-wide identification of loci associated with growth in rainbow trout. *BMC genomics*, *21*(1), 1-16.

Ali, A., Al-Tobasei, R., Lourenco, D., Leeds, T., Kenney, B., & Salem, M. (2020c). Genome-wide scan for common variants associated with intramuscular fat and moisture content in rainbow trout. *BMC genomics*, *21*(1), 529. https://doi.org/10.1186/s12864-020-06932-0

Ali, A., Al-Tobasei, R., Lourenco, D., Leeds, T., Kenney, B., & Salem, M. (2020b). Genome-wide scan for common variants associated with intramuscular fat and moisture content in rainbow trout. *BMC genomics*, *21*(1), 1-17.

Allendorf, F. W., & Thorgaard, G. H. (1984). Tetraploidy and the evolution of salmonid fishes. *Evolutionary genetics of fishes*, 1-53.

Almeida, A., Mitchell, A. L., Tarkowska, A., & Finn, R. D. (2018). Benchmarking taxonomic assignments based on 16S rRNA gene profiling of the microbiota from commonly sampled environments. *Gigascience*, *7*(5), giy054.

Amadeu, R. R., Garcia, A. A. F., Munoz, P. R., & Ferrão, L. F. V. (2023). AGHmatrix: genetic relationship matrices in R. *Bioinformatics*, *39*(7), btad445.

Amengual, J., Widjaja-Adhi, M. A. K., Rodriguez-Santiago, S., Hessel, S., Golczak, M., Palczewski, K., & Von Lintig, J. (2013). Two Carotenoid Oxygenases Contribute to Mammalian Provitamin A Metabolism*♦. *Journal of Biological Chemistry*, *288*(47), 34081-34096.

An, B., Xu, L., Xia, J., Wang, X., Miao, J., Chang, T.,…Zhang, L. (2020). Multiple association analysis of loci and candidate genes that regulate body size at three growth stages in Simmental beef cattle. *Bmc Genetics*, *21*, 1-11.

Andrews, S. (2010). FastQC: a quality control tool for high throughput sequence data. In: Cambridge, United Kingdom.

Arihara, K., Cassens, R. G., Greaser, M. L., Luchansky, J. B., & Mozdziak, P. E. (1995). Localization of metmyoglobin-reducing enzyme (NADH-cytochrome b5 reductase) system components in bovine skeletal muscle. *Meat science*, *39*(2), 205-213.

Armstrong, G. A., & Hearst, J. E. (1996). Genetics and molecular biology of carotenoid pigment biosynthesis. *The FASEB Journal*, *10*(2), 228-237.

Arredondo-Figueroa, J. L., Mora, G. I. d. l., Ponce-Palafox, J. T., Barriga-Sosa, I. d. l. A., & Vernon-Carter, E. J. (2007). Color of raw, frozen, and smoked fillets of rainbow trout (Oncorhynchus mykiss) fed diets supplemented with astaxanthin and saponified red chilli (Capsicum annuum) extracts. *Journal of Aquatic Food Product Technology*, *16*(1), 35-50.

Arya, R., Mallik, M., & Lakhotia, S. C. (2007). Heat shock genes—integrating cell survival and death. *Journal of biosciences*, *32*(3), 595-610.

Asch, R. H., Holmes, S. E., Jastreboff, A. M., Potenza, M. N., Baldassarri, S. R., Carson, R. E.,…Esterlis, I. (2022). Lower synaptic density is associated with psychiatric and cognitive alterations in obesity. *Neuropsychopharmacology*, *47*(2), 543-552.

Asker, D., & Ohta, Y. (1999). Production of canthaxanthin by extremely halophilic bacteria. *Journal of bioscience and bioengineering*, *88*(6), 617-621.

Association, A. M. S. (1991). Guidelines for meat color evaluation. proceedings: The 44th annual reciprocal meat conference. Kans, Chicago,

Aussanasuwannakul, A., Kenney, P. B., Weber, G. M., Yao, J., Slider, S. D., Manor, M. L., & Salem, M. (2011). Effect of sexual maturation on growth, fillet composition, and texture of female rainbow trout (Oncorhynchus mykiss) on a high nutritional plane. *Aquaculture*, *317*(1-4), 79-88.

Awany, D., Allali, I., Dalvie, S., Hemmings, S., Mwaikono, K. S., Thomford, N. E.,…Chimusa, E. R. (2018). Host and Microbiome Genome-Wide Association Studies: Current State and Challenges. *Front Genet*, *9*, 637. https://doi.org/10.3389/fgene.2018.00637

Bagga, S., Bracht, J., Hunter, S., Massirer, K., Holtz, J., Eachus, R., & Pasquinelli, A. E. (2005). Regulation by let-7 and lin-4 miRNAs results in target mRNA degradation. *Cell*, *122*(4), 553-563.

Bailey, A. J., & Light, N. D. (1989). *Connective tissue in meat and meat products*. Elsevier applied science.

Baker, R., Pfeiffer, A.-M., Schöner, F.-J., & Smith-Lemmon, L. (2002). Pigmenting efficacy of astaxanthin and canthaxanthin in fresh-water reared Atlantic salmon, Salmo salar. *Animal Feed Science and Technology*, *99*(1-4), 97-106.

Banerjee, R., & Vlasie, M. (2002). Controlling the reactivity of radical intermediates by coenzyme B12-dependent methylmalonyl-CoA mutase. *Biochemical Society Transactions*, *30*(4), 621-624.

Bartel, D. P. (2004). MicroRNAs: genomics, biogenesis, mechanism, and function. *cell*, *116*(2), 281-297. https://doi.org/10.1016/s0092-8674(04)00045-5

Bates, J. M., Akerlund, J., Mittge, E., & Guillemin, K. (2007). Intestinal alkaline phosphatase detoxifies lipopolysaccharide and prevents inflammation in zebrafish in response to the gut microbiota. *Cell host & microbe*, *2*(6), 371-382.

Bates, J. M., Mittge, E., Kuhlman, J., Baden, K. N., Cheesman, S. E., & Guillemin, K. (2006). Distinct signals from the microbiota promote different aspects of zebrafish gut differentiation. *Developmental biology*, *297*(2), 374-386.

Beghini, F., McIver, L. J., Blanco-Míguez, A., Dubois, L., Asnicar, F., Maharjan, S.,…Thomas, A. M. (2021). Integrating taxonomic, functional, and strain-level profiling of diverse microbial communities with bioBakery 3. *elife*, *10*, e65088.

Bellanti, F., Villani, R., Facciorusso, A., Vendemiale, G., & Serviddio, G. (2017). Lipid oxidation products in the pathogenesis of non-alcoholic steatohepatitis. *Free Radic Biol Med*, *111*, 173-185. https://doi.org/10.1016/j.freeradbiomed.2017.01.023

Ben-Dor, A., Nahum, A., Danilenko, M., Giat, Y., Stahl, W., Martin, H.-D.,…Sharoni, Y. (2001). Effects of acyclo-retinoic acid and lycopene on activation of the retinoic acid receptor and proliferation of mammary cancer cells. *Archives of Biochemistry and Biophysics*, *391*(2), 295-302.

Bernard, M., Dehaullon, A., Prchal, M., Haffray, P., Quillet, E., Dupont-Nivet, M.,…Phocas, F. (2022). Development of a high-density 665 K SNP array for rainbow trout genome-wide genotyping. *Frontiers in Genetics*, *13*, 941340.

Bharti, M., Nagar, S., Khurana, H., & Negi, R. K. (2022). Metagenomic insights to understand the role of polluted river Yamuna in shaping the gut microbial communities of two invasive fish species. *Archives of Microbiology*, *204*(8), 509.

Bilodeau, P. A., Coyne, E. S., & Wing, S. S. (2016). The ubiquitin proteasome system in atrophying skeletal muscle: roles and regulation. *American Journal of Physiology-Cell Physiology*, *311*(3), C392-C403.

Bjerkeng, B., Refstie, S., Fjalestad, K., Storebakken, T., Rødbotten, M., & Roem, A. (1997). Quality parameters of the flesh of Atlantic salmon (Salmo salar) as affected by dietary fat content and full-fat soybean meal as a partial substitute for fish meal in the diet. *Aquaculture*, *157*(3-4), 297-309.

Bjerkeng, B., Storebakken, T., & Liaaen-Jensen, S. (1992). Pigmentation of rainbow trout from start feeding to sexual maturation. *Aquaculture*, *108*(3-4), 333-346.

Blay, C., Haffray, P., Bugeon, J., D'ambrosio, J., Dechamp, N., Collewet, G.,…Corraze, G. (2021). Genetic parameters and genome-wide association studies of quality traits characterised using imaging technologies in Rainbow trout, Oncorhynchus mykiss. *Frontiers in genetics*, *12*, 219.

Boggio, G. M., Christensen, O., Legarra, A., Meynadier, A., & Marie-Etancelin, C. (2023). Microbiability of milk composition and genetic control of microbiota effects in sheep. *Journal of Dairy Science*, *106*(9), 6288-6298.

Bohn, T., Desmarchelier, C., Dragsted, L. O., Nielsen, C. S., Stahl, W., Rühl, R.,…Borel, P. (2017). Host-related factors explaining interindividual variability of carotenoid bioavailability and tissue concentrations in humans. *Molecular nutrition & food research*, *61*(6), 1600685.

Bohn, T., Desmarchelier, C., El, S. N., Keijer, J., van Schothorst, E., Rühl, R., & Borel, P. (2019). β-carotene in the human body: metabolic bioactivation pathways–from digestion to tissue distribution and excretion. *Proceedings of the Nutrition Society*, *78*(1), 68-87.

Bonder, M. J., Kurilshikov, A., Tigchelaar, E. F., Mujagic, Z., Imhann, F., Vila, A. V.,…Zhernakova, A. (2016). The effect of host genetics on the gut microbiome. *Nat Genet*, *48*(11), 1407-1412. https://doi.org/10.1038/ng.3663

Borel, P. (2003). Factors affecting intestinal absorption of highly lipophilic food microconstituents (fat-soluble vitamins, carotenoids and phytosterols).

Borel, P., Desmarchelier, C., Nowicki, M., & Bott, R. (2015a). A combination of single-nucleotide polymorphisms is associated with interindividual variability in dietary β-carotene bioavailability in healthy men. *The Journal of Nutrition*, *145*(8), 1740-1747.

Borel, P., Desmarchelier, C., Nowicki, M., & Bott, R. (2015b). Lycopene bioavailability is associated with a combination of genetic variants. *Free Radical Biology and Medicine*, *83*, 238-244.

Borel, P., Desmarchelier, C., Nowicki, M., Bott, R., Morange, S., & Lesavre, N. (2014). Interindividual variability of lutein bioavailability in healthy men: characterization, genetic variants involved, and relation with fasting plasma lutein concentration. *The American journal of clinical nutrition*, *100*(1), 168-175.

Borel, P., Grolier, P., Mekki, N., Boirie, Y., Rochette, Y., Le Roy, B.,…Azais-Braesco, V. (1998). Low and high responders to pharmacological doses of β-carotene: proportion in the population, mechanisms involved and consequences on β-carotene metabolism. *Journal of lipid research*, *39*(11), 2250-2260.

Borel, P., Lietz, G., Goncalves, A., Szabo de Edelenyi, F., Lecompte, S., Curtis, P.,…Packard, C. (2013). CD36 and SR-BI are involved in cellular uptake of provitamin A carotenoids by Caco-2 and HEK cells, and some of their genetic variants are associated with plasma concentrations of these micronutrients in humans. *The Journal of nutrition*, *143*(4), 448-456.

Bose, G. S., Kalakoti, G., Kulkarni, A. P., & Mittal, S. (2024). AP-1/C-FOS and AP-1/FRA2 differentially regulate early and late adipogenic differentiation of mesenchymal stem cells. *Journal of Cellular Biochemistry*, *125*(10), e30543.

Boussaha, M., Guyomard, R., Cabau, C., Esquerré, D., & Quillet, E. (2012). Development and characterisation of an expressed sequence tags (EST)-derived single nucleotide polymorphisms (SNPs) resource in rainbow trout. *BMC genomics*, *13*(1), 1-11.

Brennan, N. M., Ward, A. C., Beresford, T. P., Fox, P. F., Goodfellow, M., & Cogan, T. M. (2002). Biodiversity of the bacterial flora on the surface of a smear cheese. *Applied and Environmental Microbiology*, *68*(2), 820-830.

Brown, K. R., Barnes, M., Parker, T., & Fletcher, B. (2016). Retention of fillet coloration in rainbow trout after dietary astaxanthin cessation. *Fisheries & Aquaculture Journal*, *7*, 163.

Brown, R. M., Wiens, G. D., & Salinas, I. (2019). Analysis of the gut and gill microbiome of resistant and susceptible lines of rainbow trout (Oncorhynchus mykiss). *Fish & shellfish immunology*, *86*, 497-506.

Brugman, S., & Nieuwenhuis, E. E. (2010). Mucosal control of the intestinal microbial community. *Journal of Molecular Medicine*, *88*, 881-888.

Brunham, L. R., Kruit, J. K., Iqbal, J., Fievet, C., Timmins, J. M., Pape, T. D.,…Groen, A. K. (2006). Intestinal ABCA1 directly contributes to HDL biogenesis in vivo. *The Journal of clinical investigation*, *116*(4), 1052-1062.

Budanov, A. V., Sablina, A. A., Feinstein, E., Koonin, E. V., & Chumakov, P. M. (2004). Regeneration of peroxiredoxins by p53-regulated sestrins, homologs of bacterial AhpD. *Science*, *304*(5670), 596-600. https://doi.org/10.1126/science.1095569

Budanov, A. V., Shoshani, T., Faerman, A., Zelin, E., Kamer, I., Kalinski, H.,…Feinstein, E. (2002). Identification of a novel stress-responsive gene Hi95 involved in regulation of cell viability. *Oncogene*, *21*(39), 6017-6031. https://doi.org/10.1038/sj.onc.1205877

Buitenhuis, B., Lassen, J., Noel, S. J., Plichta, D. R., Sørensen, P., Difford, G. F., & Poulsen, N. A. (2019). Impact of the rumen microbiome on milk fatty acid composition of Holstein cattle. *Genetics Selection Evolution*, *51*(1), 1-8.

Busch, A. W., & Montgomery, B. L. (2015). Interdependence of tetrapyrrole metabolism, the generation of oxidative stress and the mitigative oxidative stress response. *Redox biology*, *4*, 260-271.

Buttle, L., Crampton, V., & Williams, P. (2001). The effect of feed pigment type on flesh pigment deposition and colour in farmed Atlantic salmon, Salmo salar L. *Aquaculture Research*, *32*(2), 103-111.

Byrd, A. K., Zybailov, B. L., Maddukuri, L., Gao, J., Marecki, J. C., Jaiswal, M.,…Chib, S. (2016). Evidence that G-quadruplex DNA accumulates in the cytoplasm and participates in stress granule assembly in response to oxidative stress. *Journal of Biological Chemistry*, *291*(34), 18041-18057.

Cai, W., Zhang, Y., Chang, T., Wang, Z., Zhu, B., Chen, Y.,…Gao, H. (2023). The eQTL colocalization and transcriptome-wide association study identify potentially causal genes responsible for economic traits in Simmental beef cattle. *Journal of Animal Science and Biotechnology*, *14*(1), 78.

Cai, Y.-Y., Huang, F.-Q., Lao, X., Lu, Y., Gao, X., Alolga, R. N.,…Liu, B. (2022). Integrated metagenomics identifies a crucial role for trimethylamine-producing Lachnoclostridium in promoting atherosclerosis. *NPJ biofilms and microbiomes*, *8*(1), 11.

Calegari-Santos, R., Diogo, R. A., Fontana, J. D., & Bonfim, T. M. B. (2016). Carotenoid production by halophilic archaea under different culture conditions. *Current microbiology*, *72*, 641-651.

Callahan, B. J., McMurdie, P. J., Rosen, M. J., Han, A. W., Johnson, A. J. A., & Holmes, S. P. (2016). DADA2: High-resolution sample inference from Illumina amplicon data. *Nature methods*, *13*(7), 581-583.

Camp, J. G., Jazwa, A. L., Trent, C. M., & Rawls, J. F. (2012). Intronic cis-regulatory modules mediate tissue-specific and microbial control of angptl4/fiaf transcription. *PLoS genetics*, *8*(3), e1002585.

Caporaso, J. G., Kuczynski, J., Stombaugh, J., Bittinger, K., Bushman, F. D., Costello, E. K.,…Gordon, J. I. (2010). QIIME allows analysis of high-throughput community sequencing data. *Nature methods*, *7*(5), 335-336.

Cartwright, G. M., & Scott, B. (2013). Redox regulation of an AP-1-like transcription factor, YapA, in the fungal symbiont Epichloe festucae. *Eukaryotic cell*, *12*(10), 1335-1348.

Castaño Sánchez, C., Palti, Y., & Rexroad, C. (2011). SNP analysis with duplicated fish genomes: differentiation of SNPs, paralogous sequence variants, amd multisite variants. *Next generation sequencing and whole genome selection in aquaculture*, 133-150.

Castenmiller, J. J., & West, C. E. (1998). Bioavailability and bioconversion of carotenoids. *Annu Rev Nutr*, *18*(1), 19-38. https://doi.org/10.1146/annurev.nutr.18.1.19

Cerf-Bensussan, N., & Gaboriau-Routhiau, V. (2010). The immune system and the gut microbiota: friends or foes? *Nature Reviews Immunology*, *10*(10), 735-744.
Chaijan, M., Benjakul, S., Visessanguan, W., & Faustman, C. (2007). Interaction between fish myoglobin and myosin in vitro. *Food Chemistry*, *103*(4), 1168-1175.
Chaillou, T. (2019). Ribosome specialization and its potential role in the control of protein translation and skeletal muscle size. *Journal of applied physiology*.
Chakraborty, D., Sharma, N., Kour, S., Sodhi, S. S., Gupta, M. K., Lee, S. J., & Son, Y. O. (2022). Applications of omics technology for livestock selection and improvement. *Frontiers in Genetics*, *13*, 774113.
Chan, K. M., & Decker, E. A. (1994). Endogenous skeletal muscle antioxidants. *Crit Rev Food Sci Nutr*, *34*(4), 403-426. https://doi.org/10.1080/10408399409527669
Chang, C. C., Chow, C. C., Tellier, L. C., Vattikuti, S., Purcell, S. M., & Lee, J. J. (2015). Second-generation PLINK: rising to the challenge of larger and richer datasets. *Gigascience*, *4*(1), s13742-13015-10047-13748.
Chapagain, P., Arivett, B., Cleveland, B. M., Walker, D. M., & Salem, M. (2019). Analysis of the fecal microbiota of fast-and slow-growing rainbow trout (Oncorhynchus mykiss). *BMC genomics*, *20*(1), 1-11.
Chavan, R. (2015). Indigo dye and reduction techniques. In *Denim* (pp. 37-67). Elsevier.
Chen, C., Yu, Q., Han, L., Zhang, J., & Guo, Z. (2018). Effects of aldehyde products of lipid oxidation on the color stability and metmyoglobin reducing ability of bovine Longissimus muscle. *Anim Sci J*, *89*(5), 810-816. https://doi.org/10.1111/asj.12993
Chen, J., & Tian, Y. (2021). Hexavalent chromium reducing bacteria: mechanism of reduction and characteristics. *Environmental Science and Pollution Research*, *28*, 20981-20997.
Chen, K., & Rajewsky, N. (2007). The evolution of gene regulation by transcription factors and microRNAs. *Nature Reviews Genetics*, *8*(2), 93-103.
Chen, L., & Liu, B. (2017). Relationships between stress granules, oxidative stress, and neurodegenerative diseases. *Oxidative medicine and cellular longevity*, *2017*.
Chen, M.-M., Zhao, Y.-P., Zhao, Y., Deng, S.-L., & Yu, K. (2021). Regulation of myostatin on the growth and development of skeletal muscle. *Frontiers in cell and developmental biology*, *9*, 785712.
Chen, X., Peng, M., Yang, C., Li, Q., Feng, P., Zhu, W.,…Zhao, Y. (2024). Genome-wide QTL and eQTL mapping reveal genes associated with growth rate trait of the Pacific white shrimp (Litopenaeus vannamei). *BMC genomics*, *25*(1), 414.
Chen, Y., Xie, Y., Zhong, R., Liu, L., Lin, C., Xiao, L.,…Everaert, N. (2021). Effects of xylo-oligosaccharides on growth and gut microbiota as potential replacements for antibiotic in weaning piglets. *Frontiers in microbiology*, *12*, 641172.
Cheng, M. P., Domingo, M.-C., Lévesque, S., & Yansouni, C. P. (2016). A case report of a deep surgical site infection with Terrisporobacter glycolicus/T. Mayombei and review of the literature. *BMC Infectious Diseases*, *16*, 1-4.
Chiang, J. Y. (2009). Bile acids: regulation of synthesis: thematic review series: bile acids. *Journal of lipid research*, *50*(10), 1955-1966.
Chisté, R. C., Freitas, M., Mercadante, A. Z., & Fernandes, E. (2014). Carotenoids inhibit lipid peroxidation and hemoglobin oxidation, but not the depletion of glutathione induced by ROS in human erythrocytes. *Life sciences*, *99*(1-2), 52-60.
Choubert, G., de la Noüe, J., & Blanc, J.-M. (1991). Apparent digestibility of canthaxanthin in rainbow trout: effect of dietary fat level, antibiotics and number of pyloric caeca. *Aquaculture*, *99*(3-4), 323-329.
Chung, Y.-H., Zhou, M., Holtshausen, L., Alexander, T., McAllister, T., Guan, L.,…Beauchemin, K. (2012). A fibrolytic enzyme additive for lactating Holstein cow diets: ruminal fermentation, rumen microbial populations, and enteric methane emissions. *Journal of dairy science*, *95*(3), 1419-1427.

Clark, F. N. (1928). *The Weight-length Relationship of the California Sardine:(Sardina caerulea) at San Pedro*. California state print. Office.

Cleveland, B. M., Gao, G., & Leeds, T. D. (2020). Transcriptomic response to selective breeding for fast growth in rainbow trout (Oncorhynchus mykiss). *Marine Biotechnology*, *22*(4), 539-550.

Cleveland, B. M., Radler, L. M., & Leeds, T. D. Growth, fillet yield, and muscle quality traits are not affected by a genotype by diet interaction in rainbow trout consuming diets that differ in lipid content. *Journal of the World Aquaculture Society*.

Cleveland, B. M., Radler, L. M., & Leeds, T. D. (2023). Growth, fillet yield, and muscle quality traits are not affected by a genotype by diet interaction in rainbow trout consuming diets that differ in lipid content. *Journal of the World Aquaculture Society*.

Clevidence, B. A., & Bieri, J. G. (1993). [4] Association of carotenoids with human plasma lipoproteins. In *Methods in enzymology* (Vol. 214, pp. 33-46). Elsevier.

Clop, A., Marcq, F., Takeda, H., Pirottin, D., Tordoir, X., Bibe, B.,…Georges, M. (2006). A mutation creating a potential illegitimate microRNA target site in the myostatin gene affects muscularity in sheep. *Nat Genet*, *38*(7), 813-818. https://doi.org/10.1038/ng1810

Clop, A., Marcq, F., Takeda, H., Pirottin, D., Tordoir, X., Bibé, B.,…Eychenne, F. (2006). A mutation creating a potential illegitimate microRNA target site in the myostatin gene affects muscularity in sheep. *Nature genetics*, *38*(7), 813-818.

Clugston, R. D., & Blaner, W. S. (2014). Vitamin A (retinoid) metabolism and actions: What we know and what we need to know about amphibians. *Zoo biology*, *33*(6), 527-535.

Codina, M., Montserrat, N., De La Serrana, D. G., Rallière, C., Gabillard, J. C., Navarro, I.,…Gutiérrez, J. (2006). Role of insulin and IGFs in fish muscle development and quality. Archiv fur Tierzucht,

Colihueque, N. (2010). Genetics of salmonid skin pigmentation: clues and prospects for improving the external appearance of farmed salmonids. *Reviews in Fish Biology and Fisheries*, *20*(1), 71-86.

Collins, M. P., & Forgac, M. (2020). Regulation and function of V-ATPases in physiology and disease. *Biochimica et Biophysica Acta (BBA)-Biomembranes*, *1862*(12), 183341.

Consortium, G. (2020). The GTEx Consortium atlas of genetic regulatory effects across human tissues. *Science*, *369*(6509), 1318-1330.

Consortium, G., Ardlie, K. G., Deluca, D. S., Segrè, A. V., Sullivan, T. J., Young, T. R.,…Tukiainen, T. (2015). The Genotype-Tissue Expression (GTEx) pilot analysis: multitissue gene regulation in humans. *Science*, *348*(6235), 648-660.

Crouse, C. C., Davidson, J. W., Good, C. M., May, T. C., Summerfelt, S. T., Kenney, P. B.,…Cleveland, B. M. (2018). Growth and fillet quality attributes of five genetic strains of rainbow trout (Oncorhynchus mykiss) reared in a partial water reuse system and harvested at different sizes. *Aquaculture Research*, *49*(4), 1672-1681.

Cui, X., Hou, Y., Yang, S., Xie, Y., Zhang, S., Zhang, Y.,…Sun, D. (2014). Transcriptional profiling of mammary gland in Holstein cows with extremely different milk protein and fat percentage using RNA sequencing. *BMC genomics*, *15*, 1-15.

Dallinga-Thie, G. M., Franssen, R., Mooij, H. L., Visser, M. E., Hassing, H. C., Peelman, F.,…Nieuwdorp, M. (2010). The metabolism of triglyceride-rich lipoproteins revisited: new players, new insight. *Atherosclerosis*, *211*(1), 1-8.

Damon, M., Wyszynska-Koko, J., Vincent, A., Herault, F., & Lebret, B. (2012). Comparison of muscle transcriptome between pigs with divergent meat quality phenotypes identifies genes related to muscle metabolism and structure. *PLoS One*, *7*(3), e33763.

Dandachi, I., Anani, H., Hadjadj, L., Brahimi, S., Lagier, J.-C., Daoud, Z., & Rolain, J.-M. (2021). Genome analysis of Lachnoclostridium phocaeense isolated from a patient after kidney transplantation in Marseille. *New Microbes and New Infections*, *41*, 100863.

Danecek, P., Auton, A., Abecasis, G., Albers, C. A., Banks, E., DePristo, M. A.,…Sherry, S. T. (2011). The variant call format and VCFtools. *Bioinformatics*, *27*(15), 2156-2158.

Danecek, P., Bonfield, J. K., Liddle, J., Marshall, J., Ohan, V., Pollard, M. O.,…Davies, R. M. (2021). Twelve years of SAMtools and BCFtools. *Gigascience*, *10*(2), giab008.

Danzmann, R. G., Kocmarek, A. L., Norman, J. D., Rexroad, C. E., & Palti, Y. (2016). Transcriptome profiling in fast versus slow-growing rainbow trout across seasonal gradients [Article]. *BMC genomics*, *17*(1), Article 60. https://doi.org/10.1186/s12864-016-2363-5

Dawkins, R. (2016). *The extended phenotype: The long reach of the gene*. Oxford University Press.

de los Campos, G., Pataki, A., & Pérez, P. (2015). The BGLR (Bayesian Generalized Linear Regression) R-Package. In.

de Lourdes Moreno, M., Sánchez-Porro, C., García, M. T., & Mellado, E. (2012). Carotenoids' production from halophilic bacteria. *Microbial Carotenoids from Bacteria and Microalgae: Methods and Protocols*, 207-217.

dela Seña, C., Riedl, K. M., Narayanasamy, S., Curley, R. W., Schwartz, S. J., & Harrison, E. H. (2014). The human enzyme that converts dietary provitamin A carotenoids to vitamin A is a dioxygenase. *Journal of biological chemistry*, *289*(19), 13661-13666.

Deming, D. M., & Erdman, J. W. (1999). Mammalian carotenoid absorption and metabolism. *Pure and Applied Chemistry*, *71*(12), 2213-2223.

Denstadli, V., Vegusdal, A., Krogdahl, Å., Bakke-McKellep, A., Berge, G., Holm, H.,…Ruyter, B. (2004). Lipid absorption in different segments of the gastrointestinal tract of Atlantic salmon (Salmo salar L.). *Aquaculture*, *240*(1-4), 385-398.

Desai, A. R., Links, M. G., Collins, S. A., Mansfield, G. S., Drew, M. D., Van Kessel, A. G., & Hill, J. E. (2012). Effects of plant-based diets on the distal gut microbiome of rainbow trout (Oncorhynchus mykiss). *Aquaculture*, *350*, 134-142.

Desmarchelier, C., & Borel, P. (2017). Overview of carotenoid bioavailability determinants: From dietary factors to host genetic variations. *Trends in Food Science & Technology*, *69*, 270-280.

Difford, G. F. (2018). *Genetic control of methane emission, feed efficiency and metagenomics in dairy cattle* Wageningen University and Research].

Druet, T., Macleod, I., & Hayes, B. (2014). Toward genomic prediction from whole-genome sequence data: impact of sequencing design on genotype imputation and accuracy of predictions. *Heredity*, *112*(1), 39-47.

Du, B., Cawthorn, W. P., Su, A., Doucette, C. R., Yao, Y., Hemati, N.,…Rosen, C. J. (2013). The transcription factor paired-related homeobox 1 (Prrx1) inhibits adipogenesis by activating transforming growth factor-β (TGFβ) signaling. *Journal of Biological Chemistry*, *288*(5), 3036-3047.

Dunn, A. R., Stout, K. A., Ozawa, M., Lohr, K. M., Hoffman, C. A., Bernstein, A. I.,…Sastry, N. (2017). Synaptic vesicle glycoprotein 2C (SV2C) modulates dopamine release and is disrupted in Parkinson disease. *Proceedings of the National Academy of Sciences*, *114*(11), E2253-E2262.

During, A., Dawson, H. D., & Harrison, E. H. (2005). Carotenoid transport is decreased and expression of the lipid transporters SR-BI, NPC1L1, and ABCA1 is downregulated in Caco-2 cells treated with ezetimibe. *The Journal of nutrition*, *135*(10), 2305-2312.

Déru, V., Tiezzi, F., Carillier-Jacquin, C., Blanchet, B., Cauquil, L., Zemb, O.,…Gilbert, H. (2024). The potential of microbiota information to better predict efficiency traits in growing pigs fed a conventional and a high-fiber diet. *Genetics Selection Evolution*, *56*(1), 8.

D'Ambrosio, D. N., Clugston, R. D., & Blaner, W. S. (2011). Vitamin A metabolism: an update. *Nutrients*, *3*(1), 63-103.

D'Ambrosio, J., Morvezen, R., Brard-Fudulea, S., Bestin, A., Acin Perez, A., Guéméné, D.,…Phocas, F. (2020). Genetic architecture and genomic selection of female reproduction traits in rainbow trout. *BMC genomics*, *21*, 1-14.

Eaton, A. F., Merkulova, M., & Brown, D. (2021). The H+-ATPase (V-ATPase): from proton pump to signaling complex in health and disease. *American Journal of Physiology-Cell Physiology*, *320*(3), C392-C414.

Essers, M. A., Weijzen, S., de Vries-Smits, A. M., Saarloos, I., de Ruiter, N. D., Bos, J. L., & Burgering, B. M. (2004). FOXO transcription factor activation by oxidative stress mediated by the small GTPase Ral and JNK. *The EMBO journal*, *23*(24), 4802-4812.

Esterbauer, H., Schaur, R. J., & Zollner, H. (1991). Chemistry and biochemistry of 4-hydroxynonenal, malonaldehyde and related aldehydes. *Free Radic Biol Med*, *11*(1), 81-128. https://doi.org/10.1016/0891-5849(91)90192-6

Faustman, C., Sun, Q., Mancini, R., & Suman, S. P. (2010). Myoglobin and lipid oxidation interactions: mechanistic bases and control. *Meat Sci*, *86*(1), 86-94. https://doi.org/10.1016/j.meatsci.2010.04.025

Fayemi, P., & Muchenje, V. (2018). Expression of ovine ubiquitin C-terminal hydroxylase 1, pH and colour of variety meats from head-stunned Dohne Merino sheep. *South African Journal of Animal Science*, *48*(1), 88-97.

Folkestad, A., Wold, J. P., Rørvik, K.-A., Tschudi, J., Haugholt, K. H., Kolstad, K., & Mørkøre, T. (2008). Rapid and non-invasive measurements of fat and pigment concentrations in live and slaughtered Atlantic salmon (Salmo salar L.). *Aquaculture*, *280*(1-4), 129-135.

Forcina, G., Pérez-Pardal, L., Carvalheira, J., & Beja-Pereira, A. (2022). Gut microbiome studies in livestock: achievements, challenges, and perspectives. *Animals*, *12*(23), 3375.

Forsberg, O. I., & Guttormsen, A. G. (2006). Modeling optimal dietary pigmentation strategies in farmed Atlantic salmon: Application of mixed-integer non-linear mathematical programming techniques. *Aquaculture*, *261*(1), 118-124.

Frank, A., & Groll, M. (2017). The methylerythritol phosphate pathway to isoprenoids. *Chemical Reviews*, *117*(8), 5675-5703.

Fraslin, C., Phocas, F., Bestin, A., Charles, M., Bernard, M., Krieg, F.,…Petitprez, F. (2020). Genetic determinism of spontaneous masculinisation in XX female rainbow trout: new insights using medium throughput genotyping and whole-genome sequencing. *Scientific Reports*, *10*(1), 17693.

Froese, R. (2006). Cube law, condition factor and weight–length relationships: history, meta-analysis and recommendations. *Journal of applied ichthyology*, *22*(4), 241-253.

Gagaoua, M., Bonnet, M., De Koning, L., & Picard, B. (2018). Reverse Phase Protein array for the quantification and validation of protein biomarkers of beef qualities: The case of meat color from Charolais breed. *Meat Sci*, *145*, 308-319. https://doi.org/10.1016/j.meatsci.2018.06.039

Gallagher, M. D., & Chen-Plotkin, A. S. (2018). The post-GWAS era: from association to function. *The American Journal of Human Genetics*, *102*(5), 717-730.

Galloway-Peña, J., & Hanson, B. (2020). Tools for Analysis of the Microbiome. *Digestive diseases and sciences*, *65*, 674-685.

Gao, G., Nome, T., Pearse, D. E., Moen, T., Naish, K. A., Thorgaard, G. H.,…Palti, Y. (2018). A new single nucleotide polymorphism database for rainbow trout generated through whole genome resequencing. *Frontiers in genetics*, *9*, 363858.

Gao, H., Antony, R., Srinivasan, R., Wu, P., Wang, X., & Li, Y. (2020). UCHL1 regulates oxidative activity in skeletal muscle. *PLoS One*, *15*(11), e0241716. https://doi.org/10.1371/journal.pone.0241716

Gao, H., Hartnett, S., & Li, Y. (2017). Ubiquitin C-Terminal Hydrolase L1 regulates myoblast proliferation and differentiation. *Biochem Biophys Res Commun*, *492*(1), 96-102. https://doi.org/10.1016/j.bbrc.2017.08.027

Gao, N., Chen, Y., Liu, X., Zhao, Y., Zhu, L., Liu, A.,…Chen, Y. (2019). Weighted single-step GWAS identified candidate genes associated with semen traits in a Duroc boar population. *BMC genomics*, *20*(1), 797. https://doi.org/10.1186/s12864-019-6164-5

Gao, Q., Liu, P., Li, Y., Song, D., Long, W., Wang, Z.,…Jiang, L. (2023). Gut microbiota, host genetics and phenotypes in aquatic animals: A review. *Aquaculture Reports*, *31*, 101648.

Gao, X., Wu, W., Ma, C., Li, X., & Dai, R. (2016). Postmortem changes in sarcoplasmic proteins associated with color stability in lamb muscle analyzed by proteomics. *European Food Research and Technology*, *242*(4), 527-535.

Garcia, A., Tsuruta, S., Gao, G., Palti, Y., Lourenco, D., & Leeds, T. (2023a). Genomic selection models substantially improve the accuracy of genetic merit predictions for fillet yield and body weight in rainbow trout using a multi-trait model and multi-generation progeny testing. *Genetics Selection Evolution*, *55*(1), 11.

Garcia, A., Tsuruta, S., Gao, G., Palti, Y., Lourenco, D., & Leeds, T. (2023b). Genomic selection models substantially improve the accuracy of genetic merit predictions for fillet yield and body weight in rainbow trout using a multi-trait model and multi-generation progeny testing. *Genetics Selection Evolution*, *55*(1), 1-12.

Ge, S. X., Jung, D., & Yao, R. (2020). ShinyGO: a graphical gene-set enrichment tool for animals and plants. *Bioinformatics*, *36*(8), 2628-2629.

Genet, C., Dehais, P., Palti, Y., Gao, G., Gavory, F., Wincker, P.,…Boussaha, M. (2011). Analysis of BAC-end sequences in rainbow trout: content characterization and assessment of synteny between trout and other fish genomes. *BMC genomics*, *12*, 1-8.

Georges, M., Clop, A., Marcq, F., Takeda, H., Pirottin, D., Hiard, S.,…Bibé, B. (2006). Polymorphic Polymorphic MicroRNA–Target Interactions: A Novel Source of Phenotypic Variation. Cold Spring Harbor symposia on quantitative biology,

Ghit, A., Assal, D., Al-Shami, A. S., & Hussein, D. E. E. (2021). GABAA receptors: structure, function, pharmacology, and related disorders. *Journal of Genetic Engineering and Biotechnology*, *19*(1), 123.

Gilad, Y., Rifkin, S. A., & Pritchard, J. K. (2008). Revealing the architecture of gene regulation: the promise of eQTL studies. *Trends in genetics*, *24*(8), 408-415.

Gildberg, A., Johansen, A., & Bøgwald, J. (1995). Growth and survival of Atlantic salmon (Salmo salar) fry given diets supplemented with fish protein hydrolysate and lactic acid bacteria during a challenge trial with Aeromonas salmonicida. *Aquaculture*, *138*(1-4), 23-34.

Gjerde, B. a., & Schaeffer, L. (1989). Body traits in rainbow trout: II. Estimates of heritabilities and of phenotypic and genetic correlations. *Aquaculture*, *80*(1-2), 25-44.

Gnaiger, E. (2009). Capacity of oxidative phosphorylation in human skeletal muscle: new perspectives of mitochondrial physiology. *The international journal of biochemistry & cell biology*, *41*(10), 1837-1845.

Gogarten, S. M., Sofer, T., Chen, H., Yu, C., Brody, J. A., Thornton, T. A.,…Conomos, M. P. (2019). Genetic association testing using the GENESIS R/Bioconductor package. *Bioinformatics*, *35*(24), 5346-5348.

Gonzalez-Pena, D., Gao, G., Baranski, M., Moen, T., Cleveland, B. M., Brett Kenney, P.,…Leeds, T. D. (2016). Genome-wide association study for identifying loci that affect fillet yield, carcass, and body weight traits in rainbow trout (Oncorhynchus mykiss) [Article]. *Frontiers in genetics*, *7*(NOV), Article 203. https://doi.org/10.3389/fgene.2016.00203

Gonzalez-Pena, D., Gao, G., Baranski, M., Moen, T., Cleveland, B. M., Kenney, P. B.,…Leeds, T. D. (2016). Genome-wide association study for identifying loci that affect fillet yield, carcass, and body weight traits in rainbow trout (Oncorhynchus mykiss). *Frontiers in genetics*, *7*, 203.

González-Recio, O., Toro, M. A., & Bach, A. (2015). Past, present, and future of epigenetics applied to livestock breeding. *Frontiers in genetics*, *6*, 305.

Goodwin, T. (1986). Metabolism, nutrition, and function of carotenoids. *Annual review of nutrition*, *6*(1), 273-297.

Grant, C. M., Collinson, L. P., Roe, J. H., & Dawes, I. W. (1996). Yeast glutathione reductase is required for protection against oxidative stress and is a target gene for yAP-1 transcriptional regulation. *Molecular microbiology*, *21*(1), 171-179.

Grattagliano, I., Ciampi, S. A., & Portincasa, P. (2017). Gallbladder disease: Relevance of oxidative stress. In *Gastrointestinal Tissue* (pp. 187-194). Elsevier.

Grauso, M., Lan, A., Andriamihaja, M., Bouillaud, F., & Blachier, F. (2019). Hyperosmolar environment and intestinal epithelial cells: impact on mitochondrial oxygen consumption, proliferation, and barrier function in vitro. *Sci Rep*, *9*(1), 11360. https://doi.org/10.1038/s41598-019-47851-9

Grieve, I. C., Dickens, N. J., Pravenec, M., Kren, V., Hubner, N., Cook, S. A.,…Mangion, J. (2008). Genome-wide co-expression analysis in multiple tissues. *PLoS ONE*, *3*(12), e4033. https://doi.org/10.1371/journal.pone.0004033

Guan, L., Cao, Z., Pan, Z., Zhao, C., Xue, M., Yang, F., & Chen, J. (2023). Butyrate promotes C2C12 myoblast proliferation by activating ERK/MAPK pathway. *Molecular Omics*, *19*(7), 552-559.

Guo, G., Wu, Y., Liu, Y., Wang, Z., Xu, G., Wang, X.,…Zhu, Q. (2023). Exploring the causal effects of the gut microbiome on serum lipid levels: A two-sample Mendelian randomization analysis. *Frontiers in microbiology*, *14*, 1113334.

Gupta, V. A., & Beggs, A. H. (2014). Kelch proteins: emerging roles in skeletal muscle development and diseases. *Skelet Muscle*, *4*(1), 11. https://doi.org/10.1186/2044-5040-4-11

Gupta, V. A., Ravenscroft, G., Shaheen, R., Todd, E. J., Swanson, L. C., Shiina, M.,…Darras, B. T. (2013). Identification of KLHL41 mutations implicates BTB-Kelch-mediated ubiquitination as an alternate pathway to myofibrillar disruption in nemaline myopathy. *The American Journal of Human Genetics*, *93*(6), 1108-1117.

Gutiérrez-Luna, F. M., Hernández-Domínguez, E. E., Valencia-Turcotte, L. G., & Rodríguez-Sotres, R. (2018). "Pyrophosphate and pyrophosphatases in plants, their involvement in stress responses and their possible relationship to secondary metabolism". *Plant Science*, *267*, 11-19.

Guyomard, R., Boussaha, M., Krieg, F., Hervet, C., & Quillet, E. (2012). A synthetic rainbow trout linkage map provides new insights into the salmonid whole genome duplication and the conservation of synteny among teleosts. *BMC genetics*, *13*, 1-12.

Haffray, P., Enez, F., Bugeon, J., Chapuis, H., Dupont-Nivet, M., Chatain, B., & Vandeputte, M. (2018). Accuracy of BLUP breeding values in a factorial mating design with mixed families and marker-based parentage assignment in rainbow trout Oncorhynchus mykiss. *Aquaculture*, *490*, 350-354.

Hanan, T., & Shaklai, N. (1995). Peroxidative interaction of myoglobin and myosin. *Eur J Biochem*, *233*(3), 930-936. https://doi.org/10.1111/j.1432-1033.1995.930_3.x

Hardy, R., Torrissen, O., & Scott, T. (1990). Absorption and distribution of 14C-labeled canthaxanthin in rainbow trout (Oncorhynchus mykiss). *Aquaculture*, *87*(3-4), 331-340.

Harlioglu, A. G. (2012). Fatty acid composition, fat soluble vitamins and cholesterol content of farmed rainbow trout (Oncorhynchus mykiss). *Pakistan Journal of Zoology*, *44*(4).

Harrigan, J. A., Jacq, X., Martin, N. M., & Jackson, S. P. (2018). Deubiquitylating enzymes and drug discovery: emerging opportunities. *Nat Rev Drug Discov*, *17*(1), 57-78. https://doi.org/10.1038/nrd.2017.152

Harrison, E. H. (2012). Mechanisms involved in the intestinal absorption of dietary vitamin A and provitamin A carotenoids. *Biochimica et Biophysica Acta (BBA)-Molecular and Cell Biology of Lipids*, *1821*(1), 70-77.

Hayashi, H., Inamura, K., Aida, K., Naoi, S., Horikawa, R., Nagasaka, H.,…Sugiyama, Y. (2012). AP2 adaptor complex mediates bile salt export pump internalization and modulates its hepatocanalicular expression and transport function. *Hepatology*, *55*(6), 1889-1900. https://doi.org/10.1002/hep.25591

Hayes, B., & Goddard, M. (2010). Genome-wide association and genomic selection in animal breeding. *Genome*, *53*(11), 876-883.

He, L., & Hannon, G. J. (2004). MicroRNAs: small RNAs with a big role in gene regulation. *Nat Rev Genet*, *5*(7), 522-531. https://doi.org/10.1038/nrg1379

He, S., Ran, C., Qin, C., Li, S., Zhang, H., De Vos, W. M.,…Zhou, Z. (2017). Anti-infective effect of adhesive probiotic Lactobacillus in fish is correlated with their spatial distribution in the intestinal tissue. *Scientific reports*, *7*(1), 1-12.

Heider, S. A., Peters-Wendisch, P., & Wendisch, V. F. (2012). Carotenoid biosynthesis and overproduction in Corynebacterium glutamicum. *BMC microbiology*, *12*, 1-11.

Heincke, F. (1908). *Bericht über die Untersuchungen der Biologischen Anstalt auf Helgoland zur Naturgeschichte der Nutzfische (1. April 1905 bis 1. Oktober 1907)*.

Helgeland, H., Sodeland, M., Zoric, N., Torgersen, J. S., Grammes, F., von Lintig, J.,…Vage, D. I. (2019). Genomic and functional gene studies suggest a key role of beta-carotene oxygenase 1 like (bco1l) gene in salmon flesh color. *Sci Rep*, *9*(1), 20061. https://doi.org/10.1038/s41598-019-56438-3

Helgeland, H., Sodeland, M., Zoric, N., Torgersen, J. S., Grammes, F., von Lintig, J.,…Våge, D. I. (2019). Genomic and functional gene studies suggest a key role of beta-carotene oxygenase 1 like (bco1l) gene in salmon flesh color. *Scientific reports*, *9*(1), 1-12.

Henderson, C. (1975). Use of all relatives in intraherd prediction of breeding values and producing abilities. *Journal of Dairy Science*, *58*(12), 1910-1916.

Henry, L. P., Bruijning, M., Forsberg, S. K., & Ayroles, J. F. (2021). The microbiome extends host evolutionary potential. *Nature communications*, *12*(1), 5141.

Hessel, S., Eichinger, A., Isken, A., Amengual, J., Hunzelmann, S., Hoeller, U.,…Wyss, A. (2007). CMO1 deficiency abolishes vitamin A production from beta-carotene and alters lipid metabolism in mice. *J Biol Chem*, *282*(46), 33553-33561. https://doi.org/10.1074/jbc.M706763200

Hill, G. E. (1999). Is there an immunological cost to carotenoid-based ornamental coloration? *The American Naturalist*, *154*(5), 589-595.

Hirota, K., Aino, K., Nodasaka, Y., & Yumoto, I. (2013). Oceanobacillus indicireducens sp. nov., a facultative alkaliphile that reduces an indigo dye. *International Journal of Systematic and Evolutionary Microbiology*, *63*(Pt_4), 1437-1442.

Hofer, A. (1998). Variance component estimation in animal breeding: a review. *Journal of Animal Breeding and Genetics*, *115*(1-6), 247-265.

Hollander, D., & Ruble Jr, P. E. (1978). beta-carotene intestinal absorption: bile, fatty acid, pH, and flow rate effects on transport. *American Journal of Physiology-Endocrinology and Metabolism*, *235*(6), E686.

Hong, L., Xu, D., Li, W., Wang, Y., Cao, N., Fu, X.,…Li, B. (2024). Non-coding RNA regulation of Magang geese skeletal muscle maturation via the MAPK signaling pathway. *Frontiers in Physiology*, *14*, 1331974.

Hou, Z. S., Xin, Y. R., Zeng, C., Zhao, H. K., Tian, Y., Li, J. F., & Wen, H. S. (2020). GHRH-SST-GH-IGF axis regulates crosstalk between growth and immunity in rainbow trout (Oncorhynchus mykiss) infected with Vibrio anguillarum [Article]. *Fish and Shellfish Immunology*, *106*, 887-897. https://doi.org/10.1016/j.fsi.2020.08.037

Hu, G., Gu, W., Bai, Q. L., & Wang, B. Q. (2013). Estimation of genetic parameters for growth traits in a breeding program for rainbow trout (Oncorhynchus mykiss) in China [Article]. *Genetics and Molecular Research*, *12*(2), 1457-1467. https://doi.org/10.4238/2013.April.26.7

Huang, Y., Li, J., Li, W., & Han, F. (2024). Integrative GWAS and eQTL analysis identifies genes associated with resistance to Vibrio harveyi infection in yellow drum (Nibea albiflora). *Frontiers in Marine Science*, *11*, 1435469.

Huang, Y., Zhang, L., Wang, G., & Huang, S. (2022). De novo assembly transcriptome analysis reveals the genes associated with body color formation in the freshwater ornamental shrimps Neocaridina denticulate sinensis. *Gene*, *806*, 145929. https://doi.org/10.1016/j.gene.2021.145929

Hughes, J., Oiseth, S., Purslow, P., & Warner, R. (2014). A structural approach to understanding the interactions between colour, water-holding capacity and tenderness. *Meat science*, *98*(3), 520-532.

Ibtisham, F., Zhang, L., Xiao, M., An, L., Ramzan, M. B., Nawab, A.,…Xu, Y. (2017). Genomic selection and its application in animal breeding. *The Thai Journal of Veterinary Medicine*, *47*(3), 301.

Ichiyama, S., Shimokata, K., & Tsukamura, M. (1988). Relationship between mycobacterial species and their carotenoid pigments. *Microbiology and immunology*, *32*(5), 473-479.

Jami, E., White, B. A., & Mizrahi, I. (2014). Potential role of the bovine rumen microbiome in modulating milk composition and feed efficiency. *PloS one*, *9*(1), e85423.

Janssens, V., & Goris, J. (2001). Protein phosphatase 2A: a highly regulated family of serine/threonine phosphatases implicated in cell growth and signalling. *Biochemical Journal*, *353*(3), 417-439.

Jewell, K. A., McCormick, C. A., Odt, C. L., Weimer, P. J., & Suen, G. (2015). Ruminal bacterial community composition in dairy cows is dynamic over the course of two lactations and correlates with feed efficiency. *Applied and environmental microbiology*, *81*(14), 4697-4710.

Jia, W., Zhang, R., Liu, L., Zhu, Z., Xu, M., & Shi, L. (2021). Molecular mechanism of protein dynamic change for Hengshan goat meat during freezing storage based on high-throughput proteomics. *Food Research International*, *143*, 110289.

Jia, X., Veiseth-Kent, E., Grove, H., Kuziora, P., Aass, L., Hildrum, K., & Hollung, K. (2009). Peroxiredoxin-6—a potential protein marker for meat tenderness in bovine longissimus thoracis muscle. *Journal of Animal Science*, *87*(7), 2391-2399.

Jlali, M., Graulet, B., Chauveau-Duriot, B., Chabault, M., Godet, E., Leroux, S.,…Berri, C. (2012). A mutation in the promoter of the chicken β, β-carotene 15, 15'-monooxygenase 1 gene alters xanthophyll metabolism through a selective effect on its mRNA abundance in the breast muscle. *Journal of animal science*, *90*(12), 4280-4288.

Jlali, M., Graulet, B., Chauveau-Duriot, B., Godet, E., Praud, C., Nunes, C. S.,…Duclos, M. J. (2014). Nutrigenetics of carotenoid metabolism in the chicken: a polymorphism at the β, β-carotene 15, 15'-mono-oxygenase 1 (BCMO1) locus affects the response to dietary β-carotene. *British journal of nutrition*, *111*(12), 2079-2088.

Johnston, I. A., Bower, N. I., & Macqueen, D. J. (2011). Growth and the regulation of myotomal muscle mass in teleost fish. *Journal of Experimental Biology*, *214*(10), 1617-1628.

Jones, J., Reinke, S. N., Ali, A., Palmer, D. J., & Christophersen, C. T. (2021). Fecal sample collection methods and time of day impact microbiome composition and short chain fatty acid concentrations. *Scientific reports*, *11*(1), 13964.

Joseph, P., Suman, S. P., Li, S., Beach, C. M., Steinke, L., & Fontaine, M. (2010). Characterization of bison (Bison bison) myoglobin. *Meat Sci*, *84*(1), 71-78. https://doi.org/10.1016/j.meatsci.2009.08.014

Joseph, P., Suman, S. P., Rentfrow, G., Li, S., & Beach, C. M. (2012). Proteomics of muscle-specific beef color stability. *J Agric Food Chem*, *60*(12), 3196-3203. https://doi.org/10.1021/jf204188v

Juanchich, A., Bardou, P., Rue, O., Gabillard, J. C., Gaspin, C., Bobe, J., & Guiguen, Y. (2016). Characterization of an extensive rainbow trout miRNA transcriptome by next generation sequencing. *BMC genomics*, *17*(1), 164. https://doi.org/10.1186/s12864-016-2505-9

Kah, O., Trudeau, V. L., Sloley, B. D., Chang, J. P., Dubourg, P., Yu, K. L., & Peter, R. E. (1992). Influence of GABA on gonadotrophin release in the goldfish. *Neuroendocrinology*, *55*(4), 396-404.

Kanamoto, H., Nakamura, K., & Misawa, N. (2021). Carotenoid production in oleaginous yeasts. *Carotenoids: Biosynthetic and Biofunctional Approaches*, 153-163.

Karami, A., Kania, P., Al-Jubury, A., Stefanova, D., Krych, L., Madsen, L.,…Buchmann, K. (2025). Gut microbiota in rainbow trout Oncorhynchus mykiss with different susceptibility to Flavobacterium psychrophilum infection. *Aquaculture*, *596*, 741841.

Kaulmann, A., & Bohn, T. (2014). Carotenoids, inflammation, and oxidative stress—implications of cellular signaling pathways and relation to chronic disease prevention. *Nutrition research*, *34*(11), 907-929.

Kaźmierczuk, A., & Kiliańska, Z. M. (2009). Plejotropowa aktywność białek szoku cieplnego The pleiotropic activity of heat-shock proteins. *Postepy Hig Med Dosw.(online)*, *63*, 502-521.

Khanal, P., Maltecca, C., Schwab, C., Fix, J., Bergamaschi, M., & Tiezzi, F. (2020a). Modeling host-microbiome interactions for the prediction of meat quality and carcass composition traits in swine. *Genetics Selection Evolution*, *52*, 1-13.

Khanal, P., Maltecca, C., Schwab, C., Fix, J., Bergamaschi, M., & Tiezzi, F. (2020b). Modeling host-microbiome interactions for the prediction of meat quality and carcass composition traits in swine. *Genetics Selection Evolution*, *52*(1), 1-13.

Kiessling, A., Espe, M., Ruohonen, K., & Mørkøre, T. (2004). Texture, gaping and colour of fresh and frozen Atlantic salmon flesh as affected by pre-slaughter iso-eugenol or CO2 anaesthesia. *Aquaculture*, *236*(1-4), 645-657.

Kim, J. M., Santure, A., Barton, H. J., Quinn, J., Cole, E. F., Consortium, G. T. H.,…van Oers, K. (2018). A high-density SNP chip for genotyping great tit (Parus major) populations and its application to studying the genetic architecture of exploration behaviour. *Molecular Ecology Resources*, *18*(4), 877-891.

Klassen, J. L. (2018). Defining microbiome function. *Nature microbiology*, *3*(8), 864-869.

Kobayashi, T., Winslow, S., Sunesson, L., Hellman, U., & Larsson, C. (2012). PKCα binds G3BP2 and regulates stress granule formation following cellular stress. *PloS one*, *7*(4), e35820.

Kong, H. R., Anthony, N. B., Rowland, K. C., Khatri, B., & Kong, B. C. (2018). Genome re-sequencing to identify single nucleotide polymorphism markers for muscle color traits in broiler chickens. *Asian-Australas J Anim Sci*, *31*(1), 13-18. https://doi.org/10.5713/ajas.17.0479

Koopaee, H. K., & Koshkoiyeh, A. E. (2014). SNPs Genotyping technologies and their applications in farm animals breeding programs. *Brazilian Archives of Biology and Technology*, *57*, 87-95.

Kruuk, L. E., & Hadfield, J. D. (2007). How to separate genetic and environmental causes of similarity between relatives. *Journal of evolutionary biology*, *20*(5), 1890-1903.

Krämer, A., Green, J., Pollard Jr, J., & Tugendreich, S. (2014). Causal analysis approaches in ingenuity pathway analysis. *Bioinformatics*, *30*(4), 523-530.

Kumar, S., Sandell, L. L., Trainor, P. A., Koentgen, F., & Duester, G. (2012). Alcohol and aldehyde dehydrogenases: retinoid metabolic effects in mouse knockout models. *Biochimica et Biophysica Acta (BBA)-Molecular and Cell Biology of Lipids*, *1821*(1), 198-205.

Kumari, S., Rajarani, A., Bansal, N., Dahuja, A., Praveen, S., Krishnan, V., & Kumar, S. (2019). Extraction and estimation of provitamin A carotenoids from carrot. *Omics meet Plant Biochemistry: Applications in nutritional enhancement with one health perspective*, *221*.

Kurilshikov, A., Wijmenga, C., Fu, J., & Zhernakova, A. (2017). Host genetics and gut microbiome: challenges and perspectives. *Trends in immunology*, *38*(9), 633-647.

Kutter, C., & Svoboda, P. (2008). miRNA, siRNA, piRNA: Knowns of the unknown. In: Taylor & Francis.

Kwon, H.-S., Lee, H.-S., Rubin, J., & Tomarev, S. (2008). Myocilin May Regulate Actin Cytoskeleton Through Components of Wnt Signaling Pathway. *Investigative Ophthalmology & Visual Science*, *49*(13), 5111-5111.

Lakamp, A. Breeding for the Little Things: A Look at Including Microbiome Information in Animal Breeding.

Lakshman, M., Asher, K., Attlesey, M., Satchithanandam, S., Mychkovsky, I., & Coutlakis, P. (1989). Absorption, storage, and distribution of beta-carotene in normal and beta-carotene-fed rats: roles of parenchymal and stellate cells. *Journal of Lipid Research*, *30*(10), 1545-1550.

Lam, S., Miglior, F., Fonseca, P., Gómez-Redondo, I., Zeidan, J., Suárez-Vega, A.,…Stothard, P. (2021). Identification of functional candidate variants and genes for feed efficiency in Holstein and Jersey cattle breeds using RNA-sequencing. *Journal of dairy science*, *104*(2), 1928-1950.

Langmead, B., & Salzberg, S. L. (2012). Fast gapped-read alignment with Bowtie 2. *Nature methods*, *9*(4), 357-359.

Laplante, M., & Sabatini, D. (2012). mTOR signaling. Cold Spring Harb Perspect Biol 4: a011593. In.

Le Bihan-Duval, E., Nadaf, J., Berri, C., Pitel, F., Graulet, B., Godet, E.,…Duby, C. (2011). Detection of a Cis eQTL controlling BMCO1 gene expression leads to the identification of a QTG for chicken breast meat color. *PLoS One*, *6*(7), e14825.

Le Bras, Y., Dechamp, N., Montfort, J., Le Cam, A., Krieg, F., Quillet, E.,…Le Roy, P. (2010). Acclimation to seawater in rainbow trout: a QTL/eQTL approach. 9. World Congress on Genetics Applied to Livestock Production,

Leandro, J., & Houten, S. M. (2020). The lysine degradation pathway: Subcellular compartmentalization and enzyme deficiencies. *Molecular Genetics and Metabolism*, *131*(1-2), 14-22.

LeBlanc, F., Laflamme, M., & Gagne, N. (2010). Genetic markers of the immune response of Atlantic salmon (Salmo salar) to infectious salmon anemia virus (ISAV). *Fish & Shellfish Immunology*, *29*(2), 217-232.

Lee, J., Godon, C., Lagniel, G., Spector, D., Garin, J., Labarre, J., & Toledano, M. B. (1999). Yap1 and Skn7 control two specialized oxidative stress response regulons in yeast. *J Biol Chem*, *274*(23), 16040-16046. https://doi.org/10.1074/jbc.274.23.16040

Lee, S., Park, J., Jang, J.-K., Lee, B.-H., & Park, Y.-S. (2019). Structural analysis of gluco-oligosaccharides produced by Leuconostoc lactis and their prebiotic effect. *Molecules*, *24*(21), 3998.

Lee, T. T., Ciou, J. Y., Chen, C. L., & Yu, B. (2013). Effect of Echinacea purpurea L. on oxidative status and meat quality in Arbor Acres broilers. *J Sci Food Agric*, *93*(1), 166-172. https://doi.org/10.1002/jsfa.5745

Leeds, T. D., Vallejo, R. L., Weber, G. M., Gonzalez-Pena, D., & Silverstein, J. T. (2016). Response to five generations of selection for growth performance traits in rainbow trout (Oncorhynchus mykiss). *Aquaculture*, *465*, 341-351.

Leeds, T. D., & Weber, G. M. (2019). Effects of triploidy on genetic gains in a rainbow trout (Oncorhynchus mykiss) population selectively bred for diploid growth performance. *Aquaculture*, *505*, 481-487.

Legarra, A., Aguilar, I., & Misztal, I. (2009). A relationship matrix including full pedigree and genomic information. *J Dairy Sci*, *92*(9), 4656-4663. https://doi.org/10.3168/jds.2009-2061

Lehnert, S. J. (2016). *Why are salmon red? Proximate and ultimate causes of flesh pigmentation in Chinook salmon* University of Windsor (Canada)].

Lei, C., Li, J., Zheng, Z., Du, X., & Deng, Y. (2019). Molecular cloning, expression pattern of beta-carotene 15,15-dioxygenase gene and association analysis with total carotenoid content in pearl oyster Pinctada fucata martensii. *Comp Biochem Physiol B Biochem Mol Biol*, *229*, 34-41. https://doi.org/10.1016/j.cbpb.2018.11.006

Leonardi, R., Zhang, Y.-M., Rock, C. O., & Jackowski, S. (2005). Coenzyme A: back in action. *Progress in lipid research*, *44*(2-3), 125-153.

Li, G., Martínez-Bonet, M., Wu, D., Yang, Y., Cui, J., Nguyen, H. N.,…Westra, H.-J. (2018). High-throughput identification of noncoding functional SNPs via type IIS enzyme restriction. *Nature genetics*, *50*(8), 1180-1188.

Li, H., Jiang, K., Wang, S., Liu, X., Kang, X., Jiang, R.,…Sun, G. (2015). Assessment of correlation between pre-miRNA-1757 polymorphism and chicken performance traits. *Genetics and Molecular Research*, *14*(4), 12184-12195.

Li, X., Wang, S., Xun, X., Zhang, M., Wang, S., Li, H.,…Li, T. (2019). A carotenoid oxygenase is responsible for muscle coloration in scallop. *Biochimica et Biophysica Acta (BBA)-Molecular and Cell Biology of Lipids*, *1864*(7), 966-975.

Li, Y., Sidore, C., Kang, H. M., Boehnke, M., & Abecasis, G. R. (2011). Low-coverage sequencing: implications for design of complex trait association studies. *Genome research*, *21*(6), 940-951.

Liang, J. Q., Li, T., Nakatsu, G., Chen, Y.-X., Yau, T. O., Chu, E.,…Chan, F. K. (2020). A novel faecal Lachnoclostridium marker for the non-invasive diagnosis of colorectal adenoma and cancer. *Gut*, *69*(7), 1248-1257.

Lietz, G., Oxley, A., Leung, W., & Hesketh, J. (2012). Single nucleotide polymorphisms upstream from the beta-carotene 15,15'-monoxygenase gene influence provitamin A conversion efficiency in female volunteers. *J Nutr*, *142*(1), 161S-165S. https://doi.org/10.3945/jn.111.140756

Lima, V. C., Rosen, R. B., & Farah, M. (2016). Macular pigment in retinal health and disease. *International journal of retina and vitreous*, *2*(1), 1-9.

Lin, D., & Medeiros, D. M. (2023). The microbiome as a major function of the gastrointestinal tract and its implication in micronutrient metabolism and chronic diseases. *Nutrition Research*.

Lin, H., & Peddada, S. D. (2020). Analysis of microbial compositions: a review of normalization and differential abundance analysis. *NPJ biofilms and microbiomes*, *6*(1), 60.

Liu, F., Dai, R., Zhu, J., & Li, X. (2010). Optimizing color and lipid stability of beef patties with a mixture design incorporating with tea catechins, carnosine, and α-tocopherol. *Journal of Food Engineering*, *98*(2), 170-177.

Liu, S., Gao, G., Layer, R. M., Thorgaard, G. H., Wiens, G. D., Leeds, T. D.,…Palti, Y. (2021). Identification of high-confidence structural variants in domesticated rainbow trout using whole-genome sequencing. *Frontiers in Genetics*, *12*, 639355.

Liu, S., Gao, G., Palti, Y., Cleveland, B. M., Weber, G. M., & Rexroad III, C. E. (2014). RNA-seq analysis of early hepatic response to handling and confinement stress in rainbow trout. *Plos one*, *9*(2), e88492.

Liu, S., Martin, K. E., Snelling, W. M., Long, R., Leeds, T. D., Vallejo, R. L.,…Palti, Y. (2024). Accurate genotype imputation from low-coverage whole-genome sequencing data of rainbow trout. *G3: Genes, Genomes, Genetics*, *14*(9), jkae168.

Liu, S., Vallejo, R. L., Evenhuis, J. P., Martin, K. E., Hamilton, A., Gao, G.,…Palti, Y. (2018). Retrospective evaluation of marker-assisted selection for resistance to bacterial cold water disease in three generations of a commercial rainbow trout breeding population. *Frontiers in genetics*, *9*, 374762.

Liu, X., Liu, Y., Jiang, Y., Zou, L., Liu, K., Liu, M.,…Chen, F. (2020). Homo-oxidized HSPB1 protects cardiomyocytes against oxidative stress via targeting Keap1/Nrf-2 signaling pathway. *Journal of Molecular and Cellular Cardiology*, *140*, 37-38.

Liu, X., Xiao, W., Jiang, Y., Zou, L., Chen, F., Xiao, W.,…Zhu, Y. (2021). Bmal1 Regulates the Redox Rhythm of HSPB1, and Homooxidized HSPB1 Attenuates the Oxidative Stress Injury of Cardiomyocytes. *Oxid Med Cell Longev*, *2021*, 5542815. https://doi.org/10.1155/2021/5542815

Liu, Y., Du, M., Li, X., Chen, L., Shen, Q., Tian, J., & Zhang, D. (2016). Role of the ubiquitin-proteasome pathway on proteolytic activity in postmortem proteolysis and tenderisation of sheep skeletal muscle. *International Journal of Food Science & Technology*, *51*(11), 2353-2359.

Long, T., Liu, Y., Qin, Y., DeBose-Boyd, R. A., & Li, X. (2021). Structures of dimeric human NPC1L1 provide insight into mechanisms for cholesterol absorption. *Science Advances*, *7*(34), eabh3997.

Lozano, G. A. (1994). Carotenoids, parasites, and sexual selection. *Oikos*, 309-311.

Lu, J., Breitwieser, F. P., Thielen, P., & Salzberg, S. L. (2017). Bracken: estimating species abundance in metagenomics data. *PeerJ Computer Science*, *3*, e104.

Lubzens, E., Lissauer, L., Levavi-Sivan, B., Avarre, J.-C., & Sammar, M. (2003). Carotenoid and retinoid transport to fish oocytes and eggs: what is the role of retinol binding protein? *Molecular aspects of medicine*, *24*(6), 441-457.

Lundquist, M. R., Storaska, A. J., Liu, T.-C., Larsen, S. D., Evans, T., Neubig, R. R., & Jaffrey, S. R. (2014). Redox modification of nuclear actin by MICAL-2 regulates SRF signaling. *Cell*, *156*(3), 563-576.

Luo, W., Lin, S., Li, G., Nie, Q., & Zhang, X. (2016). Integrative analyses of miRNA-mRNA interactions reveal let-7b, miR-128 and MAPK pathway involvement in muscle mass loss in sex-linked dwarf chickens. *International journal of molecular sciences*, *17*(3), 276.

Luo, Z. (1992). Computing inbreeding coefficients in large populations. *Genetics Selection Evolution*, *24*(4), 305-313.

Luo, Z., Yu, Y., Xiang, J., & Li, F. (2021). Genomic selection using a subset of SNPs identified by genome-wide association analysis for disease resistance traits in aquaculture species. *Aquaculture*, *539*, 736620.

Luther, J., Ubieta, K., Hannemann, N., Jimenez, M., Garcia, M., Zech, C.,…Bozec, A. (2014). Fra-2/AP-1 controls adipocyte differentiation and survival by regulating PPARγ and hypoxia. *Cell Death & Differentiation*, *21*(4), 655-664.

Madaro, A., Torrissen, O., Whatmore, P., Lall, S. P., Schmeisser, J., Verlhac Trichet, V., & Olsen, R. E. (2020). Red and White Chinook Salmon (Oncorhynchus tshawytscha): differences in the transcriptome profile of muscle, liver, and pylorus. *Marine Biotechnology*, *22*(4), 581-593.

Mancini, R. A., & Ramanathan, R. (2014). Effects of postmortem storage time on color and mitochondria in beef. *Meat Sci*, *98*(1), 65-70. https://doi.org/10.1016/j.meatsci.2014.04.007

Manor, M. L., Cleveland, B. M., Weber, G. M., & Kenney, P. B. (2015). Effects of sexual maturation and feeding level on fatty acid metabolism gene expression in muscle, liver, and visceral adipose tissue of diploid and triploid rainbow trout, Oncorhynchus mykiss. *Comparative Biochemistry and Physiology Part B: Biochemistry and Molecular Biology*, *179*, 17-26.

Mansfield, G. S., Desai, A. R., Nilson, S. A., Van Kessel, A. G., Drew, M. D., & Hill, J. E. (2010). Characterization of rainbow trout (Oncorhynchus mykiss) intestinal microbiota and inflammatory marker gene expression in a recirculating aquaculture system. *Aquaculture*, *307*(1-2), 95-104.

Marancik, D., Gao, G., Paneru, B., Ma, H., Hernandez, A. G., Salem, M.,…Wiens, G. D. (2015). Whole-body transcriptome of selectively bred, resistant-, control-, and susceptible-line rainbow trout following experimental challenge with Flavobacterium psychrophilum. *Frontiers in genetics*, *5*, 453.

Martin, M. (2011). Cutadapt removes adapter sequences from high-throughput sequencing reads. *EMBnet. journal*, *17*(1), 10-12.

Matthews, S. J., Ross, N. W., Lall, S. P., & Gill, T. A. (2006). Astaxanthin binding protein in Atlantic salmon. *Comp Biochem Physiol B Biochem Mol Biol*, *144*(2), 206-214. https://doi.org/10.1016/j.cbpb.2006.02.007

Mañanos, E. L., Anglade, I., Chyb, J., Saligaut, C., Breton, B., & Kah, O. (1999). Involvement of γ-aminobutyric acid in the control of GtH-1 and GtH-2 secretion in male and female rainbow trout. *Neuroendocrinology*, *69*(4), 269-280.

McCormick, R. J. (1999). Extracellular modifications to muscle collagen: implications for meat quality. *Poult Sci*, *78*(5), 785-791. https://doi.org/10.1093/ps/78.5.785

McDermaid, A., Monier, B., Zhao, J., Liu, B., & Ma, Q. (2019). Interpretation of differential gene expression results of RNA-seq data: review and integration. *Briefings in bioinformatics*, *20*(6), 2044-2054.

McGowan, K. A., Li, J. Z., Park, C. Y., Beaudry, V., Tabor, H. K., Sabnis, A. J.,…Myers, R. M. (2008). Ribosomal mutations cause p53-mediated dark skin and pleiotropic effects. *Nature genetics*, *40*(8), 963-970.

McMurdie, P. J., & Holmes, S. (2013). phyloseq: an R package for reproducible interactive analysis and graphics of microbiome census data. *PloS one*, *8*(4), e61217.

Meuwissen, T., Hayes, B., & Goddard, M. (2016). Genomic selection: a paradigm shift in animal breeding. *Animal frontiers*, *6*(1), 6-14.

Meuwissen, T. H., Hayes, B. J., & Goddard, M. (2001). Prediction of total genetic value using genome-wide dense marker maps. *genetics*, *157*(4), 1819-1829.

Michaelson, J. J., Loguercio, S., & Beyer, A. (2009). Detection and interpretation of expression quantitative trait loci (eQTL). *Methods*, *48*(3), 265-276.

Misawa, N., Maoka, T., & Takemura, M. (2022). Carotenoids: Carotenoid and apocarotenoid analysis—Use of E. coli to produce carotenoid standards. In *Methods in Enzymology* (Vol. 670, pp. 87-137). Elsevier.

Misztal, I., Tsuruta, S., Strabel, T., Auvray, B., Druet, T., & Lee, D. (2002). BLUPF90 and related programs (BGF90). Proceedings of the 7th world congress on genetics applied to livestock production,

Mora, L., Gallego, M., Aristoy, M. C., Fraser, P. D., & Toldrá, F. (2015). Peptides naturally generated from ubiquitin-60S ribosomal protein as potential biomarkers of dry-cured ham processing time. *Food Control*, *48*, 102-107.

Morais, P. V., Francisco, R., Branco, R., Chung, A. P., & Da Costa, M. S. (2004). Leucobacter chromiireducens sp. nov, and Leucobacter aridicollis sp. nov., two new species isolated from a chromium contaminated environment. *Systematic and applied microbiology*, *27*(6), 646-652.

Morimoto, R. I. (1998). Regulation of the heat shock transcriptional response: cross talk between a family of heat shock factors, molecular chaperones, and negative regulators. *Genes & development*, *12*(24), 3788-3796.

Mott, A. C., Mott, A., Preuß, S., Bennewitz, J., Tetens, J., & Falker-Gieske, C. (2022). eQTL analysis of laying hens divergently selected for feather pecking identifies KLF14 as a potential key regulator for this behavioral disorder. *Frontiers in genetics*, *13*, 969752.

Mounier, J., Irlinger, F., Leclercq-Perlat, M.-N., Sarthou, A.-S., Spinnler, H.-E., Fitzgerald, G. F., & Cogan, T. M. (2006). Growth and colour development of some surface ripening bacteria with Debaryomyces hansenii on aseptic cheese curd. *Journal of dairy research*, *73*(4), 441-448.

Mukhopadhyay, C., & Kumar, D. (2013). SNP chip development and genome wide association studies in livestock. *Phenomic and genomic tools for analysis of livestock genome*, *66*.

Napoli, J. (2000). Enzymology and biogenesis of retinoic acid. *Vitamin A and retinoids: An update of biological aspects and clinical applications*, 17-27.

Napoli, J. L. (2012). Physiological insights into all-trans-retinoic acid biosynthesis. *Biochimica et Biophysica Acta (BBA)-Molecular and Cell Biology of Lipids*, *1821*(1), 152-167.

Navarrete, P., Magne, F., Araneda, C., Fuentes, P., Barros, L., Opazo, R.,…Romero, J. (2012). PCR-TTGE analysis of 16S rRNA from rainbow trout (Oncorhynchus mykiss) gut microbiota reveals host-specific communities of active bacteria. *PloS one*, *7*(2), e31335.

Nayak, S. K. (2010). Role of gastrointestinal microbiota in fish. *Aquaculture research*, *41*(11), 1553-1573.

Nguyen, C. D., Amoroso, G., Ventura, T., & Elizur, A. (2020). Assessing the pyloric caeca and distal gut microbiota correlation with flesh color in Atlantic salmon (Salmo salar L., 1758). *Microorganisms*, *8*(8), 1244.

Nguyen, C. D., Amoroso, G., Ventura, T., Minich, J. J., & Elizur, A. (2020). Atlantic salmon (Salmo salar L., 1758) gut microbiota profile correlates with flesh pigmentation: cause or effect? *Marine Biotechnology*, *22*, 786-804.

Nickell, D., & Bromage, N. R. (1998). The effect of dietary lipid level on variation of flesh pigmentation in rainbow trout (Oncorhynchus mykiss). *Aquaculture*, *161*(1-4), 237-251.

No, H. K., & Storebakken, T. (1991). Pigmentation of rainbow trout with astaxanthin at different water temperatures. *Aquaculture*, *97*(2-3), 203-216.

Nogal, A., Louca, P., Zhang, X., Wells, P. M., Steves, C. J., Spector, T. D.,…Menni, C. (2021). Circulating levels of the short-chain fatty acid acetate mediate the effect of the gut microbiome on visceral fat. *Frontiers in microbiology*, *12*, 711359.

Nohl, H., Breuninger, V., & Hegner, D. (1978). Influence of mitochondrial radical formation on energy-linked respiration. *Eur J Biochem*, *90*(2), 385-390. https://doi.org/10.1111/j.1432-1033.1978.tb12615.x

Nonhoff, U., Ralser, M., Welzel, F., Piccini, I., Balzereit, D., Yaspo, M.-L.,…Krobitsch, S. (2007). Ataxin-2 interacts with the DEAD/H-box RNA helicase DDX6 and interferes with P-bodies and stress granules. *Molecular biology of the cell*, *18*(4), 1385-1396.

Numa, S., Bortz, W. M., & Lynen, F. (1965). Regulation of fatty acid synthesis at the acetyl-CoA carboxylation step. *Advances in enzyme regulation*, *3*, 407-423.

O'Hara, E., Neves, A. L., Song, Y., & Guan, L. L. (2020). The role of the gut microbiome in cattle production and health: driver or passenger? *Annual review of animal biosciences*, *8*(1), 199-220.

Ogasawara, S., Cheng, X. W., Inoue, A., Hu, L., Piao, L., Yu, C.,…Kuzuya, M. (2018). Cathepsin K activity controls cardiotoxin-induced skeletal muscle repair in mice. *J Cachexia Sarcopenia Muscle*, *9*(1), 160-175. https://doi.org/10.1002/jcsm.12248

Oksanen, J., Blanchet, F. G., Kindt, R., Legendre, P., Minchin, P. R., O'hara, R.,…Wagner, H. (2013). Package 'vegan'. *Community ecology package, version*, *2*(9), 1-295.

Olofsson, S. O., & Boren, J. (2005). Apolipoprotein B: a clinically important apolipoprotein which assembles atherogenic lipoproteins and promotes the development of atherosclerosis. *Journal of internal medicine*, *258*(5), 395-410.

Ong, D. E. (1982). Purification and partial characterization of cellular retinol-binding protein from human liver. *Cancer Research*, *42*(3), 1033-1037.

Opstal, E. J. v., & Bordenstein, S. R. (2015). Rethinking heritability of the microbiome. *Science*, *349*(6253), 1172-1173.

Oren, A. (2010). Industrial and environmental applications of halophilic microorganisms. *Environmental technology*, *31*(8-9), 825-834.

Ottestad, S., Sørheim, O., Heia, K., Skaret, J., & Wold, J. P. (2011). Effects of storage atmosphere and heme state on the color and visible reflectance spectra of salmon (Salmo salar) fillets. *Journal of agricultural and food chemistry*, *59*(14), 7825-7831.

Page, G., & Davies, S. (2003). Hepatic carotenoid uptake in rainbow trout (Oncorhynchus mykiss) using an isolated organ perfusion model. *Aquaculture*, *225*(1-4), 405-419.

Palti, Y., Gao, G., Liu, S., Kent, M., Lien, S., Miller, M.,…Moen, T. (2015). The development and characterization of a 57 K single nucleotide polymorphism array for rainbow trout. *Molecular ecology resources*, *15*(3), 662-672.

Palti, Y., Gao, G., Miller, M. R., Vallejo, R. L., Wheeler, P. A., Quillet, E.,…Rexroad III, C. E. (2014). A resource of single-nucleotide polymorphisms for rainbow trout generated by restriction-site associated DNA sequencing of doubled haploids. *Molecular ecology resources*, *14*(3), 588-596.

Paneru, B., Al-Tobasei, R., Palti, Y., Wiens, G. D., & Salem, M. (2016). Differential expression of long non-coding RNAs in three genetic lines of rainbow trout in response to infection with Flavobacterium psychrophilum. *Scientific reports*, *6*(1), 36032.

Panigrahi, M., Kumar, H., Saravanan, K., Rajawat, D., Nayak, S. S., Ghildiyal, K.,…Dutt, T. (2022). Trajectory of livestock genomics in South Asia: a comprehensive review. *Gene*, *843*, 146808.

Park, J. W. (1994). Functional protein additives in surimi gels. *Journal of Food Science*, *59*(3), 525-527.

Parker, R. S. (1996). Absorption, metabolism, and transport of carotenoids. *The FASEB Journal*, *10*(5), 542-551.

Paulusma, C. C., de Waart, D. R., Kunne, C., Mok, K. S., & Elferink, R. P. O. (2009). Activity of the bile salt export pump (ABCB11) is critically dependent on canalicular membrane cholesterol content. *Journal of biological chemistry*, *284*(15), 9947-9954.

Percie du Sert, N., Hurst, V., Ahluwalia, A., Alam, S., Avey, M. T., Baker, M.,…Dirnagl, U. (2020). The ARRIVE guidelines 2.0: Updated guidelines for reporting animal research. *Journal of Cerebral Blood Flow & Metabolism*, *40*(9), 1769-1777.

Piga, R., van Dartel, D., Bunschoten, A., van der Stelt, I., & Keijer, J. (2014). Role of Frizzled6 in the molecular mechanism of beta-carotene action in the lung. *Toxicology*, *320*, 67-73.

Prakash, P., Liu, C., Hu, K.-Q., Krinsky, N. I., Russell, R. M., & Wang, X.-D. (2004). β-Carotene and β-apo-14'-carotenoic acid prevent the reduction of retinoic acid receptor β in benzo [a] pyrene-treated normal human bronchial epithelial cells. *The Journal of nutrition*, *134*(3), 667-673.

Pérez-Enciso, M., Rincón, J. C., & Legarra, A. (2015). Sequence-vs. chip-assisted genomic selection: accurate biological information is advised. *Genetics Selection Evolution*, *47*, 1-14.

Quince, C., Walker, A. W., Simpson, J. T., Loman, N. J., & Segata, N. (2017). Shotgun metagenomics, from sampling to analysis. *Nature biotechnology*, *35*(9), 833-844.

Rajasingh, H., Øyehaug, L., Våge, D. I., & Omholt, S. W. (2006). Carotenoid dynamics in Atlantic salmon. *Bmc Biology*, *4*(1), 1-15.

Ram, S., Mitra, M., Shah, F., Tirkey, S. R., & Mishra, S. (2020). Bacteria as an alternate biofactory for carotenoid production: A review of its applications, opportunities and challenges. *Journal of Functional Foods*, *67*, 103867.

Ramanathan, R., Nair, M., Hunt, M., & Suman, S. (2019). Mitochondrial functionality and beef colour: A review of recent research. *South African Journal of Animal Science*, *49*(1), 9-19.

Ramazzotti, M., & Bacci, G. (2018). 16S rRNA-based taxonomy profiling in the metagenomics era. In *Metagenomics* (pp. 103-119). Elsevier.

Ramirez-Martinez, A., Cenik, B. K., Bezprozvannaya, S., Chen, B., Bassel-Duby, R., Liu, N., & Olson, E. N. (2017). KLHL41 stabilizes skeletal muscle sarcomeres by nonproteolytic ubiquitination. *Elife*, *6*, e26439. https://doi.org/10.7554/eLife.26439

Rauluseviciute, I., Riudavets-Puig, R., Blanc-Mathieu, R., Castro-Mondragon, J. A., Ferenc, K., Kumar, V.,…Baranasic, D. (2024). JASPAR 2024: 20th anniversary of the open-access database of transcription factor binding profiles. *Nucleic acids research*, *52*(D1), D174-D182.

Ravenscroft, G., Miyatake, S., Lehtokari, V. L., Todd, E. J., Vornanen, P., Yau, K. S.,…Laing, N. G. (2013). Mutations in KLHL40 are a frequent cause of severe autosomal-recessive nemaline myopathy. *Am J Hum Genet*, *93*(1), 6-18. https://doi.org/10.1016/j.ajhg.2013.05.004

Rawls, J. F., Samuel, B. S., & Gordon, J. I. (2004). Gnotobiotic zebrafish reveal evolutionarily conserved responses to the gut microbiota. *Proceedings of the National Academy of Sciences*, *101*(13), 4596-4601.

Ray, A. K., Ghosh, K., & Ringø, E. (2012). Enzyme-producing bacteria isolated from fish gut: a review. *Aquaculture Nutrition*, *18*(5), 465-492.

Raymo, G., Ali, A., Ahmed, R. O., & Salem, M. (2024). Early-Life Fecal Transplantation from High Muscle Yield Rainbow Trout to Low Muscle Yield Recipients Accelerates Somatic Growth through Respiratory and Mitochondrial Efficiency Modulation. *Microorganisms*, *12*(2), 261.

Razin, S., & Hayflick, L. (2010). Highlights of mycoplasma research—an historical perspective. *Biologicals*, *38*(2), 183-190.

Reboul, E. (2019). Mechanisms of carotenoid intestinal absorption: where do we stand? *Nutrients*, *11*(4), 838.

Reboul, E., & Borel, P. (2011). Proteins involved in uptake, intracellular transport and basolateral secretion of fat-soluble vitamins and carotenoids by mammalian enterocytes. *Progress in lipid research*, *50*(4), 388-402.

Reindl, K. M., Kittilson, J. D., Bergan, H. E., & Sheridan, M. A. (2011). Growth hormone-stimulated insulin-like growth factor-1 expression in rainbow trout (oncorhynchus mykiss) hepatocytes is mediated by ERK, PI3K-AKT, and JAK-STAT [Article]. *American Journal of Physiology - Regulatory Integrative and Comparative Physiology*, *301*(1), R236-R243. https://doi.org/10.1152/ajpregu.00414.2010

Reis Neto, R. V., Yoshida, G. M., Lhorente, J. P., & Yáñez, J. M. (2019). Genome-wide association analysis for body weight identifies candidate genes related to development and metabolism in rainbow trout (Oncorhynchus mykiss) [Article]. *Molecular Genetics and Genomics*, *294*(3), 563-571. https://doi.org/10.1007/s00438-018-1518-2

Rescan, P.-Y. (2019). Development of myofibres and associated connective tissues in fish axial muscle: Recent insights and future perspectives. *Differentiation*, *106*, 35-41.

Ringø, E., Salinas, I., Olsen, R., Nyhaug, A., Myklebust, R., & Mayhew, T. (2007). Histological changes in intestine of Atlantic salmon (Salmo salar L.) following in vitro exposure to pathogenic and probiotic bacterial strains. *Cell and tissue research*, *328*, 109-116.

Ringø, E., Strøm, E., & Tabachek, J. A. (1995). Intestinal microflora of salmonids: a review. *Aquaculture research*, *26*(10), 773-789.

Rizal, N. S. M., Neoh, H.-m., Ramli, R., Hanafiah, A., Samat, M. N. A., Tan, T. L.,…Saw, S. H. (2020). Advantages and limitations of 16S rRNA next-generation sequencing for pathogen identification in the diagnostic microbiology laboratory: perspectives from a middle-income country. *Diagnostics*, *10*(10), 816.

Robertson, P., O'Dowd, C., Burrells, C., Williams, P., & Austin, B. (2000). Use of Carnobacterium sp. as a probiotic for Atlantic salmon (Salmo salar L.) and rainbow trout (Oncorhynchus mykiss, Walbaum). *Aquaculture*, *185*(3-4), 235-243.

Rodríguez-Concepción, M. (2010). Supply of precursors for carotenoid biosynthesis in plants. *Archives of Biochemistry and Biophysics*, *504*(1), 118-122.

Rohmer, M. (1999). The discovery of a mevalonate-independent pathway for isoprenoid biosynthesis in bacteria, algae and higher plants. *Natural product reports*, *16*(5), 565-574.

Ross, A. C., & Harrison, E. H. (2007). Vitamin A: nutritional aspects of retinoids and carotenoids. *Handbook of Vitamins, 4th Edition, USA: CRC PressTaylor & Francis Group*.

Ross, E. M., Moate, P. J., Marett, L. C., Cocks, B. G., & Hayes, B. J. (2013). Metagenomic predictions: from microbiome to complex health and environmental phenotypes in humans and cattle. *PloS one*, *8*(9), e73056.

Rossi, R., Arjmand, S., Bærentzen, S. L., Gjedde, A., & Landau, A. M. (2022). Synaptic vesicle glycoprotein 2A: features and functions. *Frontiers in neuroscience*, *16*, 864514.

Rothschild, D., Weissbrod, O., Barkan, E., Kurilshikov, A., Korem, T., Zeevi, D.,…Bar, N. (2018). Environment dominates over host genetics in shaping human gut microbiota. *Nature*, *555*(7695), 210-215.

Rowlerson, A. (2001). Cellular mechanisms of post-embryonic muscle growth in aquaculture species. *Muscle Growth and Development*.

Ruan, J., Xu, J., Chen-Tsai, R. Y., & Li, K. (2017). Genome editing in livestock: Are we ready for a revolution in animal breeding industry? *Transgenic research*, *26*, 715-726.

Rubinacci, S., Hofmeister, R. J., Sousa da Mota, B., & Delaneau, O. (2023). Imputation of low-coverage sequencing data from 150,119 UK Biobank genomes. *Nature Genetics*, *55*(7), 1088-1090.

Ryter, S. W., & Tyrrell, R. M. (2000). The heme synthesis and degradation pathways: role in oxidant sensitivity: heme oxygenase has both pro-and antioxidant properties. *Free Radical Biology and Medicine*, *28*(2), 289-309.

Røsjø, C., Nordrum, S., Olli, J., Krogdahl, Å., Ruyter, B., & Holm, H. (2000). Lipid digestibility and metabolism in Atlantic salmon (Salmo salar) fed medium-chain triglycerides. *Aquaculture*, *190*(1-2), 65-76.

Sablina, A. A., Budanov, A. V., Ilyinskaya, G. V., Agapova, L. S., Kravchenko, J. E., & Chumakov, P. M. (2005). The antioxidant function of the p53 tumor suppressor. *Nat Med*, *11*(12), 1306-1313. https://doi.org/10.1038/nm1320

Saedi, N., Ye, X., Cai, Z., Lund, M. S., & Karaman, E. (2024). Genomic prediction of methane emission using microbiome data and genomic markers in Holstein cows. In *Genomic prediction of methane emission using microbiome data and genomic markers in Holstein cows*.

Salem, M., Al-Tobasei, R., Ali, A., Lourenco, D., Gao, G., Palti, Y.,…Leeds, T. D. (2018). Genome-wide association analysis with a 50K transcribed gene SNP-chip identifies QTL affecting muscle yield in rainbow trout. *Frontiers in genetics*, *9*, 387.

Salem, M., Al-Tobasei, R., Ali, A., Lourenco, D., Gao, G., Palti, Y.,…Leeds, T. D. (2018). Genome-Wide Association Analysis With a 50K Transcribed Gene SNP-Chip Identifies QTL Affecting Muscle Yield in Rainbow Trout. *Front Genet*, *9*, 387. https://doi.org/10.3389/fgene.2018.00387

Salem, M., Vallejo, R. L., Leeds, T. D., Palti, Y., Liu, S., Sabbagh, A.,…Yao, J. (2012). RNA-Seq identifies SNP markers for growth traits in rainbow trout. *PloS one*, *7*(5), e36264.

Sampels, S. (2013). Oxidation and antioxidants in fish and meat from farm to fork. *Food industry*, 114-144.

Sassone-Corsi, P., & Borrelli, E. (1986). Transcriptional regulation by trans-acting factors. *Trends in Genetics*, *2*, 215-219.

Scaife, J., Onibi, G., Murray, I., Fletcher, T., & Houlihan, D. (2000). Influence of a-tocopherol acetate on the short-and long-term storage properties of fillets from Atlantic salmon Salmo salar fed a high lipid diet. *Aquaculture Nutrition*, *6*(1), 65.

Schaeffer, C., Devuyst, O., & Rampoldi, L. (2021). Uromodulin: roles in health and disease. *Annual Review of Physiology*, *83*, 477-501.

Schaid, D. J., Rowland, C. M., Tines, D. E., Jacobson, R. M., & Poland, G. A. (2002). Score tests for association between traits and haplotypes when linkage phase is ambiguous. *The American Journal of Human Genetics*, *70*(2), 425-434.

Schmeisser, J., Verlhac-Trichet, V., Madaro, A., Lall, S. P., Torrissen, O., & Olsen, R. E. (2021). Molecular Mechanism Involved in Carotenoid Metabolism in Post-Smolt Atlantic Salmon: Astaxanthin Metabolism During Flesh Pigmentation and Its Antioxidant Properties. *Marine Biotechnology*, *23*(4), 653-670.

Schröder, J., Maus, I., Trost, E., & Tauch, A. (2011). Complete genome sequence of Corynebacterium variabile DSM 44702 isolated from the surface of smear-ripened cheeses and insights into cheese ripening and flavor generation. *BMC genomics*, *12*(1), 1-23.

Segata, N., Izard, J., Waldron, L., Gevers, D., Miropolsky, L., Garrett, W. S., & Huttenhower, C. (2011). Metagenomic biomarker discovery and explanation. *Genome biology*, *12*, 1-18.

Sellers, J. R. (2000). Myosins: a diverse superfamily. *Biochim Biophys Acta*, *1496*(1), 3-22. https://doi.org/10.1016/s0167-4889(00)00005-7

Semova, I., Carten, J. D., Stombaugh, J., Mackey, L. C., Knight, R., Farber, S. A., & Rawls, J. F. (2012). Microbiota regulate intestinal absorption and metabolism of fatty acids in the zebrafish. *Cell host & microbe*, *12*(3), 277-288.

Seyfert, M., Mancini, R. A., Hunt, M. C., Tang, J., Faustman, C., & Garcia, M. (2006). Color stability, reducing activity, and cytochrome c oxidase activity of five bovine muscles. *J Agric Food Chem*, *54*(23), 8919-8925. https://doi.org/10.1021/jf061657s

Shahidi, F., & Brown, J. A. (1998). Carotenoid pigments in seafoods and aquaculture. *Critical Reveiws in Food Science*, *38*(1), 1-67.

Shao, L., Elujoba-Bridenstine, A., Zink, K. E., Sanchez, L. M., Cox, B. J., Pollok, K. E.,…Cooper, S. H. (2021). The neurotransmitter receptor Gabbr1 regulates proliferation and function of hematopoietic stem and progenitor cells. *Blood, The Journal of the American Society of Hematology*, *137*(6), 775-787.

Sharma, P., Doultani, S., Hadiya, K., George, L., & Highland, H. (2024). Overview of marker-assisted selection in animal breeding. *HISTORY*, *9*, 11.

Shi, J., & Sun, G. (2017). Effect of pre-miRNA-1658 gene polymorphism on chicken growth and carcass traits. *Asian-Australas J Anim Sci*, *30*(4), 455-461. https://doi.org/10.5713/ajas.16.0305

Shindo, K., & Misawa, N. (2014). New and rare carotenoids isolated from marine bacteria and their antioxidant activities. *Marine drugs*, *12*(3), 1690-1698.

Shmarakov, I., Fleshman, M. K., D'Ambrosio, D. N., Piantedosi, R., Riedl, K. M., Schwartz, S. J.,…Harrison, E. H. (2010). Hepatic stellate cells are an important cellular site for β-carotene conversion to retinoid. *Archives of biochemistry and biophysics*, *504*(1), 3-10.

Singh, A., Mittal, A., & Benjakul, S. (2022). Undesirable discoloration in edible fish muscle: Impact of indigenous pigments, chemical reactions, processing, and its prevention. *Comprehensive Reviews in Food Science and Food Safety*, *21*(1), 580-603.

Singmann, H., Bolker, B., Westfall, J., Aust, F., Ben-Shachar, M., Højsgaard, S.,…Love, J. (2015). Package 'afex'. *URL http://afex. Singmann. Science/, https://github. Com/singmann/afex*.

Sinnwell, J. P., Schaid, D. J., Yu, Z., & Sinnwell, M. J. P. (2007). The haplo. stats Package.

Sinnwell, J. P., Therneau, T. M., & Schaid, D. J. (2014). The kinship2 R package for pedigree data. *Human heredity*, *78*(2), 91-93.

Smirnoff, N. (2018). Ascorbic acid metabolism and functions: A comparison of plants and mammals. *Free Radical Biology and Medicine*, *122*, 116-129.

Sousa-Victor, P., Neves, J., & Muñoz-Cánoves, P. (2020). Muscle stem cell aging: identifying ways to induce tissue rejuvenation. *Mechanisms of Ageing and Development*, *188*, 111246.

Spor, A., Koren, O., & Ley, R. (2011). Unravelling the effects of the environment and host genotype on the gut microbiome. *Nature Reviews Microbiology*, *9*(4), 279-290.

Starr, M. P., & Saperstein, S. (1953). Thiamine and the carotenoid pigments of Corynebacterium poinsettiae. *Archives of Biochemistry and Biophysics*, *43*(1), 157-168.

Stofan, M., & Guo, G. L. (2020). Bile Acids and FXR: Novel Targets for Liver Diseases. *Front Med (Lausanne)*, *7*, 544. https://doi.org/10.3389/fmed.2020.00544

Storebakken, T., & No, H. K. (1992). Pigmentation of rainbow trout. *Aquaculture*, *100*(1-3), 209-229.

Sturm, G., Brunner, S., Suvorova, E., Dempwolff, F., Reiner, J., Graumann, P.,…Gescher, J. (2018). Chromate resistance mechanisms in Leucobacter chromiiresistens. *Applied and Environmental Microbiology*, *84*(23), e02208-02218.

Su, I.-C., Su, Y.-K., Chuang, H.-Y., Yadav, V. K., Setiawan, S. A., Fong, I.-H.,…Lin, C.-M. (2022). Ubiquitin-Specific Protease 6 n-Terminal-like Protein (USP6NL) and the Epidermal Growth Factor Receptor (EGFR) signaling axis regulates ubiquitin-mediated DNA repair and temozolomide-resistance in glioblastoma. *Biomedicines*, *10*(7), 1531.

Subramaniyan, S. A., Kang, D. R., Jung, Y. C., Jung, J. H., Choi, Y. I., Lee, M. J.,…Shim, K. S. (2017). Comparative studies of meat quality traits and the proteome profile between low-and high-pH muscles in longissimus dorsi of Berkshire. *Canadian Journal of Animal Science*, *97*(4), 640-649.

Sun, H. (2012). Membrane receptors and transporters involved in the function and transport of vitamin A and its derivatives. *Biochimica et Biophysica Acta (BBA)-Molecular and Cell Biology of Lipids*, *1821*(1), 99-112.

Sánchez, C. C., Smith, T. P., Wiedmann, R. T., Vallejo, R. L., Salem, M., Yao, J., & Rexroad, C. E. (2009). Single nucleotide polymorphism discovery in rainbow trout by deep sequencing of a reduced representation library. *Bmc Genomics*, *10*, 1-8.

Taft, D. H., Ambalavanan, N., Schibler, K. R., Yu, Z., Newburg, D. S., Ward, D. V., & Morrow, A. L. (2014). Intestinal microbiota of preterm infants differ over time and between hospitals. *Microbiome*, *2*, 1-12.

Takahashi, M., Yamashita, K., Shiozawa, A., Ichiishi, A., Fukumori, F., & Fujimura, M. (2010). An AP-1-like transcription factor, NAP-1, regulates expression of the glutathione S-transferase and NADH: flavin oxidoreductase genes in Neurospora crassa. *Bioscience, biotechnology, and biochemistry*, *74*(4), 746-752.

Tan, G., & Lenhard, B. (2016). TFBSTools: an R/bioconductor package for transcription factor binding site analysis. *Bioinformatics*, *32*(10), 1555-1556.

Tan, X., He, Z., Fahey, A. G., Zhao, G., Liu, R., & Wen, J. (2023). Research progress and applications of genome-wide association study in farm animals. *Animal Research and One Health*, *1*(1), 56-77.

Tang, J., Faustman, C., Hoagland, T. A., Mancini, R. A., Seyfert, M., & Hunt, M. C. (2005). Postmortem oxygen consumption by mitochondria and its effects on myoglobin form and stability. *J Agric Food Chem*, *53*(4), 1223-1230. https://doi.org/10.1021/jf048646o

Tapio, I., Snelling, T. J., Strozzi, F., & Wallace, R. J. (2017). The ruminal microbiome associated with methane emissions from ruminant livestock. *Journal of animal science and biotechnology*, *8*, 1-11.

Tapio, M., Fischer, D., Mäntysaari, P., & Tapio, I. (2023). Rumen microbiota predicts feed efficiency of primiparous nordic red dairy cows. *Microorganisms*, *11*(5), 1116.

Tarique, T., Yang, S., Mohsina, Z., Qiu, J., Yan, Z., Chen, G., & Chen, A. (2014). Identification of genes involved in regulatory mechanism of pigments in broiler chickens. *Genetics and Molecular Research*, *13*(3), 7201-7216.

Terra, L. F., Wailemann, R. A., Dos Santos, A. F., Gomes, V. M., Silva, R. P., Laporte, A.,…Lortz, S. (2019). Heat shock protein B1 is a key mediator of prolactin-induced beta-cell cytoprotection against oxidative stress. *Free Radical Biology and Medicine*, *134*, 394-405.

Thomas, A. C. (1999). *Astaxanthin in juvenile farmed Chinook salmon (Oncorhynchus tshawytscha): effective dietary levels for flesh pigmentation and influence on fatty acid profile during cold temperature storage of fillets* University of British Columbia].

Thomas, S. E., & Harrison, E. H. (2016). Mechanisms of selective delivery of xanthophylls to retinal pigment epithelial cells by human lipoproteins. *Journal of lipid research*, *57*(10), 1865-1878.

Thorgaard, G. H., Bailey, G. S., Williams, D., Buhler, D. R., Kaattari, S. L., Ristow, S. S.,…Palti, Y. (2002). Status and opportunities for genomics research with rainbow trout. *Comp Biochem Physiol B Biochem Mol Biol*, *133*(4), 609-646. https://doi.org/10.1016/s1096-4959(02)00167-7

Tian, B., & Hua, Y. (2010). Carotenoid biosynthesis in extremophilic Deinococcus–Thermus bacteria. *Trends in microbiology*, *18*(11), 512-520.

Tigistu-Sahle, F. (2012). Lipidomics for Human Bone Marrow Mesenchymal Stem Cells.

Tintchev, F., Kuhlmann, U., Wackerbarth, H., Töpfl, S., Heinz, V., Knorr, D., & Hildebrandt, P. (2009). Redox processes in pressurised smoked salmon studied by resonance Raman spectroscopy. *Food chemistry*, *112*(2), 482-486.

Torrissen, O. (1995). Strategies for salmonid pigmentation. *Journal of Applied ichthyology*, *11*(3-4), 276-281.

Torrissen, O. J. (1989). Pigmentation of salmonids: interactions of astaxanthin and canthaxanthin on pigment deposition in rainbow trout. *Aquaculture*, *79*(1-4), 363-374.

Torrissen, O. J., & Ingebrigtsen, K. (1992). Tissue distribution of 14C-astaxanthin in the Atlantic salmon (Salmo salar). *Aquaculture*, *108*(3-4), 381-385.

Turchini, G. M., Francis, D. S., Keast, R. S., & Sinclair, A. J. (2011). Transforming salmonid aquaculture from a consumer to a producer of long chain omega-3 fatty acids. *Food Chemistry*, *124*(2), 609-614.

Turner, S. D. (2014). qqman: an R package for visualizing GWAS results using QQ and manhattan plots. *Biorxiv*, 005165.

Tyagi, A., Singh, B., Billekallu Thammegowda, N. K., & Singh, N. K. (2019). Shotgun metagenomics offers novel insights into taxonomic compositions, metabolic pathways and antibiotic resistance genes in fish gut microbiome. *Archives of microbiology*, *201*, 295-303.

Umeno, D., Tobias, A. V., & Arnold, F. H. (2005). Diversifying carotenoid biosynthetic pathways by directed evolution. *Microbiology and molecular biology reviews*, *69*(1), 51-78.

Vala, A. G., Tomar, R., & Rathod, P. J. (2023). Speed Breeding: Accelerating Crop Improvement through Controlled Environments, Genetics, and High-Throughput Phenotyping. *Int J Adv Res Sci Eng Technol*, *10*(5), 746-749.

Vallejo, R. L., Cheng, H., Fragomeni, B. O., Gao, G., Silva, R. M., Martin, K. E.,…Palti, Y. (2021). The accuracy of genomic predictions for bacterial cold water disease resistance remains higher than the pedigree-based model one generation after model training in a commercial rainbow trout breeding population. *Aquaculture*, *545*, 737164.

Vallejo, R. L., Leeds, T. D., Fragomeni, B. O., Gao, G., Hernandez, A. G., Misztal, I.,…Palti, Y. (2016). Evaluation of genome-enabled selection for bacterial cold water disease resistance using progeny performance data in rainbow trout: insights on genotyping methods and genomic prediction models. *Frontiers in genetics*, *7*, 187840.

Vallejo, R. L., Leeds, T. D., Gao, G., Parsons, J. E., Martin, K. E., Evenhuis, J. P.,…Palti, Y. (2017). Genomic selection models double the accuracy of predicted breeding values for bacterial cold water disease resistance compared to a traditional pedigree-based model in rainbow trout aquaculture. *Genetics Selection Evolution*, *49*, 1-13.

Vallejo, R. L., Silva, R. M., Evenhuis, J. P., Gao, G., Liu, S., Parsons, J. E.,…Leeds, T. D. (2018). Accurate genomic predictions for BCWD resistance in rainbow trout are achieved using low-density SNP panels: Evidence that long-range LD is a major contributing factor. *Journal of animal breeding and genetics*, *135*(4), 263-274.

Vallejo, R. L., Silva, R. M. O., Evenhuis, J. P., Gao, G., Liu, S., Parsons, J. E.,…Palti, Y. (2018). Accurate genomic predictions for BCWD resistance in rainbow trout are achieved using low-density SNP panels: Evidence that long-range LD is a major contributing factor. *J Anim Breed Genet*. https://doi.org/10.1111/jbg.12335

Van den Boogaart, K. G., & Tolosana-Delgado, R. (2008). "Compositions": a unified R package to analyze compositional data. *Computers & Geosciences*, *34*(4), 320-338.

VanRaden, P. M. (2008). Efficient methods to compute genomic predictions. *J Dairy Sci*, *91*(11), 4414-4423. https://doi.org/10.3168/jds.2007-0980

Villar, D., Flicek, P., & Odom, D. T. (2014). Evolution of transcription factor binding in metazoans—mechanisms and functional implications. *Nature Reviews Genetics*, *15*(4), 221-233.

Viney, M. E., & Riley, E. M. (2014). From immunology to eco-immunology: more than a new name. *Eco-immunology: evolutive aspects and future perspectives*, 1-19.

Vo, T. T. M., Nguyen, T. V., Amoroso, G., Ventura, T., & Elizur, A. (2021). Deploying new generation sequencing for the study of flesh color depletion in Atlantic Salmon (Salmo salar). *BMC genomics*, *22*(1), 1-21.

von Lintig, J., Moon, J., Lee, J., & Ramkumar, S. (2020). Carotenoid metabolism at the intestinal barrier. *Biochimica et Biophysica Acta (BBA)-Molecular and Cell Biology of Lipids*, *1865*(11), 158580.

Vranová, E., Coman, D., & Gruissem, W. (2013). Network analysis of the MVA and MEP pathways for isoprenoid synthesis. *Annual review of plant biology*, *64*(1), 665-700.

Võsa, U., Claringbould, A., Westra, H.-J., Bonder, M. J., Deelen, P., Zeng, B.,…Yazar, S. (2021). Large-scale cis-and trans-eQTL analyses identify thousands of genetic loci and polygenic scores that regulate blood gene expression. *Nature genetics*, *53*(9), 1300-1310.

Wakchaure, R., Ganguly, S., Praveen, P., Kumar, A., Sharma, S., & Mahajan, T. (2015). Marker assisted selection (MAS) in animal breeding: a review. *J. Drug. Metab. Toxicol*, *6*(5), e127.

Wang, A. R., Ran, C., Ringø, E., & Zhou, Z. G. (2018). Progress in fish gastrointestinal microbiota research. *Reviews in Aquaculture*, *10*(3), 626-640.

Wang, H., Misztal, I., Aguilar, I., Legarra, A., & Muir, W. (2012). Genome-wide association mapping including phenotypes from relatives without genotypes. *Genetics Research*, *94*(2), 73-83.

Wang, L., Babushkin, N., Liu, Z., & Liu, X. (2024). Trans-eQTL mapping in gene sets identifies network effects of genetic variants. *Cell Genomics*, *4*(4).

Wariso, B. A., Kester, A. S., & Thomas, R. D. (2006). Isolation and partial characterization of carotenoid mutants of Corynebacterium poinsettiae ATCC 9682. *Global Journal of Pure and Applied Sciences*, *12*(2), 203-210.

Wasik, K., Berisa, T., Pickrell, J. K., Li, J. H., Fraser, D. J., King, K., & Cox, C. (2021). Comparing low-pass sequencing and genotyping for trait mapping in pharmacogenetics. *BMC genomics*, *22*, 1-7.

Weber, K. L., Welly, B. T., Van Eenennaam, A. L., Young, A. E., Porto-Neto, L. R., Reverter, A., & Rincon, G. (2016). Identification of gene networks for residual feed intake in Angus cattle using genomic prediction and RNA-seq. *PloS one*, *11*(3), e0152274.

Weigel, K., VanRaden, P., Norman, H., & Grosu, H. (2017). A 100-Year Review: Methods and impact of genetic selection in dairy cattle—From daughter–dam comparisons to deep learning algorithms. *Journal of dairy science*, *100*(12), 10234-10250.

Weishaar, R., Wellmann, R., Camarinha-Silva, A., Rodehutscord, M., & Bennewitz, J. (2020). Selecting the hologenome to breed for an improved feed efficiency in pigs—A novel selection index. *Journal of Animal Breeding and Genetics*, *137*(1), 14-22.

Weiss, S., Xu, Z. Z., Peddada, S., Amir, A., Bittinger, K., Gonzalez, A.,…Birmingham, A. (2017). Normalization and microbial differential abundance strategies depend upon data characteristics. *Microbiome*, *5*, 1-18.

Westra, H.-J., & Franke, L. (2014). From genome to function by studying eQTLs. *Biochimica et Biophysica Acta (BBA)-molecular basis of Disease*, *1842*(10), 1896-1902.

Williams, J., & Schneider, J. (2000). Manual of Fisheries Survey Methods II: with periodic updates. *The coefficient of condition of fish. Schneider JC (ed)*.

Wing, S. S., Lecker, S. H., & Jagoe, R. T. (2011). Proteolysis in illness-associated skeletal muscle atrophy: from pathways to networks. *Critical reviews in clinical laboratory sciences*, *48*(2), 49-70.

Wiseman, S., Osachoff, H., Bassett, E., Malhotra, J., Bruno, J., VanAggelen, G.,…Vijayan, M. M. (2007). Gene expression pattern in the liver during recovery from an acute stressor in rainbow trout. *Comparative Biochemistry and Physiology Part D: Genomics and Proteomics*, *2*(3), 234-244.

Wlodarchak, N., & Xing, Y. (2016). PP2A as a master regulator of the cell cycle. *Critical reviews in biochemistry and molecular biology*, *51*(3), 162-184.

Wong, E. S., Schmitt, B. M., Kazachenka, A., Thybert, D., Redmond, A., Connor, F.,…Marioni, J. C. (2017). Interplay of cis and trans mechanisms driving transcription factor binding and gene expression evolution. *Nature communications*, *8*(1), 1092.

Wood, D. E., Lu, J., & Langmead, B. (2019). Improved metagenomic analysis with Kraken 2. *Genome biology*, *20*, 1-13.

Wu, H., Yesilyurt, H. G., Yoon, J., & Terman, J. R. (2018). The MICALs are a family of F-actin dismantling oxidoreductases conserved from Drosophila to humans. *Scientific reports*, *8*(1), 1-20.

Wu, H. J., Seib, K. L., Srikhanta, Y. N., Edwards, J., Kidd, S. P., Maguire, T. L.,…Jennings, M. P. (2010). Manganese regulation of virulence factors and oxidative stress resistance in Neisseria gonorrhoeae. *J Proteomics*, *73*(5), 899-916. https://doi.org/10.1016/j.jprot.2009.12.001

Wu, L., Fan, J., & Belasco, J. G. (2006). MicroRNAs direct rapid deadenylation of mRNA. *Proceedings of the National Academy of Sciences*, *103*(11), 4034-4039.

Wu, W., Gao, X.-G., Dai, Y., Fu, Y., Li, X.-M., & Dai, R.-T. (2015). Post-mortem changes in sarcoplasmic proteome and its relationship to meat color traits in M. semitendinosus of Chinese Luxi yellow cattle. *Food Research International*, *72*, 98-105.

Wu, W., Yu, Q.-Q., Fu, Y., Tian, X.-J., Jia, F., Li, X.-M., & Dai, R.-T. (2016). Towards muscle-specific meat color stability of Chinese Luxi yellow cattle: A proteomic insight into post-mortem storage. *Journal of proteomics*, *147*, 108-118.

Xiang, H., Sun, S., Huang, H., Hao, S., Li, L., Yang, X.,…Pan, C. (2023). Proteomics study of mitochondrial proteins in tilapia red meat and their effect on color change during storage. *Food Chemistry*, *400*, 134061.

Yabuta, S., Masaki, M., & Shidoji, Y. (2016). Associations of Buccal Cell Telomere Length with Daily Intake of beta-Carotene or alpha-Tocopherol Are Dependent on Carotenoid Metabolism-related Gene Polymorphisms in Healthy Japanese Adults. *J Nutr Health Aging*, *20*(3), 267-274. https://doi.org/10.1007/s12603-015-0577-x

Yabuuchi, H., Tanaka, K., Maeda, M., Takemura, M., Oka, M., Ohashi, R., & Tamai, I. (2008). Cloning of the dog bile salt export pump (BSEP; ABCB11) and functional comparison with the human and rat proteins. *Biopharm Drug Dispos*, *29*(8), 441-448. https://doi.org/10.1002/bdd.629

Yan, W., Jang, G.-F., Haeseleer, F., Esumi, N., Chang, J., Kerrigan, M.,…Zack, D. J. (2001). Cloning and characterization of a human β, β-carotene-15, 15′-dioxygenase that is highly expressed in the retinal pigment epithelium. *Genomics*, *72*(2), 193-202.

Yang, T., Wang, Y., Li, H., Shi, F., Xu, S., Wu, Y.,…Jiang, M. (2025). Homeobox C4 transcription factor promotes adipose tissue thermogenesis. *Diabetes*, *74*(4), 472-485.

Yang, X., Wu, S., Hopkins, D. L., Liang, R., Zhu, L., Zhang, Y., & Luo, X. (2018). Proteomic analysis to investigate color changes of chilled beef longissimus steaks held under carbon monoxide and high oxygen packaging. *Meat science*, *142*, 23-31.

Yatsunami, R., Ando, A., Yang, Y., Takaichi, S., Kohno, M., Matsumura, Y.,…Fujita, N. (2014). Identification of carotenoids from the extremely halophilic archaeon Haloarcula japonica. *Frontiers in microbiology*, *5*, 100.

Ye, S., Yuan, X., Lin, X., Gao, N., Luo, Y., Chen, Z.,…Zhang, Z. (2018). Imputation from SNP chip to sequence: a case study in a Chinese indigenous chicken population. *Journal of animal science and biotechnology*, *9*, 1-12.

Yoon, J.-H., Lee, K.-C., Weiss, N., Kang, K. H., & Park, Y.-H. (2003). Jeotgalicoccus halotolerans gen. nov., sp. nov. and Jeotgalicoccus psychrophilus sp. nov., isolated from the traditional Korean fermented seafood jeotgal. *International Journal of Systematic and Evolutionary Microbiology*, *53*(2), 595-602.

Yuan, F. L., Xu, R. S., Ye, J. X., Zhao, M. D., Ren, L. J., & Li, X. (2019). Apoptotic bodies from endplate chondrocytes enhance the oxidative stress-induced mineralization by regulating PPi metabolism. *J Cell Mol Med*, *23*(5), 3665-3675. https://doi.org/10.1111/jcmm.14268

Zeng, B., Lloyd-Jones, L. R., Montgomery, G. W., Metspalu, A., Esko, T., Franke, L.,…Quyyumi, A. A. (2019). Comprehensive multiple eQTL detection and its application to GWAS interpretation. *Genetics*, *212*(3), 905-918.

Zenger, K., Khatkar, M., Jerry, D., & Raadsma, H. (2017). The next wave in selective breeding: implementing genomic selection in aquaculture. Proc. Assoc. Advmt. Anim. Breed. Genet,

Zhang, W., Liu, M., & Dai, X. (2013). Biological characteristics and probiotic effect of Leuconostoc lactis strain isolated from the intestine of black porgy fish. *Brazilian journal of microbiology*, *44*, 685-691.

Zhang, X., & Xie, J. (2019). Analysis of proteins associated with quality deterioration of grouper fillets based on TMT quantitative proteomics during refrigerated storage. *Molecules*, *24*(14), 2641.

Zhang, Y., Johnson, K., Russell, R. G. G., Wordsworth, B. P., Carr, A. J., Terkeltaub, R. A., & Brown, M. A. (2005). Association of sporadic chondrocalcinosis with a− 4-basepair G-to-A transition in the 5′-untranslated region of ANKH that promotes enhanced expression of ANKH protein and excess generation of extracellular inorganic pyrophosphate. *Arthritis & Rheumatism*, *52*(4), 1110-1117.

ZHANG, Y.-m., ZHANG, X.-z., WANG, T.-t., Hopkins, D. L., MAO, Y.-w., LIANG, R.-r.,…ZHU, L.-x. (2018). Implications of step-chilling on meat color investigated using proteome analysis of the sarcoplasmic protein fraction of beef longissimus lumborum muscle. *Journal of Integrative Agriculture*, *17*(9), 2118-2125.

Zheng, Q., Zhang, Y., Chen, Y., Yang, N., Wang, X. J., & Zhu, D. (2009). Systematic identification of genes involved in divergent skeletal muscle growth rates of broiler and layer chickens. *BMC genomics*, *10*(1), 87. https://doi.org/10.1186/1471-2164-10-87

Zheng, X. (2013). A tutorial for the R Package SNPRelate. *University of Washington, Washington, USA*.

Zhu, W., Yang, Z., Ma, Z., & Chai, L. (2008). Reduction of high concentrations of chromate by Leucobacter sp. CRB1 isolated from Changsha, China. *World Journal of Microbiology and Biotechnology*, *24*, 991-996.

Zhu, Z., Zhang, F., Hu, H., Bakshi, A., Robinson, M. R., Powell, J. E.,…Visscher, P. M. (2016). Integration of summary data from GWAS and eQTL studies predicts complex trait gene targets. *Nature genetics*, *48*(5), 481-487.

Ziyada, A. M. A. (2023). *Evaluation of Low Coverage Whole Genome Sequencing Genotype Imputation Strategies* Hamad Bin Khalifa University (Qatar)].

Zoric, N. (2017). Characterization of genes and gene products influencing carotenoid metabolism in Atlantic salmon.

Zychowska, M., Jastrzebski, Z., Chruscinski, G., Michalowska-Sawczyn, M., & Nowak-Zaleska, A. (2015). Vitamin C, A and E supplementation decreases the expression of HSPA1A and HSPB1 genes in the leukocytes of young polish figure skaters during a 10-day training camp. *J Int Soc Sports Nutr*, *12*(1), 9. https://doi.org/10.1186/s12970-015-0069-8

Ługowska, A., Hetmańczyk-Sawicka, K., Iwanicka-Nowicka, R., Fogtman, A., Cieśla, J., Purzycka-Olewiecka, J. K.,…Lualdi, S. (2019). Gene expression profile in patients with Gaucher disease indicates activation of inflammatory processes. *Scientific reports*, *9*(1), 1-14.

Supplementary Files

Supplementary File 1:

Parameters used for the Differential Gene Expression Analyses

Adapter and low-quality reads trimming parameters

Quality trim = Yes, Quality limit = 0.05, Trim adapter list = Illumina_New trim adapter list, Automatic read-through adapter trimming = Yes, Trim homopolymers from 5' = Yes, Trim homopolymers from 3' = Yes, polyA = Yes, polyT = Yes, Remove 5' terminal nucleotides = No, Remove 3' terminal nucleotides = No, Fixed length trimming = No, Maximum length = 150, Trim from side = 3'-end, Discard short reads = No, Discard long reads = No, Save discarded sequences = Yes, Save broken pairs = No, Create report = Yes

Reads Mapping parameters.

Reference type = Genome annotated with genes and transcripts, Reference sequence = GCF_013265735.2_USDA_OmykA_1.1_genomic (Genome), Gene track GCF_013265735.2_USDA_OmykA_1.1_genomic (Gene), mRNA track = GCF_013265735.2_USDA_OmykA_1.1_genomic (mRNA), Use spike-in controls = no, Mismatch cost = 2, Insertion cost = 3, Deletion cost = 3, Length fraction = 0.8, Similarity fraction = 0.8, Global alignment = Yes, Strand specific = Both, Library type = Bulk, Maximum number of hits for a read = 20, Count paired reads as two = No, Ignore broken pairs = No, Expression value = RPKM, Calculate expression for genes without transcripts = Yes, Create reads track = No, Create report = Yes, Create fusion gene table = No, Create list of unmapped reads = No

Muscle Yield Differentially Expressed Genes (DEGs) (First 50):

id	baseMean	log2FoldChange	lfcSE	stat	pvalue	padj	FoldChange
cfh	12.65217391	-4.048360834	0.768951658	-5.26477938	1.40358E-07	1.19896E-05	-16.54542945
LOC110529382	10.47826087	-3.756503767	0.774125921	-4.85257458	1.21869E-06	6.79855E-05	-13.51513265
hpxb	16.13043478	-3.685400779	0.737508281	-4.997097489	5.81996E-07	3.74326E-05	-12.86518929
antiprot1	18.26086957	-3.630523571	0.729920386	-4.973862414	6.56319E-07	4.07738E-05	-12.3850138
apoa2	67.26086957	-3.620940596	0.784073307	-4.61811487	3.87242E-06	0.000173529	-12.30302005
LOC100499622	42.7826087	-3.546993592	0.752587537	-4.713064485	2.44019E-06	0.000120799	-11.68830311
LOC110537948	33.2173913	-3.457874305	0.771393028	-4.482636193	7.37266E-06	0.000294207	-10.98813248
apoa-i-1	40.17391304	-3.302407764	0.693198604	-4.76401387	1.89779E-06	0.000100806	-9.865606628
LOC110489027	34.13043478	-3.245111488	0.735555599	-4.411782727	1.02523E-05	0.000378161	-9.481474846
LOC110510206	20.26086957	-3.214723537	0.704868466	-4.560742452	5.09731E-06	0.000217711	-9.283852082
lect2	10.17391304	-3.189032762	0.641527307	-4.971000809	6.66082E-07	4.09154E-05	-9.119993285
c9	17.2173913	-3.162789513	0.671503805	-4.710009815	2.47705E-06	0.000120799	-8.955596405
fetub	24.39130435	-3.108251951	0.705424731	-4.40621347	1.05193E-05	0.000383395	-8.623371008
c4b	10.82608696	-2.939517884	0.679125869	-4.3283845	1.50207E-05	0.000500721	-7.671548871
LOC110534419	28.56521739	-2.935396295	0.687243649	-4.271259981	1.94372E-05	0.000621421	-7.649663545
ambp	11.86956522	-2.844348336	0.651789472	-4.363906532	1.2776E-05	0.000447734	-7.181814233
LOC110530600	8.739130435	-2.813585967	0.64888264	-4.336047527	1.45068E-05	0.000489558	-7.030298603
LOC110531464	28.34782609	-2.786788044	0.639502335	-4.357744907	1.31409E-05	0.000457589	-6.900916821
LOC100136077	16.91304348	-2.727874847	0.629942182	-4.330357491	1.48867E-05	0.0004993	-6.624790567
LOC110513729	40.34782609	-2.705058972	0.724668256	-3.732823879	0.000189345	0.004012206	-6.520845202
LOC110531328	56.17391304	-2.688466676	0.746899839	-3.599500943	0.000318828	0.006225126	-6.446279204
LOC110523946	15.17391304	-2.672273339	0.673394679	-3.968361235	7.23686E-05	0.001798359	-6.374328363
LOC110517089	12.7826087	-2.670808912	0.672193662	-3.973272976	7.08917E-05	0.001769703	-6.367861296
cp	8.913043478	-2.669850573	0.653466599	-4.085672593	4.39493E-05	0.001223775	-6.363632724
LOC110524786	11.65217391	-2.636492108	0.637593182	-4.135069478	3.54847E-05	0.001031888	-6.218178832
LOC110529383	13.73913043	-2.309448771	0.582442457	-3.965110616	7.33619E-05	0.00180662	-4.956936478
LOC110534076	15.47826087	-2.234367086	0.552754665	-4.042240126	5.2943E-05	0.001405045	-4.705562153
apoa-i-2	10.65217391	-2.200298253	0.586915723	-3.748916865	0.0001776	0.003822594	-4.595743414
LOC110531721	136.8695652	-2.17355773	0.288792392	-7.526367703	5.21713E-14	1.4261E-11	-4.511345348
tfa	42.47826087	-1.744161192	0.506492057	-3.443610155	0.000574003	0.009655609	-3.350000224
LOC100136260	62.17391304	-1.729387854	0.446957003	-3.869248817	0.000109171	0.002518308	-3.315870937
LOC110496519	9.086956522	-1.61095761	0.47935317	-3.36069043	0.000777479	0.012041015	-3.054545244
LOC110536447	111.7391304	-1.568738385	0.193734307	-8.097370112	5.616E-16	2.19305E-13	-2.96645189
LOC110486628	20.13043478	-1.560626056	0.237723181	-6.564887992	5.2072E-11	9.48925E-09	-2.949818228
LOC110525076	252.826087	-1.53920418	0.15898843	-9.6812339	3.62316E-22	3.30131E-19	-2.906341395
LOC110524069	20.30434783	-1.469154073	0.167947523	-8.747697169	2.17751E-18	9.15725E-16	-2.768595089
LOC118941202	45.34782609	-1.427186611	0.153177573	-9.317203476	1.19447E-20	7.25574E-18	-2.689217813
ATP8	58.91304348	-1.335270252	0.138616727	-9.632821926	5.81113E-22	4.53849E-19	-2.523227435
LOC110491198	168.7826087	-1.294516643	0.169688375	-7.628788044	2.36971E-14	7.19733E-12	-2.452947987
LOC110509125	67.30434783	-1.266289287	0.218733817	-5.789179295	7.07312E-09	9.20684E-07	-2.40542078
LOC110488974	67.7826087	-1.246647632	0.139751715	-8.920446022	4.64414E-19	2.14015E-16	-2.372893962
LOC110513340	1689.869565	-1.196216299	0.228335942	-5.238843654	1.61586E-07	1.31849E-05	-2.291379309
rl29	14.52173913	-1.190822373	0.194892203	-6.110159129	9.95318E-10	1.47065E-07	-2.282828331
LOC118946663	17	-1.114475765	0.323899352	-3.440808878	0.000579978	0.009717259	-2.165163188
LOC110530826	147.3913043	-1.076018726	0.159633083	-6.740574751	1.57761E-11	3.19437E-09	-2.108210211
rpl38	15.30434783	-1.022220202	0.194395478	-5.25845668	1.45269E-07	1.22183E-05	-2.031042181
LOC110506823	36.91304348	-1.019736247	0.13055494	-7.810782543	5.6834E-15	1.82771E-12	-2.02754825
LOC118965306	245.3043478	-1.002569423	0.156202715	-6.418386656	1.37726E-10	2.28166E-08	-2.003565151

Muscle Yield DEGs Enrichment Terms:

Enrichment FDR	nGenes	Pathway G	Fold Enrichment	Pathway
3.22E-23	20	141	38.73185853	Ribosome
6.29E-18	25	526	12.978118	Amide biosynthetic process
8.50E-18	17	158	29.37983066	Oxidative phosphorylation
2.36E-17	24	509	12.87510897	Peptide biosynthetic process
2.89E-17	20	299	18.26485636	Ribosome
1.21E-16	25	630	10.83569852	Cellular amide metabolic process
1.21E-16	23	502	12.51069893	Translation
1.21E-16	19	283	18.3326235	Structural constituent of ribosome
1.21E-16	24	569	11.51745248	Peptide metabolic process
1.21E-16	35	1489	6.418459431	Metabolic pathways
1.29E-16	31	1125	7.524309051	Organonitrogen compound biosynthetic process
5.36E-14	56	4835	3.162634488	Organelle
1.39E-13	55	4783	3.139928527	Intracellular organelle
1.21E-11	20	621	8.794190101	Structural molecule activity
2.23E-11	28	1427	5.35786186	Non-membrane-bounded organelle
2.23E-11	28	1427	5.35786186	Intracellular non-membrane-bounded organelle
4.94E-10	12	194	16.8902847	Mitochondrial inner membrane
9.43E-10	12	206	15.90638462	Organelle inner membrane
2.14E-09	12	222	14.75997852	Generation of precursor metabolites and energy
7.70E-09	37	3151	3.206348873	Cellular nitrogen compound biosynthetic process
9.60E-09	10	148	18.44997315	ATP metabolic process
2.17E-08	12	275	11.91532812	Mitochondrial membrane
4.99E-08	13	369	9.619986001	Organelle envelope
4.99E-08	13	369	9.619986001	Envelope
8.22E-08	12	314	10.43539883	Mitochondrial envelope
8.22E-08	40	3971	2.750537423	Biosynthetic process
1.07E-07	14	478	7.997561584	Mitochondrion
1.38E-07	8	101	21.62848338	Cardiac muscle contraction
1.42E-07	39	3891	2.736911977	Organic substance biosynthetic process
2.16E-07	38	3782	2.743591989	Cellular biosynthetic process

Body weight Differentially Expressed Genes (DEGs) (First 50)

id	baseMean	log2FoldChange	lfcSE	stat	pvalue	padj	FoldChange
smpx	50.45833333	0.998213311	0.138024604	7.232140398	4.7544E-13	1.87514E-09	1.997524657
LOC110492108	168.5833333	0.600430684	0.090984909	6.5992338	4.13288E-11	8.15004E-08	1.516169117
prkag3b	21.29166667	1.391829948	0.217604407	6.396147785	1.59346E-10	2.09487E-07	2.624113183
LOC110495406	61.79166667	1.045477522	0.165393713	6.321144271	2.59633E-10	2.19539E-07	2.064049431
LOC110486628	37.66666667	-0.995214979	0.157710357	-6.310397081	2.7832E-10	2.19539E-07	-1.99337754
LOC118965241	16.875	1.146841295	0.182845555	6.272185791	3.56014E-10	2.3402E-07	2.214285571
LOC110506823	51.25	-0.763299776	0.124256043	-6.142958969	8.09982E-10	4.56367E-07	-1.697368461
LOC110533583	102.5833333	0.579592929	0.097437097	5.948380525	2.70808E-09	1.33509E-06	1.494427521
LOC110510070	94.125	0.520313834	0.088194387	5.899625294	3.64328E-09	1.58896E-06	1.434267215
LOC110524579	40.16666667	0.708301791	0.12039792	5.883006877	4.02879E-09	1.58896E-06	1.633879731
cpt1ab	77.16666667	0.698866902	0.119282654	5.85891474	4.65902E-09	1.67047E-06	1.623229402
g0s2	154.3333333	1.132973681	0.193978452	5.840719273	5.19759E-09	1.70828E-06	2.193103168
LOC110518968	391.5	-1.058439324	0.182205098	-5.809054379	6.28267E-09	1.90606E-06	-2.082677308
LOC110505842	110.25	0.698128089	0.120542967	5.791528977	6.97485E-09	1.96492E-06	1.622398348
LOC110488303	484.125	0.404178662	0.070665386	5.719613044	1.06767E-08	2.80726E-06	1.32333531
LOC118941202	63.41666667	-0.916893616	0.16126845	-5.685511423	1.30422E-08	3.2149E-06	-1.888045609
LOC110538823	137.0416667	0.511484426	0.091072359	5.616242201	1.95155E-08	4.5276E-06	1.425516192
nfkbie	47.95833333	-0.777891139	0.139240975	-5.586653923	2.31486E-08	5.07212E-06	-1.714622689
unm_hu7910	477.0416667	0.421066785	0.075944294	5.544416325	2.94936E-08	6.12226E-06	1.338917236
LOC110526482	73.54166667	0.584962461	0.106064893	5.515137445	3.48507E-08	6.87257E-06	1.499999959
acadvl	128.2916667	0.646930603	0.118842744	5.443585224	5.22187E-08	9.80718E-06	1.56583327
LOC100136600	1224.75	0.517493979	0.095494791	5.419080679	5.99063E-08	1.07396E-05	1.431466571
LOC110525946	798.4166667	0.36329668	0.067539643	5.37901392	7.48949E-08	1.28429E-05	1.286361988
LOC110537607	69.66666667	-0.65288361	0.123217385	-5.298632241	1.16673E-07	1.91733E-05	-1.572307733
LOC110530875	95.125	-0.659615042	0.126587956	-5.210725133	1.88104E-07	2.96753E-05	-1.579661063
gatd3a	37.08333333	0.584962464	0.112509421	5.199230957	2.00115E-07	3.03559E-05	1.499999962
s10i	79.5	0.633014573	0.123568495	5.122782889	3.01059E-07	4.39769E-05	1.550802078
LOC110538293	91.45833333	0.438452754	0.085821206	5.108909245	3.24024E-07	4.44955E-05	1.355150191
svila	142.5833333	-0.549563651	0.107608165	-5.107081341	3.27173E-07	4.44955E-05	-1.463642944
LOC110513340	2134.333333	-1.000971947	0.197028762	-5.08033415	3.76772E-07	4.95329E-05	-2.001347858
LOC110520344	87.66666667	0.425442532	0.084137267	5.056529036	4.26956E-07	5.43198E-05	1.342984387
LOC110492846	98.70833333	0.403321173	0.080883279	4.986459231	6.14959E-07	7.57937E-05	1.322548998
atp5mc3b	45.33333333	0.575024222	0.115732119	4.968579392	6.74452E-07	7.97595E-05	1.489702474
bckdk	23.20833333	0.79109896	0.159340316	4.964838665	6.87582E-07	7.97595E-05	1.730392071
LOC110502871	100.75	0.476839296	0.09717774	4.906877838	9.25376E-07	0.000104277	1.391691361
hibadhb	47.91666667	0.506959956	0.103483078	4.89896479	9.63429E-07	0.000105549	1.421052599
shbgb	40.91666667	0.81428532	0.167554847	4.859813566	1.17496E-06	0.000125245	1.75842685
LOC110517608	38.91666667	0.582388513	0.120729787	4.823900793	1.40777E-06	0.000146112	1.497326158
LOC110504971	119.5416667	1.393445662	0.289253347	4.817388208	1.4545E-06	0.000147091	2.627053646
LOC110490189	34.375	0.945256902	0.197105798	4.795682892	1.62122E-06	0.000156128	1.925531736
LOC110492049	305.4166667	0.90477834	0.188674007	4.79545833	1.62303E-06	0.000156128	1.872256814
LOC110491529	142.0416667	-0.696253966	0.148292772	-4.695130835	2.66436E-06	0.000244651	-1.620292152
LOC110485647	68.95833333	0.380516738	0.081048915	4.694902282	2.66734E-06	0.000244651	1.301808048
LOC110496277	37.04166667	0.705029	0.150972319	4.669922308	3.01314E-06	0.000270087	1.630177433
LOC110485428	116.7916667	-0.735044445	0.159309794	-4.613931294	3.95123E-06	0.000346303	-1.664448745
LOC110494664	46.29166667	0.796143424	0.17379874	4.580835411	4.63122E-06	0.000397077	1.736453074
LOC110492316	19.875	-0.800230532	0.175124271	-4.569501008	4.88887E-06	0.000410249	-1.741379364
ndufc2	47.375	0.505025966	0.111261935	4.539072304	5.65023E-06	0.00046426	1.419148898
fabph	140.8333333	0.787270542	0.173804188	4.529640812	5.9084E-06	0.000475566	1.725806291

Body weight DEGs Enrichment Terms:

Enrichment FDR	nGenes	Pathway Genes	Fold Enrich	Pathway
5.28E-38	27	158	56.3678	Oxidative phosphorylation
7.17E-35	48	1489	10.63337	Metabolic pathways
9.48E-26	18	101	58.78622	Cardiac muscle contraction
2.77E-10	7	36	64.13867	Valine, leucine and isoleucine degradation
8.41E-09	6	32	61.848	Citrate cycle (TCA cycle)
1.78E-08	6	37	53.49016	Pyruvate metabolism
2.50E-08	6	40	49.4784	Tryptophan metabolism
3.28E-08	9	175	16.96402	Adrenergic signaling in cardiomyocytes
2.41E-07	6	60	32.9856	Lysine degradation
3.21E-07	5	32	51.54	Propanoate metabolism
4.67E-07	5	35	47.12229	Fatty acid degradation
9.35E-06	4	28	47.12229	Glyoxylate and dicarboxylate metabolism
1.10E-05	6	121	16.3565	Carbon metabolism
1.44E-05	5	72	22.90667	Glycolysis / Gluconeogenesis
0.000108655	4	54	24.43378	Fatty acid metabolism
0.000209205	7	309	7.472466	Salmonella infection
0.000440521	3	30	32.9856	Fatty acid elongation
0.00091805	3	39	25.37354	Glycine, serine and threonine metabolism
0.001613591	3	48	20.616	Cysteine and methionine metabolism
0.003198539	2	15	43.9808	Butanoate metabolism
0.003198539	4	141	9.357617	Ribosome
0.004742413	3	73	13.55573	PPAR signaling pathway
0.007210042	4	181	7.289635	Apoptosis
0.0105256	2	29	22.74869	Beta-Alanine metabolism
0.023872885	2	45	14.66027	Arachidonic acid metabolism
0.030592893	3	151	6.55343	Biosynthesis of cofactors
0.033002183	4	293	4.503154	Calcium signaling pathway
0.049503103	2	70	9.424457	RNA degradation

Condition Factor Differentially Expressed Genes (DEGs) (First 50):

id	baseMean	log2FoldChange	lfcSE	stat	pvalue	padj	FoldChange
eif3h	23.39269904	-1.291091181	0.142069003	-9.087775335	1.01086E-19	3.03501E-15	-2.447130741
rpl38	13.85624369	-1.643380403	0.188580106	-8.714495057	2.92057E-18	4.38437E-14	-3.123969576
LOC110523343	17.56453074	-1.494421203	0.173296427	-8.623496891	6.49399E-18	6.49919E-14	-2.817510922
rl29	12.77744411	-2.061155922	0.240871381	-8.557081004	1.15761E-17	8.68904E-14	-4.173205377
LOC110509310	133.0328009	1.532952362	0.182599618	8.395156432	4.65274E-17	2.79388E-13	2.893774217
LOC118965306	178.3587083	-1.120881292	0.141867615	-7.900896134	2.76905E-15	1.38563E-11	-2.174797827
tpd52l2b	43.93579007	0.874481417	0.111176101	7.865732046	3.66945E-15	1.57388E-11	1.833348962
ttc33	61.65972062	2.559672841	0.328181321	7.79956894	6.2119E-15	2.33133E-11	5.895739743
pigp	7.534800047	1.555827416	0.200433934	7.762295471	8.34058E-15	2.78242E-11	2.940022947
LOC110522421	25.09138735	-1.167698007	0.151501714	-7.707490429	1.28316E-14	3.85256E-11	-2.246529501
LOC110511907	7.713942273	1.599487651	0.209508024	7.63449352	2.2671E-14	6.18794E-11	3.030356761
LOC110489228	103.9003836	-0.850725997	0.113384924	-7.502990393	6.23781E-14	1.5607E-10	-1.803408213
LOC110488974	54.80324342	-1.338129443	0.178805099	-7.483731994	7.22412E-14	1.66844E-10	-2.528233028
grid2	5.83477429	2.987685785	0.401461293	7.442027003	9.91519E-14	2.12638E-10	7.932006091
LOC110503312	13.02782555	2.823550922	0.38517571	7.330552919	2.29205E-13	4.58777E-10	7.079026237
LOC110500321	17.88127938	-1.410206677	0.1928408	-7.312802463	2.61627E-13	4.77299E-10	-2.657752343
LOC110526678	15.70984374	1.057105363	0.144641643	7.308444116	2.70253E-13	4.77299E-10	2.080752489
urm1	12.95845745	1.156744611	0.160053636	7.227231087	4.92941E-13	8.22225E-10	2.229537725
cadps2	1754.506712	2.891477609	0.401178487	7.207459274	5.70055E-13	9.00807E-10	7.420300479
LOC110518867	5.964785563	2.266801222	0.317085574	7.148862669	8.74998E-13	1.31355E-09	4.812548975
samd12	33.55205848	2.731057586	0.382850776	7.133478002	9.7864E-13	1.39917E-09	6.639421697
LOC110504448	13.94662245	-1.291087369	0.181667156	-7.106883807	1.18692E-12	1.61983E-09	-2.447124275
LOC110531045	5.72946499	2.584251456	0.37031182	6.97858215	2.98174E-12	3.89234E-09	5.997043577
LOC118941202	42.35678686	-1.573825944	0.22578703	-6.970400126	3.16041E-12	3.95367E-09	-2.976931333
rpl35a	109.1310491	-0.943244633	0.135520477	-6.96016315	3.39879E-12	4.08181E-09	-1.92284788
LOC110498798	38.51864711	0.981897805	0.141561857	6.93617493	4.02859E-12	4.65209E-09	1.975061812
LOC110497946	12.0833258	2.584114639	0.373186959	6.924450534	4.37671E-12	4.8669E-09	5.996474877
LOC110509935	12.33568135	-0.954338631	0.138250141	-6.902984886	5.0921E-12	5.46019E-09	-1.937691142
LOC110530018	47.10342371	-0.711918348	0.103482515	-6.879600371	6.00207E-12	6.214E-09	-1.637980689
LOC118947810	37.68276165	-1.438358275	0.209320003	-6.871575847	6.34965E-12	6.35473E-09	-2.710122896
LOC110537744	32.56543691	1.123053535	0.164842128	6.812903665	9.56482E-12	9.26368E-09	2.178074852
LOC110513232	6.04868976	-2.076996619	0.305583612	-6.796819388	1.06954E-11	1.0035E-08	-4.219279379
LOC110506778	2.314127979	-4.497486607	0.664854289	-6.764619982	1.3366E-11	1.21606E-08	-22.58803094
LOC110537730	70.20931766	0.952549575	0.141711097	6.721771252	1.79529E-11	1.58534E-08	1.935289741
scarb2c	35.30365548	0.540001052	0.080418358	6.714897791	1.88198E-11	1.61442E-08	1.453973577
LOC110527702	3.212812779	2.56881232	0.385962875	6.655594322	2.82158E-11	2.35319E-08	5.933207836
LOC110497706	14.84305677	-0.999164148	0.150506386	-6.638682733	3.16499E-11	2.56826E-08	-1.998841599
LOC110487768	35.61351394	-0.89417424	0.135311585	-6.60826079	3.88861E-11	3.07241E-08	-1.858545799
LOC110488130	7.11798782	2.262186145	0.344262687	6.571104657	4.99433E-11	3.68967E-08	4.797178574
eps15	24.2573264	-0.867855537	0.132091882	-6.570089867	5.02849E-11	3.68967E-08	-1.824948228
LOC110534136	8.824571983	1.636409958	0.249080887	6.569793351	5.03851E-11	3.68967E-08	3.108912381
LOC110502650	5.391678076	2.711409474	0.413059254	6.564214322	5.23079E-11	3.73927E-08	6.549612138
LOC110497830	48.73486683	0.625297276	0.095370702	6.556492349	5.50881E-11	3.84643E-08	1.54252864
vamp3	60.31389143	0.595916254	0.091302667	6.526821952	6.71798E-11	4.58411E-08	1.51143219
LOC110503016	42.18699948	1.302489545	0.199967546	6.51350466	7.34173E-11	4.8984E-08	2.466541472
LOC110504215	34.47693892	1.004885186	0.154610608	6.499458214	8.06098E-11	5.26137E-08	2.006783785
LOC110513868	15.08385816	1.276148116	0.196619324	6.490451128	8.55797E-11	5.46691E-08	2.421914805
pigk	17.01359094	0.754040066	0.11699279	6.445184065	1.1546E-10	7.22204E-08	1.686509057

Condition DEGs Enrichment Terms:

Enrichment FDR	nGenes	Pathway Genes	Fold Enrichment	Pathway
3.76E-13	29	158	7.007313643	Oxidative phosphorylation
1.11E-10	91	1489	2.333228864	Metabolic pathways
4.14E-10	207	4835	1.634498449	Organelle
6.86E-10	204	4783	1.628322531	Intracellular organelle
4.93E-09	24	164	5.58699187	Spliceosome
8.15E-09	22	141	5.956816391	Ribosome
3.47E-08	163	3765	1.652849343	Membrane-bounded organelle
3.47E-08	161	3699	1.661698357	Intracellular membrane-bounded organelle
4.68E-08	22	157	5.3497523	Cell adhesion molecules
1.04E-06	30	329	3.481256332	Endocytosis
2.19E-06	22	194	4.329438717	Mitochondrial inner membrane
5.61E-06	22	206	4.077238403	Organelle inner membrane
5.61E-06	50	811	2.353747089	RNA binding
1.41E-05	18	149	4.612080537	Phagosome
1.85E-05	137	3342	1.565037569	Metal ion binding
1.95E-05	138	3380	1.558737673	Cation binding
2.08E-05	113	2622	1.645342826	Cytoplasm
3.21E-05	9	36	9.544444444	Energy coupled proton transport, down electrochemical gradient
3.21E-05	9	36	9.544444444	ATP synthesis coupled proton transport
3.21E-05	57	1052	2.068567807	Calcium ion binding
3.21E-05	9	36	9.544444444	ATP biosynthetic process
3.65E-05	24	275	3.331878788	Mitochondrial membrane
4.05E-05	17	148	4.385285285	ATP metabolic process
4.86E-05	140	3523	1.517141325	Gene expression
4.92E-05	22	242	3.470707071	Focal adhesion
0.000138544	24	299	3.064437012	Ribosome
0.000146597	32	478	2.555834496	Mitochondrion
0.000163471	27	369	2.793495935	Organelle envelope
0.000163471	27	369	2.793495935	Envelope
0.000163471	6	16	14.31666667	Proton-transporting ATP synthase activity, rotational mechanism

Genetic Line Differentially Expressed Genes (DEGs) (First 50):

id	baseMean	log2FoldChange	lfcSE	stat	pvalue	padj	FoldChange
LOC110490499	821948.7938	18.41102293	0.920359309	20.00416876	5.06561E-89	8.68954E-85	348554.0653
LOC110500299	932902.0212	17.82512637	0.896655809	19.87956382	6.11632E-88	5.24597E-84	232218.9803
cbpa1	768826.8538	16.91429537	0.853361922	19.82077584	1.97047E-87	1.12672E-83	123512.315
LOC118941542	366730.1066	17.54462052	0.906104886	19.36268174	1.59369E-83	6.83454E-80	191186.4197
LOC110523637	247394.3922	15.74304406	0.830141222	18.96429624	3.36501E-80	1.15447E-76	54843.91961
LOC110498318	133200.433	16.21704585	0.869454342	18.65198098	1.21684E-77	3.47894E-74	76175.83817
LOC110520383	169249.384	15.64832665	0.843825295	18.54451005	9.032E-77	2.21336E-73	51358.89897
LOC110537588	147891.1343	15.66862017	0.858453708	18.25214339	1.98948E-74	4.26595E-71	52086.43839
LOC110538314	178121.5691	14.5176586	0.798383636	18.18381281	6.93408E-74	1.32163E-70	23455.82455
LOC110514797	74803.33181	15.20022642	0.846659827	17.95316837	4.5329E-72	7.77574E-69	37646.45564
LOC118936721	74623.89297	15.06037787	0.84703971	17.78001395	1.00955E-70	1.57435E-67	34168.46621
LOC118959030	353583.7127	-12.53525524	0.710662599	-17.63882783	1.24007E-69	1.77268E-66	-5935.917137
LOC118948649	130497.8176	-12.39116437	0.710049356	-17.45113106	3.37483E-68	4.45322E-65	-5371.705017
LOC110527149	99932.15505	13.66312233	0.783289867	17.44325174	3.87392E-68	4.74666E-65	12972.0811
LOC110503652	133363.9197	13.36794653	0.768531507	17.39414248	9.13841E-68	1.04507E-64	10571.8961
hmgcra	24303.88885	13.93011785	0.813664055	17.12023257	1.04856E-65	1.12418E-62	15609.29601
mamdc4	737181.3879	19.46602548	1.141980037	17.04585444	3.7522E-65	3.78619E-62	724198.4098
LOC110537803	256706.668	12.32620629	0.72386283	17.02837303	5.05913E-65	4.82135E-62	5135.205466
LOC110486790	174133.202	17.0507758	1.00190929	17.01828297	6.01076E-65	5.42676E-62	135767.2324
cpb1	49006.39822	12.39701923	0.737613309	16.8069354	2.17109E-63	1.86214E-60	5393.549222
LOC110517805	951061.3664	19.95979544	1.192509164	16.73764533	6.96909E-63	5.69275E-60	1019758.035
LOC110537912	45702.62307	12.42508555	0.759287174	16.36414519	3.44836E-60	2.68878E-57	5499.503089
LOC118946663	66273.36613	-10.72254507	0.661372746	-16.21255961	4.11085E-59	3.06598E-56	-1689.692571
LOC110524716	28297.311	11.83693232	0.744122594	15.90723414	5.64529E-57	4.03497E-54	3658.235721
LOC110537812	127292.6988	10.68964673	0.677213644	15.78474803	3.96228E-56	2.71876E-53	1651.59785
LOC110510120	69527.60939	10.35787996	0.665155756	15.57211206	1.12626E-54	7.43072E-52	1312.298283
LOC110510128	10542.22886	10.78398017	0.702064423	15.36038549	3.01775E-53	1.91728E-50	1763.199702
LOC118936383	636960.8165	19.83284348	1.29212829	15.34897397	3.59833E-53	2.20449E-50	933857.8773
LOC110508116	10693.56921	-10.17440199	0.664985147	-15.30019435	7.62287E-53	4.50906E-50	-1155.580454
LOC110523005	22836.95199	14.75588333	0.970411362	15.20580231	3.23641E-52	1.85058E-49	27667.09078
ezra	613069.5635	19.5697529	1.31659101	14.86395756	5.64873E-50	3.12575E-47	778184.5961
LOC110535290	19006.64933	14.08981584	0.951697027	14.80493837	1.36112E-49	7.29644E-47	17436.41512
ahsg1	3059.493007	-9.989960495	0.681940803	-14.64930747	1.36096E-48	7.07451E-46	-1016.898869
LOC118962126	16032.92436	-8.850430924	0.609414399	-14.52284511	8.68301E-48	4.38084E-45	-461.5780867
LOC110510198	3817.65243	10.81799265	0.752016606	14.38531087	6.39899E-47	3.13624E-44	1805.262169
LOC110524789	1825.118374	-8.785734233	0.61746055	-14.22881872	6.06984E-46	2.89228E-43	-441.3361867
LOC118936646	48746.5652	15.82765167	1.112577288	14.2261143	6.30913E-46	2.92505E-43	58156.45326
elovl5	2017.608838	10.43930771	0.73420265	14.21856446	7.02799E-46	3.17258E-43	1388.496392
meltf	3592.350627	9.834622798	0.706212337	13.92587227	4.41123E-44	1.94026E-41	913.096038
fetub	4386.800819	-8.239658109	0.59180841	-13.92284728	4.60199E-44	1.97356E-41	-302.2624824
LOC110538364	2258.267949	8.727540938	0.643284096	13.56716418	6.27013E-42	2.62336E-39	423.8884768
fads2	1323.05213	9.580496848	0.711173819	13.47138574	2.30499E-41	9.41424E-39	765.6264433
LOC110537948	3422.013135	-7.752401323	0.578668991	-13.39695308	6.29968E-41	2.51313E-38	-215.6280903
LOC110490653	2683.276666	8.370033046	0.629932431	13.28719182	2.74695E-40	1.07094E-37	330.849903
LOC118940171	2619.254026	11.0774595	0.838792576	13.20643484	8.05501E-40	3.07057E-37	2160.964258
ela2l	1863.61252	8.282849109	0.630984746	13.12686109	2.31036E-39	8.61564E-37	311.4483478
LOC110537956	3221.996797	11.2397641	0.856868126	13.11726247	2.62238E-39	9.57112E-37	2418.277525
LOC110528107	1217.778666	9.735597505	0.744832294	13.07085848	4.83171E-39	1.72673E-36	852.5245121

Genetic Line DEGs Enrichment Terms:

Enrichment FDR	nGenes	Pathway Genes	Fold Enrichment	Pathway
6.77E-08	18	309	7.553031691	Salmonella infection
1.49E-05	34	1489	2.960680208	Metabolic pathways
4.32E-05	13	250	6.742339623	Regulation of actin cytoskeleton
0.000256932	65	4554	1.850664148	Organonitrogen compound metabolic process
0.000366418	15	423	4.597885722	Actin binding
0.000975922	65	4835	1.743107452	Organelle
0.000975922	5	32	20.25943396	Citrate cycle (TCA cycle)
0.000975922	8	121	8.572586933	Carbon metabolism
0.002381294	63	4783	1.707841057	Intracellular organelle
0.002604104	8	145	7.153675992	Apelin signaling pathway
0.002991679	7	109	8.326813225	Energy derivation by oxidation of organic compounds
0.003447417	40	2622	1.978037793	Cytoplasm
0.003447417	8	158	6.565082398	Oxidative phosphorylation
0.003447417	12	366	4.251159913	MAPK signaling pathway
0.003888614	17	705	3.126562291	Cytoskeletal protein binding
0.004130772	52	3846	1.753078425	Protein metabolic process
0.004130772	9	214	5.453006524	Serine-type endopeptidase activity
0.004978794	9	222	5.256501785	Generation of precursor metabolites and energy
0.009241904	4	34	15.25416204	Tricarboxylic acid cycle
0.009241904	25	1427	2.271555315	Non-membrane-bounded organelle
0.009241904	25	1427	2.271555315	Intracellular non-membrane-bounded organelle
0.010045519	9	253	4.612424491	Serine-type peptidase activity
0.010045519	9	253	4.612424491	Serine hydrolase activity
0.010045519	7	149	6.091427124	Phagosome
0.01060654	11	379	3.76322995	Actin cytoskeleton organization
0.01060654	8	204	5.084720681	Actin cytoskeleton
0.01060654	4	37	14.01733809	Protein peptidyl-prolyl isomerization
0.012280301	11	388	3.675938533	Actin filament-based process
0.012516116	4	40	12.96603774	Peptidyl-proline modification
0.016662176	6	120	6.483018868	Oocyte meiosis

Supplementary File 2

Cis-eQTL List (First 50):

id	gene name	snps	statistic	pvalue	FDR	beta
ghrl	ghrelin/obestatin prepropeptide	17_622493	-7.51589	1.44E-11	5E-08	-0.11051
ghrl	ghrelin/obestatin prepropeptide	17_622493	-7.51589	1.44E-11	5E-08	-0.11051
ghrl	ghrelin/obestatin prepropeptide	17_622493	-7.51589	1.44E-11	5E-08	-0.11051
ghrl	ghrelin/obestatin prepropeptide	17_622478	-7.44365	2.08E-11	6.83E-08	-0.10966
ghrl	ghrelin/obestatin prepropeptide	17_622478	-7.44365	2.08E-11	6.83E-08	-0.10966
ghrl	ghrelin/obestatin prepropeptide	17_622474	-7.29518	4.41E-11	1.29E-07	-0.10786
ghrl	ghrelin/obestatin prepropeptide	17_622474	-7.29518	4.41E-11	1.29E-07	-0.10786
ghrl	ghrelin/obestatin prepropeptide	17_622510	-7.05464	1.48E-10	3.58E-07	-0.13376
wu:fj39g12	C-type natriuretic peptide variant 1	3_1124810	-9.37308	8.62E-16	1.03E-11	-11.2348
wu:fj39g12	C-type natriuretic peptide variant 1	3_1124814	-9.29228	1.33E-15	1.51E-11	-11.1935
wu:fj39g12	C-type natriuretic peptide variant 1	3_1124754	-8.83633	1.49E-14	1.27E-10	-10.5743
wu:fj39g12	C-type natriuretic peptide variant 1	3_1125253	-8.75913	2.24E-14	1.82E-10	-11.1836
wu:fj39g12	C-type natriuretic peptide variant 1	3_1125062	-8.73162	2.59E-14	2.06E-10	-11.1624
wu:fj39g12	C-type natriuretic peptide variant 1	3_1161586	-8.73154	2.6E-14	2.07E-10	-10.9446
wu:fj39g12	C-type natriuretic peptide variant 1	3_1161562	-8.72453	2.69E-14	2.13E-10	-10.9379
wu:fj39g12	C-type natriuretic peptide variant 1	3_1161567	-8.72453	2.69E-14	2.13E-10	-10.9379
wu:fj39g12	C-type natriuretic peptide variant 1	3_1123611	-8.67965	3.41E-14	2.63E-10	-10.2584
wu:fj39g12	C-type natriuretic peptide variant 1	3_1139724	-8.51881	7.96E-14	5.56E-10	-10.6134
wu:fj39g12	C-type natriuretic peptide variant 1	3_1124653	-8.47769	9.88E-14	6.73E-10	-10.1055
wu:fj39g12	C-type natriuretic peptide variant 1	3_1103740	-8.13863	5.82E-13	3.17E-09	-10.3298
wu:fj39g12	C-type natriuretic peptide variant 1	3_1123605	-8.08084	7.85E-13	4.12E-09	-9.68552
wu:fj39g12	C-type natriuretic peptide variant 1	3_1103621	-8.05668	8.91E-13	4.59E-09	-10.2642
wu:fj39g12	C-type natriuretic peptide variant 1	3_1103621	-8.05668	8.91E-13	4.59E-09	-10.2642
wu:fj39g12	C-type natriuretic peptide variant 1	3_1103622	-8.03743	9.84E-13	5.01E-09	-10.2541
wu:fj39g12	C-type natriuretic peptide variant 1	3_1103583	-8.01838	1.09E-12	5.45E-09	-10.2353
wu:fj39g12	C-type natriuretic peptide variant 1	3_1103670	-8.01838	1.09E-12	5.45E-09	-10.2353
wu:fj39g12	C-type natriuretic peptide variant 1	3_1103676	-8.01838	1.09E-12	5.45E-09	-10.2353
wu:fj39g12	C-type natriuretic peptide variant 1	3_1103617	-8.01515	1.1E-12	5.53E-09	-10.2279
wu:fj39g12	C-type natriuretic peptide variant 1	3_1103619	-8.01515	1.1E-12	5.53E-09	-10.2279
wu:fj39g12	C-type natriuretic peptide variant 1	3_1103620	-8.01515	1.1E-12	5.53E-09	-10.2279
wu:fj39g12	C-type natriuretic peptide variant 1	3_1103643	-8.0101	1.13E-12	5.65E-09	-10.2329
wu:fj39g12	C-type natriuretic peptide variant 1	3_1161575	-7.96288	1.45E-12	6.99E-09	-9.99043
wu:fj39g12	C-type natriuretic peptide variant 1	3_1103651	-7.76769	3.97E-12	1.66E-08	-9.71351
wu:fj39g12	C-type natriuretic peptide variant 1	3_1103559	-7.65061	7.23E-12	2.78E-08	-9.66015
wu:fj39g12	C-type natriuretic peptide variant 1	3_1103567	-7.65061	7.23E-12	2.78E-08	-9.66015
wu:fj39g12	C-type natriuretic peptide variant 1	3_1103565	-7.64852	7.31E-12	2.8E-08	-9.65413
wu:fj39g12	C-type natriuretic peptide variant 1	3_1103565	-7.64852	7.31E-12	2.8E-08	-9.65413
wu:fj39g12	C-type natriuretic peptide variant 1	3_1124673	-7.62744	8.14E-12	3.08E-08	-9.0624
wu:fj39g12	C-type natriuretic peptide variant 1	3_1125985	-7.59399	9.66E-12	3.56E-08	-9.87423
wu:fj39g12	C-type natriuretic peptide variant 1	3_1104005	-7.35635	3.24E-11	9.95E-08	-9.37259
wu:fj39g12	C-type natriuretic peptide variant 1	3_1104035	-7.35635	3.24E-11	9.95E-08	-9.37259
wu:fj39g12	C-type natriuretic peptide variant 1	3_1161714	-7.26153	5.23E-11	1.49E-07	-10.4979
wu:fj39g12	C-type natriuretic peptide variant 1	3_1083641	7.036711	1.61E-10	3.86E-07	9.412882
gpx1	glutathione peroxidase 1	7_6071097	7.102394	1.16E-10	2.93E-07	154.9947
socs6	suppressor of cytokine signaling 6	28_190787	-9.67316	1.74E-16	2.46E-12	-1.23433
socs6	suppressor of cytokine signaling 6	28_190786	-9.64955	1.97E-16	2.75E-12	-1.23531
socs6	suppressor of cytokine signaling 6	28_190810	-9.64158	2.06E-16	2.86E-12	-1.23465

Genetic Line Prioritized eQTL (First 40) :

snps	SNP_chr	SNP_pos	gene name	statistic	pvalue	FDR	beta	Start.y	End.y	hromosom	strand	TSS	SNP_POS_MINUS_TSS
10_40479884_T_C	10	40479884	apoptosis a	7.220832	6.41E-11	1.77E-07	4.8531	40479739	40495940	10	+	40479739	145
10_40480421_C_A	10	40480421	apoptosis a	7.220832	6.41E-11	1.77E-07	4.8531	40479739	40495940	10	+	40479739	682
7_88450019_C_T	7	88450019	dual specif	7.192082	7.41E-11	2E-07	3.772073	88421430	88454090	7	-	88454090	-4071
7_88449320_C_T	7	88449320	dual specif	7.50602	1.51E-11	5.22E-08	3.786657	88421430	88454090	7	-	88454090	-4770
7_88447431_T_G	7	88447431	dual specif	7.055007	1.47E-10	3.57E-07	3.728491	88421430	88454090	7	-	88454090	-6659
18_18495752_G_C	18	18495752	ELAVlike F	7.09148	1.23E-10	3.07E-07	3.969361	18488722	18498859	18	+	18488722	7030
18_18496033_G_A	18	18496033	ELAVlike F	7.65881	6.94E-12	2.68E-08	4.171192	18488722	18498859	18	+	18488722	7311
18_18497066_A_G	18	18497066	ELAVlike F	7.65881	6.94E-12	2.68E-08	4.171192	18488722	18498859	18	+	18488722	8344
18_18492258_T_A	18	18492258	ELAVlike F	7.423605	2.3E-11	7.45E-08	4.124483	18488722	18498859	18	+	18488722	3536
18_18495810_C_T	18	18495810	ELAVlike F	7.671818	6.49E-12	2.53E-08	4.190293	18488722	18498859	18	+	18488722	7088
18_18495967_T_G	18	18495967	ELAVlike F	7.65881	6.94E-12	2.68E-08	4.171192	18488722	18498859	18	+	18488722	7245
18_18496253_A_G	18	18496253	ELAVlike F	7.319813	3.89E-11	1.16E-07	3.991041	18488722	18498859	18	+	18488722	7531
18_18496391_G_A	18	18496391	ELAVlike F	7.319813	3.89E-11	1.16E-07	3.991041	18488722	18498859	18	+	18488722	7669
25_16186514_C_T	25	16186514	LCK2	7.07011	1.37E-10	3.36E-07	0.374157	16154316	16193639	25	-	16193639	-7125
25_16185520_A_G	25	16185520	LCK2	10.06954	2.08E-17	3.68E-13	0.455341	16154316	16193639	25	-	16193639	-8119
25_16185740_C_T	25	16185740	LCK2	9.517249	3.99E-16	5.18E-12	0.442559	16154316	16193639	25	-	16193639	-7899
25_16192935_G_A	25	16192935	LCK2	10.92806	2.09E-19	6.3E-15	0.480528	16154316	16193639	25	-	16193639	-704
25_16193105_T_G	25	16193105	LCK2	7.7212	5.04E-12	2.04E-08	0.41594	16154316	16193639	25	-	16193639	-534
25_16193192_T_C	25	16193192	LCK2	8.126758	6.19E-13	3.34E-09	0.436308	16154316	16193639	25	-	16193639	-447
25_16193242_G_A	25	16193242	LCK2	8.070762	8.28E-13	4.31E-09	0.430246	16154316	16193639	25	-	16193639	-397
25_16193250_A_G	25	16193250	LCK2	8.070762	8.28E-13	4.31E-09	0.430246	16154316	16193639	25	-	16193639	-389
25_16186089_C_A	25	16186089	LCK2	7.860461	2.46E-12	1.1E-08	0.396819	16154316	16193639	25	-	16193639	-7550
25_16193435_C_A	25	16193435	LCK2	7.517634	1.43E-11	4.96E-08	0.415693	16154316	16193639	25	-	16193639	-204
25_16187211_C_T	25	16187211	LCK2	8.637166	4.27E-14	3.2E-10	0.425257	16154316	16193639	25	-	16193639	-6428
25_16187306_T_A	25	16187306	LCK2	10.52972	1.77E-18	4.17E-14	0.470489	16154316	16193639	25	-	16193639	-6333
25_16187811_A_G	25	16187811	LCK2	8.448846	1.15E-13	7.69E-10	0.430609	16154316	16193639	25	-	16193639	-5828
25_16187925_A_G	25	16187925	LCK2	8.414967	1.37E-13	9E-10	0.425085	16154316	16193639	25	-	16193639	-5714
25_16191569_G_A	25	16191569	LCK2	9.021412	5.59E-15	5.35E-11	0.437071	16154316	16193639	25	-	16193639	-2070
25_16192221_C_T	25	16192221	LCK2	9.437045	6.13E-16	7.6E-12	0.444373	16154316	16193639	25	-	16193639	-1418
25_16195864_G_T	25	16195864	LCK2	9.982867	3.31E-17	5.57E-13	0.457343	16154316	16193639	25	-	16193639	2225
25_16196017_T_A	25	16196017	LCK2	10.07205	2.05E-17	3.64E-13	0.459054	16154316	16193639	25	-	16193639	2378
25_16196263_T_G	25	16196263	LCK2	9.651399	1.95E-16	2.73E-12	0.594666	16154316	16193639	25	-	16193639	2624
25_16196389_G_T	25	16196389	LCK2	8.782342	1.98E-14	1.63E-10	0.436234	16154316	16193639	25	-	16193639	2750
25_16196403_T_C	25	16196403	LCK2	8.782342	1.98E-14	1.63E-10	0.436234	16154316	16193639	25	-	16193639	2764
25_16196404_C_G	25	16196404	LCK2	8.795418	1.85E-14	1.53E-10	0.436797	16154316	16193639	25	-	16193639	2765
25_16196416_G_A	25	16196416	LCK2	8.795418	1.85E-14	1.53E-10	0.436797	16154316	16193639	25	-	16193639	2777
25_16196521_C_T	25	16196521	LCK2	11.58672	6.17E-21	2.75E-16	0.501996	16154316	16193639	25	-	16193639	2882
25_16196703_G_T	25	16196703	LCK2	10.43158	2.99E-18	6.69E-14	0.465687	16154316	16193639	25	-	16193639	3064
25_16196788_C_T	25	16196788	LCK2	10.97291	1.64E-19	5.12E-15	0.473794	16154316	16193639	25	-	16193639	3149

Supplementary File 2b: Trans eQTL list (First 50):

id	Chr	Start	End	snps	CHROM	POS	gene.name	statistic	pvalue	FDR	beta
LOC100136661	7	79745594	79757141	1_13441788_A_T	1	13441788	1,25-dihydroxyvitamin D(3) 24-hydroxylase, mitochondrial	7.615853	8.64E-12	1.89E-06	1.315712
LOC100136661	7	79745594	79757141	1_33934325_C_T	1	33934325	1,25-dihydroxyvitamin D(3) 24-hydroxylase, mitochondrial	8.440504	1.20E-13	6.86E-08	1.552862
LOC100136661	7	79745594	79757141	1_41358827_A_G	1	41358827	1,25-dihydroxyvitamin D(3) 24-hydroxylase, mitochondrial	7.852031	2.57E-12	7.57E-07	1.284622
LOC100136661	7	79745594	79757141	1_41359003_T_C	1	41359003	1,25-dihydroxyvitamin D(3) 24-hydroxylase, mitochondrial	7.472658	1.79E-11	3.26E-06	1.176315
LOC100136661	7	79745594	79757141	1_41359005_C_G	1	41359005	1,25-dihydroxyvitamin D(3) 24-hydroxylase, mitochondrial	7.472658	1.79E-11	3.26E-06	1.176315
LOC100136661	7	79745594	79757141	1_69555437_C_T	1	69555437	1,25-dihydroxyvitamin D(3) 24-hydroxylase, mitochondrial	7.375495	2.94E-11	4.69E-06	1.021029
LOC100136661	7	79745594	79757141	1_72959567_G_T	1	72959567	1,25-dihydroxyvitamin D(3) 24-hydroxylase, mitochondrial	7.132606	9.99E-11	1.15E-05	1.278909
LOC100136661	7	79745594	79757141	1_73614191_C_A	1	73614191	1,25-dihydroxyvitamin D(3) 24-hydroxylase, mitochondrial	8.966197	7.50E-15	7.03E-09	1.638836
LOC100136661	7	79745594	79757141	1_73614193_G_A	1	73614193	1,25-dihydroxyvitamin D(3) 24-hydroxylase, mitochondrial	8.962842	7.63E-15	7.14E-09	1.63637
LOC100136661	7	79745594	79757141	1_89896499_T_G	1	89896499	1,25-dihydroxyvitamin D(3) 24-hydroxylase, mitochondrial	-8.97839	7.03E-15	6.66E-09	-1.65723
LOC100136661	7	79745594	79757141	2_232170_G_T	2	232170	1,25-dihydroxyvitamin D(3) 24-hydroxylase, mitochondrial	9.691707	1.57E-16	2.64E-10	1.511679
LOC100136661	7	79745594	79757141	2_295513_A_C	2	295513	1,25-dihydroxyvitamin D(3) 24-hydroxylase, mitochondrial	-7.79589	3.43E-12	9.44E-07	-1.3978
LOC100136661	7	79745594	79757141	2_513267_T_C	2	513267	1,25-dihydroxyvitamin D(3) 24-hydroxylase, mitochondrial	7.14445	9.41E-11	1.10E-05	1.365225
LOC100136661	7	79745594	79757141	2_2044652_T_G	2	2044652	1,25-dihydroxyvitamin D(3) 24-hydroxylase, mitochondrial	7.382315	2.84E-11	4.57E-06	1.387141
LOC100136661	7	79745594	79757141	2_2044658_G_T	2	2044658	1,25-dihydroxyvitamin D(3) 24-hydroxylase, mitochondrial	7.689801	5.92E-12	1.43E-06	1.36715
LOC100136661	7	79745594	79757141	2_2123101_C_T	2	2123101	1,25-dihydroxyvitamin D(3) 24-hydroxylase, mitochondrial	8.121856	6.35E-13	2.58E-07	1.338498
LOC100136661	7	79745594	79757141	2_4211124_A_C	2	4211124	1,25-dihydroxyvitamin D(3) 24-hydroxylase, mitochondrial	7.710162	5.33E-12	1.32E-06	1.452286
LOC100136661	7	79745594	79757141	2_4303776_T_A	2	4303776	1,25-dihydroxyvitamin D(3) 24-hydroxylase, mitochondrial	7.259601	5.28E-11	7.21E-06	1.260469
LOC100136661	7	79745594	79757141	2_4303778_C_A	2	4303778	1,25-dihydroxyvitamin D(3) 24-hydroxylase, mitochondrial	7.304842	4.20E-11	6.10E-06	1.270042
LOC100136661	7	79745594	79757141	2_11579850_T_G	2	11579850	1,25-dihydroxyvitamin D(3) 24-hydroxylase, mitochondrial	7.260143	5.26E-11	7.20E-06	1.133574
LOC100136661	7	79745594	79757141	2_15732069_T_A	2	15732069	1,25-dihydroxyvitamin D(3) 24-hydroxylase, mitochondrial	7.48846	1.66E-11	3.07E-06	1.216781
LOC100136661	7	79745594	79757141	2_15732110_C_A	2	15732110	1,25-dihydroxyvitamin D(3) 24-hydroxylase, mitochondrial	7.37914	2.88E-11	4.63E-06	1.194115
LOC100136661	7	79745594	79757141	2_15732124_A_C	2	15732124	1,25-dihydroxyvitamin D(3) 24-hydroxylase, mitochondrial	7.37914	2.88E-11	4.63E-06	1.194115
LOC100136661	7	79745594	79757141	2_15732128_C_T	2	15732128	1,25-dihydroxyvitamin D(3) 24-hydroxylase, mitochondrial	7.37914	2.88E-11	4.63E-06	1.194115
LOC100136661	7	79745594	79757141	2_15732148_A_T	2	15732148	1,25-dihydroxyvitamin D(3) 24-hydroxylase, mitochondrial	7.37914	2.88E-11	4.63E-06	1.194115
LOC100136661	7	79745594	79757141	2_15732154_C_A	2	15732154	1,25-dihydroxyvitamin D(3) 24-hydroxylase, mitochondrial	7.37914	2.88E-11	4.63E-06	1.194115
LOC100136661	7	79745594	79757141	2_21953811_C_T	2	21953811	1,25-dihydroxyvitamin D(3) 24-hydroxylase, mitochondrial	7.653706	7.12E-12	1.64E-06	1.270863
LOC100136661	7	79745594	79757141	2_21953812_T_A	2	21953812	1,25-dihydroxyvitamin D(3) 24-hydroxylase, mitochondrial	7.653706	7.12E-12	1.64E-06	1.270863
LOC100136661	7	79745594	79757141	2_26493929_G_A	2	26493929	1,25-dihydroxyvitamin D(3) 24-hydroxylase, mitochondrial	7.150621	9.13E-11	1.08E-05	1.306294
LOC100136661	7	79745594	79757141	2_27831058_T_A	2	27831058	1,25-dihydroxyvitamin D(3) 24-hydroxylase, mitochondrial	7.951686	1.53E-12	5.11E-07	1.240457
LOC100136661	7	79745594	79757141	2_27971780_G_T	2	27971780	1,25-dihydroxyvitamin D(3) 24-hydroxylase, mitochondrial	7.285153	4.64E-11	6.56E-06	1.037618
LOC100136661	7	79745594	79757141	2_28321505_T_A	2	28321505	1,25-dihydroxyvitamin D(3) 24-hydroxylase, mitochondrial	8.607111	5.00E-14	3.37E-08	1.352229
LOC100136661	7	79745594	79757141	2_29508970_A_G	2	29508970	1,25-dihydroxyvitamin D(3) 24-hydroxylase, mitochondrial	7.835956	2.79E-12	8.06E-07	1.281642
LOC100136661	7	79745594	79757141	2_31746104_G_T	2	31746104	1,25-dihydroxyvitamin D(3) 24-hydroxylase, mitochondrial	7.459635	1.92E-11	3.43E-06	1.334587
LOC100136661	7	79745594	79757141	2_31746114_G_T	2	31746114	1,25-dihydroxyvitamin D(3) 24-hydroxylase, mitochondrial	7.459635	1.92E-11	3.43E-06	1.334587
LOC100136661	7	79745594	79757141	2_37918430_T_A	2	37918430	1,25-dihydroxyvitamin D(3) 24-hydroxylase, mitochondrial	7.168635	8.34E-11	1.01E-05	1.381092
LOC100136661	7	79745594	79757141	2_37918432_C_T	2	37918432	1,25-dihydroxyvitamin D(3) 24-hydroxylase, mitochondrial	7.168635	8.34E-11	1.01E-05	1.381092
LOC100136661	7	79745594	79757141	2_69621001_G_T	2	69621001	1,25-dihydroxyvitamin D(3) 24-hydroxylase, mitochondrial	8.543662	6.98E-14	4.43E-08	1.679989
LOC100136661	7	79745594	79757141	2_73073726_T_A	2	73073726	1,25-dihydroxyvitamin D(3) 24-hydroxylase, mitochondrial	8.078488	7.95E-13	3.07E-07	1.27706
LOC100136661	7	79745594	79757141	2_73074052_C_A	2	73074052	1,25-dihydroxyvitamin D(3) 24-hydroxylase, mitochondrial	9.440425	6.02E-16	8.36E-10	1.498857
LOC100136661	7	79745594	79757141	2_76488218_G_A	2	76488218	1,25-dihydroxyvitamin D(3) 24-hydroxylase, mitochondrial	8.427636	1.28E-13	7.24E-08	1.39235
LOC100136661	7	79745594	79757141	2_79037410_A_C	2	79037410	1,25-dihydroxyvitamin D(3) 24-hydroxylase, mitochondrial	7.306814	4.16E-11	6.06E-06	1.175537
LOC100136661	7	79745594	79757141	2_81805013_A_G	2	81805013	1,25-dihydroxyvitamin D(3) 24-hydroxylase, mitochondrial	7.616939	8.59E-12	1.88E-06	1.399145
LOC100136661	7	79745594	79757141	2_81805019_A_G	2	81805019	1,25-dihydroxyvitamin D(3) 24-hydroxylase, mitochondrial	7.615127	8.67E-12	1.90E-06	1.398953
LOC100136661	7	79745594	79757141	3_1982583_T_C	3	1982583	1,25-dihydroxyvitamin D(3) 24-hydroxylase, mitochondrial	-8.93602	8.80E-15	8.03E-09	-1.61544
LOC100136661	7	79745594	79757141	3_4636314_T_A	3	4636314	1,25-dihydroxyvitamin D(3) 24-hydroxylase, mitochondrial	9.16635	2.59E-15	2.88E-09	1.402361

Supplementary File 3

GWAS Significant SNPs for Body weight (First 50):

CHR	SNP	BP	UNADJ	GC	FDR_BH	Is_Intergenic	Matched_Gene	Nearest_Gene_Right	Distance_To_Right_Gene	Nearest_Gene_Left	Distance_To_Left_Gene
8	8_6425640	64256406	2.99E-10	2.52E-07	0.00058	Yes		tmem53	43825	LOC110530324	99126
8	8_6468282	64682826	4.4E-10	3.31E-07	0.00058	No	LOC110530341	LOC110530341	0	LOC110530341	0
8	8_6299979	62999790	5.6E-10	3.89E-07	0.00058	No	LOC110530310	LOC110530310	0	LOC110530310	0
8	8_6468486	64684869	5.7E-10	3.96E-07	0.00058	No	LOC110530341	LOC110530341	0	LOC110530341	0
8	8_6468407	64684075	6.9E-10	4.47E-07	0.00058	No	LOC110530341	LOC110530341	0	LOC110530341	0
8	8_6447567	64475678	6.93E-10	4.52E-07	0.00058	No	zswim5	zswim5	0	zswim5	0
8	8_6442184	64421848	1.09E-09	6.15E-07	0.000659	Yes		zswim5	11257	elovl8a	63144
8	8_6300040	63000408	1.13E-09	6.32E-07	0.000659	No	LOC110530310	LOC110530310	0	LOC110530310	0
8	8_6468437	64684375	1.51E-09	7.75E-07	0.000659	No	LOC110530341	LOC110530341	0	LOC110530341	0
8	8_6467944	64679448	1.91E-09	9.09E-07	0.000659	No	LOC110530341	LOC110530341	0	LOC110530341	0
8	8_6467978	64679781	1.97E-09	9.28E-07	0.000659	No	LOC110530341	LOC110530341	0	LOC110530341	0
8	8_6467979	64679790	1.97E-09	9.28E-07	0.000659	No	LOC110530341	LOC110530341	0	LOC110530341	0
8	8_6467976	64679760	2.03E-09	9.47E-07	0.000659	No	LOC110530341	LOC110530341	0	LOC110530341	0
8	8_6468182	64681822	2.03E-09	9.48E-07	0.000659	No	LOC110530341	LOC110530341	0	LOC110530341	0
8	8_6468004	64680049	2.17E-09	1E-06	0.000659	No	LOC110530341	LOC110530341	0	LOC110530341	0
16	16_5516061	55160646	2.22E-09	1E-06	0.000659	Yes		sema3b	6117	sema3bl	21543
8	8_6451439	64514399	2.23E-09	9.93E-07	0.000659	No	LOC110530332	LOC110530332	0	LOC110530332	0
8	8_6468171	64681718	2.82E-09	1.19E-06	0.00074	No	LOC110530341	LOC110530341	0	LOC110530341	0
8	8_6468185	64681853	2.82E-09	1.19E-06	0.00074	No	LOC110530341	LOC110530341	0	LOC110530341	0
8	8_6425660	64256609	3.02E-09	1.24E-06	0.00074	Yes		tmem53	43622	LOC110530324	99329
8	8_6240810	62408102	3.09E-09	1.26E-06	0.00074	Yes		LOC110530307	105202	LOC110530306	95609
8	8_6347675	63476754	3.55E-09	1.38E-06	0.000811	No	LOC110530317	LOC110530317	0	LOC110530317	0
8	8_6451209	64512090	4.21E-09	1.56E-06	0.000908	No	LOC110530332	LOC110530332	0	LOC110530332	0
8	8_6442307	64423071	4.33E-09	1.59E-06	0.000908	Yes		zswim5	10034	elovl8a	64367
8	8_6392417	63924176	4.79E-09	1.71E-06	0.00093	Yes		LOC110530324	61153	klf17	31703
8	8_6392403	63924033	4.93E-09	1.74E-06	0.00093	Yes		LOC110530324	61296	klf17	31560
8	8_6425799	64257998	5.16E-09	1.79E-06	0.00093	Yes		tmem53	42233	LOC110530324	100718
8	8_6208910	62089102	5.47E-09	1.85E-06	0.00093	No	LOC110530303	LOC110530303	0	LOC110530303	0
8	8_6453894	64538943	5.72E-09	1.91E-06	0.00093	No	LOC118965543	LOC118965543	0	LOC118965543	0
8	8_6454261	64542611	6.46E-09	2.08E-06	0.00093	No	LOC110530333	LOC110530333	0	LOC110530333	0
8	8_6451944	64519444	6.65E-09	2.13E-06	0.00093	No	LOC110530332	LOC110530332	0	LOC110530332	0
8	8_6451944	64519446	6.65E-09	2.13E-06	0.00093	No	LOC110530332	LOC110530332	0	LOC110530332	0
8	8_6453059	64530592	6.79E-09	2.17E-06	0.00093	Yes		LOC118965543	1679	LOC110530332	1924
8	8_6299904	62999040	7.55E-09	2.32E-06	0.00093	No	LOC110530310	LOC110530310	0	LOC110530310	0
8	8_6294453	62944530	7.77E-09	2.37E-06	0.00093	No	LOC110530309	LOC110530309	0	LOC110530309	0
8	8_6332668	63326685	7.9E-09	2.41E-06	0.00093	Yes		LOC110530316	49356	LOC110530314	31982
8	8_6447382	64473825	8.01E-09	2.41E-06	0.00093	No	zswim5	zswim5	0	zswim5	0
8	8_6294287	62942878	8.36E-09	2.48E-06	0.00093	No	LOC110530309	LOC110530309	0	LOC110530309	0
8	8_6208930	62089303	8.74E-09	2.57E-06	0.00093	No	LOC110530303	LOC110530303	0	LOC110530303	0
16	16_5552722	55527235	8.94E-09	2.62E-06	0.00093	No	LOC110492332	LOC110492332	0	LOC110492332	0
16	16_5552722	55527236	8.94E-09	2.66E-06	0.00093	No	LOC110492332	LOC110492332	0	LOC110492332	0
16	16_5552722	55527239	8.94E-09	2.62E-06	0.00093	No	LOC110492332	LOC110492332	0	LOC110492332	0
8	8_6294444	62944446	9E-09	2.62E-06	0.00093	No	LOC110530309	LOC110530309	0	LOC110530309	0
8	8_6451692	64516928	9.17E-09	2.62E-06	0.00093	No	LOC110530332	LOC110530332	0	LOC110530332	0
8	8_6259526	62595263	9.21E-09	2.66E-06	0.00093	No	LOC110530307	LOC110530307	0	LOC110530307	0
8	8_6433243	64332435	9.61E-09	2.74E-06	0.00093	No	LOC110530325	LOC110530325	0	LOC110530325	0
8	8_6468018	64680188	9.66E-09	2.79E-06	0.00093	No	LOC110530341	LOC110530341	0	LOC110530341	0

GWAS Significant SNPs for Muscle yield (First 50) and Manhattan Plot:

CHR	SNP	BP	UNADJ	GC	FDR_BH	Is_Intergenic	Matched_Gene	Nearest_Gene_Right	Distance_To_Right_Gene	Nearest_Gene_Left	Distance_To_Left_Gene
5	5_5174072	51740724	1.09E-10	4.12E-10	0.000242	No	LOC110522962	LOC110522962	0	LOC110522962	0
5	5_6323702	63237024	4.07E-10	1.42E-09	0.000242	Yes		LOC110524282	20573	LOC110524279	22121
5	5_5174063	51740638	4.1E-10	1.43E-09	0.000242	No	LOC110522962	LOC110522962	0	LOC110522962	0
5	5_5174064	51740645	4.1E-10	1.43E-09	0.000242	No	LOC110522962	LOC110522962	0	LOC110522962	0
5	5_5174287	51742873	5.03E-10	1.73E-09	0.000242	No	LOC110522962	LOC110522962	0	LOC110522962	0
5	5_5174077	51740773	5.04E-10	1.74E-09	0.000242	No	LOC110522962	LOC110522962	0	LOC110522962	0
5	5_5174078	51740783	5.04E-10	1.74E-09	0.000242	No	LOC110522962	LOC110522962	0	LOC110522962	0
5	5_5173888	51738884	7.31E-10	2.47E-09	0.000242	No	LOC110522962	LOC110522962	0	LOC110522962	0
5	5_5173853	51738530	7.47E-10	2.52E-09	0.000242	No	LOC110522962	LOC110522962	0	LOC110522962	0
5	5_5173855	51738552	7.47E-10	2.52E-09	0.000242	No	LOC110522962	LOC110522962	0	LOC110522962	0
5	5_5174106	51741067	7.74E-10	2.62E-09	0.000242	No	LOC110522962	LOC110522962	0	LOC110522962	0
5	5_5173904	51739049	7.78E-10	2.62E-09	0.000242	No	LOC110522962	LOC110522962	0	LOC110522962	0
5	5_5173905	51739054	7.78E-10	2.6E-09	0.000242	No	LOC110522962	LOC110522962	0	LOC110522962	0
5	5_5174183	51741830	7.97E-10	2.67E-09	0.000242	No	LOC110522962	LOC110522962	0	LOC110522962	0
5	5_5174055	51740556	8.17E-10	2.74E-09	0.000242	No	LOC110522962	LOC110522962	0	LOC110522962	0
5	5_5174032	51740321	8.25E-10	2.77E-09	0.000242	No	LOC110522962	LOC110522962	0	LOC110522962	0
5	5_5173921	51739218	8.33E-10	2.79E-09	0.000242	No	LOC110522962	LOC110522962	0	LOC110522962	0
5	5_5173951	51739511	8.66E-10	2.89E-09	0.000242	No	LOC110522962	LOC110522962	0	LOC110522962	0
5	5_4023606	40236069	1.08E-09	3.58E-09	0.000287	Yes		LOC110523804	13804	LOC110523803	5200
5	5_5173843	51738437	1.18E-09	3.87E-09	0.000296	No	LOC110522962	LOC110522962	0	LOC110522962	0
5	5_5174042	51740428	1.27E-09	4.13E-09	0.000303	No	LOC110522962	LOC110522962	0	LOC110522962	0
5	5_7154362	71543622	1.44E-09	4.65E-09	0.000328	No	LOC110524493	LOC110524493	0	LOC110524493	0
5	5_4623402	46234021	1.64E-09	5.27E-09	0.000354	No	LOC110523953	LOC110523953	0	LOC110523953	0
5	5_4623372	46233722	1.73E-09	5.55E-09	0.000354	No	LOC110523953	LOC110523953	0	LOC110523953	0
5	5_3683217	36832172	1.83E-09	5.85E-09	0.000354	No	lrrc75bb	lrrc75bb	0	lrrc75bb	0
5	5_3683218	36832189	1.83E-09	5.85E-09	0.000354	No	lrrc75bb	lrrc75bb	0	lrrc75bb	0
5	5_4623362	46233621	2.43E-09	7.64E-09	0.000402	No	LOC110523953	LOC110523953	0	LOC110523953	0
5	5_6903809	69038096	2.56E-09	8.01E-09	0.000402	No	eps15	eps15	0	eps15	0
5	5_5173807	51738076	2.56E-09	8.04E-09	0.000402	No	LOC110522962	LOC110522962	0	LOC110522962	0
5	5_5173676	51736768	2.59E-09	8.13E-09	0.000402	No	LOC110522962	LOC110522962	0	LOC110522962	0
5	5_5173743	51737431	2.59E-09	8.13E-09	0.000402	No	LOC110522962	LOC110522962	0	LOC110522962	0
5	5_5173763	51737636	2.59E-09	8.13E-09	0.000402	No	LOC110522962	LOC110522962	0	LOC110522962	0
5	5_5173808	51738089	2.67E-09	8.35E-09	0.000402	No	LOC110522962	LOC110522962	0	LOC110522962	0
5	5_5173739	51737396	2.72E-09	8.49E-09	0.000402	No	LOC110522962	LOC110522962	0	LOC110522962	0
5	5_3933773	39337735	2.97E-09	9.21E-09	0.000427	No	nadk2	nadk2	0	nadk2	0
5	5_3217743	32177436	3.29E-09	1.02E-08	0.000447	Yes		LOC110523609	6308	LOC110523607	5636
5	5_3217755	32177553	3.29E-09	1.02E-08	0.000447	Yes		LOC110523609	6191	LOC110523607	5753
5	5_4623349	46233491	3.78E-09	1.21E-08	0.000501	No	LOC110523953	LOC110523953	0	LOC110523953	0
5	5_3933735	39337351	3.96E-09	1.16E-08	0.000511	No	nadk2	nadk2	0	nadk2	0
5	5_3285263	32852630	5.77E-09	1.72E-08	0.000725	No	LOC110523629	LOC110523629	0	LOC110523629	0
5	5_3933741	39337418	6.38E-09	1.89E-08	0.000782	No	nadk2	nadk2	0	nadk2	0
5	5_4623550	46235507	7.22E-09	2.13E-08	0.000864	No	LOC110523953	LOC110523953	0	LOC110523953	0
10	10_100273	10027308	1.02E-08	2.93E-08	0.001187	Yes		LOC110533311	26174	LOC110533312	60376
5	5_5875125	58751253	1.4E-08	3.98E-08	0.00157	No	LOC110522978	LOC110522978	0	LOC110522978	0
10	10_100272	10027249	1.41E-08	3.98E-08	0.00157	Yes		LOC110533311	26233	LOC110533312	60317
5	5_3134026	31340267	1.55E-08	4.39E-08	0.001647	Yes		LOC110522855	256791	LOC110523598	54068
5	5_3464074	34640749	1.56E-08	4.37E-08	0.001647	Yes		LOC110523660	446077	ppp2r2ab	123176

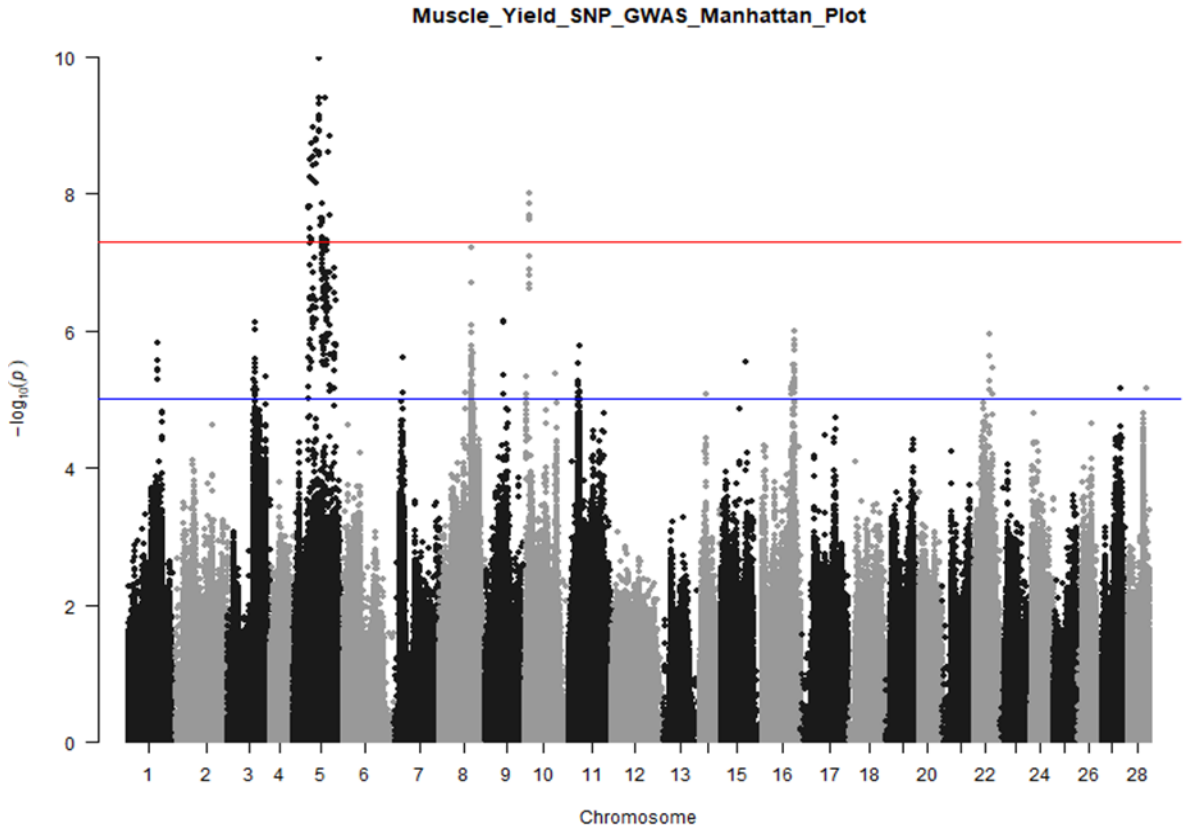
Muscle_Yield_SNP_GWAS_Manhattan_Plot
10
8
6
4
2
0
$-\log_{10}(p)$
1
2
3
4
5
6
7
8
9
10
11
12
13
15
16
17
18
20
22
24
26
28
Chromosome

GWAS Significant SNPs for Condition (First 50) and Manhattan Plot:

CHR	SNP	BP	UNADJ	GC	FDR_BH	Is_Intergenic	Matched_Gene	Nearest_Gene_Right	Distance_To_Right_Gene	Nearest_Gene_Left	Distance_To_Left_Gene
5	5_4841892	48418925	3.14E-10	7.88E-08	0.000113	No	sec16a	sec16a	0	sec16a	0
5	5_4003822	40038229	5.55E-10	1.2E-07	0.00018	Yes		LOC110523800	3532	rai14	46424
5	5_4003816	40038162	5.72E-10	1.22E-07	0.00018	Yes		LOC110523800	3599	rai14	46357
5	5_4467982	44679829	6.71E-10	1.39E-07	0.000188	No	itga1	itga1	0	itga1	0
2	2_6809408	68094085	6.74E-10	1.39E-07	0.000188	No	cdh13	cdh13	0	cdh13	0
5	5_3836704	38367041	8.56E-10	1.66E-07	0.000213	No	LOC110523766	LOC110523766	0	LOC110523766	0
5	5_4003895	40038951	9.03E-10	1.72E-07	0.000213	Yes		LOC110523800	2810	rai14	47146
5	5_3836704	38367045	9.8E-10	1.84E-07	0.000213	No	LOC110523766	LOC110523766	0	LOC110523766	0
5	5_3836708	38367083	9.8E-10	1.84E-07	0.000213	No	LOC110523766	LOC110523766	0	LOC110523766	0
5	5_3137303	31373037	9.86E-10	1.85E-07	0.000213	Yes		LOC110522855	224021	LOC110523598	86838
5	5_6161220	61612205	1.02E-09	1.89E-07	0.000213	Yes		LOC110524247	5782	nr2c2ap	12873
5	5_5656016	56560165	1.11E-09	2.02E-07	0.000215	Yes		LOC110524093	18470	LOC118964624	13471
5	5_5656038	56560386	1.11E-09	2.02E-07	0.000215	Yes		LOC110524093	18249	LOC118964624	13692
5	5_5656023	56560238	1.15E-09	2.07E-07	0.000215	Yes		LOC110524093	18397	LOC118964624	13544
5	5_4003888	40038851	1.2E-09	2.12E-07	0.000215	Yes		LOC110523800	2910	rai14	47046
5	5_4003886	40038866	1.41E-09	2.4E-07	0.000241	Yes		LOC110523800	2895	rai14	47061
5	5_3195016	31950162	1.44E-09	2.44E-07	0.000241	Yes		LOC110523606	136075	LOC110523605	7255
5	5_6161226	61612260	1.53E-09	2.6E-07	0.000244	Yes		LOC110524247	5727	nr2c2ap	12928
5	5_4003915	40039153	1.57E-09	2.56E-07	0.000244	Yes		LOC110523800	2608	rai14	47348
5	5_4003902	40039027	1.69E-09	2.74E-07	0.000244	Yes		LOC110523800	2734	rai14	47222
5	5_4003898	40038981	1.7E-09	2.76E-07	0.000244	Yes		LOC110523800	2780	rai14	47176
5	5_6161178	61611787	1.73E-09	2.82E-07	0.000244	Yes		LOC110524247	6200	nr2c2ap	12455
12	12_557948	55794852	1.89E-09	3E-07	0.000244	No	LOC110537815	LOC110537815	0	LOC110537815	0
5	5_5244036	52440365	1.91E-09	2.98E-07	0.000244	No	ptprsa	ptprsa	0	ptprsa	0
5	5_4003851	40038517	1.98E-09	3.09E-07	0.000244	Yes		LOC110523800	3244	rai14	46712
5	5_4003856	40038566	1.98E-09	3.08E-07	0.000244	Yes		LOC110523800	3195	rai14	46761
12	12_558009	55800950	2E-09	3.08E-07	0.000244	No	LOC110537815	LOC110537815	0	LOC110537815	0
12	12_557973	55797318	2E-09	3.12E-07	0.000244	No	LOC110537815	LOC110537815	0	LOC110537815	0
5	5_4841434	48414348	2.11E-09	3.29E-07	0.000244	No	sec16a	sec16a	0	sec16a	0
5	5_7684529	76845291	2.16E-09	3.29E-07	0.000244	Yes		LOC110524596	146700	LOC118964533	124159
5	5_7684531	76845313	2.16E-09	3.26E-07	0.000244	Yes		LOC110524596	146678	LOC118964533	124181
5	5_6161112	61611127	2.18E-09	3.34E-07	0.000244	Yes		LOC110524247	6860	nr2c2ap	11795
5	5_4078668	40786688	2.3E-09	3.46E-07	0.000246	No	LOC110523821	LOC110523821	0	LOC110523821	0
5	5_4078681	40786818	2.3E-09	3.46E-07	0.000246	No	LOC110523821	LOC110523821	0	LOC110523821	0
5	5_7296233	72962330	2.44E-09	3.61E-07	0.000255	Yes		LOC110524517	42925	LOC110524516	43599
5	5_3547930	35479308	2.65E-09	3.82E-07	0.000267	No	stoml2	stoml2	0	stoml2	0
5	5_4003941	40039417	2.71E-09	3.9E-07	0.000267	Yes		LOC110523800	2344	rai14	47612
5	5_5656090	56560902	2.71E-09	3.91E-07	0.000267	Yes		LOC110524093	17733	LOC118964624	14208
5	5_6936270	69362701	2.81E-09	4.01E-07	0.000268	Yes		LOC110524443	103570	LOC110524442	12150
5	5_4841751	48417519	2.82E-09	4.04E-07	0.000268	No	sec16a	sec16a	0	sec16a	0
12	12_557979	55797923	2.93E-09	4.13E-07	0.000268	No	LOC110537815	LOC110537815	0	LOC110537815	0
12	12_557985	55798571	2.94E-09	4.14E-07	0.000268	No	LOC110537815	LOC110537815	0	LOC110537815	0
5	5_5656069	56560694	3.13E-09	4.35E-07	0.000268	Yes		LOC110524093	17941	LOC118964624	14000
5	5_5655775	56557753	3.2E-09	4.43E-07	0.000268	Yes		LOC110524093	20882	LOC118964624	11059
5	5_4841875	48418756	3.32E-09	4.54E-07	0.000268	No	sec16a	sec16a	0	sec16a	0
5	5_5656103	56561039	3.32E-09	4.58E-07	0.000268	Yes		LOC110524093	17596	LOC118964624	14345

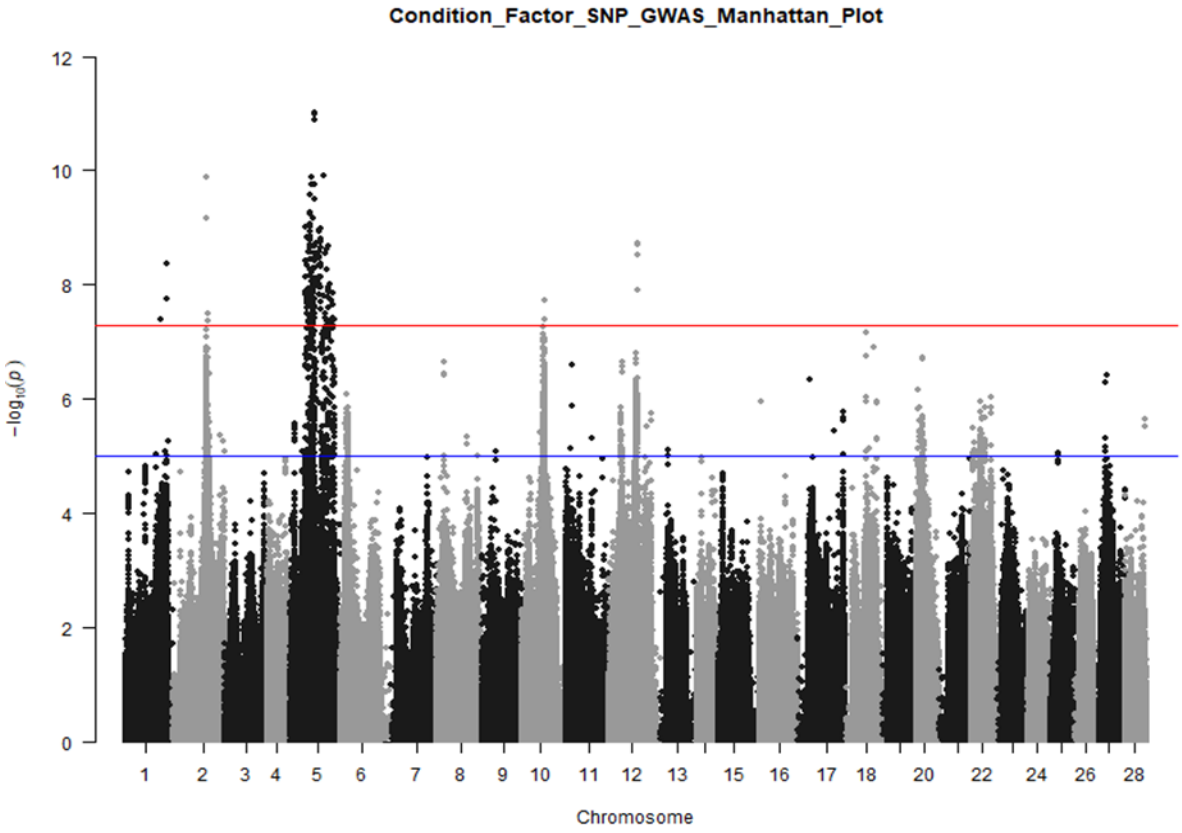

Observed Gain/Loss of Transcription Factor:

2_27321356_C_G_SNP TFBS changes:

id	Loss/Gain	**TF**
MA0634.1	Loss	ALX3
MA0658.1	Loss	LHX6
MA0699.1	Loss	LBX2
MA0700.1	Loss	LHX2
MA0722.1	Loss	VAX1
MA0723.1	Loss	VAX2
MA0725.1	Loss	VSX1
MA0726.1	Loss	VSX2
MA0914.1	Loss	ISL2
MA1128.1	Loss	FOSL1::JUN
MA1132.1	Loss	JUN::JUNB
MA1137.1	Loss	FOSL1::JUNB

19_55095320_G_A SNP TFBS changes:

id	Loss/Gain	**TF**
MA0672.1	Loss	NKX2-3
MA0673.1	Loss	NKX2-8
MA0635.1	Gain	BARHL2

2_27318690_A_G SNP TFBS changes:

id	Loss/Gain	**TF**
MA0673.1	Loss	NKX2-8

CHAPTER 6: Genomic prediction of growth traits using genomic and microbiome data in Rainbow trout

Abstract

Improving growth and muscle yield are goals of many aquaculture breeding programs. Genetic improvement for growth traits in rainbow trout have been facilitated using pedigree-information and genomic data. In recent times, the role of gut microbiome in shaping host phenotypic traits variation is gaining traction. Here, we tested if the inclusion microbiome information improves accuracy of genomic prediction for body weight and muscle yield in rainbow trout. A total of 348 rainbow trout with phenotypic, metagenomics, and genomic data were used. The microbiome information was included using two methods: Jaccard similarity and as microbiome covariance matrix.

A cross-validation approach was used to predict the traits, using seven models with different combinations of the pedigree, genomic and microbiome information; gen (genomics only), ped (pedigree only), micro (microbiome only) model The heritability of muscle yield was estimated at between 0.38 (gen), and 0.47 (ped + gen), and body weight heritability estimated as 0.48 (gen) and (0.55 (ped + gen). The microbiome composition (microbiability) explained up to 0.23, 0.21 and 0.18 of the muscle yield phenotypic variances using the pathway, taxa, and gene family abundance, respectively with the micro model. Microbiability estimates were up to 0.23, 0.22, and 0.21 for muscle yield using taxa, pathway and gene family abundance, respectively.

Compared to ped+gen model, adding microbiome information (ped+gen+micro) resulted in an improvement of the prediction accuracy for body weight by up to 7.20% (0.375 to 0.402). Including microbiome information improved the prediction accuracy of muscle yield by up to 8% (gen VS gen+micro model).Microbiome-wide association analysis using principal components that explains up to 75% of the variance in the microbiome data identified important microbiome taxa including including *Cetobacterium sp,* Lactobacillus species (*crispatus, amylovorus, kitasatonis*) and *Ligilactobacillus salivarius* as associated with muscle yield and body weight.

This study provides insight on the use of microbiome information for the phenotypic prediction of growth traits in rainbow trout. The inclusion of microbiome information in the models shows potential to improve the predictive ability of body weight and muscle yield in rainbow trout

Introduction

Globally, the aquaculture sector is the fastest growing food sector, and the United Nations estimated a fish demand rise to up to 47 million tonnes causing a fish demand-supply gap of 28 million tonnes (Burbridge et al., 2001; Cai & Leung, 2017).

Rainbow trout is one of the most widely cultured finfish in the world. In the United States, a key challenge to achieving improved productivity in rainbow trout aquaculture is the lack of genetically improve strains to provide faster growth and improved efficiency (Fornshell, 2002). A family-based selective breeding programs was established to produce rainbow trout of improved genetics, especially for faster growth (Leeds et al., 2016). Body weight and fillet yield are amenable to selective breeding as moderate to high heritabilities have been reported for them (Ali et al., 2020; Gonzalez-Pena et al., 2016).

As against relying on Most selective breeding programs rely on phenotypic and pedigree data to make selection decisions and achieve genetic improvement, recent studies have shown that incorporating genomic information into selection decisions can help to accelerate genetic gains especially for lethal traits like the fillet yield (Al-Tobasei et al., 2021).

Compared to the traditional, pedigree-based method, genomic selection allows accurate selection of breeding candidates at an early life stage (Song et al., 2023). Genomic selection has been effectively used to achieve genetic gain in several aquaculture species including tilapia (Joshi et al., 2020), Atlantic salmon (Bangera et al., 2017), catfish (Zhang et al., 2020) and rainbow trout (Al-Tobasei et al., 2021). Our previous study shows that genomic prediction accuracies outperforms pedigree-based selection accuracies by up to 35% and 42% for fillet yield and fillet texture, respectively (Al-Tobasei et al., 2021). Reducing the SNP panel densities to 500–800 SNPs in still provides predictive abilities higher than pedigree-based method. A study by Kriaridou et al. (2020) revealed the possibility of achieving genetic improvement using the same cheaper, low and medium-density SNP panels (100 to 9,000 SNPs) across four aquaculture species: Atlantic salmon, common carp, gilthead sea bream, and Pacific oyster. Vu et al. (2022) found that genomic prediction outperformed pedigree-based BLUP by 22–24% for survival status and survival time for resistance to Edwardsiella ictaluri, the causative agent of Bacillary Necrosis, in stripped catfish. A study on rainbow trout demonstrated that genomic selection with 12K–40 K SNP arrays doubled the accuracy of predicted breeding values for bacterial cold water disease resistance compared to pedigree-based methods (Vallejo et al., 2017). Genomic prediction in Yellow River carp using a 250K SNP array showed that GBLUP outperformed pedigree-based BLUP by up to 37.5% for growth and morphological traits (J. Wang et al., 2021).

Alongside the host genetic information, the microbiome, the community of microorganisms living in and on a host—plays an increasingly recognized role in shaping hosts' phenotypic variation (Gao et al., 2023). The gut microbiome can influence phenotypic traits in the host animal by modulating growth, immunity, and nutrient metabolism (Brugman & Nieuwenhuis, 2010; Cerf-Bensussan & Gaboriau-Routhiau, 2010; Wang et al., 2018). In rainbow trout, the gut microbiome

affects traits such as fillet color, a key marketing attribute. Our previous study showed that rainbow trout families with reddish-pink fillets had enriched probiotic bacteria like *Leuconostoc lactis* and *Corynebacterium variabile*, which produce carotenoid pigments, compared to pale fillet fish families (Ridwan O Ahmed et al., 2023). These microbial differences suggest a gut microbiome role in astaxanthin metabolism, impacting fillet pigmentation. We also showed that fast-growing rainbow trout are enriched in cellulose, amylose degrading and amino acid fermenting bacteria (*Clostridium*, *Leptotrichia,* and *Peptostreptococcus*) , while pathogenic bacteria (*Corynebacterium* and *Paeniclostridium*) were enriched in the slow-growing fish (Chapagain et al., 2019). Similarly, in large yellow croaker (*Larimichthys crocea*), genomic selection for swimming performance altered gut microbiota, with the selected line showing higher survival (64.8% vs. 37.3%) and feed efficiency, linked to distinct microbial profiles (Liu et al., 2025). These findings highlight the gut microbiome's role in nutrient metabolism, immune function, and phenotypic variation across aquaculture species. The microbiome composition could therefore be a valuable predictor of complex phenotypes.

Most of the selection efforts in aquaculture have been through exploiting the genomic variability present among individual fish and between fish families. However, the gut microbiome, recently identified as a key component contributing significantly to the variation of many phenotypes. The integration of gut microbiome data with genomic information has potential to enhance genomic prediction for complex traits in livestock and aquaculture species. As a result, many studies in terrestrial livestock species have investigated the integration of both information. In swine, incorporating microbiome data into genomic models improved prediction accuracy for growth and body composition by up to 10–20%, with microbiability estimates ranging from 0.02–0.52 across breeds (He et al., 2022). In sheep, and swine, the inclusion of microbiome and genomic information in genomic prediction have been reported to improve prediction accuracies for several complex traits (Khanal et al., 2020a; Ross et al., 2020). Other studies in poultry, cattle found no improvement in accuracy with the inclusion of microbiome information (Saedi et al., 2024; Xiong et al., 2024). Buitenhuis et al. (2019) found contrasting effect of microbiome information in predicting milk fatty acid composition in cattle. They found that the inclusion of microbiome information improved prediction accuracy for C15:0 and C18:3 n-3, while it was not beneficial for milk fatty acid profiles.

With the increasing drop in the cost of genome sequencing, the inclusion of genomic information in predicting the performance of aquaculture species is becoming more popular, but the inclusion of microbiome information into that prediction is limited, and absent in rainbow trout.

Thus, the objectives of this study were to conduct microbiome wide association study to identify gut microbiome features associated with growth traits, and to test the effect of the inclusion of microbiome information into genomic prediction models for body weight and muscle yield in rainbow trout.

Methods

Rainbow Trout Population and Experimental Design

We used the same experimental design and animals described in Ahmed et al. (2023). We used rainbow trout from a muscle yield genetic selection line developed at the National Center for Cool and Cold-Water Aquaculture (NCCCWA). This line started as a growth-selected line in 2002 and underwent five generations of selection for improved growth performance as described by Leeds et al. (2016). Subsequent generations were selected for muscle yield as described in Cleveland et al. (2023) and Garcia et al. (2023a). Fish from the 2020-year class (YC) were used in this study, representing the third-generation families from lines selected for high (ARS-FY-H) or low (ARS-FY-L) fillet yield.

Breeding and Hatching

Briefly, the fish used for this study were from 40 families (20 full-sib families each from the ARS-FY-H and -L lines) received from the NCCCWA at 322 days post-hatch and reared at the Crane Aquaculture facility of the University of Maryland, College Park. The aquaculture facility uses a recirculating aquaculture system (RAS) with all water quality parameters closely monitored. The fish were fed an astaxanthin-supplemented diet (BioTrout 4.0mm & 6.0mm, ~ 40ppm astaxanthin) from Bio-Oregon at an ad libitum feeding rate for approximately six months before harvest. At the age of between 450 to 485 days post-hatch, 442 fish were harvested (average body weight = 694.36g; SD = 173.76). The fish were taken off feed a day before harvesting. Tissue samples were collected on the harvest day for nucleic acid extraction. The fish were allowed to undergo rigor mortis on ice for 48 hours and manually processed into trimmed, skinless fillets on the third day. The harvest period was done for six consecutive weeks, and sampling was done so that each week, we had a representative of one to two fish per family. Sixty fish were harvested in the first and second week, while 80 were harvested in each subsequent week, and 82 in the final week. Fecal samples were collected from each fish for microbiome sequencing.

Microbiome collection and sequencing

Fecal DNA Extraction, Library preparation, and Metagenomic sequencing

DNA was extracted from fecal samples from individual fish using the ZymoBIOMICS®-96 MagBead DNA Kit (Zymo Research, Irvine, CA) and following the manufacturer's instructions. The genomic DNA extracted was used to prepare the library following Illumina® DNA Library Prep Kit (Illumina, San Diego, CA) with up to 500 ng DNA input following the manufacturer's protocol using unique dual-index 10 bp barcodes with Nextera® adapters (Illumina, San Diego, CA). All libraries were pooled in equal abundance. The final pool was quantified using qPCR and TapeStation® (Agilent Technologies, Santa Clara, CA). The final library was profiled with shotgun metagenomic sequencing on the NovaSeq X or 6000® (Illumina, San Diego, CA) platform.

The ZymoBIOMICS® Microbial Community Standard (Zymo Research, Irvine, CA) was used as a positive control for each DNA extraction. The ZymoBIOMICS® Microbial Community DNA Standard (Zymo Research, Irvine, CA) was used as a positive control for each library preparation. Negative controls (i.e. blank extraction control, blank library preparation control) were included to assess the bioburden level carried by the wet-lab process.

Metagenomics Sequence Data Processing and Analysis

The paired raw reads were checked for quality control using FastQC (Andrews, 2010). This was followed by trimming the Illumina Nexterra adapter sequences and low-quality reads using a minimum base quality of 20 Phred and length of 70bp with Cutadapt (v48) (Martin, 2011). Furthermore, host and human sequence contaminations in the trimmed reads were removed using bowtie2 (v2.5.4) (Langmead & Salzberg, 2012) using rainbow trout (Refseq assembly accession: GCA_013265735.3) and human (Refseq assembly accession: GCF_000001405.40) assemblies. The unmapped data were considered clean reads, free of human and host contamination. The resulting clean sequence reads were used for subsequent analysis.

Taxonomic Classification, Abundance Estimation, and Functional Profiling

The MetaPhlAn3 software (Beghini et al., 2021), which profiles functional taxonomy, was used for species-level taxonomic profiling using default parameters. This outputs the abundance of microbiome taxa present in each sample. The HUMAnN3 software (Beghini et al., 2021) was used to profile the gene family, and pathways from the metagenomic reads of each sample using the UniRef90 database. This outputs the abundance of each detected gene and pathway.

The three microbiome abundance data - taxa abundance, gene family abundance, and pathway abundance — represent different levels of biological organization in the microbiome and each provides unique insights into the microbial community. The taxa abundance measures the relative presence of microbial taxa, while gene family measures the abundance of protein-coding gene families capturing the functional potential of the microbial community, while pathway abundance estimates the abundance of complete metabolic pathways reflecting what biological processes are active or enriched.

Genotyping

Tissue DNA extraction, genotyping, and quality control (QC)

Genomic DNA extraction on 442 fish was carried out using a modified salting-out protocol (Salem et al., 2012). DNA quality was assessed using gel electrophoresis, while DNA quantity was measured using Qubit fluorometry (Catalog# Q32853).

Library Preparation and Sequencing

Libraries were generated using a modified protocol with the Illumina Nextera DNA Flex Library Preparation kit. Sequencing libraries were paired-end with an average insert size of approximately 350 bp. Library quality was assessed using TapeStation (Agilent), and final libraries were quantified by fluorometry prior to pooling. Adapter sequences utilized for libraries were standard Illumina adapters. The sequencing was performed on an Illumina NovaSeq 6000 (Paired End Reads 2x150).

The library was subjected to low-pass whole-genome sequencing genotyping. The samples were sequenced to an average coverage of 1x, and the imputation of genotypes was performed using L-oimpute v0.18 by Gencove, Inc. (New York, NY) , based on the imputation model developed by Rubinacci et al. (2023). Several studies have shown that low-pass sequencing could be a cost-efficient alternative to genotyping arrays and produce comparable quality (Wasik et al., 2021).

Quality control

Quality control (QC) was done using VCFtools (Danecek et al., 2011), with the following parameters: a threshold for minor allele frequency of 5% (–maf 0.05), a Hardy-Weinberg equilibrium threshold of 1e-06 (- hwe 1e-06), a maximum allele count of 2 (- max-allele 2), and a maximum missingness rate of 0.5 (- max-missing 0.5). A total of 12,047,625 SNPs were retained for further analysis.

Phenotype prediction using pedigree, genomic and microbiome data

We retained only the fish that had matched metagenomics data, phenotypes, and genotypes, resulting in 348 fish available for the analysis. To predict phenotypes using genomic, pedigree, and microbiome data, we constructed genomic (G_matrix), pedigree (A_matrix), and microbiome relationship matrices. These matrices were then integrated into the genomic prediction.

Pedigree-data processing and A_matrix

The pedigree relationship matrix (A_matrix) was computed from pedigree data (1,613 individuals) using `kinship2` package in R (Sinnwell et al., 2014). A full pedigree was created, assigning sexes (F for Dam, M for Sire, U for unknown), and the kinship matrix was calculated, doubled (2 × kinship), adjusted for positive definiteness (`Matrix::nearPD`), normalized (divided by maximum diagonal), and perturbed ((10^{-6}) on diagonal)).

Genomic data processing and Genomic Relationship matrix (G)

The genomic relationship matrix G_matrix was computed from the SNP data file using `AGHmatrix::Gmatrix` (VanRaden method, ploidy = 2) (Amadeu et al., 2023). The SNP matrix was converted to a numeric matrix, and the G_matrix was adjusted (`nearPD`), normalized, and perturbed (10^{-6}).

Microbiome data processing and Microbiome relationship matrix (M)

The microbiome data comprised the metaphlan taxa abundance, HUMAnN3 pathway, and gene family abundances. The HUMAnN3 pathway dimension is 349 samples × 6,684 features, the HUMAnN3 gene family dimension is 349 samples × 1,114,049 features, and the metaphlan taxa abundance has the 349 X 1,566 dimension. For each microbiome dataset, low-abundance features were filtered, ensuring that only meaningful taxa were retained. Prevalence filtering excluded features present in fewer than 20% of the samples. Variance filtering was performed to retain only features with non-zero variance. The filtered matrix was normalized to relative abundances per sample. A small pseudocount ($1x10^{-5}$) was added to all abundance data, and the resulting microbiome abundance is normalized to relative abundance. A centered log-ratio (CLR) transformation is subsequently applied to the relative abundance data.

M_maxtrix

Two approaches were used to construct the M_matrix: the Jaccard similarity matrix and the covariance matrix approach.

Jaccard similarity matrix

The Jaccard distance method focuses on presence-absence patterns, ideal for sparse datasets like metagenomics data (Galloway-Pena & Hanson, 2020). For the Jaccard dissimilarity calculation, a global threshold was set as the mean of all CLR values and the filtered CLR matrix (S) was binarized. Microbiome features with CLR values greater than the threshold are set to 1, while features with CLR values less than the threshold are set to 0 to reflect feature presence or absence of each feature per sample. The Jaccard dissimilarity was computed using `vegan::vegdist` (Oksanen et al., 2013), defined as:

$$J_{ij} = 1 - \frac{|A_i \cap A_j|}{|A_i \cup A_j|}$$

where (A_i) and (A_j) are the sets of features present in samples (i) and (j). The dissimilarity matrix was transformed into a similarity matrix using a Gaussian radial basis function (RBF) kernel as:

$$S_{ij} = \exp(-\frac{jaccard\ matrix^2}{mean\ jaccard})$$

Where the mean jaccard is the mean of squared jaccard distance (i.e, mean jaccard = mean (jaccard matrix^2)). The similarity matrix is adjusted for positive definiteness, normalized, and perturbed with a diagonal term (10^{-4}) to form the M_matrix (microbiome relationship matrix). This method

is robust to zero-inflated data, capturing ecological similarities based on shared microbial presence.

Microbiome covariance

Principal component analysis was performed on the CLR-transformed microbiome data using the prcomp function in R. This captures the majar variability within each microbiome data. Subsequently, microbiome features contributing most (top 10%) to the first two principal components (PC1 and PC2) were selected and their CLR-transformed abundance data was used for the microbiome relationship matrix construction (covariance). Selecting microbiome features to include in genomic prediction based on PCA was also done by Alemu et al. (2025) in sheep. The relationship matrix (M_matrix) is computed from the scaled CLR-transformed abundance data as $M = \frac{SS^t}{n}$ where S is matrix of scaled CLR transformed abundance data of dimension n x p (p is the number of features and n is the number of animals. This is the microbiome relationship matrix formula used in Deru et al. (2024).

Genomic Prediction Models

The genomic prediction framework used the R package Bayesian Generalized Linear Regression (BGLR) (de los Campos et al., 2015) to model the phenotypic trait, integrating A_matrix, G_matrix, and M_matrix. Déru et al. (2024) also used the BGLR model framework. This is a mixed-model framework that utilizes Bayesian Reproducing Kernel Hilbert Spaces (RKHS) regression, a non-linear kernel model, to predict phenotypes based on relationships among individual fish. It uses the MCMC (Markov Chain Monte Carlo) algorithm to estimate model parameters, including the fixed effect coefficients, variance components, and random effects. The standardized phenotype (mean = 0, SD = 1) was used as the response variable.

Fixed effects (Harvest_date, Genetic_Line, and/or Tank_Assignment) included in the model were identified as significant ($p < 0.05$) via preliminary mixed-effects analysis (`lme4::lmer`) (Singmann et al., 2015).

Seven BGLR models were fitted:

1. Ped Model: Used only the A-matrix.
2. Gen Model: Used only the G-matrix.
3. Micro Model: Used only the M-matrix.
4. Ped+Gen Model: Combined A- and G-matrices.
5. Ped+Micro Model: Combined A- and M-matrices.
6. Micro+Gen Model: Combined M- and G-matrices.

7. Ped+Gen+Micro Model: Combined all three matrices.

Each model is specified as a full or subset of the below depending on which random effect is included:

$$y = X\beta + Z_g g + Z_m m + Z_p P + e$$

Where y = vector of phenotype

Xβ= Includes fixed effects of Harvest date and/or tank assignment.

The *g*,*m,* and *p* are random effects for genomic, microbiome, and pedigree components following a multivariate normal distribution with g∼*N*(0,cG), m∼*N*(0, σ^2_mM), p∼*N*(0, σ^2_pP), and e∼*N*(0, σ^2_eI) is the residual. For all the models, the random effects variance components were assigned the default BGLR's RKHS prior densities (scaled inverse chi-square prior), with hyperparameters of 5 degrees of freedom and a scale parameter based on the phenotypic variance. The fixed effects are assigned a Gaussian prior with mean zero and a constant variance of 10^{10} as proposed by the default in the BGLR package. An MCMC chain was run for each model with 120,000 iterations, 20,000 burn-in iteration, and a thinning interval of 20 to ensure the stability of the estimated parameters.

Model Evaluation

A stratified four-fold cross-validation (CV) was performed to assess predictive accuracy of the models. Samples were stratified by "Tank Assignment" and "Harvest date" to ensure balanced representation across folds. Fold sizes were approximately balanced (e.g., 88, 87, 87, 87 samples), assigned using a greedy algorithm to distribute samples proportionally across strata. The dataset was split into training (~261 samples) and test (~88 samples) sets for each fold. Model accuracy was calculated as the correlation between the predicted and observed phenotypes.

Estimation of variance components, heritability, and microbiability

The full dataset was used to estimate variance components (varE, varA, varG, varM) and compute heritabilities/microbiability (varComponent / total variance).

For each model, heritability/microbiability is calculated as the ratio of each random effect kernel's variance component (σ^2_i) to the total phenotypic variance (σ^2_p), where $\sigma^2_p = \sigma^2_e + \sum\sigma^2_i$. That is, the proportion of the total phenotypic variance explained by the random effect(s) in each model. For instance, for the ped + gen + micro model, the total phenotypic variance is: $\sigma^2_p = \sigma^2_A + \sigma^2_G + \sigma^2_M + \sigma^2_e$, in which case $h^2_A = \frac{\sigma^2_A}{\sigma^2_p}$, $h^2_G = \frac{\sigma^2_G}{\sigma^2_p}$, and microbiability $h^2_M = \frac{\sigma^2_M}{\sigma^2_p}$.

Microbiome-Wide Association Study (MWAS)

A microbiome-wide association study (MWAS) was performed to investigate the relationship between gut microbiome composition and phenotypic traits. The analysis integrated genomic, phenotypic, and microbiome abundance data, employing principal component analysis (PCA) to summarize microbiome variation and linear mixed models to test associations.

Genomic Data Processing

Genomic data was sourced from the 1X WGS data with imputation containing 12,047,625 SNPs from 351 fish samples. The SNP data file was filtered using `bcftools` (version 1.15) (Danecek et al., 2021), to retain SNPs with missingness ≤10% and minor allele frequency ≥5. This resulted in a filtered SNP set of ~5.72 million SNPs. A genetic relationship matrix (GRM) was computed using the GCTA method `SNPRelate::snpgdsGRM`, capturing population structure for downstream analyses.

Microbiome Data Processing and PCA

Microbiome abundance data were preprocessed to address zero inflation and sparsity. The abundance matrix was filtered to exclude features with low counts ($<5 \times 10^{-6}$ in >95% samples), low prevalence (<10% of samples), or low variance ($<10^{-6}$). Samples with zero total abundance were also removed. To handle zero counts, a pseudo-count of 10^{-5} was added, followed by normalization to relative abundances. The data were then transformed using centered log-ratio (CLR) transformation with the `compositions` package (Van den Boogaart & Tolosana-Delgado, 2008) to account for compositional effects. PCA was performed on the CLR-transformed data using the `prcomp` function in R to derive principal components (PCs), selecting up to 10 PCs that explained up to 80% of the variance (minimum 5 PCs). The resulting PCs were used for association testing.

In total, 348 samples were aligned across phenotype, genomic, and microbiome datasets and are used for the association analysis. The phenotype was standardized using median absolute deviation to ensure robust scaling.

MWAS Analysis

The MWAS tested associations between each microbiome PC (PC1–PC10) and the standardized phenotype (body weight and muscle yield), adjusting for covariates of harvest date, tank assignment, and genetic PCs (gPC1–gPC5).

The five genetic PCs (gPC1–gPC5) were computed using `SNPRelate::snpgdsPCA` on the SNP data GDS file to adjust for population structure. A mixed model was fitted for each PC using `GENESIS::fitNullModel` (Gogarten et al., 2019) with a Gaussian family.. The fixed effects include the microbiome PC as the primary predictor, harvest date, tank, and genetic PCs as covariates to control for population structure and other environmental variables. The random effect

accounted for genetic relatedness among individuals, modelled as a genetic relationship matrix (GRM) computed from the SNP data

$$y_i = \beta_0 + \beta_1 PC_{i,k} + \sum_{j=1}^{J} \beta_{2j}\, HD_{i,j} + \sum_{m=1}^{M} \beta_{3m} Tank_{i,m} + \sum_{n=1}^{5} \beta_{4n} \mathrm{gPC}_{i,n} + \mu_i + \epsilon_i$$

Where:

- HD = Harvest date
- y_i: Phenotype (standardized) for individual i.
- β_0: Intercept.
- β_1: Fixed effect coefficient for the k-th microbiome PC ($PC_{i,k}$)
- β_{2j} : Fixed effect coefficients for the J levels of harvest date (categorical).
- β_{3m}: Fixed effect coefficients for the M levels of tank (categorical).
- β_{4n}: Fixed effect coefficients for the five genetic PCs ($gPC_{i,n}$)
- μ_i: Random genetic effect for individual i, distributed as $u \sim N(0, \sigma^2_g K)$, where K is the GRM and σ^2_g is the genetic variance.
- ϵ_i: Residual error, distributed as $\epsilon \sim N(0, \sigma^2_e)$, where σ^2_e is the residual variance.
- i: Individual index (1 to ~348).
- k: Microbiome PC index (1 up to 10).

Results and Discussion

Phenotypic Summary

The descriptive statistics of the phenotypes are shown in Table 1. The means of body weight and muscle yield are 710.5g and 47.87g, respectively. There is a moderate positive correlation ($r = 0.41$, $p < 1.02X10^{-15}$) between body weight and muscle yield.

Table 1. Descriptive statistics of the phenotypes

Trait	N	Mean	SD	Min	Max	CV (%)
Muscle yield	348	47.87	3.61	29.14	67.08	7.54
Body weight	349	710.51	174.69	161.2	1373.8	24.59

Heritability and Microbiability

The heritability and microbiability estimates are shown in Table 2 and 3.

Analogous to heritability, the microbiability (m^2) has been defined as the relative proportion of the total phenotypic variance that can be attributed to the gut microbiome community.

Table 2. Heritability and microbiability estimates for muscle yield across all models

Muscle yield Jaccard Similarity							
Gene Family							
Heritability Component	Ped Model	Gen Model	Micro Model	Ped+Gen Model	Ped+Micro Model	Micro+Gen Model	Ped+Gen+Micro Model
h2_A	0.40 ± 0.1000	–	–	0.24 ± 0.1100	0.34 ± 0.1100	–	0.20 ± 0.1100
h2_G	–	0.39 ± 0.090	–	0.24 ± 0.0800	–	0.32 ± 0.1000	0.21 ± 0.0900
h2_M	–	–	0.18 ± 0.0600	–	0.14 ± 0.0500	0.14 ± 0.0500	0.12 ± 0.0400
Pathway							
Heritability Component	Ped Model	Gen Model	Micro Model	Ped+Gen Model	Ped+Micro Model	Micro+Gen Model	Ped+Gen+Micro Model
h2_A	0.40 ± 0.0013	–	–	0.23 ± 0.0014	0.32 ± 0.0014	–	0.20 ± 0.0015
h2_G	–	0.38 ± 0.001	–	0.25 ± 0.0010	–	0.30 ± 0.0012	0.19 ± 0.0011
h2_M	–	–	0.23 ± 0.0008	–	0.17 ± 0.0007	0.18 ± 0.0007	0.15 ± 0.0006
Taxa							
Heritability Component	Ped Model	Gen Model	Micro Model	Ped+Gen Model	Ped+Micro Model	Micro+Gen Model	Ped+Gen+Micro Model
h2_A	0.40 ± 0.0013	–	–	0.24 ± 0.0014	0.33 ± 0.0014	–	0.24 ± 0.0014
h2_G	–	0.38 ± 0.001	–	0.24 ± 0.0011	–	0.31 ± 0.0013	0.24 ± 0.0010
h2_M	–	–	0.21 ± 0.0009	–	0.15 ± 0.0007	0.16 ± 0.0007	0.15 ± 0.0007
Muscle yield Covariance Matrix							
Gene Family							
Heritability Component	Ped Model	Gen Model	Micro Model	Ped+Gen Model	Ped+Micro Model	Micro+Gen Model	Ped+Gen+Micro Model
h2_A	0.41 ± 0.0013	–	–	0.23 ± 0.0013	0.33 ± 0.0013	–	0.20 ± 0.0014
h2_G	–	0.39 ± 0.001	–	0.24 ± 0.0011	–	0.30 ± 0.0012	0.19 ± 0.0011
h2_M	–	–	0.23 ± 0.0009	–	0.17 ± 0.0007	0.17 ± 0.0007	0.14 ± 0.0007
Pathway							
Heritability Component	Ped Model	Gen Model	Micro Model	Ped+Gen Model	Ped+Micro Model	Micro+Gen Model	Ped+Gen+Micro Model
h2_A	0.40 ± 0.0013	–	–	0.24 ± 0.0014	0.33 ± 0.0013	–	0.20 ± 0.0013
h2_G	–	0.39 ± 0.001	–	0.24 ± 0.0012	–	0.30 ± 0.0012	0.20 ± 0.0011
h2_M	–	–	0.21 ± 0.0008	–	0.15 ± 0.0007	0.15 ± 0.0006	0.13 ± 0.0007
Taxa							
Heritability Component	Ped Model	Gen Model	Micro Model	Ped+Gen Model	Ped+Micro Model	Micro+Gen Model	Ped+Gen+Micro Model
h2_A	0.40 ± 0.0013	–	–	0.24 ± 0.0014	0.34 ± 0.0013	–	0.20 ± 0.0014
h2_G	–	0.38 ± 0.001	–	0.24 ± 0.0011	–	0.33 ± 0.0012	0.21 ± 0.0012
h2_M	–	–	0.16 ± 0.0006	–	0.11 ± 0.0005	0.12 ± 0.0005	0.10 ± 0.0004

Muscle yield

Jaccard method

Heritability for muscle yield ranges between ~0.40 (ped model), 0.38 (gen model), and 0.47(ped+gen). Microbiability for muscle yield in the micro model is higher for pathway abundance (0.23), followed by taxa abundance (0.21), and gene family (0.18). Similar pattern for microbiability was observed for the gen+micro model with the highest microbiability for pathway abundance (0.18), followed by taxa abundance (0.16), and gene family (0.14). The ped+gen+micro model follows the same trend.

Covariance matrix method

Heritability estimates remain the same with the Jaccard method above for the gen model. The microbiome composition explained 0.23, 0.21 and 0.17 of the phenotypic variances using gene family, pathway, and taxa abundance, respectively. Microbiability followed the same pattern in the

gen+micro and the ped+gen+micro model: highest with gene family abundance, followed by pathway abundance, and taxa abundance.

Body weight

Jaccard method

The heritability estimates for body weight is between 0.51 (ped), 0.48 (gen model), and 0.55 (ped + gen) model. In the micro model, microbiability is highest using the taxa abundance (0.23), followed by pathway abundance (0.22), and gene family abundance (0.21). Microbiability is highest using the taxa abundance, followed by gene family abundance, and the pathway abundance in the gen+micro and the ped+gen+micro models.

Covariance matrix method

Heritability is as reported in Jaccard method above. Microbiability for body weight in the micro model is 0.21, 0.18, and 0.15 when using gene family, pathway, and taxa abundance, respectively. For the gen+micro, microbiability ranges from 0.15,0.13, and 0.11, for gene family, pathway, and taxa abundance, respectively. Microbiability in the ped+gen+micro model ranges from 0.12,0.11 and 0.08 for gene family, pathway, and taxa abundance, respectively.

Comparably, the body weight has greater heritabilities than the muscle yield; suggesting that host additive genetic variance play more important role in the regulation of body weight in comparison to muscle yield. Notably, For both traits, the additive genomic variance was reduced in models where microbiome information was included suggesting a possible interaction between host genetics and gut microbiome, a trend similarly reported in a Swine study by Khanal et al. (2020b).

Table 3. Heritability and microbiability estimates for body weight across all models

Body weight Jaccard Similarity							
Gene Family							
Heritability Component	Ped Model	Gen Model	Micro Model	Ped+Gen Model	Ped+Micro Model	Micro+Gen Model	Ped+Gen+Micro Model
h2_A	0.52 ± 0.0014	–	–	0.33 ± 0.0017	0.44 ± 0.0014	–	0.29 ± 0.0018
h2_G	–	0.48 ± 0.0013	–	0.22 ± 0.0012	–	0.40 ± 0.0014	0.18 ± 0.0013
h2_M	–	–	0.21 ± 0.0009	–	0.15 ± 0.0007	0.15 ± 0.0007	0.12 ± 0.0006
Pathway							
Heritability Component	Ped Model	Gen Model	Micro Model	Ped+Gen Model	Ped+Micro Model	Micro+Gen Model	Ped+Gen+Micro Model
h2_A	0.51 ± 0.0014	–	–	0.34 ± 0.0017	0.42 ± 0.0014	–	0.29 ± 0.0017
h2_G	–	0.48 ± 0.0014	–	0.22 ± 0.0012	–	0.40 ± 0.0014	0.17 ± 0.0013
h2_M	–	–	0.22 ± 0.0009	–	0.14 ± 0.0007	0.15 ± 0.0007	0.12 ± 0.0007
Taxa							
Heritability Component	Ped Model	Gen Model	Micro Model	Ped+Gen Model	Ped+Micro Model	Micro+Gen Model	Ped+Gen+Micro Model
h2_A	0.52 ± 0.0014	–	–	0.33 ± 0.0017	0.43 ± 0.0014	–	0.28 ± 0.0018
h2_G	–	0.48 ± 0.0013	–	0.22 ± 0.0012	–	0.42 ± 0.0014	0.20 ± 0.0015
h2_M	–	–	0.23 ± 0.0010	–	0.17 ± 0.0008	0.19 ± 0.0008	0.15 ± 0.0007
Body weight Covariance Matrix							
Gene Family							
Heritability Component	Ped Model	Gen Model	Micro Model	Ped+Gen Model	Ped+Micro Model	Micro+Gen Model	Ped+Gen+Micro Model
h2_A	0.52 ± 0.0014	–	–	0.34 ± 0.0017	0.44 ± 0.0014	–	0.30 ± 0.0017
h2_G	–	0.48 ± 0.0013	–	0.21 ± 0.0012	–	0.41 ± 0.0014	0.18 ± 0.0013
h2_M	–	–	0.21 ± 0.0010	–	0.15 ± 0.0008	0.15 ± 0.0008	0.12 ± 0.0008
Pathway							
Heritability Component	Ped Model	Gen Model	Micro Model	Ped+Gen Model	Ped+Micro Model	Micro+Gen Model	Ped+Gen+Micro Model
h2_A	0.52 ± 0.0014	–	–	0.34 ± 0.0017	0.44 ± 0.0014	–	0.30 ± 0.0017
h2_G	–	0.48 ± 0.0014	–	0.21 ± 0.0012	–	0.40 ± 0.0014	0.18 ± 0.0012
h2_M	–	–	0.18 ± 0.0008	–	0.12 ± 0.0006	0.13 ± 0.0006	0.11 ± 0.0005
Taxa							
Heritability Component	Ped Model	Gen Model	Micro Model	Ped+Gen Model	Ped+Micro Model	Micro+Gen Model	Ped+Gen+Micro Model
h2_A	0.52 ± 0.0014	–	–	0.33 ± 0.0017	0.45 ± 0.0014	–	0.29 ± 0.0018
h2_G	–	0.48 ± 0.0013	–	0.22 ± 0.0012	–	0.43 ± 0.0014	0.19 ± 0.0014
h2_M	–	–	0.15 ± 0.0006	–	0.10 ± 0.0004	0.11 ± 0.0005	0.08 ± 0.0004

Phenotypic predictions

We investigated the effectiveness of various models by estimating correlations between the predicted and actual phenotypic values in a 4-fold cross validation. Results of this analysis is presented in Figures 1, and 2 and a summary of the predictive abilities and their standard deviation for both traits are reported supplementary table 1.

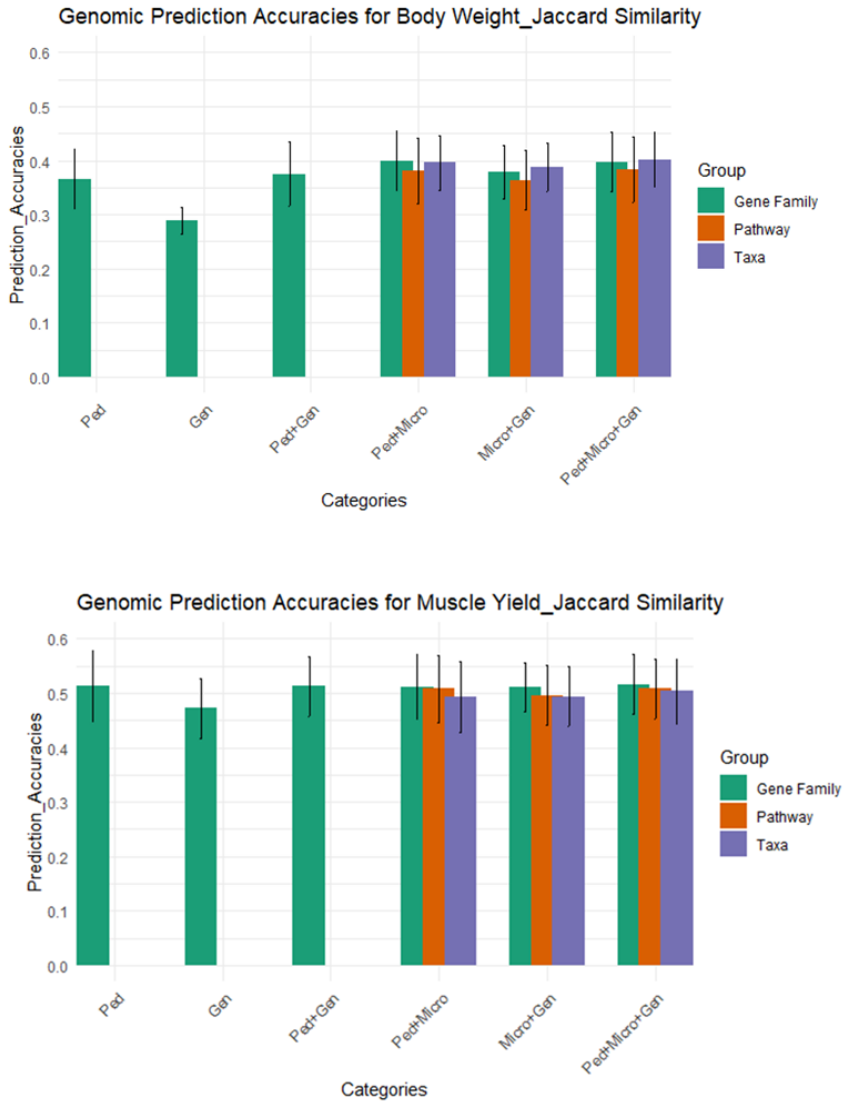

Figure 1. Mean prediction accuracies across all models for body weight and muscle yield using Jaccard similarity approach. Ped indicates pedigree-only model, Gen: genomic information only, Ped+Gen: A combination of pedigree and Genomic data.

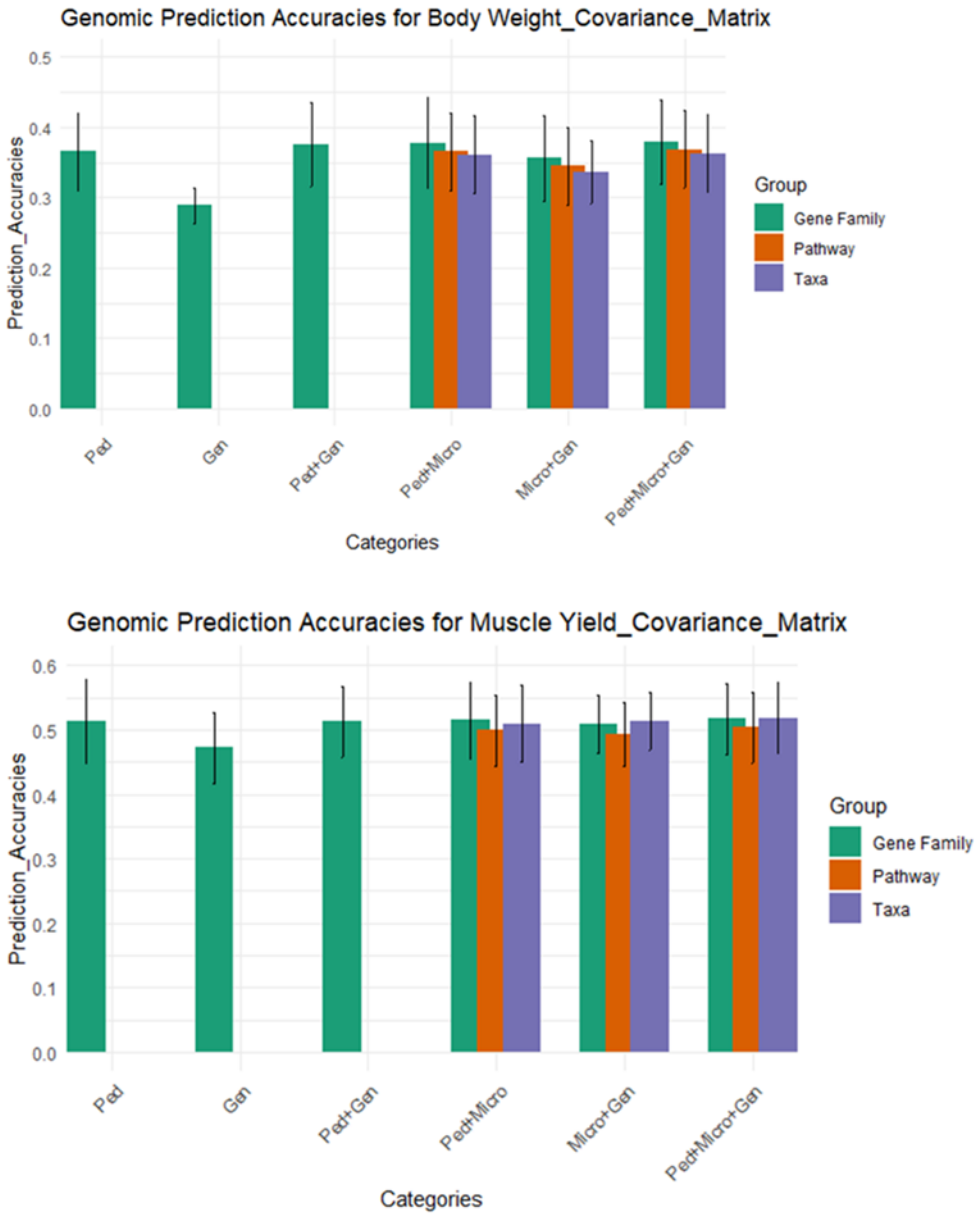

Figure 2. Mean prediction accuracies across all models for body weight and muscle yield using the Covariance matrix approach. Ped indicates pedigree-only model, Gen: genomic information only, Ped+Gen: A combination of pedigree and Genomic data.

Comparing the ped+gen with the ped+gen+micro model with jaccard similarity method microbiome processing, including microbiome information could improve the prediction accuracy of body weight by up to 7.2% (0.402 to 0.375), 2.13% (0.383 to 0.375), and 6.13% (0.398 to 0.375) using taxonomic, pathway, and gene family abundance, respectively. With the covariance approach to processing microbiome data, only the microbiome gene family resulted in a 1.06% improvement in genomic prediction accuracy for body weight (0.375 to 0.379).

When comparing ped+gen to ped+gen+micro, including microbiome information did not improve prediction accuracy for muscle yield. The only marginal improvements found were up to 0.58% (jaccard similarity method with gene family abundance), 0.77% (covariance approach with gene family abundance), and 1.17% improvement (covariance approach with taxa abundance). However, comparing the gen model to the gen+micro shows that the addition of microbiome information improves the prediction accuracy of muscle yield by up to 8.03% (jaccarad approach with gene family abundance) and 8.66% (covariance approach with taxa abundance).

Overall, the prediction accuracy with microbiome alone model (micro) were small and significantly lower than gen and ped models.

Microbiome Features associated with Body weight and Muscle yield

As discussed in the review by Wang et al. (2016), the associations that can be identified by MWAS are not limited to finding associated taxa alone, but should include the identification of microbial functions which can be achieved using microbiome gene family and pathway abundance data.

We used MWAS to test associations between microbiome principal components and the standardized phenotype (body weight and muscle yield). For body weight and taxa abundance, principal components 3 (PC3) and PC5 which explains 7.2% and 5.1%, respectively, of the microbiome variance are significantly associated with body weight (Tabe 4). The beta coefficient values show that PC3 and PC5 are negatively and positively associated with body weight, respectively.

Table 4. The MWAS predictor principal components associated with body weight and muscle yield

BW	**TA**	Beta	SE	P_value	% contribution		**PA**	Beta	SE	P_value	% contribution		**GFA**	Beta	SE	P_value	% contribution
	PC1	0.0140	0.009	0.132	45.928		PC1	0.0014	0.008	0.852	25.339		PC1	0.0005	0.0002	0.026*	22.327
	PC2	0.0010	0.020	0.960	10.881		PC2	-0.0069	0.012	0.555	9.565		PC2	-0.0002	0.0004	0.606	7.819
	PC3	-0.0652	0.023	0.005*	7.189		PC3	-0.0364	0.013	0.004*	8.309		PC3	0.0007	0.0006	0.285	2.939
	PC4	0.0145	0.024	0.543	6.773		PC4	0.0294	0.017	0.080	4.945		PC4	-0.0005	0.0008	0.510	1.768
	PC5	0.0628	0.027	0.020*	5.099		PC5	-0.0310	0.019	0.094	3.913		PC5	-0.0004	0.0009	0.599	1.462
MY	**TA**	Beta	SE	P_value	% contribution		**PA**	Beta	SE	P_value	% contribution		**GFA**	Beta	SE	P_value	% contribution
	PC1	-0.0287	0.010	0.004*	45.928		PC1	0.0075	0.008	0.362	25.339		PC1	-0.0005	0.0002	0.050	22.327
	PC2	0.0464	0.021	0.030*	10.881		PC2	-0.0215	0.013	0.094	9.565		PC2	-0.0003	0.0004	0.383	7.819
	PC3	0.0023	0.025	0.929	7.189		PC3	0.0214	0.014	0.124	8.309		PC3	-0.0003	0.0007	0.676	2.939
	PC4	-0.0285	0.026	0.270	6.773		PC4	-0.0161	0.019	0.408	4.945		PC4	-0.0007	0.0009	0.452	1.768
	PC5	0.0276	0.030	0.350	5.099		PC5	-0.0053	0.020	0.795	3.913		PC5	-0.0005	0.0009	0.559	1.462

BW: Body weight, MY: Muscle yield, TA: Taxa abundance, PA: Pathway abundance, GFA: Gene family abundance.

The identified taxa within PC3 (*Aeromonas bestiarum, Obesumbacterium proteus, Peptostreptococcus russellii, Mycobacterium frederiksbergense, Carnobacterium*

maltaromaticum, Lactococcus garvieae, Craterilacuibacter sp, Shewanella sp, Cetobacterium sp, and Ligilactobacillus salivarius) are associated with body weight (Table 5). *Cetobacterium sp* and *Ligilactobacillus salivarius* are often associated with gut health, which can indirectly affect growth through nutrient absorption. Wange et al. (2021) found that zebrafish higher gut abundance of *Cetobacterium somerae* to be correlated with improved glucose homeostasis, higher insulin expression, and more efficient carbohydrate utilization in zebrafish. The supplementation of *Lactobacillus salivarius* in the diet of piglets improved their weight gain and gut morphology. Other studies in poultry have shown *Ligilactobacillus salivarius* to be a potent probiotic for improving growth and intestinal health (Yang et al., 2023; Zhao et al., 2025).

The microbiome taxa from PC5 associated with body weight includes *Polynucleobacter yangtzensis, Peptostreptococcus russellii, Obesumbacterium proteus, Lactobacillus kitasatonis, Lactobacillus amylovorus, and Ligilactobacillus salivarius (*Table 5). Lactobacillus species (kitasatonis, amylovorus, and salivarius) are known for their roles in gut health and improved nutrient utilization (Giraffa et al., 2010; Walter, 2008), which may positively affect body weight and growth.

The microbiome taxa from PC1 associated with muscle yield includes *Shewanella sp, Cetobacterium sp, Lactococcus lactis, Lactobacillus crispatus, Streptococcus parauberis Clostridium perfringens, Ligilactobacillus salvarius, Streptococcus dysgalactiae, Lactobacillus amylovorus, Lactococcus garvieae, Peptostreptococcus russellii*, and *Lactobacillus kitasatonis* (Table 5). Those within PC2 associated with muscle yield are *Polynucleobacter yangtzensis , Enterococcus gilvis, Carnobacterium maltaromaticum, Lactobacillus kitasatonis, Ligalactobacillus salivarius, Peptostreptococcus russellii, Cetobacterium sp, Craterilacuibacter sp, Lactococcus garvieae, Streptococcus dysgalactiae*, and *Clostridium perfringens* (Table 5).

Some of the taxa associated with muscle yield such as Lactobacillus species (crispatus, amylovorus, kitasatonis) and *Ligilactobacillus salivarius*, are known to support gut health and nutrient absorption (Walter, 2008), which could indirectly enhance muscle yield by improving protein metabolism. *Cetobacterium sp* may influence short-chain fatty acid production, potentially aiding energy availability for muscle development (Wang et al., 2021).

Table 5: Body weight and Muscle yield significant principal components and their features (Taxa)

	Body weight		Muscle yield
	Taxa		**Taxa**
PC3	Aeromonas bestiarum	PC1	Shewanella sp
	Obesumbacterium proteus		Cetobacterium sp
	Peptostreptococcus russellii		Lactococcus lactis
	Mycobacterium frederiksbergense		Lactobacillus crispatus
	Carnobacterium maltaromaticum		Streptococcus parauberis
	Lactococcus garvieae		Clostridium perfringens
	Craterilacuibacter sp		Ligilactobacillus salvarius
	Shewanella sp		Streptococcus dysgalactiae
	Cetobacterium sp		Lactobacillus amylovorus
	Ligilactobacillus salivarius		Lactococcus garvieae
			Peptostreptococcus russellii
PC5	Polynucleobacter yangtzensis		Lactobacillus kitasatonis
	Peptostreptococcus russellii		
	Obesumbacterium proteus	PC2	Polynucleobacter yangtzensis
	Lactobacillus kitasatonis		Enterococcus gilvis
	Lactobacillus amylovorus		Carnobacterium maltaromaticum
	Ligilactobacillus salivarius		Lactobacillus kitasatonis
			Ligalactobacillus salivarius
			Peptostreptococcus russellii
			Cetobacterium sp
			Craterilacuibacter sp
			Lactococcus garvieae
			Streptococcus dysgalactiae
			Clostridium perfringens

For body weight pathway abundance, we identified principal component 3 as significantly associated with body weight (Table 6). No pathway abundance principal components are associated with muscle yield.

Table 6: Body weight significant principal components and their features (Pathways)

	Body weight
	Pathway
PC3	L-histidine degradation III
	Superpathway of N-acetylglusamine N-acetylmannosamine and N-acetylneuraminate degradation
	D-galactose degradation I (Leloir pathway)
	Stachyose degradation
	Thiazole component of thiamine diphosphate biosynthesis I
	Formaldehyde assimilation III (dihydroxyacetone cycle)
	Lactose and galactose degradation I
	UDP-N-acetylmuramoyl-pentapeptide biosynthesis I (meso-diaminopimelate containing)
	Peptidoglycan biosynthesis III (mycobacteria)
	Peptidoglycan biosynthesis I (meso-diaminopimelate containing)
	Superpathway of glycerol degradation to 1,3-propanediol
	Phosphopantothenate biosynthesis
	Peptidoglycan biosynthesis II (staphylococci)
	(S)-propane-1,-diol degradation
	Myo- chiro- and scyllo-inositol degradation
	L-valine biosynthesis
	Gondoate biosynthesis (anaerobic)
	L-isoleucine biosynthesis I (from threonine)
	Pyruvate fermentation to isobutanol (engineered)
	Fatty acid & beta coefficient oxidation II (plant perisome)
	Mixed acid fermentation
	L-isoleucine biosynthesis III
	Superpathway of pyrimidine nucleobases salvage
	(5Z) – dodecenoate biosynthesis I
	Glyoxylate cycle
	Oleate biosynthesis IV (anaerobic)
	Palmitoleate biosynthesis I (from (5Z)-dodec-5-enoate)
	Peptidoglycan maturation (meso-diaminopimelate containing)
	Superpathway of branched chain amino acid biosynthesis
	Fatty acid elongation –saturated
	(5Z) – dodecenoate biosynthesis II
	Stearate biosynthesis II (bacteria and plants)
	Inosine 5'-phosphate degradation

Microbiome gene family PC1, which explains 22.3% of the variance in microbiome data, is significantly associated with body weight. Gene families within PC1 are presented in Table 7. There were no significant microbiome gene family PCs associated with muscle yield.

The microbiome gene family PC1 (22% of the variance) was significantly associated with body weight (Table 7).

Table 7: Body weight significant principal components and their features (Gene families)

	Body weight
	Gene Family
PC1	UniRef90_N0D1A2 – Rep52
	UniRef90_A0A1D4S2G3 – Replication protein Rep
	UniRef90_P06107 | g__Staphylococcus.s__Staphylococcus_cohnii – Lincosamide resistance protein
	UniRef90_A0A0E1VB08 – Plasmid replication protein
	UniRef90_A0A178P106 – CopG family transcriptional regulator

Conclusions

This study reveals the impact of using genomic and gut microbiome information on improving growth traits in rainbow trout breeding programs. Including microbiome in the model improved prediction accuracy for body weight by up to 7.2%, but with no profound benefit on muscle yield prediction.

References

Ahmed, R. O., Ali, A., Leeds, T., & Salem, M. (2023). Fecal Microbiome Analysis Distinguishes Bacterial Taxa Biomarkers Associated with Red Fillet Color in Rainbow Trout. *Microorganisms*, *11*(11), 2704.

Ahmed, R. O., Ali, A., Leeds, T., & Salem, M. (2023). RNA-Seq analysis of the pyloric caecum, liver, and muscle reveals molecular mechanisms regulating fillet color in rainbow trout. *BMC genomics*, *24*(1), 579. https://doi.org/10.1186/s12864-023-09688-5

Al-Tobasei, R., Ali, A., Garcia, A. L., Lourenco, D., Leeds, T., & Salem, M. (2021). Genomic predictions for fillet yield and firmness in rainbow trout using reduced-density SNP panels. *BMC genomics*, *22*, 1-11.

Alemu, S. W., Bilton, T. P., Johnson, P. L., Perry, B. J., Henry, H., Dodds, K. G.,…Rowe, S. J. (2025). Improving genomic prediction accuracy for methane emission and feed efficiency in sheep: integrating rumen microbial PCA with host genomic variation using neural network GBLUP (NN-GBLUP). *Genetics Selection Evolution*, *57*(1), 41.

Ali, A., Al-Tobasei, R., Lourenco, D., Leeds, T., Kenney, B., & Salem, M. (2020). Genome-wide identification of loci associated with growth in rainbow trout. *BMC genomics*, *21*(1), 1-16.

Amadeu, R. R., Garcia, A. A. F., Munoz, P. R., & Ferrao, L. F. V. (2023). AGHmatrix: genetic relationship matrices in R. *Bioinformatics*, *39*(7), btad445. https://doi.org/10.1093/bioinformatics/btad445

Andrews, S. (2010). FastQC: a quality control tool for high throughput sequence data. In: Cambridge, United Kingdom.

Bangera, R., Correa, K., Lhorente, J. P., Figueroa, R., & Yáñez, J. M. (2017). Genomic predictions can accelerate selection for resistance against Piscirickettsia salmonis in Atlantic salmon (Salmo salar). *BMC genomics*, *18*(1), 121.

Beghini, F., McIver, L. J., Blanco-Miguez, A., Dubois, L., Asnicar, F., Maharjan, S.,…Segata, N. (2021). Integrating taxonomic, functional, and strain-level profiling of diverse microbial communities with bioBakery 3. *Elife*, *10*, e65088. https://doi.org/10.7554/eLife.65088

Brugman, S., & Nieuwenhuis, E. E. (2010). Mucosal control of the intestinal microbial community. *Journal of Molecular Medicine*, *88*, 881-888.

Buitenhuis, B., Lassen, J., Noel, S. J., Plichta, D. R., Sørensen, P., Difford, G. F., & Poulsen, N. A. (2019). Impact of the rumen microbiome on milk fatty acid composition of Holstein cattle. *Genetics Selection Evolution*, *51*, 1-8.

Burbridge, Hendrick, Roth, & Rosenthal. (2001). Social and economic policy issues relevant to marine aquaculture. *Journal of Applied Ichthyology*, *17*(4), 194-206.

Cai, J., & Leung, P. (2017). *Short-term projection of global fish demand and supply gaps*. FAO;.

Cerf-Bensussan, N., & Gaboriau-Routhiau, V. (2010). The immune system and the gut microbiota: friends or foes? *Nature Reviews Immunology*, *10*(10), 735-744.

Chapagain, P., Arivett, B., Cleveland, B. M., Walker, D. M., & Salem, M. (2019). Analysis of the fecal microbiota of fast-and slow-growing rainbow trout (Oncorhynchus mykiss). *BMC genomics*, *20*(1), 1-11.

Danecek, P., Bonfield, J. K., Liddle, J., Marshall, J., Ohan, V., Pollard, M. O.,…Li, H. (2021). Twelve years of SAMtools and BCFtools. *Gigascience*, *10*(2), giab008. https://doi.org/10.1093/gigascience/giab008

de los Campos, G., Pataki, A., & Pérez, P. (2015). The BGLR (Bayesian Generalized Linear Regression) R-Package. In.

Déru, V., Tiezzi, F., Carillier-Jacquin, C., Blanchet, B., Cauquil, L., Zemb, O.,…Gilbert, H. (2024). The potential of microbiota information to better predict efficiency traits in growing pigs fed a conventional and a high-fiber diet. *Genetics Selection Evolution*, *56*(1), 8.

Fornshell, G. (2002). Rainbow trout—challenges and solutions. *Reviews in Fisheries Science*, *10*(3-4), 545-557.

Galloway-Pena, J., & Hanson, B. (2020). Tools for Analysis of the Microbiome. *Dig Dis Sci*, *65*(3), 674-685. https://doi.org/10.1007/s10620-020-06091-y

Giraffa, G., Chanishvili, N., & Widyastuti, Y. (2010). Importance of lactobacilli in food and feed biotechnology. *Research in microbiology*, *161*(6), 480-487.

Gogarten, S. M., Sofer, T., Chen, H., Yu, C., Brody, J. A., Thornton, T. A.,…Conomos, M. P. (2019). Genetic association testing using the GENESIS R/Bioconductor package. *Bioinformatics*, *35*(24), 5346-5348. https://doi.org/10.1093/bioinformatics/btz567

Gonzalez-Pena, D., Gao, G., Baranski, M., Kenney, P. B., Vallejo, R. L., Palti, Y., & Leeds, T. D. (2016). Genome-wide association study for identifying loci that affect fillet yield, carcass, and body weight traits in rainbow trout (Oncorhynchus mykiss). *Frontiers in genetics*, *7*, 224917.

He, Y., Tiezzi, F., Jiang, J., Howard, J. T., Huang, Y., Gray, K.,…Maltecca, C. (2022). Use of host feeding behavior and gut microbiome data in estimating variance components and predicting growth and body composition traits in swine. *Genes*, *13*(5), 767.

Joshi, R., Skaarud, A., de Vera, M., Alvarez, A. T., & Ødegård, J. (2020). Genomic prediction for commercial traits using univariate and multivariate approaches in Nile tilapia (Oreochromis niloticus). *Aquaculture*, *516*, 734641.

Khanal, P., Maltecca, C., Schwab, C., Fix, J., Bergamaschi, M., & Tiezzi, F. (2020a). Modeling host-microbiome interactions for the prediction of meat quality and carcass composition traits in swine. *Genetics Selection Evolution*, *52*, 1-13.

Khanal, P., Maltecca, C., Schwab, C., Fix, J., Bergamaschi, M., & Tiezzi, F. (2020b). Modeling host-microbiome interactions for the prediction of meat quality and carcass composition traits in swine. *Genetics Selection Evolution*, *52*(1), 1-13.

Kriaridou, C., Tsairidou, S., Houston, R. D., & Robledo, D. (2020). Genomic prediction using low density marker panels in aquaculture: performance across species, traits, and genotyping platforms. *Frontiers in genetics*, *11*, 124.

Langmead, B., & Salzberg, S. L. (2012). Fast gapped-read alignment with Bowtie 2. *Nat Methods*, *9*(4), 357-359. https://doi.org/10.1038/nmeth.1923

Leeds, T. D., Vallejo, R. L., Weber, G. M., Gonzalez-Pena, D., & Silverstein, J. T. (2016). Response to five generations of selection for growth performance traits in rainbow trout (Oncorhynchus mykiss). *Aquaculture*, *465*, 341-351.

Liu, W., Zeng, J., Suo, N., Ke, Q., Zhao, J., Wang, J.,…Wang, Y. (2025). Dynamic changes in gut microbiota and production phenotypes driven by host genetic background in large yellow croaker. *Aquaculture*, *598*, 741948.

Martin, M. (2011). Cutadapt removes adapter sequences from high-throughput sequencing reads. *EMBnet. journal*, *17*(1), 10-12.

Oksanen, J., Blanchet, F. G., Kindt, R., Legendre, P., Minchin, P. R., O'hara, R.,…Wagner, H. (2013). Package 'vegan'. *Community ecology package, version*, *2*(9), 1-295.

Ross, E. M., Hayes, B. J., Tucker, D., Bond, J., Denman, S. E., & Oddy, V. H. (2020). Genomic predictions for enteric methane production are improved by metabolome and microbiome data in sheep (Ovis aries). *Journal of animal science*, *98*(10), skaa262.

Saedi, N., Ye, X., Cai, Z., Lund, M. S., & Karaman, E. (2024). Genomic prediction of methane emission using microbiome data and genomic markers in Holstein cows. In *Genomic prediction of methane emission using microbiome data and genomic markers in Holstein cows*.

Singmann, H., Bolker, B., Westfall, J., Aust, F., Ben-Shachar, M., Højsgaard, S.,…Love, J. (2015). Package 'afex'. *URL http://afex. Singmann. Science/, https://github. Com/singmann/afex*.

Sinnwell, J. P., Therneau, T. M., & Schaid, D. J. (2014). The kinship2 R package for pedigree data. *Hum Hered*, *78*(2), 91-93. https://doi.org/10.1159/000363105

Song, H., Dong, T., Yan, X., Wang, W., Tian, Z., Sun, A.,…Hu, H. (2023). Genomic selection and its research progress in aquaculture breeding. *Reviews in aquaculture*, *15*(1), 274-291.

Vallejo, R. L., Leeds, T. D., Gao, G., Parsons, J. E., Martin, K. E., Evenhuis, J. P.,…Palti, Y. (2017). Genomic selection models double the accuracy of predicted breeding values for bacterial cold water disease resistance compared to a traditional pedigree-based model in rainbow trout aquaculture. *Genetics Selection Evolution*, *49*, 1-13.

Van den Boogaart, K. G., & Tolosana-Delgado, R. (2008). "Compositions": a unified R package to analyze compositional data. *Computers & Geosciences*, *34*(4), 320-338.

Vu, N. T., Phuc, T. H., Oanh, K. T. P., Sang, N. V., Trang, T. T., & Nguyen, N. H. (2022). Accuracies of genomic predictions for disease resistance of striped catfish to Edwardsiella ictaluri using artificial intelligence algorithms. *G3*, *12*(1), jkab361.

Walter, J. (2008). Ecological role of lactobacilli in the gastrointestinal tract: implications for fundamental and biomedical research. *Applied and environmental microbiology*, *74*(16), 4985-4996.

Wang, A., Zhang, Z., Ding, Q., Yang, Y., Bindelle, J., Ran, C., & Zhou, Z. (2021). Intestinal Cetobacterium and acetate modify glucose homeostasis via parasympathetic activation in zebrafish. *Gut microbes*, *13*(1), 1-15.

Wang, A. R., Ran, C., Ringø, E., & Zhou, Z. G. (2018). Progress in fish gastrointestinal microbiota research. *Reviews in Aquaculture*, *10*(3), 626-640.

Wang, J., Chen, L., Li, B., Xu, J., Feng, J., Dong, C.,…Xu, P. (2021). Performance of genome prediction for morphological and growth-related traits in Yellow River carp. *Aquaculture*, *536*, 736463.

Wang, J., & Jia, H. (2016). Metagenome-wide association studies: fine-mining the microbiome. *Nature Reviews Microbiology*, *14*(8), 508-522.

Wasik, K., Berisa, T., Pickrell, J. K., Li, J. H., Fraser, D. J., King, K., & Cox, C. (2021). Comparing low-pass sequencing and genotyping for trait mapping in pharmacogenetics. *BMC genomics*, *22*(1), 197. https://doi.org/10.1186/s12864-021-07508-2

Xiong, X., Yu, C., Qiu, M., Zhang, Z., Hu, C., Zhu, S.,…Chen, J. (2024). Genomic and Gut Microbiome Evaluations of Growth and Feed Efficiency Traits in Broilers. *Animals*, *14*(24), 3615.

Yang, J., Wang, J., Liu, Z., Chen, J., Jiang, J., Zhao, M., & Gong, D. (2023). Ligilactobacillus Salivarius improve body growth and anti-oxidation capacity of broiler chickens via regulation of the microbiota-gut-brain axis. *BMC microbiology*, *23*(1), 395.

Zhang, Y., Liu, Z., & Li, H. (2020). Genomic prediction of columnaris disease resistance in catfish. *Marine Biotechnology*, *22*(1), 145-151.

Zhao, P., Li, Y., Yang, Y., Xiao, Q., Zhang, Z., Hong, X.,…Yang, S. (2025). Probiotic efficacy and mechanism of a pigeon derived Ligilactobacillus salivarius strain in promoting growth and intestinal development of pigeons. *Frontiers in Microbiology*, *16*, 1584380.

Supplementary Table 1: Summary of the predictive abilities and their standard deviation for body weight and muscle yield

Body weight							
Jaccard similarity	**Ped**	**Gen**	**Micro**	**Ped+Gen**	**Ped+Micro**	**Micro+Gen**	**Ped+Micro+Gen**
Gene Family	0.366 ± 0.11	0.289 ± 0.05	-0.09± 0.10	0.375 ± 0.12	0.40 ± 0.11	0.379 ± 0.10	0.398 ± 0.11
Pathway	0.366 ± 0.11	0.289 ± 0.05	-0.214 ± 0.09	0.375 ± 0.12	0.381 ± 0.12	0.364 ± 0.11	0.383 ± 0.12
Taxa	0.366 ± 0.11	0.289 ± 0.05	-0.042 ± 0.08	0.375 ± 0.12	0.396 ± 0.10	0.387 ± 0.09	0.402 ± 0.10
Covariance Matrix Method	Ped	Gen	Micro	Ped+Gen	Ped+Micro	Micro+Gen	Ped+Micro+Gen
Gene Family	0.366 ± 0.11	0.289 ± 0.05	-0.042± 0.06	0.375 ± 0.12	0.378 ± 0.13	0.356 ± 0.12	0.379 ± 0.12
Pathway	0.366 ± 0.11	0.289 ± 0.05	0.047 ± 0.09	0.375 ± 0.12	0.366 ± 0.11	0.345 ± 0.11	0.369 ± 0.11
Taxa	0.366 ± 0.11	0.289 ± 0.05	0.028 ± 0.15	0.375 ± 0.12	0.361 ± 0.11	0.337 ± 0.09	0.363 ± 0.11
Muscle Yield							
Jaccard similarity							
Gene Family	0.513 ± 0.13	0.473± 0.11	0.05 ± 0.17	0.513 ± 0.11	0.512 ± 0.12	0.511 ± 0.09	0.516 ± 0.11
Pathway	0.513 ± 0.13	0.473± 0.11	0.106 ± 0.16	0.513 ± 0.11	0.508 ± 0.123	0.496 ± 0.11	0.509 ± 0.11
Taxa	0.513 ± 0.13	0.473± 0.11	0.138± 0.25	0.513 ± 0.11	0.493 ± 0.13	0.494 ± 0.11	0.504 ± 0.12
Covariance Matrix Method							
Gene Family	0.513 ± 0.13	0.473± 0.11	0.02 ± 0.09	0.513 ± 0.11	0.515 ± 0.12	0.509 ± 0.09	0.517 ± 0.11
Pathway	0.513 ± 0.13	0.473± 0.11	-0.02 ± 0.13	0.513 ± 0.11	0.500 ± 0.11	0.493 ± 0.10	0.504 ± 0.11
Taxa	0.513 ± 0.13	0.473± 0.11	0.152± 0.09	0.513 ± 0.11	0.510 ± 0.12	0.514 ± 0.09	0.519 ± 0.11

Overall Conclusion

Rainbow trout is the most cultivated, cool, freshwater fish in the United States. Rainbow trout are reared to produce fillets, and high production efficiency is needed to meet the ever-increasing demand for quality products. A significant constraint is the lack of genetically improved fish strains with high fillet yields and good-quality fillets. The industry has worked to remedy the situation by introducing breeding programs to select the best animals mainly through traditional pedigree selection. However, traditional breeding programs can be time-consuming and inefficient, especially for lethal traits such as fillet yield and color that cannot be accurately measured on live fish. The use of genomic information in breeding programs offers a faster and more accurate method of achieving genetic progress, especially for lethally measured traits like muscle yield and fillet coloration that cannot be directly measured on selection candidates. Even with genomic information, the phenotypic variance is still not completely explained, leading to the concept of "missing heritability". The gut microbiome is a key component of aquaculture and other mammalian species and may contribute to the variation of many phenotypes. The microbiome information may explain some of the "missing" heritability.

This dissertation sought to investigate the genomic and microbiome architecture in rainbow trout fish families from the USDA and utilize this information to improve fillet yield and quality traits in rainbow trout. We approached this research with "system genetics" and the "holobiont" concept, which integrates several omics approaches and views each component as complementary to understanding complex traits and how genetic improvement can be achieved.

First, we used GWAS and RNA-seq differential expression analysis to identify candidate genes and understand the genetic architecture underlying the variability in these traits. The GWAS analysis identified several SNP windows explaining up to 3.5%, 2.5%, and 1.6% of the additive genetic variance for fillet redness, yellowness, and whiteness, respectively. SNPs are located within genes implicated in carotenoid metabolism (*BCO1, retinol dehydrogenase*) and myoglobin homeostasis (*ATP5F1B*). Other identified genes are involved in maintaining muscle structural integrity (*klh41b, COL28A1*, and *CTSK*) and protecting against lipid oxidation (*SOD2, sestrin-1, USP10*). Using RNA-Seq to study the transcriptome profile in the pyloric caecum, liver, and muscle from fish families with pink-reddish fillet coloration (red) versus those with lighter pale coloration (white), we identified genes involved in lipid/carotenoid metabolism and transport, ribosomal activities, mitochondrial functions, and stress homeostasis were uniquely enriched in the muscle and liver. For instance, the two beta carotene genes (*BCO1* and *BCO2*) were significantly under-represented in the muscle of the red fillet group, favoring more carotenoid retention. Enriched genes in the pyloric caecum were involved in intestinal absorption and transport of carotenoids and lipids. In addition, the analysis revealed the modulation of several genes with immune functions in the pyloric caecum, liver, and muscle.

The majority of the GWAS-associated variants lie in the non-coding regions, limiting our understanding of how they regulate the phenotype and making functional characterization

challenging. Expression quantitative trait loci (eQTL) mapping bridges this gap by integrating gene expression and genotype data to identify variants regulating gene expression, explaining how the genetic variants influence phenotypic variability. By integrating eQTL mapping with GWAS and differential gene expression data, we aimed to prioritize candidate genes and regulatory variants that contribute to the genetic architecture of growth. We identified 234,630 cis-eQTLs and over 5.3 million trans-eQTLs, highlighting widespread regulatory variation across the genome. A subset of 6,275 cis-eQTLs located near gene promoters was integrated with GWAS and transcriptomic data to prioritize genes involved in somatic growth processes. Key candidate genes include GABRR1-like, AZIN1, and ATP6V1 for body weight; TNNI2, PDLIM3, CDK5, and CYP3A27 for tissue robustness; and GATD3A, PPP2R1BB, and USP6NL for muscle development. The eQTL SNPs identified are located in genomic regions enriched with active enhancers. The SNPs associated with these traits could be prioritized for genomic selection to breed rainbow trout with faster growth and improved fillet quality.

We used 16S and shotgun metagenomics to investigate gut microbial taxa and pathways predictive of fillet color in rainbow trout. The red fillet group has enrichment (LDA score > 1.5) of taxa *Leuconostoc lactis*, *Corynebacterium variabile*, *Jeotgalicoccus halotolerans*, and *Leucobacter chromiireducens*. In contrast, the white fillet group has an enriched presence of *mycoplasma*, *Lachnoclostridium*, and *Oceanobacillus indicireducens*. The enriched bacterial taxa in the red fillet group have probiotic functions and can generate carotenoid pigments. Bacteria taxa enriched in the white fillet group are either commensal, parasitic, or capable of reducing indigo dye. The Methylerythritol Phosphate (MEP) pathway, capable of producing carotenoids, is enriched in the red fillet family. Other pathways enriched in the red fillet group include Coenzyme A Biosynthesis Pathways, Fatty Acid and Phospholipid Biosynthesis pathways, Retinol Biosynthesis, and tetrapyrrole and Heme Biosynthesis pathways. Microbiome-wide association analysis (MWAS) revealed microbial taxa and pathways associated with growth traits. Microbiome taxa involved in fatty acid elongation, fatty acid oxidation II, pyruvate fermentation to isobutanol, mixed acid fermentation, super-pathway of branched chain amino acid biosynthesis, glyoxylate cycle and Peptidoglycan biosynthesis II pathways influence growth traits in rainbow trout.

Finally, we investigated the feasibility of using 1x WGS with imputation and microbiome information for genomic prediction for these traits. Our results show that 1x WGS data can achieve comparable results to pedigree information. Including microbiome information in the genomic prediction model could improve prediction accuracy by up to 7.2%, and 8.66% for body weight and muscle yield, respectively. This improvement could translate into significant gains if achieved consistently over generations. The implications of improved prediction accuracies are earlier selection, faster growth, and rapid genetic progress. Microbiome information did not improve the prediction accuracy for muscle yield.

Altogether, these findings show the possibility of utilizing genomic and microbiome information to genetically improve rainbow trout fish populations, enhancing food security and providing economic benefits to the United States.

Future Directions

1. The direct impact of the candidate SNPs and genes identified in this study should be used for functional genomics studies, such as genome editing, to confirm their relationship with growth and fillet quality.
2. Investigate the potential of structural variants in explaining some components of the "missing" heritability. The 1X WGS and imputation data includes structural variants that could be used for INDEL-based GWAS and INDEL-based eQTL analysis.
3. Utilize several other models for genomic prediction. Investigate the accuracy of the prediction if the microbiome principal components are used to construct the microbiome relationship matrix. Use machine learning to model the genomic and microbiome components of the genomic prediction.
4. Prioritize the GWAS and eQTL SNPs identified in this study and use them for genomic prediction of fillet yield and quality traits.